frontiers | Research Topics

# Current advances in genetic dementia and aging, volume II

**Edited by**
Yuzhen Xu, Ulises Gomez-Pinedo, Jun Liu, Daojun Hong and Jun Xu

**Published in**
Frontiers in Aging Neuroscience

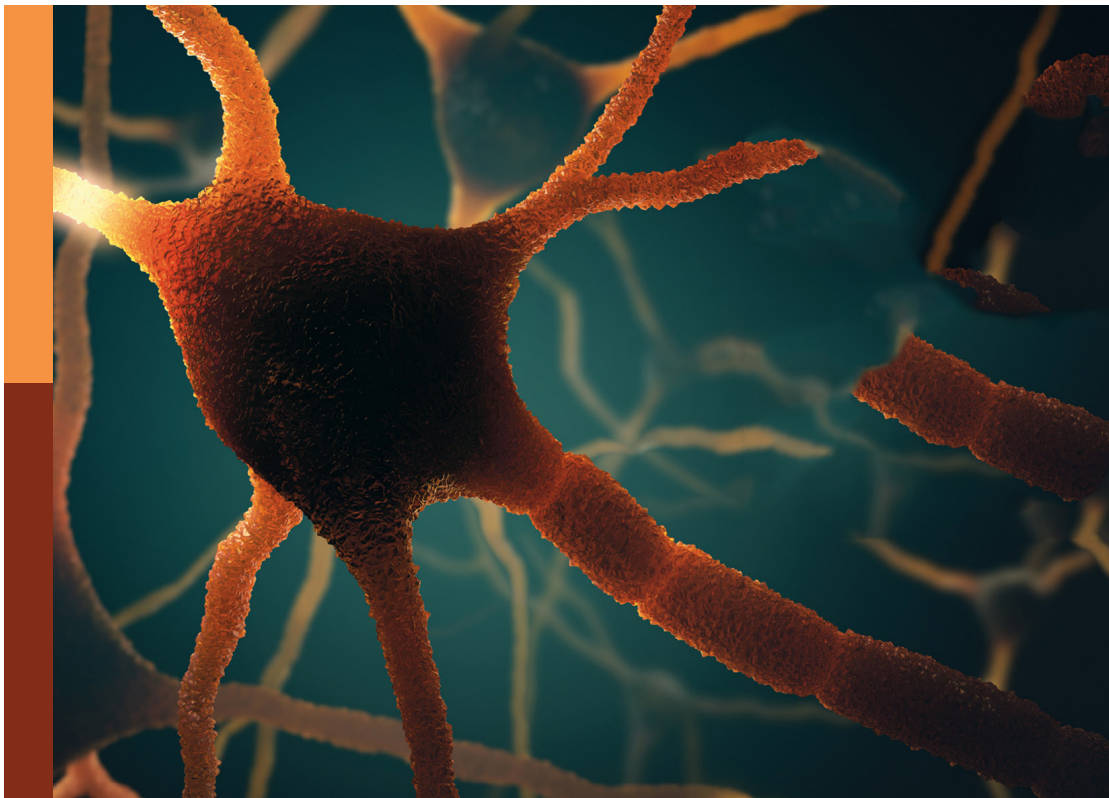

ISSN 1664-8714
ISBN 978-2-8325-2694-1
DOI 10.3389/978-2-8325-2694-1

## About Frontiers

Frontiers is more than just an open access publisher of scholarly articles: it is a pioneering approach to the world of academia, radically improving the way scholarly research is managed. The grand vision of Frontiers is a world where all people have an equal opportunity to seek, share and generate knowledge. Frontiers provides immediate and permanent online open access to all its publications, but this alone is not enough to realize our grand goals.

## Frontiers journal series

The Frontiers journal series is a multi-tier and interdisciplinary set of open-access, online journals, promising a paradigm shift from the current review, selection and dissemination processes in academic publishing. All Frontiers journals are driven by researchers for researchers; therefore, they constitute a service to the scholarly community. At the same time, the *Frontiers journal series* operates on a revolutionary invention, the tiered publishing system, initially addressing specific communities of scholars, and gradually climbing up to broader public understanding, thus serving the interests of the lay society, too.

## Dedication to quality

Each Frontiers article is a landmark of the highest quality, thanks to genuinely collaborative interactions between authors and review editors, who include some of the world's best academicians. Research must be certified by peers before entering a stream of knowledge that may eventually reach the public - and shape society; therefore, Frontiers only applies the most rigorous and unbiased reviews. Frontiers revolutionizes research publishing by freely delivering the most outstanding research, evaluated with no bias from both the academic and social point of view. By applying the most advanced information technologies, Frontiers is catapulting scholarly publishing into a new generation.

## What are Frontiers Research Topics?

Frontiers Research Topics are very popular trademarks of the *Frontiers journals series*: they are collections of at least ten articles, all centered on a particular subject. With their unique mix of varied contributions from Original Research to Review Articles, Frontiers Research Topics unify the most influential researchers, the latest key findings and historical advances in a hot research area.

Find out more on how to host your own Frontiers Research Topic or contribute to one as an author by contacting the Frontiers editorial office: frontiersin.org/about/contact

# Current advances in genetic dementia and aging, volume II

**Topic editors**

Yuzhen Xu — Tongji University, China

Ulises Gomez-Pinedo — Institute of Neurosciences, Health Research Institute of Hospital Clínico San Carlos, Spain

Jun Liu — The Second Affiliated Hospital of Guangzhou Medical University, China

Daojun Hong — The First Affiliated Hospital of Nanchang University, China

Jun Xu — Capital Medical University, China

**Citation**

Xu, Y., Gomez-Pinedo, U., Liu, J., Hong, D., Xu, J., eds. (2023). *Current advances in genetic dementia and aging, volume II*. Lausanne: Frontiers Media SA.

doi: 10.3389/978-2-8325-2694-1

# Table of contents

frontiers | Frontiers in Aging Neuroscience

TYPE Editorial
PUBLISHED 31 May 2023
DOI 10.3389/fnagi.2023.1202532



OPEN ACCESS

EDITED AND REVIEWED BY
Agustin Ibanez,
Latin American Brain Health Institute (BrainLat), Chile

*CORRESPONDENCE
Jun Xu
✉ neurojun@126.com

RECEIVED 08 April 2023
ACCEPTED 18 May 2023
PUBLISHED 31 May 2023

CITATION
Xu Y, Gomez-Pinedo U, Liu J, Hong D and Xu J (2023) Editorial: Current advances in genetic presentations of dementia and aging, volume II. *Front. Aging Neurosci.* 15:1202532. doi: 10.3389/fnagi.2023.1202532



# Editorial: Current advances in genetic presentations of dementia and aging, volume II

Yuzhen Xu[1], Ulises Gomez-Pinedo[2], Jun Liu[3], Daojun Hong[4] and Jun Xu[5,6]*

[1]Department of Rehabilitation, The Second Affiliated Hospital of Shandong First Medical University, Taian, China, [2]Laboratory of Neurobiology, Department of Neurology, Institute of Neurosciences, IdISSC, Hospital Clínico San Carlos, Universidad Complutense de Madrid, Madrid, Spain, [3]Department of Neurology, The Second Affiliated Hospital, Guangzhou Medical University, Guangzhou, China, [4]Department of Neurology, The First Affiliated Hospital of Nanchang University, Nanchang, China, [5]Department of Neurology, Beijing Tiantan Hospital, Capital Medical University, Beijing, China, [6]China National Clinical Research Center for Neurological Diseases, Beijing Tiantan Hospital, Capital Medical University, Beijing, China

KEYWORDS

**genetic, aging, dementia, advance, Alzheimer's disease**

Editorial on the Research Topic
Current advances in genetic presentations of dementia and aging, volume II

Dementia associated with causative genes refers to a group of inherited disorders that cause progressive cognitive decline and dementia. These disorders are caused by mutations in certain genes that are involved in the normal function of the brain (Loy et al., 2014). The most common dementia associated with the causative gene is Huntington's disease. Aging is a natural process that affects all organisms, and it is a major risk factor for many diseases, including dementia. As we age, the structure and function of the brain change, and this can lead to cognitive decline and an increased risk of developing dementia (Singh et al., 2019). Some forms of genetic presentations of dementia are associated with accelerated aging and an earlier onset of cognitive decline. Similarly, mutations in certain genes can lead to accelerated aging and an earlier onset of cognitive decline. However, it is important to note that not all forms of genetic presentations of dementia are associated with accelerated aging, and the relationship between genetics, aging, and dementia is complex and not fully understood.

This topic aims to address the relationship between dementia associated with causative genes and aging, including the mechanism of action of various dementia risk genes during aging, identification of aging biomarkers associated with dementia associated with causative genes and strategies for aging prevention and treatment associated with dementia The topic will provide a comprehensive overview of the aging risk genes associated with causative genes and strategies to prevent and treat aging. This publication focuses on Alzheimer's disease (AD), neuronal intranuclear inclusion disease (NIID), type 2 diabetes mellitus (T2DM)-related cognitive impairment, Schizophrenia (SCZ), and co-morbid RNA-binding proteins (RBPs) of glioma and cerebral ischemia. This topic will provide potential new therapeutic strategies for aging-related dementia associated with causative genes.

AD is the most common type of dementia attributed to aging. The ε4 allele of the apolipoprotein E (APOE) gene is recognized as a strong genetic risk factor for AD. However, the role of cerebral blood flow (CBF) in cognition-related brain regions in mediating the association of APOE with cognition is unknown. The clinical study of Wang et al. proposed for the first time that CBF based on arterial spin labeling (ASL) technology could partially mediate the correlation between APOE genotype and cognition. Neurotrophic factors and their receptors have long been promising targets for the treatment of AD. The results of animal experiments by Wei et al. showed that the MET protein showed an age-dependent progressive decrease in the early stage of AD, and affected the activity of its ligand hepatocyte growth factor (HGF), suggesting that the decrease of the HGF/MET signaling pathway may be a potential cause of AD. One of the pathogenic mechanisms. Heart fatty acid binding protein (HFABP) is a regulatory factor in lipid metabolism and is considered to be a novel biomarker involved in the pathogenesis of AD. Fu et al. found that the level of HFABP in cerebrospinal fluid was correlated with the classic AD pathological marker p-Tau, which may affect the longitudinal changes of cognitive function by mediating the level of p-Tau. Visuospatial impairment is common in AD patients. Tokushige et al. investigated whether gaze exploration patterns during visual tasks could help predict cognitive decline in the early stages of AD.

Unlike AD, NIID, first reported in 1968, is a rare neurodegenerative disease that affects cognitive function. The current diagnosis of NIID relies on CGG repeat expansion in the 50 UTR of the *NOTCH2 NLC* gene, or p62-positive intranuclear inclusions in skin biopsy. Skin biopsies are limited in scope due to their novelty. The study of Zhou et al. suggested that urine cytology is a sensitive and reliable non-invasive method for diagnosing NIID, although its accuracy is not as good as that of skin biopsy.

T2DM is an important risk factor affecting cognitive function in the elderly. Liu G. et al. found that T2DM may be related to dementia by affecting the volume of the fourth ventricle in a cross-sectional study of Chinese elderly communities, but this conclusion still needs further large-scale and multi-center verification. Zhang Y. et al. used astragaloside IV (AS-IV) to intervene in T2DM model rats, and found that its therapeutic effect may be achieved by regulating the Nrf2/Keap1/HO1/NQO1 pathway to reduce oxidative stress and neuroinflammation. In addition to AS-IV, quercetin, a traditional Chinese medicine, has recently been considered to prevent diabetic cerebrovascular endothelial cell injury by targeting VCAM1 (Huang et al., 2022).

SCZ is a multi-etiological mental illness that can cause cognitive impairment and neuropsychological disorders. It currently affects about 20 million people worldwide and is one of the leading causes of disability. The results of bioinformatics-based research by Zhang C. et al. showed that NEUROD6, NMU, PVALB, and NECAB1 may be potential biomarkers for predicting SCZ. In addition, Lin et al. also explored the comorbid RBPs of glioma and ischemic stroke, namely POLR2F, DYNC1H1, SMAD9, TRIM21, BRCA1, and ERI1. Among them, upregulated SMAD9 is associated with dementia, while downregulated POLR2F is associated with aging-related hypoxic stress. In the future, RBP is expected to be used as a comorbidity biomarker of glioma and ischemic stroke to guide clinical prevention and treatment.

ASL and urine cytology techniques offer no innovative options for early diagnosis and treatment of AD and NIID. The mechanisms of HGF/MET, HFABP in the pathogenesis of AD have been further explored. T2DM-related cognitive impairment has been at the forefront of research, and the detection of Nrf2/Keap1/HO1/NQO1 signaling pathway and fourth ventricular volume has helped to unravel the pathogenic mechanisms of the disease. Interestingly, bioinformatics has an increasingly prominent role in predicting neurological diseases such as SCZ, glioma and cerebral ischemic comorbidity RBPs. In addition, gaze exploration patterns may also be important indicators of response to early AD. In conclusion, the genetic manifestations of dementia are complex and current studies are insufficient to present the full picture of the disease, especially its concomitant aging manifestations deserve further investigation.

## Author contributions

YX drafted the manuscript. All authors contributed to the article and approved the submitted version.

## Funding

The present study was funded by the Shandong Medical and Health Technology Development Fund (202103070325), the Shandong Province Traditional Chinese Medicine Science and Technology Project (M-2022216), the Natural Science Foundation of Shandong Province (ZR2022MH124), the Nursery Project of the Shandong First Medical University Youth Science Fund Cultivation Funding Program (202201-105), the National Key Research and Development Program of China (2021YFC2500103), the National Natural Science Foundation (Grant Nos. 82071187, 81870821, and 81471215), and Beijing Youth Talent Team Support Program (2018000021223TD08).

## Acknowledgments

We would like to thank all the authors who participated in the subject collection and all the reviewers who were involved in the review process, and we are very grateful to all the editors who assisted us in processing the manuscripts.

## Conflict of interest

The authors declare that the research was conducted in the absence of any commercial or financial relationships that could be construed as a potential conflict of interest.

## Publisher's note

the editors and the reviewers. Any product that may be evaluated in this article, or claim that may be made by its manufacturer, is not guaranteed or endorsed by the publisher.

## References

Huang, J., Lin, W., Sun, Y., Wang, Q., He, S., Han, Z., et al. (2022). Quercetin targets VCAM1 to prevent diabetic cerebrovascular endothelial cell injury. *Front Aging Neurosci.* 14, 944195, doi: 10.3389/fnagi.2022.944195

Loy, C. T., Schofield, P. R., Turner, A. M., and Kwok, J. B. (2014). Genetics of dementia. *The Lancet.* 383, 828–840. doi: 10.1016/S0140-6736(13)60630-3

Singh, P. P., Demmitt, B. A., Nath, R. D., and Brunet, A. (2019). The genetics of aging: a vertebrate perspective. *Cell* 177, 200–220. doi: 10.1016/j.cell.2019.02.038

frontiers | Frontiers in Aging Neuroscience

ORIGINAL RESEARCH
published: 30 June 2022
doi: 10.3389/fnagi.2022.928925

# Mediation of the APOE Associations With Cognition Through Cerebral Blood Flow: The CIBL Study

*Yan-Li Wang[1,2], Mengfan Sun[1], Fang-Ze Wang[3], Xiaohong Wang[4], Ziyan Jia[1], Yuan Zhang[1], Runzhi Li[1], Jiwei Jiang[1], Linlin Wang[1], Wenyi Li[1], Yongan Sun[5], Jinglong Chen[6], Cuicui Zhang[7], Baolin Shi[8], Jianjian Liu[9], Xiangrong Liu[2] and Jun Xu[1,2]**

[1] Department of Neurology, Beijing Tiantan Hospital, Capital Medical University, Beijing, China, [2] China National Clinical Research Center for Neurological Diseases, Beijing Tiantan Hospital, Capital Medical University, Beijing, China, [3] Department of Cardiology, Weifang People's Hospital, Weifang Medical University, Weifang, China, [4] Institute of Translational Medicine, Medical College, Yangzhou University, Yangzhou, China, [5] Department of Neurology, Peking University First Hospital, Peking University, Beijing, China, [6] Division of Neurology, Department of Geriatrics, National Clinical Key Specialty, Guangzhou First People's Hospital, School of Medicine, South China University of Technology, Guangzhou, China, [7] Department of Neurology, The Second Affiliated Hospital of Xuzhou Medical University, Xuzhou, China, [8] Department of Neurology, Weifang People's Hospital, Weifang Medical University, Weifang, China, [9] Department of Neurology, Fuxing Hospital, Capital Medical University, Beijing, China

OPEN ACCESS

**Edited by:**
*Boon-Seng Wong, Singapore Institute of Technology, Singapore*

**Reviewed by:**
*Jing Cai, Guizhou University of Traditional Chinese Medicine, China*
*Nan Zhang, Tianjin Medical University General Hospital, China*

***Correspondence:**
*Jun Xu*
*neurojun@126.com*

**Specialty section:**
*This article was submitted to Alzheimer's Disease and Related Dementias, a section of the journal Frontiers in Aging Neuroscience*

**Received:** *26 April 2022*
**Accepted:** *02 June 2022*
**Published:** *30 June 2022*

**Citation:**
*Wang Y-L, Sun M, Wang F-Z, Wang X, Jia Z, Zhang Y, Li R, Jiang J, Wang L, Li W, Sun Y, Chen J, Zhang C, Shi B, Liu J, Liu X and Xu J (2022) Mediation of the APOE Associations With Cognition Through Cerebral Blood Flow: The CIBL Study. Front. Aging Neurosci. 14:928925. doi: 10.3389/fnagi.2022.928925*

**Background:** The ε4 allele of the apolipoprotein E (APOE) gene is a strong genetic risk factor for aging-related cognitive decline. However, the causal connection between ε4 alleles and cognition is not well understood. The objective of this study was to identify the roles of cerebral blood flow (CBF) in cognitive-related brain areas in mediating the associations of APOE with cognition.

**Methods:** The multiple linear regression analyses were conducted on 369 subjects (mean age of 68.8 years; 62.9% of women; 29.3% of APOE ε4 allele carriers). Causal mediation analyses with 5,000 bootstrapped iterations were conducted to explore the mediation effects.

**Result:** APOE ε4 allele was negatively associated with cognition ($P < 0.05$) and CBF in the amygdala, hippocampus, middle temporal gyrus, posterior cingulate, and precuneus (all $P < 0.05$). The effect of the APOE genotype on cognition was partly mediated by the above CBF (all $P < 0.05$).

**Conclusion:** CBF partially mediates the potential links between APOE genotype and cognition. Overall, the APOE ε4 allele may lead to a dysregulation of the vascular structure and function with reduced cerebral perfusion, which in turn leads to cognitive impairment.

**Keywords: APOE ε4, cerebral blood flow, cognition, causal mediation, CIBL study**

## INTRODUCTION

According to World Alzheimer Report 2019, the number of people with dementia is over 50 million currently, which is projected to be 82 million in 2030 and 152 million in 2050 (Sheet, 2019). According to the latest epidemiological survey, the incidence of mild cognitive impairment is 15.5% among people aged over 60 years in China (Jia et al., 2020). The vascular factor and apolipoprotein

E gene (APOE) ε4 allele are important factors associated with cognitive impairment (Bretsky et al., 2003; Strickland, 2018). Previous studies have drawn conflicting conclusions concerning the association between CBF and cognition. Some argued that reduced cerebral blood flow (CBF) is independently associated with worse cognitive performance (Bracko et al., 2020; Visser et al., 2020), especially, in the hippocampus, posterior cingulate, precuneus, thalamus, and caudate (Nation et al., 2013; Okonkwo et al., 2014). However, Steffener et al. suggested that cognition is negatively correlated with CBF in the posterior central gyrus, hippocampus, and part of the temporal cortex. Therefore, the relationship between cognition and CBF still needs further exploration. Besides, the relationship between CBF and APOE is still contradictory (Zlatar et al., 2014; Michels et al., 2016; Dounavi et al., 2021). The PREVENT-Dementia study shows that CBF is higher in ε4 carriers than in non-carriers across the general population (Dounavi et al., 2021), whereby a small-sample study of 48 subjects finds an inverse relationship between CBF and APOE ε4 (Michels et al., 2016). Moreover, the relationship is inconclusive at different stages of Alzheimer's disease (AD) (Wierenga et al., 2012; Kim et al., 2013; Michels et al., 2016; McKiernan et al., 2020). CBF is significantly increased in the cognitively normal (CN) ε4 carriers, (Wierenga et al., 2012; McKiernan et al., 2020) and decreased in mild cognitive impairment (MCI) ε4 carriers (Wierenga et al., 2012). However, the results are exactly the opposite in an age-matched cohort study (Kim et al., 2013). However, it has been widely accepted that APOE ε4 is the most common genetic risk factor for cognitive decline, and the mechanism underlying ε4 allele effects on cognition is not clear. Previous mediation analyses reveal that APOE ε2 may exert a protective effect on neurofibrillary tangles by two pathways: a direct effect of the ε2 allele (direct pathway) and *via* its effect on neuritic plaques (indirect pathway) (Serrano-Pozo et al., 2015). Thus, it could be speculated that the ε4 allele exerts its effects on cognition by both direct and indirect pathways. To date, the roles of CBF on the associations of APOE genotype with cognition have not been studied carefully. Herein, we aimed (1) to explore the relationships of APOE genotype with CBF and cognition and (2) to test whether the influences of APOE genotype on cognition is mediated by CBF.

# MATERIALS AND METHODS

## The Chinese Imaging, Biomarkers and Lifestyle Database

The Chinese Imaging, Biomarkers and Lifestyle (CIBL) Study of Alzheimer's Disease is an ongoing large-scale study mainly focused on radiographic changes, biomarkers, and risk factors of AD, aiming to construct prediction models for early diagnosis of AD. The samples were recruited at Beijing Tiantan Hospital Affiliated with Capital Medical University since September 2020. All enrolled participants underwent neuroimaging examination, blood collection, and clinical and neuropsychological assessments *via* a structured questionnaire. The clinically cognitive diagnoses of MCI and AD were aligned with the National Institute on Aging-Alzheimer's Association (NIA-AA) criteria (Albert et al., 2011; McKhann et al., 2011). Exclusion criteria for this study were (1) education illiterate groups; (2) cognitive impairment attributable to alcohol use, depression, medication use, or medical illness; (3) magnetic resonance imaging (MRI) contraindications; (4) using drugs or substance that affected cerebral perfusion on the same day as the MRI; (5) history of significant psychiatric disorder or neurological disease (e.g., central nervous system infection, traumatic brain injury, epilepsy, or other major neurological disorders); (6) life-threatening somatic disease; and (7) family history of Mendelian inheritance. All participants provided written informed consent prior to enrollment in the CIBL study, which was approved by the Research Ethics Committee of Beijing Tiantan Hospital in accordance with the Declaration of Helsinki.

## Participants

In this study, participants who had data seen as extreme values (situated outside ± 3 standard deviations) were removed from the analysis. Finally, 369 participants without a history of stroke or other structural brain abnormality were included in the CIBL study. Individual information including gender, age, APOE ε4 genotyping, educational level, systolic blood pressure (SBP), body mass index (BMI), history of hypertension, Mini-Mental State Examination (MMSE), Montreal Cognitive Assessment (MoCA), and CBF values was derived from arterial spin labeling (ASL). Age status was categorized as midlife ($40 < \text{age} < 65$) and late-life ($\text{age} \geq 65$).

## Apolipoprotein E Genotypes and Cognitive Assessment

DNA samples were extracted from 10 ml ethylene diamine tetraacetic acid (EDTA) overnight fasting blood samples. All individuals were genotyped at WeGene Lab using a customized Illumina WeGene V3 Array by Illumina iScan System, which contains roughly 700,000 markers. APOE genotypes comprising ε2, ε3, and ε4 alleles were defined by single nucleotide polymorphisms (SNPs) rs429358 and rs7412. Participants in this study were classified as APOE ε4 non-carriers and APOE ε4 carriers (presence of at least one APOE ε4 allele). Global cognitive function was assessed for all participants using the MoCA test (Hemmy et al., 2020).

## Brain Magnetic Resonance Imaging

All participants in this study underwent brain MRI using a 3.0-T MR scanner (SIGNA Premier; GE Healthcare, Milwaukee, WI, United States) with the 48-channelhead coil. The imaging parameters for high-resolution three-dimensional (3D) T1-weighted scans were as follows: repetition time, 1,900 ms; echo time, 3.0 ms; flip angle, 12°; slice thickness, 1.0 mm; number of slices, 176; field of view, 256 × 256 $mm^2$; acquisition matrix, 256 × 256; and scan time, 4 min 56 s. The perfusion-weighted MRI was performed using 3D pseudocontinuous arterial spin labeling (pCASL) sequences.

The acquisition parameters for eASL were as follows: repetition time, 4,849 ms; echo time, 10.6 ms; field of view,

220 × 220 mm$^2$; acquisition matrix, 512 × 512; slice thickness, 4 mm; number of slices, 36; and scan time, 4 min 22 s. CBF of PLD (2,025 ms) was calculated according to the standard one-compartment model (Alsop et al., 2015). The perfusion regions of interest (ROIs) included the amygdala, hippocampus, parahippocampal gyrus, middle temporal gyrus, posterior cingulate, precuneus, and thalamus.

## Statistical Analyses

The statistical analyses and figure preparation were performed using SPSS version 24.0, R version 4.0.3, and GraphPad Prism version 8.0. According to the APOE genotypes, subjects were categorized into APOE ε4 carrier and non-carrier groups, and *t*-test (for continuous variables) and chi-square test (for categorical variables) were used to test the difference of baseline between-group characteristics. *P*-values were corrected for multiple hypotheses using the Benjamini–Hochberg method (Klipper-Aurbach et al., 1995).

First, multiple linear regressions (MLRs) were used to explore associations of cognition with APOE genotypes and CBF averaged across left and right hemispheres, adjusting for different covariates. Then, to assess the influence of hemispheric dominance on cognitive ability, CBF of both left and right hemispheres was included in the same MLR model (DELETED). Furthermore, to examine whether cerebral perfusion could modulate the relationship between APOE and cognition, causal mediation analyses were conducted based on the method suggested by Baron and Kenny (Baron and Kenny, 1986). The relative indirect effects ($\beta_{IE}$) through CBF, natural direct effect ($\beta_{DE}$), total effect ($\beta_{total}$), and proportion of mediation ($\beta_{IE}/\beta_{total}$) were analyzed using bootstrapping with 5,000 iterations. A two-tailed *P*-value less than 0.05 was considered statistically significant.

# RESULTS

## Description of the Subjects

Patient demographics and baseline characteristics are shown in **Table 1**. A total of 369 subjects were recruited for the study, including 92 CN, 124 MCI, and 153 Alzheimer's dementia. The mean age was 68.82 ± 11.24 years and 62.87% were women. Of these, 108 (29.26%) were APOE ε4 allele carriers (≥ 1 ε4 allele). Compared with APOE ε4 non-carriers, APOE ε4 carriers were less educated ($P = 0.02$) (Araque Caballero et al., 2018) and performed significantly less well on the MMSE and the MoCA ($P < 0.0001$). No differences were registered in terms of age, gender, blood pressure, BMI, and history of hypertension ($P > 0.05$).

## Associations of Apolipoprotein E Genotype With Cerebral Blood Flow and Cognition

As can be seen in **Figure 1**, in the general study population, mean CBF of middle temporal gyrus ($P = 0.004$), hippocampus ($P = 0.036$), posterior cingulate ($P = 0.009$), and precuneus ($P = 0.011$) was significantly higher in the APOE ε4 non-carriers than in carriers. Similarly, as presented in **Table 1**, APOE ε4 carriers had lower value of all the above regional CBF in both left-hemisphere and right-hemisphere than non-carriers (all $P < 0.05$). APOE genotype was associated with CBF of amygdala ($P = 0.04$), hippocampus ($P = 0.03$), middle temporal gyrus ($P = 0.02$), posterior cingulate ($P = 0.02$), and precuneus ($P = 0.04$) but not in parahippocampal gyrus ($P = 0.126$) and thalamus ($P = 0.593$). Besides, comparison of the CBF among different APOE allele types is shown in **Supplementary Table 1**.

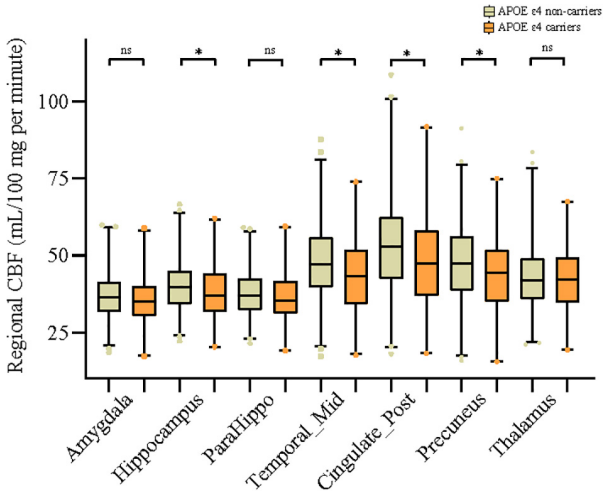


**FIGURE 1 |** Associations of APOE ε4 allele with mean cerebral blood flow (CBF) of 7 different brain regions. Comparisons between groups were analyzed using *t*-tests. The asterisks mean significant, and ns indicates non-significant.

As shown in **Table 2**, APOE genotype correlated negatively with MoCA ($\beta = -0.215$, $P < 0.001$), after adjusting for age, gender, and years of education (model 1). Additionally, adjusting for SBP and BMI (model 2), the association of APOE and MoCA became weaker ($\beta = -0.167$, $P = 0.002$), indicating that blood pressure and BMI are important risk factors for cognition. Besides, the APOE genotype was significantly associated with lower mean CBFs of the amygdala, hippocampus, parahippocampal gyrus, middle temporal gyrus, posterior cingulate, precuneus, and thalamus (all $P < 0.001$). In model 3, as for model 2 and additionally adjusting for APOE genotype, CBF of different brain areas was positively correlated with MoCA (β range from 0.193 to 0.454, all $P < 0.001$). Among these, the most significantly associated region was middle temporal gyrus ($\beta = 0.454$, $P < 0.001$), followed by posterior cingulate ($\beta = 0.447$, $P < 0.001$) and precuneus ($\beta = 0.438$, $P < 0.001$). Subgroup analysis was performed according to age, all but the relationship of thalamic CBF with cognition in the late-life group remained, as in **Supplementary Table 2**. In addition, correlation values were higher in the midlife group than that in the late-life group.

To further explore the influence of the dominant hand hemisphere, we performed a subgroup analysis of the left

**TABLE 1 |** Characteristics of subjects.

| | All subjects (*N* = 369) | APOE ε4 non-carriers (*N* = 261) | APOE ε4 carriers (*N* = 108) | *P*-value | FDR_BH |
|---|---|---|---|---|---|
| Female (N, %) | 232,62.87 | 165,63.22 | 67,62.04 | 0.831[a] | |
| Age, years | 68.82 ± 11.24 | 64.2 ± 11.53 | 66.31 ± 10.43 | 0.102 | |
| Education, years | 10.74 ± 4.56 | 11.11 ± 4.33 | 9.86 ± 5.00 | **0.02** | |
| MMSE score | 21.97 ± 7.58 | 23.22 ± 7.03 | 18.94 ± 8.03 | **6.92E-07** | |
| MoCA score | 17.19 ± 7.96 | 18.49 ± 7.51 | 13.95 ± 8.15 | **6.03E-07** | |
| SBP, mmHg | 128.62 ± 17.88 | 127.68 ± 17.07 | 131.38 ± 19.94 | 0.124 | |
| BMI, kg/m$^2$ | 23.92 ± 3.33 | 24.54 ± 9.48 | 23.83 ± 3.34 | 0.461 | |
| Hypertension (N, %) | 138, 37.40 | 100,38.61 | 38,36.19 | 0.666[a] | |
| **Regional CBF, mL/100 mg per minute** | | | | | |
| Amygdala_L | 37.12 ± 7.89 | 37.61 ± 7.7 | 35.95 ± 8.27 | 0.067 | 0.094 |
| Amygdala_R | 35.76 ± 7.74 | 36.27 ± 7.74 | 34.52 ± 7.64 | 0.05 | 0.078 |
| Hippocampus_L | 39.92 ± 8.34 | 40.5 ± 8.07 | 38.54 ± 8.84 | **0.041** | 0.071 |
| Hippocampus_R | 39.27 ± 8.87 | 39.88 ± 8.46 | 37.79 ± 9.69 | **0.04** | 0.071 |
| ParaHippocampal_L | 36.54 ± 7.37 | 36.86 ± 7.24 | 35.76 ± 7.66 | 0.193 | 0.225 |
| ParaHippocampal_R | 38.2 ± 8.25 | 38.69 ± 8.04 | 37.02 ± 8.67 | 0.076 | 0.097 |
| Temporal_Mid_L | 48.8 ± 13.26 | 49.99 ± 12.96 | 45.91 ± 13.61 | **0.007** | **0.028** |
| Temporal_Mid_R | 44.09 ± 11.67 | 45.22 ± 11.37 | 41.33 ± 11.98 | **0.003** | **0.028** |
| Cingulate_Post_L | 55.1 ± 17.74 | 56.7 ± 17.18 | 51.22 ± 18.54 | **0.007** | **0.028** |
| Cingulate_Post_R | 48.42 ± 14.82 | 49.58 ± 14.69 | 45.62 ± 14.81 | **0.019** | **0.044** |
| Precuneus_L | 46.57 ± 13.79 | 47.78 ± 13.75 | 43.63 ± 13.49 | **0.008** | **0.028** |
| Precuneus_R | 46.24 ± 13.64 | 47.33 ± 13.49 | 43.62 ± 13.7 | **0.017** | **0.044** |
| Thalamus_L | 42.1 ± 10.32 | 42.49 ± 10.34 | 41.17 ± 10.25 | 0.264 | 0.284 |
| Thalamus_R | 42.99 ± 10.03 | 43.13 ± 9.82 | 42.66 ± 10.55 | 0.684 | 0.684 |

*Continuous variables are shown as mean ± standard deviation (SD) and examined by the t-test. a, Categorical variables are shown as number (N) and percent and examined by chi-square test. FDR_BH indicates the Benjamini–Hochberg method corrected P-value. Bold indicates that the results were significant. FDR, false discovery rate; APOE, apolipoprotein E gene; MMSE, Mini-Mental State Examination; MoCA, Montreal Cognitive Assessment; SBP, systolic blood pressure; BMI, body mass index; Temporal_Mid, middletemporalgyrus; Cingulate_Post, posterior cingulate; L, left; R, right.*

and right hemispheres. When the left CBF and the right CBF were simultaneously included in the linear regression model, as shown in **Table 3**, the significances of correlations between MoCA and right amygdala, right hippocampus, right parahippocampal gyrus, right middle temporal gyrus, and right precuneus were lost (DELETED).

## Mediation Analysis Identified Indirect Effects Through Cerebral Blood Flow in the Associations of Apolipoprotein E Genotype With Cognition

The above findings demonstrated that there may be possible pathobiological pathways leading from APOE genotype to impaired cognition. We identified CBF of 5 regions mediating the effect of APOE genotype on cognition, after correcting for age, gender, education (refer to **Figure 2**). Of them, middle temporal gyrus ($\beta_{IE}$ = −0.74, 95% $CI_{IE}$ = −0.56 to −0.93), posterior cingulate ($\beta_{IE}$ = −0.65, 95% $CI_{IE}$ = −0.48 to −0.84), and precuneus ($\beta_{IE}$ = −0.63, 95% $CI_{IE}$ = −0.47 to −0.79) showed strong mediating effects, accounting for 24.41%, 21.51%, and 20.88% of the total effects of APOE genotype on cognition, respectively. Besides, CBF of the hippocampus (Proportion $_{IE}$ = 11.51%) and amygdala (Proportion $_{IE}$ = 7.92%) was also a potential modulator of APOE. Results of the left and right hemispheres are congruent with the results in **Figure 2**, and we found that brain regions of the left side have a stronger mediation than the right side (refer to **Supplementary Figure 1**).

# DISCUSSION

In this prospective cohort study, three main findings were summarized as follows: (1) APOE ε4 carriers had lower perfusion in multiple brain areas compared with non-carriers; (2) cerebral perfusion had a positive association with cognition, particularly for the left (dominant) hemisphere; (3) APOE was related to cognition through a CBF-mediated pathway. Taken together, our results clearly demonstrated that APOE genotypes could associate not only with cognition but also with cerebral perfusion. Cerebral perfusion of multiple brain regions could mediate the influences of APOE on cognition, suggesting the potentially causal connections between APOE and neurodegenerative changes in the brain.

Consistent with previous theoretical work, we found that APOE ε4 carriers had reduced CBF, (Hays et al., 2016, 2019) especially in the middle temporal gyrus, hippocampus, posterior cingulate, and precuneus. In addition, the BLSA study reported that the carriers had a more rapid cerebral perfusion decline than that of non-carriers (Beason-Held et al., 2007). One longitudinal

**TABLE 2 |** Associations of cognition with APOE and different regional CBF.

| | Model 1 | | Model 2 | | Model 3 | | Model 4 | |
|---|---|---|---|---|---|---|---|---|
| | β | *P*-value | β | *P*-value | β | *P*-value | β | *P*-value |
| APOE genotype | −4.542 | < 0.001 | −0.215 | < 0.001 | −0.167 | 0.002 | −0.167 | 0.002 |
| Amygdala | 0.250 | < 0.001 | 0.179 | < 0.001 | 0.200 | < 0.001 | 0.193 | < 0.001 |
| Hippocampus | 0.278 | < 0.001 | 0.245 | < 0.001 | 0.293 | < 0.001 | 0.286 | < 0.001 |
| Parahippocampal gyrus | 0.294 | < 0.001 | 0.219 | < 0.001 | 0.268 | < 0.001 | 0.264 | < 0.001 |
| Middle temporal gyrus | 0.311 | < 0.001 | 0.448 | < 0.001 | 0.458 | < 0.001 | 0.454 | < 0.001 |
| Posterior cingulate | 0.219 | < 0.001 | 0.403 | < 0.001 | 0.454 | < 0.001 | 0.447 | < 0.001 |
| Precuneus | 0.260 | < 0.001 | 0.420 | < 0.001 | 0.443 | < 0.001 | 0.438 | < 0.001 |
| Thalamus | 0.146 | < 0.001 | 0.182 | < 0.001 | 0.214 | < 0.001 | 0.214 | < 0.001 |

*Model 1: univariate linear regression of the relationship between cognition and variables in the first column.*
*Model 2: adjusting for age, sex, and years of education.*
*Model 3: adjusting for age, sex, years of education, systolic blood pressure, and BMI.*
*Model 4: adjusting for age, sex, years of education, systolic blood pressure, BMI, and APOE.*
*APOE, apolipoprotein E gene; CBF, cerebral blood flow; BMI, body mass index.*

**TABLE 3 |** Associations of CBF with cognition (DELETED).

| | $R^2$ | t | B | 95% CI | | *P*-value |
|---|---|---|---|---|---|---|
| | | | | Lower | Upper | |
| Amygdala_L | 0.323 | 2.285 | 0.228 | 0.032 | 0.425 | **0.023** |
| Amygdala_R | | −0.520 | −0.055 | −0.262 | 0.152 | 0.603 |
| Hippocampus_L | 0.347 | 2.443 | 0.318 | 0.062 | 0.574 | **0.015** |
| Hippocampus_R | | −0.527 | −0.064 | −0.304 | 0.176 | 0.599 |
| Parahippocampal gyrus _L | 0.338 | 2.801 | 0.387 | 0.115 | 0.659 | **0.005** |
| Parahippocampal gyrus _R | | −1.096 | −0.135 | −0.377 | 0.108 | 0.274 |
| Middle temporal gyrus _L | 0.450 | 4.127 | 0.260 | 0.136 | 0.384 | **<0.001** |
| Middle temporal gyrus _R | | 0.143 | 0.011 | −0.135 | 0.157 | 0.886 |
| Posterior cingulate _L | 0.461 | 6.075 | 0.307 | 0.207 | 0.406 | **<0.001** |
| Posterior cingulate _R | | −2.310 | −0.140 | −0.260 | −0.021 | **0.022** |
| Precuneus_L | 0.439 | 4.007 | 0.313 | 0.159 | 0.467 | **<0.001** |
| Precuneus_R | | −0.882 | −0.070 | −0.226 | 0.086 | 0.379 |
| Thalamus_L | 0.341 | 3.812 | 0.355 | 0.172 | 0.538 | **<0.001** |
| Thalamus_R | | −2.264 | −0.208 | −0.389 | −0.027 | **0.024** |

*All models were adjusted for age, gender, education, APOE genotype, systolic blood pressure, BMI, and CBF of the specific brain area (left and right). Bold indicates that the results were significant (P < 0.05). L, left; R, right; CBF, cerebral blood flow.*

study of cognitively unimpaired older individuals showed that the hippocampus, posterior cingulate, and precuneus declined faster than other gray matter regions (McKiernan et al., 2020; Wang et al., 2021), and the heterogeneity in different brain regions may result from different causative mechanisms. A cross-sectional study from the PREVEBT-Dementia cohort also concluded that the compensatory hyperperfusion would occur at the early stages of neurodegeneration, conversely decreasing CBF at the subclinical phase of AD (McKiernan et al., 2020). During the spectrum of AD, relationships between APOE ε4 and CBF were incongruent. CBF was decreased in CN APOE ε4 carriers (Kim et al., 2013; Michels et al., 2016), but others were not (Wierenga et al., 2012; McKiernan et al., 2020). In addition, for MCI APOE ε4 carriers, findings were also contradictory (Wierenga et al., 2012; Kim et al., 2013).

However, the precise mechanisms underlying the effects of APOE on CBF and cognition are poorly defined. A study in ApoE-4 targeted replacement mice demonstrated that reduced resting CBF of APOE ε4 carriers was associated with vascular rarefaction rather than the slow velocity of a microvascular red blood cell (Koizumi et al., 2018). Besides, Østergaard et al. (2013) summarized that APOE ε4 can increase the likelihood of heterogeneity of capillary blood flow, reducing CBF, ultimately resulting in oxidative stress, activation of inflammatory pathways, and neurodegeneration. A randomized, double-blinded, placebo-controlled crossover study found that vascular function was impaired in ε4 carriers, and the peak time and magnitude of the blood oxygenation level-dependent hemodynamic response to breath-hold significantly decreased with age (Rasmussen et al., 2019). In addition, functional magnetic resonance imaging studies show that APOE ε4 carriers

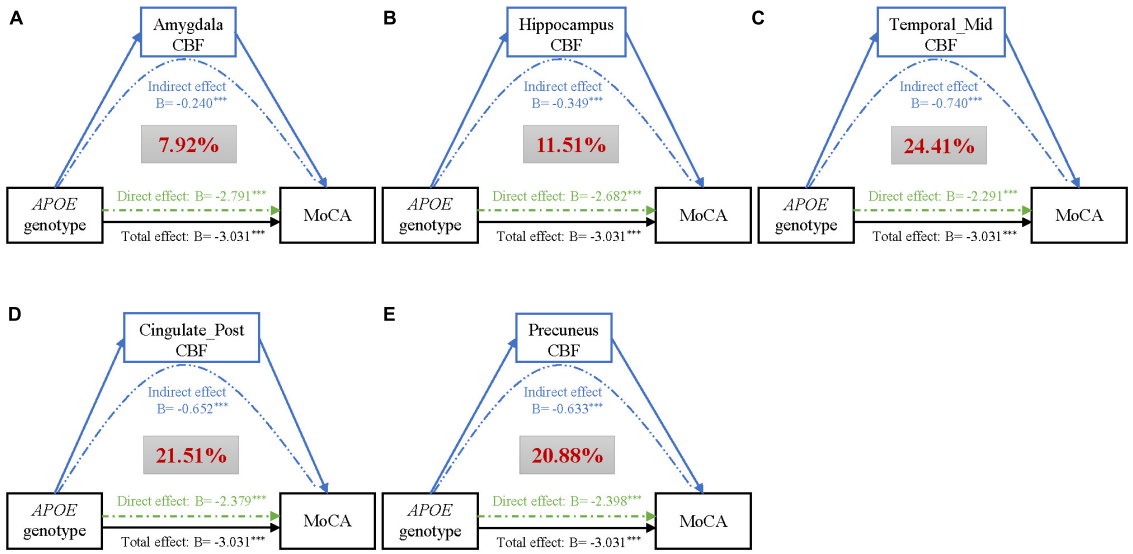


**FIGURE 2 |** Mediation analyses of CBF of different brain regions **(A–E)** on the association of APOE genotype with MoCA, adjusting for age, gender, and education. Black lines show the total effect of APOE genotype on MoCA, green lines show the direct effect (i.e., without mediation), and blue lines depict the CBF mediation effect. Path weights are presented in *B*-values (unstandardized coefficients), and the asterisks mean that the indirect/direct/total effect is significant. Significance was determined using bootstrapping with 5,000 iterations. Additionally, the red figure within the gray box represents the proportion of mediation. Abbreviations: CBF, cerebral blood flow; MoCA, Montreal Cognitive Assessment; ParaHippo, parahippocampal gyrus; Temporal_Mid, middletemporalgyrus; Cingulate_Post, posterior cingulate.

experienced reduced cerebrovascular reactivity, indicating highly sensitive to hypoperfusion and hypoxia (Suri et al., 2015; Koizumi et al., 2018). This conclusion is supported by preclinical and human studies, suggesting that the APOE ε4 allele was associated with higher oxidative stress and a higher pro-inflammatory state (Jofre-Monseny et al., 2008). A multimodal meta-analysis noted that APOE ε4 carriers presented a higher risk of developing white matter hyperintensity (Schilling et al., 2013), which had been widely accepted that was clearly associated with cognition decline (Wang et al., 2020).

The mediating finding in our study provided first that the causal relationship between APOE and cognition can be explained in terms of CBF. Mouse models carrying the APOE ε4 also experienced reduced CBF, and glucose metabolism and rapamycin could rescue cerebrovascular functions, CBF and incipient learning, and memory deficits in young ApoE4 mice (Lin et al., 2017). The above results increased our belief that the CBF was a mediator. Further experimental validation of this causality was required *in vitro* and *in vivo*. However, whether APOE ε4 is beneficial or aggravating remains controversial and seems to depend on the age. For example, Mondadori et al. (2007) and McKiernan et al. (2020) found that relative hyperperfusion and better cognition were observed in young APOE ε4 carriers. But ε4 carriers exhibited lower resting CBF in old age and increased the risk of AD (Thambisetty et al., 2010; Wierenga et al., 2013). When additional correction for age was applied to the association of CBF and cognition in our study, the effect size was much reduced especially in the elderly, indicating significantly affected by age. In addition, a few small studies (sample size $< 100$) revealed no significant correlation of APOE ε4 with CBF and cognition (Su et al., 2015; Matura et al., 2016).

This study had several strengths. We had a population-based design with a large sample size and imaging data. The data reported in this study will serve as a baseline for follow-up studies and be conducted to pursue an in-depth understanding in this regard. CBF was obtained by non-invasive ASL MRI, which had good agreements with quantitative CBF values derived from $^{15}O$-$H_2O$ PET (Kamano et al., 2013). Additionally, an imaging examination was performed after overnight fasting for 8 h, minimizing the effects of metabolic factors. However, several potential limitations should be addressed. First, our study was hospital-based, and the generalizability of conclusions warrants further validation in large community-based longitudinal studies. Second, ASL measurements were not corrected for partial volume effect (PVE), until now, the correction approaches are inconsistent, and the consistent benefit of adjusting for PVE has not been shown (Chappell et al., 2021). In addition, we did not consider the influence of the whole brain CBF. Currently, examination of serum or cerebrospinal fluid biomarkers related to neurodegenerative diseases has been not performed in the CIBL cohort. Besides, multi-delay ASL was required to verify these results, due to the effect of different arterial transit times.

## CONCLUSION

Results demonstrated cerebral perfusion as an independent risk factor not only for cognitive impairments but also an important mediator for the effects of APOE genotype on the cognitive deficiency. The adverse genetic influence of APOE

ε4 on cognition may be moderated by improved cerebral vasculature and CBF.

## DATA AVAILABILITY STATEMENT

The raw data supporting the conclusions of this article will be made available by the authors, without undue reservation.

## ETHICS STATEMENT

The studies involving human participants were reviewed and approved by the Research Ethics Committee of Beijing Tiantan Hospital. The patients/participants provided their written informed consent to participate in this study.

## AUTHOR CONTRIBUTIONS

JX, XL, and Y-LW conceived and designed the study. Y-LW contributed to generation of the manuscript. All authors contributed to the editing of the manuscript.

## FUNDING

This study was supported by the National Key Research and Development Program of China (2021YFC2500103), the National Natural Science Foundation (Grant numbers: 82071187, 81870821, and 81471215), the Beijing Youth Talent Team Support Program (2018000021223TD08), the National Key Research and Development Program (2019YFC0120902), and the Beijing Natural Science Foundation Grant (L182055).

## ACKNOWLEDGMENTS

We would like to thank AnImage (Beijing) Technology Co., Ltd., and WeGene Lab for technical guidance.

## SUPPLEMENTARY MATERIAL

The Supplementary Material for this article can be found online at: https://www.frontiersin.org/articles/10.3389/fnagi.2022.928925/full#supplementary-material

## REFERENCES

Albert, M. S., DeKosky, S. T., Dickson, D., Dubois, B., Feldman, H. H., Fox, N. C., et al. (2011). The diagnosis of mild cognitive impairment due to Alzheimer's disease: recommendations from the National Institute on Aging-Alzheimer's Association workgroups on diagnostic guidelines for Alzheimer's disease. *Alzheimers Dement.* 7, 270–279. doi: 10.1016/j.jalz.2011.03.008

Alsop, D. C., Detre, J. A., Golay, X., Günther, M., Hendrikse, J., Hernandez-Garcia, L., et al. (2015). Recommended implementation of arterial spin-labeled perfusion MRI for clinical applications: a consensus of the ISMRM perfusion study group and the European consortium for ASL in dementia. *Magn. Reson. Med.* 73, 102–116. doi: 10.1002/mrm.25197

Araque Caballero, M., Suárez-Calvet, M., Duering, M., Franzmeier, N., Benzinger, T., Fagan, A. M., et al. (2018). White matter diffusion alterations precede symptom onset in autosomal dominant Alzheimer's disease. *Brain* 141, 3065–3080. doi: 10.1093/brain/awy229

Baron, R. M., and Kenny, D. A. (1986). The moderator-mediator variable distinction in social psychological research: conceptual, strategic, and statistical considerations. *J. Pers. Soc. Psychol.* 51, 1173–1182.

Beason-Held, L. L., Moghekar, A., Zonderman, A. B., Kraut, M. A., and Resnick, S. M. (2007). Longitudinal changes in cerebral blood flow in the older hypertensive brain. *Stroke* 38, 1766–1773. doi: 10.1161/STROKEAHA.106.477109

Bracko, O., Njiru, B. N., Swallow, M., Ali, M., Haft-Javaherian, M., and Schaffer, C. B. (2020). Increasing cerebral blood flow improves cognition into late stages in Alzheimer's disease mice. *J. Cereb. Blood Flow Metab.* 40, 1441–1452. doi: 10.1177/0271678X19873658

Bretsky, P., Guralnik, J. M., Launer, L., Albert, M., and Seeman, T. E. (2003). The role of APOE-epsilon4 in longitudinal cognitive decline: macArthur Studies of Successful Aging. *Neurology* 60, 1077–1081. doi: 10.1212/01.wnl.0000055875.26908.24

Chappell, M. A., McConnell, F. A. K., Golay, X., Günther, M., Hernandez-Tamames, J. A., van Osch, M. J., et al. (2021). Partial volume correction in arterial spin labeling perfusion MRI: a method to disentangle anatomy from physiology or an analysis step too far? *Neuroimage* 238:118236.

Dounavi, M. E., Low, A., McKiernan, E. F., Mak, E., Muniz-Terrera, G., Ritchie, K., et al. (2021). Evidence of cerebral hemodynamic dysregulation in middle-aged APOE ε4 carriers: the PREVENT-Dementia study. *J. Cereb. Blood Flow Metab.* 41, 2844–2855. doi: 10.1177/0271678X211020863

Hays, C. C., Zlatar, Z. Z., and Wierenga, C. E. (2016). The Utility of Cerebral Blood Flow as a Biomarker of Preclinical Alzheimer's Disease. *Cell. Mol. Neurobiol.* 36, 167–179. doi: 10.1007/s10571-015-0261-z

Hays, C. C., Zlatar, Z. Z., Meloy, M. J., Bondi, M. W., Gilbert, P. E., Liu, T. T., et al. (2019). APOE modifies the interaction of entorhinal cerebral blood flow and cortical thickness on memory function in cognitively normal older adults. *Neuroimage* 202:116162. doi: 10.1016/j.neuroimage.2019.116162

Hemmy, L. S., Linskens, E. J., Silverman, P. C., Miller, M. A., Talley, K. M. C., Taylor, B. C., et al. (2020). Brief Cognitive Tests for Distinguishing Clinical Alzheimer-Type Dementia From Mild Cognitive Impairment or Normal Cognition in Older Adults With Suspected Cognitive Impairment. *Ann. Intern. Med.* 172, 678–687. doi: 10.7326/M19-3889

Jia, L., Du, Y., Chu, L., Zhang, Z., Li, F., Lyu, D., et al. (2020). Prevalence, risk factors, and management of dementia and mild cognitive impairment in adults aged 60 years or older in China: a cross-sectional study. *Lancet Public Health* 5, e661–e671. doi: 10.1016/S2468-2667(20)30185-7

Jofre-Monseny, L., Minihane, A. M., and Rimbach, G. (2008). Impact of apoE genotype on oxidative stress, inflammation and disease risk. *Mol. Nutr. Food Res.* 52, 131–145. doi: 10.1002/mnfr.200700322

Kamano, H., Yoshiura, T., Hiwatashi, A., Abe, K., Togao, O., Yamashita, K., et al. (2013). Arterial spin labeling in patients with chronic cerebral artery steno-occlusive disease: correlation with (15)O-PET. *Acta Radiol.* 54, 99–106. doi: 10.1258/ar.2012.120450

Kim, S. M., Kim, M. J., Rhee, H. Y., Ryu, C. W., Kim, E. J., Petersen, E. T., et al. (2013). Regional cerebral perfusion in patients with Alzheimer's disease and mild cognitive impairment: effect of APOE epsilon4 allele. *Neuroradiology* 55, 25–34. doi: 10.1007/s00234-012-1077-x

Klipper-Aurbach, Y., Wasserman, M., Braunspiegel-Weintrob, N., Borstein, D., Peleg, S., Assa, S., et al. (1995). Mathematical formulae for the prediction of the residual beta cell function during the first two years of disease in children and adolescents with insulin-dependent diabetes mellitus. *Med. Hypotheses* 45, 486–490. doi: 10.1016/0306-9877(95)90228-7

Koizumi, K., Hattori, Y., Ahn, S. J., Buendia, I., Ciacciarelli, A., Uekawa, K., et al. (2018). Apoε4 disrupts neurovascular regulation and undermines white matter integrity and cognitive function. *Nat. Commun.* 9:3816. doi: 10.1038/s41467-018-06301-2

Lin, A. L., Jahrling, J. B., Zhang, W., DeRosa, N., Bakshi, V., Romero, P., et al. (2017). Rapamycin rescues vascular, metabolic and learning deficits in

apolipoprotein E4 transgenic mice with pre-symptomatic Alzheimer's disease. *J. Cereb. Blood Flow Metab.* 37, 217–226. doi: 10.1177/0271678X15621575

Matura, S., Prvulovic, D., Hartmann, D., Scheibe, M., Sepanski, B., Butz, M., et al. (2016). Age-Related Effects of the Apolipoprotein E Gene on Brain Function. *J. Alzheimers Dis.* 52, 317–331. doi: 10.3233/JAD-150990

McKhann, G. M., Knopman, D. S., Chertkow, H., Hyman, B. T., Jack, C. R. Jr., and Kawas, C. H. (2011). The diagnosis of dementia due to Alzheimer's disease: recommendations from the National Institute on Aging-Alzheimer's Association workgroups on diagnostic guidelines for Alzheimer's disease. *Alzheimers Dement.* 7, 263–269. doi: 10.1016/j.jalz.2011.03.005

McKiernan, E. F., Mak, E., Dounavi, M. E., Wells, K., Ritchie, C., Williams, G., et al. (2020). Regional hyperperfusion in cognitively normal APOE ε4 allele carriers in mid-life: analysis of ASL pilot data from the PREVENT-Dementia cohort. *J. Neurol. Neurosurg. Psychiatry* 91, 861–866. doi: 10.1136/jnnp-2020-322924

Michels, L., Warnock, G., Buck, A., Macauda, G., Leh, S. E., Kaelin, A. M., et al. (2016). Arterial spin labeling imaging reveals widespread and Aβ-independent reductions in cerebral blood flow in elderly apolipoprotein epsilon-4 carriers. *J. Cereb. Blood Flow Metab.* 36, 581–595. doi: 10.1177/0271678X15605847

Mondadori, C. R., de Quervain, D. J., Buchmann, A., Mustovic, H., Wollmer, M. A., Schmidt, C. F., et al. (2007). Better memory and neural efficiency in young apolipoprotein E epsilon4 carriers. *Cereb. Cortex* 17, 1934–1947. doi: 10.1093/cercor/bhl103

Nation, D. A., Wierenga, C. E., Clark, L. R., Dev, S. I., Stricker, N. H., Jak, A. J., et al. (2013). Cortical and subcortical cerebrovascular resistance index in mild cognitive impairment and Alzheimer's disease. *J. Alzheimers Dis.* 36, 689–698. doi: 10.3233/JAD-130086

Okonkwo, O. C., Xu, G., Oh, J. M., Dowling, N. M., Carlsson, C. M., Gallagher, C. L., et al. (2014). Cerebral blood flow is diminished in asymptomatic middle-aged adults with maternal history of Alzheimer's disease. *Cereb. Cortex* 24, 978–988. doi: 10.1093/cercor/bhs381

Østergaard, L., Aamand, R., Gutiérrez-Jiménez, E., Ho, Y. C., Blicher, J. U., Madsen, S. M., et al. (2013). The capillary dysfunction hypothesis of Alzheimer's disease. *Neurobiol. Aging* 34, 1018–1031. doi: 10.1016/j.neurobiolaging.2012.09.011

Rasmussen, P. M., Aamand, R., Weitzberg, E., Christiansen, M., Østergaard, L., and Lund, T. E. (2019). APOE gene-dependent BOLD responses to a breath-hold across the adult lifespan. *Neuroimage Clin.* 24:101955. doi: 10.1016/j.nicl.2019.101955

Schilling, S., DeStefano, A. L., Sachdev, P. S., Choi, S. H., Mather, K. A., DeCarli, C. D., et al. (2013). APOE genotype and MRI markers of cerebrovascular disease: systematic review and meta-analysis. *Neurology* 81, 292–300. doi: 10.1212/WNL.0b013e31829bfda4

Serrano-Pozo, A., Qian, J., Monsell, S. E., Betensky, R. A., and Hyman, B. T. (2015). APOEε2 is associated with milder clinical and pathological Alzheimer disease. *Ann. Neurol.* 77, 917–929.

World Health Organization [WHO] (2019). *Dementia Fact Sheet.* Available online at: https://www.who.int/news-room/fact-sheets/detail/dementia (accessed September 2, 2021).

Strickland, S. (2018). Blood will out: vascular contributions to Alzheimer's disease. *J. Clin. Invest.* 128, 556–563. doi: 10.1172/JCI97509

Su, Y. Y., Liang, X., Schoepf, U. J., Varga-Szemes, A., West, H. C., Qi, R., et al. (2015). APOE Polymorphism Affects Brain Default Mode Network in Healthy Young Adults: a STROBE Article. *Medicine* 94:e1734. doi: 10.1097/MD.0000000000001734

Suri, S., Mackay, C. E., Kelly, M. E., Germuska, M., Tunbridge, E. M., Frisoni, G. B., et al. (2015). Reduced cerebrovascular reactivity in young adults carrying the APOE ε4 allele. *Alzheimers Dement.* 11, 648–57.e1. doi: 10.1016/j.jalz.2014.05.1755

Thambisetty, M., Beason-Held, L., An, Y., Kraut, M. A., and Resnick, S. M. (2010). APOE epsilon4 genotype and longitudinal changes in cerebral blood flow in normal aging. *Arch. Neurol.* 67, 93–98. doi: 10.1001/archneurol.2009.913

Visser, D., Wolters, E. E., Verfaillie, S. C. J., Coomans, E. M., Timmers, T., Tuncel, H., et al. (2020). Tau pathology and relative cerebral blood flow are independently associated with cognition in Alzheimer's disease. *Eur. J. Nucl. Med. Mol. Imaging* 47, 3165–3175. doi: 10.1007/s00259-020-04831-w

Wang, R., Oh, J. M., Motovylyak, A., Ma, Y., Sager, M. A., Rowley, H. A., et al. (2021). Impact of sex and APOE ε4 on age-related cerebral perfusion trajectories in cognitively asymptomatic middle-aged and older adults: a longitudinal study. *J. Cereb. Blood Flow Metab.* 41, 3016–3027. doi: 10.1177/0271678X211021313

Wang, Y. L., Chen, W., Cai, W. J., Hu, H., Xu, W., Wang, Z. T., et al. (2020). Associations of White Matter Hyperintensities with Cognitive Decline: a Longitudinal Study. *J. Alzheimers Dis.* 73, 759–768. doi: 10.3233/JAD-191005

Wierenga, C. E., Clark, L. R., Dev, S. I., Shin, D. D., Jurick, S. M., Rissman, R. A., et al. (2013). Interaction of age and APOE genotype on cerebral blood flow at rest. *J. Alzheimers Dis.* 34, 921–935. doi: 10.3233/JAD-121897

Wierenga, C. E., Dev, S. I., Shin, D. D., Clark, L. R., Bangen, K. J., Jak, A. J., et al. (2012). Effect of mild cognitive impairment and APOE genotype on resting cerebral blood flow and its association with cognition. *J. Cereb. Blood Flow Metab.* 32, 1589–1599. doi: 10.1038/jcbfm.2012.58

Zlatar, Z. Z., Wierenga, C. E., Bangen, K. J., Liu, T. T., and Jak, A. J. (2014). Increased hippocampal blood flow in sedentary older adults at genetic risk for Alzheimer's disease. *J. Alzheimers Dis.* 41, 809–817. doi: 10.3233/JAD-132252

**Conflict of Interest:** The authors declare that the research was conducted in the absence of any commercial or financial relationships that could be construed as a potential conflict of interest.

**Publisher's Note:** All claims expressed in this article are solely those of the authors and do not necessarily represent those of their affiliated organizations, or those of the publisher, the editors and the reviewers. Any product that may be evaluated in this article, or claim that may be made by its manufacturer, is not guaranteed or endorsed by the publisher.

frontiers | Frontiers in Aging Neuroscience

ORIGINAL RESEARCH
published: 12 July 2022
doi: 10.3389/fnagi.2022.954266

# Reduced HGF/MET Signaling May Contribute to the Synaptic Pathology in an Alzheimer's Disease Mouse Model

*Jing Wei, Xiaokuang Ma, Antoine Nehme, Yuehua Cui, Le Zhang and Shenfeng Qiu**

*Basic Medical Sciences, University of Arizona College of Medicine-Phoenix, Phoenix, AZ, United States*

Alzheimer's disease (AD) is a neurodegenerative disorder strongly associates with aging. While amyloid plagues and neurofibrillary tangles are pathological hallmarks of AD, recent evidence suggests synaptic dysfunction and physical loss may be the key mechanisms that determine the clinical syndrome and dementia onset. Currently, no effective therapy prevents neuropathological changes and cognitive decline. Neurotrophic factors and their receptors represent novel therapeutic targets to treat AD and dementia. Recent clinical literature revealed that MET receptor tyrosine kinase protein is reduced in AD patient's brain. Activation of MET by its ligand hepatocyte growth factor (HGF) initiates pleiotropic signaling in the developing brain that promotes neurogenesis, survival, synaptogenesis, and plasticity. We hypothesize that if reduced MET signaling plays a role in AD pathogenesis, this might be reflected in the AD mouse models and as such provides opportunities for mechanistic studies on the role of HGF/MET in AD. Examining the 5XFAD mouse model revealed that MET protein exhibits age-dependent progressive reduction prior to overt neuronal pathology, which cannot be explained by indiscriminate loss of total synaptic proteins. In addition, genetic ablation of MET protein in cortical excitatory neurons exacerbates amyloid-related neuropathology in 5XFAD mice. We further found that HGF enhances prefrontal layer 5 neuron synaptic plasticity measured by long-term potentiation (LTP). However, the degree of LTP enhancement is significantly reduced in 5XFAD mice brain slices. Taken together, our study revealed that early reduction of HGF/MET signaling may contribute to the synaptic pathology observed in AD.

**Keywords: Alzheimer's disease, MET receptor tyrosine kinase, hepatocyte growth factor, synaptic plasticity, regeneration**

OPEN ACCESS

***Edited by:***
*Yuzhen Xu,*
*Tongji University, China*

***Reviewed by:***
*Qiang Liu,*
*Tianjin Medical University General Hospital, China*
*Dexiao Zhu,*
*The University of Texas Health Science Center at San Antonio, United States*

****Correspondence:***
*Shenfeng Qiu*
*sqiu@arizona.edu*

***Specialty section:***
*This article was submitted to Alzheimer's Disease and Related Dementias, a section of the journal Frontiers in Aging Neuroscience*

***Received:*** *27 May 2022*
***Accepted:*** *13 June 2022*
***Published:*** *12 July 2022*

***Citation:***
*Wei J, Ma X, Nehme A, Cui Y, Zhang L and Qiu S (2022) Reduced HGF/MET Signaling May Contribute to the Synaptic Pathology in an Alzheimer's Disease Mouse Model. Front. Aging Neurosci. 14:954266. doi: 10.3389/fnagi.2022.954266*

## INTRODUCTION

An estimated 50 million people worldwide are currently living with dementia (Scheltens et al., 2021), among which Alzheimer's disease (AD) accounts for the majority of these cases (Masters et al., 2015). AD is increasingly a global public health priority as the aging population increases. The current lack of effective therapeutics derives from our limited understanding of the mechanisms underlying AD pathogenesis, which hinders development of novel therapeutic and interventional

approaches (Alexiou et al., 2019). Aside from the well-characterized extracellular amyloid plaques and neurofibrillary tangles composed of β-amyloid (Aβ) and phosphorylated tau proteins, an early pathology in AD is the loss of functional synapse and disruption in synaptic plasticity that occur before overt neurodegeneration (Cleary et al., 2005; Hsieh et al., 2006; Lacor et al., 2007; Shankar et al., 2007; Chen et al., 2010; Kim et al., 2014; Chung et al., 2016). Disruption of molecular mechanisms governing synaptic homeostasis and plasticity, such as activity-dependent long-term potentiation (LTP) (Gonzalez Burgos et al., 2012; Koch et al., 2012; Vanleeuwen and Penzes, 2012; Megill et al., 2015; Prieto et al., 2017), may render synapses dysfunctional and is considered an early pathological hallmark that instigates AD progression (Huh et al., 2016; Mango et al., 2019). While AD treatment strategies have been largely focused on Aβ and tau protein, the synapse itself could be a direct target to consider regarding disease intervention. Synaptic function may be preserved by preventing mechanisms of synapse degeneration and/or promoting mechanisms favoring homeostasis or regeneration (Smith et al., 2009).

Mesenchymal epithelial transition factor (MET) receptor tyrosine kinase and its ligand, hepatocyte growth factor (HGF), are expressed in the nervous system from prenatal development to adult life. The human *MET* gene plays a pleiotropic role in cell proliferation, morphogenesis, differentiation, survival, and regeneration of many tissue types. Upon HGF binding, MET is activated by autophosphorylation of intracellular tyrosine residues that serve as multi-substrate docking sites for signaling adaptors (Naldini et al., 1991a,b; Ponzetto et al., 1994). These adaptor proteins in turn activate pleiotropic molecular cascades including PI3K-AKT, MAPK/ERK, mTOR, and STAT (Stefan et al., 2001; Trusolino et al., 2010) to elicit a repertoire of cell behaviors collectively known as mitogenic, motogenic, and morphogenic. Our recent work reveals that MET in the developing cortical circuits controls dendritic spine formation and synaptogenesis (Qiu et al., 2011), refinement of circuit connectivity (Qiu et al., 2014; Peng et al., 2016), and the timing of excitatory synapse maturation (Qiu et al., 2011; Ising et al., 2019). Importantly, MET signaling persists in the adult brain but is restricted to the site of excitatory synapse (Akimoto et al., 2004; Eagleson et al., 2013) and is capable of modifying synaptic function and plasticity.

Existing literature supports that MET signaling is neurotrophic and neuroprotective in multiple neurodegenerative mouse models ranging from multiple sclerosis (Bai et al., 2012; Benkhoucha et al., 2014; Matsumoto et al., 2014), Parkinson's disease (Koike et al., 2006), to ALS (Genestine et al., 2011). HGF has also been shown to confer neuroprotection during stroke (Doeppner et al., 2011), ischemia (Shibuki et al., 2002), and Aβ-induced cognitive impairment in mice (Takeuchi et al., 2008). Moreover, the HGF-MET duo modifies central and peripheral immune functions (Benkhoucha et al., 2010), which are emerging as the key regulators of AD pathogenesis (Labzin et al., 2018; Ising et al., 2019; Gate et al., 2020). AD pathology accompanies numerous molecular changes that may coalesce into key signaling components, such as PI3K, STAT, PTEN, and mTOR (Oddo, 2012; Sanabria-Castro et al., 2017; Chen and Mobley, 2019; Yamazaki et al., 2019), which are also downstream players of MET signaling (Peng et al., 2013). Consistent with the posited neuroprotective role of MET signaling in AD, recent clinical literature demonstrated *reduced* levels of MET protein in the cerebral cortex and hippocampus of patients with AD (Hamasaki et al., 2014; Matsumoto et al., 2014). In addition, a transcriptome study also revealed *MET* as one of the major downregulated genes in AD brain (Liu et al., 2018). In this study, we further appraised the role of potential reduction of HGF/MET signaling in a 5XFAD AD mouse model. Our data support a novel contributory role of reduced HGF/MET signaling to the synaptic pathophysiology in this mouse model.

# MATERIALS AND METHODS

## Animals and Disease Model

The 5XFAD mice used in this study were purchased from The Jackson Laboratory (Catalog #34848-JAX). This line overexpresses both mutant forms of human amyloid precursor protein gene *APP* (K670N/M671L, V717I, and I716V) and mutant forms of human *PS1* gene (M146L and L286V) under the Thy1 promoter (Oakley et al., 2006). Mice genotypes were identified according to JAX protocol. Mutant and wild-type alleles were amplified by polymerase chain reaction (PCR) using pairs of three primers ("wild type," ACC TGC ATG TGA ACC CAG TAT TCT ATC; "common," CTA CAG CCC CTC TCC AAG GTT TAT AG; and "mutant," AAG CTA GCT GCA GTA ACG CCA TTT). All 5XFAD mice used in this study are heterozygotes. The forebrain-specific *Met* conditional knockout mice (cKO) were generated by breeding hemizygote male mice with a floxed *Met* gene ($Met^{fx/+}$) and $emx1^{Cre}$ knock-in allele (Gorski et al., 2002) to homozygous female $Met^{fx/fx}$ mice (Judson et al., 2009; Qiu et al., 2014). Both $Met^{fx/fx}$ and $emx1^{Cre}$ lines were backcrossed onto the C57Bl/6 background and were genotyped by PCR as we previously reported (Xia et al., 2021). To obtain the $Met^{fx/fx}$:$emx1^{cre}$:5XFAD mice, $Met^{fx/+}$:$emx1^{cre}$:5XFAD mice were used as breeders. 5XFAD:$Met^{fx/fx}$:$emx1^{cre}$ mice (aka. 5XFAD:$Met^{cKO}$) and their 5XFAD littermates (no *cre* transgene, irrespective of floxed *Met* allele status) were used for neuropathological comparisons. All experimental procedures conformed to NIH guidelines and were approved by the Institutional Animal Care and Use Committee of the University of Arizona.

## Immunohistochemistry / Immunofluorescence

Mice were euthanized with 3–5% isoflurane and transcardially cleared with cold 0.01 M PBS. Four percent paraformaldehyde (PFA) formulated in 0.1 M phosphate buffer (pH 7.4) was then perfused. Brains were dissected and postfixed in cold 4% PFA overnight. After cryoprotection in 30% sucrose for 2 days, brains were embedded in OCT cutting compound and sectioned on a sliding microtome (Leica SR-2000). About 40-μm-thick floating brain sections were washed 3X in 0.01 M PBS and permeabilized in PBS-0.2% Triton. For APP/Aβ+Iba1+Thio-S staining, the free-floating sections were blocked in primary antibody dilution

solution (0.01M PBS containing 0.2% Triton, 5% normal goat serum, and 1% BSA) for 2 h. Anti-APP/Aβ primary antibody (clone 6E10, Biolegend, Cat# SIG-39320. Antibody Registry ID: AB_662798. 1:500 dilution) mixed with anti-Iba1 (#019-19741, Wako, 1:500 dilution) was applied for 24 h with slow rotation. Sections were washed 3X in 0.01 M PBS and further incubated with Alexa 555-conjugated goat anti-mouse antibody and Alexa 647-conjugated goat anti-rabbit antibody for 2 h. Sections were extensively washed in 0.01 M PBS and further stained with 0.025% Thio-S (prepared in 50% ethanol−50% PBS) for 10 min. After briefly destaining in 50% ethanol, sections were washed in 0.01 M PBS and mounted on the SuperFrost Plus slides (VWR Scientific, West Chester, PA) using DAPI-containing Vectashield mounting medium (H-1200, Vector Laboratories). Images were acquired on a LSM 710 confocal microscope (Zeiss GmbH, Germany) with appropriate laser lines and filters. We kept all the acquisition parameters constant through different experiments to allow comparisons, including photomultiplier tube detector gain, pinhole size, laser intensity, and image sizes. To count the number of Iba1+ microglia and coverage of APP/Aβ and Thio-S, we used maximum projection images from a 25-μm-Z stack plane (with 1-μm Z interval). Pseudo-colors of confocal image channels may be redefined to enhance visualization in figure preparation. To quantify signal area/size and co-localizations between channels, confocal .czi files were imported into Imaris or ImageJ for customized analyses.

## Western Blot Analysis

Western blots was performed using specific antibodies to detect proteins of interest. Total protein content of the micro-dissected PFC and CA1 tissues was quantified using a micro-BCA assay, after being homogenized in NP40 lysis buffer (FNN0021, Invitrogen) supplemented with proteinase inhibitor cocktail (Sigma-Aldrich, P8340, 1:100). The samples are then mixed with equal amount of 2 × Laemmli loading buffer and boiled for 5 min. Samples were separated by electrophoresis on 4–15% SDS-polyacrylamide gels. Proteins were then transferred to PVDF membrane (Immobilon-P, Sigma-Aldrich) and blocked with 0.01 M PBS-Tween 20 with 5% non-fat dry milk. Primary antibody was diluted in the same blocking solution and applied to the PVDF membrane in a humidified chamber on a glass plate covered with parafilm. After overnight primary antibody incubation, the PVDF membrane was washed three times in 0.01 M PBS-Tween 20. Secondary antibodies directed to the correct species that are conjugated to horseradish peroxidase were applied for 2 h. The protein signal was developed using an enhanced chemiluminescence method (SignalFire, Cell Signaling Technology) and captured on an X-ray film (Amersham ECL Hyperfilm). The following antibodies were used for this study: From Santa Cruz Biotechnology, mouse anti-MET (Cat# sc-8057); from Millipore/Chemicon, rabbit anti-GluA1 (AB5849), rabbit anti-PSD95 (AB9708); from Cell Signaling Technology, rabbit anti-phospho-MET (Y1234/1235) (#3077), rabbit anti-GAPDH (#5174). The final dilutions of antibodies were between 1:1,000 and 1:2,000. The optical intensity of protein signal band captured on Hyperfilm was digitized by a film scanner (Epson V850) into an 8-bit gray scale image and quantified by densitometry using ImageJ/FIJI.

## Synaptic Plasticity/Long-Term Potentiation

Standard extracellular field excitatory postsynaptic potential (fEPSP) recording was used to investigate long-term potentiation (LTP) changes in the prefrontal cortex (PFC) layer 5 (L5) region. Mice were euthanized using 3–5% isoflurane, followed by intra-cardiac perfusion of ice-cold choline solution (in mM: 110 choline chloride, 25 $NaHCO_3$, 2.5 KCl, 1.25 $NaH_2PO_4$, 0.5 $CaCl_2$, 7 $MgSO_4$, 25-d glucose, 11.6 sodium ascorbate, and 3.1 sodium pyruvate, saturated with 95% $O_2$/5% $CO_2$) to improve brain slice viability. The brains were quickly harvested, and 350-μm-thick parasagittal slices were made on a vibratome (VT-1200S, Leica) at an angle that preserves intra-cortical L23>L5 connectivity (Qiu et al., 2011). Slices were cut in ice-cold choline solution, after which they were kept in artificial cerebrospinal fluid (ACSF, contains in mM: 126 NaCl, 2.5 KCl, 26 $NaHCO_3$, 2 $CaCl_2$, 2 $MgCl_2$, 1.25 $NaH_2PO_4$, and 10-d glucose; saturated with 95% $O_2$ /5% $CO_2$) for 30 min at 35°C and then maintained at 24°C RT until recording.

Brain slices were transferred to an interface chamber (AutoMate Scientific) that is maintained at 32°C and superfused with ACSF saturated with 95% $O_2$/5% $CO_2$. This facilitates long-term slice viability. fEPSPs were recorded using a glass patch electrode in the PFC L5 region, while a bipolar tungsten stimulating electrode (FHC, Bowdoin, ME) was placed on the L23. The patch electrode had an electrical resistance of 1–2 MΩ at 1 kHz when filled with ACSF. Biphasic electrical stimuli were generated through a Digidata 1440A device (Molecular Devices, San Jose, CA) and delivered through an optic isolator (Iso-flex, A.M.P.I). Stimulus (100-μs duration) intensity ranged from 10 to 50 μA and was delivered at 0.05Hz for baseline and LTP recordings. fEPSP signals were amplified using a differential amplifier (model 1800, A–M Systems, Carlsborg, WA), low-pass filtered at 2 kHz, and digitized at 10 kHz through the Digidata 1440A board.

For each of the fEPSP recordings in PFC slices, a stimulus-response (input–output) curve was first obtained by measuring the fEPSP slope (first 1-ms response after fiber volley) as a function of the fiber volley amplitude. This curve was then used to quantify the strength of basal synaptic transmission. We adopted a stimulus intensity that produces a ∼40–50% maximum monosynaptic fEPSP responses throughout the experiments. A 10-min stable baseline responses of stimulus-evoked fEPSPs were first obtained, and the paired-pulse responses at inter-pulse intervals ranging from 20 to 200 ms were recorded to assess potential changes in presynaptic transmission. Another pre-LTP 10-min baseline was then recorded, and LTP was induced by a theta-burst stimulation protocol, which consists of a 2-s long 5 Hz train (each train consists four pulses at 100 Hz) repeated 5 times at a 10-s interval (Qiu et al., 2006; Ma et al., 2019). fEPSP responses were recorded for an additional 1 h after LTP induction. Quantification of LTP amplitude was conducted in Clampfit 10.6, or using MATLAB by reading the .abf file with the *abf2load.m* function. To test the effects of HGF on LTP in control and 5XFAD slices, 10 nM recombinant human HGF (Millipore

Sigma, Cat# GF116) was added to the ACSF perfusate for 30 min prior to the LTP induction. A subset of slices were collected after LTP studies, and L5 region was micro-dissected for western blot detection of phospho-MET (Tyr1234/1235), which was used as a surrogate of MET activation.

## ELISA Measurement of Aβ1-42 Levels

Brains were weighed, sliced, and subjected to sequential Aβ extraction. Prefrontal cortical tissues (L5 region) were dissected and homogenized in 2% SDS-RIPA buffer (containing: 150 mM NaCl, 1% NP-40, 50 mM Tris-base, 2% SDS in aqueous solution, 5 mM EDTA, and 0.5% Na-deoxycholate). The SDS-RIPA buffer also contains protease inhibitor cocktail (1:100, Sigma P8340). Tissue homogenates were incubated on ice for 15 min to extract proteins, followed by centrifugation at 16,000 g for 90 min at 4 C. The supernatant containing RIPA-soluble fraction of $A\beta_{1-42}$ was collected. The pellet containing the insoluble fraction was further incubated for 30 min with 15X volume 70% fomic acid at room temperature and further centrifuged at 16,000 g for 60 min at 4°C. The supernatant collected now contains the RIPA-insoluble fractions of $A\beta_{1-42}$. For both soluble and insoluble fractions, total protein content was determined using the micro-BCA method. $A\beta_{1-42}$ levels were measured using an amyloid beta 42 mouse colorimetric ELISA Kit (Cat# KMB3441, Thermo Fisher) that is provided in a 96-well format, according to the manufacturers' instructions. A microplate reader (Tecan) was used to measure absorption at 450 nm.

## Statistical Analyses

The experimenters were blinded to grouping/genotype information during data collection and analyses. Sample sizes and number of independent experiments were estimated by power analyses using an R script ("pwr" package on CRAN) that takes pre-specified effect size, type I and II errors as input arguments. Shapiro–Wilk test and $F$ test were first employed to test normality and equal variance. All data that passed normality/equal variance tests were reported as mean ± SEM (standard error of the mean). For normal-distributed/equal variance data, Student's $t$-test or multiple $t$-tests were used. Statistical analyses and graphing were performed using GraphPad Prism 8.0, Microsoft Excel, and MATLAB. $P$-Value $< 0.05$ was considered statistically significant for all tests. Figures were prepared using Adobe Creative Cloud.

# RESULTS

## 5xFAD Mice Show Age-Dependent Decrease of MET Protein in Prefrontal Cortex and Hippocampus

It has been reported that AD brain shows early reduction of MET (Hamasaki et al., 2014; Matsumoto et al., 2014). We examined MET protein levels in the heterozygote 5xFAD mice PFC- L5 and HPC-CA1 tissues at three different ages (**Figure 1**): P21-25, during which the brain shows no overt Aβ/amyloid pathology; P45-50, a pre-symptomatic stage when Aβ is dramatically increased; and P105-120, during which amyloid plaques are prominent (Oakley et al., 2006). Western blot analyses revealed that compared to littermate controls, MET proteins in 5xFAD tissues were of similar levels at P21-25 in both PFC-L5 and HPC-CA1 tissues (**Figures 1A,B**), but were dramatically reduced at P45-50 in both regions (**Figures 1A,C**, PFC-L5, $p = 0.019$, $n = 4$; HPC-CA1, $n = 4$, quantification not shown). At P105-120, MET is severely depleted in both brain regions in 5XFAD brain (**Figures 1A,C**, PFC-L5, $p = 0.012$, $n = 4$; HPC-CA1, $n = 4$, quantification not shown). MET protein reduction in PFC and HPC parallels the abrupt, qualitative increase in Aβ load in the 5XFAD mice at this age (**Figure 1B**).

The early reduction of MET proteins in 5XFAD brain can be due to specific reduction of HGF/MET signaling that is related to AD pathology or APP/Aβ overloading, or it could be simply a non-specific effects of early synapse loss. We therefore probed levels of PSD95, a postsynaptic protein, and GluA1, an AMPA receptor subunit of the excitatory synapse, in the PFC-L5 tissues. After normalizing to the GAPDH loading controls, quantification of MET, PSD95, and GluA1 is shown in **Figure 1C**. We found that PSD95 and GluA1 protein levels were not changed in PFC at all three ages (**Figure 1C**, $p > 0.05$ for quantification of PSD95 and GluA1 at P45-50, $n = 4$; other ages, data not shown). As such, the early reduction of MET protein in PFC and HPC at P45-50 or later cannot be explained by the gross loss of synapse at this stage, as other synaptic proteins markers were not affected.

## Genetic Ablation of MET Signaling Exacerbates Aβ-Related Neuropathology in 5XFAD Mice

The early reduction in MET protein in 5XFAD mice, together with reported neuroprotective role of HGF/MET in animal models (Doeppner et al., 2011), suggests that MET could be a protective factor in AD. If this is the case, ablation of MET signaling, which could be achieved through the cre-loxP technology, may aggravate neuropathology in the 5XFAD mice. We crossed the forebrain excitatory neuron-specific *Met* cKO mice ($Met^{fx/fx}$:$emx1^{cre}$) to the 5XFAD mice (refer to Methods). $Emx1^{cre}$ drives inactivation of the *Met* gene from mid-gestation stage. We compared the 5XFAD mice (no *cre* transgene, irrespective of floxed *Met* allele status) with their littermate mice harboring the inactivated *Met* gene (5XFAD:$Met^{cKO}$) for their neuropathological markers. We immunostained PFC sections for Iba1, a marker for reactive microglia; APP/Aβ, and Thio-S, a marker for non-soluble fibrillary β-sheet forms of amyloid plaques (**Figure 2A**).

We first counted the number and density of Iba1+ microglia from L5 mPFC regions in 12-week-old (postnatal days 82–89) 5XFAD and the 5XFAD:$Met^{cKO}$ mice. 5XFAD:$Met^{cKO}$ mice show significantly increased Iba1+ microglia density [**Figure 2B**, number of cells/mm$^2$: 5XFAD, 1827 ± 67; 5XFAD:$Met^{cKO}$, 2518 ± 188. $t_{(10)} = 2.43$, $p = 0.006$]. Next, we quantified the APP/Aβ+ plaque coverage as a percentage of the imaged L5 area. 5XFAD:$Met^{cKO}$ mice show significantly increased percentage areal coverage of APP/Aβ [**Figure 2C**, 5XFAD, 2.85 ± 0.19; 5XFAD:$Met^{cKO}$, 3.93 ± 0.23. $t_{(10)} = 3.58$, $p = 0.005$]. To estimate the density of non-soluble fibrillary forms of amyloid plaques, we quantified the Thio-S+ areas. 5XFAD:$Met^{cKO}$ mice also

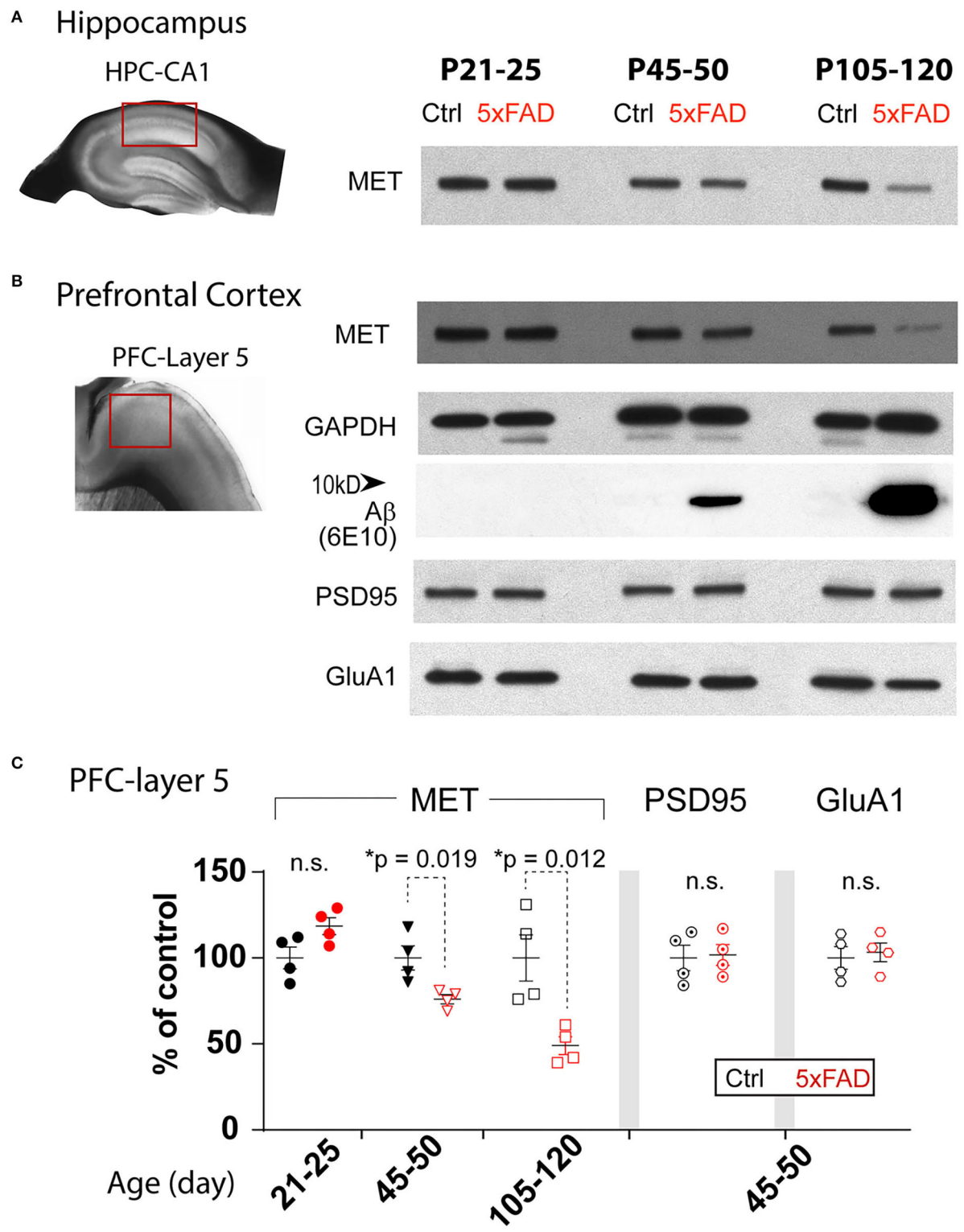


**FIGURE 1 |** Age-dependent decrease of MET protein in PFC and HPC in 5XFAD mice. **(A)** Western blot showing MET protein levels from control and 5XFAD hippocampus CA1 regions at three ages: P21-25, P45-50, and P105-120. **(B)** MET and other synaptic protein levels in micro-dissected L5 PFC tissues. The same age-dependent reduction of MET protein is observed (signals normalized to GAPDH loading control). Abrupt increase in Aβ levels was seen in P45-50 and older tissues. Other synaptic proteins, including PSD95 and GluA1, were not different between control and 5XFAD PFC L5 tissues. **(C)** Quantification of western blot results in PFC tissues. MET protein shows a significant reduction at P45-50 (*$p = 0.019$) and P105-120 (*$p = 0.012$). No difference in the levels of PSD95 and GluA1 was seen.

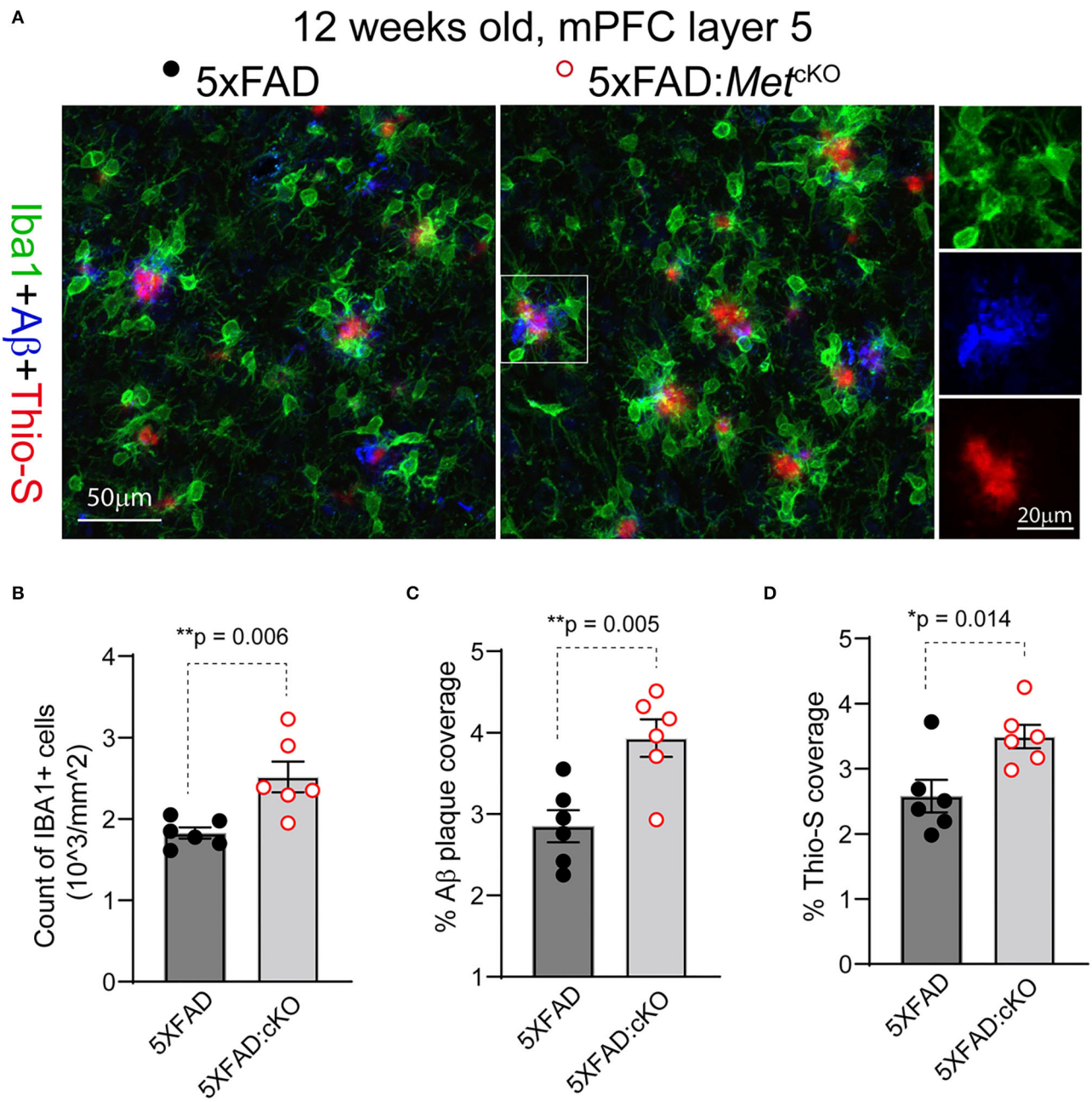


**FIGURE 2 |** Genetic ablation of MET signaling exacerbates Aβ-related neuropathology. **(A)** Representative confocal images showing triple staining of Iba1/APP-Aβ/Thio-S in 12-week-old 5XFAD and 5XFAD:*Met*$^{cKO}$ mice mPFC L5 regions. **(B)** Quantification of density of Iba1+ active microglia. 5XFAD:*Met*$^{cKO}$ mice show significantly increased microglia density (**$p = 0.006$). **(C)** Quantification of density of APP/Aβ+ plaque area. 5XFAD:*Met*$^{cKO}$ mice show significantly increased plaque coverage (**$p = 0.005$). **(D)** Quantification of Thio-S+ percentage areas. Increased Thio-S+ coverage was seen in 5XFAD:*Met*$^{cKO}$ mice (*$p = 0.014$).

show significantly increased percentage areal coverage of Thio-S staining [**Figure 2D**, 5XFAD, $2.58 \pm 0.25$; 5XFAD:*Met*$^{cKO}$, $3.49 \pm 0.18$. $t_{(10)} = 2.98$, $p = 0.014$]. Taken together, these data show that genetic ablation of MET signaling developmentally aggravates or accelerates neuropathology in the 5XFAD mouse model.

## Genetic Ablation of MET Signaling Increases Production of Aβ in 5XFAD Mice

Based on the observed changes in neuropathology, we asked whether *Met* cKO may exacerbate production of Aβ, which is an essential component of the phenotypic signature of AD. We

again used the ∼12-week-old mPFC tissues and micro-dissected the L5 regions (**Figure 3A**). We biochemically isolated the 2% SDS soluble and insoluble forms of beta-amyloid and used an ELISA kit to measure the $A\beta_{1-42}$ species (refer to Methods). We found that *Met* cKO significantly increased the levels of soluble $A\beta_{1-42}$ [**Figure 3B**, 5XFAD, 1.14 ± 0.10 ng/mg total protein; 5XFAD:*Met*$^{cKO}$, 1.77 ± 0.25. $t_{(8)} = 2.33$, $p = 0.04$]. In addition, the amyloid plaque associated insoluble fraction of $A\beta_{1-42}$ was even more dramatically elevated [**Figure 3C**, 5XFAD, 26.0 ± 2.31 ng/mg total protein; 5XFAD:*Met*$^{cKO}$, 35.9 ± 2.39. $t_{(8)} = 2.99$, $p = 0.017$]. These data are consistent with the neuropathological findings and suggest that MET signaling could be a neuroprotective factor during AD pathogenesis.

## Differential Responses to HGF-Induced Plasticity in the PFC L5 Synapses in 5XFAD Mice

It has been previously shown that HGF, when acutely applied to juvenile rat hippocampus slices, enhanced synaptic LTP in the HPC-CA1 region. This enhancement is most likely due to augmenting NMDA receptor-mediated currents in slices by HGF (Akimoto et al., 2004). Our recent work also suggests the timing of HGF/MET signaling affects the age-dependent synaptic plasticity in the hippocampus (Ma et al., 2019). We next investigated how synaptic plasticity in 5XFAD and control PFC slices response acutely to HGF application, and any potential differences may be due to the differential MET signaling state. We chose to study the plasticity measures in ∼2-month (P55-68)-old 5XFAD mice and littermate controls by conducting fEPSP recording at the PFC L23>L5 synapse. After obtaining stable baseline fEPSP responses, LTP was induced by theta-burst stimulation (**Figure 4A**). It was found that in control slices, theta-burst stimulation on its own leads to robust LTP that lasts at least 1 h postinduction (**Figure 4B**). This LTP magnitude was dramatically elevated when HGF (10 nM) was pre-applied for 30 min (**Figure 4B**). In comparison, LTP magnitude induced by theta-burst alone was smaller in 5XFAD PFC slices, although

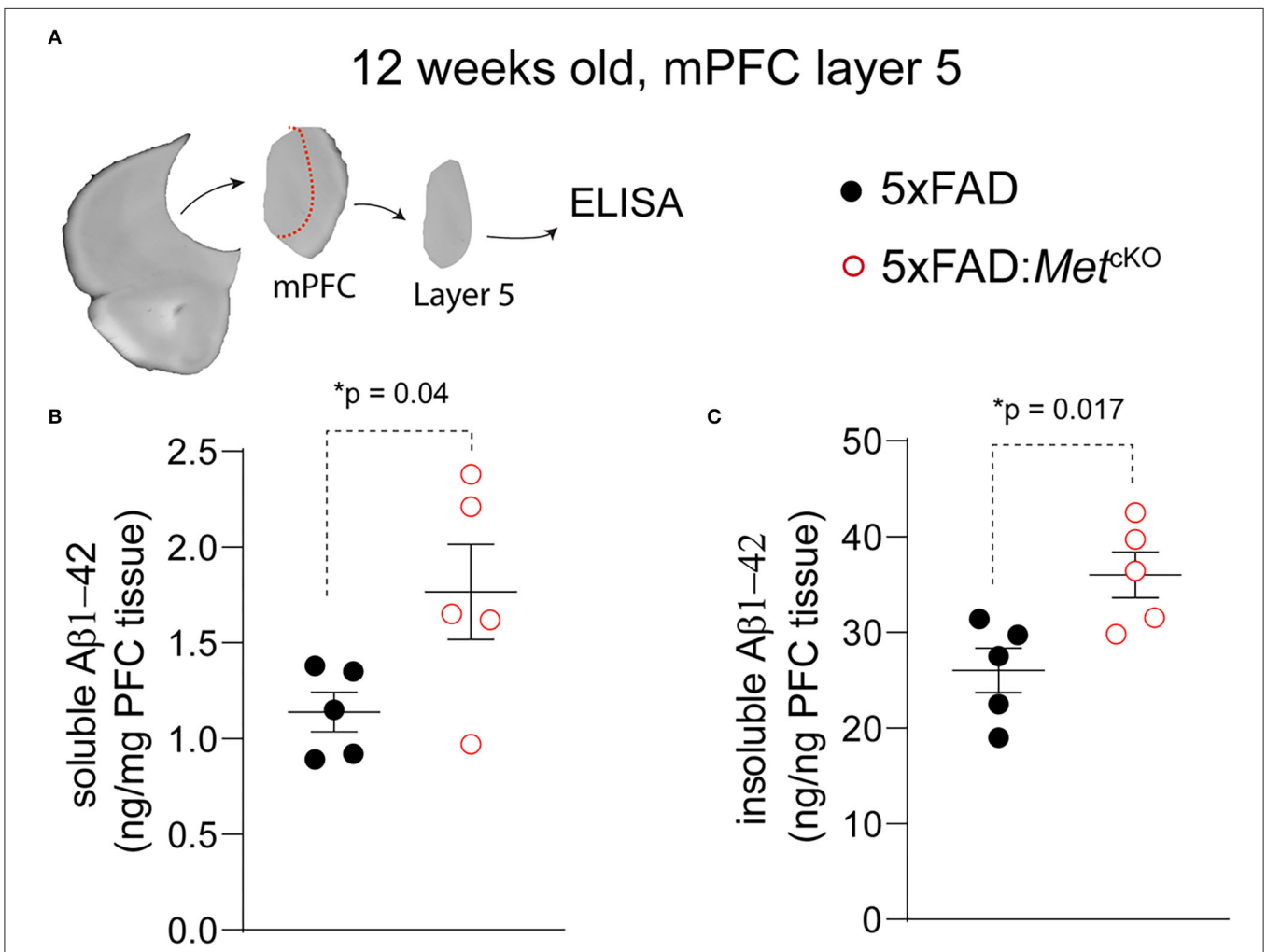


**FIGURE 3 |** Genetic ablation of MET signaling increases Aβ production in 5XFAD mice. **(A)** Schematic illustration of micro-dissected mPFC L5 tissues that are used for ELISA measurement of $A\beta_{1-42}$. **(B)** 5XFAD:*Met*$^{cKO}$ mice L5 mPFC tissues show significantly increased soluble forms of $A\beta_{1-42}$ (*$p = 0.04$). **(C)** Compared to 5XFAD tissues, 5XFAD:*Met*$^{cKO}$ mice L5 mPFC tissue shows significantly increased insoluble forms of $A\beta_{1-42}$ (*$p = 0.017$).

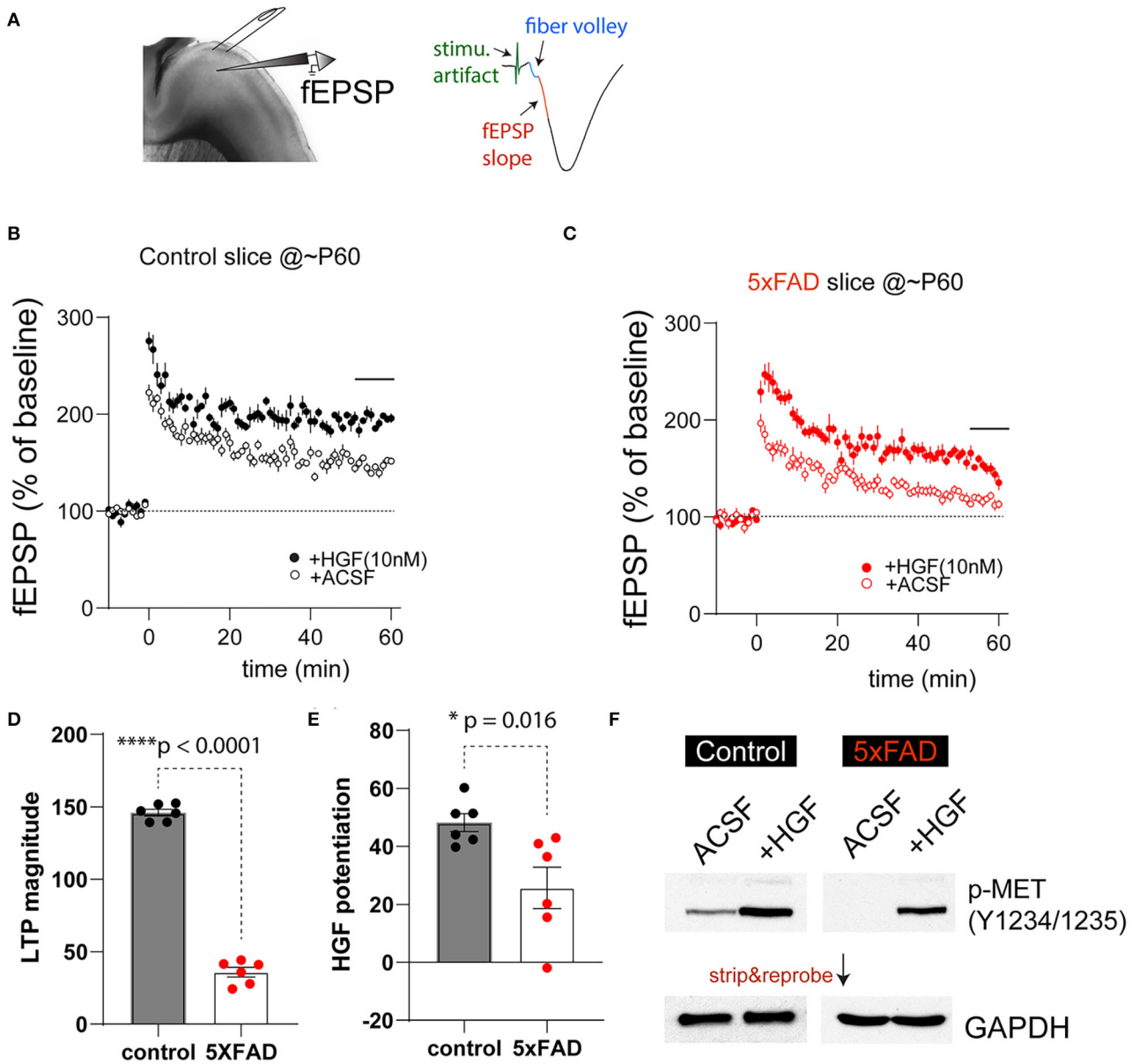


**FIGURE 4 |** 5XFAD mice show impaired PFC-L5 synaptic plasticity and HGF-induced LTP enhancement. **(A)** Schematic illustration of LTP recording in PFC-L5. A bipolar stimulating electrode was placed in L23 to elicit monosynaptic fEPSP responses (*right*). The first 1-ms fEPSP response after fiber volley was used to calculate slope of response. **(B)** LTP time course in control slices in the absence (ACSF) and the presence of 10 nM HGF. HGF clearly elevates LTP magnitude. **(C)** LTP time course in 5XFAD slices in the absence (ACSF) and the presence of 10 nM HGF. HGF shows smaller enhancement of LTP magnitude in 5XFAD slices compared to that from control slices. **(D)** Quantification of theta-burst-induced LTP magnitude in control and 5XFAD slices (last 6-min recordings were used). LTP magnitude in 5XFAD slices was dramatically reduced compared to that from control slices (****$p < 0.0001$). **(E)** Quantification of HGF-induced potentiation of the LTP magnitude. 5XFAD slices show significantly reduced HGF-induced LTP enhancement compared to that from control slices (*$p = 0.016$). **(F)** Differential basal levels of p-MET (Y1234/1235) and HGF-induced p-MET levels in 5XFAD vs. control slices that were collected after LTP recordings. $N = 4$, quantification not shown.

HGF was capable of leading to an enhancement (**Figure 4C**). When LTP magnitude was quantified using the last 6-min recording, it was found that theta-burst-induced LTP magnitude was significantly reduced in 5XFAD slices [**Figure 4D**, 5XFAD, 35.8 ± 3.3%; control, 145.9 ± 2.3%. $t_{(10)} = 27.2$, $p < 0.0001$]. We also quantified HGF-induced LTP enhancement. HGF leads to significantly lower LTP enhancement in 5XFAD slices [**Figure 4E**, Control, 41.2 ± 3.1; 5XFAD, 25.7 ± 7.2. $t_{(10)} = 2.88$, $p = 0.016$].

The reduced level of theta-burst-induced LTP and HGF enhancement of LTP magnitude in 5XFAD PFC slices may reflect the overall lower levels of MET at this age (**Figures 1B,C**)

or reduced baseline MET signaling levels at this age. We next quantified p-MET (Tyr1234/1235) levels in micro-dissected L5 tissues after recording under the above four experimental conditions. Strikingly, we found that p-MET levels in 5XFAD slices were very low, so that it is practically undetectable in 5XFAD slices under ACSF condition (**Figure 4F**). In comparison, p-MET is clearly detectable in control littermate slices. More importantly, 10 nM HGF application, which results in enhanced LTP (**Figures 4B,C**), also leads to quantitatively or qualitatively increased p-MET levels in control and 5XFAD slices (**Figure 4F**, $N = 4$ biological replicates, quantification now shown). These data suggest that baseline activation of MET is much lower in 5XFAD mouse brain at a pre-symptomatic age, yet the endogenous level of MET is still capable of responding to HGF-induced signaling.

## DISCUSSION

In this study, we found early reduction of MET receptor tyrosine kinase in the 5XFAD mouse model for AD. This is consistent with clinical literature reporting a reduction of MET protein in the AD brain, including the hippocampus and cortical regions (Hamasaki et al., 2014; Matsumoto et al., 2014; Liu et al., 2018). Importantly, early MET reduction in the 5XFAD mice cannot be due to overall early loss of synapse, as other synaptic proteins (PSD95, GluA1) were not changed at early ages. It is also likely the reduction of MET signaling promotes AD progression and severity, as genetic ablation of *Met* results in exacerbated pathological changes in the 5XFAD mice. These are reflected by the increased amyloid plaque deposition, dense core fibrillar forms of plaque, increased soluble and insoluble forms of Aβ, and increased microglia activation. All of these observations suggest that HGF/MET reduction may contribute to AD pathogenesis in this mouse model featuring aggressive amyloid deposition.

Our findings have translational implications for AD therapeutics. The pathophysiology of AD is extremely complex. Existing literature suggests that protein aggregation, neuroinflammation, disrupted energy metabolism, vascular pathology, and immune dysregulation all play a role (Kinney et al., 2018; Guo et al., 2020; Yu et al., 2021). HGF/MET signaling is also pleiotropic, engaging a plethora of molecular pathways that are reportedly disrupted in AD (Wright and Harding, 2015; Desole et al., 2021). At cellular level, early synaptic loss and impairment of plasticity occur prior to overt neuronal loss and degeneration (Oakley et al., 2006; Richard et al., 2015; Forner et al., 2021; Oblak et al., 2021), which may instigate progressive decline in memory and cognition. As such, focusing on the synaptic regeneration and preserving plasticity across the lifespan presents some important conceptual and strategic issues regarding translational AD research, may inform future clinical practice with the aim to preserve synapse and circuit connectivity, and restore cognitive function in AD and other neurodegenerative diseases.

The HGF/MET signaling is highly pleiotropic and influences a plethora of early neurodevelopmental events, including neural induction (Streit et al., 1995), proliferation (Ieraci et al., 2002), neurite outgrowth (Maina et al., 1997, 1998; Korhonen et al., 2000; Gutierrez et al., 2004), and survival and regeneration (Hamanoue et al., 1996; Wong et al., 1997; Davey et al., 2000; Maina et al., 2001). We and others have shown that MET is a temporally- and spatially-regulated receptor enriched in dorsal pallial-derived structures during mouse forebrain development. Peak levels of MET expression in cortex coincide with periods of rapid neuronal growth and synaptogenesis. MET in developing cortical circuits controls dendritic spine formation and synaptogenesis (Qiu et al., 2011), refinement of circuit connectivity (Qiu et al., 2014; Peng et al., 2016), and the timing of excitatory synapse maturation (Qiu et al., 2011; Ising et al., 2019). The cellular and circuit origins of HGF, on the other hand, are less understood. Early immunohistochemistry staining suggests astrocytes and a small number of microglia may be the main source of HGF (Yamada et al., 1994, 1997; Yamagata et al., 1995). It is thus likely that the HGF/MET signaling duo involves multiple cellular types and may be modified by physiology states of the brain. In contrast to its neurodevelopmental role, MET signaling in adult brain is less understood. However, MET protein persists in adult brain but is restricted to the site of excitatory synapse (Eagleson et al., 2013) and is capable of modifying synaptic function and plasticity (Akimoto et al., 2004). We recently found that in *Met* conditional knockout (cKO, $Met^{fx/fx}$:$emx1^{cre}$) mice, there was a disruption in hippocampus LTP and an early cognitive decline (Ma et al., 2019); conversely, in transgenic mice overexpressing *Met*, cortical excitatory neurons exhibit altered synaptic proteins and the timing of critical period plasticity (Chen et al., 2020). MET signaling also engages molecular mechanisms governing *de novo* spine morphogenesis; for example, MET signaling activates small GTPases (Cdc42, Rac1) to control actin dynamics (e.g., cofilin phosphorylation). The signaling is capable of promoting dendritic spines/synapses morphogenesis *de novo* in response to neuronal activity (Qiu et al., 2014; Chen et al., 2020). Therefore, existing literature suggests that MET signaling is neuroprotective, modifies synaptic function and plasticity, and has synapse regeneration potential.

In summary, our study revealed that MET protein and its mediated signaling are reduced in the 5XFAD mouse model for AD. The study complements recent clinical literature reporting reduced MET protein levels in AD patient's brain and the posited beneficial effects of HGF/MET activation in AD therapeutics (Sharma, 2010; Hua et al., 2022) and further supports the view that HGF/MET signaling is neurotrophic and neuroprotective. The current findings, combined with our recent work in developmental neurobiology that revealed molecular mechanisms that controls *de novo* spine genesis (Qiu et al., 2014; Peng et al., 2016; Chen et al., 2020), suggest that restoring/enhancing MET signaling levels may represent a promising direction in AD therapeutics.

## DATA AVAILABILITY STATEMENT

The original contributions presented in the study are included in the article/supplementary material, further inquiries can be directed to the corresponding author/s.

## ETHICS STATEMENT

The animal study was reviewed and approved by Institutional Animal Care and Use Committee of the University of Arizona.

## AUTHOR CONTRIBUTIONS

JW and XM performed the experiments. AN and YC conducted partial data analyses. LZ performed animal husbandry and genotyping. YC performed coded data analysis in MATLAB. SQ designed and supervised the study and acquired funding. All authors contributed to the article and approved the submitted version.

## FUNDING

This work was supported by institutional startup funding from the University of Arizona (SQ).

## REFERENCES

Akimoto, M., Baba, A., Ikeda-Matsuo, Y., Yamada, M. K., Itamura, R., Nishiyama, N., et al. (2004). Hepatocyte growth factor as an enhancer of nmda currents and synaptic plasticity in the hippocampus. *Neuroscience* 128, 155–162. doi: 10.1016/j.neuroscience.2004.06.031

Alexiou, A., Kamal, M. A., and Ashraf, G. M. (2019). Editorial: the Alzheimer's disease challenge. *Front. Neurosci.* 13, 768. doi: 10.3389/fnins.2019.00768

Bai, L., Lennon, D. P., Caplan, A. I., DeChant, A., Hecker, J., Kranso, J., et al. (2012). Hepatocyte growth factor mediates mesenchymal stem cell-induced recovery in multiple sclerosis models. *Nat. Neurosci.* 15, 862–870. doi: 10.1038/nn.3109

Benkhoucha, M., Molnarfi, N., Dunand-Sauthier, I., Merkler, D., Schneiter, G., Bruscoli, S., et al. (2014). Hepatocyte growth factor limits autoimmune neuroinflammation via glucocorticoid-induced leucine zipper expression in dendritic cells. *J. Immunol.* 193, 2743–2752. doi: 10.4049/jimmunol.1302338

Benkhoucha, M., Santiago-Raber, M. L., Schneiter, G., Chofflon, M., Funakoshi, H., Nakamura, T., et al. (2010). Hepatocyte growth factor inhibits CNS autoimmunity by inducing tolerogenic dendritic cells and CD25+Foxp3+ regulatory T cells. *Proc. Natl. Acad. Sci. U. S. A.* 107, 6424–6429. doi: 10.1073/pnas.0912437107

Chen, K., Ma, X., Nehme, A., Wei, J., Cui, Y., Cui, Y., et al. (2020). Time-delimited signaling of MET receptor tyrosine kinase regulates cortical circuit development and critical period plasticity. *Mol. Psychiatry* 26, 3723–3736. doi: 10.1038/s41380-019-0635-6

Chen, X. Q., and Mobley, W. C. (2019). Alzheimer disease pathogenesis: insights from molecular and cellular biology studies of oligomeric abeta and tau species. *Front. Neurosci.* 13, 659. doi: 10.3389/fnins.2019.00659

Chen, Y., Durakoglugil, M. S., Xian, X., and Herz, J. (2010). ApoE4 reduces glutamate receptor function and synaptic plasticity by selectively impairing ApoE receptor recycling. *Proc. Natl. Acad. Sci. U. S. A.* 107, 12011–12016. doi: 10.1073/pnas.0914984107

Chung, W. S., Verghese, P. B., Chakraborty, C., Joung, J., Hyman, B. T., Ulrich, J. D., et al. (2016). Novel allele-dependent role for APOE in controlling the rate of synapse pruning by astrocytes. *Proc. Natl. Acad. Sci. U. S. A.* 113, 10186–10191. doi: 10.1073/pnas.1609896113

Cleary, J. P., Walsh, D. M., Hofmeister, J. J., Shankar, G. M., Kuskowski, M. A., Selkoe, D. J., et al. (2005). Natural oligomers of the amyloid-beta protein specifically disrupt cognitive function. *Nat. Neurosci.* 8, 79–84. doi: 10.1038/nn1372

Davey, F., Hilton, M., and Davies, A. M. (2000). Cooperation between HGF and CNTF in promoting the survival and growth of sensory and parasympathetic neurons. *Mol. Cell. Neurosci.* 15, 79–87. doi: 10.1006/mcne.1999.0803

Desole, C., Gallo, S., Vitacolonna, A., Montarolo, F., Bertolotto, A., Vivien, D., et al. (2021). HGF and MET: from brain development to neurological disorders. *Front Cell Dev Biol* 9, 683609. doi: 10.3389/fcell.2021.683609

Doeppner, T. R., Kaltwasser, B., ElAli, A., Zechariah, A., Hermann, D. M., and Bahr, M. (2011). Acute hepatocyte growth factor treatment induces long-term neuroprotection and stroke recovery via mechanisms involving neural precursor cell proliferation and differentiation. *J. Cereb. Blood Flow Metab.* 31, 1251–1262. doi: 10.1038/jcbfm.2010.211

Eagleson, K. L., Milner, T. A., Xie, Z., and Levitt, P. (2013). Synaptic and extrasynaptic location of the receptor tyrosine kinase met during postnatal development in the mouse neocortex and hippocampus. *J. Comp. Neurol.* 521, 3241–3259. doi: 10.1002/cne.23343

Forner, S., Kawauchi, S., Balderrama-Gutierrez, G., Kramár, E. A., Matheos, D. P., Phan, J., et al. (2021). Systematic phenotyping and characterization of the 5xFAD mouse model of Alzheimer's disease. *Sci Data* 8, 270. doi: 10.1038/s41597-021-01054-y

Gate, D., Saligrama, N., Leventhal, O., Yang, A. C., Unger, M. S., Middeldorp, J., et al. (2020). Clonally expanded CD8 T cells patrol the cerebrospinal fluid in Alzheimer's disease. *Nature* 577, 399–404. doi: 10.1038/s41586-019-1895-7

Genestine, M., Caricati, E., Fico, A., Richelme, S., Hassani, H., Sunyach, C., et al. (2011). Enhanced neuronal Met signalling levels in ALS mice delay disease onset. *Cell Death Dis.* 2, e130. doi: 10.1038/cddis.2011.11

Gonzalez Burgos, I., Nikonenko, I., and Korz, V. (2012). Dendritic spine plasticity and cognition. *Neural Plast.* 2012, 875156. doi: 10.1155/2012/875156

Gorski, J. A., Talley, T., Qiu, M., Puelles, L., Rubenstein, J. L., and Jones, K. R. (2002). Cortical excitatory neurons and glia, but not GABAergic neurons, are produced in the Emx1-expressing lineage. *J. Neurosci.* 22, 6309–6314. doi: 10.1523/JNEUROSCI.22-15-06309.2002

Guo, T., Zhang, D., Zeng, Y., Huang, T. Y., Xu, H., and Zhao, Y. (2020). Molecular and cellular mechanisms underlying the pathogenesis of Alzheimer's disease. *Mol. Neurodegener.* 15, 40. doi: 10.1186/s13024-020-00391-7

Gutierrez, H., Dolcet, X., Tolcos, M., and Davies, A. (2004). HGF regulates the development of cortical pyramidal dendrites. *Development* 131, 3717–3726. doi: 10.1242/dev.01209

Hamanoue, M., Takemoto, N., Matsumoto, K., Nakamura, T., Nakajima, K., and Kohsaka, S. (1996). Neurotrophic effect of hepatocyte growth factor on central nervous system neurons *in vitro*. *J. Neurosci. Res.* 43, 554–564.

Hamasaki, H., Honda, H., Suzuki, S. O., Hokama, M., Kiyohara, Y., Nakabeppu, Y., et al. (2014). Down-regulation of MET in hippocampal neurons of Alzheimer's disease brains. *Neuropathology* 34, 284–290. doi: 10.1111/neup.12095

Hsieh, H., Boehm, J., Sato, C., Iwatsubo, T., Tomita, T., Sisodia, S., et al. (2006). AMPAR removal underlies Abeta-induced synaptic depression and dendritic spine loss. *Neuron* 52, 831–843. doi: 10.1016/j.neuron.2006.10.035

Hua, X., Church, K., Walker, W., L'Hostis, P., Viardot, G., Danjou, P., et al. (2022). Safety, tolerability, pharmacokinetics, and pharmacodynamics of the positive modulator of HGF/MET, fosgonimeton, in healthy volunteers and subjects with Alzheimer's disease: randomized, placebo-controlled, double-blind, phase I clinical trial. *J. Alzheimers. Dis.* 86, 1399–1413. doi: 10.3233/JAD-215511

Huh, S., Baek, S. J., Lee, K. H., Whitcomb, D. J., Jo, J., Choi, S. M., et al. (2016). The reemergence of long-term potentiation in aged Alzheimer's disease mouse model. *Sci. Rep.* 6, 29152. doi: 10.1038/srep29152

Ieraci, A., Forni, P. E., and Ponzetto, C. (2002). Viable hypomorphic signaling mutant of the Met receptor reveals a role for hepatocyte growth factor in postnatal cerebellar development. *Proc. Natl. Acad. Sci. U. S. A.* 99, 15200–15205. doi: 10.1073/pnas.222362099

Ising, C., Venegas, C., Zhang, S., Scheiblich, H, Schmidt, S. V., Vieira-Saecker, A., Schwartz, S., et al. (2019). NLRP3 inflammasome activation drives tau pathology. *Nature* 575, 669–673. doi: 10.1038/s41586-019-1769-z

Judson, M. C., Bergman, M. Y., Campbell, D. B., Eagleson, K. L., and Levitt, P. (2009). Dynamic gene and protein expression patterns of the autism-associated met receptor tyrosine kinase in the developing mouse forebrain. *J. Comp. Neurol.* 513, 511–531. doi: 10.1002/cne.21969

Kim, J., Yoon, H., Basak, J., and Kim, J. (2014). Apolipoprotein E in synaptic plasticity and Alzheimer's disease: potential cellular and molecular mechanisms. *Mol. Cells* 37, 767–776. doi: 10.14348/molcells.2014.0248

Kinney, J. W., Bemiller, S. M., Murtishaw, A. S., Leisgang, A. M., Salazar, A. M., and Lamb, B. T. (2018). Inflammation as a central mechanism in Alzheimer's disease. *Alzheimers Dement.* 4, 575–590. doi: 10.1016/j.trci.2018.06.014

Koch, G., Di Lorenzo, F., Bonni, S., Ponzo, V., Caltagirone, C., and Martorana, A. (2012). Impaired LTP- but not LTD-like cortical plasticity in Alzheimer's disease patients. *J. Alzheimers. Dis.* 31, 593–599. doi: 10.3233/JAD-2012-120532

Koike, H., Ishida, A., Shimamura, M., Mizuno, S., Nakamura, T., Ogihara, T., et al. (2006). Prevention of onset of Parkinson's disease by *in vivo* gene transfer of human hepatocyte growth factor in rodent model: a model of gene therapy for Parkinson's disease. *Gene Ther.* 13, 1639–1644. doi: 10.1038/sj.gt.3302810

Korhonen, L., Sjoholm, U., Takei, N., Kern, M. A., Schirmacher, P., Castren, E., et al. (2000). Expression of c-Met in developing rat hippocampus: evidence for HGF as a neurotrophic factor for calbindin D-expressing neurons. *Eur. J. Neurosci.* 12, 3453–3461. doi: 10.1046/j.1460-9568.2000.00260.x

Labzin, L. I., Heneka, M. T., and Latz, E. (2018). Innate Immunity and Neurodegeneration. *Annu. Rev. Med.* 69, 437–449. doi: 10.1146/annurev-med-050715-104343

Lacor, P. N., Buniel, M. C., Furlow, P. W., Clemente, A. S., Velasco, P. T., Wood, M., et al. (2007). Abeta oligomer-induced aberrations in synapse composition, shape, and density provide a molecular basis for loss of connectivity in Alzheimer's disease. *J. Neurosci.* 27, 796–807. doi: 10.1523/JNEUROSCI.3501-06.2007

Liu, H., Luo, K., and Luo, D. (2018). Guanosine monophosphate reductase 1 is a potential therapeutic target for Alzheimer's disease. *Sci. Rep.* 8, 2759. doi: 10.1038/s41598-018-21256-6

Ma, X., Chen, K., Lu, Z., Piechowicz, M., Liu, Q., Wu, J., et al. (2019). Disruption of MET receptor tyrosine kinase, an autism risk factor, impairs developmental synaptic plasticity in the hippocampus. *Dev. Neurobiol.* 79, 36–50. doi: 10.1002/dneu.22645

Maina, F., Hilton, M. C., Andres, R., Wyatt, S., Klein, R., and Davies, A. M. (1998). Multiple roles for hepatocyte growth factor in sympathetic neuron development. *Neuron* 20, 835–846. doi: 10.1016/S0896-6273(00)80466-3

Maina, F., Hilton, M. C., Ponzetto, C., Davies, A. M., and Klein, R. (1997). Met receptor signaling is required for sensory nerve development and HGF promotes axonal growth and survival of sensory neurons. *Genes Dev.* 11, 3341–3350. doi: 10.1101/gad.11.24.3341

Maina, F., Pante, G., Helmbacher, F., Andres, R., Porthin, A., Davies, A. M., et al. (2001). Coupling Met to specific pathways results in distinct developmental outcomes. *Mol. Cell* 7, 1293–1306. doi: 10.1016/S1097-2765(01)00261-1

Mango, D., Saidi, A., Cisale, G. Y., Feligioni, M., Corbo, M., and Nistico, R. (2019). Targeting synaptic plasticity in experimental models of Alzheimer's disease. *Front. Pharmacol.* 10, 778. doi: 10.3389/fphar.2019.00778

Masters, C. L., Bateman, R., Blennow, K., Rowe, C. C., Sperling, R. A., and Cummings, J. L. (2015). Alzheimer's disease. *Nat Rev Dis Primers* 1, 15056. doi: 10.1038/nrdp.2015.56

Matsumoto, K., Funakoshi, H., Takahashi, H., and Sakai, K. (2014). HGF-met pathway in regeneration and drug discovery. *Biomedicines* 2, 275–300. doi: 10.3390/biomedicines2040275

Megill, A., Tran, T., Eldred, K., Lee, N. J., Wong, P. C., Hoe, H. S., et al. (2015). Defective age-dependent metaplasticity in a mouse model of Alzheimer's disease. *J. Neurosci.* 35, 11346–11357. doi: 10.1523/JNEUROSCI.5289-14.2015

Naldini, L., Vigna, E., Ferracini, R., Longati, P., Gandino, L., Prat, M., et al. (1991a). The tyrosine kinase encoded by the MET proto-oncogene is activated by autophosphorylation. *Mol. Cell. Biol.* 11, 1793–1803. doi: 10.1128/MCB.11.4.1793

Naldini, L., Weidner, K. M., Vigna, E., Gaudino, G., Bardelli, A., Ponzetto, C., et al. (1991b). Scatter factor and hepatocyte growth factor are indistinguishable ligands for the MET receptor. *EMBO J.* 10, 2867–2878. doi: 10.1002/j.1460-2075.1991.tb07836.x

Oakley, H., Cole, S. L., Logan, S., Maus, E., Shao, P., Craft, J., et al. (2006). Intraneuronal beta-amyloid aggregates, neurodegeneration, and neuron loss in transgenic mice with five familial Alzheimer's disease mutations: potential factors in amyloid plaque formation. *J. Neurosci.* 26, 10129–10140. doi: 10.1523/JNEUROSCI.1202-06.2006

Oblak, A. L., Lin, P. B., Kotredes, K. P., Pandey, R. S., Garceau, D., Williams, H, M., et al. (2021). Comprehensive evaluation of the 5XFAD mouse model for preclinical testing applications: a MODEL-AD study. *Front. Aging Neurosci.* 13, 713726. doi: 10.3389/fnagi.2021.713726

Oddo, S. (2012). The role of mTOR signaling in Alzheimer disease. *Front Biosci.* 4, 941–952. doi: 10.2741/s310

Peng, Y., Huentelman, M., Smith, C., and Qiu, S. (2013). MET receptor tyrosine kinase as an autism genetic risk factor. *Int. Rev. Neurobiol.* 113, 135–165. doi: 10.1016/B978-0-12-418700-9.00005-8

Peng, Y., Lu, Z., Li, G., Piechowicz, M., Anderson, M. A., Uddin, Y., et al. (2016). The autism associated MET receptor tyrosine kinase engages early neuronal growth mechanism and controls glutamatergic circuits development in the forebrain. *Mol. Psychiatry*. 21, 925–935. doi: 10.1038/mp.2015.182

Ponzetto, C., Bardelli, A., Zhen, Z., Maina, F., dalla Zonca, P., Giordano, S., et al. (1994). A multifunctional docking site mediates signaling and transformation by the hepatocyte growth factor/scatter factor receptor family. *Cell* 77, 261–271. doi: 10.1016/0092-8674(94)90318-2

Prieto, G. A., Trieu, B. H., Dang, C. T., Bilousova, T., Gylys, K. H., Berchtold, N. C., et al. (2017). Pharmacological rescue of long-term potentiation in Alzheimer diseased synapses. *J. Neurosci.* 37, 1197–1212. doi: 10.1523/JNEUROSCI.2774-16.2016

Qiu, S., Anderson, C. T., Levitt, P., and Shepherd, G. M. (2011). Circuit-specific intracortical hyperconnectivity in mice with deletion of the autism-associated Met receptor tyrosine kinase. *J. Neurosci.* 31, 5855–5864. doi: 10.1523/JNEUROSCI.6569-10.2011

Qiu, S., Lu, Z., and Levitt, P. (2014). MET receptor tyrosine kinase controls dendritic complexity, spine morphogenesis, and glutamatergic synapse maturation in the hippocampus. *J. Neurosci.* 34, 16166–16179. doi: 10.1523/JNEUROSCI.2580-14.2014

Qiu, S., Zhao, L. F., Korwek, K. M., and Weeber, E. J. (2006). Differential reelin-induced enhancement of NMDA and AMPA receptor activity in the adult hippocampus. *J. Neurosci.* 26, 12943–12955. doi: 10.1523/JNEUROSCI.2561-06.2006

Richard, B. C., Kurdakova, A., Baches, S., Bayer, T. A., Weggen, S., and Wirths, O. (2015). Gene dosage dependent aggravation of the neurological phenotype in the 5XFAD mouse model of Alzheimer's disease. *J. Alzheimers. Dis.* 45, 1223–1236. doi: 10.3233/JAD-143120

Sanabria-Castro, A., Alvarado-Echeverria, I., and Monge-Bonilla, C. (2017). Molecular pathogenesis of Alzheimer's disease: an update. *Ann. Neurosci.* 24, 46–54. doi: 10.1159/000464422

Scheltens, P., De Strooper, B., Kivipelto, M., Holstege, H., Chetelat, G., Teunissen, C. E., et al. (2021). Alzheimer's disease. *Lancet* 397, 1577–1590. doi: 10.1016/S0140-6736(20)32205-4

Shankar, G. M., Bloodgood, B. L., Townsend, M., Walsh, D. M., Selkoe, D. J., and Sabatini, B. L. (2007). Natural oligomers of the Alzheimer amyloid-beta protein induce reversible synapse loss by modulating an NMDA-type glutamate receptor-dependent signaling pathway. *J. Neurosci.* 27, 2866–2875. doi: 10.1523/JNEUROSCI.4970-06.2007

Sharma, S. (2010). Hepatocyte growth factor in synaptic plasticity and Alzheimer's disease. *Sci. World J.* 10, 457–461. doi: 10.1100/tsw.2010.49

Shibuki, H., Katai, N., Kuroiwa, S., Kurokawa, T., Arai, J., Matsumoto, K., et al. (2002). Expression and neuroprotective effect of hepatocyte growth factor in retinal ischemia-reperfusion injury. *Invest. Ophthalmol. Vis. Sci.* 43, 528–536.

Smith, D. L., Pozueta, J., Gong, B., Arancio, O., and Shelanski, M. (2009). Reversal of long-term dendritic spine alterations in Alzheimer disease models. *Proc. Natl. Acad. Sci. U. S. A.* 106, 16877–16882. doi: 10.1073/pnas.0908706106

Stefan, M., Koch, A., Mancini, A., Mohr, A., Weidner, K. M., Niemann, H., et al. (2001). Src homology 2-containing inositol 5-phosphatase 1 binds to the multifunctional docking site of c-Met and potentiates hepatocyte growth factor-induced branching tubulogenesis. *J. Biol. Chem.* 276, 3017–3023. doi: 10.1074/jbc.M009333200

Streit, A., Stern, C. D., Thery, C., Ireland, G. W., Aparicio, S., Sharpe, M. J., et al. (1995). A role for HGF/SF in neural induction and its expression in Hensen's node during gastrulation. *Development* 121, 813–824. doi: 10.1242/dev.121.3.813

Takeuchi, D., Sato, N., Shimamura, M., Kurinami, H., Takeda, S., Shinohara, M., et al. (2008). Alleviation of Abeta-induced cognitive impairment by ultrasound-mediated gene transfer of HGF in a mouse model. *Gene Ther.* 15, 561–571. doi: 10.1038/sj.gt.3303094

Trusolino, L., Bertotti, A., and Comoglio, P. M. (2010). MET signalling: principles and functions in development, organ regeneration and cancer. *Nat. Rev. Mol. Cell Biol.* 11, 834–848. doi: 10.1038/nrm3012

Vanleeuwen, J. E., and Penzes, P. (2012). Long-term perturbation of spine plasticity results in distinct impairments of cognitive function. *J. Neurochem.* 123, 781–789. doi: 10.1111/j.1471-4159.2012.07899.x

Wong, V., Glass, D. J., Arriaga, R., Yancopoulos, G. D., Lindsay, R. M., and Conn, G. (1997). Hepatocyte growth factor promotes motor neuron survival and synergizes with ciliary neurotrophic factor. *J. Biol. Chem.* 272, 5187–5191. doi: 10.1074/jbc.272.8.5187

Wright, J. W., and Harding, J. W. (2015). The brain hepatocyte growth factor/c-met receptor system: a new target for the treatment of Alzheimer's disease. *J. Alzheimers. Dis.* 45, 985–1000. doi: 10.3233/JAD-142814

Xia, B., Wei, J., Ma, X., Nehme, A., Liong, K., Cui, Y., et al. (2021). Conditional knockout of MET receptor tyrosine kinase in cortical excitatory neurons leads to enhanced learning and memory in young adult mice but early cognitive decline in older adult mice. *Neurobiol. Learn. Mem.* 179, 107397. doi: 10.1016/j.nlm.2021.107397

Yamada, T., Tsubouchi, H., Daikuhara, Y., Prat, M., Comoglio, P. M., McGeer, P. L., et al. (1994). Immunohistochemistry with antibodies to hepatocyte growth factor and its receptor protein *(c-MET)* in human brain tissues. *Brain Res.* 637, 308–312. doi: 10.1016/0006-8993(94)91250-5

Yamada, T., Yoshiyama, Y., Tsuboi, Y., and Shimomura, T. (1997). Astroglial expression of hepatocyte growth factor and hepatocyte growth factor activator in human brain tissues. *Brain Res.* 762, 251–255. doi: 10.1016/S0006-8993(97)00504-0

Yamagata, T., Muroya, K., Mukasa, T., Igarashi, H., Momoi, M., Tsukahara, T., et al. (1995). Hepatocyte growth factor specifically expressed in microglia activated Ras in the neurons, similar to the action of neurotrophic factors. *Biochem. Biophys. Res. Commun.* 210, 231–237. doi: 10.1006/bbrc.1995.1651

Yamazaki, Y., Zhao, N., Caulfield, T. R., Liu, C. C., and Bu, G. (2019). Apolipoprotein E and Alzheimer disease: pathobiology and targeting strategies. *Nat. Rev. Neurol.* 15, 501–518. doi: 10.1038/s41582-019-0228-7

Yu, M., Sporns, O., and Saykin, A. J. (2021). The human connectome in Alzheimer disease - relationship to biomarkers and genetics. *Nat. Rev. Neurol.* 17, 545–563. doi: 10.1038/s41582-021-00529-1

**Conflict of Interest:** The authors declare that the research was conducted in the absence of any commercial or financial relationships that could be construed as a potential conflict of interest.

**Publisher's Note:** All claims expressed in this article are solely those of the authors and do not necessarily represent those of their affiliated organizations, or those of the publisher, the editors and the reviewers. Any product that may be evaluated in this article, or claim that may be made by its manufacturer, is not guaranteed or endorsed by the publisher.

frontiers | Frontiers in Aging Neuroscience

TYPE Original Research
PUBLISHED 01 September 2022
DOI 10.3389/fnagi.2022.951197



OPEN ACCESS

EDITED BY
Jun Xu,
Capital Medical University, China

REVIEWED BY
Shu-Ping Zhou,
Ningbo College of Health Sciences, China
Donghua Liu,
The Second People's Hospital of Yinchuan, China

*CORRESPONDENCE
Qian Wang
qianqianwangxi@163.com
Yongjian Zhu
neurosurgery@zju.edu.cn

†These authors have contributed equally to this work

SPECIALTY SECTION
This article was submitted to Alzheimer's Disease and Related Dementias, a section of the journal Frontiers in Aging Neuroscience

RECEIVED 23 May 2022
ACCEPTED 25 July 2022
PUBLISHED 01 September 2022

CITATION
Lin W, Wang Q, Chen Y, Wang N, Ni Q, Qi C, Wang Q and Zhu Y (2022) Identification of a 6-RBP gene signature for a comprehensive analysis of glioma and ischemic stroke: Cognitive impairment and aging-related hypoxic stress. *Front. Aging Neurosci.* 14:951197. doi: 10.3389/fnagi.2022.951197



# Identification of a 6-RBP gene signature for a comprehensive analysis of glioma and ischemic stroke: Cognitive impairment and aging-related hypoxic stress

Weiwei Lin[1,2†], Qiangwei Wang[1,2†], Yisheng Chen[3†], Ning Wang[4†], Qingbin Ni[5], Chunhua Qi[5], Qian Wang[5*] and Yongjian Zhu[1,2,6*]

[1]Department of Neurosurgery, The Second Affiliated Hospital of Zhejiang University School of Medicine, Hangzhou, China, [2]Key Laboratory of Precise Treatment and Clinical Translational Research of Neurological Diseases of Zhejiang, Hangzhou, China, [3]Department of Orthopedics, Shanghai General Hospital, Shanghai Jiao Tong University School of Medicine, Shanghai, China, [4]Brain Center, Affiliated Zhejiang Hospital, Zhejiang University School of Medicine, Hangzhou, China, [5]Postdoctoral Workstation, Department of Central Laboratory, The Affiliated Taian City Central Hospital of Qingdao University, Taian, China, [6]College of Mathematical Medicine, Zhejiang Normal University, Jinhua, China

There is mounting evidence that ischemic cerebral infarction contributes to vascular cognitive impairment and dementia in elderly. Ischemic stroke and glioma are two majorly fatal diseases worldwide, which promote each other's development based on some common underlying mechanisms. As a post-transcriptional regulatory protein, RNA-binding protein is important in the development of a tumor and ischemic stroke (IS). The purpose of this study was to search for a group of RNA-binding protein (RBP) gene markers related to the prognosis of glioma and the occurrence of IS, and elucidate their underlying mechanisms in glioma and IS. First, a 6-RBP (*POLR2F*, *DYNC1H1*, *SMAD9*, *TRIM21*, *BRCA1*, and *ERI1*) gene signature (RBPS) showing an independent overall survival prognostic prediction was identified using the transcriptome data from TCGA-glioma cohort ($n$ = 677); following which, it was independently verified in the CGGA-glioma cohort ($n$ = 970). A nomogram, including RBPS, 1p19q codeletion, radiotherapy, chemotherapy, grade, and age, was established to predict the overall survival of patients with glioma, convenient for further clinical transformation. In addition, an automatic machine learning classification model based on radiomics features from MRI was developed to stratify according to the RBPS risk. The RBPS was associated with immunosuppression, energy metabolism, and tumor growth of gliomas. Subsequently, the six RBP genes from blood samples showed good classification performance for IS diagnosis (AUC = 0.95, 95% CI: 0.902–0.997). The RBPS was associated with hypoxic responses, angiogenesis, and increased coagulation in IS. Upregulation of *SMAD9* was associated with dementia, while downregulation of *POLR2F* was associated with aging-related hypoxic stress. *Irf5*/*Trim21*

in microglia and *Taf7*/*Trim21* in pericytes from the mouse cerebral cortex were identified as RBPS-related molecules in each cell type under hypoxic conditions. The RBPS is expected to serve as a novel biomarker for studying the common mechanisms underlying glioma and IS.

KEYWORDS

**elderly, glioma, ischemic stroke, RNA binding protein (RBP), dementia**

## Introduction

There is mounting evidence that ischemic cerebral infarction contributes to vascular cognitive impairment and dementia in elderly, but the origins of ischemic cerebral infarction are unclear. Understanding the vascular pathologies that cause ischemic cerebral infarction may yield strategies to prevent their occurrence and reduce their deleterious effects on brain function (Hartmann et al., 2018). Worldwide, ischemic stroke (IS) accounts for about 70% of all stroke events, with a proportion as high as 87% in the United States, and is also the second leading cause of death (Musuka et al., 2015; Benjamin et al., 2019; Phipps and Cronin, 2020). Glioma is a common type of invasive brain tumor and the leading cause of primary brain tumor-related deaths (Musuka et al., 2015; Velasco et al., 2019; Wang E. et al., 2019). Among them, glioblastoma multiforme (GBM; WHO IV) accounts for 45.2% of all primary malignant tumors of the central nervous system (CNS) and is one of the fatal tumor types, with a median survival time of fewer than 15 months (Ostrom et al., 2013; Bi et al., 2020; Wang et al., 2020).

Clinical studies show that glioma and cerebral ischemia can promote each other's occurrence during disease development and treatment (Fraum et al., 2011; Seidel et al., 2013; Wojtasiewicz et al., 2013; Farkas et al., 2018; Noda et al., 2022). Previous studies have reported that the incidence of brain tumors is higher in a cohort of patients with IS than in those without a history of IS (Qureshi et al., 2015; Chen et al., 2017; Tanislav et al., 2019). Similarly, stroke is a common complication among patients with tumor. A postmortem-based study reported that about 14.6% of non-CNS cancer cases showed cerebrovascular disease (CVD) (Graus et al., 1985). Moreover, embolic strokes are the most common cause of strokes in patients with cancer, possibly due to intravascular coagulopathy (Cestari et al., 2004); patients with active cancer show multiple infarcts (Kikuno et al., 2021). Gliomas account for 60% of ischemic strokes secondary to primary brain tumors, whereby complications due to surgery and radiotherapy form the majority (Kreisl et al., 2008). In these coexisting diseases, stroke is usually missed, often leading to increased neurological disabilities and injuries in susceptible individuals. Therefore, the pathogenesis of glioma could provide potential mechanisms for cerebral ischemia.

RNA-binding protein (RBP) is a large protein family, which plays a vital role in regulating gene expression through interactions with RNA. These proteins participate in many biological processes, such as splicing, lysis, and polyadenylation, as well as mRNA editing, localization, stabilization, and translation (Kedde et al., 2007; Liao et al., 2020; Van Nostrand et al., 2020). In addition, some studies suggest that the interaction between RBP and RNA plays a vital role in the occurrence and development of cancers (including renal cell carcinoma, triple-negative breast cancer, and lung squamous cell carcinoma) (Mohibi et al., 2019; Duan and Zhang, 2020; Kim et al., 2020; Li et al., 2020; Qin et al., 2020). In this context, many RBPs are reportedly associated with a poor prognosis of gliomas (Shao et al., 2013; Barbagallo et al., 2018; Lan et al., 2020). In IS, several RBPs participate in the development and influence the prognoses of these patients by promoting inflammatory reactions (Zhou et al., 2014; Sharma et al., 2021), increasing cerebrovascular permeability, promoting vasogenic cerebral edema (Ardelt et al., 2017), regulating apoptosis (Si et al., 2020; Zhang et al., 2020), and protecting neurons (Fang et al., 2021).

In the development of glioma and ischemic stroke events, some common pathways, such as hypoxia, brain inflammation, angiogenesis, and hypercoagulability, have been identified (Ghosh et al., 2019). Among them, hypoxia is the most widely accepted basis for building research models for studying the common mechanisms underlying glioma and IS (Søndergaard et al., 2002; Kasivisvanathan et al., 2011). However, the specific mechanism of co-occurrence or mutual promotion of glioma and ischemic stroke remains unclear. Many clinical studies have described this problem from a clinical perspective and expounded the possible common pathway underlying the pathogenesis from the perspective of each disease. Several RBP molecular or molecular combination markers are used to identify specific subgroups of patients with glioma, showing

Abbreviations: TCGA, The cancer genome atlas; CGGA, Chinese glioma genome atlas; LGG, Lower-grade gliomas; GBM, Glioblastomas; RBP, RNA-binding protein; LASSO, Least absolute shrinkage and selection operator; GO, Gene ontology; GSEA, Gene set enrichment analysis; IDH, Isocitrate dehydrogenases; MGMT, O6-methylguanine-DNA methyltransferase; IS, Ischemic stroke.

poor survival. Similarly, several RBPs are involved in the development of IS. However, there is a lack of a comprehensive analysis of the RBP family of genes in the common pathway underlying glioma and IS. Through an in-depth study on the role of RBPs, we hypothesized that RBP signature could not only provide an effective identification for molecular subtypes of patients with glioma with a poor prognosis but also yield certain reference values for the diagnosis of IS. Such biomarkers will also provide more reliable risk stratification and treatment targets for the clinicians to customize more accurate personalized treatment plans and ultimately improve the treatment efficacy.

Bioinformatics based on medical big data has solid advantages for analyzing the common molecular mechanisms and pathways for such coexisting diseases. In addition, the combination of radiomics and machine learning shows a good performance in image-based diagnosis or molecular subtype prediction and is more convenient for clinical application (Acs et al., 2020). The primary purpose of this study was to identify a group of RBP genes related to the prognosis of glioma and the occurrence of IS, and elucidate their mechanism in glioma, dementia, and IS. First, we identified a panel of RBP genes related to the prognosis and analyzed the pathogenesis of these genes in glioma. Next, using the radiomics features from MRI images, an automatic machine learning classifier was used to predict risk stratification based on this RBP gene signature in glioma. Finally, using bulk RNA sequencing (RNA-seq) and single-cell RNA sequencing (scRNA-seq) data, the classificatory performance and the potential mechanism of these RBP genes in IS were analyzed.

# Materials and methods

## Research design and data extraction

According to the research purpose, the study design was divided into two stages. The first stage involved the identification of a 6-RBP gene signature (RBPS) and functional analysis of the RBPS in glioma. The second stage was evaluating the expression and functions of the RBPS in IS and mouse cerebral cortex cells under hypoxic conditions.

The first stage could be subdivided into three steps as follows: the discovery and verification of biological gene markers and automatic machine learning prediction based on radiomics features. First, the standardized RNA expression profile data of 677 patients with glioma (including 698 tumor tissues and 5 adjacent normal tissue samples) were downloaded from TCGA (https://portal.gdc.cancer.gov/), and a 6-RBP gene signature related to the prognosis of glioma was identified. Next, the identified biomarkers were verified in independent clinical data sets using the transcriptome RNA expression profile data and clinical characteristics of patients with glioma (N = 970; Verification Cohort 1) in CGGA (https://www.cgga.org.cn/). Moreover, the clinical data of patients with Grade IV glioma in the GSE72951 data set (Erdem-Eraslan et al., 2016) (N = 110; Validation Cohort 2) and the gene expression profile data from gene chip analysis were obtained from the Gene Expression Omnibus (GEO) database for verification. Finally, using MRI-based radiomics features, an automatic machine learning classifier was constructed to predict the RBPS. MRI-based radiomics feature data from 132 patients with glioma were downloaded from TCIA (Clark et al., 2013) and used to train classifiers for predicting RBPS risk stratification (Bakas et al., 2017; Beers et al., 2018).

In the second stage, the possible mechanism underlying the six RBP genes in stroke and dementia was evaluated, and the gene regulatory network related to hypoxia was analyzed in mouse cerebral cortex cells. First, the GSE16561 dataset was retrieved from the GEO database to examine differentially expressed genes (DEGs) related to ischemic stroke. RNA-seq data in this dataset were derived from peripheral blood samples of 39 patients with ischemic stroke and 24 healthy controls (Barr et al., 2010; O'Connell et al., 2016, 2017). The GSE36980 dataset was used to explore DEGs associated with Alzheimer's disease, which included 33 patients with AD and 47 non-AD controls (Hokama et al., 2014). In addition, to study the expressions of the related genes at a single-cell level, RNA-seq data from 7,925 isolated mouse cerebral cortex cells were obtained from the GSE125708 dataset. In this data set, mice were divided into two groups: one group living in indoor air for 7 days was the normal oxygen concentration group, and the other group living in 7.5% oxygen concentration for 7 days was the hypoxia concentration group. Using this dataset, we examined the regulatory changes for the RBPS-related genes with changes in the oxygen concentration (Heng et al., 2019).

## Analysis of differentially expressed RBP genes

A total of 1,542 RNA-binding protein genes were collected from a published dataset (Gerstberger et al., 2014). Differentially expressed RBP genes were analyzed between tumor samples and normal samples adjacent to cancer in the TCGA-glioma dataset. An adjusted $p$ value $< 0.05$ using the Benjamini-Hochberg false discovery rate (FDR) method (FDR $< 0.05$) and a logarithmic value of fold change $>1$ ($|\log_2 FC| > 1$) were used as the cut-off criteria to screen differentially expressed RBP genes. Differentially expressed genes (DEGs) were used to perform Gene Ontology (GO) and Kyoto Encyclopedia of Genes and Genomes (KEGG) pathway enrichment analysis using the online DAVID database. The protein-protein interaction (PPI) analysis of DE-RBP genes was performed using STRING software (https://string-db.org/). Cytoscape software was used to build a sub-network to identify the PPI network's core DEGs.

The "limma" (Ritchie et al., 2015) and "sva" (Leek et al., 2012) R packages were used to remove the batch effect for the gene expression data of the shared RBP genes in TCGA, CGGA, and GSE72951 datasets.

## Construction of a 6-RBP gene signature

To identify a clinically translatable RBP gene signature, the univariate Cox proportional hazard regression model and the Lasso penalty Cox regression model were used for evaluating the association of RBP genes in predicting overall survival (OS) in patients with glioma. Next, RBPS was constructed, and its value in predicting OS was evaluated. The risk score (RS) of the RBPS was calculated based on the linear combination of the gene expression ($EXP_i$) multiplied by the corresponding coefficient ($Coef_i$).

$$RS = \sum_{i=1}^{n} Coef_i \times EXP_i \quad (1)$$

The median value of the gene signature risk score was used as a cut-off threshold to divide the entire patients with glioma into high- and low-risk groups. The Kaplan-Meier (K-M) method was used to plot survivor curves. The log-rank test was used to calculate the statistical difference between the two groups to evaluate the correlation of the RBPS with the OS outcome. Receiver operator characteristic (ROC) curve analysis of the RBPS with prognosis was performed using the "survivalROC" package (https://CRAN.R-project.org/package=survivalROC), and 95% confidence intervals (CI) of the area under the curve (AUC) were calculated by the "timeROC" (Blanche et al., 2013) package.

## Risk stratification of the RBPS

The expressions of the RBPS genes in samples were analyzed using the "pheatmap" package. The risk scores of RBPS were sorted from low to high to evaluate the relationship between the risk scores and patients' living status and overall survival time. Circosplot was drawn using the "RCircos" (Zhang et al., 2013) package to show the copy number variant status distribution of the RBPS genes and their position on chromosomes. To explore the relationship between the expression and copy number variant status of the RBPS genes, the differential expression analyses of RBPS genes among different copy number variants were performed to explore the role of a gene copy number variant in RBPS genes expression.

## Gene set enrichment analysis

Gene set enrichment analysis (GSEA) is a bioinformatics algorithm used to identify the differential expression of biological pathways between two biological states (Subramanian et al., 2005). GSEA was used to identify the pathway related to the RBPS. The "c2.cp.kegg.v7.1.symbols.gmt[Curated]" gene set collection from the Molecular Signatures Database (MSigDB) was used as a reference for enrichment analysis (Subramanian et al., 2005; Liberzon et al., 2011, 2015). The false discovery rate (FDR) and the normalized enrichment score (NES) were used to sort the KEGG pathways.

## Association between the RBPS and glioma stemness

The tumor stemness index refers to the gradual loss of cell differentiation phenotype and acquisition of progenitor cell and stem-cell-like characteristics during tumor progression (Malta et al., 2018). Two types of glioma stemness indices, namely, the RNA expression-based stemness score (RNAss) and the DNA methylation-based stemness score (DNAss) were downloaded from UCSC Xena (Goldman et al., 2020) to evaluate the correlation between the RBPS and glioma stemness indices. The stemness indices range from 0 to 1, where 0 indicates a high degree of differentiation, and 1 indicates undifferentiated.

## Immune-related tumor microenvironment and potential compounds

First, the "ESTIMATE" algorithm (Yoshihara et al., 2013) was used to calculate the immune-related tumor microenvironment features from gene expression data, including stromal, immune, and ESTIMATE scores. The profiles of six immune subtype categories representing TME features and potential therapeutic and prognostic implications were downloaded from UCSC Xena (Thorsson et al., 2018). In addition, the abundance of 22 infiltrating immune cell types was calculated and inferred from RNA expression profiles using CIBERSORTx (Newman et al., 2019). Moreover, a list of important immune checkpoint molecules, including *PD-1*, *PDL1*, and *CTLA-4*, was obtained. In the TCGA-glioma cohort, the correlations between these immune-related features and RBPS were analyzed. Finally, to identify the potential drugs targeting these RBPS genes, drug concentration and gene expression profiles were downloaded from CellMiner (Reinhold et al., 2012) to perform correlation analysis. Drugs were filtered according to FDA's approval results for clinical trials.

## Radiomics-based TPOT analysis

Radiomics features data were downloaded from TCIA to establish an Automatic Machine Learning (AutoML) prediction model. Radiomics features were extracted from T1WI, T2WI, Flair, and T1Gd images (Bakas et al., 2017; Beers et al., 2018), including 483 usable features. Univariate logistic regression analysis evaluated the association between each Radiomics feature and RBPS in patients with glioma, and RBPS-related radiomics features were selected for autoML model training. The steps of autoML model construction include features selection, parameters selection, and final model selection, which were fully automated using the Tree-based Pipeline Optimization Tool (TPOT) (Le et al., 2020). TPOT is an automated machine learning tool based on Python, which uses genetic algorithm programming (https://github.com/rhiever/tpot) to optimize the machine learning pipeline. Before TPOT analysis, the dataset was randomly divided into a training set (99 patients) and a test set (33 patients) according to 3:1, and the random number state was fixed at 42. The training process was set as follows: generations = 100, population size = 100, and 10-fold cross-validation on the training set. Finally, TPOT will return a model with the best classification performance and parameters. The TPOT was repeated 20 times, and the models were sorted by the area under the curve (AUC). After that, the top 10 models with the best performance were screened out. In addition, ROC curves and precision-recall curves were also used to compare the performance of these ten models. By comparing the sensitivity, specificity, accuracy, AUC, and average precision (AP) of these ten models, the best model was finally determined based on the accuracy metrics (Su et al., 2019).

## Single-cell analysis

RNA-seq data of 7,925 single cells from the mouse cerebral cortex under normoxia and hypoxia conditions were analyzed using the "Seurat" package (Stuart et al., 2019). Based on pre-set filter conditions (at least 200 expressed genes but no more than 6,000 expressed genes, RNA counts >1,000, mitochondrial gene expression <20%, and hemoglobin-related gene expression <1%), a total of 7,789 cells and 14,271 gene features were filtered for further single-cell analysis. The scRNA-seq data were integrated with the "SCTransform" function and then processed using "RunPCA" and "RunUMAP" functions, including noise removal, information extraction, and cell dimension reduction. The results of cell dimensionality reduction were visualized with uniform manifold propagation and projection (UMAP) (Becht et al., 2019) to observe the effect of batch effect removal between groups. The "FindNeighbors" and "FindClusters" functions were used to detect cell clusters. Finally, each cell cluster was annotated according to the commonly used marker genes of cell types. After cell annotation, microglia, astrocytes, and pericytes were extracted as cell subsets, and "FindMarker" was used to calculate differentially expressed genes in those cell types between hypoxia and normoxia conditions.

## Single-cell regulatory network inference and clustering

Single-cell regulatory network inference and clustering (SCENIC) was used to identify the main gene regulatory networks in each cell type between different groups from single-cell transcripts (Aibar et al., 2017). First, pySCENIC (version 0.11) was used to identify the major transcription factors and their corresponding gene regulatory networks in mouse cerebral cortex cells. Transcription factors and their gene regulatory networks constitute a regulatory module called regulon. Based on the expression of transcription factors and downstream-regulated molecules in the regulon, the regulon activity score (RAS) is used to measure the regulatory ability of each regulon in each cell. Finally, based on the RAS, the regulon activity score (RSS) is calculated to describe the regulatory power of each regulon in each cell subtype, and the regulons in each cell type are ranked according to RSS so as to infer the influence of each regulon on cell transcription regulation in a specific cell type.

## Pseudotime analysis and cell trajectory inference

Monoclec3 (version 1.0) and Monoclec2 (version 2.4) (Trapnell et al., 2014; Qiu et al., 2017a,b; Cao et al., 2019) were used to calculate the pseudotime and analyze cell trajectory based on scRNA-seq transcripts from the mouse cerebral cortex for further identifying transcriptional differences among these cells and examining changes in RBPS and its transcription factors during cell fate transition. First, differentially expressed genes were determined for each cell type between normoxia and hypoxia groups. Then, the "DDRTree" method was used to calculate the cell state for each cell type. The velocyto.py (version 11.2) was used to calculate the RNA velocity in each cell. The workflow, annotation files, and visual tools can be obtained following the methods described in the previous studies (Vidal et al., 2019; Lin et al., 2021).

## Statistical analysis

All statistical analyses were performed using the R software (version 4.0.2, R Foundation for Statistical Computing, Vienna, Austria; http://www.r-project.org/) and Python (version 3.8). The "rms" R package was used to draw the nomogram. Spearman correlation coefficient and the Benjamini-Hochberg method adjusted-$p$ value (FDR) were used for correlation

analysis. All $p$-values were two-sided, and $p < 0.05$ was considered statistically significant.

# Results

## Differentially expressed RBP genes

First, a panel of 1,542 RBP genes was collected. Among them, 1,472 were selected to analyze the differentially expressed RBP genes between tumor and normal samples in TCGA. A total of 170 DEGs were identified according to the preset filter conditions, and the results are shown in the heat map (Supplementary Figure 1A). Subsequently, the GO and KEGG pathways for DEGs were analyzed, and the results showed that the differentially expressed RBP genes were mainly enriched in RNA processing-related pathways (Table 1). Furthermore, the protein-protein interactions (PPI) of DEGs were predicted and analyzed using the STRING website, following which a PPI sub-network analysis of DEGs was performed using the Cytoscape software (Supplementary Figures 1B,C). The core genes and molecular interaction networks related to the differential RBP genes were obtained through PPI analysis.

TABLE 1 GO function and KEGG pathway enrichment result.

| ID | Term | *P*-value |
|---|---|---|
| hsa03010 | Ribosome | <0.001 |
| hsa03015 | mRNA surveillance pathway | <0.001 |
| hsa03018 | RNA degradation | <0.001 |
| hsa03013 | RNA transport | 0.011 |
| hsa03040 | Spliceosome | 0.022 |
| GO:0000956 | Nuclear-transcribed mRNA catabolic process | <0.001 |
| GO:0006401 | RNA catabolic process | <0.001 |
| GO:0006402 | mRNA catabolic process | <0.001 |
| GO:0022626 | Cytosolic ribosome | <0.001 |
| GO:0000184 | Nuclear-transcribed mRNA catabolic process, nonsense-mediated decay | <0.001 |
| hsa03013 | RNA transport | <0.001 |
| hsa03018 | RNA degradation | 0.020 |
| hsa03015 | mRNA surveillance pathway | 0.020 |
| hsa04914 | Progesterone-mediated oocyte maturation | 0.020 |
| hsa03008 | Ribosome biogenesis in eukaryotes | 0.022 |
| hsa04114 | Oocyte meiosis | 0.027 |
| hsa04962 | Vasopressin-regulated water reabsorption | 0.028 |
| hsa05134 | Legionellosis | 0.040 |
| GO:0008380 | RNA splicing | <0.001 |
| GO:0043484 | Regulation of RNA splicing | <0.001 |
| GO:0050684 | Regulation of mRNA processing | <0.001 |
| GO:0048024 | Regulation of mRNA splicing, *via* spliceosome | <0.001 |
| GO:0000377 | RNA splicing, *via* transesterification reactions with bulged adenosine as nucleophile | <0.001 |

## Identification of the 6-RBP gene signature

First, 170 differentially expressed RBP genes were screened and the commonly shared intersecting genes in RNA expression profiles of patients with glioma in TCGA, CGGA, and GSE72951 datasets were obtained. The filtered expression profiles from these three datasets were further processed to remove batch effects. Next, by univariate Cox analysis for TCGA glioma expression profile data, a total of 100 RBP genes were analyzed along with the total survival time data, and the top 17 RBP genes significantly related to survival were screened out (Figure 1A). Finally, in the TCGA training set, the Lasso penalty Cox regression analysis was performed to screen gene variables, and a prognosis model was constructed according to the multivariate Cox regression model. Using the lambda.min threshold (Figure 1G), a 6-RBP gene signature (RBPS) was identified, comprising 6 RBP genes (*TRIM21*, *BRCA1*, *ERI1*, *POLR2F*, *DYNC1H1*, and *SMAD9*). The RBPS was associated with the adverse OS in glioma. The volcanic plot showed the differential analysis results of these six RBP genes, which showed that *POLR2F* and *DYNC1H1* were downregulated in glioma, while *TRIM21*, *BRCA1*, *ERI1*, and *SMAD9* were upregulated in glioma (Figure 2A). Figure 2B showed the copy number variation of these six RBP genes and their positions on 24 chromosomes. The RBPS risk score (RS) was calculated based on the linear combination of the expression values of the six RBP genes multiplied by their corresponding coefficients. The formula for calculating the RBPS RS was as follows:

$$RS_{RBPS} = 0.294 \times EXP_{TRIM21} + 0.525 \times EXP_{BRCA1} + 0.400 \times EXP_{ERI1} - 0.313 \times EXP_{POLR2F} - 0.303 \times EXP_{DYNC1H1} - 0.432 \times EXP_{SMAD9} \quad (2)$$

Among the six RBP genes constituting the RBPS, higher expression levels of *POLR2F*, *DYNC1H1*, and *SMAD9* were associated with a lower risk of death (HR < 1). In contrast, higher expressions of *TRIM21*, *BRCA1*, and *ERI1* were associated with poorer overall survival (HR > 1; Figure 1B; Supplementary Table 1). Patients with glioma were stratified according to the median value of the RBPS risk score in the TCGA cohort and were divided into high-risk and low-risk groups. The 5-year OS rates for RBPS-derived high- and low-risk patients were 19 and 75%, respectively; WHO II-IV (HR: 6.76, 95% CI: 4.84–9.44; $p < 0.001$), WHO II (HR: 3.47, 95% CI:

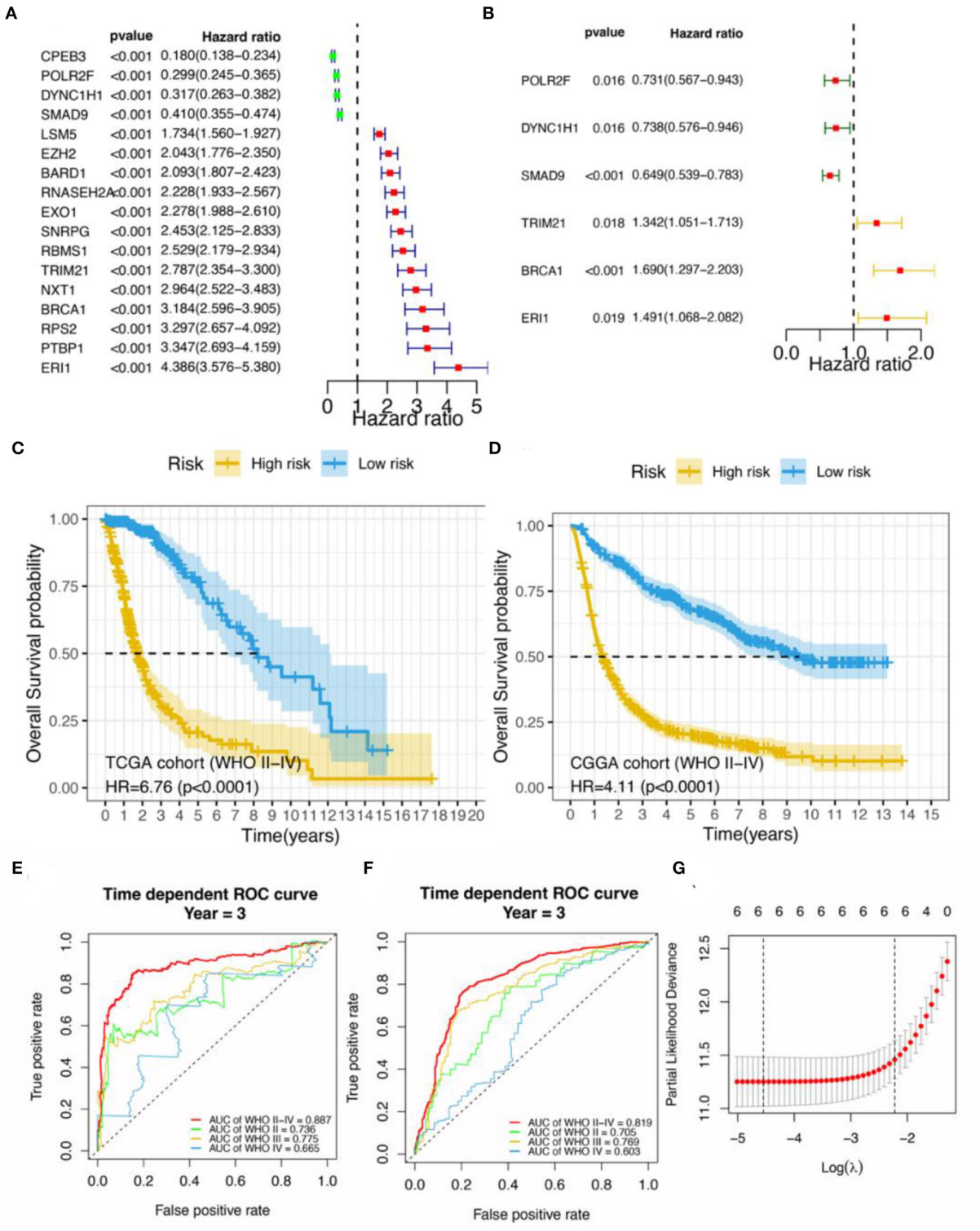


FIGURE 1
Construction of a prognostic signature based on OS events in glioma. **(A)** Univariate Cox analysis for the top 17 RBP genes. **(B)** Multivariate Cox analysis for six RBP genes. Survival analysis for patients with glioma between the high- and low-risk groups in **(C)** TCGA and **(D)** CGGA datasets. Yellow indicates high risk and blue indicates low risk for glioma. Bioinformatics analyses for the 6-gene risk stratification signature; receiver operator characteristic curve analysis for the 6-gene signature in **(E)** TCGA and **(F)** CGGA datasets. **(G)** Selection of the tuning parameter (lambda) in Cox-penalized regression analysis *via* 10-fold cross-validation in the TCGA cohort. The vertical dotted lines on the left and the right indicate "lambda.min" and "lambda.1se" criteria, respectively. The red dots represent partial likelihood deviation values, while the gray lines are the corresponding standard errors. AUC, the area under the curve.

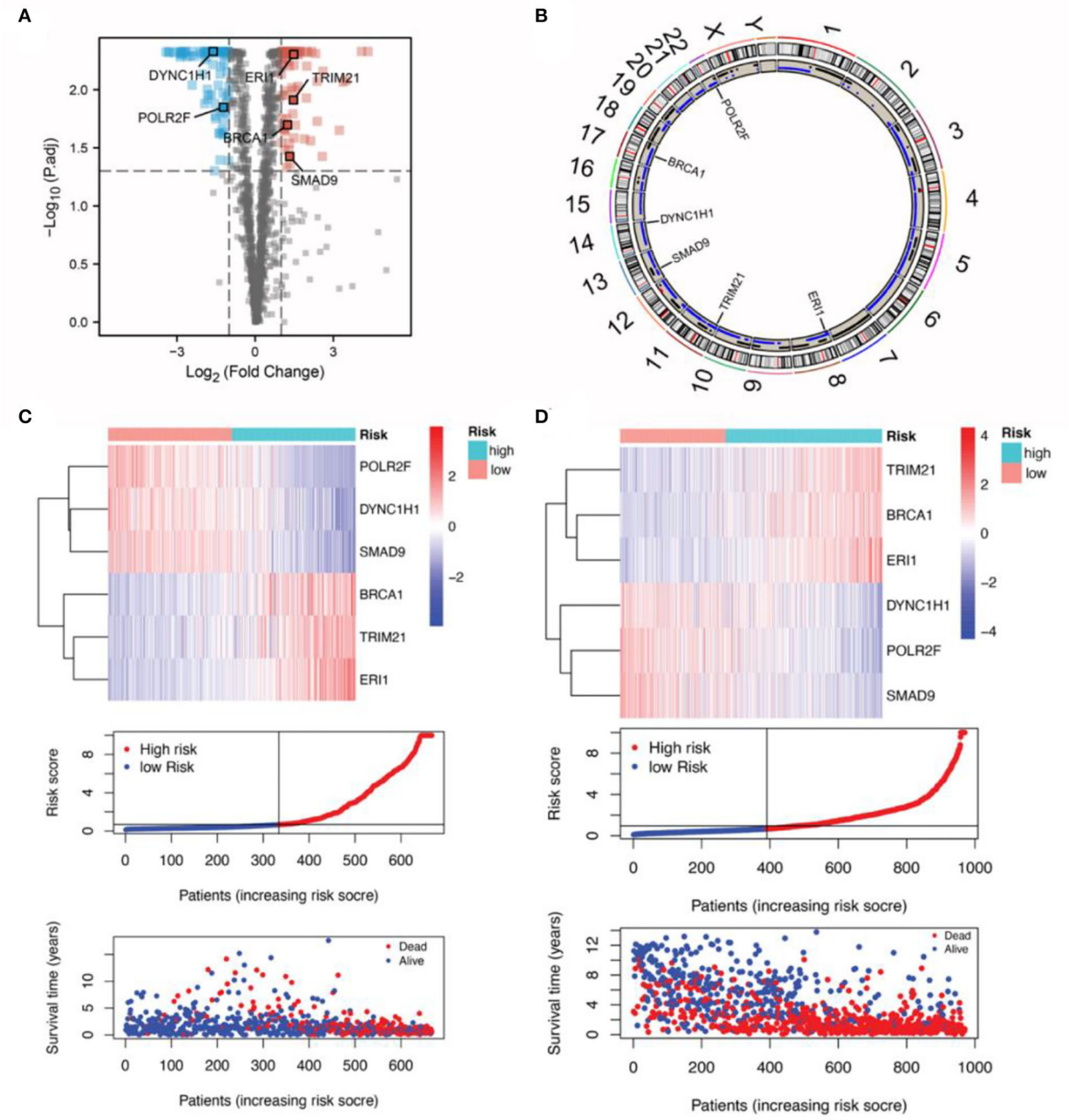


FIGURE 2
Characteristics of the six RBP genes in the RBPS. **(A)** Differently expressed genes between the normal and tumor samples are shown in the volcano plot. The dots in red represent upregulated genes (Yang et al., 2020), while those in green are signed downregulated genes (Boucas et al., 2015) in tumor samples. Significant differences were determined using the thresholds of$|\log_2 FC|> 1$ and FDR $< 0.05$. **(B)** The location of the six RBP genes on the 24 chromosomes, as well as the copy number variation events. The expression of the six RBP genes, distribution of the RBPS risk scores, survivor status, and survival time of the patients with glioma ranked by their risk scores in **(C)** TCGA and **(D)** the CGGA datasets.

1.68–7.18, $p < 0.001$), WHO III (HR: 2.85, 95% CI: 1.75–4.64, $p < 0.001$), WHO IV (HR: 1.54, 95% CI: 1.04–2.26, $p = 0.028$; Figure 1C; Supplementary Figures 2A–C).

Subsequent validation in the CGGA dataset showed the outcomes were consistent with the findings in the TCGA cohort; WHO II-IV (HR: 4.11, 95% CI: 3.40–4.95; $p < 0.001$), WHO II (HR: 2.02, 95% CI: 1.32–3.10; $p = 0.001$), WHO III (HR: 3.12, 95% CI: 2.32–4.19; $p < 0.001$), and WHO IV (HR: 1.28, 95% CI: 1.03–1.60, $p = 0.027$; Figure 1D; Supplementary Figures 2D–F). These findings indicated that Subsequent validation in tRBPS could predict adverse prognosis for patients with glioma as well as the glioma subgroups based on the WHO grades. In

addition, the gene expression differences for these six RBP genes with respect to copy number variation events were analyzed (Supplementary Figures 3A–F). The results showed that copy number variants were significantly associated with mRNA expressions of *POLR2F* ($p < 0.001$), *DYNC1H1* ($p < 0.001$), *TRIM21* ($p < 0.001$), *SMAD9* ($p < 0.001$), and *ERI1* ($p = 0.005$). This suggests that copy number variants may be an important factor in the poor prognosis of RBPS.

## RBPS is associated with a poor OS for glioma

In the TCGA discovery cohort, the RBPS showed robustness for identifying the poor survival of gliomas, as evidenced by the good AUC values for WHO grades: WHO II-IV (AUC = 0.887, 95% CI: 0.854–0.937), WHO II (0.736, 95% CI: 0.577–0.919), WHO III (0.775, 95% CI: 0.7–0.893) and WHO IV (0.665, 95% CI: 0.417–0.855; Figure 1E). Similarly, in the CGGA validation cohort, the AUC value of RBPS for identifying poor OS prognoses in all patients with glioma was 0.819 (95% CI: 0.794–0.851): WHO II (0.705, 95% CI: 0.622–0.799), WHO III (0.769, 95% CI: 0.721–0.829), and WHO IV (0.603, 95% CI: 0.507–0.687; Figure 1F). These results indicated that the RBPS had a potential clinical value, and the gene signature comprised of the six RBP genes could be used to identify the adverse OS in patients with glioma with various WHO grades. Additionally, in the CGGA validation cohort, the expression of the six RBP genes, survival status, and survival time distribution for patients according to their RBPS risk scores are shown in Figures 2C,D.

## RBPS is an independent predictor of glioma risk and survival outcome

To further evaluate the performance of RBPS as a clinical marker for risk stratification, its utility was analyzed along with clinical features for predicting survival and prognosis. First, in the TCGA cohort, univariate and multivariate Cox regression analyses were performed for various clinical features, including age, sex, WHO grade, and histopathology, along with the RBPS. In univariate analysis, age ($p < 0.001$), WHO grade ($p < 0.001$), histopathology ($p < 0.001$), and RBPS ($p < 0.001$) were important predictors for adverse OS (Supplementary Figure 3G). Subsequently, multivariate Cox regression analysis showed that age ($p < 0.001$), grade ($p < 0.001$), and RBPS ($p < 0.001$) were independent risk factors in predicting adverse OS in patients with glioma (Supplementary Figure 3H). In the CGGA cohort, univariate and multivariate cox regression analyses were conducted. Apart from age, WHO grade, and histopathology, the clinical features included radiotherapy, chemotherapy, IDH mutation, 1p19q codeletion, and methylation status of the MGMT gene promoter region (MGMTp). The results showed that WHO classification ($p < 0.001$), age ($p = 0.012$), and RBPS ($p < 0.001$) remained independent risk factors in predicting adverse OS (Supplementary Figures 3I,J). These results verified that RBPS based on these six RBP genes was reliable in predicting OS and could be used as an independent predictor of survival outcomes in patients with glioma.

The GSE72951 dataset included patients with recurrent glioblastoma only. In this dataset, K-M analysis showed that the median survival time in the high-RBPS-risk group was longer than that in the low-RBPS-risk group ($p = 0.010$, Supplementary Figures 4A,B), while univariate and multivariate Cox analyses suggested no statistical correlation between RBPS and survival outcomes (Supplementary Figures 4C,D). According to statistical significance and comparison of RBPS risk scores of WHO IV glioma in the three data sets, it was speculated that the RBPS risk scores of patients with WHO IV glioma in the GSE72951 dataset were relatively close to each other, thereby resulting in no statistically significant correlation between RBPS and survival outcomes (Supplementary Figures 4E–L). In addition, the expressions of protective genes (*POLR2F*, *DYNC1H1,* and *SMAD9*) for glioma in the GSE72951 dataset increased, while those of the risk genes (*TRIM21*, *BRCA1,* and *ERI1*) decreased so that the risk scores of patients in GSE72951 were the lowest among the three groups, but the median overall survival time was the shortest among the three datasets. The survival time of patients with WHO IV in the GSE72951 data set was the shortest, which could be attributed to the fact that the total survival time in this data set was calculated from the first recurrence and could be related to the inclusion of patients with recurrent glioblastoma. In addition, these patients received CCNU and/or bevacizumab treatment, which may be the reason why gliomas in the GSE72951 data set have lower RBPS risk scores. These findings suggested that the RBPS risk score may show dynamic changes with chemotherapy, which may, in turn, reflect the therapeutic efficacy.

## Construction of a nomogram for predicting the OS for patients with glioma

In order to further improve the predictive ability and applicability of RBPS in clinical practice, RBPS, and other critical clinical features (WHO grade, age, radiotherapy, chemotherapy, and 1p19q codeletion) were used to construct a multivariate Cox regression model and a risk nomogram for ease of use in clinical settings for predicting survival probabilities of patients with glioma. The parameters of this model are listed in Table 2. As shown in Figure 3A, the total score was calculated based on the sum of scores for each factor. The higher the total score, the lower the OS rate for 1 year, 3 years, and 5 years. As shown in the

TABLE 2 Prediction factors for survival in glioma.

| Variables | Prediction model | | |
|---|---|---|---|
| | *β* | Hazard ratio (95% CI) | *P* value |
| Grade (III vs. II) | 1.074 | 2.928 (2.506–3.421) | <0.001 |
| Grade (IV vs. II) | 1.753 | 5.773 (4.905–6.795) | <0.001 |
| Age | 0.011 | 1.011 (1.007–1.014) | 0.006 |
| Radiotherapy (yes vs. no) | −0.252 | 0.777 (0.689–0.876) | 0.035 |
| Chemotherapy (yes vs. no) | −0.357 | 0.7 (0.623–0.785) | 0.002 |
| 1p19q codeletion (yes vs. no) | −1.043 | 0.352 (0.3–0.413) | <0.001 |
| Risk score | 0.062 | 1.064 (1.048–1.079) | <0.001 |

β is the Cox regression coefficient. For grade, radiotherapy, and 1p19q codeletion, HR represents the average HR over the entire time period.

example (the red dot) in the figure, a patient with WHO grade III and an RBPS risk score of 1 (wherein no radiotherapy, no chemotherapy, and no 1p19q codeletion all corresponded to 34 points, WHO grade III corresponded to 70 points, and the RBPS risk score of 1 corresponded to 33 points in the nomogram), the total score corresponding to all characteristics was 233 points, and the predicted survival probabilities for 3 years and 5 years based on this total score were 0.344 and 0.219, respectively. Figure 3B shows the AUC of the model between 0.74 and 0.85 for predicting the overall survival rate for 1–5 years. The calibration curve showed that the predicted values using the model were in good agreement with the actual values (Figure 3C), suggesting a good prediction performance.

## Gene set enrichment analysis for RBPS

GSEA was performed using MSigDB Collection [c2. cp.kegg. v7.1. symbols (curated)] to identify differentially expressed signaling pathways in gliomas between high- and low-risk groups of patients with glioma. All genes were ranked according to their fold changes between the high- and low-risk groups, following which a GSEA was performed. FDR < 0.05 was used to filter and select significant enrichment signaling pathways. The results showed that a high RBPS risk score was related to the carcinogenesis of glioma, including multiple pathways related to cellular metabolism, immunity, and proliferation (Figures 3D,E). Furthermore, based on the sharing signaling pathways in TCGA and CGGA datasets, GSEA showed that the RBPS was associated with cytokine-cytokine receptor interaction (TCGA: NES = 1.72, size = 264, FDR = 0.046; CGGA: NES = 1.91; size = 209; FDR = 0.037) and intestinal immune network for IgA production (TCGA: NES = 1.75, size = 46, FDR = 0.048; CGGA: NES = 1.86; size = 42; FDR = 0.040). Taken together, the activity of immune, metabolic, and proliferative pathways may be enhanced, which may be related to the enhanced carcinogenic phenotype in patients with a high RBPS risk score.

## Relationship between RBPS and glioma stemness

To evaluate the relationship between RBPS and tumor stemness of glioma, the correlation of the RBPS score with DNAss and RNAss was calculated (Figure 4A). In all WHO grade II-IV gliomas, DNAss was positively correlated with the RBPS score, *ERI1*, *BRCA1*, and *TRIM21*, while negatively correlated with *POLR2F*, *DYNC1H1*, and *SMAD9* [Spearman correlation, Benjamini-Hochberg (BH)-adjusted $p < 0.05$]. However, RNAss was negatively correlated with the RBPS score, *ERI1*, *BRCA1*, and *TRIM21*, while positively correlated with *POLR2F*, *DYNC1H1*, and *SMAD9* (Spearman, BH-adjusted $p < 0.05$). In WHO grade II and III gliomas, the correlation of RBPS with DNAss and RNAss also showed a similar pattern in the overall glioma cohort. However, no significant correlation between RBPS and stemness index was observed in WHO grade IV gliomas, which may be attributed to their high malignancy and stemness.

## Correlation between RBPS and tumor microenvironment

GSEA showed that RBPS was associated with immune-related pathways. In order to evaluate the relationship between RBPS and the immune microenvironment of glioma, the correlation between RBPS and immune-related characteristics was analyzed. Figure 4A shows that RBPS and these six RBP genes were significantly correlated with the stromal score (Spearman, BH-adjusted $p < 0.05$), the immune score (Spearman, BH-adjusted $p < 0.05$), the ESTIMATE score (Spearman, BH-adjusted $p < 0.05$), and tumor purity (Spearman, BH-adjusted $p < 0.05$), as, also, tumors of all WHO subtypes.

As shown in Figure 4B, significant correlations between RBPS and individual immune cell types were observed. Specifically, RBPS was positively correlated with $CD8^+$ T cells, M1 and M0 macrophages, activated memory $CD4^+$ T cells, regulatory T cells, γδ T cells, and neutrophils (Spearman, BH-adjusted $p < 0.05$), and negatively correlated with naive B cells, naive $CD4^+$ T cells, eosinophils, activated mast cells, activated NK cells, monocytes, and dendritic cells (Spearman, BH-adjusted $p < 0.05$). In addition, the RBPS scores and the expressions of the six RBP genes were significantly different among the immune subtypes C1, C3, C4, C5, and C6 (the Kruskal-Wallis test, $p < 0.05$; Figure 4C). Among the WHO subtypes of glioma, the expression differences for RBPS and the

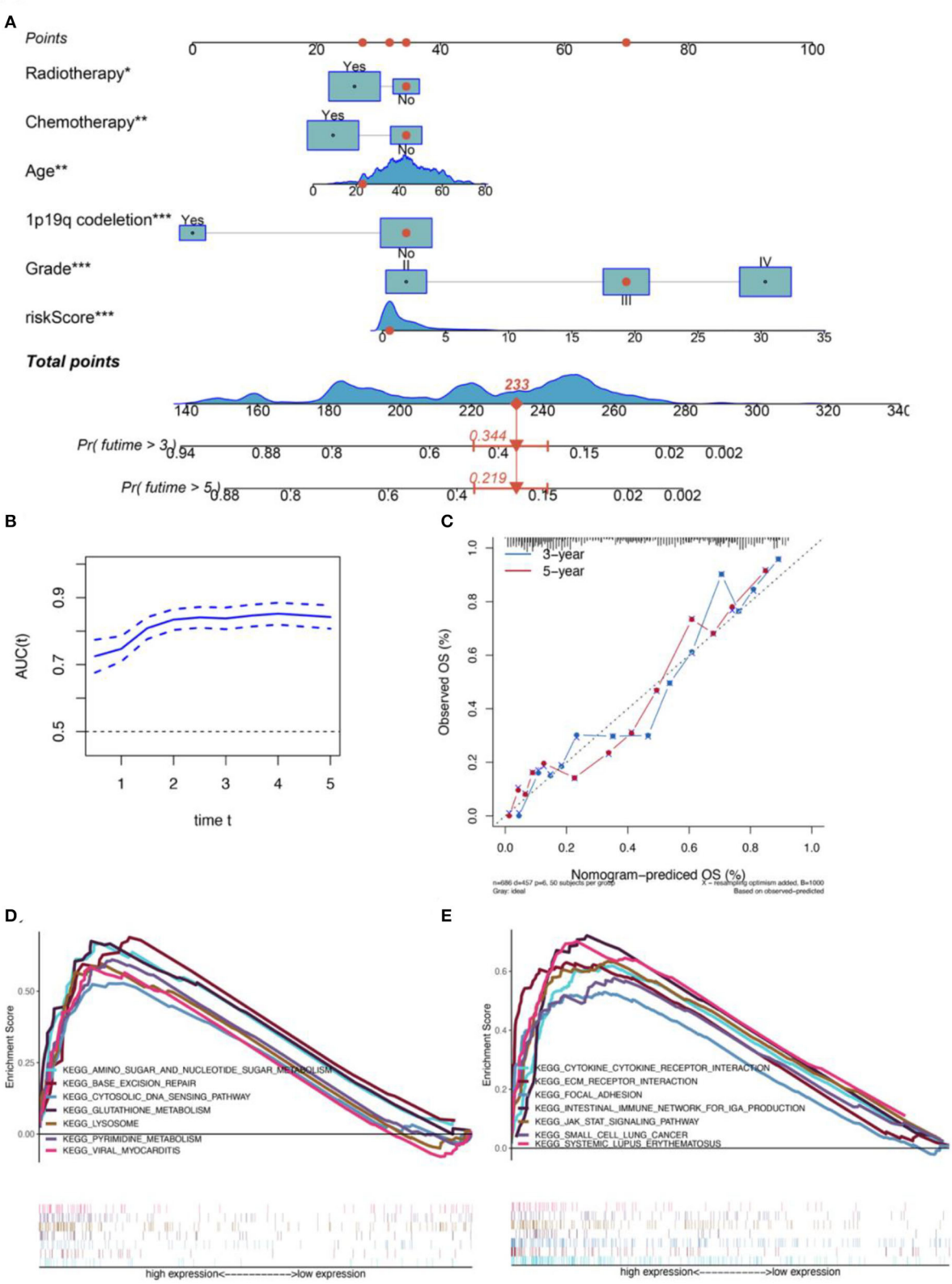


FIGURE 3
Construction of a CGGA-based clinical prediction model. **(A)** The nomogram for predicting the 3- and 5-year overall survival of patients with glioma based on the six independent prognostic factors from the CGGA dataset. **(B)** Relationship between the AUC values for the prognostic

*(Continued)*

FIGURE 3 (Continued)
prediction model and the correspondingly predicted survival times. **(C)** The calibration plot shows that the prediction using the model is in good agreement with the actual situation. **(D)** Glutathione metabolism, an amino sugar, and nucleotide sugar metabolism, lysosome, pyrimidine metabolism, viral myocarditis, base exception repair, and cytosolic DNA-sensing path were significantly differentially enriched between the high- and low-risk-score groups in the TCGA dataset. **(E)** JAK-STAT signaling, ECM-receptor interaction, cytokine-cytokine receptor interaction, systematic lupus erythematosus, intestinal immune network for IgA production, focal adhesion, and small cell lung cancer pathways were differentially enriched between the high- and low-risk groups in the CGGA database.

six RBP genes among different immune subtypes were analyzed, and the results are illustrated in Supplementary Figure 5.

To further elucidate the potential role of RBPS in immunotherapy, the correlations of RBPS and six RBP genes with common immune checkpoint molecules were analyzed. The results showed that, for glioma, the RBPS scores were positively correlated with the expression of immune checkpoint molecules, *PDCD1*, *CD274*, *PDCD1LG2*, *CTLA4*, *CD86*, *CD80*, *CD276*, and *FAS* (Spearman, BH-adjusted $p < 0.05$) but negatively correlated with *VTCN1* (Spearman, BH-adjusted $p < 0.05$; Figure 4C). In WHO grades II, III, and IV gliomas, RBPS was positively correlated with *CD274*, *CD276*, *CD80*, *CD86*, *CTLA4*, *FAS*, and *PDCD1LG2*. Finally, to identify potential drugs that targeted RBPS, the potential drugs related to the expression of these six RBP genes were queried in the database, and a correlation analysis was performed. The top 16 compounds with the highest correlation with the six RBP genes are shown (Supplementary Figure 5D). As shown, the top 16 predicted compounds were mainly related to *DYNC1H1* and *POLR2F*.

## Radiomics features for RBPS and automatic machine learning prediction model

First, by univariate logistic regression analysis, 180 radiomics features were selected according to $p < 0.05$ and included in the automatic machine learning model (Figure 5A). When splitting the training and test sets from the whole dataset to reduce the randomness in selecting patients for high- and low-RBPS risk between training different models and comparing their performances, the samples of the two sets were fixed (the random state was set at 42) and standard TPOT was performed. TPOT was used to calculate the average cross-validation score (AC) for each model in the training set (each model was trained 100 times/generation) and return the model with the best accuracy in the test set. Finally, by repeating the TPOT process ten times, ten independent classificatory models were obtained to predict the risk stratification according to RBPS. Overall, these 10 models showed good classification performances in training and test sets, along with high accuracy (Accuracy, ACC) (Supplementary Tables 2, 3). During the training process, each model showed the following performance in training and test sets: Model 1 (AC = 0.829, ACC = 0.727), Model 2 (AC = 0.868, ACC = 0.758), Model 3 (AC = 0.868, ACC = 0.667), Model 4 (AC = 0.829, ACC = 0.697), Model 5 (AC = 0.858, ACC = 0.818), Model 6 (AC = 0.859, ACC = 0.697), Model 7 (AC = 0.858, ACC = 0.697), Model 8 (AC = 0.839, ACC = 0.727), Model 9 (AC = 0.848, ACC = 0.788), Model 10 (AC = 0.829, ACC = 0.727), and 10 Average of models generated based on TPOT (AC = 0.848, ACC = 0.736). Among them, according to the accuracy in the test set, Model 5 was selected as it showed the best classification performance. Figures 5B,C show the average accuracy (AP) and the area under the curve (AUC) for the 10 models in the test set. The parameters of Model 5 are as follows: Model [5] = make_pipeline [binarizer (threshold = 0.3), OneHotEncoder (minimum_fraction = 0.15, sparse = false, threshold = 10], GradientBoostingClassifier [the learning_rate = 0.5, max_depth = 8, max_features = 0.3, min_samples_leaf = 1, min_samples_split = 3, n_estimators = 1t00, subsample = 0.95)]. In this model, Binarizer and OneHotEncoder were used to process the radiomics features (see Supplementary Table 4 for detailed parameter descriptions of the other nine models).

## The six RBP genes are associated with ischemic stroke, dementia, and aging

In order to examine the potential role of RBPS genes in ischemic stroke, RNA transcripts from peripheral blood samples of 39 patients with ischemic stroke and 24 healthy controls were analyzed. The six RBP genes included in the RBPS could distinguish IS from the healthy control group (Figure 6A, AUC = 0.950). Differentially expressed analysis showed that *POLR2F*, *BRCA1*, and *TRIM21* in this RBPS were associated with ischemic stroke. Among them, *TRIM21* and *BRCA1* were upregulated, while *POLR2F* was downregulated in IS (Figure 6B). GSEA showed that the upregulation of *TRIM21* was significantly related to upregulated pathways, including (REACTOME) response to elevated platelet cytosolic $Ca^{2+}$, (REACTOME) cellular response to hypoxia, (KEGG) complex and coagulation cascades, and (KEGG) focal adhesion (Figure 6C). In *BRCA1*-upregulated samples, (REACTOME) oncogenic MAPK signaling, (REACTOME) platelet activation

10.3389/fnagi.2022.951197

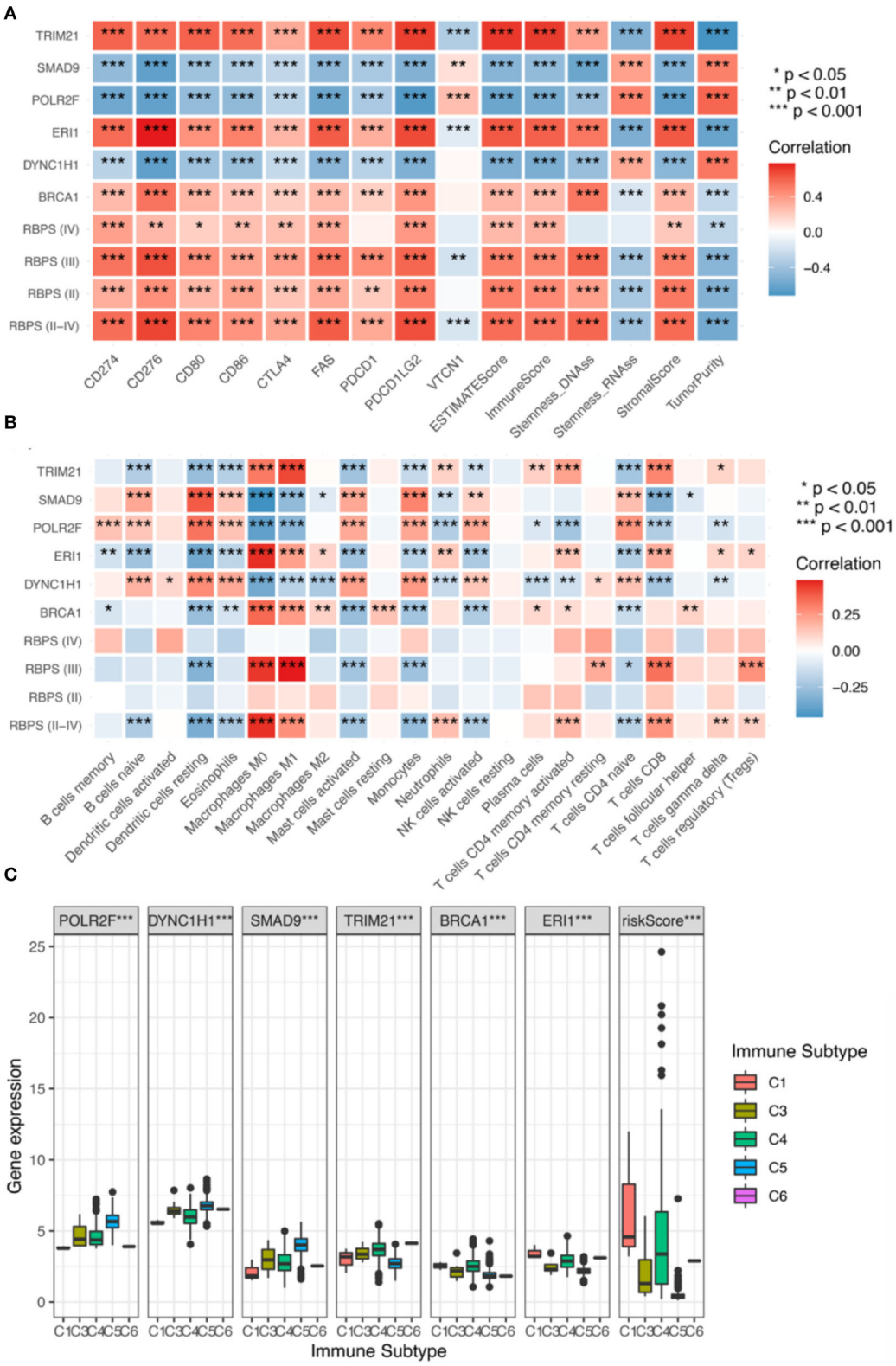


FIGURE 4
**(A)** Correlation analysis for the expression of the six RBPs and the RBPS with stemness (RNAss and DNAss), TME (the stromal score, the immune score, the ESTIMATE score, and tumor purity), and immune checkpoints (*CD274*, *CD276*, *CD80*, *CD86*, *CTLA4*, *PDCD1*, *PDCD1LG2*, and *VTCN1*). Correlation analysis of RBPS for Grades II, III, and IV glioma, respectively; red: positive correlation and blue: negative correlation. Relationship of the expressions of the six RBP genes (*POLR2F*, *DYNC1H1*, *SMAD9*, *TRIM21*, *BRCA1*, and *ERI1*) and RBPS with **(B)** infiltration of eight types of immune cells (B cells, $CD8^+$ T cells, $CD4^+$ T cells, NK cells, monocytes, macrophages, dendritic cells, neutrophils), and **(C)** immune subtypes in TCGA.

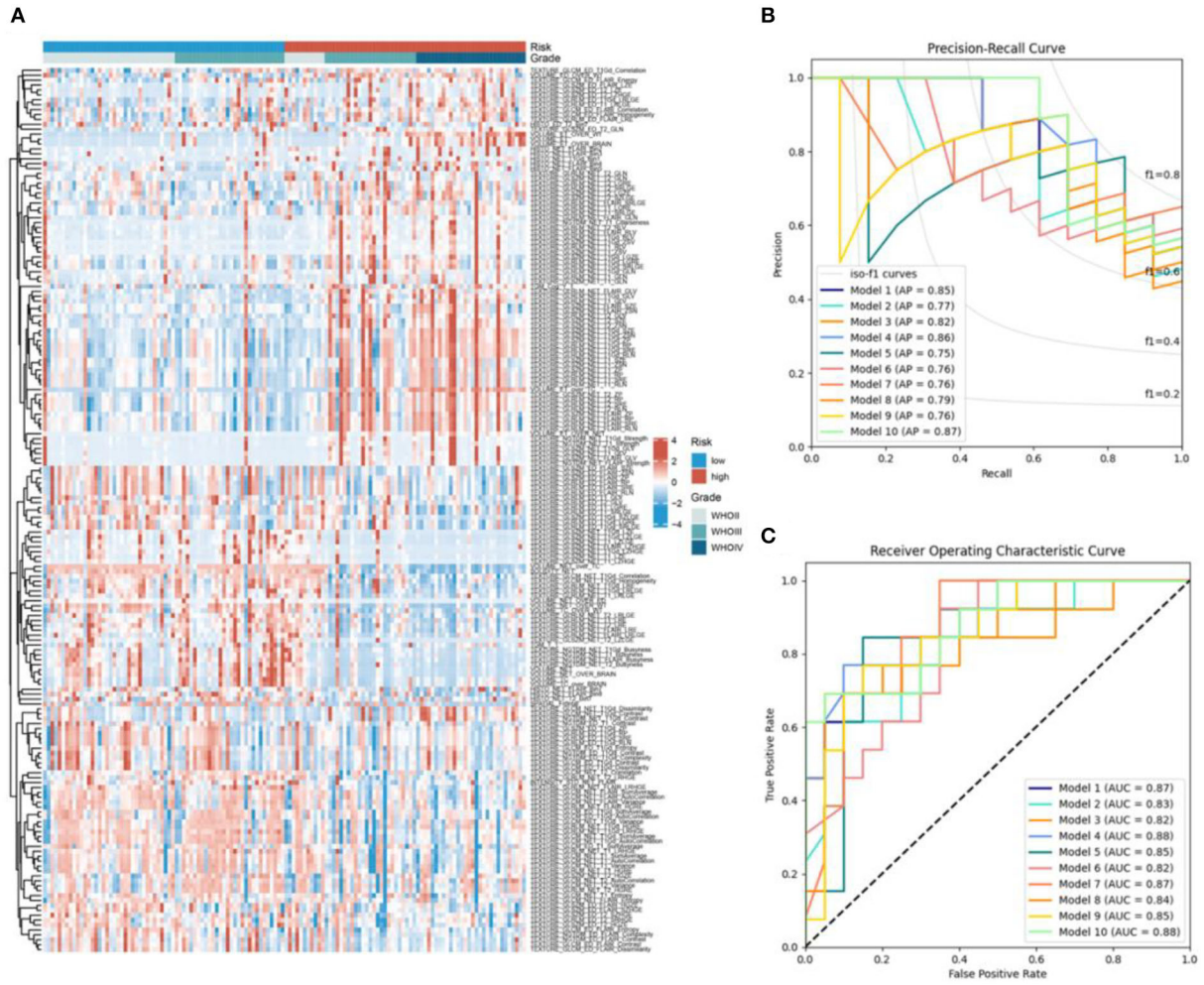


FIGURE 5
**(A)** The heatmap of the 180 radiomics features between the high- and low-RBPS-risk-score samples. **(B)** Receiver operating characteristic curves and **(C)** precision-recall curves for 10 models based on the testing set. AP, average precision; AUC, area under the curve.

signaling and aggregation, (WP) angiogenesis, and the (PID) VEGFR1 and VEGFR2 pathway were upregulated, while the (REACTOME) respiratory electron transport pathway was downregulated significantly (Figure 6D). In *POLR2F*-upregulated samples, (REACTOME) response to elevated platelet cytosolic $Ca^{2+}$, (KEGG) complement and coagulation cascades, and (KEGG) focal adhesion pathways were downregulated, while (REACTOME) cellular response to hypoxia was upregulated (Figure 6E). In IS, the upregulation of *TRIM21* was related to platelet function activation, increased coagulation, and response to hypoxia. Upregulation of *BRCA1* was related to tumor progression, platelet activation, and angiogenesis. The downregulation of *POLR2F* was accompanied by an upregulation of platelet reaction and coagulation, and downregulation of hypoxia-related response.

Further analyses revealed that *SMAD9* in the RBPS was associated with the Alzheimer's disease onset (Figure 6F). In addition, aging was positively associated with *ERI1* expression and negatively with *POLR2F* expression (Figure 6G).

## Cell clustering shows the highest proportion of microglia and astrocytes

First, quality control for single-cell RNA-seq (scRNA-seq) data (Supplementary Figures 6A–G) was performed according to cell characteristic distributions and preset quality filtering conditions. UMAP showed no significant batch effects

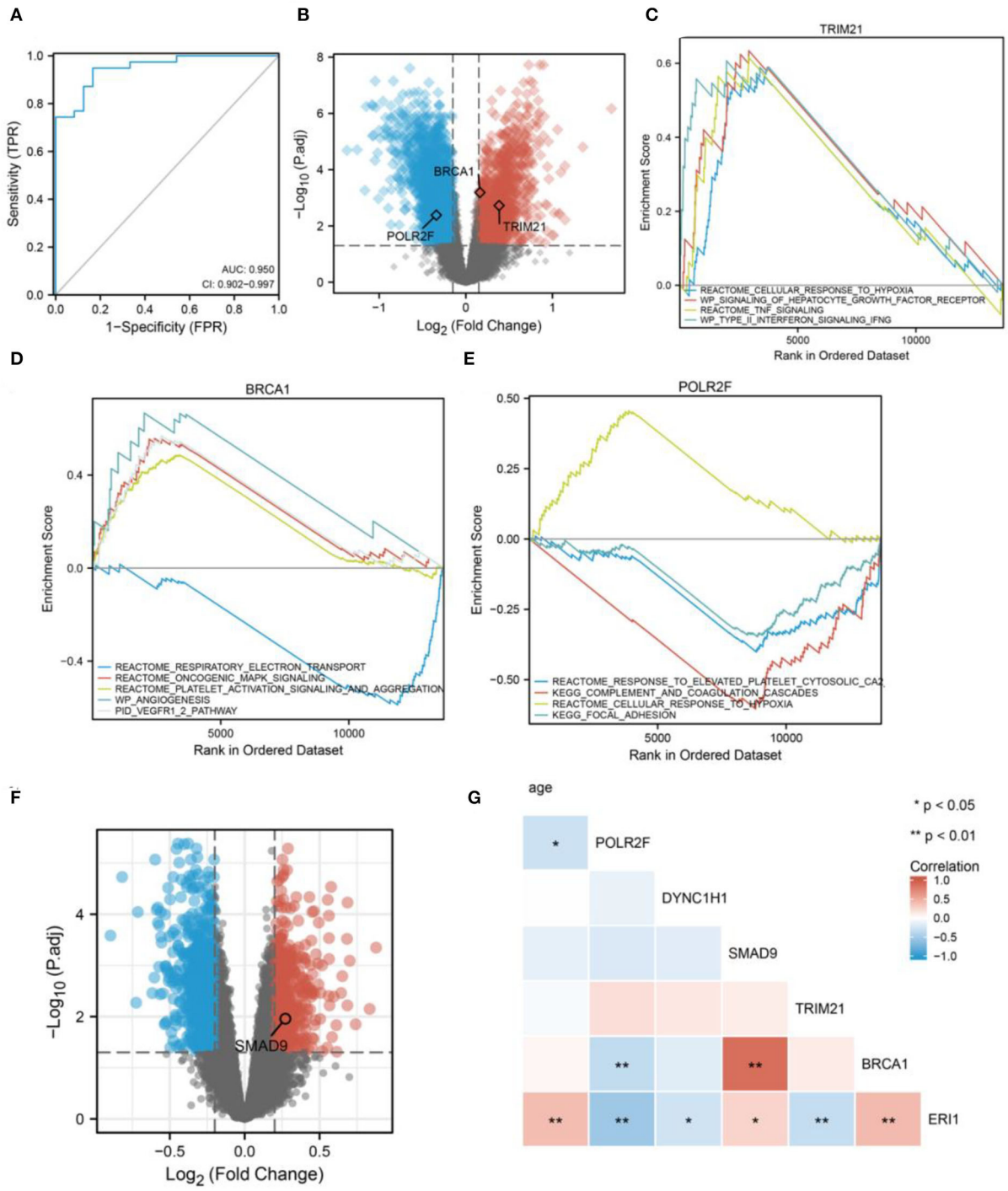


FIGURE 6
Diagnostic efficacy of the six RBP genes for IS. **(A)** Diagnostic efficacy of the six RBP genes for IS using blood samples (AUC = 0.950, 95% CI: 0.902–0.994). **(B)** The volcano plot shows the DERBPs associated with IS. GSEA for **(C)** *TRIM21*, **(D)** *BRCA1*, and **(E)** *POLR2F* in IS. **(F)** The volcano plot shows *SMAD9* is associated with dementia. **(G)** The correlation heatmap shows that aging correlates with *POLR2F* and *ERI1* expression.

for cells between the two groups after integration analysis (Supplementary Figure 6H). By clustering, 16 cell clusters were finally identified, and 11 cell types were annotated (Figures 7A–C; Supplementary Figures 6I, 7). Among them, microglia and astrocytes had the highest proportion (Figure 7D).

10.3389/fnagi.2022.951197

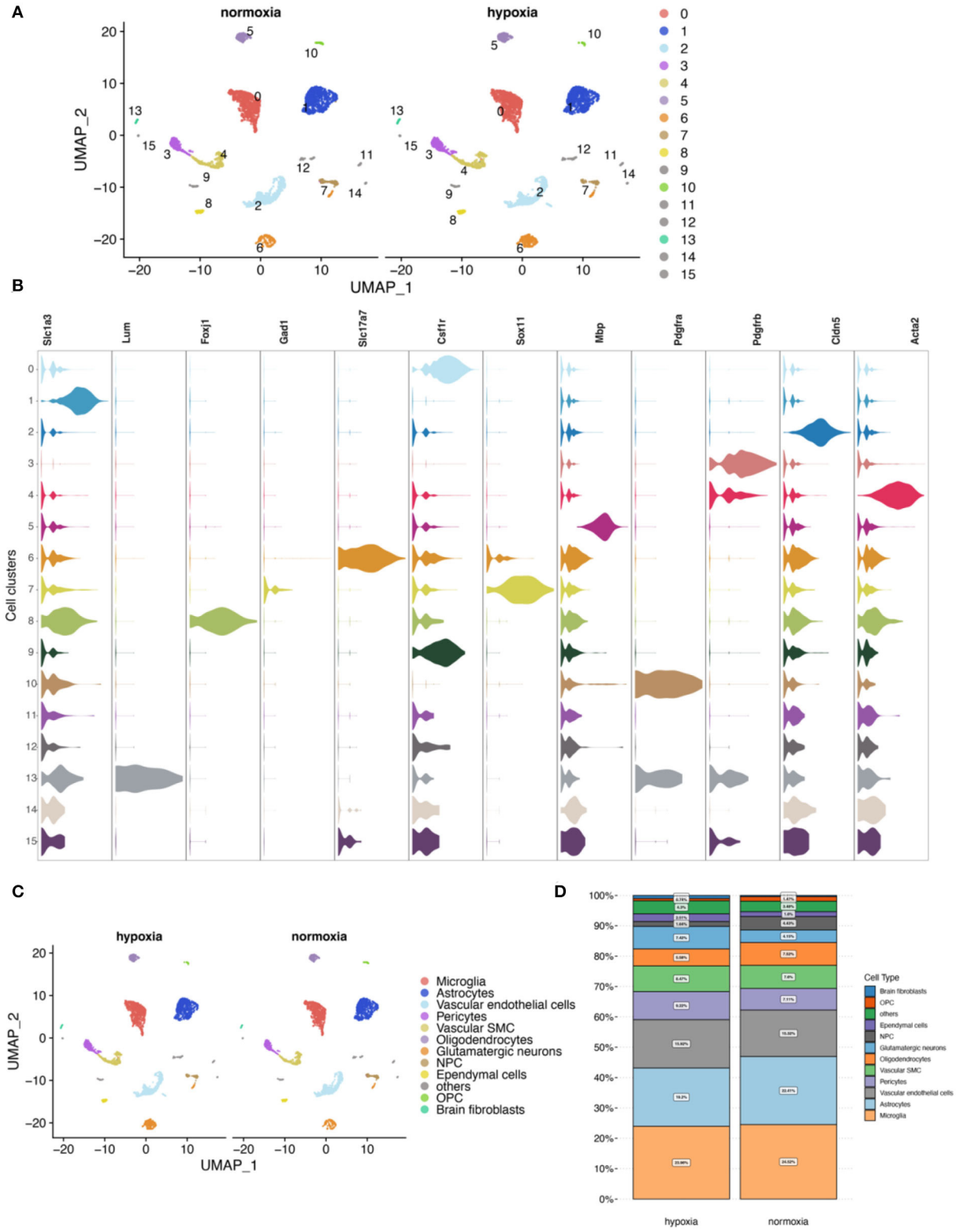


FIGURE 7
Cell clustering and annotation for the mouse cerebral cortex. **(A)** Single-cell analysis shows 16 cell clusters in hypoxic and normoxic conditions. **(B)** Expression of marker genes for cell annotation between the cell clusters. **(C)** Cell annotation results show 11 cell types. **(D)** Comparison of proportions of cells between the normoxia and the hypoxia groups.

## RBPS-related genes associated with pseudotime in microglia

Pseudotime analysis showed three main cell stages of microglia at normal- and low-oxygen concentrations (Figures 8A,B, Supplementary Figure 8). In microglia, *Sox4* and *Tcf7l2*, which regulated *Brca1*, and *Irf5*, which regulated *Trim21*, were significantly related to the pseudotime of these cells (Figures 8C,D). The expression of transcription factors and RBPs in microglia during the transition from hypoxia to normal oxygen concentrations (Figures 8A,E) were observed using the pseudotime distribution plot. *Sox4*, *Irf5,* and *Tcf7l2* were downregulated at the early stages of pseudotime but upregulated at normal-oxygen concentrations. These results suggested that *Sox4* and *Tcf7l2*, which regulated *Brca1*, and *Irf5*, which regulated *Trim21*, may change under hypoxia, thus participating in cellular phenotypic changes.

## RBPS-related genes associated with pseudotime in astrocytes

Pseudotime analysis showed that astrocytes went through eight major cell stages in normal-oxygen concentration and hypoxia conditions (Figures 9A,B; Supplementary Figure 9). According to SCENIC analysis, a regulatory relationship between *Tcf7l2* and *Brca1* was observed (Figure 9C). In astrocytes, *Tcf7l2* was an important pseudotime-related gene (Figure 9D). In addition, from the pseudotime distribution map, astrocytes were found in the early, middle, and late pseudotime stages in the normal oxygen concentration group, while, in the hypoxia group, astrocytes were dominant in the middle stage and lesser in the early and late stages; *Tcf7l2* increased in the early stages and decreased toward the later stage (Figures 9A,E). These results suggested that (*Brca1*-related) *Tcf712* may play a role in the transition to a hypoxic environment.

## RBPS-related genes associated with pseudotime in pericytes

Pseudotime analysis showed that pericytes went through six cell stages (Figures 10A,B; Supplementary Figure 10) in normal oxygen concentration and hypoxia conditions. According to the prediction of the gene regulatory network by SCENIC analysis, a regulatory relationship between *Taf7* and *Trim21* was obtained (Figure 10C). In astrocytes, *Taf7* was an important pseudotime-related gene (Figure 10D). In addition, as shown in the pseudotime distribution plot, pericytes were obviously stagnating in the early pseudotime stages under hypoxia (Figure 10A). *Taf7* increased at an early stage of pseudotime but decreased toward the end stage; pericytes under hypoxia were mostly dominant in the early stage of pseudotime (Figure 10E). These results suggested that *Taf7* may play an important role in cell-state transition between hypoxia and normal oxygen conditions.

## Pseudotime-related regulons

SCENIC analysis was performed for single-cell data to identify important regulons of each cell subtype. In the SCENIC analysis flow, UMAP and tSNE showed single-cell dimension reduction results and the distributions for each cell type (Supplementary Figure 11). Figures 11A–C show the distribution of microglia, astrocytes, and pericytes under normal- and low-oxygen conditions. Irf5 was an essential and specific regulon of microglia in the normal oxygen and hypoxia concentration groups (Figures 11D,G,J). The RSS and rank of Tcf7l2 were related to oxygen concentration. The rank of Tcf7l2 in the normoxia group was higher than that in the hypoxic group (Figures 11E,H,K). The Taf7 regulon played a regulatory role in many other cells apart from pericytes (Figures 11F,I,L).

# Discussion

The RBP family of proteins plays an important regulatory role in glioma and IS (Shao et al., 2013; Zhou et al., 2014; Barbagallo et al., 2018; Lan et al., 2020; Si et al., 2020; Zhang et al., 2020; Sharma et al., 2021); however, there is a lack of a systematic analysis of the role of RBP in both these diseases. Herein, we describe a set of previously unreported six RBP genes that can be used to predict the prognosis of glioma and diagnostic classification for IS. In particular, we found that the RBPS was associated with tumor immunosuppression in glioma and hypoxia and coagulation in IS. In addition, automatic machine learning was used to predict the risk stratification based on RBPS in glioma. In this RBPS, *SMAD9* was found to be associated with dementia; *POLR2F* and *ERI1* were identified to be associated with aging. In view of hypoxia as the basis of common models for studying glioma and IS, the expressions of these six RBP genes in microglia, astrocytes, and pericytes, along with their gene regulatory networks, were analyzed using single-cell data from the mouse cerebral cortex. The six RBP genes and the transcription factors in their gene regulatory networks were analyzed using pseudotime analyses between normal oxygen and hypoxia conditions. *Irf5*/*Trim21* and *Tcf712*/*Brca1* in microglia, *Tcf712*/*Brca1* in astrocytes, and *Taf7*/*Trim21* in pericytes were identified as RBPS-related genes that were regulated in response to hypoxia. These new findings indicated that RBPs, post-transcriptional regulators, are essential regulatory molecules involved in the underlying common pathways in the development of glioma and IS.

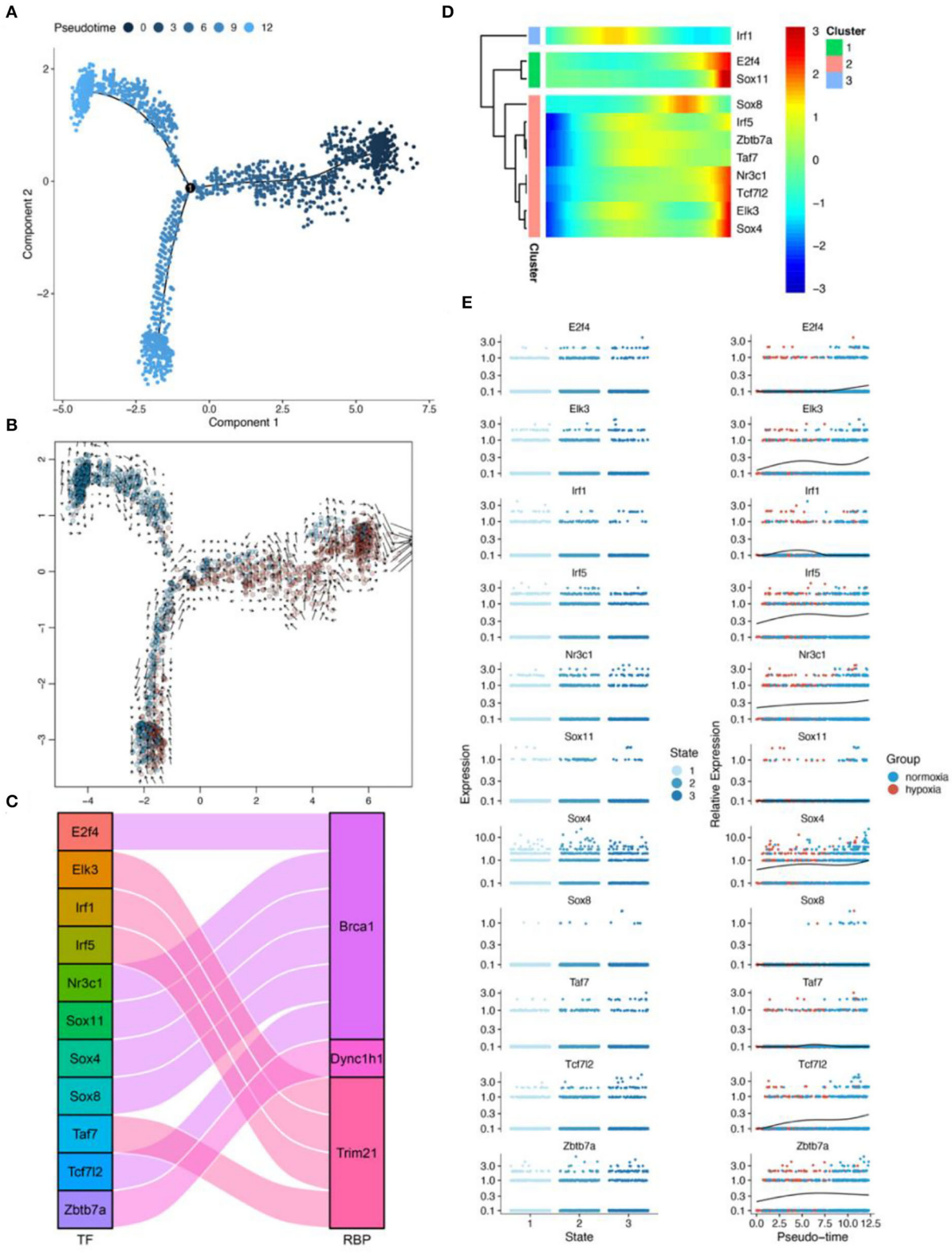


FIGURE 8
Results of pseudotime analysis for microglia. **(A)** The pseudotime distribution plot of microglia. **(B)** The RNA velocity plot; the longer is the arrow, the stronger is the transcriptional activity. **(C)** The Sankey diagram shows the RBPS-related transcription factors (*E2f4*, *Elk3*, *Irf1*, *Irf5*, *Nr3c1*, *Sox11*, *Sox4*, *Sox8*, *Taf7*, *Tcf712*, and *Zbtb7a*), which are associated with the pseudotime. **(D,E)** Changes in the expression of these RBPS-related transcription factors with changes in pseudotime.

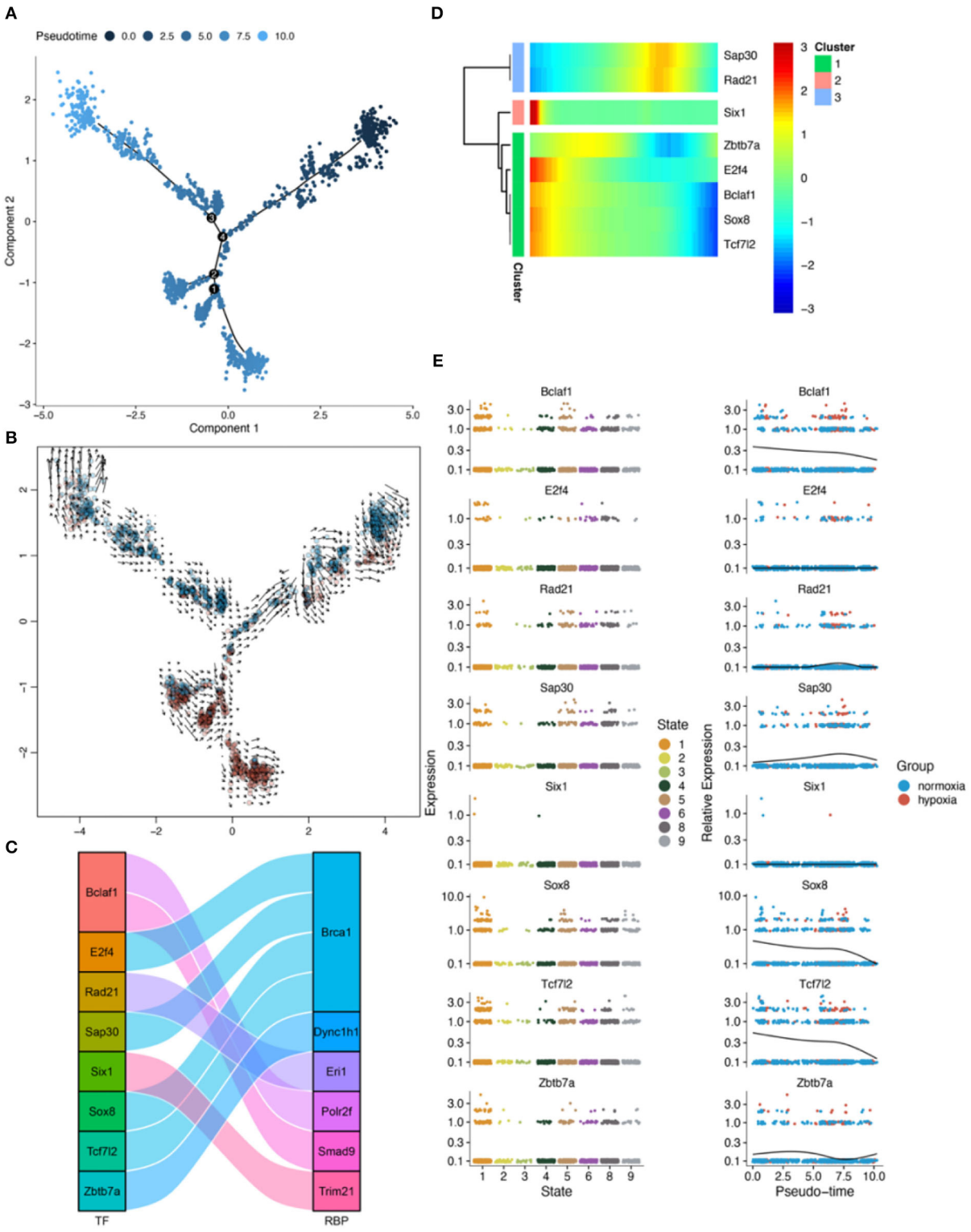


FIGURE 9
Results of pseudotime analysis for astrocytes. **(A)** The pseudotime distribution plot of astrocytes. **(B)** The RNA velocity plot, wherein the longer the arrow, the stronger the transcriptional activity. **(C)** The Sankey diagram shows the RBPS-related transcription factors (*Bclaf1*, *E2f4*, *Rad21*, *Sap30*, *Six1*, *Sox8*, *Tcf712*, and *Zbtb7a*), which are associated with the pseudotime. **(D,E)** Changes in the expression of these RBPS-related transcription factors with changes in pseudotime.

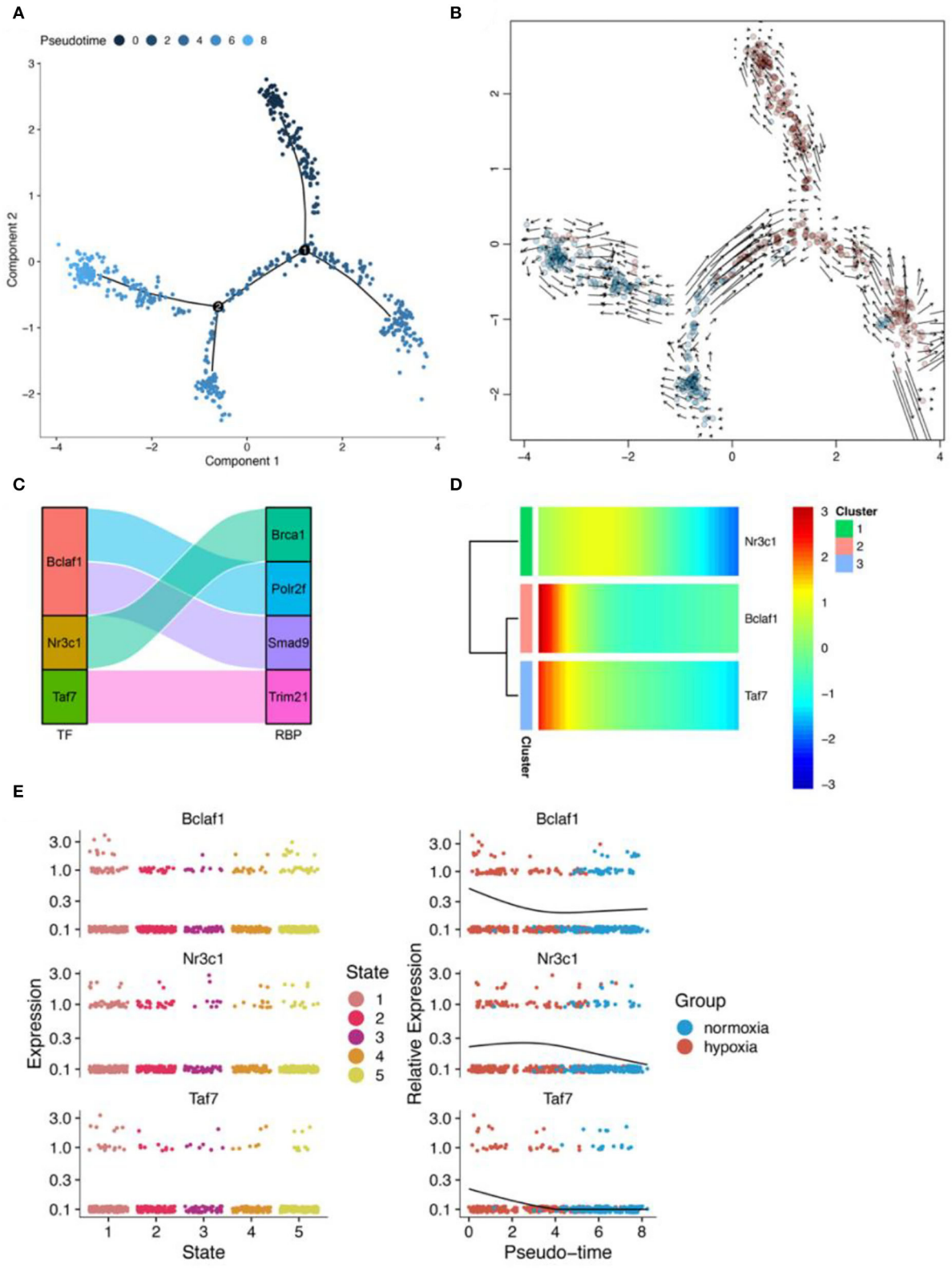


FIGURE 10
Results of pseudotime analysis for pericytes. **(A)** The pseudotime distribution plot of pericytes. **(B)** The RNA velocity plot, wherein the longer the arrow, the stronger is the transcriptional activity. **(C)** The Sankey diagram shows the RBPS-related transcription factors (Bclaf1, Nr3c1, Taf7), which are associated with the pseudotime. **(D,E)** Changes in the expression of these RBPS-related transcription factors with changes in pseudotime.

10.3389/fnagi.2022.951197

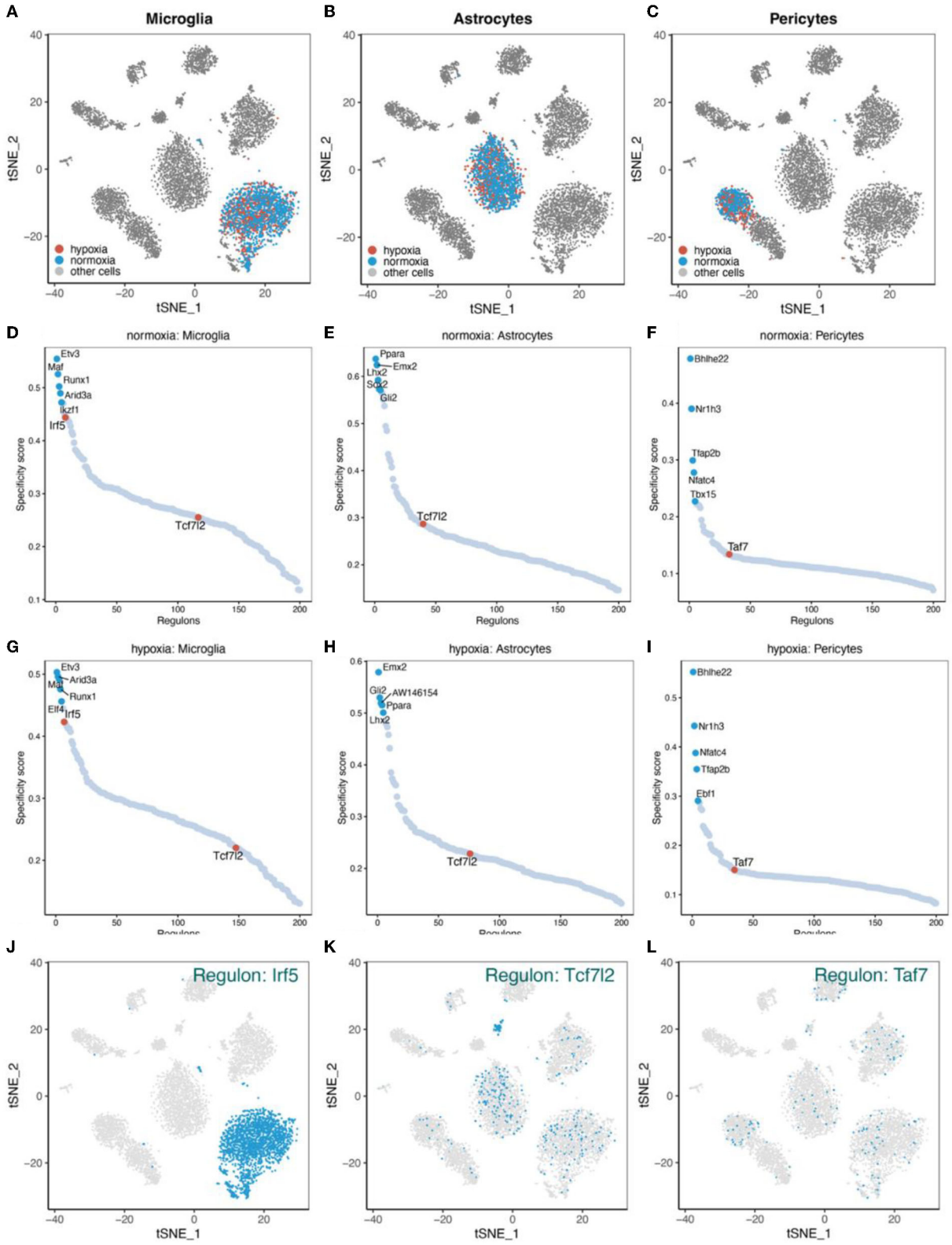


FIGURE 11
Major regulons in microglia, astrocytes, and pericytes. **(A–C)** tSNE shows the distribution of microglia, astrocytes, and pericytes. **(D–F)** Major gene regulatory networks in the three types of cells under normoxia condition, wherein red dots represent the gene regulatory networks regulated by corresponding transcription factor related to the RBPS. **(G–I)** Major gene regulatory networks in the three types of cells under hypoxia condition. **(J–L)** Distribution of regulons associated with the RBPS in cells.

## Significance of identification of molecular markers for glioma

Glioma is the most common primary intracranial tumor with high mortality, among which glioblastoma is the most malignant type (Liu et al., 2020). According to molecular genetic characteristics, some important glioma subtypes, including IDH mutation, TERT promoter, and 1p/19q codeletion, improve the therapeutic efficacy for glioma (Wang et al., 2020). It is worth trying to identify biomarkers that are robust and can guide the treatment and predict a prognosis so as to stratify the patients according to the risk and help choose appropriate treatment methods.

## Role of RBP in tumors

Previous studies have shown that RBP plays a vital role in tumor progression. For example, in the progression of HCC, global changes in RBP are more evident than those of transcription factors (Dang et al., 2017). In immunity, RBP CAPRIN1 promotes innate immunity mediated by IFN-γ-STAT1 by stabilizing the Stat1 mRNA (Xu H. et al., 2019). In addition, some studies suggest that the genetic system of RBP dysfunction can provide methods for describing different immunological conditions (Kafasla et al., 2014). In AML, the effects of RBM39 deletion on splicing further lead to preferential lethality for AML with spliceosome mutations, which provides a strategy for the treatment of those carrying RBP-splicing mutations (Wang E. et al., 2019; Villanueva et al., 2020). In glioma, although some studies report several RBPs related to a poor prognosis of these patients (Boucas et al., 2015; Bhargava et al., 2017; Barbagallo et al., 2018; Velasco et al., 2019; Wang J. et al., 2019; Lan et al., 2020; Wang et al., 2020), their potential clinical application, including for an individual prognostic risk assessment, lacks systematic evaluation. In the research on RBPs, some new technologies have been developed to enrich and extract RBPs and their homologous RNAs, such as the orthogonal organic phase separation (OOPS) (Villanueva et al., 2020), which is a fast, efficient, and reproducible method to purify cross-linked RNA-protein complexes in an unbiased manner, thus making it more efficient for identifying and studying new RBPs. Taken together, we first developed a risk stratification gene signature based on RBP gene expression profiles and an automatic machine learning prediction model based on radiomics for individualized risk assessment of patients with glioma. Below, we discuss the roles of these core RBPs in glioma genesis.

## Identification of RBPS and the role of the six RBP genes in glioma

First, six prognostic-related RBP genes (*POLR2F*, *DYNC1H1*, *SMAD9*, *TRIM21*, *BRCA1*, and *ERI1*) were obtained from the TCGA-glioma dataset. Based on these six RBP genes, a 6-RBP gene signature (RBPS) with risk stratification characteristics was constructed. Among them, *POLR2F*, *DYNC1H1*, and *SMAD9* in tumor tissues of patients with glioma were downregulated as compared to normal tissues adjacent to cancer, while *TRIM21*, *BRCA1*, and *ERI1* were upregulated. In literature, only *BRCA1*, *TRIM21*, and *POLR2F* have been implicated in the progression of glioma (Rasmussen et al., 2016; Yang et al., 2020; Zhao et al., 2020). Breast cancer susceptibility gene (*BRCA*) mutations, including *BRCA1*, are found in several tumors (Sun et al., 2020). Umphlett et al. (2020) reported a case of a patient with GBM with extensive metastases, whereby *BRCA1* (p.I571T) was considered the possible driving mutation. Through bioinformatics analyses based on the GSE53733 dataset, Yang et al. (2020) report that *POLR2F* is one of the four potential key genes that affect the OS in GBM. Higher levels of *TRIM21* expression are associated with a poor prognosis of glioma and promote proliferation, drug resistance, and migration of glioma cells (Zhao et al., 2020). *SMAD9* mutations have been reported in the progression of gastrointestinal ganglioma. In addition, a low expression of SMAD9 is related to a poor OS in lung adenocarcinoma (Ngeow et al., 2015; Zhai et al., 2021). The microtubule motor protein encoded by *DYNC1H1* is involved in many cellular processes, such as mitosis and intracellular transport. *DYNC1H1* mutations have been implicated in nervous system diseases (Hoang et al., 2017) and pancreatic cancer (Furukawa et al., 2011), and these mutations are consistent with a high immune activity of tumor mutation load in various cancer types (Bai et al., 2020). In addition, *DYC1H1* is upregulated in gastric cancer (Gong et al., 2019) and downregulated in primary gallbladder carcinoma (Huang et al., 2014). In mice, Eri1 is a histone mRNA-related protein involved in RNA metabolism pathways and various cellular processes regulated by RNA (Thomas et al., 2014). Declercq et al. (2020) show that the exogenous nuclease, ERI1, interacts with PB2, PB1, and NP components of the viral ribonucleoprotein, thus promoting viral transcription. Previous studies have reported that gene copy number variations in glioma may lead to changes in RBP gene expression (Bhargava et al., 2017), which was also observed in this study. In addition, in tumor stemness, RBPS was positively correlated with DNAss but negatively correlated with RNAss. For results of RBP genes and tumor stemness, we speculated that, due to the characteristics of post-transcriptional regulation of RBPs, the correlations of DNAss and RNAss with RBP would be different, and the underlying mechanism needs to be elucidated in the future.

## A high risk of RBPS in glioma is related to immunosuppression

GSEA showed differences in immune-related functional pathways between high- and low-RBPS-risk-score groups. By evaluating the relationship between RBPS and immune-related characteristics, it was possible to improve the understanding of the anti-tumor immune intervention and highlight feasible immunotherapeutic strategies. Therefore, the associations of RBPS with the tumor microenvironment, immune subtypes, immune cell types, and immune checkpoint molecules were further analyzed. Xu et al. (2021) report that higher stromal and immune scores predict a poor prognosis in patients with LGG. In LGG and GBM of this study, gliomas with higher RBPS risk are related to higher immune and stromal scores, thus indicating that the RBPS index was related to immune responses in gliomas. A previous study reports that macrophage infiltration indicates a worse OS in GBM (Iglesia et al., 2016). Differentiated GBM cells promote GSC-dependent tumor progression by enhancing macrophage infiltration into tumor tissues (Uneda et al., 2021). RBPS also showed a positive correlation with the proportion of infiltrated macrophages in the tumor, which indicated that RBPS may play a potential role in the involvement of macrophage infiltration in the development of glioma. Conventional type-1 dendritic cells (cDC1) play an important role in immunotherapy-mediated reactivation of tumor-specific $CD8^+$ T cells to promote tumor regression (Liang et al., 2021). In this study, RBPS was negatively correlated with dendritic cell infiltration and positively correlated with $CD8^+$ T cells, which implied that, in gliomas with a high RBPS risk, a complete $CD8^+$ T cell reactivation for immunotherapy may be difficult due to the lack of dendritic cells, thus making the anti-tumor effects difficult to be achieved. Due to several reasons, including inherent challenges in drug application, a unique immune environment of the brain, and heterogeneity between and within tumors, immune checkpoint blockade therapy has not been effective for GBM (Khasraw et al., 2020). A comprehensive understanding of the unique tumor microenvironment of the brain is important for glioma immunotherapy with immune checkpoint blockade (Qi et al., 2020). In this study, RBPS was positively correlated with the expressions of *CD274*, *CD276*, *CD80*, *CD86*, *CTLA4*, *FAS*, *PD1*, and *PDL1* in gliomas, indicating that the expressions of immune checkpoint-related genes increased with a high RBPS risk, thus leading to a worse prognosis. The relationship between RBPS and immune checkpoint molecules needs further studies.

## Automatic machine learning model predicts RBPS

Generally, the RBPS showed reliable prognostic value for predicting the OS and immune-related characteristics of glioma and comprised only six RBP genes, making its clinical translation convenient. Recently, with the development of computing power, researchers have tried to replace some expensive molecular detection techniques using MR image-based artificial intelligence so as to stratify the risk of tumor phenotypes, screen patients with cancer, and predict their responsiveness to treatment (Acs et al., 2020). Therefore, using MRI-based radiomics features, we developed an automatic machine learning classification model to predict the risk of RBPS in glioma, thus making the molecular signature more convenient and attractive for preoperative evaluation.

## Diagnostic performance and the roles of the six RBP genes in IS

The prediction model based on the six RBP genes from blood samples could also predict the occurrence of IS, suggesting their association with IS. Among the six RBP genes, *TRIM21* and *BRCA1* were upregulated in IS, while *POLR2F* was downregulated in IS. Functional pathway enrichment analysis showed that *TRIM21* upregulation was related to platelet activation, enhanced coagulation, and response to hypoxia. Previous studies have shown that *TRIM21* is mainly expressed in hematopoietic cells, wherein it is induced by IFNs in case of infections and autoimmune diseases (Sjöstrand et al., 2013). Pan et al. (2016) show that TRIM21 modulates redox homeostasis through the ubiquitination of p62, and *TRIM21*-deficient cells exhibit enhanced antioxidant responses and reduced cell death under oxidative stress. In addition, TRIM21 deficiency induces naive T cells to differentiate into Th17 and promotes IL-17 expression, along with a stable atherosclerotic plaques phenotype formation (Brauner et al., 2018). In cerebral ischemia/reperfusion (I/R), BRCA1 overexpression can alleviate or prevent nerve injury caused by I/R due to reduced production of reactive oxygen species (ROS) and lipid peroxidation (Xu et al., 2018). Overexpression of BRCA1 in neural stem cells (NSCs) reduces apoptosis and oxidative stress after the oxygen-glucose deprivation/reoxygenation (OGD/R) insert, stimulating their proliferation, thus improving the therapeutic effects of NSC transplantation in cases of ischemic stroke (Xu P. et al., 2019). Genome-wide association analysis shows that *POLR2F* (22q13.1) is associated with periventricular white matter hyperintensions (PVWMH), and PVWMH are associated with ischemic stroke (Armstrong et al., 2020).

## Dual action of ROS under hypoxia

In the cerebrovascular unit, hypoxia can induce astrocytes, microglia, pericytes, and neuronal cells to produce ROS and reactive nitrogen species (RNS) (Sumbayev and Yasinska, 2007; Chen et al., 2013). ROS and RNS play dual roles in the

neurovascular unit, destroying tissues and macromolecules upon injury (global cerebral ischemia and reperfusion injury) while promoting cellular proliferation, tissue repair and regeneration, and angiogenesis in the recovery stage (acute ischemic stroke and hypoxic tumor core) (Kalogeris et al., 2014).

## The role of hypoxic stress in tumor immunity and angiogenesis

In tumors, hypoxic stress plays an important role in tumor progression and immune escape by controlling angiogenesis, promoting immunosuppression, and tumor resistance (Noman et al., 2015). Several hypoxia-induced immunosuppressive cells in the hypoxic zones of solid tumors, such as myeloid-derived suppressor cells, tumor-associated macrophages (MDSCs), and T-regulatory (Treg) cells, have been reported (Mantovani et al., 2002; Ohta et al., 2011). Hypoxia increases MDSC-mediated T cell tolerance by upregulating the tumoral MDSC expression of PD-L1 (Noman et al., 2014); hypoxia-inducible factor-1 (HIF-1) is the primary regulator of PD-L1 (Barsoum et al., 2014). Hypoxia decreases the expression of several molecular markers of differentiation and maturation of DCs in response to lipopolysaccharide and inhibits the stimulating ability of DCs to activate T cell functions (Mancino et al., 2008). In addition, VEGF produced by human tumors can inhibit the functional maturation of DCs and promote the escape of tumor cells (Gabrilovich et al., 1996). Hypoxic stress increases the lytic functions of $CD8^+$ T cells and decreases their proliferation and differentiation (Noman et al., 2015). Hypoxia attracts Treg cells to the tumor bed by affecting the distribution of cytokines in the tumor microenvironment and enhancing the immunosuppressive functions of Treg cells (Noman et al., 2015). For cancer stem cells (CSCs), hypoxia and HIFs are considered to induce tumor cells to dedifferentiate into immature phenotypes and maintain their stemness (Kallergi et al., 2009; Semenza, 2012). In this study, RBPS in glioma was related to tumor immunosuppression. Glucose and amino acid metabolism increased in gliomas with a high RBPS risk score. This may serve the increased demand for energy and oxygen of highly proliferating tumor masses. In addition, among these six RBP genes, the upregulation of *TRIM21* and *BRCA1* in IS was related to angiogenesis and responses to hypoxia. The upregulation of *TRIM21* and *BRCA1* and the downregulation of *POLR2F* were related to platelet activation and increased coagulation, thus suggesting that an imbalance among these genes may result in a state of hypercoagulation, which could easily lead to an ischemic cerebral infarction. Along with aging, *POLR2F* was downregulated, while *ERI1* was upregulated. In IS, downregulated *POLR2F* was associated with downregulation of pathways in response to hypoxic responses, implying that *POLR2F* may be associated with aging-related hypoxic stress.

Astrocytes, microglia, and pericytes are important cells that maintain brain homeostasis. In order to observe the regulation and potential mechanism underlying the six RBP genes in the hypoxic environment at the cellular level, the gene regulatory network in various cell types was investigated.

## Gene regulatory networks in astrocytes

Astrocytes are the most abundant cell types in the central nervous system. As an integral part of the neuron-glial system, astrocytes serve as housekeeping functions, including the formation of the blood-brain barrier (BBB), regulation of cerebral blood flow, repair of blood vessels (Williamson et al., 2021), and the resistance to oxidative stress (Blanc et al., 1998; Ransom and Ransom, 2012). After an ischemic stroke, reactive astrogliosis involving astrocytes exerts harmful and beneficial effects on neuronal survival and nerve recovery (Liu and Chopp, 2016; Xu et al., 2020). The upregulation of *BRCA1* in IS was related to tumor promotion, platelet activation, and angiogenesis. On examining the gene regulatory network in astrocytes, *Brca1* was identified in Tcf712 regulon that was upregulated under hypoxia. These results suggested that *Tcf712*/*Brca1* may play an important role in the response of astrocytes to hypoxic stress.

## Gene regulatory networks and immune responses of microglia

As resident macrophages in the central nervous system, microglia are the first immune cells that perceive and respond immediately during cerebral ischemia (Lambertsen et al., 2019). During a stroke, with the dynamic changes in pathology, microglia undergo polarization (Tsuyama et al., 2018). According to the phenotypic changes in microglia, they can be roughly classified into pro-inflammatory (M1) or anti-inflammatory (M2) types (Ransohoff, 2016). The interferon regulatory factor (IRF) family of proteins has an important relationship with microglial polarization after stroke (Zhao et al., 2017; Al Mamun et al., 2018). For instance, IRF4 negatively regulates inflammation and promotes M2 polarization of macrophages (Eguchi et al., 2013), while IRF5 induces M1 polarization (Paun et al., 2008). Recent studies have shown that the IRF5-IRF4 regulatory axis in microglia regulates neuroinflammation after ischemic stroke and affects stroke outcomes (Al Mamun et al., 2020). IRF5 mediates pro-inflammatory activation of microglia and affects anti-inflammatory responses (Fan et al., 2020; Al Mamun et al., 2021). We found that Irf5 regulon was an important regulator in microglia, and *Trim21* was a downstream molecule in this gene regulatory network. The expression of *Irf5* was

downregulated under hypoxia, which may be related to the time of experimental conditions, suggesting that the main microglia types may be changing toward the anti-inflammatory phenotype after living in 7.5% oxygen concentration for 7 days. The Tcf712 regulon was another important gene regulatory network identified in microglia, and Brca1 was a member of this network. The expression of *Tcf712* was also downregulated under hypoxia.

### Multiple microvascular regulatory functions of pericytes

Pericytes play an important role in regulating various microvascular functions, such as angiogenesis (Winkler et al., 2011), the formation and maintenance of the BBB (Armulik et al., 2010; Daneman et al., 2010), capillary blood flow regulation (Hall et al., 2014; Korte et al., 2022), neuroinflammatory regulation (Stark et al., 2013; Korte et al., 2022), glial plaque formation (Göritz et al., 2011), and stem cell characterization (Özen et al., 2014; Nakagomi et al., 2015). Pericytes are important therapeutic targets in stroke, glioma, Alzheimer's disease, spinal cord injury, and other diseases due to their vital role in the nervous system diseases (Cheng et al., 2018). Variable permeability of BBB can be observed in the high cell proliferation regions, which may be related to an increase in the NG2-expressing pericytes herein (Jackson et al., 2017). In addition, hypoxic regions of tumors recruit activated pericytes through the regulation of hypoxia-inducible factors (Svensson et al., 2015). In acute ischemic stroke, pericyte HIF-1 can destroy BBB and affect the prognosis of stroke (Tsao et al., 2021). In addition, glioma stem cells can also differentiate into pericytes, thus supporting BBB integrity and angiogenesis (Cheng et al., 2013; Segura-Collar et al., 2021). Under hypoxia, *in vitro*, pericytes derived from the human brain acquire a microglial phenotype and are a new source of inflammatory cells during cerebral ischemia (Özen et al., 2014). Interestingly, *Trim21* (Irf5 and Taf7 regulon) is present in different gene regulatory networks of microglia and pericytes in response to hypoxia. This suggests that RBPs, as post-transcriptional regulators, participate in different regulatory pathways, thus performing various cellular functions.

Owing to the heterogeneity of pericytes (Armulik et al., 2011), the selection of specific cell markers and the correct identification of pericytes in "-omics" studies pose a challenge (Cheng et al., 2018). Using transcriptomics and proteomics, mRNA and protein expressions in pericytes at different positions of the capillary bed would be accurately defined.

This study is the first attempt to comprehensively evaluate the role of RBPs in glioma and IS using computational biology, thus providing a panoramic map of a panel of genes between the two diseases and a research paradigm for the study of such scientific issues. Using bulk RNA-seq and scRNA-seq data, we examined the important roles of a panel of RBP genes in glioma and IS and identified the relationship between the two diseases. In this study, a prognostic RBPS consisting of six RBP genes was identified for glioma. These six RBP genes obtained from blood samples had a high classificatory performance for diagnosing IS. RBPS was associated with immunosuppression, enhanced energy metabolism, and tumor growth in glioma, and hypoxia response, angiogenesis, and enhanced coagulation in IS. In this RBPS, *SMAD9* was found to be associated with dementia; *POLR2F* and *ERI1* were identified to be associated with aging. Under hypoxia, *Irf5*/*Trim21* in microglia and *Taf7*/*Trim21* in pericytes were identified as RBPS-related networks. There are some limitations to this study. The gene signature was developed based on large publicly available databases and retrospective cohorts. However, no independent clinical cohort in local hospitals for validation was evaluated. In addition, the properties of these RBP genes need to be verified at cellular levels and using animal models. With the identification of new RBP molecules, computational biological analyses need to be updated to identify important molecules in the occurrence and development of glioma and IS.

## Conclusion

In conclusion, we developed a 6-RBP gene signature associated with a glioma prognosis and an IS diagnosis. In addition, an automatic machine learning classification model based on radiomics features from MRI was developed to stratify the RBPS risk. The RBPS was associated with immunosuppression, energy metabolism, and enhanced tumor growth in glioma, and hypoxia response, angiogenesis, and increased coagulation in IS. Upregulation of *SMAD9* was associated with dementia, while downregulation of *POLR2F* was associated with aging-related hypoxic stress. The RBPS is expected to serve as a biomarker to study the common mechanism between glioma and IS. These six RBP gene markers play a critical role in the association of IS with glioma, as revealed by our study.

## Data availability statement

The original contributions presented in the study are included in the article/Supplementary material, further inquiries can be directed to the corresponding author/s.

## Author contributions

WL conceptualized the data, involved in formal analysis and methodology, investigated the study, and wrote the original draft. QW, YC, NW, QN, CQ, and QW participated in literature review, data collection, and statistical analysis. YZ conceptualized the study, supervised the data, and reviewed and

edited the manuscript. All the authors read and approved the final manuscript.

## Funding

This study was funded by Provincial Key R&D Program, Science and Technology Department of Zhejiang Province (Grant No. 2017C03018), Key Program of Administration of Traditional Chinese Medicine, Zhejiang Province (Grant No. 2018ZZ015), Nursery Project of the Affiliated Tai'an City Central Hospital of Qingdao University (Grant No. 2022M PM06), Shandong Medical and Health Technology Development Fund (Grant No.202103070325), and 2021 Zhejiang Normal University Interdisciplinary Advance Research Fund.

## Acknowledgments

Sincere thanks to all the reviewers for their valuable comments on the study.

## Conflict of interest

The authors declare that the research was conducted in the absence of any commercial or financial relationships that could be construed as a potential conflict of interest.

## Publisher's note

All claims expressed in this article are solely those of the authors and do not necessarily represent those of their affiliated organizations, or those of the publisher, the editors and the reviewers. Any product that may be evaluated in this article, or claim that may be made by its manufacturer, is not guaranteed or endorsed by the publisher.

## Supplementary material

The Supplementary Material for this article can be found online at: https://www.frontiersin.org/articles/10.3389/fnagi.2022.951197/full#supplementary-material

## References

Acs, B., Rantalainen, M., and Hartman, J. (2020). Artificial intelligence as the next step towards precision pathology. *J. Intern. Med.* 288, 62–81. doi: 10.1111/joim.13030

Aibar, S., González-Blas, C. B., Moerman, T., Huynh-Thu, V. A., Imrichova, H., Hulselmans, G., et al. (2017). SCENIC: single-cell regulatory network inference and clustering. *Nat. Methods* 14, 1083–1086. doi: 10.1038/nmeth.4463

Al Mamun, A., Chauhan, A., Qi, S., Ngwa, C., Xu, Y., Sharmeen, R., et al. (2020). Microglial IRF5-IRF4 regulatory axis regulates neuroinflammation after cerebral ischemia and impacts stroke outcomes. *Proc. Natl. Acad. Sci. USA* 117, 1742–1752. doi: 10.1073/pnas.1914742117

Al Mamun, A., Chauhan, A., Yu, H., Xu, Y., Sharmeen, R., Liu, F., et al. (2018). Interferon regulatory factor 4/5 signaling impacts on microglial activation after ischemic stroke in mice. *Eur. J. Neurosci.* 47, 140–149. doi: 10.1111/ejn.13778

Al Mamun, A., Yu, H., Sharmeen, R., McCullough, L. D., and Liu, F. (2021). IRF5 signaling in phagocytes is detrimental to neonatal hypoxic ischemic encephalopathy. *Transl. Stroke Res.* 12, 602–614. doi: 10.1007/s12975-020-00832-x

Ardelt, A. A., Carpenter, R. S., Iwuchukwu, I., Zhang, A., Lin, W., Kosciuczuk, E., et al. (2017). Transgenic expression of HuR increases vasogenic edema and impedes functional recovery in rodent ischemic stroke. *Neurosci. Lett.* 661, 126–131. doi: 10.1016/j.neulet.2017.09.062

Armstrong, N. J., Mather, K. A., Sargurupremraj, M., Knol, M. J., Malik, R., Satizabal, C. L., et al. (2020). Common genetic variation indicates separate causes for periventricular and deep white matter hyperintensities. *Stroke* 51, 2111–2121. doi: 10.1161/STROKEAHA.119.027544

Armulik, A., Genové, G., and Betsholtz, C. (2011). Pericytes: developmental, physiological, and pathological perspectives, problems, and promises. *Dev. Cell* 21, 193–215. doi: 10.1016/j.devcel.2011.07.001

Armulik, A., Genové, G., Mäe, M., Nisancioglu, M. H., Wallgard, E., Niaudet, C., et al. (2010). Pericytes regulate the blood-brain barrier. *Nature* 468, 557–561. doi: 10.1038/nature09522

Bai, J., Yang, B., Shi, R., Shao, X., Yang, Y., Wang, F., et al. (2020). Could microtubule inhibitors be the best choice of therapy in gastric cancer with high immune activity: mutant DYNC1H1 as a biomarker. *Aging (Albany, NY)* 12, 25101–25119. doi: 10.18632/aging.104084

Bakas, S., Akbari, H., Sotiras, A., Bilello, M., Rozycki, M., Kirby, J. S., et al. (2017). Advancing the Cancer Genome Atlas glioma MRI collections with expert segmentation labels and radiomic features. *Sci. Data* 4, 170117. doi: 10.1038/sdata.2017.117

Barbagallo, D., Caponnetto, A., Cirnigliaro, M., Brex, D., Barbagallo, C., D'Angeli, F., et al. (2018). CircSMARCA5 inhibits migration of glioblastoma multiforme cells by regulating a molecular axis involving splicing factors SRSF1/SRSF3/PTB. *Int. J. Mol. Sci.* 19, 480. doi: 10.3390/ijms19020480

Barr, T. L., Conley, Y., Ding, J., Dillman, A., Warach, S., Singleton, A., et al. (2010). Genomic biomarkers and cellular pathways of ischemic stroke by RNA gene expression profiling. *Neurology* 75, 1009–1014. doi: 10.1212/WNL.0b013e3181f2b37f

Barsoum, I. B., Smallwood, C. A., Siemens, D. R., and Graham, C. H. (2014). A mechanism of hypoxia-mediated escape from adaptive immunity in cancer cells. *Cancer Res.* 74, 665–674. doi: 10.1158/0008-5472.CAN-13-0992

Becht, E., McInnes, L., Healy, J., Dutertre, C.-A., and Kwok, I. W. H., Ng, L. G., et al. (2019). Dimensionality reduction for visualizing single-cell data using UMAP. *Nat. Biotechnol.* 37, 38–44. doi: 10.1038/nbt.4314

Beers, A., Gerstner, E., Rosen, B., Clunie, D., Pieper, S., Fedorov, A., et al. (2018). Dicom-seg conversions for TCGA-LGG, and TCGA-GBM segmentation datasets. *Cancer Imaging Arch.* doi: 10.7937/TCIA.2018.ow6ce3ml

Benjamin, E. J., Muntner, P., Alonso, A., Bittencourt, M. S., Callaway, C. W., Carson, A. P., et al. (2019). Heart disease and stroke statistics-2019 update: a report from the American Heart Association. *Circulation* 139, e56–e528. doi: 10.1161/CIR.0000000000000659

Bhargava, S., Patil, V., Mahalingam, K., and Somasundaram, K. (2017). Elucidation of the genetic and epigenetic landscape alterations in RNA binding proteins in glioblastoma. *Oncotarget* 8, 16650–16668. doi: 10.18632/oncotarget.14287

Bi, J., Chowdhry, S., Wu, S., Zhang, W., Masui, K., Mischel, P. S., et al. (2020). Altered cellular metabolism in gliomas—an emerging landscape of actionable co-dependency targets. *Nat. Rev. Cancer* 20, 57–70. doi: 10.1038/s41568-019-0226-5

Blanc, E. M., Bruce-Keller, A. J., and Mattson, M. P. (1998). Astrocytic gap junctional communication decreases neuronal vulnerability to oxidative stress-induced disruption of $Ca^{2+}$ homeostasis and cell death. *J. Neurochem.* 70, 958–970. doi: 10.1046/j.1471-4159.1998.70030958.x

Blanche, P., Dartigues, J.-F., and Jacqmin-Gadda, H. (2013). Estimating and comparing time-dependent areas under receiver operating characteristic curves for censored event times with competing risks. *Statist. Med.* 32, 5381–5397. doi: 10.1002/sim.5958

Boucas, J., Fritz, C., Schmitt, A., Riabinska, A., Thelen, L., Peifer, M., et al. (2015). Label-free protein-RNA interactome analysis identifies khsrp signaling downstream of the p38/Mk2 kinase complex as a critical modulator of cell cycle progression. *PLoS ONE* 10, e0125745. doi: 10.1371/journal.pone.0125745

Brauner, S., Jiang, X., Thorlacius, G. E., Lundberg, A. M., Östberg, T., Yan, Z.-Q., et al. (2018). Augmented Th17 differentiation in Trim21 deficiency promotes a stable phenotype of atherosclerotic plaques with high collagen content. *Cardiovasc. Res.* 114, 158–167. doi: 10.1093/cvr/cvx181

Cao, J., Spielmann, M., Qiu, X., Huang, X., Ibrahim, D. M., Hill, A. J., et al. (2019). The single-cell transcriptional landscape of mammalian organogenesis. *Nature* 566, 496–502. doi: 10.1038/s41586-019-0969-x

Cestari, D. M., Weine, D. M., Panageas, K. S., Segal, A. Z., and Deangelis, L. M. (2004). Stroke in patients with cancer: incidence and etiology. *Neurology* 62, 2025. doi: 10.1212/01.WNL.0000129912.56486.2B

Chen, C.-W., Cheng, T.-J., Ho, C.-H., Wang, J.-J., Weng, S.-F., Hou, Y.-C., et al. (2017). Increased risk of brain cancer incidence in stroke patients: a clinical case series, population-based and longitudinal follow-up study. *Oncotarget* 8, 108989–108999. doi: 10.18632/oncotarget.22480

Chen, X., Chen, H., Xu, M., and Shen, J. (2013). Targeting reactive nitrogen species: a promising therapeutic strategy for cerebral ischemia-reperfusion injury. *Acta Pharmacol. Sin.* 34, 67–77. doi: 10.1038/aps.2012.82

Cheng, J., Korte, N., Nortley, R., Sethi, H., Tang, Y., Attwell, D., et al. (2018). Targeting pericytes for therapeutic approaches to neurological disorders. *Acta Neuropathol.* 136, 507–523. doi: 10.1007/s00401-018-1893-0

Cheng, L., Huang, Z., Zhou, W., Wu, Q., Donnola, S., Liu, J. K., et al. (2013). Glioblastoma stem cells generate vascular pericytes to support vessel function and tumor growth. *Cell* 153, 139–152. doi: 10.1016/j.cell.2013.02.021

Clark, K., Vendt, B., Smith, K., Freymann, J., Kirby, J., Koppel, P., et al. (2013). The Cancer Imaging Archive (TCIA): maintaining and operating a public information repository. *J. Digit. Imaging* 26, 1045–1057. doi: 10.1007/s10278-013-9622-7

Daneman, R., Zhou, L., Kebede, A. A., and Barres, B. A. (2010). Pericytes are required for blood-brain barrier integrity during embryogenesis. *Nature* 468, 562–566. doi: 10.1038/nature09513

Dang, H., Takai, A., Forgues, M., Pomyen, Y., Mou, H., Xue, W., et al. (2017). Oncogenic activation of the RNA binding protein NELFE and MYC signaling in hepatocellular carcinoma. *Cancer Cell.* 32, 101–114.e8. doi: 10.1016/j.ccell.2017.06.002

Declercq, M., Biquand, E., Karim, M., Pietrosemoli, N., Jacob, Y., Demeret, C., et al. (2020). Influenza A virus co-opts ERI1 exonuclease bound to histone mRNA to promote viral transcription. *Nucleic Acids Res.* 48, 10428–10440. doi: 10.1093/nar/gkaa771

Duan, Y., and Zhang, D. (2020). Identification of novel prognostic alternative splicing signature in papillary renal cell carcinoma. *J. Cell. Biochem.* 121, 672–689. doi: 10.1002/jcb.29314

Eguchi, J., Kong, X., Tenta, M., Wang, X., Kang, S., Rosen, E. D., et al. (2013). Interferon regulatory factor 4 regulates obesity-induced inflammation through regulation of adipose tissue macrophage polarization. *Diabetes* 62, 3394–3403. doi: 10.2337/db12-1327

Erdem-Eraslan, L., van den Bent, M. J., Hoogstrate, Y., Naz-Khan, H., Stubbs, A., van der Spek, P., et al. (2016). Identification of patients with recurrent glioblastoma who may benefit from combined bevacizumab and CCNU therapy: a report from the BELOB trial. *Cancer Res.* 76, 525–534. doi: 10.1158/0008-5472.CAN-15-0776

Fan, Z., Zhao, S., Zhu, Y., Li, Z., Liu, Z., Yan, Y., et al. (2020). Interferon regulatory factor 5 mediates lipopolysaccharide-induced neuroinflammation. *Front. Immunol.* 11, 600479. doi: 10.3389/fimmu.2020.600479

Fang, Z., Wu, D., Deng, J., Yang, Q., Zhang, X., Chen, J., et al. (2021). An MD2-perturbing peptide has therapeutic effects in rodent and rhesus monkey models of stroke. *Sci. Transl. Med.* 13:eabb6716. doi: 10.1126/scitranslmed.abb6716

Farkas, A., Schlakman, B., Khan, M., and Joyner, D. (2018). Glioblastoma presenting with acute middle cerebral artery territory infarct. *J. Stroke Cerebrovasc. Dis.* 27, e113–e114. doi: 10.1016/j.jstrokecerebrovasdis.2018.01.019

Fraum, T. J., Kreisl, T. N., Sul, J., Fine, H. A., and Iwamoto, F. M. (2011). Ischemic stroke and intracranial hemorrhage in glioma patients on antiangiogenic therapy. *J. Neurooncol.* 105, 281–289. doi: 10.1007/s11060-011-0579-4

Furukawa, T., Kuboki, Y., Tanji, E., Yoshida, S., Hatori, T., Yamamoto, M., et al. (2011). Whole-exome sequencing uncovers frequent GNAS mutations in intraductal papillary mucinous neoplasms of the pancreas. *Sci. Rep.* 1, 161. doi: 10.1038/srep00161

Gabrilovich, D. I., Chen, H. L., Girgis, K. R., Cunningham, H. T., Meny, G. M., Nadaf, S., et al. (1996). Production of vascular endothelial growth factor by human tumors inhibits the functional maturation of dendritic cells. *Nat. Med.* 2, 1096–1103. doi: 10.1038/nm1096-1096

Gerstberger, S., Hafner, M., and Tuschl, T. A. (2014). census of human RNA-binding proteins. *Nat. Rev. Genet.* 15, 829–845. doi: 10.1038/nrg3813

Ghosh, M. K., Chakraborty, D., Sarkar, S., Bhowmik, A., and Basu, M. (2019). The interrelationship between cerebral ischemic stroke and glioma: a comprehensive study of recent reports. *Signal Transduct Target Ther.* 4, 42. doi: 10.1038/s41392-019-0075-4

Goldman, M. J., Craft, B., Hastie, M., Repečka, K., McDade, F., Kamath, A., et al. (2020). Visualizing and interpreting cancer genomics data via the Xena platform. *Nat. Biotechnol.* 38, 675–678. doi: 10.1038/s41587-020-0546-8

Gong, L.-B., Wen, T., Li, Z., Xin, X., Che, X.-F., Wang, J., et al. (2019). DYNC1I1 promotes the proliferation and migration of gastric cancer by up-regulating IL-6 expression. *Front. Oncol.* (2019). 9:491. doi: 10.3389/fonc.2019.00491

Göritz, C., Dias, D. O., Tomilin, N., Barbacid, M., Shupliakov, O., Frisén, J., et al. (2011). A pericyte origin of spinal cord scar tissue. *Science.* 333, 238–242. doi: 10.1126/science.1203165

Graus, F., Rogers, L. R., and Posner, J. B. (1985). Cerebrovascular complications in patients with cancer. *Medicine (Baltimore)* 64, 16–35. doi: 10.1097/00005792-198501000-00002

Hall, C. N., Reynell, C., Gesslein, B., Hamilton, N. B., Mishra, A., Sutherland, B. A., et al. (2014). Capillary pericytes regulate cerebral blood flow in health and disease. *Nature* 508, 55–60. doi: 10.1038/nature13165

Hartmann, D. A., Hyacinth, H. I., Liao, F., and Shih, A. Y. (2018). Does pathology of small venules contribute to cerebral microinfarcts and dementia? *J. Neurochem.* 144, 517–526. doi: 10.1111/jnc.14228

Heng, J. S., Rattner, A., Stein-O'Brien, G. L., Winer, B. L., Jones, B. W., Vernon, H. J., et al. (2019). Hypoxia tolerance in the Norrin-deficient retina and the chronically hypoxic brain studied at single-cell resolution. *Proc. Natl. Acad. Sci. USA* 116, 9103–9114. doi: 10.1073/pnas.1821122116

Hoang, H. T., Schlager, M. A., Carter, A. P., and Bullock, S. L. (2017). DYNC1H1 mutations associated with neurological diseases compromise processivity of dynein-dynactin-cargo adaptor complexes. *Proc. Natl. Acad. Sci. USA* 114, E1597–E1606. doi: 10.1073/pnas.1620141114

Hokama, M., Oka, S., Leon, J., Ninomiya, T., Honda, H., Sasaki, K., et al. (2014). Altered expression of diabetes-related genes in Alzheimer's disease brains: the Hisayama study. *Cereb Cortex* 24, 2476–2488. doi: 10.1093/cercor/bht101

Huang, H.-L., Yao, H.-S., Wang, Y., Wang, W.-J., Hu, Z.-Q., and Jin, K.-Z., et al. (2014). Proteomic identification of tumor biomarkers associated with primary gallbladder cancer. *World J. Gastroenterol.* 20, 5511–5518. doi: 10.3748/wjg.v20.i18.5511

Iglesia, M. D., Parker, J. S., Hoadley, K. A., Serody, J. S., Perou, C. M., Vincent, B. G., et al. (2016). Genomic analysis of immune cell infiltrates across 11 tumor types. *J. Natl. Cancer Inst.* 108:djw144. doi: 10.1093/jnci/djw144

Jackson, S., ElAli, A., Virgintino, D., and Gilbert, M. R. (2017). Blood-brain barrier pericyte importance in malignant gliomas: what we can learn from stroke and Alzheimer's disease. *Neuro-oncology* 19, 1173–1182. doi: 10.1093/neuonc/nox058

Kafasla, P., Skliris, A., and Kontoyiannis, D. L. (2014). Post-transcriptional coordination of immunological responses by RNA-binding proteins. *Nat. Immunol.* 15, 492–502. doi: 10.1038/ni.2884

Kallergi, G., Markomanolaki, H., Giannoukaraki, V., Papadaki, M. A., Strati, A., Lianidou, E. S., et al. (2009). Hypoxia-inducible factor-1alpha and vascular endothelial growth factor expression in circulating tumor cells of breast cancer patients. *Breast Cancer Res.* 11, R84. doi: 10.1186/bcr2452

Kalogeris, T., Bao, Y., and Korthuis, R. J. (2014). Mitochondrial reactive oxygen species: a double edged sword in ischemia/reperfusion vs preconditioning. *Redox Biol.* 2, 702–714. doi: 10.1016/j.redox.2014.05.006

Kasivisvanathan, V., Shalhoub, J., Lim, C. S., Shepherd, A. C., Thapar, A., Davies, A. H., et al. (2011). Hypoxia-inducible factor-1 in arterial disease: a putative therapeutic target. *Curr. Vasc. Pharmacol.* 9, 333–349. doi: 10.2174/157016111795495602

Kedde, M., Strasser, M. J., Boldajipour, B., Vrielink, J. A. F. O., Slanchev, K., le Sage, C., Nagel, R. (2007). RNA-binding protein Dnd1 inhibits microRNA access to target mRNA. *Cell* 131, 1273–1286. doi: 10.1016/j.cell.2007.11.034

Khasraw, M., Reardon, D. A., Weller, M., and Sampson, J. H. (2020). PD-1 inhibitors: do they have a future in the treatment of glioblastoma? *Clin. Cancer Res.* 26, 5287–5296. doi: 10.1158/1078-0432.CCR-20-1135

Kikuno, M., Ueno, Y., Takekawa, H., Kanemaru, K., Shimizu, T., Kuriki, A., et al. (2021). Distinction in prevalence of atherosclerotic embolic sources in cryptogenic stroke with cancer status. *J. Am. Heart Assoc.* 10, e021375. doi: 10.1161/JAHA.120.021375

Kim, S.-J., Ju, J.-S., Kang, M.-H., Won, J. E., and Kim, Y. H., Raninga, P. V., et al. (2020). RNA-binding protein NONO contributes to cancer cell growth and confers drug resistance as a theranostic target in TNBC. *Theranostics* 10, 7974–7992. doi: 10.7150/thno.45037

Korte, N., Ilkan, Z., Pearson, C. L., Pfeiffer, T., Singhal, P., Rock, J. R., et al. (2022). The Ca2+-gated channel TMEM16A amplifies capillary pericyte contraction and reduces cerebral blood flow after ischemia. *J. Clin. Invest.* 2022, e154118. doi: 10.1101/2022.02.03.479031

Kreisl, T. N., Toothaker, T., Karimi, S., and DeAngelis, L. M. (2008). Ischemic stroke in patients with primary brain tumors. *Neurology* 70, 2314–2320. doi: 10.1212/01.wnl.0000314648.82924.6f

Lambertsen, K. L., Finsen, B., and Clausen, B. H. (2019). Post-stroke inflammation-target or tool for therapy? *Acta Neuropathol.* 137, 693–714. doi: 10.1007/s00401-018-1930-z

Lan, Y., Lou, J., Hu, J., Yu, Z., Lyu, W., Zhang, B., et al. (2020). Downregulation of SNRPG induces cell cycle arrest and sensitizes human glioblastoma cells to temozolomide by targeting Myc through a p53-dependent signaling pathway. *Cancer Biol. Med.* 17, 112–131. doi: 10.20892/j.issn.2095-3941.2019.0164

Le, T. T., Fu, W., and Moore, J. H. (2020). Scaling tree-based automated machine learning to biomedical big data with a feature set selector. *Bioinformatics* 36, 250–256. doi: 10.1093/bioinformatics/btz470

Leek, J. T., Johnson, W. E., Parker, H. S., Jaffe, A. E., and Storey, J. D. (2012). The sva package for removing batch effects and other unwanted variation in high-throughput experiments. *Bioinformatics* 28, 882–883. doi: 10.1093/bioinformatics/bts034

Li, W., Li, X., Gao, L.-N., and You, C.-G. (2020). Integrated analysis of the functions and prognostic values of RNA binding proteins in lung squamous cell carcinoma. *Front. Genet.* 11, 185. doi: 10.3389/fgene.2020.00185

Liang, Y., Hannan, R., and Fu, Y.-X. (2021). Type I IFN activating type I dendritic cells for antitumor immunity. *Clin. Cancer Res.* 27, 3818–3824. doi: 10.1158/1078-0432.CCR-20-2564

Liao, J.-Y., Yang, B., Zhang, Y.-C., Wang, X.-J., Ye, Y., Peng, J.-W., et al. (2020). EuRBPDB: a comprehensive resource for annotation, functional and oncological investigation of eukaryotic RNA binding proteins (RBPs). *Nucleic Acids Res.* 48, D307–D313. doi: 10.1093/nar/gkz823

Liberzon, A., Birger, C., Thorvaldsdóttir, H., Ghandi, M., Mesirov, J., Tamayo, P., et al. (2015). The Molecular Signatures Database (MSigDB) hallmark gene set collection. *Cell Syst.* 1, 417–425. doi: 10.1016/j.cels.2015.12.004

Liberzon, A., Subramanian, A., Pinchback, R., Thorvaldsdottir, H., Tamayo, P., Mesirov, J. P., et al. (2011). Molecular signatures database (MSigDB) 3.0. *Bioinformatics* 27, 1739–1740. doi: 10.1093/bioinformatics/btr260

Lin, W., Wang, Y., Chen, Y., Wang, Q., Gu, Z., Zhu, Y., et al. (2021). Role of calcium signaling pathway-related gene regulatory networks in ischemic stroke based on multiple WGCNA and single-cell analysis. *Oxid. Med. Cell. Longev.* 2021, 1–35. doi: 10.1155/2021/8060477

Liu, W., Xu, Z., Zhou, J., Xing, S., Li, Z., Gao, X., et al. (2020). High levels of HIST1H2BK in low-grade glioma predicts poor prognosis: a study using CGGA and TCGA data. *Front. Oncol.* 10, 627. doi: 10.3389/fonc.2020.00627

Liu, Z., and Chopp, M. (2016). Astrocytes, therapeutic targets for neuroprotection and neurorestoration in ischemic stroke. *Prog. Neurobiol.* 144, 103–120. doi: 10.1016/j.pneurobio.2015.09.008

Malta, T. M., Sokolov, A., Gentles, A. J., Burzykowski, T., Poisson, L., Weinstein, J. N., et al. (2018). Machine learning identifies stemness features associated with oncogenic dedifferentiation. *Cell* 173, 338–354.e15. doi: 10.1016/j.cell.2018.03.034

Mancino, A., Schioppa, T., Larghi, P., Pasqualini, F., Nebuloni, M., and Chen, I.-H., et al. (2008). Divergent effects of hypoxia on dendritic cell functions. *Blood* 112, 3723–3734. doi: 10.1182/blood-2008-02-142091

Mantovani, A., Sozzani, S., Locati, M., Allavena, P., and Sica, A. (2002). Macrophage polarization: tumor-associated macrophages as a paradigm for polarized M2 mononuclear phagocytes. *Trends Immunol.* 23, 549–555. doi: 10.1016/S1471-4906(02)02302-5

Mohibi, S., Chen, X., and Zhang, J. (2019). Cancer the'RBP'eutics-RNA-binding proteins as therapeutic targets for cancer. *Pharmacol. Therap.* 203, 107390. doi: 10.1016/j.pharmthera.2019.07.001

Musuka, T. D., Wilton, S. B., Traboulsi, M., and Hill, M. D. (2015). Diagnosis and management of acute ischemic stroke: speed is critical. *CMAJ Can. Med. Assoc. J.* 2015, 887. doi: 10.1503/cmaj.140355

Nakagomi, T., Kubo, S., Nakano-Doi, A., Sakuma, R., Lu, S., Narita, A., et al. (2015). Brain vascular pericytes following ischemia have multipotential stem cell activity to differentiate into neural and vascular lineage cells. *Stem Cells* 33, 1962–1974. doi: 10.1002/stem.1977

Newman, A. M., Steen, C. B., Liu, C. L., Gentles, A. J., Chaudhuri, A. A., Scherer, F., et al. (2019). Determining cell type abundance and expression from bulk tissues with digital cytometry. *Nat. Biotechnol.* 37, 773–782. doi: 10.1038/s41587-019-0114-2

Ngeow, J., Yu, W., Yehia, L., Niazi, F., Chen, J., Tang, X., et al. (2015). Exome sequencing reveals germline SMAD9 mutation that reduces phosphatase and tensin homolog expression and is associated with hamartomatous polyposis and gastrointestinal ganglioneuromas. *Gastroenterology.* 149, 886–889.e5. doi: 10.1053/j.gastro.2015.06.027

Noda, M., Inaji, M., Karakama, J., Arai, Y., Kuroha, M., Tamura, K., et al. (2022). Ischemic stroke with multiple cerebral artery stenosis in a patient with an anaplastic astrocytoma during bevacizumab treatment: a case report. *NMC Case Rep. J.* 9, 13–17. doi: 10.2176/jns-nmc.2021-0297

Noman, M. Z., Desantis, G., Janji, B., Hasmim, M., Karray, S., Dessen, P., et al. (2014). PD-L1 is a novel direct target of HIF-1α, and its blockade under hypoxia enhanced MDSC-mediated T cell activation. *J. Exp. Med.* 211, 781–790. doi: 10.1084/jem.20131916

Noman, M. Z., Hasmim, M., Messai, Y., Terry, S., Kieda, C., Janji, B., et al. (2015). Hypoxia: a key player in antitumor immune response. A review in the theme: cellular responses to hypoxia. *Am. J. Physiol. Cell Physiol.* 309, C569–C579. doi: 10.1152/ajpcell.00207.2015

O'Connell, G. C., Petrone, A. B., Treadway, M. B., Tennant, C. S., Lucke-Wold, N., Chantler, P. D., et al. (2016). Machine-learning approach identifies a pattern of gene expression in peripheral blood that can accurately detect ischaemic stroke. *NPJ Genomic Med.* 1, 16038. doi: 10.1038/npjgenmed.2016.38

O'Connell, G. C., Treadway, M. B., Petrone, A. B., Tennant, C. S., Lucke-Wold, N., Chantler, P. D., et al. (2017). Peripheral blood AKAP7 expression as an early marker for lymphocyte-mediated post-stroke blood brain barrier disruption. *Sci. Rep.* 7, 1172. doi: 10.1038/s41598-017-01178-5

Ohta, A., Diwanji, R., Kini, R., Subramanian, M., Ohta, A., Sitkovsky, M., et al. (2011). In vivo T cell activation in lymphoid tissues is inhibited in the oxygen-poor microenvironment. *Front. Immunol.* 2, 27. doi: 10.3389/fimmu.2011.00027

Ostrom, Q. T., Gittleman, H., Farah, P., Ondracek, A., Chen, Y., Wolinsky, Y., et al. (2013). Statistical report: primary brain and central nervous system tumors diagnosed in the United States in 2006–2010. *Neuro-Oncology* 15, ii1–ii56. doi: 10.1093/neuonc/not151

Özen, I., Deierborg, T., Miharada, K., Padel, T., and Englund, E., Genové, G., et al. (2014). Brain pericytes acquire a microglial phenotype after stroke. *Acta Neuropathol.* 128, 381–396. doi: 10.1007/s00401-014-1295-x

Pan, J.-A., Sun, Y., Jiang, Y.-P., Bott, A. J., Jaber, N., Dou, Z., et al. (2016). TRIM21 ubiquitylates SQSTM1/p62 and suppresses protein sequestration to regulate redox homeostasis. *Mol. Cell* 61, 720–733. doi: 10.1016/j.molcel.2016.02.007

Paun, A., Reinert, J. T., Jiang, Z., Medin, C., Balkhi, M. Y., Fitzgerald, K. A., et al. (2008). Functional characterization of murine interferon regulatory factor 5 (IRF-5) and its role in the innate antiviral response. *J. Biol. Chem.* 283, 14295–14308. doi: 10.1074/jbc.M800501200

Phipps, M. S., and Cronin, C. A. (2020). Management of acute ischemic stroke. *BMJ* 368, l6983. doi: 10.1136/bmj.l6983

Qi, Y., Liu, B., Sun, Q., Xiong, X., and Chen, Q. (2020). Immune checkpoint targeted therapy in glioma: status and hopes. *Front. Immunol.* 11, 578877. doi: 10.3389/fimmu.2020.578877

Qin, H., Ni, H., Liu, Y., Yuan, Y., Xi, T., Li, X., et al. (2020). RNA-binding proteins in tumor progression. *J. Hematol. Oncol.* 13, 90. doi: 10.1186/s13045-020-00927-w

Qiu, X., Hill, A., Packer, J., Lin, D., Ma, Y.-A., Trapnell, C., et al. (2017a). Single-cell mRNA quantification and differential analysis with Census. *Nat. Methods* 14, 309–315. doi: 10.1038/nmeth.4150

Qiu, X., Mao, Q., Tang, Y., Wang, L., Chawla, R., Pliner, H., et al. (2017b). Reversed graph embedding resolves complex single-cell developmental trajectories. *Genomics*. 14, 979–982. doi: 10.1101/110668

Qureshi, A. I., Malik, A. A., Saeed, O., Adil, M. M., Rodriguez, G. J., Suri, M. F. K., et al. (2015). Incident cancer in a cohort of 3,247 cancer diagnosis free ischemic stroke patients. *Cerebrovasc. Dis.* 39, 262–268. doi: 10.1159/000375154

Ransohoff, R. M. A. (2016). polarizing question: do M1 and M2 microglia exist? *Nat. Neurosci.* 19, 987–991. doi: 10.1038/nn.4338

Ransom, B. R., and Ransom, C. B. (2012). Astrocytes: multitalented stars of the central nervous system. *Methods Mol. Biol.* 814, 3–7. doi: 10.1007/978-1-61779-452-0_1

Rasmussen, R. D., Gajjar, M. K., Tuckova, L., Jensen, K. E., Maya-Mendoza, A., Holst, C. B., et al. (2016). BRCA1-regulated RRM2 expression protects glioblastoma cells from endogenous replication stress and promotes tumorigenicity. *Nat. Commun.* 7, 13398. doi: 10.1038/ncomms13398

Reinhold, W. C., Sunshine, M., Liu, H., Varma, S., Kohn, K. W., Morris, J., et al. (2012). CellMiner: a web-based suite of genomic and pharmacologic tools to explore transcript and drug patterns in the NCI-60 cell line set. *Cancer Res.* 72, 3499–3511. doi: 10.1158/0008-5472.CAN-12-1370

Ritchie, M. E., Phipson, B., Wu, D., Hu, Y., Law, C. W., Shi, W., et al. (2015). limma powers differential expression analyses for RNA-sequencing and microarray studies. *Nucleic Acids Res.* 43, e47–e47. doi: 10.1093/nar/gkv007

Segura-Collar, B., Garranzo-Asensio, M., Herranz, B., Hernández-SanMiguel, E., Cejalvo, T., Casas, B. S., et al. (2021). Tumor-derived pericytes driven by EGFR mutations govern the vascular and immune microenvironment of gliomas. *Cancer Res.* 81, 2142–2156. doi: 10.1158/0008-5472.CAN-20-3558

Seidel, C., Hentschel, B., Simon, M., Schnell, O., Heese, O., Tatagiba, M., et al. (2013). A comprehensive analysis of vascular complications in 3,889 glioma patients from the German Glioma Network. *J. Neurol.* 260, 847–855. doi: 10.1007/s00415-012-6718-9

Semenza, G. L. (2012). Hypoxia-inducible factors: mediators of cancer progression and targets for cancer therapy. *Trends Pharmacol. Sci.* 33, 207–214. doi: 10.1016/j.tips.2012.01.005

Shao, J., Zhang, J., Zhang, Z., Jiang, H., Lou, X., Huang, B., et al. (2013). Alternative polyadenylation in glioblastoma multiforme and changes in predicted RNA binding protein profiles. *OMICS J Integr. Biol.* 17, 136–149. doi: 10.1089/omi.2012.0098

Sharma, A., Brenner, M., Jacob, A., Marambaud, P., and Wang, P. (2021). Extracellular CIRP activates the IL-6Rα/STAT3/Cdk5 pathway in neurons. *Mol. Neurobiol.* 58, 3628–3640. doi: 10.1007/s12035-021-02368-z

Si, W., Li, Z., Huang, Z., Ye, S., Li, X., Li, Y., et al. (2020). Binding protein Motif 3 inhibits oxygen-glucose deprivation/reoxygenation-induced apoptosis through promoting stress granules formation in PC12 cells and rat primary cortical neurons. *Front. Cell. Neurosci.* 14, 559384. doi: 10.3389/fncel.2020.559384

Sjöstrand, M., Ambrosi, A., Brauner, S., Sullivan, J., Malin, S., Kuchroo, V. K., et al. (2013). Expression of the immune regulator tripartite-motif 21 is controlled by IFN regulatory factors. *JI* 191, 3753–3763. doi: 10.4049/jimmunol.1202341

Søndergaard, K. L., Hilton, D. A., Penney, M., Ollerenshaw, M., and Demaine, A. G. (2002). Expression of hypoxia-inducible factor 1alpha in tumours of patients with glioblastoma. *Neuropathol. Appl. Neurobiol.* 28, 210–217. doi: 10.1046/j.1365-2990.2002.00391.x

Stark, K., Eckart, A., Haidari, S., Tirniceriu, A., Lorenz, M., and von Brühl, M.-L., et al. (2013). Capillary and arteriolar pericytes attract innate leukocytes exiting through venules and "instruct" them with pattern-recognition and motility programs. *Nat. Immunol.* 14, 41–51. doi: 10.1038/ni.2477

Stuart, T., Butler, A., Hoffman, P., Hafemeister, C., Papalexi, E., Mauck, W. M., et al. (2019). Comprehensive integration of single-cell data. *Cell.* 177, 1888–1902.e21. doi: 10.1016/j.cell.2019.05.031

Su, X., Chen, N., Sun, H., Liu, Y., Yang, X., Wang, W., et al. (2019). Automated machine learning based on radiomics features predicts H3 K27M mutation in midline gliomas of the brain. *Neuro-Oncology.* 2019:noz184. doi: 10.1093/neuonc/noz184

Subramanian, A., Tamayo, P., Mootha, V. K., Mukherjee, S., Ebert, B. L., Gillette, M. A., et al. (2005). Gene set enrichment analysis: a knowledgE-based approach for interpreting genome-wide expression profiles. *Proc. Natl. Acad. Sci. USA.* 102, 15545–15550. doi: 10.1073/pnas.0506580102

Sumbayev, V. V., and Yasinska, I. M. (2007). Mechanisms of hypoxic signal transduction regulated by reactive nitrogen species. *Scand. J. Immunol.* 65, 399–406. doi: 10.1111/j.1365-3083.2007.01919.x

Sun, P., Li, Y., Chao, X., Li, J., Luo, R., Li, M., et al. (2020). Clinical characteristics and prognostic implications of BRCA-associated tumors in males: a pan-tumor survey. *BMC Cancer* 20, 994. doi: 10.1186/s12885-020-07481-1

Svensson, A., Özen, I., Genové, G., Paul, G., and Bengzon, J. (2015). Endogenous brain pericytes are widely activated and contribute to mouse glioma microvasculature. *PLoS ONE* 10, e0123553. doi: 10.1371/journal.pone.0123553

Tanislav, C., Adarkwah, C. C., Jakob, L., and Kostev, K. (2019). Increased risk for cancer after stroke at a young age: etiological relevance or incidental finding? *J. Cancer Res. Clin. Oncol.* 145, 3047–3054. doi: 10.1007/s00432-019-03022-x

Thomas, M. F., L'Etoile, N. D., and Ansel, K. M. (2014). Eri1: a conserved enzyme at the crossroads of multiple RNA-processing pathways. *Trends Genet.* 30, 298–307. doi: 10.1016/j.tig.2014.05.003

Thorsson, V., Gibbs, D. L., Brown, S. D., Wolf, D., Bortone, D. S., Yang, T.-H. O., et al. (2018). The immune landscape of cancer. *Immunity.* 48, 812–830.e14. doi: 10.1016/j.immuni.2018.03.023

Trapnell, C., Cacchiarelli, D., Grimsby, J., Pokharel, P., Li, S., Morse, M., et al. (2014). The dynamics and regulators of cell fate decisions are revealed by pseudotemporal ordering of single cells. *Nat. Biotechnol.* 32, 381–386. doi: 10.1038/nbt.2859

Tsao, C.-C., Baumann, J., Huang, S.-F., Kindler, D., Schroeter, A., Kachappilly, N., et al. (2021). Pericyte hypoxia-inducible factor-1 (HIF-1) drives blood-brain barrier disruption and impacts acute ischemic stroke outcome. *Angiogenesis* 24, 823–842. doi: 10.1007/s10456-021-09796-4

Tsuyama, J., Nakamura, A., Ooboshi, H., Yoshimura, A., and Shichita, T. (2018). Pivotal role of innate myeloid cells in cerebral post-ischemic sterile inflammation. *Semin. Immunopathol.* 40, 523–538. doi: 10.1007/s00281-018-0707-8

Umphlett, M., Shea, S., Tome-Garcia, J., Zhang, Y., Hormigo, A., Fowkes, M., et al. (2020). Widely metastatic glioblastoma with BRCA1 and ARID1A mutations: a case report. *BMC Cancer* 20, 47. doi: 10.1186/s12885-020-6540-1

Uneda, A., Kurozumi, K., Fujimura, A., Fujii, K., Ishida, J., Shimazu, Y., et al. (2021). Differentiated glioblastoma cells accelerate tumor progression by shaping the tumor microenvironment via CCN1-mediated macrophage infiltration. *Acta Neuropathol Commun.* 9, 29. doi: 10.1186/s40478-021-01124-7

Van Nostrand, E. L., Freese, P., Pratt, G. A., Wang, X., Wei, X., Xiao, R., et al. (2020). A large-scale binding and functional map of human RNA-binding proteins. *Nature* 583, 711–719. doi: 10.1038/s41586-020-2077-3

Velasco, M. X., Kosti, A., Penalva, L. O. F., and Hernández, G. (2019). The diverse roles of RNA-binding proteins in glioma development. *Adv. Exp. Med. Biol.* 1157, 29–39. doi: 10.1007/978-3-030-19966-1_2

Vidal, R., Wagner, J. U. G., Braeuning, C., Fischer, C., Patrick, R., Tombor, L., et al. (2019). Transcriptional heterogeneity of fibroblasts is a hallmark of the aging heart. *JCI Insight* 4, 131092. doi: 10.1172/jci.insight.131092

Villanueva, E., Smith, T., Queiroz, R. M. L., Monti, M., Pizzinga, M., Elzek, M., et al. (2020). Efficient recovery of the RNA-bound proteome and protein-bound transcriptome using phase separation (OOPS). *Nat. Protoc.* 15, 2568–2588. doi: 10.1038/s41596-020-0344-2

Wang, E., Lu, S. X., Pastore, A., Chen, X., Imig, J., Chun-Wei Lee, S., et al. (2019). Targeting an RNA-binding protein network in acute myeloid leukemia. *Cancer Cell* 35, 369–384.e7. doi: 10.1016/j.ccell.2019.01.010

Wang, J., Qi, J., and Hou, X. (2019). Systematically dissecting the function of RNA-binding proteins during glioma progression. *Front. Genet.* 10, 1394. doi: 10.3389/fgene.2019.01394

Wang, Z., Tang, W., Yuan, J., Qiang, B., Han, W., Peng, X., et al. (2020). Integrated analysis of RNA-binding proteins in glioma. *Cancers (Basel)* 12, E892. doi: 10.3390/cancers12040892

Williamson, M. R., Fuertes, C. J. A., Dunn, A. K., Drew, M. R., and Jones, T. A. (2021). Reactive astrocytes facilitate vascular repair and remodeling after stroke. *Cell Rep.* 35, 109048. doi: 10.1016/j.celrep.2021.109048

Winkler, E. A., Bell, R. D., and Zlokovic, B. V. (2011). Central nervous system pericytes in health and disease. *Nat. Neurosci.* 14, 1398–1405. doi: 10.1038/nn.2946

Wojtasiewicz, T. J., Ducruet, A. F., Noticewala, S. S., Canoll, P., and McKhann, G. M. (2013). De novo glioblastoma in the territory of a prior middle cerebral artery infarct. *Case Rep. Neurol. Med.* 2013, 1–5. doi: 10.1155/2013/356526

Xu, H., Jiang, Y., Xu, X., Su, X., Liu, Y., Ma, Y., et al. (2019). Inducible degradation of lncRNA Sros1 promotes IFN-γ-mediated activation of innate immune responses by stabilizing Stat1 mRNA. *Nat. Immunol.* 20, 1621–1630. doi: 10.1038/s41590-019-0542-7

Xu, P., Liu, Q., Xie, Y., Shi, X., Li, Y., Peng, M., et al. (2018). Breast cancer susceptibility protein 1 (BRCA1) rescues neurons from cerebral ischemia/reperfusion injury through NRF2-mediated antioxidant pathway. *Redox Biol.* 18, 158–172. doi: 10.1016/j.redox.2018.06.012

Xu, P., Shi, X., Zhang, X., Liu, Q., Xie, Y., Hong, Y., et al. (2019). Overexpression of BRCA1 in neural stem cells enhances cell survival and functional recovery after transplantation into experimental ischemic stroke. *Oxid. Med. Cell. Longev.* 2019, 8739730. doi: 10.1155/2019/8739730

Xu, S., Lu, J., Shao, A., Zhang, J. H., and Zhang, J. (2020). Glial cells: role of the immune response in ischemic stroke. *Front. Immunol.* 11, 294. doi: 10.3389/fimmu.2020.00294

Xu, S., Tang, L., Dai, G., Luo, C., and Liu, Z. (2021). Immune-related genes with APA in microenvironment indicate risk stratification and

clinical prognosis in grade II/III gliomas. *Mol. Therap. Nucl. Acids* 23, 1229–1242. doi: 10.1016/j.omtn.2021.01.033

Yang, Y., Yan, R., Zhang, L., Meng, X., and Sun, W. (2020). Primary glioblastoma transcriptome data analysis for screening survival-related genes. *J. Cell. Biochem.* 121, 1901–1910. doi: 10.1002/jcb.29425

Yoshihara, K., Shahmoradgoli, M., Martínez, E., Vegesna, R., Kim, H., Torres-Garcia, W., et al. (2013). Inferring tumour purity and stromal and immune cell admixture from expression data. *Nat. Commun.* 4, 2612. doi: 10.1038/ncomms3612

Zhai, Y., Zhao, B., Wang, Y., Li, L., Li, J., Li, X., et al. (2021). Construction of the optimization prognostic model based on differentially expressed immune genes of lung adenocarcinoma. *BMC Cancer* 21, 213. doi: 10.1186/s12885-021-07911-8

Zhang, H., Meltzer, P., and Davis, S. (2013). RCircos: an R package for Circos 2D track plots. *BMC Bioinform.* 14, 244. doi: 10.1186/1471-2105-14-244

Zhang, Z., Guo, M., Liu, Y., Liu, P., Cao, X., Xu, Y., et al. (2020). RNPS1 inhibition aggravates ischemic brain injury and promotes neuronal death. *Biochem. Biophys. Res. Commun.* 523, 39–45. doi: 10.1016/j.bbrc.2019.11.185

Zhao, S.-C., Wang, C., Xu, H., Wu, W.-Q., Chu, Z.-H., Ma, L.-S., et al. (2017). Age-related differences in interferon regulatory factor-4 and−5 signaling in ischemic brains of mice. *Acta Pharmacol. Sin.* 38, 1425–1434. doi: 10.1038/aps.2017.122

Zhao, Z., Wang, Y., Yun, D., Huang, Q., Meng, D., Li, Q., et al. (2020). TRIM21 overexpression promotes tumor progression by regulating cell proliferation, cell migration and cell senescence in human glioma. *Am. J. Cancer Res.* 10, 114–130.

Zhou, M., Yang, W.-L., Ji, Y., Qiang, X., and Wang, P. (2014). Cold-inducible RNA-binding protein mediates neuroinflammation in cerebral ischemia. *Biochim. Biophys. Acta General Subjects* 1840, 2253–2261. doi: 10.1016/j.bbagen.2014.02.027

frontiers | Frontiers in Aging Neuroscience

TYPE Original Research
PUBLISHED 12 September 2022
DOI 10.3389/fnagi.2022.977604



OPEN ACCESS

EDITED BY
Gang Wang,
Shanghai Jiao Tong University, China

REVIEWED BY
Yun Tian,
Central South University, China
Qiying Sun,
Central South University, China

*CORRESPONDENCE
Daojun Hong
hongdaojun@hotmail.com
Zhaoxia Wang
drwangzx@163.com

†These authors have contributed equally to this work

SPECIALTY SECTION
This article was submitted to Alzheimer's Disease and Related Dementias,
a section of the journal
Frontiers in Aging Neuroscience

RECEIVED 24 June 2022
ACCEPTED 25 August 2022
PUBLISHED 12 September 2022

CITATION
Zhou Y, Huang P, Huang Z, Peng Y, Zheng Y, Yu Y, Zhu M, Deng J, Wang Z and Hong D (2022) Urine cytological study in patients with clinicopathologically confirmed neuronal intranuclear inclusion disease.
*Front. Aging Neurosci.* 14:977604.
doi: 10.3389/fnagi.2022.977604



# Urine cytological study in patients with clinicopathologically confirmed neuronal intranuclear inclusion disease

Yiyi Zhou[1†], Pengcheng Huang[1†], Zhaojun Huang[1], Yun Peng[1], Yilei Zheng[1], Yaqing Yu[1], Min Zhu[1], Jianwen Deng[2], Zhaoxia Wang[2*] and Daojun Hong[1,3*]

[1]Department of Neurology, The First Affiliated Hospital of Nanchang University, Nanchang, China, [2]Department of Neurology, Peking University First Hospital, Beijing, China, [3]Department of Medical Genetics, The First Affiliated Hospital of Nanchang University, Nanchang, China

**Objective:** The diagnosis of neuronal intranuclear inclusion disease (NIID) is currently based on CGG repeat expansion in the 5′UTR of the *NOTCH2NLC* gene, or p62-positive intranuclear inclusions in skin biopsy. The purpose of this study is to explore the value of non-invasive pathological findings in urine sediment cells from NIID patients.

**Materials and methods:** Ten patients with clinically suspected NIID were enrolled for skin biopsy and gene screening. Morning urine (500 ml) was collected from each patient, and cell sediment was obtained by centrifugation. Urine cytology, including Giemsa staining, p62 immunostaining, and electron microscopic examination, were conducted on cell sediment.

**Results:** The main clinical symptoms of 10 patients included episodic disturbance of consciousness, cognitive impairment, tremor, limb weakness, and so on. Cerebral MRI showed that 9 patients had linear DWI high signal in the corticomedullary junction. Genetic testing found that the number of CGG repeat ranged from 96 to 158 in the *NOTCH2NLC* gene. Skin biopsy revealed that all patients showed p62-positive intranuclear inclusions in 18.5 ± 6.3% of the duct epithelial cells of sweat gland. In contrast, urine sediment smears revealed that only 3 patients had p62 positive intranuclear inclusions in 3.5 ± 1.2% of the sedimentary cells. Ultrastructural examinations showed that intranuclear inclusions were also identified in the cell sediment of the 3 patients.

**Conclusion:** Urine cytology may be a new and non-invasive pathological diagnosis technique for some NIID patients, although the positive rate is not as high as that of skin biopsy, which is a sensitive and reliable pathological method for NIID.

KEYWORDS

neuronal intranuclear inclusion disease, skin biopsy, urine cytology, *NOTCH2NLC* gene, pathological diagnosis

## Introduction

Neuronal intranuclear inclusion disease (NIID) is a rare neurodegenerative disease, initially named after the pathological features characterized by eosinophilic intranuclear inclusions in neurons (Liufu et al., 2022). Further studies have found that eosinophilic intranuclear inclusions also exist in the cells of peripheral nervous system and the most other organs (Miki et al., 2022). Abnormal CGG repeat expansion in the 5′-untranslated region (5′UTR) of the *NOTCH2NLC* gene is the genetic cause of NIID (Deng et al., 2019; Ishiura et al., 2019; Sone et al., 2019; Tian et al., 2019). In addition, studies have shown that the repeat expansion is also associated with Parkinson's disease (PD) (Shi et al., 2021), essential tremor (Sun et al., 2020), multiple system atrophy (Fang et al., 2020), motor neuron disease (Yuan et al., 2020), peripheral neuropathy (Wang et al., 2021), and oculopharyngodistal myopathy (OPDM) (Yu et al., 2021). Collectively, these phenotypes are referred to as *NOTCH2NLC*-related repeat expansion disorders (NREDs) (Lu and Hong, 2021). Among them, NIID is the most common subtype, and its clinical manifestations show great heterogeneities, such as sudden disturbance of consciousness, episodic psychiatric or cognitive impairments, seizures, limb weakness, tremor, miosis, and autonomic dysfunctions (Sone et al., 2016; Liang et al., 2020; Wang et al., 2020). Although the causative gene of the NIID has been identified, the relationship between the phenotype and genotype remains uncertain in some NIID patients. Therefore, pathological examination still plays a crucial role in the accurate and timely diagnosis of NIID (Chen et al., 2020b).

Skin biopsy has been developed as a sensitive and specific method for pathological diagnosis of NIID, which is characterized by p62-positive eosinophilic intranuclear inclusions in fibroblasts, adipocytes, and duct epithelial cells of sweat gland (Sone et al., 2011). As an invasive examination, open skin biopsy usually takes specimens deep into the dermis and subcutaneous adipose tissue, thus increasing the risk of potential infection and pain in patients. In addition, the genetic screening is expensive and unavailable to most patients. Therefore, it is necessary to find a non-invasive and economic examination for the diagnosis of NIID patients. In this study, 10 patients with NIID were diagnosed according to the clinical, radiological, pathological and genetic characteristics, and then the urine of 10 patients was collected in the acute phase of hospitalization to explore whether urine cytology was helpful to the diagnosis of NIID.

## Materials and methods

### Subjects

A total of 10 NIID patients who were referred to the Department of Neurology, the First Affiliated Hospital of Nanchang University were recruited from January 2021 to February 2022. The clinical features and radiological data of the patients were collected, and their family history and symptoms of family members were obtained from the subjects and their relatives. This study was approved by the Ethics Committee of The First Affiliated Hospital of Nanchang University. The tissue samples of the patients and controls were obtained under a written consent signed by each individual in compliance with the bioethics laws of China as well as the Declaration of Helsinki.

### Genetic screening

Peripheral blood was taken from each patient in 3 ml for DNA extraction. Repeat-primed polymerase chain reaction (RP-PCR) was initially used to identify the repeat expansion in the *NOTCH2NLC* gene. RP-PCR was performed as described in our previous study (Deng et al., 2019). The PCR primer mix contained three primers: NOTCH2NLC-F:5′-FAM-GGCATTTGCGCCTGTGCTTCGGACCGT-3′, M13-(GGC)4(GGA)2-R:5′-CAGGAAACAGCTATGACCTCCTCCGCCGCCGCCGCC-3′, and M13-linker-R: 5′-CAGGAAACAGCTATGACC-3′. A saw-tooth tail pattern in the electropherogram was considered to be the disease-associated repeat expansion. Fluorescence amplicon length polymerase chain reaction (AL-PCR) was used to detect the length of GGC repeat expansion. The composition of PCR mix was identical to that of RP-PCR

except for the use of 50 ng genomic DNA as a template and a different primer pair: NOTCH2NLC-AL-F: 5′-VIC-CATTTGCGCCTGTGCTTCGGAC-3′; NOTCH2NLC-AL-R: 5′-AGAGCGGCGCAGGGCGGGCATCTT-3′. The PCR conditions were the same as for RP-PCR. Electrophoresis was performed on a 3500xl Genetic analyzer (Thermo Fisher Scientific, Waltham, MA, United States) and the data were analyzed using GeneMapper software (Thermo Fisher Scientific). The length of the highest signal peak of expanded allele was used to calculate the repeat number.

## Pathological examination of skin biopsy

Skin biopsy in the distal part of the leg (10 cm above the external malleous) was performed in the 10 patients. A part of the specimen was fixed by 4% formalin solution, embedded in paraffin, cut into 4-mm thick sections, and stained with hematoxylin and eosin (H&E). The immunohistochemical and immunofluorescent staining were performed with anti-p62 antibody (sc-28359, Santa Cruz Biotechnology, CA, United States). The rate of p62-positive intranuclear inclusions was calculated by the number of positive cells to the total number of the duct epithelial cells of sweat gland. For electron microscopy, a portion of the specimens were initially fixed in 2.5% glutaraldehyde, subsequently fixed in 1% osmium tetroxide, and embed in Epon 812. Ultrathin sections were examined through electron microscope (JEOL-1230, Japan).

## Pathological examination of urine sediment

Five hundred milliliters of morning urine were collected in the 10 NIID patients and 6 healthy controls, subsequently centrifuged at 1500 rpm/min for 5 min, discarded the supernatant, and collected the urine sediment into a cell cryopreservation tube. Suspending a small amount of sediment with phosphate buffered saline (PBS) for suspension, and then 100 μl of the suspension was drawn and dropped on the glass slide for natural drying, and were used for Wright's Giemsa staining and anti-p62 immunostaining, respectively. The rate of p62-positive intranuclear inclusions was calculated by the number of positive nuclei to the total number of the nuclei on six random 100× microscopic fields. The remaining urine sediment were centrifuged at 5000 rpm/min for 5 min, discarded the supernatant. 1 ml 2.5% glutaraldehyde solution was added to the urine sediment for fixation, subsequently embedded in epoxy resin, stained with uranyl acetate and lead citrate. Ultrastructural pathological changes were observed under transmission electron microscope (JEOL-1230, Japan).

# Results

## Clinical features

Half of the patients (5/10) had family history (only the probands included), and 5 (5/10) patients were sporadic cases, including 4 male and 6 female patients. The age of onset was 54–73 (65.90 ± 4.95) years old, and the disease duration was 0.5–20 (6.95 ± 6.90) years. The presenting symptoms included episodic disturbance of consciousness (4/10), episodic headache (2/10), tremor (2/10), cognitive impairment (1/10), and episodic psychiatric disorder (1/10). The episodic disturbance of consciousness or mental disorder usually lasted from a few hours to several weeks, and most of them could return to their pre-onset state. Episodic headaches were similar to migraine attacks, lasting from a few hours to a few days, and usually relieved within a day. The main neurological clinical symptoms at visit included cognitive impairments (7/10), tremor (4/10), limb weakness (4/10), bradykinesia (2/10), psychiatric symptoms (2/10), sensory dysfunction (2/10), visual dysfunction (2/10), and seizures (1/10). Other multi-system symptoms included urinary dysfunction (4/10), dry cough (3/10), episodic fever (3/10), constipation (3/10), episodic abdominal pain (2/10), episodic nausea/vomiting (2/10), and diabetes (2/10). Physical examination revealed paresthesias in 4 patients (4/10), hyporeflexia of lower limb in 4 patients (4/10), decreased muscle tone in 4 patients (4/10), increased muscle tone in 3 patients (3/10), pyramidal signs in 3 patients (3/10), cerebellar ataxia in 2 patients (2/10), and miosis in one patient (1/10) (**Table 1**).

Nerve conduction studies revealed that all patients had different degrees of peripheral neuropathy, including demyelinating sensorimotor neuropathy in 6 patients (6/10), mixed sensorimotor neuropathy in 3 patients (3/10), and demyelinating sensory neuropathy in one patients (1/10) (**Table 2**). Cerebral magnetic resonance imaging (MRI) showed 9 patients (9/10) with abnormal curve-like hyperintensity along the corticomedullary junction on diffusion weighted imaging (DWI) (**Figure 1A**), and 2 patients (2/10) had involvements in the corpus callosum (**Figure 1B**). White matter hyperintensities were symmetrically observed in the corona radiata, the center of the semiovale, and the lateral ventricle in 9 patients (9/10) (**Figure 1C**). One patient (1/10) presented with edema of the left temporo-occipital cortex, which was significantly enhanced on contrast scan (**Figure 1D**).

## Genetic mutation

Repeat-primed PCR amplification of the 5′UTR of the *NOTCH2NLC* gene revealed that the chromatograms of all patients showed long saw-tooth curves, indicating the presence of CGG repeat expansion variant (**Figure 2A**). In addition, the

10.3389/fnagi.2022.977604

TABLE 1 Clinical data of 10 patients with neuronal intranuclear inclusion disease (NIID).

| Variables | P1 | P2 | P3 | P4 | P5 | P6 | P7 | P8 | P9 | P10 |
|---|---|---|---|---|---|---|---|---|---|---|
| Age (years) | 70 | 54 | 69 | 73 | 66 | 67 | 64 | 63 | 64 | 69 |
| Sex | M | F | F | M | F | F | M | F | M | F |
| Disease duration (years) | 3 | 3 | 2 | 5 | 17 | 20 | 2 | 15 | 2 | 0.5 |
| Family history | + | + | + | + | + | − | − | − | − | − |
| Cognitive impairment | + | + | + | + | − | − | + | + | + | − |
| Tremor | − | + | − | − | + | + | + | − | − | − |
| Limb weakness | − | − | − | + | + | + | − | − | − | + |
| Bradykinesia | − | − | − | − | − | − | − | + | + | − |
| Psychiatric symptoms | − | + | − | + | − | − | − | − | − | − |
| Sensory dysfunction | − | − | − | + | − | − | − | + | − | − |
| Visual dysfunction | − | + | − | − | − | − | − | − | − | + |
| Seizures | − | − | − | − | − | + | − | − | − | − |
| Urinary dysfunction | + | − | − | + | − | + | + | − | − | − |
| Dry cough | − | + | − | − | + | − | − | − | + | − |
| Episodic fever | + | − | − | + | − | − | − | + | − | − |
| Constipation | + | − | − | + | − | − | + | − | − | − |
| Episodic abdominal pain | − | − | − | + | − | − | − | + | − | − |
| Episodic nausea and vomiting | − | + | − | − | + | − | − | − | − | − |
| Diabetes | − | + | − | − | − | − | − | − | − | + |
| Paresthesia | − | − | − | + | − | + | − | + | − | + |
| Reduced reflex | − | − | − | + | − | + | − | + | − | + |
| Increased muscle tension | − | + | − | − | + | − | − | − | + | − |
| Pathological signs | − | + | − | − | + | − | − | − | + | − |
| Ataxia | − | − | − | − | − | − | − | + | + | − |
| Miosis | − | − | − | − | − | + | − | − | − | − |

AL-PCR amplification showed that the number of CGG repeat in these patients ranged from 96 to 158, with an average number of 119 ± 23 (Figure 2B).

## Skin pathological features

Skin biopsies were performed in all 10 patients. The skin had no structural abnormalities and inflammatory cell infiltrations in the subcutaneous fatty tissue. Eosinophilic intranuclear inclusions were observed in the nuclei of fibroblasts, adipocytes, and duct epithelial cells of sweat gland (Figures 3A,D), and some of the inclusions presented with halo, especially in the nuclei of sweat gland duct epithelial cells. Occasionally, multiple inclusions were observed in a single nucleus. P62 antibody staining showed that positive intranuclear inclusions were observed in the nuclei of sweat gland duct epithelial cells, fibroblasts, and adipocytes in all patients (Figures 3B,E). The mean rate of p62-positive intranuclear inclusions accounted for 18.5 ± 6.3% of the duct epithelial cells of sweat gland in all patients. Electron microscopy revealed that intranuclear inclusions included filamentous materials with no membrane components around or within them (Figures 3C,F).

## Pathological changes of urinary sediment

Different degrees of leukocytes, epithelial cells, erythrocytes, bacteria, and casts were observed in the urine sediment smear of all patients, while no intranuclear inclusions could be observed in the nuclei of the nucleated cells on Giemsa staining (Figure 4A). Five patients (5/10) received indwelling catheterization before or during hospitalization, and three patients (3/5) showed urinary tract infection in routine urine examination. Therefore, more urine sediments were collected from these 3 patients, and more nucleated cells were observed under the light microscope. Urine sediment smears of all patients were stained for p62 antibody through both immunohistochemistry and immunofluorescence. P62-positive materials could be observed in the cytoplasm of sediment cells in all patients and controls (Figure 4B), but p62-positive intranuclear inclusions were only observed in 3 patients with urinary tract infection (Figures 4C–F). The mean rate of cells with p62-positive inclusions accounted for only 3.5 ± 1.2% of the sedimentary cells in the 3 patients (3.2, 2.5, and 4.9%, respectively). The positive rate of skin biopsy was significantly higher than that of urine sediment ($p < 0.01$). Electron

10.3389/fnagi.2022.977604

TABLE 2 Electrophysiological changes in 10 patients with neuronal intranuclear inclusion disease (NIID).

| P | Age (y)* | Motor NCV | | | | | | | | | | | | Sensory NCV | | | | | |
|---|---|---|---|---|---|---|---|---|---|---|---|---|---|---|---|---|---|---|---|
| | | Median nerve | | | Ulnar nerve | | | Peroneal nerve | | | Tibial nerve | | | Median nerve | | Sup peron. nerve | | Sural nerve | |
| | | DML (≤4.0 ms) | CV (≥50 m/s) | CMAP (≥4.0 mV) | DML (≤3.0 ms) | CV (≥50 m/s) | CMAP (≥3.5 mV) | DML (≤5.3 ms) | CV (≥40 m/s) | CMAP (≥2.0 mV) | DML (≤5.0 ms) | CV (≥40 m/s) | CMAP (≥3.5 mV) | CV (≥50 m/s) | SNAP (≥5 μV) | CV (≥40 m/s) | SNAP (≥1 μV) | CV (≥40 m/s) | SNAP (≥1 μV) |
| 1 | 70 | 3.7 | 45 | 7.4 | 3.3 | 49 | 8.2 | 4.9 | 55 | 3.3 | 4.5 | 36 | 6.5 | 46 | 3.5 | NA | NA | 38 | 4.8 |
| 2 | 54 | 4.3 | 47 | 4.8 | 3.5 | 48 | 5.5 | 3.8 | 38 | 3.0 | NA | NA | NA | 40 | 5.7 | NA | NA | NR | NR |
| 3 | 69 | 3.6 | 48 | 5.3 | 2.1 | 55 | 8.8 | 4.7 | 36 | 2.7 | 4.5 | 33 | 8.8 | 46 | 2.3 | 44 | 2.6 | NA | NA |
| 4 | 73 | 4.2 | 50 | 6.4 | 2.9 | 52 | 7.2 | 5.9 | 37 | 0.1 | 4.0 | 36 | 7.3 | 45 | 16.7 | NA | NA | 48 | 6.7 |
| 5 | 66 | 4.1 | 33 | 3.3 | 3.0 | 37 | 2.7 | 6.5 | 26 | 0.8 | 6.7 | 29 | 1.5 | 38 | 3.1 | NR | NR | 30 | 0.9 |
| 6 | 67 | 4.3 | 52 | 5.5 | 2.8 | 51 | 7.1 | 3.8 | 40 | 5.5 | 4.5 | 40 | 5.7 | 54 | 11.9 | 42 | 2.8 | 35 | 4.5 |
| 7 | 64 | 3.6 | 38 | 3.5 | 2.7 | 40 | 3.4 | 4.1 | 38 | 1.5 | 3.7 | 34 | 4.2 | 39 | 9.3 | 27 | 3.2 | 32 | 5.9 |
| 8 | 63 | 3.3 | 45 | 6.6 | 3.6 | 47 | 4.2 | 3.8 | 33 | 3.6 | NA | NA | NA | 48 | 4.8 | NR | NR | NR | NR |
| 9 | 64 | 4.7 | 37 | 3.8 | 2.5 | 50 | 4.5 | 3.9 | 35 | 1.4 | 4.4 | 36 | 3.4 | 35 | 4.2 | 42 | 4.6 | NA | NA |
| 10 | 69 | 3.9 | 48 | 9.7 | 2.6 | 53 | 5.7 | 6.0 | 37 | 2.6 | 6.5 | 39 | 3.8 | 46 | 6.4 | 31 | 4.2 | NA | NA |

*Age at examination; reference value at age of 65 years in our lab. CMAP, compound motor action potential; CV, conduction velocity; DML, distal motor latency; SNAP, sensory nerve action potential; NA, not available; NR, no response; NCV, nerve conduction velocity.




FIGURE 1
Cerebral magnetic resonance imaging (MRI) features of neuronal intranuclear inclusion disease (NIID) patients. Diffusion weighted imaging (DWI) showed curve-like hyperintensity along the corticomedullary junction **(A)**; DWI also showed lesions in the corpus callosum **(B)**; T2-weighted showed symmetrical white matter lesions **(C)**; Contrast T1-weighted showed the left temporal occipital cortical edema with enhancement **(D)**.

microscopy revealed filamentous inclusions in the nuclei of urinary neutrophils (Figures 5A–C) or monocyte (Figures 5D–F) in the patients.

## Discussion

In the period when autopsy pathology was the main diagnostic method, our understanding for the NIID was mainly limited to the nervous system (Cao et al., 2021; Fan et al., 2022; Huang et al., 2022). However, with the discovery of the NIID causative gene, the understanding about the disease was already beyond the scope of the previous cognition (Deng et al., 2019; Ishiura et al., 2019; Sone et al., 2019; Tian et al., 2019). In this study, the NIID patients showed great clinical heterogeneity, while deep analysis of the phenotypic features of the patients revealed some clues to the diagnosis. First, episodic symptoms were very common in our patients. Seven patients presented with episodic symptoms, including sudden disturbance of consciousness, sudden psychiatric disorder, and sudden headache, and some patients also experienced multiple episodes of fever, abdominal pain, and nausea and vomiting in the course of the disease. The duration of these episodic symptoms could vary greatly, but the symptoms were reversible after symptomatic treatment. Second, all patients in this

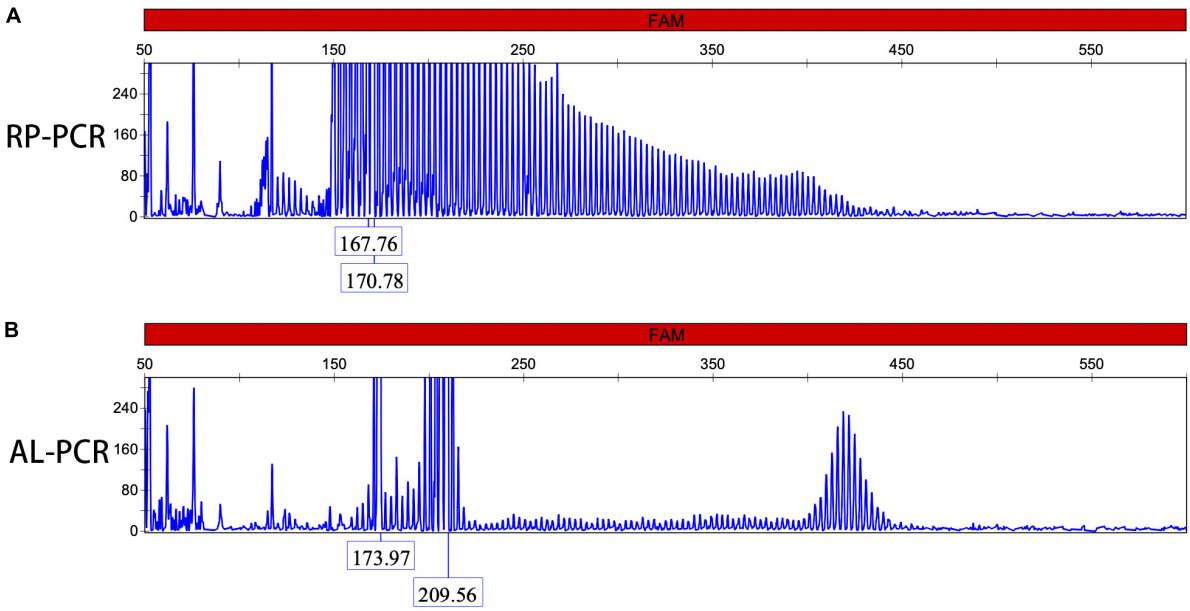


FIGURE 2
Dynamic variant of the *NOTCH2NLC* gene. Repeat-primed polymerase chain reaction (RP-PCR) chromatogram of patients 1 showed a long saw-tooth curve, indicating the presence of CGG repeat expansion **(A)**; Amplicon length polymerase chain reaction (AL-PCR) showed that the number of CGG repeat was 102 **(B)**.

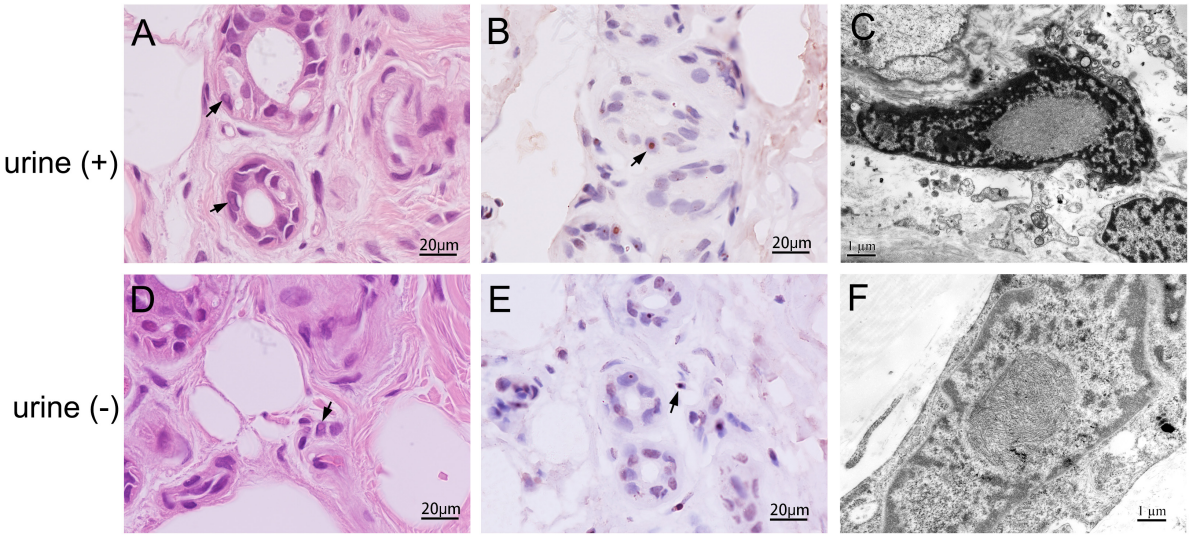


FIGURE 3
Skin pathology of neuronal intranuclear inclusion disease (NIID) patients with positive and negative urine sediment. H&E staining showed eosinophilic intranuclear inclusions in the nuclei of epithelial cells of the skin sweat gland ducts (Panels **A,D**, arrow); anti-p62 immunohistochemical staining showed positive intranuclear inclusions (Panels **B,E**, arrow); The intranuclear inclusions were seen as filamentous materials under electron microscope **(C,F)**.

cohort showed varying degrees of peripheral neuropathy. Some patients had no clinical symptoms of peripheral neuropathy, but electrophysiological studies exhibited that there were length-dependent sensorimotor demyelinating neuropathy, mainly characterized by mild NCV reduction and latency delay (Liao et al., 2022). Demyelinating impairment in these patients was more extensive and severe than axonal impairment, which might partly explain the absence of obvious neuropathy symptoms in some NIID cases. Third, in addition to the prominent neurological symptoms, these patients also showed

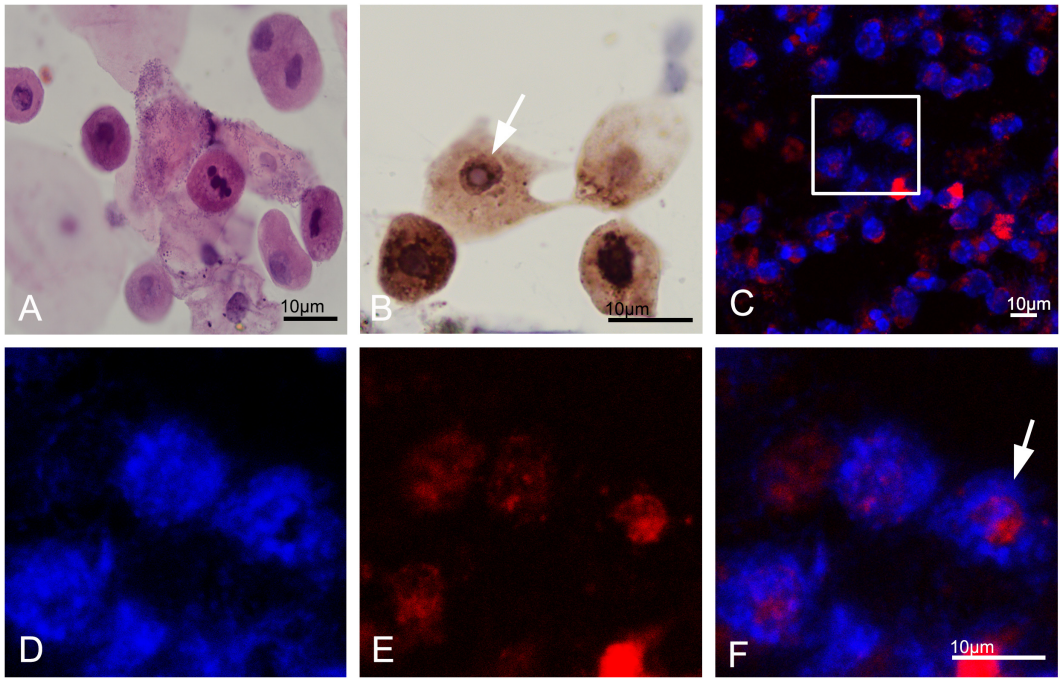


FIGURE 4
Urine cytology in neuronal intranuclear inclusion disease (NIID) patients. Leukocytes, epithelial cells, and epithelial cells were observed in the urinary sediment on Giemsa staining **(A)**. Immunohistochemistry showed p62-positive materials in the cytoplasm of sediment cells in patient 1 (Panel **B**, arrow). Immunofluorescence revealed that p62-positive intranuclear inclusions were observed in patient 1 (Panels **C–F** were magnification, arrow).

multi-system symptoms, such as dry cough, paroxysmal abdominal pain, and paroxysmal nausea and vomiting (Chen et al., 2020a). Finally, the symptoms in some NIID patients were non-specific. Whether it was paroxysmal symptoms, autonomic nervous disorders or other visceral symptoms, they were easily neglected in the context of chronic degenerative diseases. In fact, the timely diagnosis in most our patients benefited from the characteristic features of cerebral MRI rather than the clinical phenotype.

In this study, nine of ten patients showed curve-like DWI high-intensity along the corticomedullary junction mainly in the fronto-parietal lobe, which was common in adult NIID patients, and also a specific radiological biomarker for the clinical diagnosis of NIID patients (Sone et al., 2014). The pathological basis of these imaging change may be associated with the progressive spongiform degeneration of subcortical U fibers (Yokoi et al., 2016). Our patients also presented with symmetrical distribution of white matter lesions, which were thought to be closely associated with oligodendrocyte degeneration. Abnormal CGG repeat expansion in the *NOTCH2NLC* gene was a major cause of non-vascular white matter lesions, so the characteristics of white matter lesions should be emphasized when interpreting the images of NIID patients (Liu et al., 2022). Meanwhile, two patients had persistent DWI hyperintensities in the corpus callosum. Previous study had reported this imaging feature, which might be related to degeneration of the large projective fibers of the corpus callosum (Wang et al., 2020). Notably, one patient did not have curve-like DWI high intensity and no white matter lesions, but temporo-occipital cortex edema and enhancement were the main image changes, similar to mitochondrial encephalomyopathy. Previous studies had reported a few cases of this distinct subtype of NIID (Liang et al., 2020).

Since the discovery of CGG repeat expansion in the 5′UTR of *NOTCH2NLC*, there have been more and more reports of expansion mutation, and the reported cases were mainly concentrated in Asia rather than Europe (Chen et al., 2020b). At present, it was believed that the number of CGG repeat in *NOTCH2NLC* was less than 40 in the normal controls. The number of CGG repeat between 41 and 60 was intermediate and might be associated with a few Parkinson's disease or essential tremor (Fan et al., 2022). The number of CGG repeat more than 60 was pathogenic, and the typical phenotype of NIID usually had about 120 repeats. The number of CGG repeat in the 10 patients was more than 60, and the average number was approximately to 120. Therefore it was necessary to measure the CGG repeat number to determine its pathogenicity in the genetic diagnosis of NIID patients. The repeat expansion in *NOTCH2NLC* also showed some rare clinical phenotypes, such as neurodegenerative dementia (Jiao et al., 2020), non-vascular

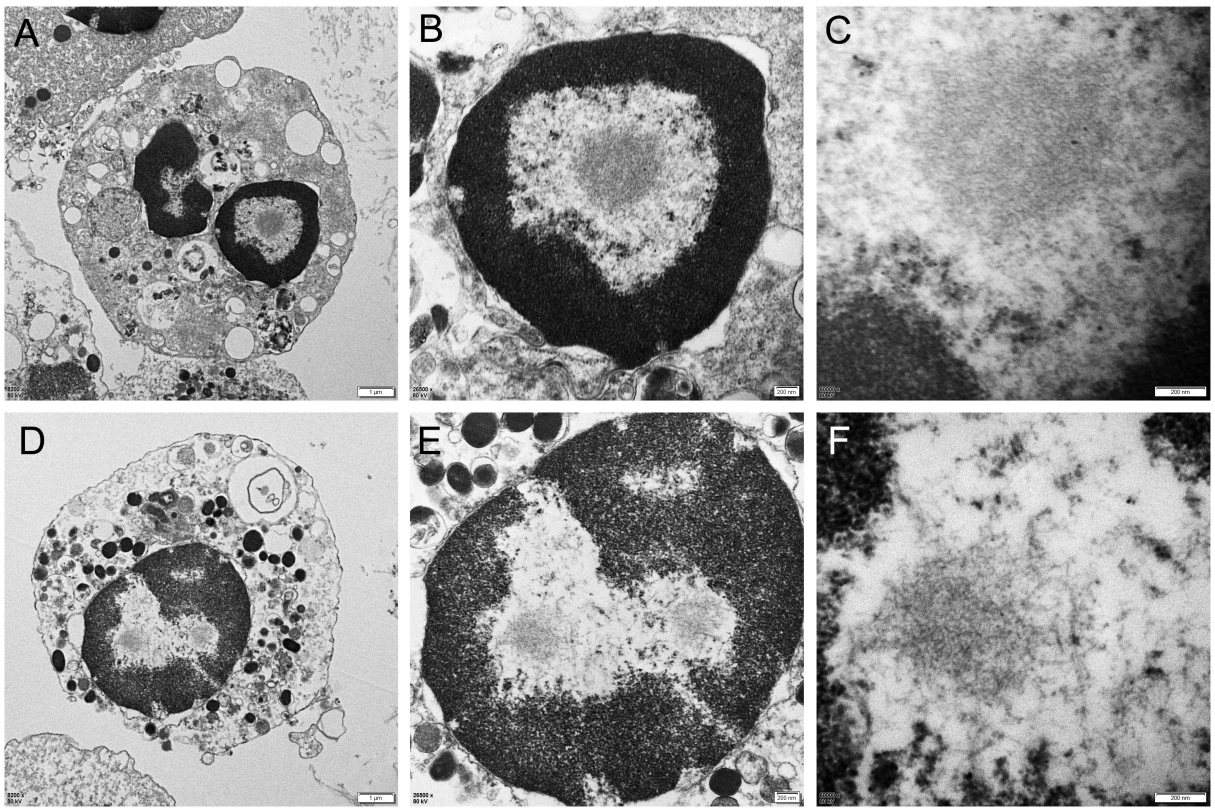


FIGURE 5
Electron microscopy of urine sediment cells. In the patient 1, electron microscopy showed the appearance of filamentous inclusions in a neutrophil (Panels **A–C** were magnification). In the patient 6, electron microscopy showed the appearance of filamentous inclusions in a monocyte (Panels **D–F** were magnification).

leukoencephalopathy (Liu et al., 2022), motor neuron disease (Yuan et al., 2020), sensorimotor with autonomic neuropathy (Wang et al., 2021), distal motor neuropathy (Wu et al., 2022), as well as oculopharyngeal distal myopathy (OPDM) (Yu et al., 2021). Because of the small number of these cases, the relationship between the clinical phenotype and the number of CGG repeat had not been established, but distal motor neuropathy and OPDM were generally considered to have more repeats. In addition, some studies had shown that carriers with more than 300 repeats exhibited very mild symptoms or no symptoms (Deng et al., 2022).

Neuronal intranuclear inclusion disease was named after its pathological characteristics. Therefore, the pathological examination of the intranuclear inclusions was still considered as one of the indispensable procedures for diagnosing the disease, although the disease-causative gene had been cloned. Sone et al. (2011) found that there were eosinophilic inclusions in the nuclei of sweat gland duct epithelial cells, adipocytes, and fibroblasts in the skin biopsies of NIID patients, and their composition and structural characteristics were almost the same as those in the CNS (Sone et al., 2011). Subsequent studies also confirmed the high consistency between the intranuclear inclusions of skin cells and the abnormal CGG repeat expansion in *NOTCH2NLC* (Deng et al., 2019). Our study also confirmed this association between genetic mutation and skin pathology. Collectively, skin biopsy had become the most important pathological diagnosis method for NIID.

Due to the great heterogeneity of NIID, especially when patients lacked typical features, such as DWI high-intensity along the corticomedullary junction, we needed more evidence to support the diagnosis of NIID or distinguish the diseases from other neurodegenerative diseases. However, open skin biopsy should not be routinely performed for every patient clinically suspected as NIID. In addition, conventional genetic screening was expensive and time-consuming. Considering that there were eosinophilic inclusions in the nuclei of renal tubular epithelial cells, we intended to search the intranuclear inclusions in the exfoliative cells in urine sediment cells (Sone et al., 2016). Among the 10 NIID patients confirmed by genetic screening and skin biopsy pathology, we found typical intranuclear inclusions in urine sediment cells of 3 patients by immunostaining, but the cell type could not be determined based the cell morphology alone. We further confirmed the filamentous inclusions in the nuclei of neutrophils and monocytes from the urine sediment by

electron microscopy. Although the sensitivity of urine sediment was relatively lower than that of skin biopsy, it showed a certain value of application as a non-invasive examination.

In this study, there were some limitations in the pathological examination of urinary sediment cells. (1) The quantity and quality of cell sediment of 500 ml urine were quite different in these NIID patients, which directly affected the quality of subsequent cell smears and electron microscope examination. It might improve the positive rate of examination to collect more urine for cell sediment. (2) Because of the small amount of urine sediment, we could not conduct quantitative analysis before preparing the cell smear, resulting in a great difference in the cell density of the smear. The number of smear cells in some patients was too sparse to be observed, but the number of smear cells in other patients was too crowded to interfere with the observations. This might partly explain the low positive rate of urine sediment cytology for the pathological diagnosis of NIID. (3) Since the protocol characteristics of the study design and the relatively insufficient number of NIID cases, the area under curve (AUC) of receiver operating characteristic curve (ROC) could not be calculated in this study. In order to evaluate the diagnostic significance of urine cytology, a large-sample controlled trial will be needed in the future. (4) We found that p62-positive intranuclear inclusions were only observed in the three patients with urinary tract infection or indwelling catheterization, indicating that this method had some limitations, and urinary tract infection could improve the quantity and quality of urine sediment cells. Conversely, the limitation might be improved in patients with urinary tract infection, if urine cytology was performed before antibiotic treatment. (5) Most nucleated cells on the urine smear showed p62-positive materials in the cytoplasm. The epithelial cells and inflammatory cells in urine might gradually degenerate and lead to an increase in p62 levels in the cytoplasm (Ruppert et al., 2015), although the exact mechanism of p62 cytoplasmic positivity needed to be further explored. The p62-positive cytoplasmic materials greatly interfered with the rapid determination of intranuclear inclusions. If some specific antibodies can easily identify cell types and sources of urine sediment, the positive rate of urine cytology may be further improved.

In summary, our study showed that NIID had great clinical heterogeneity, of which episodic symptoms were various and non-specific. Skin biopsy had almost identical diagnostic value to the CGG repeat expansion in the *NOTCH2NLC* gene. Cytological pathology, a non-invasive and convenient pathological examination, showed p62-positive intranuclear inclusions in urine sediment cells of some patients with urinary tract infection, although the positive rate of urine sediment was not as high as that of skin biopsy. The method of urine cytology needed to be further optimized to improve the positive rate, and the number of patients needed to be further expanded.

## Data availability statement

The datasets presented in this study can be found in online repositories. The names of the repository/repositories and accession number(s) can be found in the article/supplementary material.

## Ethics statement

This research was approved by Ethics Committee of the First Affiliated Hospital of Nanchang University. The patients/participants provided their written informed consent to participate in this study. Written informed consent was obtained from the individual(s) for the publication of any potentially identifiable images or data included in this article.

## Author contributions

YYZ and PH: manuscript writing and data management. ZH, YP, YLZ, and MZ: data collection, data management, methodology, and biopsy. YY: specimen processing. ZW and JD: genetic testing, resources, supervision, and funding. DH: supervision, conceptualization, research, writing, and funding. All authors contributed to the article and approved the submitted version.

## Funding

This work was supported by the National Natural Science Foundation of China (Grants 82071409, 82171846, 82160252, 82270688, and U20A20356), Science and Technology Project of Jiangxi Health Commission (202110028), Double Thousand Talents Program of Jiangxi Province (jxsq2019101021), Peking University Medicine Fund of Fostering, Young Scholars' Scientific and Technological Innovation (BMU2021PY003), and Capital's Funds for Health Improvement and Research (2022-4-40716).

## Acknowledgments

The authors would like to appreciate the patients and their families for their enthusiasm and participation in this study.

## Conflict of interest

The authors declare that the research was conducted in the absence of any commercial or financial relationships that could be construed as a potential conflict of interest.

## Publisher's note



## References

Cao, L., Yan, Y., and Zhao, G. (2021). NOTCH2NLC-related repeat expansion disorders: An expanding group of neurodegenerative disorders. *Neurol. Sci.* 42, 4055–4062.

Chen, Z., Yan, Y. W., Jaunmuktane, Z., Tucci, A., Sivakumar, P., Gagliano Taliun, S. A., et al. (2020b). Neuronal intranuclear inclusion disease is genetically heterogeneous. *Ann. Clin. Transl. Neurol.* 7, 1716–1725.

Chen, H., Lu, L., Wang, B., Cui, G., Wang, X., Wang, Y., et al. (2020a). Re-defining the clinicopathological spectrum of neuronal intranuclear inclusion disease. *Ann. Clin. Transl. Neurol.* 7, 1930–1941. doi: 10.1002/acn3.51189

Deng, J., Gu, M., Miao, Y., Yao, S., Zhu, M., Fang, P., et al. (2019). Long-read sequencing identified repeat expansions in the 5'UTR of the NOTCH2NLC gene from Chinese patients with neuronal intranuclear inclusion disease. *J. Med. Genet.* 56, 758–764. doi: 10.1136/jmedgenet-2019-106268

Deng, J., Zhou, B., Yu, J., Han, X., Fu, J., Li, X., et al. (2022). Genetic origin of sporadic cases and RNA toxicity in neuronal intranuclear inclusion disease. *J. Med. Genet.* 59, 462–469. doi: 10.1136/jmedgenet-2020-107649

Fan, Y., Xu, Y., and Shi, C. (2022). NOTCH2NLC-related disorders: The widening spectrum and genotype-phenotype correlation. *J. Med. Genet.* 59, 1–09. doi: 10.1136/jmedgenet-2021-107883

Fang, P., Yu, Y., Yao, S., Chen, S., Zhu, M., Chen, Y., et al. (2020). Repeat expansion scanning of the NOTCH2NLC gene in patients with multiple system atrophy. *Ann. Clin. Transl. Neurol.* 7, 517–526. doi: 10.1002/acn3.51021

Huang, X. R., Tang, B. S., Jin, P., and Guo, J. F. (2022). The phenotypes and mechanisms of NOTCH2NLC-related GGC repeat expansion disorders: A comprehensive review. *Mol. Neurobiol.* 59, 523–534. doi: 10.1007/s12035-021-02616-2

Ishiura, H., Shibata, S., Yoshimura, J., Suzuki, Y., Qu, W., Doi, K., et al. (2019). Noncoding CGG repeat expansions in neuronal intranuclear inclusion disease, oculopharyngodistal myopathy and an overlapping disease. *Nat. Genet.* 51, 1222–1232. doi: 10.1038/s41588-019-0458-z

Jiao, B., Zhou, L., Zhou, Y., Weng, L., Liao, X., Tian, Y., et al. (2020). Identification of expanded repeats in NOTCH2NLC in neurodegenerative dementias. *Neurobiol. Aging* 89, 141–142. doi: 10.1016/j.neurobiolaging.2020.01.010

Liang, H., Wang, B., Li, Q., Deng, J., Wang, L., Wang, H., et al. (2020). Clinical and pathological features in adult-onset NIID patients with cortical enhancement. *J. Neurol.* 267, 3187–3198. doi: 10.1007/s00415-020-09945-7

Liao, Y. C., Chang, F. P., Huang, H. W., Chen, T. B., Chou, Y. T., Hsu, S. L., et al. (2022). GGC repeat expansion of NOTCH2NLC in Taiwanese patients with inherited neuropathies. *Neurology* 98, e199–e206. doi: 10.1212/WNL.0000000000013008

Liu, Y. H., Chou, Y. T., Chang, F. P., Lee, W. J., Guo, Y. C., Chou, C. T., et al. (2022). Neuronal intranuclear inclusion disease in patients with adult-onset non-vascular leukoencephalopathy. *Brain* 12:awac135. doi: 10.1093/brain/awac135

Liufu, T., Zheng, Y., Yu, J., Yuan, Y., Wang, Z., Deng, J., et al. (2022). The polyG diseases: A new disease entity. *Acta Neuropathol. Commun.* 10:79. doi: 10.1186/s40478-022-01383-y

Lu, X., and Hong, D. (2021). Neuronal intranuclear inclusion disease: Recognition and update. *J. Neural Transm.* 128, 295–303. doi: 10.1007/s00702-021-02313-3

Miki, Y., Kamata, K., Goto, S., Sakuraba, H., Mori, F., Yamagata, K., et al. (2022). The clinical and neuropathological picture of adult neuronal intranuclear inclusion disease with no radiological abnormality. *Neuropathology.* 42, 204–211. doi: 10.1111/neup.12792

Ruppert, T., Schumann, A., Gröne, H. J., Okun, J. G., Kölker, S., Morath, M. A., et al. (2015). Molecular and biochemical alterations in tubular epithelial cells of patients with isolated methylmalonic aciduria. *Hum. Mol. Genet.* 24, 7049–7059. doi: 10.1093/hmg/ddv405

Shi, C. H., Fan, Y., Yang, J., Yuan, Y. P., Shen, S., Liu, F., et al. (2021). NOTCH2NLC intermediate-length repeat expansions are associated with Parkinson disease. *Ann. Neurol.* 89, 182–187.

Sone, J., Kitagawa, N., Sugawara, E., Iguchi, M., Nakamura, R., Koike, H., et al. (2014). Neuronal intranuclear inclusion disease cases with leukoencephalopathy diagnosed via skin biopsy. *J. Neurol. Neurosurg Psychiatry.* 85, 354–356. doi: 10.1136/jnnp-2013-306084

Sone, J., Mitsuhashi, S., Fujita, A., Mizuguchi, T., Hamanaka, K., Mori, K., et al. (2019). Long-read sequencing identifies GGC repeat expansions in NOTCH2NLC associated with neuronal intranuclear inclusion disease. *Nat. Genet.* 51, 1215–1221.

Sone, J., Mori, K., Inagaki, T., Katsumata, R., Takagi, S., Yokoi, S., et al. (2016). Clinicopathological features of adult-onset neuronal intranuclear inclusion disease. *Brain* 139, 3170–3186.

Sone, J., Tanaka, F., Koike, H., Inukai, A., Katsuno, M., Yoshida, M., et al. (2011). Skin biopsy is useful for the antemortem diagnosis of neuronal intranuclear inclusion disease. *Neurology* 76, 1372–1376.

Sun, Q. Y., Xu, Q., Tian, Y., Hu, Z. M., Qin, L. X., Yang, J. X., et al. (2020). Expansion of GGC repeat in the human-specific NOTCH2NLC gene is associated with essential tremor. *Brain* 143, 222–233. doi: 10.1093/brain/awz372

Tian, Y., Wang, J. L., Huang, W., Zeng, S., Jiao, B., Liu, Z., et al. (2019). Expansion of human-specific GGC repeat in neuronal intranuclear inclusion disease-related disorders. *Am. J. Hum. Genet.* 105, 166–176. doi: 10.1016/j.ajhg.2019.05.013

Wang, H., Yu, J., Yu, M., Deng, J., Zhang, W., Lv, H., et al. (2021). GGC repeat expansion in the NOTCH2NLC gene is associated with a phenotype of predominant motor-sensory and autonomic neuropathy. *Front. Genet.* 12:694790.

Wang, Y., Wang, B., Wang, L., Yao, S., Zhao, J., Zhong, S., et al. (2020). Diagnostic indicators for adult-onset neuronal intranuclear inclusion disease. *Clin. Neuropathol.* 39, 7–18.

Wu, C., Xiang, H., Chen, R., Zheng, Y., Zhu, M., Chen, S., et al. (2022). Genetic spectrum in a cohort of patients with distal hereditary motor neuropathy. *Ann. Clin. Transl. Neurol.* 9, 633–643. doi: 10.1002/acn3.51543

Yokoi, S., Yasui, K., Hasegawa, Y., Niwa, K., Noguchi, Y., Tsuzuki, T., et al. (2016). Pathological background of subcortical hyperintensities on diffusion-weighted images in a case of neuronal intranuclear inclusion disease. *Clin. Neuropathol.* 35, 375–380. doi: 10.5414/NP300961

Yu, J., Deng, J., Guo, X., Shan, J., Luan, X., Cao, L., et al. (2021). The GGC repeat expansion in NOTCH2NLC is associated with oculopharyngodistal myopathy type 3. *Brain* 144, 1819–1832. doi: 10.3389/fgene.2021.694790

Yuan, Y., Liu, Z., Hou, X., Li, W., Ni, J., Huang, L., et al. (2020). Identification of GGC repeat expansion in the NOTCH2NLC gene in amyotrophic lateral sclerosis. *Neurology* 95, e3394–e3405. doi: 10.1212/WNL.0000000000010945

frontiers | Frontiers in Aging Neuroscience

TYPE Review
PUBLISHED 13 September 2022
DOI 10.3389/fnagi.2022.934725



OPEN ACCESS

EDITED BY
Ulises Gomez-Pinedo,
Health Research Institute of the Hospital Clínico San Carlos, Spain

REVIEWED BY
María José Gil Moreno,
Hospital Clínico San Carlos, Spain
Dimitra Dafou,
Aristotle University of Thessaloniki, Greece

*CORRESPONDENCE
Xingshun Xu
xingshunxu@suda.edu.cn
Miao Sun
miaosunsuda@163.com
Bo Wan
wanbo@suda.edu.cn

†These authors have contributed equally to this work

SPECIALTY SECTION
This article was submitted to Alzheimer's Disease and Related Dementias, a section of the journal Frontiers in Aging Neuroscience

RECEIVED 03 May 2022
ACCEPTED 22 August 2022
PUBLISHED 13 September 2022

CITATION
Liu Y, Li H, Liu X, Wang B, Yang H, Wan B, Sun M and Xu X (2022) Clinical and mechanism advances of neuronal intranuclear inclusion disease. *Front. Aging Neurosci.* 14:934725. doi: 10.3389/fnagi.2022.934725



# Clinical and mechanism advances of neuronal intranuclear inclusion disease

Yueqi Liu[1,2†], Hao Li[1,2†], Xuan Liu[1], Bin Wang[2,3], Hao Yang[3], Bo Wan[2*], Miao Sun[3*] and Xingshun Xu[1,2,4*]

[1]Department of Neurology, The First Affiliated Hospital of Soochow University, Suzhou, China, [2]Institute of Neuroscience, Soochow University, Suzhou, China, [3]Institute for Fetology, The First Affiliated Hospital of Soochow University, Suzhou, China, [4]Jiangsu Key Laboratory of Neuropsychiatric Diseases, Soochow University, Suzhou, Jiangsu, China

Due to the high clinical heterogeneity of neuronal intranuclear inclusion disease (NIID), it is easy to misdiagnose this condition and is considered to be a rare progressive neurodegenerative disease. More evidence demonstrates that NIID involves not only the central nervous system but also multiple systems of the body and shows a variety of symptoms, which makes a clinical diagnosis of NIID more difficult. This review summarizes the clinical symptoms in different systems and demonstrates that NIID is a multiple-system intranuclear inclusion disease. In addition, the core triad symptoms in the central nervous system, such as dementia, parkinsonism, and psychiatric symptoms, are proposed as an important clue for the clinical diagnosis of NIID. Recent studies have demonstrated that expanded GGC repeats in the 5′-untranslated region of the NOTCH2NLC gene are the cause of NIID. The genetic advances and possible underlying mechanisms of NIID (expanded GGC repeat-induced DNA damage, RNA toxicity, and polyglycine-NOTCH2NLC protein toxicity) are briefly summarized in this review. Interestingly, inflammatory cell infiltration and inflammation were observed in the affected tissues of patients with NIID. As a downstream pathological process of NIID, inflammation could be a therapeutic target for NIID.

KEYWORDS

**neuronal intranuclear inclusion disease, neurodegenerative diseases, inflammation, NOTCH2NLC, nucleotide repeat expansion disorders**

## Introduction

Neuronal intranuclear inclusion disease (NIID) was first described in 1968 and is considered to be a rare neurodegenerative disease (Lindenberg et al., 1968). With the development of imaging technology and the increasing knowledge about this disease, more NIID cases have been reported in many countries (Takahashi-Fujigasaki et al., 2016); however, compared with other neurodegenerative diseases, its incidence is still extremely low according to current case reports. The characterization of its

clinical manifestations is symptom heterogeneity, including cognitive dysfunction, Parkinsonism-like behavior, peripheral neuropathy, cerebellar ataxia, tremor, gait instability, myotonia, involuntary movement, muscle weakness, seizure, and headache (Sone et al., 2016; Takahashi-Fujigasaki et al., 2016; Tian et al., 2019; Wang et al., 2019a). Similar to amyloid plaques in Alzheimer's disease (AD) and α-synuclein aggregates in Parkinson's disease (PD), intranuclear eosinophil inclusion bodies are the main characteristic pathological changes in the central and peripheral nervous systems, as well as in various organs (Takahashi-Fujigasaki, 2003). However, unlike AD and PD, which are most sporadic in the population, most recently reported NIID cases are familial (Sone et al., 2016).

Repeated GGC expansion in the 5′UTR of the NOTCH2NLC gene was identified as the causative mutation for NIID in Japan and China in 2019 (Ishiura et al., 2019; Sone et al., 2019; Tian et al., 2019). These findings provide a potential and important criterion for the diagnosis of NIID, owing to the rapidly increased number of reported NIID cases. However, some studies also reported that some symptoms or signs, such as essential tremor and leukoencephalopathy, are associated with GGC repeat expansion in the NOTCH2NLC gene (Okubo et al., 2019; Sun et al., 2020). Moreover, in many studies, patients previously diagnosed with AD, PD, or frontotemporal dementia (FTD) were found to have this GGC repeat expansion in the NOTCH2NLC gene (Sone et al., 2019; Jiao et al., 2020; Sun et al., 2020). Due to the heterogeneity of the clinical phenotypes of NIID, clinical diagnosis of NIID is still difficult. In this review, we summarize the advances in the clinical features, pathology, genetics, and diagnosis of NIID, as well as NOTCH2NLC-related repeat expansion disorders.

## Clinical symptoms of neuronal intranuclear inclusion disease

Hundreds of NIID cases have been reported so far, and the most common feature of NIID is symptom heterogeneity; different families and individuals have different symptoms of NIID. In early clinical studies, the major clinical manifestations of previously described cases were cerebral cortical dysfunction and extrapyramidal symptoms, including cognitive dysfunction and dementia (Wang et al., 2020a; Zhang et al., 2020), PD-like behavior (Wang et al., 2020c), tremor (Kitagawa et al., 2014), ataxia (Imai et al., 2018), muscle weakness (Qin et al., 2021), bradykinesia, paroxysmal encephalopathy (Li et al., 2020b), and stroke-like episodes (Lin et al., 2020). However, except for nervous system symptoms, other symptoms, such as cough, vomiting (Okamura et al., 2020), retinal degeneration (Nakamura et al., 2020), and bladder dysfunction (Chen et al., 2020c), have been increasingly reported in many cases (Schuffler et al., 1978; Kimber et al., 1998; Horino et al., 2018). Here, we summarize the common nervous system symptoms and non-nervous system symptoms related to NIID, the details are presented in **Figure 1** and **Table 1**.

### Nervous system symptoms

#### Dementia

Dementia was one of the main symptoms described in a patient with NIID in 1978 (Schuffler et al., 1978). Since then, an increasing number of NIID patients with dementia have been reported, and patients with dementia are considered to be a subtype group of patients with NIID (Tian et al., 2019). Sone et al. (2016) analyzed the clinical features in 54 patients with NIID and found that dementia was the most prominent initial symptom in sporadic adult-onset NIID and familial NIID patients who are more than 40 years old. Araki et al. (2016) performed neuropsychological assessments in patients with NIID and revealed that language and executive functions were more prominent in these patients with dementia. In these patients, brain magnetic resonance imaging (MRI) showed leukoaraiosis and global cortical atrophy, especially in the cingulate and the temporal cortex regions (Cupidi et al., 2019). Moreover, a decline in the Mini-Mental State Examination score was found in both sporadic and familial NIID cases (Sone et al., 2016). Some patients previously diagnosed with AD were found to have GGC repeat expansions in the NOTCH2NLC gene (Tian et al., 2019), implicating that NIID should be considered as a differential diagnosis of AD.

#### Parkinson's disease-like symptoms

Parkinson's disease-like symptoms are regarded as another common and typical representative symptom in patients with NIID (Tian et al., 2019). PD-like symptoms in patients with NIID include resting tremors, rigidity, walking difficulty, clumsiness, and ataxia (Sone et al., 2016). Patients with PD-like symptoms usually respond well to levodopa treatment but easily develop dopa-induced motor fluctuations (O'Sullivan et al., 2000; Vermilion et al., 2019). Typical NIID pathology was found in some families with symptoms of PD (Tian et al., 2019). Recently, more groups found that patients with a diagnosis of PD or essential tremor have expended GGC repeats in the NOTCH2NLC gene (Tian et al., 2019; Ma et al., 2020; Sun et al., 2020; Shi et al., 2021). However, some groups showed that PD-like symptoms were the early-stage symptoms of NIID (Chen et al., 2020b; Yang et al., 2021). Therefore, PD-like symptoms are the dominant phenotypes of NIID (Huang et al., 2021). Patients with familial PD or essential tremors should be considered for the diagnosis of NIID or NOTCH2NLC gene-related disorders.

#### Personality changes and mood disorders

It is worth noting that a significant proportion of patients with NIID have adverse changes in terms of mood and personality (Sone et al., 2016; Chen et al., 2020a), but due

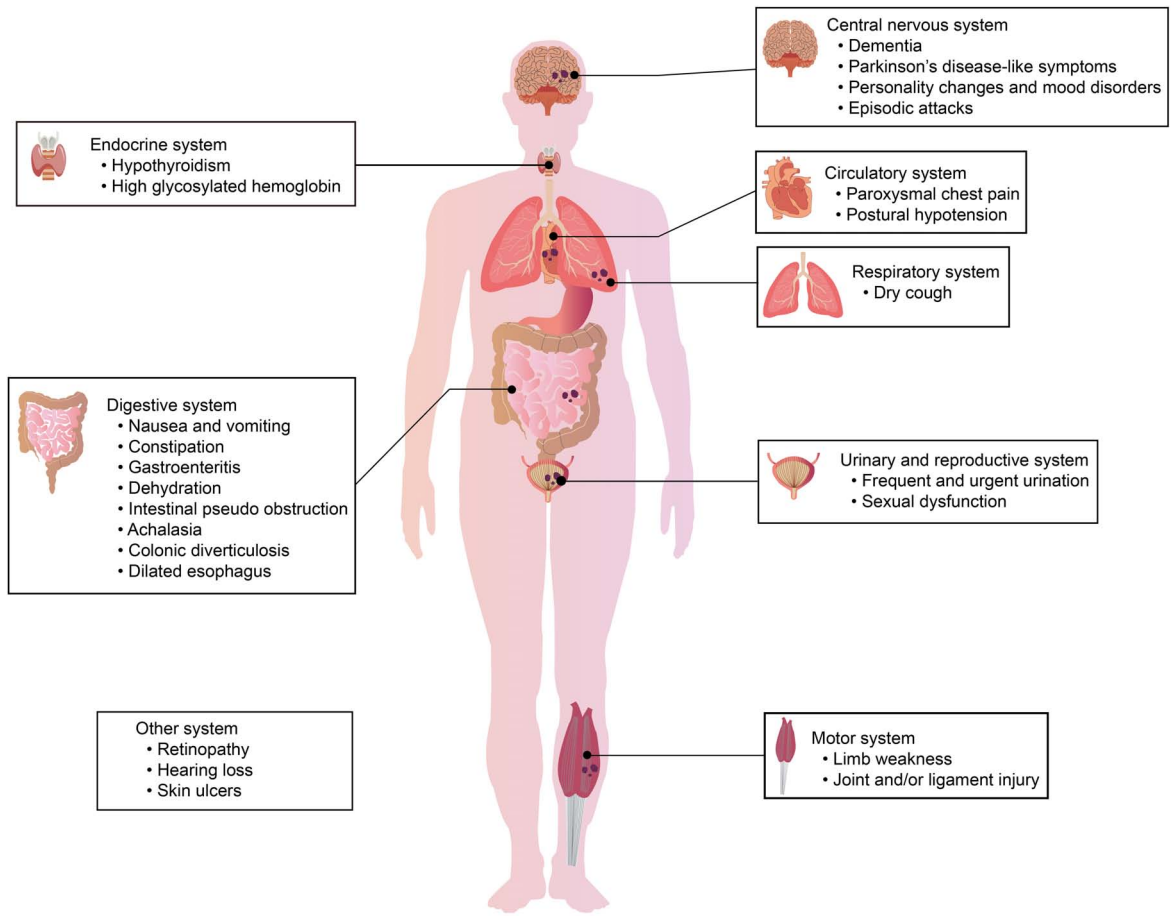


FIGURE 1
Clinical symptoms in different systems of patients with NIID. The clinical manifestations of NIID are highly heterogeneous. Patients with NIID may have symptoms/signs of the nervous system and/or symptoms/signs of other systems, including the respiratory system, urinary system, digestive system, and motor system.

to the non-specificity of these symptoms, personality changes and mood disorders are usually ignored in patients with NIID. Many patients with familial NIID gradually develop emotional instability, such as apathy, irritability, depression, and anxiety (Chen et al., 2020a). A previous case report also showed the presence of behavioral abnormalities in patients with NIID. Malandrini et al. (1996) reported a patient with NIID confirmed by a rectal biopsy having episodes of rage and aggressiveness that preceded other symptoms. Vermilion et al. (2019) reported that a NIID patient developed depression and anxiety at the age of 11 years, social isolation at 16 years, and increasing impulsivity at 17 years. Kawarabayashi et al. (2018) described a patient with NIID with the acute onset of apathy, and symptoms existed for a long time. In a recent study, approximately 60.8% of patients with NIID identified with genetic tests had different extents of abnormal behaviors, such as irritability, anxiety, depression, obsession, and impulsivity (Chen et al., 2020a). Based on the pathological and imaging results in patients with NIID (Sone et al., 2016; Chen et al., 2020a), it is reasonable that diffuse brain damage by neuronal intranuclear inclusion causes behavioral abnormalities. Therefore, abnormal behaviors or mood disorders are an ignored but important sub-phenotype of NIID.

## Peripheral nervous symptoms

Sone et al. (2016) showed the involvement of peripheral nerve injury in patients with NIID and found a delay in conduction velocity or a decrease in amplitude in the electromyogram of motor and sensory nerves. Hirose et al. (2018) proposed that abnormalities in nerve conduction velocity and somatosensory-evoked potentials may be the diagnostic basis of NIID. In addition, the reflexes in some patients with NIID were hyporeflexia (Hirose et al., 2018). A recent study reported a case of NIID with mitochondrial encephalomyopathy, lactic acidosis, and stroke (MELAS)-like episodes in chronic polyneuropathy, and this patient developed slowly progressing muscle weakness and paraesthesia in all extremities (Ishihara et al., 2020).

TABLE 1 The clinical symptoms of NIID in different systems.

| Systems | Symptoms and signs | References |
|---|---|---|
| **Nervous systems** | **Dementia-related symptoms** | |
| | Cognitive impairment | Kish et al., 1985; Goutieres et al., 1990; Lai et al., 2010; Aiba et al., 2016; Araki et al., 2016; Takeshita et al., 2017; Takumida et al., 2017; Hirose et al., 2018; Imai et al., 2018; Kawarabayashi et al., 2018; Nakamura et al., 2018; Liu et al., 2019b; Shindo et al., 2019; Yadav et al., 2019 |
| | Dementia | Sung et al., 1980; Garen et al., 1986; Sone et al., 2014; Aiba et al., 2016; Araki et al., 2016; Abe and Fujita, 2017; Yamada et al., 2017; Nakamura et al., 2018; Chen et al., 2019; Yadav et al., 2019 |
| | **PD-related symptoms** | |
| | Classic PD symptoms | Iizuka and Spalke, 1972; Kish et al., 1985; O'Sullivan et al., 2000; Lai et al., 2010; Wiltshire et al., 2010; Yoshimoto et al., 2017; Cupidi et al., 2019; Vermilion et al., 2019 |
| | Tremor | Haltia et al., 1984; Kish et al., 1985; Goutieres et al., 1990; Afshari and Kamarei, 2005; Kitagawa et al., 2014; Yamaguchi et al., 2018; Yadav et al., 2019 |
| | Ataxia | Lindenberg et al., 1968; Schuffler et al., 1978; Janota, 1979; Haltia et al., 1984; Soffer, 1985; Munoz-Garcia and Ludwin, 1986; Goutieres et al., 1990; Imai et al., 2018; Xiao et al., 2018; Yamaguchi et al., 2018 |
| | Dystonia | Haltia et al., 1984; Paviour et al., 2005; Lai et al., 2010; Takumida et al., 2017; Chen et al., 2018; Kawarabayashi et al., 2018; Liu et al., 2019a; Vermilion et al., 2019 |
| | Involuntary movements | Sung et al., 1980; Paviour et al., 2005; Takeshita et al., 2017; Hirose et al., 2018; Yamanaka et al., 2019 |
| | Gait disturbance/dyskinesia | Janota, 1979; O'Sullivan et al., 2000; Wiltshire et al., 2010; Yamada et al., 2017; Yoshimoto et al., 2017; Horino et al., 2018; Xiao et al., 2018; Liu et al., 2019b; Yadav et al., 2019 |
| | Hyporeflexia/ hyperreflexia | Kimber et al., 1998; O'Sullivan et al., 2000; Afshari and Kamarei, 2005; Araki et al., 2016; Imai et al., 2018; Kawarabayashi et al., 2018; Nakamura et al., 2018; Liu et al., 2019a,b |
| | **Mood-related symptoms** | |
| | Emotional lability | Sung et al., 1980; Haltia et al., 1984; Lai et al., 2010; Wiltshire et al., 2010; Hirose et al., 2018; Kawarabayashi et al., 2018; Yamaguchi et al., 2018; Vermilion et al., 2019 |
| | Abnormal behaviors | Goutieres et al., 1990; Sone et al., 2014; Han et al., 2019; Wang et al., 2019b |
| | **Others** | |
| | Muscle wasting | Malandrini et al., 1998; Yoshimoto et al., 2017; Omoto et al., 2018; Pilson et al., 2018; Xiao et al., 2018 |
| | Paroxysmal encephalopathy | Xiao et al., 2018; Wang et al., 2019b |
| | Recurrent headaches | Han et al., 2019; Qin et al., 2020 |
| | Sensory disturbance | Aiba et al., 2016; Araki et al., 2016; Sakurai et al., 2016; Abe and Fujita, 2017; Takeshita et al., 2017; Takumida et al., 2017; Nakamura et al., 2018; Omoto et al., 2018; Yamanaka et al., 2019 |
| | Epileptic episodes | Haltia et al., 1984; Patel et al., 1985; Pilson et al., 2018; Shindo et al., 2019; Vermilion et al., 2019 |
| **Circulatory system** | Cardiomyopathy | Oyer et al., 1991; Takumida et al., 2017; Yoshimoto et al., 2017; Yadav et al., 2019 |
| | Coronary atherosclerosis | Parker et al., 1987 |
| | Orthostatic hypotension | Aiba et al., 2016; Araki et al., 2016; Sakurai et al., 2016; Nakamura et al., 2018; Liu et al., 2019a; Vermilion et al., 2019 |
| **Digestive system** | Nausea and vomiting | Barnett et al., 1992; El-Rifai et al., 2006; Xiao et al., 2018; Han et al., 2019; Shindo et al., 2019 |
| | Constipation/diverticulosis | Lindenberg et al., 1968; Schuffler et al., 1978; Barnett et al., 1992; Aiba et al., 2016; Yamada et al., 2017; Vermilion et al., 2019 |
| | Gastroenteritis | Lindenberg et al., 1968; El-Rifai et al., 2006 |
| | Intestinal obstruction | El-Rifai et al., 2006; Yamaguchi et al., 2018 |
| **Respiratory system** | Bronchopneumonia | Kimber et al., 1998; Wiltshire et al., 2010; Takumida et al., 2017; Pilson et al., 2018; Shindo et al., 2019; Vermilion et al., 2019; Qin et al., 2020 |
| | Respiratory failure | Afshari and Kamarei, 2005; Paviour et al., 2005 |
| | Respiratory distress | Malandrini et al., 1998 |
| **Urinary and reproductive system** | Urinary dysfunction | Cupidi et al., 2019; Haltia et al., 1984; Han et al., 2019; Hirose et al., 2018; Horino et al., 2018; Imai et al., 2018; Kawarabayashi et al., 2018; Liu et al., 2019a; Nakamura et al., 2018; Shindo et al., 2019; Takumida et al., 2017; Yadav et al., 2019; Yamaguchi et al., 2018 |
| | Sexual dysfunction | Zannolli et al., 2002; Han et al., 2019 |
| | Glomerular lesion | Horino et al., 2018; Motoki et al., 2018 |
| **Other systems** | Oculogyric crisis | Afshari and Kamarei, 2005; Wiltshire et al., 2010; Vermilion et al., 2019 |
| | Pupillary dysfunction/miosis | Barnett et al., 1992; Kimber et al., 1998; Yamanaka et al., 2019 |

*(Coninued)*

TABLE 1 (Coninued)

| Systems | Symptoms and signs | References |
|---|---|---|
| | Vision disorder/ptosis | Michaud and Gilbert, 1981; Chen et al., 2018; Hirose et al., 2018; Imai et al., 2018; Omoto et al., 2018; Hayashi et al., 2019; Yadav et al., 2019 |
| | Nystagmus | Haltia et al., 1984; O'Sullivan et al., 2000; Lai et al., 2010; Imai et al., 2018; Liu et al., 2019a; Wang et al., 2019b |
| | Dysarthria | Janota, 1979; Tateishi et al., 1984; Patel et al., 1985; Malandrini et al., 1998; Takeshita et al., 2017; Imai et al., 2018; Nakamura et al., 2018 |
| | Hearing losing | Soffer, 1985; Yoshimoto et al., 2017 |
| | Dysphagia | Michaud and Gilbert, 1981; Tateishi et al., 1984; Malandrini et al., 1998; O'Sullivan et al., 2000; Afshari and Kamarei, 2005; Takumida et al., 2017; Chen et al., 2018; Vermilion et al., 2019 |

Limb weakness was found in many patients with NIID and is one of the key phenotypes of NIID (Sone et al., 2016; Chen et al., 2020a). A previous study reported that a NIID patient had dyskinesia and upper limb chorea and could not walk or sit up without support (Pilson et al., 2018). Tian et al. (2019) demonstrated that the average onset age of muscle weakness in NIID patients with initial clinical manifestations was approximately 36 years. Muscle weakness tends to begin in the distal lower limbs and then move to the throat muscles and face. Recent studies have shown that many diseases with limb weakness, such as amyotrophic lateral sclerosis and oculopharyngodistal myopathy, are associated with NIID or NOTCH2NLC-related GGC repeat expansion disorders (Ogasawara et al., 2020; Yuan et al., 2020; Jih et al., 2021; Sugiyama et al., 2021). A recent clinical study indicated that 62.7% of patients with NIID had muscle weakness (Chen et al., 2020a). Due to the high occurrence of limb weakness in patients with NIID, the limb weakness-dominant subtype was proposed as one of the clinical phenotypes of patients with NIID (Sone et al., 2016).

### Episodic attacks

Although progressive symptoms, such as cognitive impairment and parkinsonism, are key features of NIID as a neurodegenerative disease, episodic attacks are also found in some patients with NIID, such as encephalitis-like, vestibular migraine-like attacks, or MELAS-like or epileptic episodes (Xiao et al., 2018; Yamanaka et al., 2019; Ishihara et al., 2020; Li et al., 2020b; Ataka et al., 2021; Zhao et al., 2021).

Han et al. (2019) reported a 63-year-old male with NIID who had recurrent acute encephalopathy syndrome, including recurrent headaches, personality changes, and abnormal mental behavior for 3 years. Shindo et al. (2019) reported that a 65-year-old patient with NIID had recurrent paroxysmal nausea and vomiting that lasted 2–3 days for each episode, and this patient later developed a non-convulsive epileptic status with generalized periodic electrical discharge identified by an EEG test. In addition to case reports, Sone et al. (2016) found that sporadic patients with NIID had generalized convulsions (13.2%), disturbance of consciousness (39.5%), and encephalitic episodes (21%). These findings demonstrated that episodic attacks are common symptoms in patients with NIID. Recently, Wang et al. (2020b) proposed that episodic encephalopathy prior to other neurological symptoms was a valuable diagnostic indicator for adult-onset NIID.

### Other symptoms in the nervous system

Several ophthalmological manifestations have been reported in patients with NIID, such as abnormal pupillary functions, miosis, oculogyric crisis (Vermilion et al., 2019), reduced eye movements, nystagmus, blepharospasm (Ogasawara et al., 2020), ptosis (Ogasawara et al., 2020), and loss of pigment in the retinal pigment epithelium (Haltia et al., 1986; Arrindell et al., 1991; Yamada et al., 2017). Pupillary dysfunction was reported to be a sensitive indicator of NIID (Arrindell et al., 1991). Adult-onset NIID patients with CGG repeat expansion in the NOTCH2NLC gene had similar ophthalmological characteristics, including rod-cone dysfunction with progressive retinal degeneration in the peripapillary and midperipheral regions; the most common symptoms in these patients were reduced visual acuity and night blindness (Nakamura et al., 2020). Therefore, retinal dystrophy was proposed as a NOTCH2NLC-related GGC repeat expansion disorder (Hayashi et al., 2020; Nakamura et al., 2020). In addition, pupil constriction (56.9%) and neurogenic bladder (23.5%) were found to be very common symptoms in patients with NIID and were considered to involve the autonomic nervous system (Chen et al., 2020a).

## Non-nervous system symptoms and signs

Except for the nervous system, many studies have indicated that other systems are involved in the pathology of NIID (Sone et al., 2016; Chen et al., 2020a). The non-nervous system manifestations of NIID make the diagnosis of NIID more difficult.

## Respiratory system symptoms

A recent study showed that ubiquitin and p62-positive cells are found in the lung tissues of patients with NIID, indicating the presence of intranuclear inclusion bodies in the lung (Chen et al., 2020a). By interviewing the symptoms of patients with NIID, approximately 78.4% of patients had respiratory system symptoms, and the most common symptoms were intractable irritant dry cough (51.0%) (Chen et al., 2020a). Among these patients, 89.5% had positive chest CT results, and chronic inflammation signs, lung nodules, and interstitial changes were found in chest CT (Chen et al., 2020a). Lung biopsy showed the infiltration of neutrophil monocytes in the pulmonary interstitium, suggesting chronic inflammation in the lungs of patients with NIID (Chen et al., 2020a). In an overview of all the NIID-reported cases, a surprising and unexpected finding was that some reported patients eventually died of respiratory diseases, such as respiratory distress (Malandrini et al., 1998), bronchopneumonia (Kimber et al., 1998), or aspiration pneumonia (Pilson et al., 2018; Vermilion et al., 2019); however, the underlying mechanisms are still unclear.

## Circulatory system symptoms

Cardiomyopathy and coronary atherosclerosis are reported to be associated with circulatory symptoms in patients with NIID. Oyer et al. (1991) found the presence of cardiomyopathy with intranuclear inclusions in myocytes in a NIID patient confirmed on postmortem, which expanded the known pathological spectrum of NIID. Parker et al. (1987) reported a 23-year-old patient with NIID with severe premature coronary atherosclerosis but no known risk factors. A recent study showed that approximately 72.5% of patients had circulatory system symptoms and signs (Chen et al., 2020a). In this study, paroxysmal chest pain (35.3%) and postural hypotension (29.4%) were common symptoms in the circulatory system (Chen et al., 2020a). Some non-specific changes in electrocardiograms, such as T wave or ST-T changes and atrial or ventricular premature beats, were found in patients with NIID. Cells in blood vessels from different tissues were found to be ubiquitin- and p62-positive (Chen et al., 2020a), suggesting the presence of intranuclear inclusions in the blood vessels.

## Urinary system symptoms

In previous studies, intranuclear inclusions were found in the kidneys of patients with NIID (Horino et al., 2018; Motoki et al., 2018; Nakamura et al., 2018), but urinary system symptoms were not obvious. A case report showed an eosinophilic intranuclear inclusion in a renal biopsy obtained 12 years prior to the diagnosis of NIID, suggesting the possibility that the formation of intranuclear inclusions in kidneys may occur prior to neuronal degeneration for years (Motoki et al., 2018). Clinical symptoms and laboratory examinations by a clinical evaluation demonstrated the involvement of the urinary system in 66.7% of patients; common clinical manifestations, such as frequent and urgent urination, were found in 49.0% of patients with NIID (Chen et al., 2020a). Renal function insufficiency and abnormal urine routine tests were found in some patients with NIID; intranuclear inclusions detected by p62 and ubiquitin antibodies were observed in kidney and bladder tissues (Chen et al., 2020a). Bladder biopsy in three cases showed diffuse inflammatory cell infiltration, suggesting an inflammatory response by intranuclear inclusions in NIID (Chen et al., 2020a). A recent urodynamic report demonstrated bladder dysfunction in patients with NIID, including detrusor overactivity, decreased bladder sensation, and large post-void residual urine (Aiba et al., 2020). Current evidence shows the involvement of the urinary system in NIID.

## Digestive system symptoms

Digestive system symptoms in patients with NIID commonly manifest as severe nausea and vomiting, which can occur alone, but in most cases, nausea and vomiting occur together. A case report showed that a patient with NIID repeatedly vomited for 7 years before the apparent abnormality in DWI was found, suggesting that periodic vomiting could be the only symptom of NIID in the early stages of NIID (Okamura et al., 2020). Gastrointestinal symptoms that presented in patients with NIID included bouts of constipation, gastroenteritis, dehydration, intestinal pseudo-obstruction, achalasia, colonic diverticulosis, and dilated esophagus (Barnett et al., 1992). Two siblings of patients with NIID were reported to present primary gastrointestinal dysfunction, such as abdominal pain, distention, and vomiting for 40 years (Schuffler et al., 1978). A systemic clinical evaluation showed that approximately 64.7% of patients had digestive system symptoms, including nausea, vomiting, and constipation; a portion of patients (15.6%) had abnormal liver functions, and 83.3% of patients had gastrointestinal polyps (Chen et al., 2020a). Diffused ubiquitin- and p62-positive cells were found in esophageal, stomach, gallbladder, and rectal tissues (Chen et al., 2020a), indicating the high involvement of digestive organs in NIID.

## Other system symptoms

The patients with familial NIID were reported to have erectile dysfunction beginning in the first or second decade of life (Zannolli et al., 2002). Chen et al. (2020a) reported that approximately 43.1% of patients with NIID had sexual dysfunction. Many cases have reported prostatic hyperplasia in over 60-year-old male patients with NIID (Sone et al., 2014; Araki et al., 2016; Yamada et al., 2017; Chen et al., 2020a). Joint and spine MRI/CT showed joint degeneration and joint and/or ligament injury in all patients (Chen et al., 2020a). Approximately one-third of patients with NIID have endocrine abnormalities, such as high glycosylated hemoglobin and hypothyroidism (Chen et al., 2020a). In addition, blurred vision, hearing loss, and skin ulcers are common symptoms in patients with NIID (Chen et al., 2020a).

### The sequences of involvement in different systems

Although different systems and organs are involved in NIID, the sequences of involvement in different systems may vary in individual patients according to previous case reports; for example, the existence of intranuclear inclusions and symptoms in systemic organs, such as the stomach and kidneys, precedes the onset of nervous system symptoms in NIID case reports (Morimoto et al., 2017; Motoki et al., 2018). Therefore, the age of onset in different systems may indirectly reflect the involvement of different systems. In a recent study, the median onset age was used to evaluate the sequence of involvement of different systems (Chen et al., 2020a). The median onset age in different systems was as follows; the locomotor system (3 years), reproductive system (28.5 years), digestive system (30 years), circulatory system (38.5 years), respiratory system (40 years), nervous system (50 years), and urinary system (55 years) (Chen et al., 2020a). Therefore, the nervous system was affected by NIID much later than most other systems.

## Brain imaging features of neuronal intranuclear inclusion disease

Imaging examination is of great value in the clinical diagnosis of NIID. The earlier reported MRI findings were atrophy of the cerebellar hemispheres and no specific imaging for NIID (Zannolli et al., 2002). With the development of MRI technologies, high intensity of bilateral cerebral white matter on T2 and FLAIR, as well as a specific high-intensity signal in the corticomedullary junction on DWI (as shown in **Figure 2**) was found in patients with NIID identified by skin biopsy (Sone et al., 2014). These specific changes in the DWI sequence of MRI were further confirmed in a large number of patients with NIID and case reports (Sone et al., 2014, 2016; Chen et al., 2020a). Therefore, DWI high-intensity signals along the corticomedullary junction became a strong clue for the diagnosis of NIID (Sone et al., 2016). Usually, the DWI high-intensity signal in the corticomedullary junction extends with the disease worsening from a small regional portion in the frontal lobe to the cerebellum but does not expand into the deep white matter even with T2 widely expanded leukoencephalopathy (Sone et al., 2016); however, some cases also reported that the DWI high-intensity signal disappears several years later (Yokoi et al., 2016; Chen et al., 2018; Kawarabayashi et al., 2018). In the T2 flair sequence of MRI, except for abnormal intensity signals in the corticomedullary junction and periventricular areas, abnormal signals are also found in the callosum, cerebellum, and brainstem, indicating diffuse lesions in the brains of patients with NIID (Chen et al., 2020a). Recent studies also demonstrated that the high-intensity signal in the corticomedullary junction is consistent with the neuropathological findings that are spongiotic changes proximal to the U-fibers in subcortical white matter (Yokoi et al., 2016; Cupidi et al., 2019).

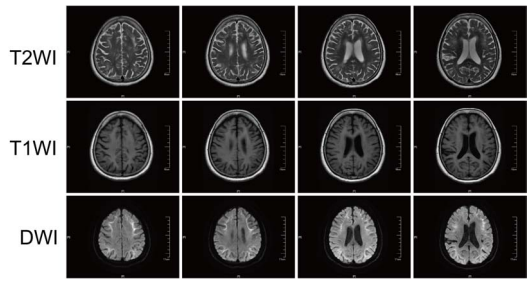


FIGURE 2
The typical brain magnetic resonance imaging (MRI) in patients with NIID. Curved or ribbon-like high signals along the corticomedullary junction, a strong clue for NIID, are found in the DWI sequence of head MRI of some patients with NIID.

## Neuronal nuclear inclusions, the typical pathological changes in neuronal intranuclear inclusion disease

Neuronal nuclear inclusions (NIIs) in the skin or biopsy samples of other tissues are the characteristic histopathologic findings of NIID. NIIs are not limited to NIID, but are also present in a variety of multiple neurodegenerative diseases, such as fragile X-associated tremor/ataxia syndrome (FXTAS), distal ophthalmopharyngeal myopathy, and oropharyngeal myopathy, which have overlapping clinical symptoms and similar pathological outcomes, and even have some commonalities in genetic diagnosis (Boivin and Charlet-Berguerand, 2022; Ogasawara et al., 2022; Zhou et al., 2022). The existence of NIIs and the dysfunction of the ubiquitin-proteasome system (UPS) are the shared pathological features in NIID and other neurodegenerative diseases. Similar to these neurodegenerative diseases, the impairment of the UPS, such as the increase of ubiquitinated proteins and P62 protein, is found in the pathological changes of NIID (Oh et al., 2015; Hagerman and Hagerman, 2021; Boivin and Charlet-Berguerand, 2022; Ogasawara et al., 2022; Ribot et al., 2022; Zhou et al., 2022). However, how expanded GGC repeats cause the formation of NIIs and dysfunction of the UPS is generally unknown in the pathogenesis of NIID.

The NIID was defined as an intranuclear inclusion disease when it was first described in Lindenberg et al. (1968). In 1980, a case with progressive behavioral abnormalities, involuntary movements, ataxia, and dementia was reported, and pathological findings indicated that intranuclear inclusions were found in all types of central, peripheral, and autonomic neurons from almost all neuronal systems; therefore, this disease was

proposed as NIID (Sung et al., 1980). Some studies confirmed the existence of NIIs in the cerebral cortex, basal ganglia, brain stem, and spinal cord, as well as in neurons and astrocyte glial cells (Greco et al., 2002; Zannolli et al., 2002; Takahashi-Fujigasaki, 2003; Nakamura et al., 2014; Sone et al., 2016; Yamaguchi et al., 2018). Intranuclear inclusions in glial cells were more commonly found in adult cases (Weidenheim and Dickson, 1995; Nakamura et al., 2014). However, later studies found that intranuclear inclusions involved multiple systems and not occurred only in the nervous system (Yamaguchi et al., 2018). Intranuclear inclusions have been observed in the following systems: the respiratory system, including the lungs (Yamaguchi et al., 2018); the gastrointestinal system, including the liver, spleen, pancreas, esophagus, stomach, jejunum, ileum, colon, and rectum (Sloane et al., 1994; El-Rifai et al., 2006; Mori et al., 2011); the endocrine system, including the parathyroid gland, pituitary gland, thyroid gland, and adrenal gland (Tateishi et al., 1984; Patel et al., 1985); the urinary system, including the kidney and urinary bladder (Motoki et al., 2018; Yamaguchi et al., 2018); the circulatory system, including the heart and lymph nodes (Oyer et al., 1991; Sone et al., 2016; Yamaguchi et al., 2018); the reproductive system, including ovaries and uterus (Yamaguchi et al., 2018); the locomotor system, including muscles (Morimoto et al., 2017); and the miscellaneous system, including the skin (Takumida et al., 2017; Hirose et al., 2018). A recent study systemically examined the distribution of NII detected by ubiquitin and P62 antibodies in tissue samples and found that NIID was in different systems except for the nervous system, indicating that NIID actually is a systemic intranuclear inclusion disease (Chen et al., 2020a). The spatial and temporal distribution in different systems may explain the highly heterogeneous phenotypes of NIID.

These inclusion bodies are circular, 1.5–10 μm in diameter, and are located near nucleoli, and ubiquitin/p62 staining, but not tau epitope, can be seen around NIIs (Bergmann et al., 1994; Takahashi et al., 2000). Electron microscopy showed a cluster of circular halo-shaped filamentous materials (8–12 nm) without limiting the membrane structure in the nucleus center (Deng et al., 2019). Intranuclear inclusions are considered to be formed when there is an excessive accumulation of proteins in the nucleus, and the abnormal alteration of nuclear bodies might be related to the pathogenesis of NIID (Takahashi et al., 2010; Nakano et al., 2017). Excessive protein accumulation in intranuclear inclusions might impair the ubiquitin-dependent degradation process and consequently result in the dysfunction of neurons or somatic cells (Liu et al., 2019a). The exact components of intranuclear inclusions are still unknown; previous studies have demonstrated that many nonspecific proteins, such as glucocorticoid receptor, promyelocytic leukemia protein (PML), histone deacetylase 4 (HDAC4), small ubiquitin modifier-1 (Sumo-1), fused in sarcoma, optineurin, myosin 6, heat shock protein 90, and dynamin-1, were found to be present in intranuclear inclusions by immunostaining (McFadden et al., 2005; Takahashi-Fujigasaki et al., 2006; Pountney et al., 2008; Nakamura et al., 2014; Nakano et al., 2017). The roles of these proteins and why these proteins are trapped in the intranuclear inclusions are still unclear and need further investigation.

Except for the NIIs in the different tissues, in the pathological examination of NIID tissues, diffuse inflammatory cell infiltration near the intranuclear inclusions, such as neutrophil monocytes and macrophages, was found in the affected tissues, including the brain, lung, bladder, and prostate gland (Chen et al., 2020a), indicating that inflammatory cell infiltration or inflammation in tissues are related to intranuclear inclusions. The inflammatory injury and edema can be seen in the brain from the DWI sequence of MRI as shown in the corticomedullary junction (Sone et al., 2014). In addition, edema was also found in the tissues of patients with NIID, supporting that dehydrate and anti-inflammatory drugs can be used for NIID treatment (Chen et al., 2020a; Liang et al., 2020). So far, a lack of clinical data supports the use of anti-inflammatory drugs in patients with NIID.

## Genetic and epigenetic progress of neuronal intranuclear inclusion disease

### NOTCH2NLC gene

In 2019, studies reported GGC repeat expansion at the 5′ region of NOTCH2NLC as the genetic cause of NIID (Deng et al., 2019; Sone et al., 2019; Tian et al., 2019). NOTCH2NLC is one of the three human-specific NOTCH2-derived genes (NOTCH2NLA, NOTCH2NLB, and NOTCH2NLC) on chromosome 1q21.1 and is highly expressed in the brain. The genomic sequences of the NOTCH2NL paralogs are similar to NOTCH2, including the NOTCH2 promoter and six N-terminal epidermal growth factor (EGF)-like domains from NOTCH2 exons 1 to 4 but without the transmembrane and cytoplasmic domains of NOTCH2 (Fiddes et al., 2018; Suzuki et al., 2018). These genes are considered to be involved in the evolutionary expansion of the human brain, and the mutations in these genes result in the reduction of brain size (Fiddes et al., 2018; Suzuki et al., 2018). NOTCH2NLC mRNA levels are unaltered in individuals with NIID (Ishiura et al., 2019; Sone et al., 2019; Tian et al., 2019), suggesting that GGC repeat RNA may change the functions of NOTCH2NLC mRNA/protein but not change the expression of NOTCH2NLC mRNA/protein to play an important role in the molecular pathogenesis of NIID.

Sun et al. (2020) identified that abnormal GGC repeat expansion in the 5′ region of the NOTCH2NLC gene is associated with essential tremor, which may explain tremor

as a kind of symptom and sign of NIID in some relevant cases. Whether dynamic and/or postural tremors are the phenotypes of NIID requires a longer follow-up clinical and pathological examination (Chen et al., 2020b). Later studies demonstrated that many different diseases, such as amyotrophic lateral sclerosis, PD, dementia, oculopharyngodistal myopathy, leukoencephalopathy, and multiple system atrophy, were associated with GGC repeat expansion in the NOTCH2NLC gene (Okubo et al., 2019; Fang et al., 2020; Jiao et al., 2020; Ma et al., 2020; Ogasawara et al., 2020; Yuan et al., 2020). These studies showed two aspects: on the one hand, these diseases showed similar symptoms as NIID, indicating the symptom heterogenicity of NIID; on the other hand, similar to different variants of the same gene associated with distinct genetic diseases, different lengths of GGC repeat expansion in the NOTCH2NLC gene may cause different diseases with variable phenotypes, which are already reported in some studies (Sone et al., 2019; Tian et al., 2019). However, the association between GGC repeat size and different phenotypes is inconclusive (Huang et al., 2021). Therefore, to avoid confusion, NOTCH2NLC-related repeat expansion disorders were proposed to name symptom-heterogeneous diseases associated with GGC repeat expansion in the NOTCH2NLC gene (Westenberger and Klein, 2020).

Based on a multiethnic cohort of gene-confirmed patients with NIID from Southeast Asia, it was suggested that the presence of GGA interruptions in the repeated expansion of GGC may play a role in modifying the disease in terms of age at symptom onset (Chen et al., 2020c). Based on an in-depth study of NIID patients with European ancestry, GGC expansion in the NOTCH2NLC gene had a very low occurrence in Europe, suggesting that NOTCH2NLC repeat expansion is not the only cause of NIID onset or NII formation (Chen et al., 2020d); however, there was no evidence to support the hypothesis of gene heterogenicity of NIID (Li et al., 2020a).

## Epigenetic regulation of neuronal intranuclear inclusion disease

A previous study demonstrated that the NIIs in sporadic and familial NIID contained Sumo-1 and SUMOylation substrate PML and HDAC4 (Takahashi-Fujigasaki et al., 2006). Based on their results, both PML and Sumo-1 are major components of nucleosomes, suggesting that intranuclear inclusions in polyglutamine disease may originate from these functional domains that act as ubiquitin-related protein degradation sites. HDAC4 is also a major part of NIIs. HDAC is a transcriptional suppressor that regulates histone remodeling, and nucleosome is thought to be a site that controls histone acetylation levels. The presence of PML, Sumo-1, and HDAC4 in NIIs suggests that transcriptional activity regulated by histone acetylation may contribute to the disease process of NIID (Takahashi et al., 2010). In addition, previous studies also reported abnormal methylation in the CpG islands of the NOTCH2NLC gene (Tian et al., 2019; Deng et al., 2021). Hypermethylated CpG islands in the NOTCH2NLC gene were found in patients and asymptomatic carriers (Tian et al., 2019; Deng et al., 2021), suggesting that the hypermethylation status of the NOTCH2NLC gene may be related to the number of GGC repeats but not clinical symptoms. However, the mechanisms by which GGC expansion in the NOTCH2NLC gene influences methylation itself are still unclear (Tian et al., 2019).

# Possible mechanisms of neuronal intranuclear inclusion disease

Although GGC repeat expansion in the NOTCH2NLC gene has been proven to be the cause of NIID, the molecular mechanisms underlying NIID remain unclear. Similar to FXTAS (GGC repeats in the FMR1 gene), Huntington's disease (CAG repeats in the HTT gene), amyotrophic lateral sclerosis/FTD (GGGGCC repeats in the C9ORF72 gene), and myotonic dystrophy (DM1, CUG repeats in the DMPK gene), NIID is one kind of nucleotide repeat expansion disorder or microsatellite repeat expansion disorder with expanded GGC repeats in the NOTCH2NLC gene. Therefore, NIID may share some similar mechanisms to these microsatellite repeat expansion disorders. Here, we briefly propose some possible mechanistic models of NIID at the DNA, RNA, and protein levels (**Figure 3**). For more details, excellent review articles thoroughly discuss the various molecular mechanisms underlying pathogenesis in microsatellite diseases (Rodriguez and Todd, 2019; Boivin et al., 2021; Depienne and Mandel, 2021; Malik et al., 2021; Guo et al., 2022).

## Polyglycine protein toxicity

Unconventional translation, named repeat-associated non-AUG translation (RAN), of expanded repeats in toxic proteins has been identified in a variety of microsatellite disorders (Zu et al., 2011; Gao and Richter, 2017; Cleary et al., 2018; Cheng et al., 2019). For example, expanded GGC repeats located within the 5′UTR sequence of the FMR1 gene are embedded in a small upstream ORF (uORF), which is translated through initiation at a near-cognate ACG codon in a small polyglycine-containing protein, FMRpolyG (Krans et al., 2016, 2019; Sellier et al., 2017). The expression of FMRpolyG in cell and/or animal models forms protein inclusions and is toxic for neuronal cells, which could be associated with the presence of typical ubiquitin-positive intranuclear inclusions and neuronal cell death in the Fragile X Tremor Ataxia Syndrome (FXTAS) neurodegenerative disease (Glineburg et al., 2018; Hagerman and Hagerman, 2021; Zhao and Usdin, 2021). Similarly, two recent reports

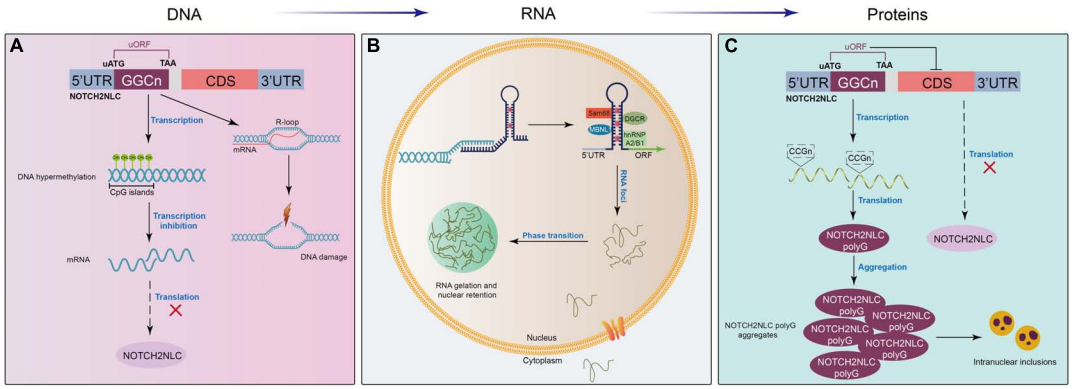


FIGURE 3
Proposed mechanistic models of NIID at different levels. **(A)** At the DNA level, expanded GGC repeats in the NOTCH2NLC gene induce the formation of RNA-DNA hybridization R-loops during transcription, promoting DNA damage and neuronal death. In addition, the hypermethylation of the NOTCH2NLC gene leads to gene silencing and the subsequent loss of protein function. **(B)** After transcription, extended GGC repeats sequester many RNA-binding proteins, forming RNA foci in the nucleus and resulting in the functional loss of RNA-binding proteins. **(C)** GGC repeat expansion initiates a near-homologous ACG codon located upstream of the GGC repeats in the NOTCH2NLC gene and is translated into the polyglycine (polyG)-NOTCH2NLC protein, which inhibits nucleocytoplasmic transport, leading to the accumulation of polyG-NOTCH2NLC and protein toxicity.

suggest that expanded GGC repeats embedded in the 5′UTR of the NOTCH2NLC gene are located in a small uORF, in which translation initiation starts at a canonical AUG codon, resulting in the expression of small polyglycine-containing proteins either named uN2CpolyG or N2NLCpolyG (Boivin et al., 2021; Zhong et al., 2021). Alike in FXTAS, the expression of uN2CpolyG/N2NLCpolyG forms protein aggregates and is toxic in cell and animal models. Moreover, antibodies directed against this polyglycine-containing protein stain the ubiquitin-positive intranuclear inclusions typical of NIID (Boivin et al., 2021; Zhong et al., 2021). Overall, these results may explain the origin of intranuclear inclusions and neuronal cell dysfunctions in NIID. Of interest, in both FXTAS and NIID, expanded CGG/GGC repeats are located in uORFs, in which translation starts ahead of the repeats and expression is independent of the downstream main FMRP or NOTCH2NLC proteins (Malik et al., 2021; Boivin and Charlet-Berguerand, 2022). Finally, these FMRpolyG and uN2CpolyG/N2NLCpolyG proteins were found to have liquid phase separation properties and impair nucleocytoplasmic transport, potentially illuminating putative molecular pathogenic mechanisms (Asamitsu et al., 2021; Zhong et al., 2021).

## RNA toxicity and RNA foci

Previous studies have demonstrated that repeat expansion-containing RNAs from the non-coding regions of genes linked to diverse human diseases, such as myotonic dystrophy type 1 and FXTAS, can form intramolecular hairpin secondary structures, bind to many RNA-binding proteins, and form RNA-protein aggregates in the pathology of these neurodegenerative diseases, resulting in toxic gain-of-function of these mRNAs (La Spada and Taylor, 2010; Xu et al., 2021). NOTCH2NLC mRNAs were supposed to have similar toxic gain-of-function; however, no evidence has shown the toxicity of NOTCH2NLC mRNAs in the pathology of NIID thus far. Recently, many reports have shown that these NOTCH2NLC mRNAs containing extended GGC repeats colocalize with p62 in nuclear inclusion bodies of patients with NIID, as well as in many RNA-binding proteins (Sam68, hnRNPA2/B1, MBNL1, DGCR, etc.) sequestered in the secondary structure of NOTCH2NLC mRNAs (Glineburg et al., 2018; Deng et al., 2021). These findings also indirectly support the RNA toxicity theory of NIID. Different repeat sizes, repeat locations, and sequestered RNA-binding proteins may influence RNA toxicity (Huang et al., 2021). Among them, sequestered RNA-binding proteins may play a critical role in RNA toxicity. Previous studies have shown that extended GGC repeats sequester many RNA-binding proteins and form RNA foci in the nucleus, resulting in the loss of RNA-binding protein functions and the occurrence of neurodegenerative diseases (Jain and Vale, 2017; Kong et al., 2017; Sanders and Brangwynne, 2017; Deng et al., 2021). RNA FISH technology combined with immunofluorescence demonstrated that RNA foci were observed in NIID-affected patients but not in the controls or asymptomatic carriers (Deng et al., 2021). However, the RNA-binding proteins that are specifically affected and their downstream signaling pathways need to be further identified.

## DNA damage and neuronal death

Extended GGC repeats may cause the pathology of neurodegenerative diseases not only at the protein level and

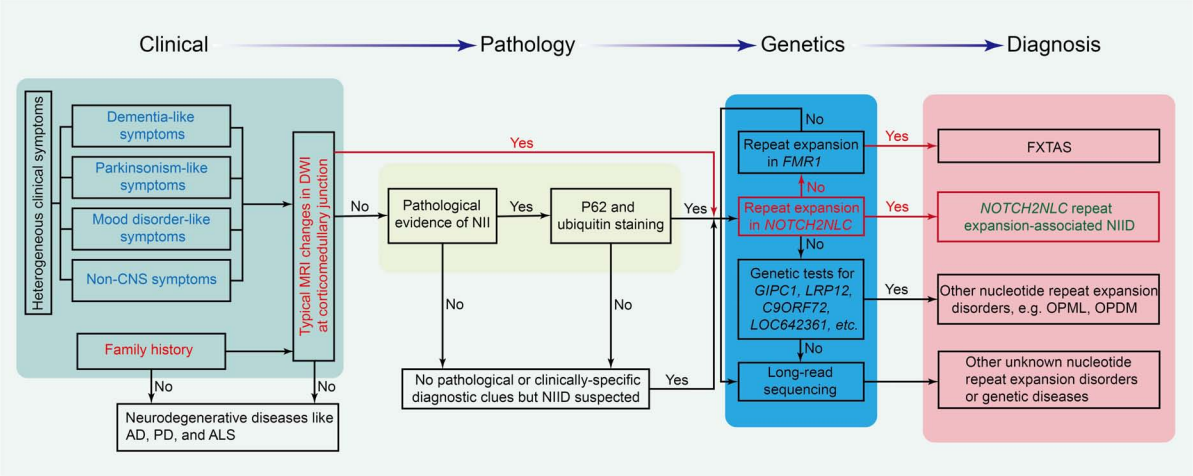


FIGURE 4
The flowchart for the diagnosis of NIID and its differential diseases. Different background colors in the chart show the four critical parts of the diagnosis protocol. AD, Alzheimer's disease; ALS, amyotrophic lateral sclerosis; FXTAS, fragile X-associated tremor/ataxia syndrome; NII, neuronal intranuclear inclusion; PD, Parkinson's disease.

the RNA level but also at the DNA level. A previous study indicated that GC enrichment in the extended GGC repeats of the FMR1 gene increases the propensity of the formation of RNA-DNA hybrid R-loops (Hamperl and Cimprich, 2014; Kong et al., 2017). These cotranscriptional R-loops can activate the DNA damage response and a series of signaling events, which result in DNA breakage and neuronal death (Barzilai, 2010; Kong et al., 2017). Due to similar extended GGC repeats in the NOTCH2NLC gene as in the FMR1 gene, extended GGC repeat-induced RNA-DNA hybrid R-loops and neuronal death may also contribute to the pathophysiology of NIID, which needs more investigation. In addition, recent studies have shown changes in the methylation level of the NOTCH2NLC gene (Deng et al., 2021; Huang et al., 2021). This methylation modification may also influence the transcriptional and translational levels that are linked to RNA toxicity and protein toxicity in the mechanisms of NIID. Therefore, different mechanisms of NIID may crosstalk or interact and contribute to the pathology of NIID.

# Diagnosis of neuronal intranuclear inclusion disease and differential diagnosis

## Diagnosis of neuronal intranuclear inclusion disease

In early case reports, autopsy, rectal biopsy, and nerve biopsy were mostly used to diagnose patients with NIID (Lindenberg et al., 1968; Funata et al., 1990; Goutieres et al., 1990; Zannolli et al., 2002; Yadav et al., 2019). Sone et al. (2011) found that the p62-positive nuclei of eosinophils detected by skin biopsy could be used for pathological diagnosis for NIID. Since then, many clinical cases have been confirmed by skin biopsy (Sone et al., 2014, 2016). With imaging development, the DWI sequence of head MRI showed a specific high signal along the corticomedullary junction (Sone et al., 2014). Therefore, the DWI imaging of head MRI became the key cue for the clinical diagnosis of NIID (Sone et al., 2016; Yu et al., 2019). After repeat GGC expansion in the NOTCH2NLC gene was confirmed as the cause of NIID in 2019 (Ishiura et al., 2019; Sone et al., 2019; Tian et al., 2019), genetic testing for GGC repeats in the NOTCH2NLC gene was performed and became the criteria for the diagnosis of NIID. The flowchart for the diagnosis of NIID and its differential diagnosis is shown in **Figure 4**.

Due to the high heterogeneity and multisystem symptoms of this disease, it is difficult to reach the diagnosis of NIID in clinical practice. The diagnosis of NIID can be considered from typical MRI signals, clinical manifestations, pathology of NIIs, and genetic tests. DWI high-intensity signals in head MRI are the strong indicators for the diagnosis of NIID. If patients had no typical MRI changes, the triad of clinical manifestations such as dementia, PD-like behaviors, and personality changes is a good cue for the diagnosis of NIID. For patients without the triad of NIID and DWI high-intensity signals, NIIs in the pathological findings from skin or other tissues are also a cue to suspect the diagnosis of NIID. Once the diagnosis of NIID is suspected, a genetic test for GGC repeats in the NOTCH2NLC gene should be performed to confirm or rule out the diagnosis of NIID, as shown in **Figure 4**.

## Differential diagnosis of neuronal intranuclear inclusion disease

Because NIID is a symptom-heterogeneous disease and shares similar imaging features with some diseases, NIID has many differential diagnoses from other diseases.

Because FXTAS and NIID are both autosomal-dominant GGC trinucleotide repeat expansion diseases in different genes (FMR1 gene and NOTCH2NLC gene, respectively) (Padilha et al., 2018; Toko et al., 2021), FXTAS is an important disease to differentiate from NIID. More importantly, FXTAS has similar clinical symptoms and radiological features to late-onset NIID, such as ataxia, tremor, Parkinsonism, cognitive decline, and bilateral high-signal abnormalities along the corticomedullary junction in DWI sequences (Leehey, 2009; Padilha et al., 2018). Therefore, genetic tests for the GGC repeats in the FMR1 gene and NOTCH2NLC gene may be a suitable method to distinguish FXTAS and NIID.

Neuronal intranuclear inclusion disease should be distinguished from Creutzfeldt–Jakob disease and some diseases with leukoencephalopathy or dementia. Creutzfeldt–Jakob disease has progressive cognitive impairment and myoclonus in the extremities, as well as characteristic lacy high-intensity signals in the cortex, caudate nucleus, or putamen on brain DWI. A recent study proposed that brain DWI is the key to differentiate from Creutzfeldt–Jakob disease and different leukoencephalopathy grades (Tokumaru et al., 2021).

Middle cerebellar peduncle lesions are considered to be a characteristic finding of NIID (Okamoto et al., 2003), but they can be found in other neurodegenerative disorders, such as multiple system atrophy and spinocerebellar ataxia, and diseases due to other etiologies (neoplasm, metabolic, cerebrovascular, inflammatory, and demyelinating diseases). Many neurodegenerative diseases, such as progressive supranuclear palsy, corticobasal degeneration, dementia with Lewy bodies, Perry syndrome, Huntington's disease, dopa-responsive dystonia, Wilson disease, and neurodegeneration with brain iron accumulation, have PD-like behavior. Therefore, sometimes it is very difficult to differentiate these diseases from clinical symptoms. High-intensity signals along the corticomedullary junction on DWI at the late stage may also help clinicians distinguish NIID from the above neurodegenerative diseases and gelsolin amyloidosis, which can present with neuropathy, ataxia, and dementia (Pihlamaa et al., 2012).

# Treatment of neuronal intranuclear inclusion disease

Currently, there is no treatment to cure or slow down the process of NIID, but medications that control symptoms, such as muscle weakness, impaired consciousness, abnormal behavior, and sensory impairment, can improve a patient's quality of life (Raza et al., 2020). Clinical treatment methods mainly adopt symptomatic treatment (Shindo et al., 2019). According to previous case reports, most patients with NIID are responsive to symptomatic treatment; for example, patients with NIID with Parkinsonism are sensitive to levodopa treatment (Lai et al., 2010; Ma et al., 2020), and patients with NIID with seizures are relieved by intravenous phenytoin and then carbamazepine (Fujita et al., 2017). However, some patients may experience relapse after effective treatment and/or develop other symptoms (Imai et al., 2018; Liu et al., 2019a; Li et al., 2020b). Because previous NIID cases eventually died of respiratory diseases, such as bronchopneumonia or aspiration pneumonia (Kimber et al., 1998; Malandrini et al., 1998; Pilson et al., 2018; Vermilion et al., 2019), it is necessary to prevent pulmonary infection and respiratory aspiration, particularly in patients with disturbed consciousness. Because diffuse inflammatory cell infiltration and edema were found in different tissues containing intranuclear inclusions (Chen et al., 2020a), dehydrate and anti-inflammatory drugs could be used to relieve the inflammation in patients with NIID, particularly in those with episodic attacks. In addition, nutritional support and psychotherapy should be provided during clinical treatments.

Recently, different therapeutic strategies have been proposed for NIID, for example, antisense oligonucleotide therapy, RNA interference, small molecule RNA drugs, and CRISPR-based therapy (Xu et al., 2021). Although these strategies are promising, the major challenge is the low specificity and high possibility of out-of-target therapies.

# Conclusion and future directions

With an increasing number of reported cases of NIID, the clinical manifestations of NIID are well characterized. Early studies showed that NIID mainly has neurological symptoms; the latest studies demonstrated that there are a variety of symptoms and signs in various systems, indicating the high heterogeneity of clinical symptoms and signs of NIID. This increases the difficulty in the clinical diagnosis of NIID. Although patients with NIID present heterogeneous symptoms, they also show some core symptoms, such as triad symptoms in the central nervous system (dementia, Parkinsonism, and psychiatric symptoms). Before the NOTCH2NLC gene was linked to the etiology of NIID, tissues/skin biopsy and DWI high-intensity signals along the corticomedullary junction were strong clues for the diagnosis of NIID; now, genetic tests for expanded GGC repeats in the NOTCH2NLC gene have become the gold standard for NIID.

Expanded GGC repeats in the NOTCH2NLC gene have been confirmed as the cause of NIID, but how expanded GGC repeats in the NOTCH2NLC gene cause pathological

changes and the accumulation of NII in the nucleus remains unclear. As a nucleotide repeat expansion disorder, NIID may share similar mechanisms to other nucleotide repeat expansion disorders, such as expanded nucleotide repeat-induced DNA damage, RNA toxicity, and abnormal encoded protein toxicity. Although recent studies have demonstrated the presence of polyG-NOTCH2NLC protein in the animal models and tissues of patients with NIID, the mechanism by which the polyG-NOTCH2NLC protein causes toxicity still needs more investigation. RNA toxicity and DNA instability theory need to be identified in the mechanisms of NIID. How do expanded GGC repeats in the NOTCH2NLC gene induce the formation of NIIs? What are the components in expanded GGC repeat-induced RNA foci? Which RNA-binding proteins are involved in the pathogenesis of NIID? These questions await more investigation, and the answers to these questions will help to guide the treatment of NIID. To date, no effective treatment is available. Even though different gene therapies, such as antisense oligonucleotide therapy and RNA interference, have been proposed, many great challenges must be overcome, such as the specificity and out-of-target nature of RNA drugs. Recent findings have shown that inflammation is involved in the pathological changes of NIID and may be downstream of expanded GGC repeat-induced RNA/protein toxicity. Therefore, the role of inflammation should be further identified in the pathology of NIID, and anti-inflammation could be a promising therapeutic strategy for NIID.

## Author contributions

XX, MS, and BoW designed and revised the manuscript. YL and HL collected the literature and made the first draft. XL, BiW, HY, BoW, and MS discussed and interpreted the analysis. All authors contributed to the article and approved the submitted version.

## Funding

This work was supported by grants from the National Natural Science Foundation of China (82071511), the National Key R&D Program of China (2017YFE0103700), the Shandong Provincial Natural Science Foundation (ZR2019ZD32), and the Priority Academic Program Development of Jiangsu Higher Education Institutions of China.

## Acknowledgments

We appreciate the contributions of NIID-related authors.

## Conflict of interest

The authors declare that the research was conducted in the absence of any commercial or financial relationships that could be construed as a potential conflict of interest.

## Publisher's note



## References

Abe, K., and Fujita, M. (2017). Over 10 years MRI observation of a patient with neuronal intranuclear inclusion disease. *BMJ Case Rep.* 2017:bcr2016218790. doi: 10.1136/bcr-2016-218790

Afshari, H., and Kamarei, M. (2005). Neuronal intranuclear inclusion disease without polyglutamine inclusions in a child. *J. Neuropathol. Exp. Neurol.* 64:545. doi: 10.1093/jnen/64.6.545

Aiba, Y., Sakakibara, R., Abe, F., Higuchi, T., Tokuyama, W., Hiruta, N., et al. (2016). Neuronal intranuclear inclusion disease with leukoencephalopathy and light motor-sensory and autonomic neuropathy diagnosed by skin biopsy. *J. Neurol. Sci.* 368, 263–265. doi: 10.1016/j.jns.2016.07.042

Aiba, Y., Sakakibara, R., Lee, F. C., and Tateno, F. (2020). Urodynamic assessment of neuronal intranuclear inclusion disease. *Eur. Neurol.* 83, 312–316. doi: 10.1159/000508746

Araki, K., Sone, J., Fujioka, Y., Masuda, M., Ohdake, R., Tanaka, Y., et al. (2016). Memory loss and frontal cognitive dysfunction in a patient with adult-onset neuronal intranuclear inclusion disease. *Intern. Med.* 55, 2281–2284. doi: 10.2169/internalmedicine.55.5544

Arrindell, E. L., Trobe, J. D., Sieving, P. A., and Barnett, J. L. (1991). Pupillary and electroretinographic abnormalities in a family with neuronal intranuclear hyaline inclusion disease. *Arch. Ophthalmol.* 109, 373–378. doi: 10.1001/archopht.1991.01080030075043

Asamitsu, S., Yabuki, Y., Ikenoshita, S., Kawakubo, K., Kawasaki, M., Usuki, S., et al. (2021). CGG repeat RNA G-quadruplexes interact with FMRpolyG to cause neuronal dysfunction in fragile X-related tremor/ataxia syndrome. *Sci. Adv.* 7:eabd9440. doi: 10.1126/sciadv.abd9440

Ataka, T., Kimura, N., and Matsubara, E. (2021). Temporal changes in brain perfusion in neuronal intranuclear inclusion disease. *Int. Med.* 60, 941–944. doi: 10.2169/internalmedicine.5743-20

Barnett, J. L., McDonnell, W. M., Appelman, H. D., and Dobbins, W. O. (1992). Familial visceral neuropathy with neuronal intranuclear inclusions: diagnosis by rectal biopsy. *Gastroenterology* 102, 684–691. doi: 10.1016/0016-5085(92)90121-e

Barzilai, A. (2010). DNA damage, neuronal and glial cell death and neurodegeneration. *Apoptosis* 15, 1371–1381.

Bergmann, M., Kuchelmeister, K., Gullotta, F., Kryne-Kubat, B., Burwinkel, E., and Harms, K. (1994). Infantile multiple system atrophy with cytoplasmic and intranuclear glioneuronal inclusions. *Acta Neuropathol.* 87, 642–647. doi: 10.1007/BF00293326

Boivin, M., and Charlet-Berguerand, N. (2022). Trinucleotide CGG repeat diseases: an expanding field of polyglycine proteins? *Front. Genet.* 13:843014. doi: 10.3389/fgene.2022.843014

Boivin, M., Deng, J., Pfister, V., Grandgirard, E., Oulad-Abdelghani, M., Morlet, B., et al. (2021). Translation of GGC repeat expansions into a toxic polyglycine protein in NIID defines a novel class of human genetic disorders: the polyG diseases. *Neuron* 109, 1825–1835.e5. doi: 10.1016/j.neuron.2021.03.038

Chen, H., Lu, L., Wang, B., Cui, G., Wang, X., Wang, Y., et al. (2020a). Re-defining the clinicopathological spectrum of neuronal intranuclear inclusion disease. *Ann. Clin. Transl. Neurol.* 7, 1930–1941. doi: 10.1002/acn3.51189

Chen, H., Lu, L., Wang, B., Hua, X., Wan, B., Sun, M., et al. (2020b). Essential tremor as the early symptom of NOTCH2NLC gene-related repeat expansion disorder. *Brain* 143:e56. doi: 10.1093/brain/awaa142

Chen, L., Chen, A., Lei, S., He, L., and Zhou, M. (2019). Teaching NeuroImages: the zigzag edging sign of adult-onset neuronal intranuclear inclusion disease. *Neurology* 92, e2295–e2296.

Chen, L., Wu, L., Li, S., Huang, Q., Xiong, J., Hong, D., et al. (2018). A long time radiological follow-up of neuronal intranuclear inclusion disease: two case reports. *Medicine* 97:e13544. doi: 10.1097/MD.0000000000013544

Chen, Z., Xu, Z., Cheng, Q., Tan, Y., Ong, H., Zhao, Y., et al. (2020c). Phenotypic bases of NOTCH2NLC GGC expansion positive neuronal intranuclear inclusion disease in a Southeast Asian cohort. *Clin. Genet.* 98, 274–281. doi: 10.1111/cge.13802

Chen, Z., Yan Yau, W., Jaunmuktane, Z., Tucci, A., Sivakumar, P., Gagliano Taliun, S., et al. (2020d). Neuronal intranuclear inclusion disease is genetically heterogeneous. *Ann. Clin. Trans. Neurol.* 7, 1716–1725.

Cheng, W., Wang, S., Zhang, Z., Morgens, D. W., Hayes, L. R., Lee, S., et al. (2019). CRISPR-Cas9 screens identify the RNA helicase DDX3X as a repressor of C9ORF72 (GGGGCC)n repeat-associated Non-AUG translation. *Neuron* 104, 885–98.e8. doi: 10.1016/j.neuron.2019.09.003

Cleary, J. D., Pattamatta, A., and Ranum, L. P. W. (2018). Repeat-associated non-ATG (RAN) translation. *J. Biol. Chem.* 293, 16127–16141.

Cupidi, C., Dijkstra, A. A., Melhem, S., Vernooij, M. W., Severijnen, L. A., Hukema, R. K., et al. (2019). Refining the spectrum of neuronal intranuclear inclusion disease: a case report. *J. Neuropathol. Exp. Neurol.* 78, 665–670. doi: 10.1093/jnen/nlz043

Deng, J., Gu, M., Miao, Y., Yao, S., Zhu, M., Fang, P., et al. (2019). Long-read sequencing identified repeat expansions in the 5'UTR of the NOTCH2NLC gene from Chinese patients with neuronal intranuclear inclusion disease. *J. Med. Genet.* 56, 758–764. doi: 10.1136/jmedgenet-2019-106268

Deng, J., Zhou, B., Yu, J., Han, X., Fu, J., Li, X., et al. (2021). Genetic origin of sporadic cases and RNA toxicity in neuronal intranuclear inclusion disease. *J. Med. Genet.* 59, 462–469. doi: 10.1136/jmedgenet-2020-107649

Depienne, C., and Mandel, J. L. (2021). 30 years of repeat expansion disorders: what have we learned and what are the remaining challenges? *Am. J. Hum. Genet.* 108, 764–785. doi: 10.1016/j.ajhg.2021.03.011

El-Rifai, N., Daoud, N., Tayyarah, K., Baydoun, A., and Jaubert, F. (2006). Neuronal intranuclear inclusion disease presenting as chronic intestinal pseudo-obstruction in the neonatal period in the absence of neurologic symptoms. *J. Pediatr. Gastroenterol. Nutr.* 42, 321–323. doi: 10.1097/01.mpg.0000189331.39527.0b

Fang, P., Yu, Y., Yao, S., Chen, S., Zhu, M., Chen, Y., et al. (2020). Repeat expansion scanning of the NOTCH2NLC gene in patients with multiple system atrophy. *Ann. Clin. Transl. Neurol.* 7, 517–526. doi: 10.1002/acn3.51021

Fiddes, I. T., Lodewijk, G. A., Mooring, M., Bosworth, C. M., Ewing, A. D., Mantalas, G. L., et al. (2018). Human-Specific NOTCH2NL genes affect notch signaling and cortical neurogenesis. *Cell* 173, 1370–1384.e16. doi: 10.1016/j.cell.2018.03.051

Fujita, K., Osaki, Y., Miyamoto, R., Shimatani, Y., Abe, T., Sumikura, H., et al. (2017). Neurologic attack and dynamic perfusion abnormality in neuronal intranuclear inclusion disease. *Neurol. Clin. Practice* 7, e39–e42. doi: 10.1212/CPJ.0000000000000389

Funata, N., Maeda, Y., Koike, M., Yano, Y., Kaseda, M., Muro, T., et al. (1990). Neuronal intranuclear hyaline inclusion disease: report of a case and review of the literature. *Clin. Neuropathol.* 9, 89–96.

Gao, F. B., and Richter, J. D. (2017). Microsatellite expansion diseases: repeat toxicity found in translation. *Neuron* 93, 249–251.

Garen, P. D., Powers, J. M., Young, G. F., and Lee, V. (1986). Neuronal intranuclear hyaline inclusion disease in a nine year old. *Acta Neuropathol.* 70, 327–332. doi: 10.1007/BF00686092

Glineburg, M. R., Todd, P. K., Charlet-Berguerand, N., and Sellier, C. (2018). Repeat-associated non-AUG (RAN) translation and other molecular mechanisms in Fragile X Tremor Ataxia syndrome. *Brain Res.* 1693(Pt A), 43–54. doi: 10.1016/j.brainres.2018.02.006

Goutieres, F., Mikol, J., and Aicardi, J. (1990). Neuronal intranuclear inclusion disease in a child: diagnosis by rectal biopsy. *Ann. Neurol.* 27, 103–106. doi: 10.1002/ana.410270117

Greco, C. M., Hagerman, R. J., Tassone, F., Chudley, A. E., Del Bigio, M. R., Jacquemont, S., et al. (2002). Neuronal intranuclear inclusions in a new cerebellar tremor/ataxia syndrome among fragile X carriers. *Brain* 125(Pt 8), 1760–1771. doi: 10.1093/brain/awf184

Guo, S., Nguyen, L., and Ranum, L. P. W. (2022). RAN proteins in neurodegenerative disease: repeating themes and unifying therapeutic strategies. *Curr. Opin. Neurobiol.* 72, 160–170. doi: 10.1016/j.conb.2021.11.001

Hagerman, R., and Hagerman, P. (2021). Fragile X-associated tremor/ataxia syndrome: pathophysiology and management. *Curr. Opin. Neurol.* 34, 541–546.

Haltia, M., Somer, H., Palo, J., and Johnson, W. G. (1984). Neuronal intranuclear inclusion disease in identical twins. *Ann. Neurol.* 15, 316–321.

Haltia, M., Tarkkanen, A., Somer, H., Palo, J., and Karli, H. (1986). Neuronal intranuclear inclusion disease. clinical ophthalmological features and ophthalmic pathology. *Acta Ophthalmol.* 64, 637–643.

Hamperl, S., and Cimprich, K. A. (2014). The contribution of co-transcriptional RNA:DNA hybrid structures to DNA damage and genome instability. *DNA Repair (Amst)* 19, 84–94.

Han, X., Han, M., Liu, N., Xu, J., Zhang, Y., Zhang, Y., et al. (2019). Adult-onset neuronal intranuclear inclusion disease presenting with typical MRI changes. *Brain Behav.* 9:e01477.

Hayashi, K., Hamaguchi, T., Sakai, K., Nakamura, K., Wakabayashi, K., Shirasaki, H., et al. (2019). Neuronal intranuclear inclusion disease showing blepharoptosis and positive serum anti-acetylcholine receptor antibody without myasthenia gravis. *J. Neurol. Sci.* 400, 119–121. doi: 10.1016/j.jns.2019.03.013

Hayashi, T., Katagiri, S., Mizobuchi, K., Yoshitake, K., Kameya, S., Matsuura, T., et al. (2020). NOTCH2NLCHeterozygous GGC repeat expansion of in a patient with neuronal intranuclear inclusion disease and progressive retinal dystrophy. *Ophthalmic Genet.* 41, 93–95. doi: 10.1080/13816810.2020.1723119

Hirose, B., Hisahara, S., Uesugi, H., Sone, J., Sobue, G., and Shimohama, S. (2018). [Sporadic adult-onset neuronal intranuclear inclusion disease with abnormal electroretinogram, nerve conduction studies and somatosensory evoked potential]. *Rinsho Shinkeigaku* 58, 407–410. doi: 10.5692/clinicalneurol.cn-001154

Horino, T., Matsumoto, T., Inoue, K., Ichii, O., and Terada, Y. (2018). A case of neuronal intranuclear inclusion disease associated with lupus nephritis-like nephropathy. *eNeurological. Sci.* 10, 28–30. doi: 10.1016/j.ensci.2018.01.002

Huang, X. R., Tang, B. S., Jin, P., and Guo, J. F. (2021). The Phenotypes and mechanisms of NOTCH2NLC-Related GGC repeat expansion disorders: a comprehensive review. *Mol. Neurobiol.* 59, 523–534. doi: 10.1007/s12035-021-02616-2

Iizuka, R., and Spalke, G. (1972). [Virus-like filaments and crystalloid inclusions in a case of "primary" reticuloendotheliosis of the brain]. *Acta Neuropathol.* 21, 39–49.

Imai, T., Kato, B., Ohsima, J., and Hasegawa, Y. (2018). [An adult onset sporadic neuronal intranuclear inclusion disease case reminiscent with Fisher syndrome]. *Rinsho Shinkeigaku* 58, 505–508. doi: 10.5692/clinicalneurol.cn-001139

Ishihara, T., Okamoto, T., Saida, K., Saitoh, Y., Oda, S., Sano, T., et al. (2020). Neuronal intranuclear inclusion disease presenting with an MELAS-like episode in chronic polyneuropathy. *Neurol. Genet.* 6:e531. doi: 10.1212/NXG.0000000000000531

Ishiura, H., Shibata, S., Yoshimura, J., Suzuki, Y., Qu, W., Doi, K., et al. (2019). Noncoding CGG repeat expansions in neuronal intranuclear inclusion disease, oculopharyngodistal myopathy and an overlapping disease. *Nat. Genet.* 51, 1222–1232. doi: 10.1038/s41588-019-0458-z

Jain, A., and Vale, R. D. (2017). RNA phase transitions in repeat expansion disorders. *Nature* 546, 243–247.

Janota, I. (1979). Widespread intranuclear neuronal corpuscles (Marinesco bodies) associated with a familial spinal degeneration with cranial and peripheral nerve involvement. *Neuropathol. Appl. Neurobiol.* 5, 311–317. doi: 10.1111/j.1365-2990.1979.tb00630.x

Jiao, B., Zhou, L., Zhou, Y., Weng, L., Liao, X., Tian, Y., et al. (2020). Identification of expanded repeats in NOTCH2NLC in neurodegenerative dementias. *Neurobiol. Aging* 89, e1–e7. doi: 10.1016/j.neurobiolaging.2020.01.010

Jih, K. Y., Chou, Y. T., Tsai, P. C., Liao, Y. C., and Lee, Y. C. (2021). Analysis of NOTCH2NLC GGC repeat expansion in Taiwanese patients with amyotrophic lateral sclerosis. *Neurobiol. Aging* 108, 210–212. doi: 10.1016/j.neurobiolaging.2021.07.011

Kawarabayashi, T., Nakamura, T., Seino, Y., Hirohata, M., Mori, F., Wakabayashi, K., et al. (2018). Disappearance of MRI imaging signals in a patient with neuronal intranuclear inclusion disease. *J. Neurol. Sci.* 388, 1–3. doi: 10.1016/j.jns.2018.02.038

Kimber, T. E., Blumbergs, P. C., Rice, J. P., Hallpike, J. F., Edis, R., Thompson, P. D., et al. (1998). Familial neuronal intranuclear inclusion disease with ubiquitin positive inclusions. *J. Neurol. Sci.* 160, 33–40.

Kish, S. J., Gilbert, J. J., Chang, L. J., Mirchandani, L., Shannak, K., and Hornykiewicz, O. (1985). Brain neurotransmitter abnormalities in neuronal intranuclear inclusion body disorder. *Ann. Neurol.* 17, 405–407.

Kitagawa, N., Sone, J., Sobue, G., Kuroda, M., and Sakurai, M. (2014). Neuronal intranuclear inclusion disease presenting with resting tremor. *Case Rep. Neurol.* 6, 176–180.

Kong, H. E., Zhao, J., Xu, S., Jin, P., and Jin, Y. (2017). Fragile X-Associated Tremor/Ataxia syndrome: from molecular pathogenesis to development of therapeutics. *Front. Cell Neurosci.* 11:128. doi: 10.3389/fncel.2017.00128

Krans, A., Kearse, M. G., and Todd, P. K. (2016). Repeat-associated non-AUG translation from antisense CCG repeats in fragile X tremor/ataxia syndrome. *Ann. Neurol.* 80, 871–881.

Krans, A., Skariah, G., Zhang, Y., Bayly, B., and Todd, P. K. (2019). Neuropathology of RAN translation proteins in fragile X-associated tremor/ataxia syndrome. *Acta Neuropathol. Commun.* 7:152. doi: 10.1186/s40478-019-0782-7

La Spada, A. R., and Taylor, J. P. (2010). Repeat expansion disease: progress and puzzles in disease pathogenesis. *Nat. Rev. Genet.* 11, 247–258.

Lai, S. C., Jung, S. M., Grattan-Smith, P., Sugo, E., Lin, Y. W., Chen, R. S., et al. (2010). Neuronal intranuclear inclusion disease: two cases of dopa-responsive juvenile parkinsonism with drug-induced dyskinesia. *Mov. Disord.* 25, 1274–1279. doi: 10.1002/mds.22876

Leehey, M. A. (2009). Fragile X-associated tremor/ataxia syndrome: clinical phenotype, diagnosis, and treatment. *J. Investig. Med.* 57, 830–836. doi: 10.2310/JIM.0b013e3181af59c4

Li, H., Sun, M., Wan, B., and Xu, X. (2020a). No evidence supports the genetic heterogeneity of neuronal intranuclear inclusion disease. *Ann. Clin. Transl. Neurol.* 7, 2542–2543.

Li, M., Li, K., Li, X., Tian, Y., Shen, L., Wu, G., et al. (2020b). Multiple reversible encephalitic attacks: a rare manifestation of neuronal intranuclear inclusion disease. *BMC Neurol.* 20:125. doi: 10.1186/s12883-020-01712-5

Liang, H., Wang, B., Li, Q., Deng, J., Wang, L., Wang, H., et al. (2020). Clinical and pathological features in adult-onset NIID patients with cortical enhancement. *J. Neurol.* 267, 3187–3198. doi: 10.1007/s00415-020-09945-7

Lin, P., Jin, H., Yi, K., He, X., Lin, S., Wu, G., et al. (2020). A case report of sporadic adult Neuronal Intranuclear Inclusion Disease (NIID) with stroke-like onset. *Front. Neurol.* 11:530. doi: 10.3389/fneur.2020.00530

Lindenberg, R., Rubinstein, L. J., Herman, M. M., and Haydon, G. B. (1968). A light and electron microscopy study of an unusual widespread nuclear inclusion body disease. a possible residuum of an old herpesvirus infection. *Acta Neuropathol.* 10, 54–73. doi: 10.1007/BF00690510

Liu, X., Liu, X., Du, Y., Lin, Y., Li, C., Liu, C., et al. (2019b). A case of recurrent vomiting: extending the spectrum of neuronal intranuclear inclusion disease. *Neurol. Sci.* 40, 2661–2664. doi: 10.1007/s10072-019-03986-1

Liu, Y., Lu, J., Li, K., Zhao, H., Feng, Y., Zhang, Z., et al. (2019a). A multimodal imaging features of the brain in adult-onset neuronal intranuclear inclusion disease. *Neurol. Sci.* 40, 1495–1497.

Ma, D., Tan, Y. J., Ng, A. S. L., Ong, H. L., Sim, W., Lim, W. K., et al. (2020). Association of NOTCH2NLC repeat expansions with Parkinson disease. *JAMA Neurol.* 77, 1559–1563.

Malandrini, A., Fabrizi, G. M., Cavallaro, T., Zazzi, M., Parrotta, E., Romano, L., et al. (1996). Neuronal intranuclear inclusion disease: polymerase chain reaction and ultrastructural study of rectal biopsy specimen in a new case. *Acta Neuropathol.* 91, 215–218. doi: 10.1007/s004010050417

Malandrini, A., Villanova, M., Tripodi, S., Palmeri, S., Sicurelli, F., Parrotta, E., et al. (1998). Neuronal intranuclear inclusion disease: neuropathologic study of a case. *Brain Dev.* 20, 290–294. doi: 10.1016/s0387-7604(98)00032-1

Malik, I., Kelley, C. P., Wang, E. T., and Todd, P. K. (2021). Molecular mechanisms underlying nucleotide repeat expansion disorders. *Nat. Rev. Mol. Cell Biol.* 22, 589–607.

McFadden, K., Hamilton, R. L., Insalaco, S. J., Lavine, L., Al-Mateen, M., Wang, G., et al. (2005). Neuronal intranuclear inclusion disease without polyglutamine inclusions in a child. *J. Neuropathol. Exp. Neurol.* 64, 545–552.

Michaud, J., and Gilbert, J. J. (1981). Multiple system atrophy with neuronal intranuclear hyaline inclusions. report of a new case with light and electron microscopic studies. *Acta Neuropathol.* 54, 113–119. doi: 10.1007/BF00689403

Mori, F., Miki, Y., Tanji, K., Ogura, E., Yagihashi, N., Jensen, P. H., et al. (2011). Incipient intranuclear inclusion body disease in a 78-year-old woman. *Neuropathology* 31, 188–193. doi: 10.1111/j.1440-1789.2010.01150.x

Morimoto, S., Hatsuta, H., Komiya, T., Kanemaru, K., Tokumaru, A. M., and Murayama, S. (2017). Simultaneous skin-nerve-muscle biopsy and abnormal mitochondrial inclusions in intranuclear hyaline inclusion body disease. *J. Neurol. Sci.* 372, 447–449. doi: 10.1016/j.jns.2016.10.042

Motoki, M., Nakajima, H., Sato, T., Tada, M., Kakita, A., and Arawaka, S. (2018). Neuronal intranuclear inclusion disease showing intranuclear inclusions in renal biopsy 12 years earlier. *Neurology* 91, 884–886.

Munoz-Garcia, D., and Ludwin, S. K. (1986). Adult-onset neuronal intranuclear hyaline inclusion disease. *Neurology* 36, 785–790.

Nakamura, M., Murray, M. E., Lin, W. L., Kusaka, H., and Dickson, D. W. (2014). Optineurin immunoreactivity in neuronal and glial intranuclear inclusions in adult-onset neuronal intranuclear inclusion disease. *Am. J. Neurodegener. Dis.* 3, 93–102.

Nakamura, M., Ueki, S., Kubo, M., Yagi, H., Sasaki, R., Okada, Y., et al. (2018). Two cases of sporadic adult-onset neuronal intranuclear inclusion disease preceded by urinary disturbance for many years. *J. Neurol. Sci.* 392, 89–93. doi: 10.1016/j.jns.2018.07.012

Nakamura, N., Tsunoda, K., Mitsutake, A., Shibata, S., Mano, T., Nagashima, Y., et al. (2020). Clinical characteristics of neuronal intranuclear inclusion disease-related retinopathy with CGG repeat expansions in the NOTCH2NLC gene. *Invest. Ophthalmol. Vis. Sci.* 61:27. doi: 10.1167/iovs.61.11.27

Nakano, Y., Takahashi-Fujigasaki, J., Sengoku, R., Kanemaru, K., Arai, T., Kanda, T., et al. (2017). PML nuclear bodies are altered in adult-onset neuronal intranuclear hyaline inclusion disease. *J. Neuropathol. Exp. Neurol.* 76, 585–594. doi: 10.1093/jnen/nlx039

Ogasawara, M., Eura, N., Nagaoka, U., Sato, T., Arahata, H., Hayashi, T., et al. (2022). Intranuclear inclusions in skin biopsies are not limited to neuronal intranuclear inclusion disease but can also be seen in oculopharyngodistal myopathy. *Neuropathol. Appl. Neurobiol.* 48:e12787.

Ogasawara, M., Iida, A., Kumutpongpanich, T., Ozaki, A., Oya, Y., Konishi, H., et al. (2020). CGG expansion in NOTCH2NLC is associated with oculopharyngodistal myopathy with neurological manifestations. *Acta Neuropathol. Commun.* 8:204.

Oh, S. Y., He, F., Krans, A., Frazer, M., Taylor, J. P., Paulson, H. L., et al. (2015). RAN translation at CGG repeats induces ubiquitin proteasome system impairment in models of fragile X-associated tremor ataxia syndrome. *Hum. Mol. Genet.* 24, 4317–4326. doi: 10.1093/hmg/ddv165

Okamoto, K., Tokiguchi, S., Furusawa, T., Ishikawa, K., Quardery, A. F., Shinbo, S., et al. (2003). MR features of diseases involving bilateral middle cerebellar peduncles. *AJNR Am. J. Neuroradiol.* 24, 1946–1954.

Okamura, S., Takahashi, M., Abe, K., Inaba, A., Sone, J., and Orimo, S. (2020). A case of neuronal intranuclear inclusion disease with recurrent vomiting and without apparent DWI abnormality for the first seven years. *Heliyon* 6:e04675. doi: 10.1016/j.heliyon.2020.e04675

Okubo, M., Doi, H., Fukai, R., Fujita, A., Mitsuhashi, S., Hashiguchi, S., et al. (2019). GGC repeat expansion of NOTCH2NLC in adult patients with leukoencephalopathy. *Ann. Neurol.* 86, 962–968.

Omoto, S., Hayashi, T., Matsuno, H., Higa, H., Kameya, S., Sengoku, R., et al. (2018). Neuronal intranuclear hyaline inclusion disease presenting with childhood-onset night blindness associated with progressive retinal dystrophy. *J. Neurol. Sci.* 388, 84–86. doi: 10.1016/j.jns.2018.03.010

O'Sullivan, J. D., Hanagasi, H. A., Daniel, S. E., Tidswell, P., Davies, S. W., and Lees, A. J. (2000). Neuronal intranuclear inclusion disease and juvenile parkinsonism. *Movement Disord.* 15, 990–995.

Oyer, C. E., Cortez, S., O'Shea, P., and Popovic, M. (1991). Cardiomyopathy and myocyte intranuclear inclusions in neuronal intranuclear inclusion disease: a case report. *Hum. Pathol.* 22, 722–724. doi: 10.1016/0046-8177(91)90296-2

Padilha, I. G., Nunes, R. H., Scortegagna, F. A., Pedroso, J. L., Marussi, V. H., Rodrigues Goncalves, M. R., et al. (2018). MR imaging features of adult-onset neuronal intranuclear inclusion disease may be indistinguishable from fragile X-associated tremor/ataxia syndrome. *AJNR Am. J. Neuroradiol.* 39, E100–E101. doi: 10.3174/ajnr.A5729

Parker, J. C. Jr., Dyer, M. L., and Paulsen, W. A. (1987). Neuronal intranuclear hyaline inclusion disease associated with premature coronary atherosclerosis. *J. Clin. Neuro-ophthalmol.* 7, 244–249.

Patel, H., Norman, M. G., Perry, T. L., and Berry, K. E. (1985). Multiple system atrophy with neuronal intranuclear hyaline inclusions. report of a case and review of the literature. *J. Neurol. Sci.* 67, 57–65. doi: 10.1016/0022-510x(85)90022-x

Paviour, D. C., Revesz, T., Holton, J. L., Evans, A., Olsson, J. E., and Lees, A. J. (2005). Neuronal intranuclear inclusion disease: report on a case originally diagnosed as dopa-responsive dystonia with Lewy bodies. *Movement Disord.* 20, 1345–1349. doi: 10.1002/mds.20559

Pihlamaa, T., Suominen, S., and Kiuru-Enari, S. (2012). Familial amyloidotic polyneuropathy type IV–gelsolin amyloidosis. *Amyloid* 19(Suppl. 1), 30–33. doi: 10.3109/13506129.2012.674076

Pilson, K., Farrell, M., Lynch, B., and Devaney, D. (2018). A case of juvenile onset neuronal intranuclear inclusion disease with a negative antemortem skin biopsy. *Pediatr. Dev. Pathol.* 21, 494–496. doi: 10.1177/1093526617724293

Pountney, D. L., Raftery, M. J., Chegini, F., Blumbergs, P. C., and Gai, W. P. (2008). NSF, Unc-18-1, dynamin-1 and HSP90 are inclusion body components in neuronal intranuclear inclusion disease identified by anti-SUMO-1-immunocapture. *Acta Neuropathol.* 116, 603–614. doi: 10.1007/s00401-008-0437-4

Qin, C., Huang, B. X., Yang, K. K., Chu, K. J., Tian, D. S., and Bu, B. T. (2020). Recurrent headaches with cerebral white matter lesions. *J. Neurol. Sci.* 408:116557.

Qin, X., Chen, H., Zhou, C., Wang, X., Gao, J., Guo, N., et al. (2021). Neuronal intranuclear inclusion disease: two case report and literature review. *Neurol. Sci.* 42, 293–296.

Raza, H. K., Singh, S., Rai, P., Chansysouphanthong, T., Amir, A., Cui, G., et al. (2020). Recent progress in neuronal intranuclear inclusion disease: a review of the literature. *Neurol. Sci.* 41, 1019–1025. doi: 10.1007/s10072-019-04195-6

Ribot, C., Soler, C., Chartier, A., Al Hayek, S., Nait-Saidi, R., Barbezier, N., et al. (2022). Activation of the ubiquitin-proteasome system contributes to oculopharyngeal muscular dystrophy through muscle atrophy. *PLoS Genet.* 18:e1010015. doi: 10.1371/journal.pgen.1010015

Rodriguez, C. M., and Todd, P. K. (2019). New pathologic mechanisms in nucleotide repeat expansion disorders. *Neurobiol. Dis.* 130:104515.

Sakurai, T., Harada, S., Wakida, K., Yoshida, M., and Nishida, H. (2016). Sporadic adult-onset neuronal intranuclear inclusion disease with the main presentation of repeated cerebellar ataxia: a case study. *Rinsho Shinkeigaku* 56, 439–443. doi: 10.5692/clinicalneurol.cn-000875

Sanders, D. W., and Brangwynne, C. P. (2017). Neurodegenerative disease: RNA repeats put a freeze on cells. *Nature* 546, 215–216. doi: 10.1038/nature22503

Schuffler, M. D., Bird, T. D., Sumi, S. M., and Cook, A. (1978). A familial neuronal disease presenting as intestinal pseudoobstruction. *Gastroenterology* 75, 889–898.

Sellier, C., Buijsen, R. A. M., He, F., Natla, S., Jung, L., Tropel, P., et al. (2017). Translation of expanded CGG repeats into FMRpolyG is pathogenic and may contribute to fragile X tremor ataxia syndrome. *Neuron* 93, 331–347.

Shi, C. H., Fan, Y., Yang, J., Yuan, Y. P., Shen, S., Liu, F., et al. (2021). NOTCH2NLC intermediate-length repeat expansions are associated with parkinson disease. *Ann. Neurol.* 89, 182–187.

Shindo, K., Tsuchiya, M., Hata, T., Ichinose, Y., Koh, K., Sone, J., et al. (2019). Non-convulsive status epilepticus associated with neuronal intranuclear inclusion disease: a case report and literature review. *Epilepsy Behav. Case Rep.* 11, 103–106. doi: 10.1016/j.ebcr.2019.01.007

Sloane, A. E., Becker, L. E., Ang, L. C., Wark, J., and Haslam, R. H. (1994). Neuronal intranuclear hyaline inclusion disease with progressive cerebellar ataxia. *Pediatr. Neurol.* 10, 61–66.

Soffer, D. (1985). Neuronal intranuclear hyaline inclusion disease presenting as Friedreich's ataxia. *Acta Neuropathol.* 65, 322–329. doi: 10.1007/BF00687016

Sone, J., Kitagawa, N., Sugawara, E., Iguchi, M., Nakamura, R., Koike, H., et al. (2014). Neuronal intranuclear inclusion disease cases with leukoencephalopathy diagnosed via skin biopsy. *J. Neurol. Neurosurg. Psychiatry* 85, 354–356. doi: 10.1136/jnnp-2013-306084

Sone, J., Mitsuhashi, S., Fujita, A., Mizuguchi, T., Hamanaka, K., Mori, K., et al. (2019). Long-read sequencing identifies GGC repeat expansions in NOTCH2NLC associated with neuronal intranuclear inclusion disease. *Nat. Genet.* 51, 1215–1221.

Sone, J., Mori, K., Inagaki, T., Katsumata, R., Takagi, S., Yokoi, S., et al. (2016). Clinicopathological features of adult-onset neuronal intranuclear inclusion disease. *Brain* 139(Pt 12), 3170–3186.

Sone, J., Tanaka, F., Koike, H., Inukai, A., Katsuno, M., Yoshida, M., et al. (2011). Skin biopsy is useful for the antemortem diagnosis of neuronal intranuclear inclusion disease. *Neurology* 76, 1372–1376.

Sugiyama, A., Takeda, T., Koide, M., Yokota, H., Mukai, H., Kitayama, Y., et al. (2021). Coexistence of neuronal intranuclear inclusion disease and amyotrophic lateral sclerosis: an autopsy case. *BMC Neurol.* 21:273. doi: 10.1186/s12883-021-02306-5

Sun, Q. Y., Xu, Q., Tian, Y., Hu, Z. M., Qin, L. X., Yang, J. X., et al. (2020). Expansion of GGC repeat in the human-specific NOTCH2NLC gene is associated with essential tremor. *Brain* 143, 222–233. doi: 10.1093/brain/awz372

Sung, J. H., Ramirez-Lassepas, M., Mastri, A. R., and Larkin, S. M. (1980). An unusual degenerative disorder of neurons associated with a novel intranuclear hyaline inclusion (neuronal intranuclear hyaline inclusion disease). a clinicopathological study of a case. *J. Neuropathol. Exp. Neurol.* 39, 107–130. doi: 10.1097/00005072-198003000-00001

Suzuki, I. K., Gacquer, D., Van Heurck, R., Kumar, D., Wojno, M., Bilheu, A., et al. (2018). Human-Specific NOTCH2NL genes expand cortical neurogenesis through delta/notch regulation. *Cell* 173, 1370–1384.e16. doi: 10.1016/j.cell.2018.03.067

Takahashi, F. J., Arai, K., Funata, N., and Fujigasaki, H. (2010). SUMOylation substrates in neuronal intranuclear inclusion disease. *Neuropathol. Appl. Neurobiol.* 32, 92–100.

Takahashi, J., Fukuda, T., Tanaka, J., Minamitani, M., Fujigasaki, H., and Uchihara, T. (2000). Neuronal intranuclear hyaline inclusion disease with polyglutamine-immunoreactive inclusions. *Acta Neuropathol.* 99, 589–594. doi: 10.1007/s004010051166

Takahashi-Fujigasaki, J. (2003). Neuronal intranuclear hyaline inclusion disease. *Neuropathology* 23, 351–359.

Takahashi-Fujigasaki, J., Arai, K., Funata, N., and Fujigasaki, H. (2006). SUMOylation substrates in neuronal intranuclear inclusion disease. *Neuropathol. Appl. Neurobiol.* 32, 92–100. doi: 10.1111/j.1365-2990.2005.00705.x

Takahashi-Fujigasaki, J., Nakano, Y., Uchino, A., and Murayama, S. (2016). Adult-onset neuronal intranuclear hyaline inclusion disease is not rare in older adults. *Geriatrics Gerontol. Int.* 16(Suppl. 1), 51–56.

Takeshita, J., Kobayashi, H., Shimoe, Y., Sone, J., Sobue, G., and Kuriyama, M. (2017). Adult-onset neuronal intranuclear inclusion disease presented transient global amnesia-a case report. *Rinsho Shinkeigaku* 57, 303–306. doi: 10.5692/clinicalneurol.cn-000994

Takumida, H., Yakabe, M., Mori, H., Shibasaki, K., Umeda-Kameyama, Y., Urano, T., et al. (2017). Case of a 78-year-old woman with a neuronal intranuclear inclusion disease. *Geriatr. Gerontol. Int.* 17, 2623–2625. doi: 10.1111/ggi.13174

Tateishi, J., Nagara, H., Ohta, M., Matsumoto, T., Fukunaga, H., and Shida, K. (1984). Intranuclear inclusions in muscle, nervous tissue, and adrenal gland. *Acta Neuropathol.* 63, 24–32. doi: 10.1007/BF00688467

Tian, Y., Wang, J. L., Huang, W., Zeng, S., Jiao, B., Liu, Z., et al. (2019). Expansion of human-specific GGC repeat in neuronal intranuclear inclusion disease-related disorders. *Am. J. Hum. Genet.* 105, 166–176. doi: 10.1016/j.ajhg.2019.05.013

Toko, M., Ohshita, T., Kurashige, T., Morino, H., Kume, K., Yamashita, H., et al. (2021). FXTAS is difficult to differentiate from neuronal intranuclear inclusion disease through skin biopsy: a case report. *BMC Neurol.* 21:396. doi: 10.1186/s12883-021-02425-z

Tokumaru, A. M., Saito, Y., and Murayma, S. (2021). Diffusion-Weighted imaging is key to diagnosing specific diseases. *Magn. Reson. Imaging Clin. N. Am.* 29, 163–183.

Vermilion, J., Johnson, M., Srinivasan, J., and Mink, J. W. (2019). Neuronal intranuclear inclusion disease: longitudinal case report of motor and nonmotor symptoms. *J. Child Neurol.* 34, 801–805. doi: 10.1177/0883073819860566

Wang, F., Ma, X., Shi, Y., Jia, L., Zuo, X., Yu, Y., et al. (2020a). Cognitive profiles in adult-onset neuronal intranuclear inclusion disease: a case series from the memory clinic. *Neurol. Sci.* 42, 2487–2495. doi: 10.1007/s10072-020-04864-x

Wang, R., Nie, X., Xu, S., Zhang, M., Dong, Z., and Yu, S. (2019a). Interrelated pathogenesis? neuronal intranuclear inclusion disease combining with hemiplegic migraine. *Headache* 60, 382–395. doi: 10.1111/head.13687

Wang, Y., Wang, B., Wang, L., Yao, S., Zhao, J., Zhong, S., et al. (2020b). Diagnostic indicators for adult-onset neuronal intranuclear inclusion disease. *Clin. Neuropathol.* 39, 7–18.

Wang, Y., Yi, Y. H., Li, X. B., Hou, D. R., Wang, B. H., and Chen, W. A. (2019b). [Sporadic adult-onset neuronal intranuclear inclusion disease: a case report]. *Zhonghua Nei Ke Za Zhi* 58, 606–608.

Wang, Z., Guo, J., Wang, M., Wang, Z., Hong, D., and Yu, X. (2020c). Adult-onset neuronal intranuclear inclusion disease mimicking Parkinson's disease in a Chinese patient: a case report and literature reviews. *Neuro Endocrinol. Lett.* 41, 155–161.

Weidenheim, K. M., and Dickson, D. W. (1995). Intranuclear inclusion bodies in an elderly demented woman: a form of intranuclear inclusion body disease. *Clin. Neuropathol.* 14, 93–99.

Westenberger, A., and Klein, C. (2020). Essential phenotypes of NOTCH2NLC-related repeat expansion disorder. *Brain* 143, 5–8.

Wiltshire, K. M., Dunham, C., Reid, S., Auer, R. N., and Suchowersky, O. (2010). Neuronal Intranuclear Inclusion Disease presenting as juvenile Parkinsonism. *Canadian J. Neurol. Sci.* 37, 213–218.

Xiao, F., Tian, X., and Wang, X. F. (2018). Cerebral atrophy and leukoencephalopathy in a young man presenting with encephalitic episodes. *JAMA Neurol.* 75, 1563–1564. doi: 10.1001/jamaneurol.2018.2333

Xu, K., Li, Y., Allen, E. G., and Jin, P. (2021). Therapeutic development for CGG repeat expansion-associated neurodegeneration. *Front. Cell Neurosci.* 15:655568. doi: 10.3389/fncel.2021.655568

Yadav, N., Raja, P., Shetty, S. S., Jitender, S., Prasad, C., Kamble, N. L., et al. (2019). Neuronal intranuclear inclusion disease: a rare etiology for rapidly progressive dementia. *Alzheimer Dis. Assoc. Disord.* 33, 359–361. doi: 10.1097/WAD.0000000000000312

Yamada, W., Takekoshi, A., Ishida, K., Mochizuki, K., Sone, J., Sobue, G., et al. (2017). Case of adult-onset neuronal intranuclear hyaline inclusion disease with negative electroretinogram. *Documenta Ophthalmol. Adv. Ophthalmol.* 134, 221–226. doi: 10.1007/s10633-017-9584-z

Yamaguchi, N., Mano, T., Ohtomo, R., Ishiura, H., Almansour, M. A., Mori, H., et al. (2018). An autopsy case of familial neuronal intranuclear inclusion disease with dementia and neuropathy. *Int. Med.* 57, 3459–3462.

Yamanaka, H., Hashimoto, S., and Suenaga, T. (2019). [Neuronal intranuclear inclusion disease with prolonged impaired consciousness and status epilepticus: a case report]. *Rinsho Shinkeigaku* 59, 425–430. doi: 10.5692/clinicalneurol.cn-001264

Yang, D., Cen, Z., Wang, L., Chen, X., Liu, P., Wang, H., et al. (2021). Neuronal intranuclear inclusion disease tremor-dominant subtype: a mimicker of essential tremor. *Eur. J. Neurol.* 29, 450–458. doi: 10.1111/ene.15169

Yokoi, S., Yasui, K., Hasegawa, Y., Niwa, K., Noguchi, Y., Tsuzuki, T., et al. (2016). Pathological background of subcortical hyperintensities on diffusion-weighted images in a case of neuronal intranuclear inclusion disease. *Clin. Neuropathol.* 35, 375–380. doi: 10.5414/NP300961

Yoshimoto, T., Takamatsu, K., Kurashige, T., Sone, J., Sobue, G., and Kuriyama, M. (2017). [Adult-Onset neuronal intranuclear inclusion disease in two female siblings]. *Brain Nerve* 69, 267–274. doi: 10.11477/mf.1416200737

Yu, W. Y., Xu, Z., Lee, H. Y., Tokumaru, A., Tan, J. M. M., Ng, A., et al. (2019). Identifying patients with neuronal intranuclear inclusion disease in Singapore using characteristic diffusion-weighted MR images. *Neuroradiology* 61, 1281–1290. doi: 10.1007/s00234-019-02257-2

Yuan, Y., Liu, Z., Hou, X., Li, W., Ni, J., Huang, L., et al. (2020). Identification of GGC repeat expansion in the NOTCH2NLC gene in amyotrophic lateral sclerosis. *Neurology* 95, e3394–e3405. doi: 10.1212/WNL.0000000000010945

Zannolli, R., Gilman, S., Rossi, S., Volpi, N., Bernini, A., Galluzzi, P., et al. (2002). Hereditary neuronal intranuclear inclusion disease with autonomic failure and cerebellar degeneration. *Arch. Neurol.* 59, 1319–1326. doi: 10.1001/archneur.59.8.1319

Zhang, S., Gong, Q., Wu, D., Tian, Y., Shen, L., Lu, J., et al. (2020). Genetic and pathological characteristic patterns of a family with neuronal intranuclear inclusion disease. *J. Neuropathol. Exp. Neurol.* 79, 1293–1302.

Zhao, D., Zhu, S., Xu, Q., Deng, J., Wang, Z., and Liu, X. (2021). Neuronal intranuclear inclusion disease presented with recurrent vestibular migraine-like attack: a case presentation. *BMC Neurol.* 21:334. doi: 10.1186/s12883-021-02367-6

Zhao, X., and Usdin, K. (2021). (Dys)function follows form: nucleic acid structure, repeat expansion, and disease pathology in FMR1 disorders. *Int. J. Mol. Sci.* 22:9167. doi: 10.3390/ijms22179167

Zhong, S., Lian, Y., Luo, W., Luo, R., Wu, X., Ji, J., et al. (2021). Upstream open reading frame with NOTCH2NLC GGC expansion generates polyglycine aggregates and disrupts nucleocytoplasmic transport: implications for polyglycine diseases. *Acta Neuropathol.* 142, 1003–1023. doi: 10.1007/s00401-021-02375-3

Zhou, Z. D., Jankovic, J., Ashizawa, T., and Tan, E. K. (2022). Neurodegenerative diseases associated with non-coding CGG tandem repeat expansions. *Nat. Rev. Neurol.* 18, 145–157.

Zu, T., Gibbens, B., Doty, N. S., Gomes-Pereira, M., Huguet, A., Stone, M. D., et al. (2011). Non-ATG-initiated translation directed by microsatellite expansions. *Proc. Natl. Acad. Sci. U S A.* 108, 260–265. doi: 10.1073/pnas.1013343108

frontiers | Frontiers in Aging Neuroscience

TYPE Original Research
PUBLISHED 16 September 2022
DOI 10.3389/fnagi.2022.1004954



OPEN ACCESS

EDITED BY
Vijay Karkal Hegde,
Texas Tech University, United States

REVIEWED BY
Xiaolong Zhao,
Sichuan Academy of Medical Sciences and Sichuan Provincial People's Hospital, China
Wu Wenbin,
Hospital of Chengdu University of Traditional Chinese Medicine, China

*CORRESPONDENCE
Wei Li
822203867@qq.com
Yuzhen Xu
xuyuzhen@sdfmu.edu.cn

†These authors share first authorship

SPECIALTY SECTION
This article was submitted to Alzheimer's Disease and Related Dementias, a section of the journal Frontiers in Aging Neuroscience

RECEIVED 27 July 2022
ACCEPTED 29 August 2022
PUBLISHED 16 September 2022

CITATION
Liu G, Li Y, Xu Y and Li W (2022) Type 2 diabetes is associated with increased risk of dementia, but not mild cognitive impairment: a cross-sectional study among the elderly in Chinese communities.
Front. Aging Neurosci. 14:1004954.
doi: 10.3389/fnagi.2022.1004954



# Type 2 diabetes is associated with increased risk of dementia, but not mild cognitive impairment: a cross-sectional study among the elderly in Chinese communities

Guojun Liu[1†], Yong Li[2,3,4†], Yuzhen Xu[5*] and Wei Li[6,7*]

[1]Department of Rehabilitation Medicine, The Third People's Hospital of Lanzhou, Lanzhou, China, [2]Department of Nephrology, Hubei Provincial Hospital of Traditional Chinese Medicine, Wuhan, China, [3]Department of Nephrology, Affiliated Hospital of Hubei University of Chinese Medicine, Wuhan, China, [4]Hubei Provincial Academy of Traditional Chinese Medicine, Wuhan, China, [5]Department of Rehabilitation, The Second Affiliated Hospital of Shandong First Medical University, Taian, China, [6]Department of Geriatric Psychiatry, Shanghai Mental Health Center, Shanghai Jiao Tong University School of Medicine, Shanghai, China, [7]Alzheimer's Disease and Related Disorders Center, Shanghai Jiao Tong University, Shanghai, China

**Background:** Previous studies have confirmed that diabetes is associated with cognitive impairment, but there is little data on this among older Chinese.

**Methods:** This study included 192 dementia patients, 610 patients with mild cognitive impairment (MCI), and 2,218 normal controls. Their general demographic information (such as gender, age, education, etc.), disease-related information (hypertension), and diabetes information (such as whether you have diabetes, course of the disease, etc) were collected by standardized questionnaires. The mini-mental state examination (MMSE) and Montreal Cognitive Assessment (MoCA) were used to assess their overall cognitive function, Moreover, 84 healthy, randomly selected older adults also underwent brain MRI scans at the same time, and the target brain regions included the hippocampus, the third, fourth, and fifth ventricles.

**Results:** The proportion of type 2 diabetes was significantly higher in the dementia group (25.5%) than that in the normal elderly group (15.6%) and the MCI group (17.7%). By using stepwise multiple logistics regression analysis, we found that type 2 diabetes was associated with dementia ($p$ = 0.005*, OR = 1.805, 95%CI: 1.199–2.761), but not with MCI ($p > 0.05$). The volume of the fourth ventricle of the healthy elderly with diabetes was significantly larger than that of the healthy elderly without diabetes ($p < 0.05$), but there was no statistical difference ($p > 0.05$) in the volume of the hippocampus, the third ventricle, and the fifth ventricle between the two groups. However, we did not find an association between the fourth ventricle and cognitive scores (MMSE and MoCA).

**Conclusions:** In conclusion, type 2 diabetes in elderly Chinese people is associated with dementia, but not MCI. Type 2 diabetes may impair cognitive function by affecting the volume of the fourth ventricle. However, larger longitudinal follow-up studies are needed to confirm these conclusions.

KEYWORDS

type 2 diabetes, cognition, elderly, MRI, the fourth ventricle

# Introduction

Dementia is a serious neurodegenerative disease that increases in incidence with age (Reddy and Hashmi, 2020). A recent meta-analysis suggested that the pooled prevalence of all-cause dementia among individuals aged 50 and over in the community was 697 (CI95%: 546–864) per 10,000 persons, and the number approximately doubles every 5 years (Cao et al., 2020). China has 249.49 million people aged 60 and above, accounting for 17.9% of the total population (140 million), indicating a higher prevalence of dementia (Cao et al., 2020). There is no doubt that caring for these dementia patients will place a heavy burden on the public and healthcare systems (Jia et al., 2020a). To make matters worse, there are currently no effective strategies to treat dementia or delay cognitive decline.

Mild cognitive impairment (MCI) is considered a transitional stage between unimpaired cognitive function and dementia (Jia et al., 2020b). It is defined as objective cognitive impairment relative to a person's age and is associated with cognitive symptoms in a person with basically normal functional activities but without dementia (Cooper et al., 2015). According to some epidemiological studies, the prevalence of MCI is about 6 percent in the general population, while rising to 20 percent in people 65 and older (Lopez et al., 2007; Sachdev et al., 2015). People with MCI generally have a higher risk of developing dementia, with about 46 percent developing dementia within 3 years, compared with 3 percent of the same age group (Tschanz et al., 2006). However, not all patients with MCI will necessarily develop dementia, and a significant proportion of patients with MCI will revert to normal status after appropriate intervention (Karssemeijer et al., 2017). Therefore, there is a consensus that cognitive intervention should be initiated at the MCI stage (Jia et al., 2020b).

Of all the risk factors for dementia and MCI, diabetes stands out. Epidemiological studies confirm that people with diabetes are at increased risk of developing dementia and MCI (Biessels et al., 2006; Koekkoek et al., 2015), suggests that diabetes may play an important role in the pathogenesis of cognitive decline. Current information from neuroimaging and neuropathologic studies suggests that elderly patients with diabetes have significant evidence of subclinical infarction and cerebral atrophy (Mayeda et al., 2015). More interestingly, patients with diabetes often exhibit pathologic changes similar to those seen in early Alzheimer's disease (AD; Ninomiya, 2014), and the mechanism may involve immunity, inflammation, and insulin resistance (Li et al., 2015). However, similar studies in China are relatively scarce, and their conclusions are also inconsistent. For example, in Jia et al. (2020b) study, they found that diabetes was a risk factor for both dementia and MCI, while other studies have not reached the same conclusion (Li et al., 2016; Qin et al., 2020).

In the current study, we used data from a large community sample of older adults to specifically explore the relationship between diabetes, dementia, and MCI. Unlike other studies, we also added structural magnetic resonance data to a subset of healthy people. Our hypothesis is that diabetes has an impact on both dementia and MCI, and that patients with diabetes already have changes in brain structure even when there is no significant change in their cognitive function.

# Methods

## The study population

Data were obtained from the China Longitudinal Aging Study (CLAS), which has been described in detail in our previous studies (Xiao et al., 2013; Lin et al., 2019). A total of 3,020 community-based individuals aged 60 years or older [including 610 patients with mild cognitive impairment (MCI), 192 patients with dementia, and 2,218 normal controls] were included in the current study. All subjects need to meet the following conditions: (1) age 60 and older; (2) vision and hearing were normal; (3) without a combination of life-threatening diseases, such as myocardial infarction, cerebral infarction, etc.; and (4) without serious mental illness, such as schizophrenia, major depression, etc. If these subjects were: (1) younger than 60 years of age; (2) associated with type 1 diabetes; (3) associated with diseases that affect blood glucose metabolism, such as Cushing's syndrome; (4) associated with diseases that affect cognitive functions, such as syphilis and vitamin B12 deficiency, would be excluded; and (5) hyperthyroidism, Cushing syndrome, primary hyperaldosteronism or other diseases that affect glucose metabolism of the elderly would

also be excluded. Then all the eligible elderly were required to complete a general demographic survey, neuropsychological assessment, and clinical assessment. The diagnosis of MCI was according to Petersen's criteria (Petersen, 2011), while the diagnosis of dementia was according to DSM IV. All the diagnostic and evaluation procedures were performed by experienced clinicians (Biedermann and Fleischhacker, 2016). Moreover, T1 phase Brain MRI scans were also performed on 84 older adults with normal cognitive function in a random lottery.

This study was approved by the Ethics Committee of Shanghai Mental Health Center, and informed consent was signed by patients or their families before the study began. The whole study was carried out in accordance with the principles of the Declaration of Helsinki.

## Diagnosis of type 2 diabetes

Participants were considered to have type 2 diabetes if their fasting serum glucose level was ≥7.0 mmol/L (126 mg/dl) or their 2-h value in an oral glucose tolerance test was ≥11.1 mmol/L. Moreover, self-reported physician's diagnosis or treatment with oral hypoglycemic agents and/or insulin were also considered to have type 2 diabetes (Gao et al., 2015).

## Cognitive assessment

The Mini-Mental State Examination (MMSE; Folstein et al., 1975) and Montreal Cognitive Assessment (MoCA; Nasreddine et al., 2005) are the most commonly used assessment tools in the field of geriatric cognition. Both of them have a total score of 30, and both have good sensitivity and specificity. However, compared with MMSE, the MoCA scale has better sensitivity. Therefore, the former was mainly used to screen for dementia, while the latter was mainly used to screen for MCI (Ciesielska et al., 2016).

## T1 phase structure MRI

Baseline cranial MRI was performed on 84 elderly subjects with normal cognitive function. T1 structural images were obtained using the Magnetom Verio 3.0 T scanner (Siemens, Munich, Germany), and the parameters were as follows: TR = 2,300 ms, TE = 2.98 ms, flip angle 9°, slice thickness 1.2 mm, matrix size 240*256, field of view (FOV) 240*256 mm, and 17,614 slices. All sMRI data were processed using FreeSurfer V6.0 software Clinica (Brown et al., 2020), including spatial registration, cortical thickness estimation, cortical surface segmentation, extraction of subcortical structures, and inclusion of blocks to 46 global structures. Previous studies have shown that the hippocampus is most closely related to cognitive function, while diabetes is often related to the increase in ventricular volume (Sadykova and Nazhmutdinova, 2009; Opitz, 2014; Eichenbaum, 2017; Lisman et al., 2017; Boutouyrie et al., 2022). Therefore, our target brain regions mainly included the hippocampus, third ventricle, fourth ventricle, and fifth brain region.

## Covariates

We also collected general demographic information (age, sex, education level), lifestyle information (smoking, drinking, tea drinking, physical exercise hobbies), and disease-related information (hypertension) through standardized questionnaires. Among these variables, those that differed among the MCI group, the dementia group, and the normal control group were considered covariates.

# Statistical methods

Continuous variables were expressed by Mean ± Standard Deviation (SD), while classified variables were expressed by frequency (%). Univariate ANOVA and Chi-square test were used to compare continuous and categorical variables among the MCI group, dementia group, and normal control group, respectively. Stepwise multivariate logistic regression analysis was used to explore the association between type 2 diabetes and cognitive impairment (Model 1 only contained type 2 diabetes; model 2 contained type 2 diabetes, age, sex, and education levels; model 3 contained type 2 diabetes, age, sex, education levels, smoker, tea drinker, hobby, physical exercise, and hypertension). Next, the ROC curve was used to explore the sensitivity and specificity of type 2 diabetes in predicting dementia. Then the independent sample *T*-test was used to detect differences in brain area volume between the diabetes group and the non-diabetes group. Then the correlation analysis was used to explore the correlation between type 2 diabetes and cognitive scores and cognitive brain regions (gender, age, and education are controlled). Two-tailed tests were used at a significance level of $p < 0.05$ for all analyzes. The data were analyzed using SPSS 22.0 (IBM Corporation, Armonk, NY, USA).

# Results

## General demographic data of the research object

**Table 1** presents the general demographic data of the research object. The proportion of type 2 diabetes was

TABLE 1 Demography, lifestyle, type 2 diabetes, and cognitive function in the overall database of study participants.

| Variables | Dementia ($n$ = 192) | MCI ($n$ = 610) | Normal ($n$ = 2,218) | F/X$^2$ | $p$ |
|---|---|---|---|---|---|
| Age, years | 78.83 ± 7.54 | 73.86 ± 8.24 | 70.10 ± 7.53 | 145.76 | <0.001* |
| Education, years | 4.34 ± 4.77 | 5.67 ± 5.02 | 9.25 ± 5.72 | 138.34 | <0.001* |
| Males, n (%) | 71 (37.0) | 233 (38.2) | 1,074 (48.4) | 26.347 | <0.001* |
| Smoker, n (%) | 43 (22.4) | 147 (24.1) | 650 (29.3) | 9.46 | 0.009* |
| Drinker, n (%) | 31 (16.1) | 119 (19.5) | 475 (21.4) | 3.65 | 0.162 |
| Tea drinker, n (%) | 57 (29.7) | 220 (36.1) | 1,116 (50.3) | 61.39 | <0.001* |
| Hobby, n (%) | 48 (25.0) | 267 (43.8) | 1,318 (59.4) | 116.98 | <0.001* |
| Diabetes, n (%) | 49 (25.5) | 108 (17.7) | 346 (15.6) | 13.136 | <0.001* |
| Hypertension, n (%) | 112 (58.3) | 294 (48.2) | 1,029 (46.4) | 10.244 | 0.006* |
| Physical Exercise, n (%) | 92 (47.9) | 389 (63.8) | 1,689 (76.1) | 94.35 | <0.001* |
| MMSE | 13.97 ± 7.41 | 22.38 ± 5.73 | 26.80 ± 3.51 | 877.04 | <0.001* |
| MoCA | 9.10 ± 6.25 | 16.72 ± 6.15 | 22.79 ± 5.18 | 724.15 | <0.001* |

Note: *$p < 0.05$; MoCA, Montreal Cognitive Assessment; MMSE, Mini-mental State Examination; MCI, mild cognitive impairment.

significantly higher in the dementia group (25.5%) than that in the normal elderly group (15.6%) and the MCI group (17.7%), while there was no statistical difference between the latter two groups. In addition, there were also statistical differences in age ($p < 0.001$), education ($p < 0.001$), gender ($p < 0.001$), smoker ($p = 0.009$), tea drinker ($p < 0.001$), hobby ($p < 0.001$), hypertension ($p = 0.006$), physical exercise ($p < 0.001$), MMSE ($P < 0.001$), and MoCA ($p < 0.001$) among the three groups, so these variables would eventually be considered as covariables.

## Stepwise logistic regression model was used to investigate the relationship between type 2 diabetes, dementia, and MCI

Stepwise multivariate logistic regression models were used to explore the association between type 2 diabetes and dementia/MCI. In model 1, without controlling for any variables, we found that type 2 diabetes was only associated with dementia ($p < 0.001$* OR = 1.854, 95%CI: 1.314–2.615), but not MCI ($p > 0.05$); In model 2, after controlling for age, education, and gender, we found that type 2 diabetes was also an influential factor for dementia ($p = 0.003$*, OR = 1.836, 95%CI: 1.237–2.724), but not MCI ($p > 0.05$); In model 3, smoker, tea drinker, hobbies, diabetes, and physical exercise were further controlled on the basis of Model 2, and the above association still existed (dementia: $p = 0.005$*, OR = 1.805, 95%CI: 1.199–2.761, MCI: $p > 0.05$). Then the Receiver Operating Characteristic (ROC) curve was used to investigate the sensitivity and specificity of type 2 diabetes in predicting dementia, and the area under the curve was 0.453 ($P = 0.028$, 95%CI: 0.409–0.497). Table 2 and Figure 1 presents the results.

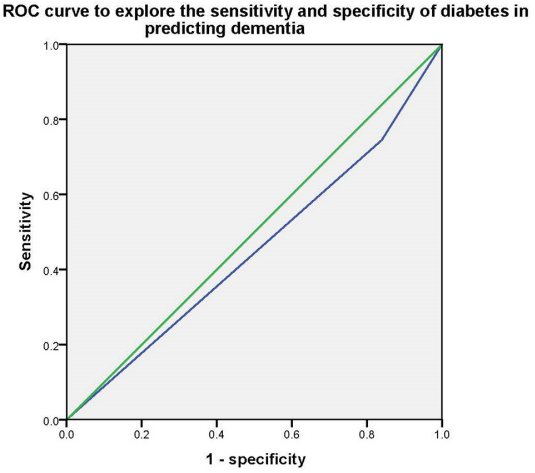


FIGURE 1
ROC curve to explore the sensitivity and specificity of diabetes in predicting dementia.

## The association between type 2 diabetes and brain structure

To investigate the possible mechanism of type 2 diabetes affecting cognitive function, T1 structural cranial magnetic resonance imaging was performed on a random sample of healthy elderly people. Based on type 2 diabetes, 84 cognitively normal adults (their average age was 69.06 ± 6.66; there were 42 males and 42 females) were divided into two groups: diabetes ($n$ = 36) and non-diabetes ($n$ = 48). There were no statistically significant differences ($p > 0.05$) in age, education, sex, smoking, alcohol consumption, tea consumption, physical exercise, hobbies, hypertension, total brain volume, MMSE score, and MoCA score between the two groups. Therefore, in this study, the hippocampus volume and ventricular volume were mainly used as our main observation indicators. Finally, we found that the fourth ventricle volume of diabetic patients was significantly larger ($p > 0.05$) than that of non-diabetic patients, while there were no statistical differences in hippocampus, third ventricle volume, and fifth ventricle volume between the two groups. Table 3 and Figure 2 presents the results. However, we

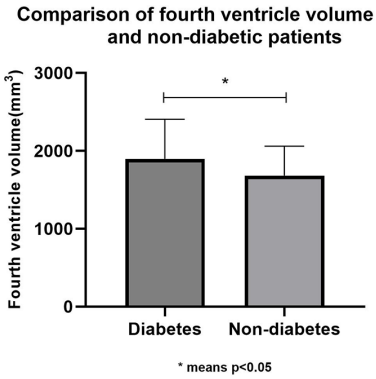


FIGURE 2
Comparison of fourth ventricle volume between diabetic and non-diabetic patients. *means $p < 0.05$.

did not find any specific association between the fourth ventricle volume and cognitive score.

## Discussion

Both cognitive dysfunction and diabetes are common diseases among the elderly, and cognitive dysfunction is one of the important comorbidities of diabetes mellitus. There are different stages of diabetes-related cognitive dysfunction, each with different cognitive characteristics, affected age groups, and outcomes, which may also have different underlying mechanisms (Biessels and Despa, 2018). In the current study, we investigated the association between type 2 diabetes and cognitive dysfunction among the elderly in the Chinese community and found that: (1) type 2 diabetes was associated with dementia, but not MCI; and (2) older cognitively normal adults with type 2 diabetes had greater fourth ventricle volume compared with older cognitively normal adults without type 2 diabetes.

In our study, we found that dementia patients had a significantly higher rate of diabetes than normal elderly and MCI patients. Using stepwise logistic regression analysis,

TABLE 2 Different regression models were used to explore the association between diabetes and dementia.

| Variables | B | S.E | Wald | df | *p* | OR | 95% confidence interval |
|---|---|---|---|---|---|---|---|
| Dementia | | | | | | | |
| Diabetes (model 1) | 0.617 | 0.176 | 12.362 | 1 | <0.001* | 1.854 | 1.314–2.615 |
| Diabetes (model 2) | 0.607 | 0.201 | 9.101 | 1 | 0.003* | 1.836 | 1.237–2.724 |
| Age (model 2) | 0.118 | 0.011 | 107.672 | 1 | <0.001* | 1.125 | 1.100–1.151 |
| Education (model 2) | −0.117 | 0.019 | 38.090 | 1 | <0.001* | 0.889 | 0.857–0.923 |
| Male (model 2) | 0.171 | 0.183 | 0.876 | 1 | 0.349 | 1.187 | 0.829–1.699 |
| Diabetes (model 3) | 0.591 | 0.208 | 8.023 | 1 | 0.005* | 1.805 | 1.199–2.761 |
| Age (model 3) | 0.106 | 0.012 | 84.782 | 1 | <0.001* | 1.112 | 1.087–1.138 |
| Education (model 3) | −0.098 | 0.020 | 23.564 | 1 | <0.001* | 0.907 | 0.871–0.943 |
| Male (model 3) | 0.091 | 0.216 | 0.179 | 1 | 0.672 | 1.096 | 0.718–1.673 |
| Smoker (model 3) | 0.023 | 0.240 | 0.009 | 1 | 0.923 | 1.024 | 0.639–1.639 |
| Tea (model 3) | −0.777 | 0.201 | 14.910 | 1 | <0.001* | 0.460 | 0.310–0.682 |
| Physical exercise (model 3) | −0.691 | 0.177 | 15.202 | 1 | <0.001* | 0.501 | 0.345–0.709 |
| Hobby (model 3) | −0.771 | 0.203 | 14.385 | 1 | <0.001* | 0.463 | 0.311–0.689 |
| Hypertension (model 3) | 0.322 | 0.177 | 3.332 | 1 | 0.068 | 1.380 | 0.977–1.951 |

Note: *$p < 0.05$.

TABLE 3 Comparison of brain region structure and neuropsychological tests between diabetic and non-diabetic patients.

| Variables | Diabetes ($n = 36$) | Non-diabetes ($n = 48$) | $X^2$ or t | *p* |
|---|---|---|---|---|
| Age, years | 68.50 ± 7.01 | 69.48 ± 6.43 | −0.665 | 0.508 |
| Education, years | 9.18 ± 3.95 | 9.81 ± 4.15 | −0.697 | 0.488 |
| Male, n (%) | 17 (47.2) | 25 (52.1) | 0.194 | 0.826 |
| Smoker, n (%) | 10 (27.8) | 15 (31.3) | 0.119 | 0.812 |
| Drinker, n (%) | 10 (27.8) | 7 (14.6) | 2.219 | 0.174 |
| Tea drinker, n (%) | 17 (47.2) | 17 (35.4) | 1.190 | 0.369 |
| Take exercise, n (%) | 22 (61.1) | 30 (62.) | 0.017 | 1.000 |
| Hobby, n (%) | 23 (63.9) | 33 (68.8) | 0.219 | 0.649 |
| Hypertension, n (%) | 29 (80.6) | 45 (93.8) | 3.415 | 0.091 |
| Total brain volume, $cm^3$ | 1,013.77 ± 104.35 | 1,012.08 ± 106.08 | 0.073 | 0.942 |
| Left hippocampus, $mm^3$ | 3,681.67 ± 417.06 | 3,710.50 ± 397.92 | −0.322 | 0.748 |
| Right hippocampus, $mm^3$ | 3,925.16 ± 453.41 | 3,843.64 ± 454.51 | 0.814 | 0.418 |
| 3rd ventricle, $mm^3$ | 1,546.58 ± 468.30 | 1,618.72 ± 622.81 | −0.582 | 0.562 |
| 4th ventricle, $mm^3$ | 1,898.39 ± 508.09 | 1,684.74 ± 376.02 | 2.216 | 0.029* |
| 5th ventricle, $mm^3$ | 0.00 ± 0.000 | 0.04 ± 0.202 | −1.236 | 0.220 |
| MMSE | 27.50 ± 2.336 | 27.91 ± 2.244 | −0.820 | 0.415 |
| MoCA | 23.50 ± 5.755 | 24.04 ± 3.759 | −0.518 | 0.606 |

*$p < 0.05$. MoCA, Montreal Cognitive Assessment; MMSE, Mini-mental State Examination; MCI, mild cognitive impairment.

we found that type 2 diabetes was an important predictor of dementia, independent of gender, age, and education. However, no association was shown between type 2 diabetes and MCI. In Fei et al. (2013) study, they found that type 2 diabetes was associated with dementia and its subtypes amongst elderly people in the Chinese population. In Wang and Liu (2021) study, they found that early-onset diabetes had a stronger association with an increased risk of stroke, all dementia, and Alzheimer's disease (AD) dementia than later-onset. In Shang et al. (2020) study, they found that diabetes, but not prediabetes, was associated with an increased risk of ischemic stroke and post-stroke dementia. In Jia L. et al.'s study, they found that type 2 diabetes was a risk factor for both dementia and MCI, but we did not find an association between type 2 diabetes and MCI. The reasons for the above differences may be as follows: (1) MCI was not divided into specific groups to distinguish between amnestic MCI and vascular MCI; (2) the sensitivity of males and females to diabetes was different; and (3) some confounding factors, such as APOE E4, may have a significant impact on the study results. Therefore, we are relatively certain that type 2 diabetes is closely associated with dementia, but the association with MCI needs to be further verified.

To investigate the possible mechanism of type 2 diabetes affecting the progression of dementia, we randomly selected some healthy elderly people with normal cognitive function and performed cranial magnetic resonance imaging of the T1 structural phase. Based on whether they had type 2 diabetes, those 84 cognitively normal elderly people were divided into diabetes ($n$ = 36) and non-diabetes groups ($n$ = 48), with no differences in gender, age, education, daily biochemical variables, disease-related variables, or cognitive scores. Although there was no difference in hippocampal volume or total brain volume between the two groups, the fourth ventricle volume was significantly larger in individuals with type 2 diabetes than in individuals without type 2 diabetes. Unfortunately, we did not find an association between the fourth ventricle and cognitive scores (MMSE and MoCA).

The fourth ventricle, also known as the cerebellum medulla cistern, is a closed chamber between the cerebellum and the medulla oblongata. The fourth ventricle is filled with cerebrospinal fluid. Its main function is buffering and nutritional support, and it is an important structure for cerebrospinal fluid to flow down and return to venous blood for reabsorption. Accumulated evidence shows that the fourth ventricle is closely related to blood glucose regulation, for example, in 1854, Claude Bernard, a French physiologist, discovered that a lesion at the base of the fourth ventricle in rabbits would cause sugar levels to rise in the blood (Tups et al., 2017). Moreover, it is now thought that the fourth ventricle may be an important medium for the brain to regulate blood sugar (Coppari, 2015). Since our sample size was small and no association between the fourth ventricle and cognitive score was found, we could not determine whether type 2 diabetes affected cognitive function by affecting the volume of the fourth ventricle. But the significance of our study is that it may provide new ideas for future research and new targets for finding brain structures in which glucose metabolism affects cognitive function.

We have to admit that there were some limitations in our study. Firstly, since this study was only a cross-sectional study, it could not indicate the causal effect between type 2 diabetes and cognitive impairment; secondly, information on diabetes was obtained through self-report rather than objective assessment, so there was the possibility of recall bias; thirdly, the sample size was relatively small, so we did not find an association between the fourth ventricle and cognitive function, so further expansion of the sample size is needed in the future; fourthly, we did not further distinguish between dementia and MCI subtypes, which may have influenced the results of the study.

## Conclusions

In conclusion, type 2 diabetes among the Chinese elderly is associated with a higher risk of dementia, but not MCI, and type 2 diabetes may impair cognitive function by affecting the volume of the fourth ventricle.

## Data availability statement

The raw data supporting the conclusions of this article will be made available by the authors, without undue reservation.

## Ethics statement

The studies involving human participants were reviewed and approved by The Third People's Hospital of Lanzhou. The patients/participants provided their written informed consent to participate in this study.

## Author contributions

WL, YL, and GL contributed to the study concept and design. WL wrote this article. YX analyzed the data and drafted the manuscript. All authors contributed to the article and approved the submitted version.

## Funding

This study was supported by grants from the clinical research center project of Shanghai Mental Health Center (CRC2017ZD02), Shanghai Clinical Research Center for Mental Health (19MC1911100), the Cultivation of Multidisciplinary Interdisciplinary Project in Shanghai Jiaotong University (YG2019QNA10), curriculum reform of Medical College of Shanghai Jiaotong University, the Feixiang Program of Shanghai Mental Health Center (2020-FX-03), the National Natural Science Foundation of China (82101564), Chinese Academy of Sciences (XDA12040101), Shanghai Clinical Research Center for Mental Health (SCRC-MH, 19MC1911100), the National Natural Science Foundation of China (82001123), the Shanghai Science and Technology Committee (20Y11906800), Shandong Medical and Health Technology Development Fund (202103070325), Shandong Province Traditional Chinese Medicine Science and Technology Project (M-2022216), and Traditional Chinese medicine for chronic kidney disease (Provincial Key Laboratory Scientific Research special-19).

## Conflict of interest

The authors declare that the research was conducted in the absence of any commercial or financial relationships that could be construed as a potential conflict of interest.

## Publisher's note

All claims expressed in this article are solely those of the authors and do not necessarily represent those of their affiliated organizations, or those of the publisher, the editors and the reviewers. Any product that may be evaluated in this article, or claim that may be made by its manufacturer, is not guaranteed or endorsed by the publisher.

## References

Biedermann, F., and Fleischhacker, W. W. (2016). Psychotic disorders in DSM-5 and ICD-11. *CNS Spectr.* 21, 349–354. doi: 10.1017/S1092852916000316

Biessels, G. J., and Despa, F. (2018). Cognitive decline and dementia in diabetes mellitus: mechanisms and clinical implications. *Nat. Rev. Endocrinol.* 14, 591–604. doi: 10.1038/s41574-018-0048-7

Biessels, G. J., Staekenborg, S., Brunner, E., Brayne, C., and Scheltens, P. (2006). Risk of dementia in diabetes mellitus: a systematic review. *Lancet Neurol.* 5, 64–74. doi: 10.1016/S1474-4422(05)70284-2

Boutouyrie, P., Climie, R. E., and Bruno, R. M. (2022). Type 2 diabetes mellitus, interaction between left ventricle and large arteries. *Am. J. Hypertens.* 35, 388–390. doi: 10.1093/ajh/hpac007

Brown, E. M., Pierce, M. E., Clark, D. C., Fischl, B. R., Iglesias, J. E., Milberg, W. P., et al. (2020). Test-retest reliability of freesurfer automated hippocampal subfield segmentation within and across scanners. *Neuroimage* 210:116563. doi: 10.1016/j.neuroimage.2020.116563

Cao, Q., Tan, C. C., Xu, W., Hu, H., Cao, X.-P., Dong, Q., et al. (2020). The prevalence of dementia: a systematic review and meta-analysis. *J. Alzheimers Dis.* 73, 1157–1166. doi: 10.3233/JAD-191092

Ciesielska, N., Sokołowski, R., Mazur, E., Podhorecka, M., Polak-Szabela, A., and Kędziora-Kornatowska, K. (2016). Is the montreal cognitive assessment (MoCA) test better suited than the mini-mental state examination (MMSE) in mild cognitive impairment (MCI) detection among people aged over 60? Meta-analysis. *Psychiatr. Pol.* 50, 1039–1052. doi: 10.12740/PP/45368

Cooper, C., Sommerlad, A., Lyketsos, C. G., and Livingston, G. (2015). Modifiable predictors of dementia in mild cognitive impairment: a systematic review and meta-analysis. *Am. J. Psychiatry* 172, 323–334. doi: 10.1176/appi.ajp.2014.14070878

Coppari, R. (2015). Hypothalamic neurones governing glucose homeostasis. *J. Neuroendocrinol.* 27, 399–405. doi: 10.1111/jne.12276

Eichenbaum, H. (2017). The role of the hippocampus in navigation is memory. *J. Neurophysiol.* 117, 1785–1796. doi: 10.1152/jn.00005.2017

Fei, M., Yan Ping, Z., Ru Juan, M., Ning Ning, L., and Lin, G. (2013). Risk factors for dementia with type 2 diabetes mellitus among elderly people in China. *Age Ageing* 42, 398–400. doi: 10.1093/ageing/afs188

Folstein, M. F., Folstein, S. E., and McHugh, P. R. (1975). "Mini-mental state". A practical method for grading the cognitive state of patients for the clinician. *J. Psychiatr. Res.* 12, 189–198. doi: 10.1016/0022-3956(75)90026-6

Gao, Y., Xiao, Y., Miao, R., Zhao, J., Zhang, W., Huang, G., et al. (2015). The characteristic of cognitive function in type 2 diabetes mellitus. *Diabetes Res. Clin. Pract.* 109, 299–305. doi: 10.1016/j.diabres.2015.05.019

Jia, L., Quan, M., Fu, Y., Zhao, T., Li, Y., Wei, C., et al. (2020a). Dementia in China: epidemiology, clinical management and research advances. *Lancet Neurol.* 19, 81–92. doi: 10.1016/S1474-4422(19)30290-X

Jia, L., Du, Y., Chu, L., Zhang, Z., Li, F., Lyu, D., et al. (2020b). Prevalence, risk factors and management of dementia and mild cognitive impairment in adults aged 60 years or older in China: a cross-sectional study. *Lancet Public Health* 5, e661–e671. doi: 10.1016/S2468-2667(20)30185-7

Karssemeijer, E. G. A., Aaronson, J. A., Bossers, W. J., Smits, T., Olde Rikkert, M. G. M., and Kessels, R. P. C. (2017). Positive effects of combined cognitive and physical exercise training on cognitive function in older adults with mild cognitive impairment or dementia: a meta-analysis. *Ageing Res. Rev.* 40, 75–83. doi: 10.1016/j.arr.2017.09.003

Koekkoek, P. S., Kappelle, L. J., van den Berg, E., Rutten, G. E., and Biessels, G. J. (2015). Cognitive function in patients with diabetes mellitus: guidance for daily care. *Lancet Neurol.* 14, 329–340. doi: 10.1016/S1474-4422(14)70249-2

Li, W., Wang, T., and Xiao, S. (2016). Type 2 diabetes mellitus might be a risk factor for mild cognitive impairment progressing to Alzheimer's disease. *Neuropsychiatr. Dis. Treat.* 12, 2489–2495. doi: 10.2147/NDT.S111298

Li, X., Song, D., and Leng, S. X. (2015). Link between type 2 diabetes and Alzheimer's disease: from epidemiology to mechanism and treatment. *Clin. Interv. Aging* 10, 549–560. doi: 10.2147/CIA.S74042

Lin, S., Yang, Y., Qi, Q., Wei, L., Jing, N., Jie, Z., et al. (2019). The beneficial effect of physical exercise on cognitive function in a non-dementia aging Chinese population. *Front. Aging Neurosci.* 11:238. doi: 10.3389/fnagi.2019.00238

Lisman, J., Buzsáki, G., Eichenbaum, H., Nadel, L., Ranganath, C., and Redish, A. D. (2017). Viewpoints: how the hippocampus contributes to memory, navigation and cognition. *Nat. Neurosci.* 20, 1434–1447. doi: 10.1038/nn.4661

Lopez, O. L., Kuller, L. H., Becker, J. T., Dulberg, C., Sweet, R. A., Gach, H. M., et al. (2007). Incidence of dementia in mild cognitive impairment in the cardiovascular health study cognition study. *Arch. Neurol.* 64, 416–420. doi: 10.1001/archneur.64.3.416

Mayeda, E. R., Whitmer, R. A., and Yaffe, K. (2015). Diabetes and cognition. *Clin. Geriatr. Med.* 31, 101–115, ix. doi: 10.1016/j.cger.2014.08.021

Nasreddine, Z. S., Phillips, N. A., Bédirian, V., Charbonneau, S., Whitehead, V., Collin, I., et al. (2005). The montreal cognitive assessment, MoCA: a brief

screening tool for mild cognitive impairment. *J. Am. Geriatr. Soc.* 53, 695–699. doi: 10.1111/j.1532-5415.2005.53221.x

Ninomiya, T. (2014). Diabetes mellitus and dementia. *Curr. Diabetes Rep.* 14:487. doi: 10.1007/s11892-014-0487-z

Opitz, B. (2014). Memory function and the hippocampus. *Front. Neurol. Neurosci.* 34, 51–59. doi: 10.1159/000356422

Petersen, R. C. (2011). Clinical practice. Mild cognitive impairment. *N. Engl. J. Med.* 364, 2227–2234. doi: 10.1056/NEJMcp0910237

Qin, H., Zhu, B., Hu, C., and Zhao, X. (2020). Later-onset hypertension is associated with higher risk of dementia in mild cognitive impairment. *Front. Neurol.* 11:557977. doi: 10.3389/fneur.2020.557977

Reddy, S., and Hashmi, A. (2020). Managing diabetes and dementia. *Clin. Geriatr. Med.* 36, 419–429. doi: 10.1016/j.cger.2020.04.003

Sachdev, P. S., Lipnicki, D. M., Kochan, N. A., Crawford, J. D., Thalamuthu, A., Andrews, G., et al. (2015). The prevalence of mild cognitive impairment in diverse geographical and ethnocultural regions: the COSMIC collaboration. *PLoS One* 10:e0142388. doi: 10.1371/journal.pone.0142388

Sadykova, H. G., and Nazhmutdinova, D. K. (2009). [Structural and functional condition of the left ventricle in patients with type 2 diabetes mellitus complicated with diabetic autonomic neuropathy]. *Lik. Sprava* 22–28.

Shang, Y., Fratiglioni, L., Marseglia, A., Plym, A., Welmer, A.-K., Wang, H.-X., et al. (2020). Association of diabetes with stroke and post-stroke dementia: a population-based cohort study. *Alzheimers Dement.* 16, 1003–1012. doi: 10.1002/alz.12101

Tschanz, J. T., Welsh-Bohmer, K. A., Lyketsos, C. G., Corcoran, C., Green, R. C., Hayden, K., et al. (2006). Conversion to dementia from mild cognitive disorder: the cache county study. *Neurology* 67, 229–234. doi: 10.1212/01.wnl.0000224748.48011.84

Tups, A., Benzler, J., Sergi, D., Ladyman, S. R., and Williams, L. M. (2017). Central regulation of glucose homeostasis. *Compr. Physiol.* 7, 741–764. doi: 10.1002/cphy.c160015

Wang, K., and Liu, H. (2021). Early-onset subgroup of type 2 diabetes and risk of dementia, Alzheimer's disease and stroke: a cohort study. *J. Prev. Alzheimers Dis.* 8, 442–447. doi: 10.14283/jpad.2021.35

Xiao, S., Li, J., Tang, M., Chen, W., Bao, F., Wang, H., et al. (2013). Methodology of China's national study on the evaluation, early recognition and treatment of psychological problems in the elderly: the China Longitudinal Aging Study (CLAS). *Shanghai Arch. Psychiatry* 25, 91–98. doi: 10.3969/j.issn.1002-0829.2013.02.005

frontiers | Frontiers in Aging Neuroscience

TYPE Original Research
PUBLISHED 29 September 2022
DOI 10.3389/fnagi.2022.1004557



OPEN ACCESS

EDITED BY
Yuzhen Xu,
Tongji University, China

REVIEWED BY
You Yin,
Naval Medical University, China
Yanxin Zhao,
Tongji University, China

*CORRESPONDENCE
Jianliang Fu
fujianliang@163.com

†These authors have contributed equally to this work

SPECIALTY SECTION
This article was submitted to Alzheimer's Disease and Related Dementias, a section of the journal Frontiers in Aging Neuroscience

RECEIVED 27 July 2022
ACCEPTED 19 August 2022
PUBLISHED 29 September 2022

CITATION
Zhang Y, Yuan Y, Zhang J, Zhao Y, Zhang Y and Fu J (2022) Astragaloside IV supplementation attenuates cognitive impairment by inhibiting neuroinflammation and oxidative stress in type 2 diabetic mice. Front. Aging Neurosci. 14:1004557. doi: 10.3389/fnagi.2022.1004557.



# Astragaloside IV supplementation attenuates cognitive impairment by inhibiting neuroinflammation and oxidative stress in type 2 diabetic mice

Yaxuan Zhang†, Yuan Yuan†, Jiawei Zhang, Yao Zhao, Yueqi Zhang and Jianliang Fu*

Department of Neurology, Shanghai Jiao Tong University Affiliated Sixth People's Hospital, Shanghai, China

Although diabetic cognitive impairment is one of the most common complications of type 2 diabetes mellitus (T2DM), optimized therapeutic strategies are not available yet. Astragalosides IV (AS-IV) is a traditional Chinese medicine possessing diverse pharmacological properties including anti-inflammatory and antioxidant effects. However, the effects of AS-IV on diabetes-related cognitive impairment and its precise mechanisms remain largely unknown. T2DM mice, induced by a high-fat diet (HFD) and an intraperitoneal injection of low-dose streptozotocin (STZ) were administrated with AS-IV every other day for eight consecutive weeks. Learning and memory abilities were assessed subsequently using the Ymaze test and the anxious behavior was evaluated using an open field test. Then, the morphology and number of neurons and microglia were observed by HE staining or immunohistochemistry. Oxidative stress biomarkers and pro-inflammatory cytokines were determined using relevant kits. In addition, the expression levels of Nrf2, Keap1, HO-1, and NQO1 were determined by Western blot analyses. The results indicated that AS-IV administration significantly improved neuronal damage and cognitive deficit in T2DM mice. Meanwhile, oxidative stress and neuroinflammation were also ameliorated in T2DM mice, which might be attributed to the regulation of Nrf2/Keap1/HO-1/NQO1 pathway in T2DM mice. Taken together, these data suggested that AS-IV ameliorates cognitive impairment in T2DM mice by attenuating oxidative stress and neuroinflammation, possibly through modulating the Nrf2/Keap1/HO1/NQO1 pathway.

KEYWORDS

**astragalosides IV, cognitive impairment, type 2 diabetes mellitus, neuroinflammation, oxidative stress**

# Introduction

Type 2 diabetes mellitus (T2DM) is a lifelong metabolic disease that results in various complications and is thus becoming a main public health problem. Diabetes-related cognitive impairment is a common but grossly underestimated complication of T2DM (Biessels and Despa, 2018; Srikanth et al., 2020). T2DM has been reported to significantly accelerate the deterioration of cognitive function. Clinical and epidemiological studies have also demonstrated that patients with T2DM have nearly twice the risk of developing dementia (Feil et al., 2011). Given the prevalence of T2DM, the incidence of diabetes-related cognitive impairment is expected to surge and cause an unpredictable social and economic burden. Thus, it is of great importance to decipher the underlying mechanisms of diabetes-related cognitive impairment and to develop effective therapeutic agents for the disease.

An increasing number of studies have indicated that oxidative stress and neuroinflammation are key contributors to the initiation and progression of diabetes-related cognitive impairment (Piatkowska-Chmiel et al., 2021; Wang et al., 2021; Wu et al., 2022). For example, increased oxidative stress was associated with neuronal damage and memory deficit in T2DM (Hoyos et al., 2022). Besides, excessive neuroinflammation leading to a cognitive deficit was also observed in T2DM (Marioni et al., 2010; Zhao et al., 2019; Ko et al., 2021). Nuclear factor erythroid 2-related factor 2 (Nrf2) is a redox-sensitive transcription factor that has been proved to be a master regulator of both neuroinflammation and oxidative stress (Ma, 2013; Ahmed et al., 2017). A growing body of studies has established the protective role of Nrf2 against oxidative stress and neuroinflammation in T2DM. It has been reported that Nrf2 increases the transcription of heme oxygenase-1 (HO-1) and NAD(P)H: quinone oxidoreductase 1 (NQO1) that mitigates the oxidative stress and inflammation of the brain and eventually improves the cognitive impairment in T2DM (Feng et al., 2018; Wang G. et al., 2020; Pang et al., 2021).

Astragaloside IV (AS-IV), a major active component extracted from Astragalus membranaceus, exerts multiple pharmacological activities including anti-inflammation and anti-oxidation (Gui et al., 2013b; Zhang and Frei, 2015). The protective effect of AS-IV against diabetes complications and neurological disease has been widely investigated in numerous literatures (Qiao et al., 2017; Wang et al., 2017, Wang E. et al., 2020; Xia et al., 2020). However, whether AS-IV treatment improves diabetes-related cognitive impairment and if so, what are the underlying mechanisms, are still unrevealed. Therefore, in the present study, we explored the hypothesis that AS-IV might improve diabetes-related cognitive impairment in T2DM mice by modulating the Nrf2/Keap1/HO-1/NQO1 pathway.

# Materials and methods

## Animals and experimental protocols

Four-week-old male C57BL/6J mice were housed in an SPF-barrier environment under standard conditions of temperature (22 ± 2°C), humidity (55%–65%), and light (12:12 h light/dark cycle) and were randomly divided into three groups: wild type group (WT; $n$ = 10), T2DM model group (T2DM; $n$ = 10) and T2DM + AS-IV treatment group (AS-IV; $n$ = 10). The mice in the WT group were given a normal diet (10% calories from fat; Research Diet, New Jersey, United States), while the mice in the other groups were fed with HFD (60% calories from fat; Research Diet, New Jersey, United States) during the whole experimental period. After 4 weeks of HFD (Zhu et al., 2022), mice in the T2DM and AS-IV group were fasted for 8 h overnight and then injected intraperitoneally with STZ (35 mg/kg, dissolved at 0.1 mm cold citrate buffer, pH 4.4; Yeasen Biotechnology, Shanghai, China) for three consecutive days to induce T2DM (Zhang et al., 2018). The mice were considered diabetic when the blood glucose levels were higher than 11.6 mmol/L 3 days after STZ injection. Then, referring to previous reports, mice in AS-IV group were intragastrically administered with 40 mg/kg of AS-IV (Song et al., 2018; Yuanye Biotechnology, Shanghai, China) every other day for 8 weeks while mice in T2DM and WT group were intragastrically administered with a vehicle. The fasting blood glucose levels of each mouse in all groups were tested every 4 weeks. All animal experiments were carried out according to the ethical committee on animal welfare of Shanghai Jiao Tong University Affiliated Sixth People's Hospital and the principles outlined in the National Institutes of Health (NIH) Guide for the Care and Use of Laboratory Animals.

## Y maze test

Learning and memory abilities were measured using a Y maze apparatus that was made up of three similar arms (A, B, C) with dimensions of 33 cm long, 15 cm high, and 10 cm wide at 120° angles to each other. After at least 30 min of acclimatization in the test room, the mouse was placed in the center of the apparatus and was allowed to move freely for 5 min. Spontaneous alternation was evaluated by the pattern of complete entry into each arm (the mouse's hind paws go entirely into the arm). Actual alternation was defined as the number of consecutive entries into the three arms on overlapping triplet sets, and the alternation behavior (%) was calculated as follows (You et al., 2020):

$$\text{Alternation behavior (\%)} = (\text{Actual alternation})/(\text{Total number of arms entries} - 2)$$

## Open field test

Anxiety-like behavior was measured using an open field apparatus of 50 cm long, 50 cm wide, and 50 cm high. After at least 30 min of acclimatization in the test room. Each mouse was placed in the center of the apparatus and was allowed to explore freely for 5 min. The apparatus was disinfected with 75% alcohol after each test. The central area was defined as half of the total area located in the center of the apparatus. Time spent in the center area and the number of times entering the center area of each mouse were recorded for data analysis (Yoshizaki et al., 2020).

## Hematoxylin and eosin staining

After the behavioral tests of cognitive ability, mice were anesthetized deeply and transcardially perfused with 400 ml phosphate buffer saline (PBS) followed by 400 ml 4% paraformaldehyde. Then, the brain was removed and postfixed in 4% paraformaldehyde for 24 h at 4°C. After dehydration in graded series of alcohol, the brain tissue was embedded in paraffin and cut into 5 μm thickness. The sections were further stained with hematoxylin and eosin and were observed under a light microscope (IX53, Olympus, Tokyo, Japan).

## Dihydroethidium staining

After postfixed for 24 h, the formalin preserved brain tissue was kept in 30% sucrose until it sank to the bottom. Then, the brain tissue was embedded in OCT and cut into 10 μm thick frozen sections. Dihydroethidium (DHE) staining detecting ROS level in situs was performed as previously described (Zhao et al., 2021). Briefly, the brain sections were incubated with 10 mmol/L DHE (Sigma-Aldrich, St. Louis, MO, USA) at 37°C for 30 min in a humidified chamber protected from light. 1 μg/ml 4,6-diamidino-2-phenylindole, dilactate (DAPI; Thermo Scientific, Waltham, MA, USA) was used before the sections were coverslipped. The brain sections were then visualized under a fluorescence microscope (IX53, Olympus, Tokyo, Japan).

## MDA level and SOD activity evaluation

MDA is one of the end products of lipid peroxidation and is considered as a marker of oxidative stress, while SOD activity is used as an antioxidant marker. Hippocampal tissues of different groups were homogenized to obtain the supernatant for subsequent analyses and the level of MDA and SOD activity was detected using biochemical assay kits (Nanjingjiancheng, Nanjing, China) following the manufacturer's protocol.

## Immunohistochemistry

To detect the status of microglia, immunohistochemical staining was performed. After deparaffinization and antigen retrieval (0.05% citraconic acid), the sections were treated with endogenous peroxidase (3% $H_2O_2$ in PBS) for 10 min, followed by a blocking buffer containing 10% bovine serum albumin in PBS for 1 h. Next, the sections were incubated with the antibody of ionized calcium-binding adapter molecule 1 (Iba1; Abcam, Cambridge, United Kingdom) overnight, and followed by incubation with biotinylated secondary antibodies (1:500) for 30 min the following day. The sections were then incubated with the avidin-biotin complex (Vector Laboratories, Burlingame, CA, USA) for 30 min, and visualized by 3,3-diaminobenzidine (DAB; Vector Laboratories) reaction. After dehydration in ethanol and clarification in xylene, the sections were visualized under a microscope (IX53, Olympus, Tokyo, Japan).

## ELISA assays

The levels of pro-inflammatory cytokines including tumor necrosis factor alpha (TNF-α), interleukin 6 (IL-6), and interleukin one beta (IL-1β) of cerebral hemispheres were determined using ELISA kits (Multisciences, Hangzhou, China) following the procedures of the manufacturer.

## Western blot analysis

Samples of hippocampal tissue of different groups stored at −80°C were homogenized in prechilled radioimmunoprecipitation assay (RIPA) buffer containing protease and phosphatase inhibitors (Beyotime, Shanghai, China). The protein concentration of the samples was determined using the BCA kit (Beyotime, Shanghai, China). The same amounts (20–30 μg) of brain protein were separated by sodium dodecyl sulfate-polyacrylamide gel electrophoresis (SDS-PAGE) on 7.5% or 12% gels and then transferred onto a polyvinylidene difluoride membranes (PVDF). The membranes were incubated overnight at 4°C with different primary antibodies. The primary antibodies used were as follows: Nrf2 (1:1,000, Abcam), Keap1(1:1,000, Abcam), HO-1(1:1,000, ABclonal), NQO1(1:1,000, Servicebio), and β-actin (1:5,000, CST). The next day, the membranes were incubated with relevant secondary antibodies at room temperature for 1 h. The immunocomplexes were detected using a

chemiluminescence reagent (Thermo Scientific, Waltham, MA, USA) with automatic chemiluminescence apparatus (BIO-RAD, USA) and the images with a specific molecular band were analyzed using ImageJ.

## Statistical analysis

Data in our study were expressed as the mean ± standard error of the mean (SEM). Statistical significance was assessed by two-way ANOVA with posttest (Turkey) for data of fasting blood glucose, and the other data were assessed by one-way ANOVA with posttest (Turkey). Values of $P < 0.05$ were considered statistically significant. Statistical data were analyzed using GraphPad Prism 7.0.

# Results

## Astragalosides IV ameliorates the hyperglycemia in T2DM mice

The experimental design is shown in Figure 1A. After 4 weeks of HFD treatment, mice in T2DM and AS-IV groups were injected with STZ for 3 days. One week after the STZ injection, the fasting blood glucose levels of the mice in T2DM and AS-IV groups were detected. The results showed that fasting blood glucose levels of the mice were higher than 11.6 mmol/L, which suggests that the T2DM model was successfully established (Figure 1B). To evaluate whether AS-IV had effects on the metabolic parameters of T2DM mice, the fasting blood glucose levels of mice in each group were detected. We found that the fasting blood glucose levels were consistently

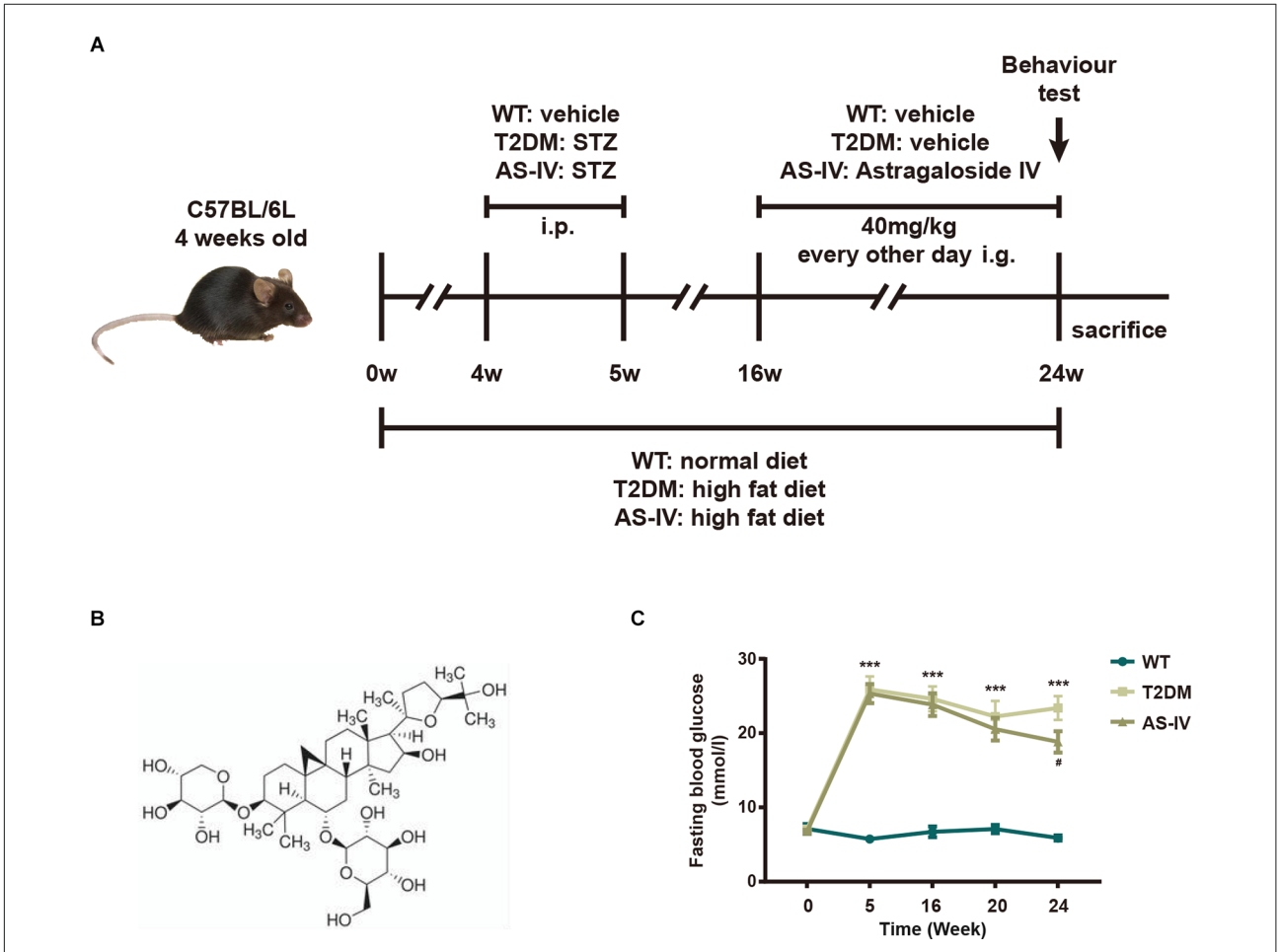


FIGURE 1
Effects of AS-IV on body weight and fasting blood glucose of type 2 diabetes mellitus (T2DM) mice. **(A)** The experimental design scheme for high-fat diet (HFD)/STZ-induced T2DM. Male 4-week-old C57BL/6J mice were fed with either the normal diet or HFD for 4 weeks. The HFD-fed mice were injected intraperitoneally (i.p.). with freshly prepared STZ (35 mg/kg) for 3 days to induce T2DM. From week 16 the T2DM mice were intragastrically (i.g.) administered with AS-IV (40 mg/kg) or vehicle for another 8 weeks. WT mice on a normal diet received vehicle administration. **(B)** 2-D structure of AS-IV. **(C)** Fasting blood glucose levels. Data are presented as the mean ± standard error of the mean (SEM; $n = 8$). $^{**}P < 0.01$; $^{***}P < 0.001$ T2DM vs. WT; $\#P < 0.05$; $\#\#\#P < 0.001$ AS-IV vs. T2DM.

high in T2DM mice, while decreased fasting blood glucose levels were observed after 8 weeks of AS-IV treatment (Figure 1C). Therefore, these findings illustrated that AS-IV treatment could partly reverse the glucose metabolism abnormalities in T2DM mice.

## Astragalosides IV improves cognitive impairment in T2DM mice

Y maze test and Open field test were performed to evaluate the effects of AS-IV on cognitive impairment in T2DM mice. Y maze test, based on the general tendency of rodents to explore new environments, was used to evaluate the learning and memory abilities of mice in each group. Mice with normal learning and memory abilities usually tend to alternate among the three arms of the Y maze (You et al., 2020). However, the results showed that compared to the WT group, the percentage of spontaneous alternations in the T2DM group was significantly decreased, while AS-IV treatment reversed the decline (Figure 2A). Meanwhile, an Open field test was used to investigate the autonomous exploratory behavior of mice in the new environment, which can reflect the anxiety phenotype of mice. An increase in the frequency of exploration behavior often means a decrease in anxiety phenotype. Compared to the WT group, mice in T2DM group tended to spend less time in the center area and the number of entries in the center area was also decreased, while AS-IV treatment significantly reversed the decrease (Figures 2B–D). Together, these results indicated that AS-IV treatment improved cognitive impairment including learning and memory deficiency and anxiety in T2DM mice.

## Astragalosides IV attenuates neuronal damage in T2DM mice

HE staining was used to detect the change in the number and morphology of neurons in the cortex and hippocampal CA1 regions that play important roles in memory formation and retrieval (Zhao et al., 2021). We found

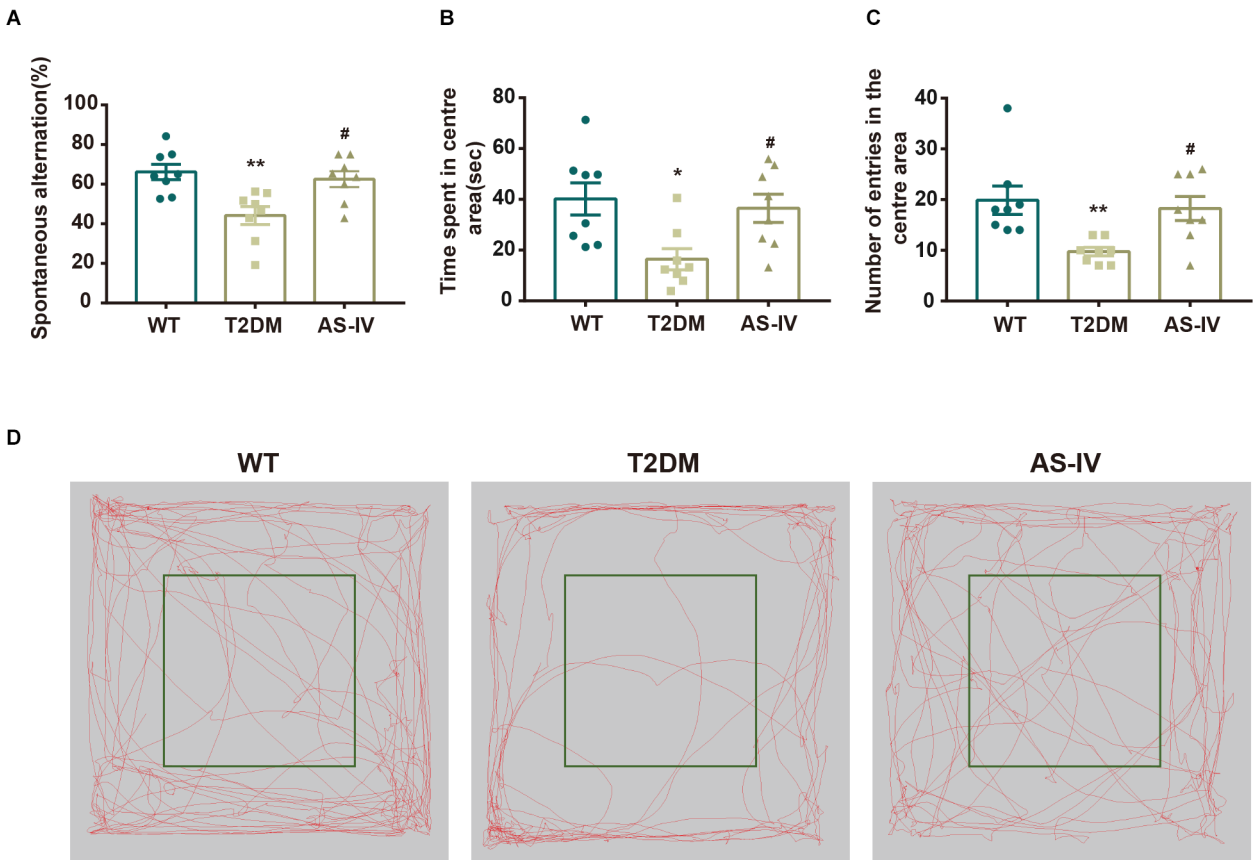


FIGURE 2
AS-IV ameliorated cognitive impairment in T2DM. **(A)** The representative exploring traces of mice in the open field. **(B)** The percentage of spontaneous alternation in the Y maze. **(C)** Time spent in the center area of the open field. **(D)** Number of entries in the center area of the open field. Data are presented as the mean ± SEM ($n$ = 8). *$P$ < 0.05; **$P$ < 0.01 T2DM vs. WT; #$P$ < 0.05 AS-IV vs. T2DM.

10.3389/fnagi.2022.1004557

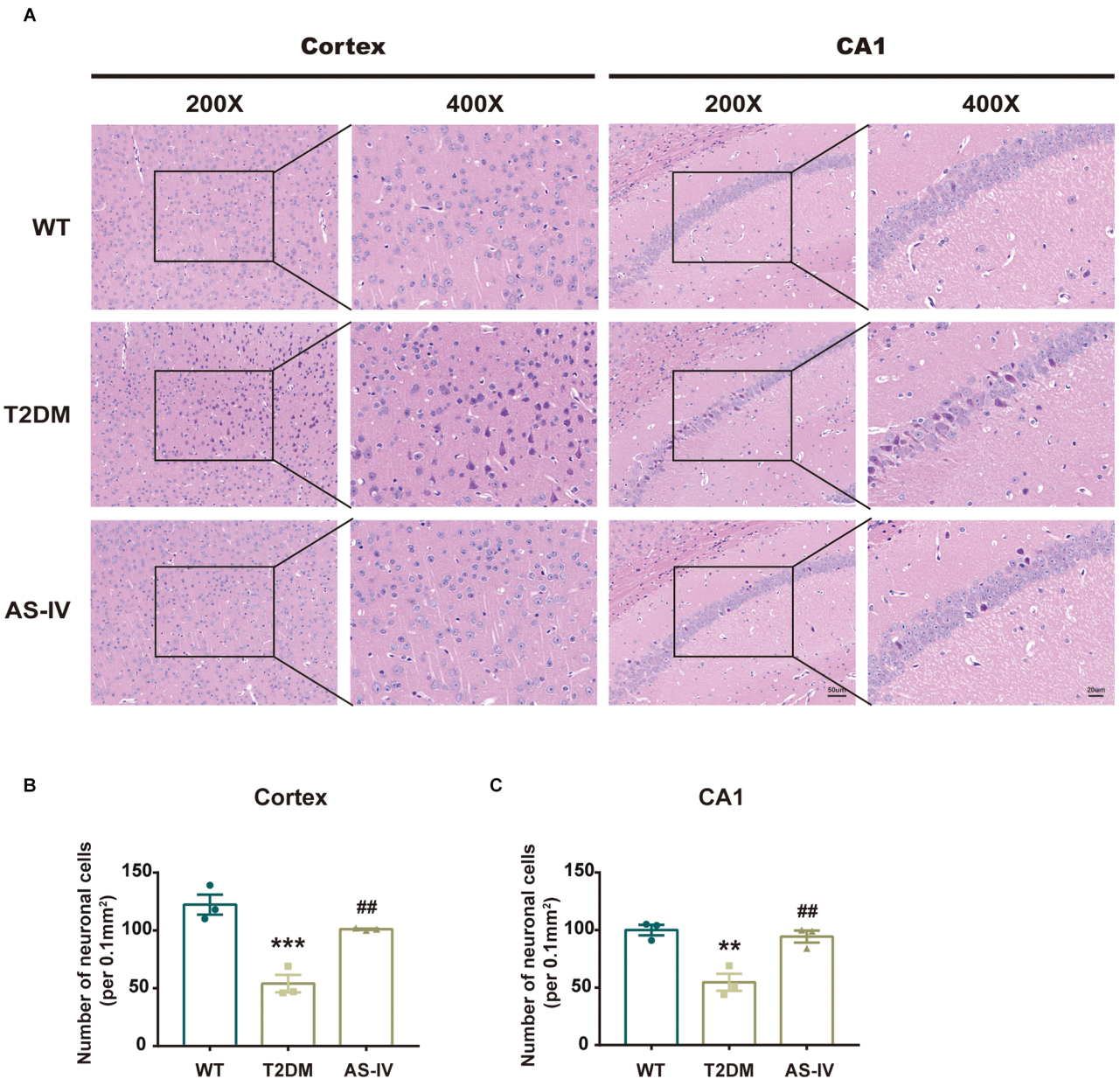


FIGURE 3
AS-IV reduced neuronal death in the cortex and hippocampus CA1 of T2DM mice. **(A)** Represented photomicrographs of HE staining in the cortex and hippocampus CA1 (magnification ×200 or ×400, scale bar = 50 μm or 20 μm). **(B)** Number of neuronal cells in the cortex. **(C)** Number of neuronal cells in hippocampus CA1. Data are presented as the mean ± SEM ($n$ = 3). $^{**}P < 0.01$; $^{***}P < 0.001$ T2DM vs. WT; $\#\#P < 0.01$ AS-IV vs. T2DM.

that AS-IV treatment noticeably reversed the reduction in neuronal number in T2DM mice (Figures 3A–C). Compared with the WT group, neurons of mice in T2DM group were shrunk and the nucleus was deeply stained, while AS-IV treatment rescued these morphological abnormalities in neurons of T2DM mice (Figure 3A). These findings indicated that AS-IV treatment alleviated neuronal damage in T2DM mice.

## Astragalosides IV alleviates oxidative stress in T2DM mice

Oxidative stress is implicated in neuronal damage in various neurological diseases (Chong et al., 2005). To examine whether AS-IV could protect the brain tissue from oxidative stress damage in T2DM, the ROS, MDA levels, and SOD activities were measured. The ROS levels were detected using DHE

10.3389/fnagi.2022.1004557

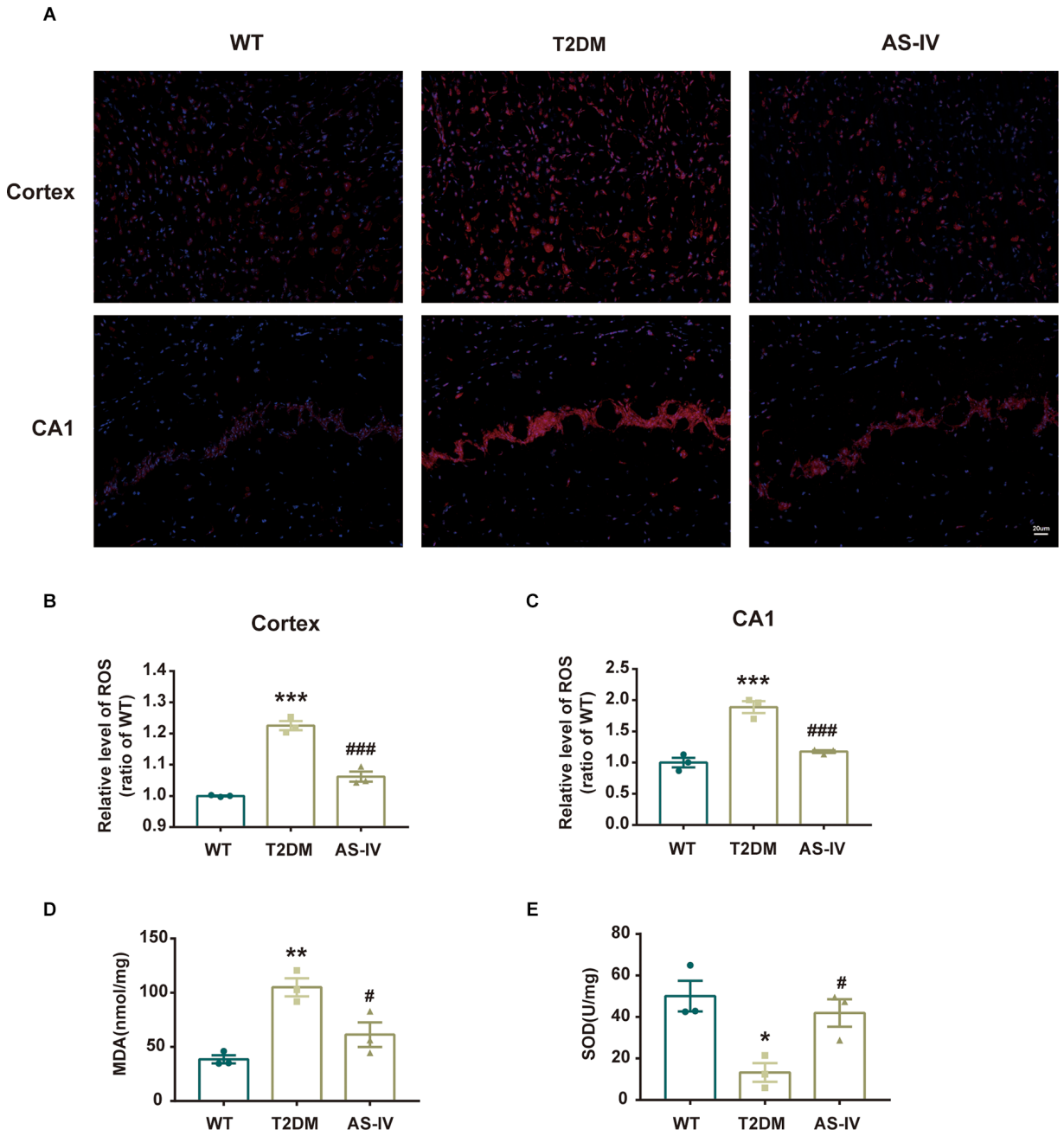


FIGURE 4
AS-IV ameliorated oxidative stress in T2DM mice. **(A)** Represented photomicrographs of dihydroethidium (DHE) staining for ROS in the cortex and hippocampus CA1 (magnification ×200, scale bar = 50 μm). **(B)** The relative level of ROS (ratio to WT group) in the cortex. **(C)** The relative level of ROS (ratio to WT group) in hippocampus CA1. **(D)** MDA levels of the hippocampus . **(E)** SOD activity of the hippocampus. Data are presented as the mean ± SEM ($n$ = 3). *$P$ < 0.05; **$P$ < 0.01; ***$P$ < 0.001 T2DM vs. WT; #$P$ < 0.05; ###$P$ < 0.001 AS-IV vs. T2DM.

staining and the results showed that AS-IV treatment markedly ameliorated ROS increase in the cortex and hippocampus CA1 of T2DM mice (Figures 4A–C). In addition, MDA levels and SOD activities of the hippocampus were also detected using the relevant kits. In T2DM group, MDA levels were dramatically increased, while SOD activities were dramatically decreased. Treatment with AS-IV reduced MDA levels and increased SOD activities of T2DM mice (Figures 4D,E). Collectively, these data demonstrated that AS-IV treatment attenuated oxidative stress in T2DM mice.

## Astragalosides IV mitigates neuroinflammation in T2DM mice

Microglia are innate immune cells of the central nervous system that play an important role in the development of neuroinflammation. Therefore, to investigate whether T2DM could promote microglia activation and the subsequent production of neurotoxic pro-inflammatory cytokines, we analyzed the number and morphology of microglia in cortex and hippocampus CA1 using immunohistochemistry. We found that T2DM produced an increase of Iba-1-positive microglia that had been transitioned from a lacy, highly ramified morphology indicative of a quiescent state to morphology with shortened processes and larger size, indicative of inflammatory activation (**Figures 5A–C**). After 8 weeks of treatment with AS-IV, the number and morphological changes of microglia in T2DM mice were significantly improved (**Figures 5A–C**). Furthermore, we detected the level of pro-inflammatory cytokines including IL-1β, IL-6, and TNF-α of hippocampus using ELISA kits. We found that when compared with the WT group, the levels of IL-1β, IL-6, and TNF-α were much higher in T2DM group, while AS-IV treatment suppressed the levels of pro-inflammatory cytokines (IL-1β, IL-6, and TNF-α) in the brain (**Figures 5D–F**). Overall, these findings indicated that AS-IV exerts anti-inflammatory effects in T2DM mice.

## The effects of astragalosides IV were involved in Nrf2/Keap1/HO-1/NQO1 pathway

To further reveal the mechanism underlying the neuroprotective effects of AS-IV on T2DM mice, we measured the expression levels of Nrf2 pathway-related proteins including Nrf2, Keap1, HO-1, and NQO1 using Western blot analysis. As the results showed, compared to the mice in the WT group, the protein expressions of Nrf2, HO-1, and NQO1 in T2DM mice were significantly decreased while the protein expression level of Keap1 was increased (**Figures 6A–E**). After 8 weeks of treatment of AS-IV, the protein expression levels of Nrf2, HO-1, and NQO1 were all increased, while the protein expression level of Keap1 was decreased (**Figures 6A–E**). These findings suggested that the neuroprotective effects of AS-IV on T2DM mice might be due to the Nrf2/Keap1/HO-1/NQO1 pathway.

# Discussion

Diabetes and cognitive impairment are two highly prevalent chronic disorders that frequently coexist in people older than 65 years old worldwide (Srikanth et al., 2020). Currently, increasing evidence shows that T2DM is an independent risk factor for cognitive impairment (Biessels et al., 2006; Biessels and Despa, 2018). However, the mechanisms by which T2DM causes cognitive impairment remain largely unknown, and there are still no effective strategies to prevent or delay the progression of cognitive impairment in T2DM (Srikanth et al., 2020). Thus, it is of great importance to find effective drugs for the treatment of diabetes-related cognitive impairment. AS-IV is a multifunction molecule with great oral bioavailability and brain-blood barrier penetration (Wang E. et al., 2020). The protective effects of AS-IV have been extensively studied in various neurodegenerative diseases and diabetic complications. It has been reported that AS-IV improves cognitive dysfunction in Alzheimer's disease (AD) and chronic cerebral hypoperfusion-induced dementia (Kim et al., 2015; Wang et al., 2017). Moreover, a previous study reported that AS-IV improved blood glucose levels and attenuated renal dysfunction in diabetic rats (Zhang Y. et al., 2020). However, its role in diabetes-related cognitive impairment remains unknown. Therefore, in this study, we sought to explore whether AS-IV exerted neuroprotective effects on T2DM-related cognitive impairment and the possible mechanisms involved. Herein, a combination of HFD and low-dose STZ, which closely resembles human T2DM development, was used to induce T2DM in mice (Chen et al., 2022). We observed that AS-IV treatment slightly reduced the blood glucose levels and significantly improved cognitive dysfunction in T2DM mice.

Numerous studies have reported that both oxidative stress and neuroinflammation are the underlying pathogeneses of diabetes-related cognitive impairment (Piatkowska-Chmiel et al., 2021; Hoyos et al., 2022; Wu et al., 2022). Oxidative stress is one of the major factors that contribute to the development of cognitive impairment in T2DM. Multiple studies have demonstrated that excessive oxidative stress accompanied by impaired antioxidant capacity in T2DM encouraged the generation of ROS that further led to neuronal damage and cognitive dysfunction in T2DM (Valko et al., 2007; Gocmez et al., 2019; Michailidis et al., 2022). Furthermore, studies have shown that AS-IV exerts neuroprotective effects on AD and chronic cerebral hypoperfusion-induced dementia depending on the inhibition of oxidation stress (Kim et al., 2015; Chen et al., 2021). Consistent with the preceding studies, our current study showed that the activities of SOD were decreased, while the MDA levels were increased in T2DM mice. Treatment with AS-IV reversed the decline in SOD activity, while concomitantly reducing MDA levels in the brain of T2DM mice. On the other hand, oxidative stress has also been shown to be a facilitator of neuroinflammation, which is another primary contributor to the progression of cognitive decline in T2DM (Pang et al., 2021). A clinical study showed that pro-inflammatory cytokines including TNF-α, IL-6, and IL-1β were strongly associated with poor cognitive performance

10.3389/fnagi.2022.1004557

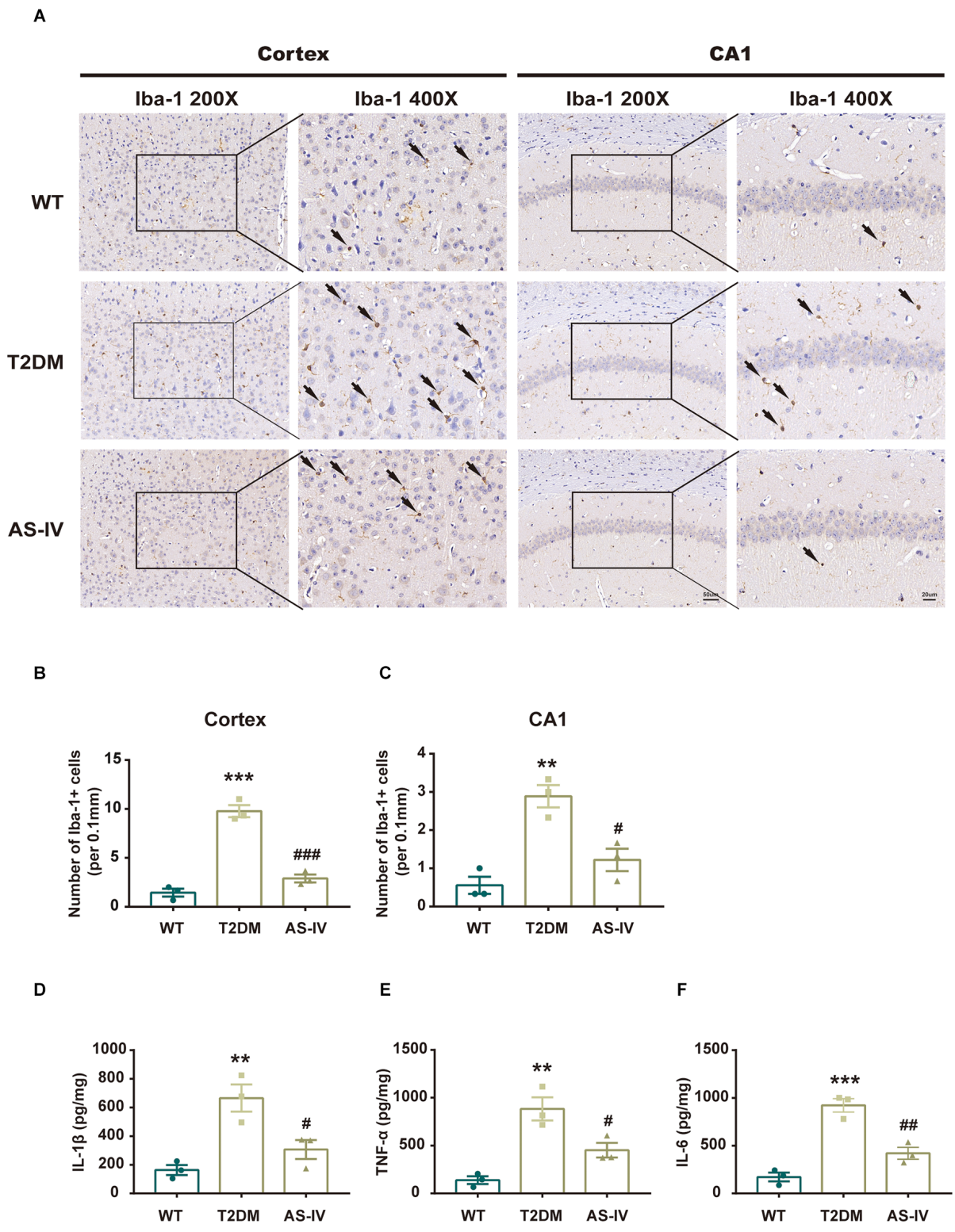


FIGURE 5
AS-IV reduced microglia activation and pro-inflammatory cytokines production in T2DM mice. **(A)** Represented photomicrographs of immunohistochemistry using Iba-1 in the cortex and hippocampus CA1 (magnification ×200 or ×400, scale bar = 50 μm or 20 μm). **(B)** Number of Iba-1 positive cells in the cortex. **(C)** Number of Iba-1 positive cells in hippocampus CA1. **(D)** IL-1β levels of the hippocampus. **(E)** TNF-α levels of the hippocampus. **(F)** IL-6 levels of the hippocampus. Data are presented as the mean ± SEM ($n$ = 3). $^{**}P < 0.01$; $^{***}P < 0.001$ T2DM vs. WT; $\#P < 0.05$; $\#\#P < 0.01$; $\#\#\#P < 0.001$ AS-IV vs. T2DM.

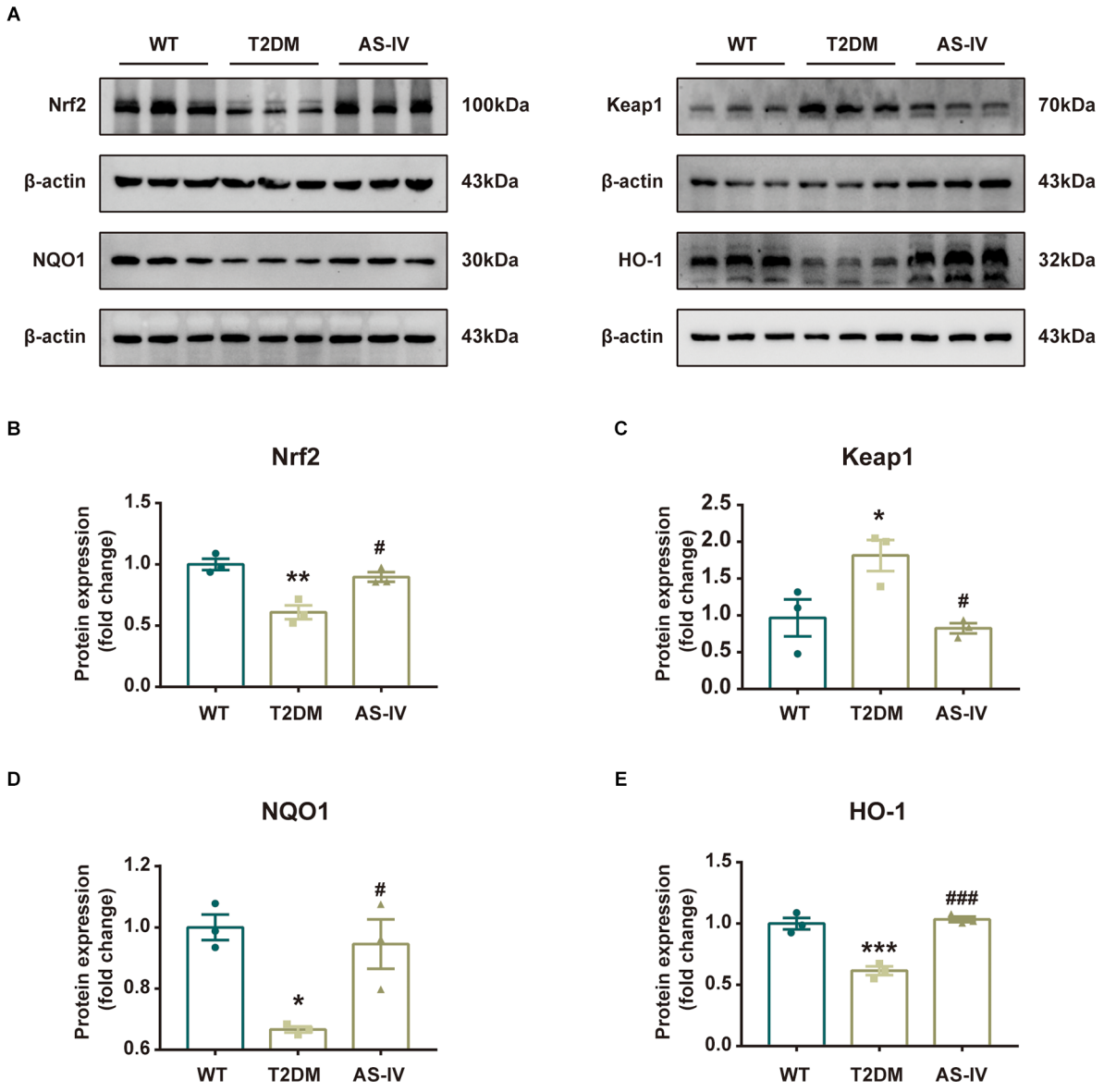


FIGURE 6
Nrf2/Keap1/HO-1/NQO1 signaling pathway was involved in the protective effect of AS-IV. **(A)** Representative bands of Western blot data. **(B)** Quantitative analysis of the Western blot bands of Nrf2. **(C)** Quantitative analysis of the Western blot bands of Keap1. **(D)** Quantitative analysis of the Western blot bands of NQO1. **(E)** Quantitative analysis of the Western blot bands of HO-1. Data are presented as the mean ± SEM ($n$ = 3). $^{*}P < 0.05$; $^{**}P < 0.01$; $^{***}P < 0.001$ T2DM vs. WT; $\#P < 0.05$; $\#\#\#P < 0.001$ AS-IV vs. T2DM.

in T2DM (Piatkowska-Chmiel et al., 2021) and the elevated pro-inflammatory cytokines have been reported to directly destroy the brain-blood barrier and inhibit the synaptic activity, resulting in the neuronal damage and cognitive dysfunction (Zhao et al., 2019; Michailidis et al., 2022). Moreover, AS-IV has been proven to exert potent protective effects on diabetic nephropathy *via* inhibiting the expressions of inflammatory genes in a rat model of T2DM (Gui et al., 2013a). Meanwhile, a previous study indicated that AS-IV was an effective anti-inflammatory agent in the treatment of an AD mouse model (Chen et al., 2021). In our study, the levels of TNF-α, IL-6, and IL-1β were increased in T2DM mice, while treatment with AS-IV exhibited a significantly anti-inflammatory prowess by decreasing the levels of those pro-inflammatory cytokines in T2DM mice.

Nrf2 is a transcription factor that forms a complex with Keap1 under physiological conditions. However, when oxidative stress or inflammation occurs, Nrf2 separates from Keap1, and translocates to the nucleus, inducing the expressions of antioxidant enzymes including HO-1 and

NQO1, etc. (He et al., 2020). Nrf2 signaling pathway has been demonstrated to be a multifunctional signaling pathway related to anti-oxidative stress and anti-neuroinflammatory response. It has been reported that Nrf2 knockout markedly exacerbated the oxidative stress and neuroinflammatory damage and aggravated learning and memory deficits of the AD mice (Rojo et al., 2017). In addition, activation of Nrf2/HO1 signaling pathway has been demonstrated to provide neuroprotective effects against T2DM-related cognitive impairment by ameliorating oxidative stress and neuroinflammation (Zhao et al., 2019; Zhang L. et al., 2020; Pang et al., 2021). Similarly, in the present study, the expressions of Nrf2, HO-1, and NOQ1 were decreased while Keap1 was increased in T2DM mice. AS-IV administration suppress the expression of Keap1 and reversed the reduction of Nrf2, HO-1, and NOQ1. These data suggested that AS-IV ameliorated cognitive impairment in T2DM mice possibly through modulating Nrf2/Keap1/HO1/NQO1 pathway. However, we still do not know how AS-IV stimulates Nrf2, which is a limitation of this study. AS-IV may either directly or indirectly impact Nrf2, which then promotes the expression of HO-1 and NQO-1 and finally results in the improvement of neuroinflammation and oxidative stress. This will be addressed in further researches.

Overall, our study illustrated that AS-IV decreases the fasting blood glucose levels, alleviates oxidative stress and neuroinflammation, and ultimately improves cognitive impairment probably *via* Nrf2/Keap1/HO-1/NQO1 pathway in T2DM mice. It is the first time to demonstrate the neuroprotective effects of AS-IV in diabetes-related cognitive impairment, indicating that AS-IV may be a therapeutic agent for the treatment of cognitive dysfunction in T2DM.

## Data availability statement

The raw data supporting the conclusions of this article will be made available by the authors, without undue reservation.

## Ethics statement

The animal study was reviewed and approved by Ethical Committee on Animal Welfare of Shanghai Jiao Tong University Affiliated Sixth People's Hospital.

## Author contributions

YaZ and JZ carried out the study and participated in the production of the manuscript. JF supervised the research. YaZ and YY treated the animals and preformed the animal experiment. YZhao and YuZ contributed to the discussion and analysis of the data. All authors contributed to the article and approved the submitted version.

## Funding

This study was supported by the research grants from National Natural Science Foundation of China (Grant No. 81871103, 82171179, and 81870952).

## Conflict of interest

The authors declare that the research was conducted in the absence of any commercial or financial relationships that could be construed as a potential conflict of interest.

## Publisher's note

All claims expressed in this article are solely those of the authors and do not necessarily represent those of their affiliated organizations, or those of the publisher, the editors and the reviewers. Any product that may be evaluated in this article, or claim that may be made by its manufacturer, is not guaranteed or endorsed by the publisher.

## References

Ahmed, S. M., Luo, L., Namani, A., Wang, X. J., and Tang, X. (2017). Nrf2 signaling pathway: pivotal roles in inflammation. *Biochim. Biophys. Acta Mol. Basis Dis.* 1863, 585–597. doi: 10.1016/j.bbadis.2016.11.005

Biessels, G. J., and Despa, F. (2018). Cognitive decline and dementia in diabetes mellitus: mechanisms and clinical implications. *Nat. Rev. Endocrinol.* 14, 591–604. doi: 10.1038/s41574-018-0048-7

Biessels, G. J., Staekenborg, S., Brunner, E., Brayne, C., and Scheltens, P. (2006). Risk of dementia in diabetes mellitus: a systematic review. *Lancet Neurol.* 5, 64–74. doi: 10.1016/S1474-4422(05)70284-2

Chen, F., Yang, D., Cheng, X. Y., Yang, H., Yang, X. H., Liu, H. T., et al. (2021). Astragaloside IV ameliorates cognitive impairment and neuroinflammation in an oligomeric aβ induced Alzheimer's disease mouse model via inhibition of microglial activation and NADPH oxidase expression. *Biol. Pharm. Bull.* 44, 1688–1696. doi: 10.1248/bpb.b21-00381

Chen, X., Famurewa, A. C., Tang, J., Olatunde, O. O., and Olatunji, O. J. (2022). Hyperoside attenuates neuroinflammation, cognitive impairment and oxidative stress via suppressing TNF-α/NF-κB/caspase-3 signaling in type 2 diabetes rats. *Nutr. Neurosci.* 25, 1774–1784. doi: 10.1080/1028415X.2021.1901047

Chong, Z. Z., Li, F., and Maiese, K. (2005). Oxidative stress in the brain: novel cellular targets that govern survival during neurodegenerative disease. *Prog. Neurobiol.* 75, 207–246. doi: 10.1016/j.pneurobio.2005.02.004

Feil, D. G., Rajan, M., Soroka, O., Tseng, C. L., Miller, D. R., and Pogach, L. M. (2011). Risk of hypoglycemia in older veterans with dementia and cognitive impairment: implications for practice and policy. *J. Am. Geriatr. Soc.* 59, 2263–2272. doi: 10.1111/j.1532-5415.2011.03726.x

Feng, Y., Chu, A., Luo, Q., Wu, M., Shi, X., and Chen, Y. (2018). The protective effect of astaxanthin on cognitive function via inhibition of oxidative stress and inflammation in the brains of chronic T2DM rats. *Front. Pharmacol.* 9:748. doi: 10.3389/fphar.2018.00748

Gocmez, S. S., Sahin, T. D., Yazir, Y., Duruksu, G., Eraldemir, F. C., Polat, S., et al. (2019). Resveratrol prevents cognitive deficits by attenuating oxidative damage and inflammation in rat model of streptozotocin diabetes induced vascular dementia. *Physiol. Behav.* 201, 198–207. doi: 10.1016/j.physbeh.2018.12.012

Gui, D., Huang, J., Guo, Y., Chen, J., Chen, Y., Xiao, W., et al. (2013a). Astragaloside IV ameliorates renal injury in streptozotocin-induced diabetic rats through inhibiting NF-κB-mediated inflammatory genes expression. *Cytokine* 61, 970–977. doi: 10.1016/j.cyto.2013.01.008

Gui, D., Huang, J., Liu, W., Guo, Y., Xiao, W., and Wang, N. (2013b). Astragaloside IV prevents acute kidney injury in two rodent models by inhibiting oxidative stress and apoptosis pathways. *Apoptosis* 18, 409–422. doi: 10.1007/s10495-013-0801-2

He, F., Ru, X., and Wen, T. (2020). NRF2, a transcription factor for stress response and beyond. *Int. J. Mol. Sci.* 21:4777. doi: 10.3390/ijms21134777

Hoyos, C. M., Stephen, C., Turner, A., Ireland, C., Naismith, S. L., and Duffy, S. L. (2022). Brain oxidative stress and cognitive function in older adults with diabetes and pre-diabetes who are at risk for dementia. *Diabetes Res. Clin. Pract.* 184:109178. doi: 10.1016/j.diabres.2021.109178

Kim, S., Kang, I. H., Nam, J. B., Cho, Y., Chung, D. Y., Kim, S. H., et al. (2015). Ameliorating the effect of astragaloside IV on learning and memory deficit after chronic cerebral hypoperfusion in rats. *Molecules* 20, 1904–1921. doi: 10.3390/molecules20021904

Ko, C. Y., Xu, J. H., Lo, Y. M., Tu, R. S., Wu, J. S., Huang, W. C., et al. (2021). Alleviative effect of alpha-lipoic acid on cognitive impairment in high-fat diet and streptozotocin-induced type 2 diabetic rats. *Front Aging Neurosci* 13:774477. doi: 10.3389/fnagi.2021.774477

Ma, Q. (2013). Role of nrf2 in oxidative stress and toxicity. *Annu. Rev. Pharmacol. Toxicol.* 53, 401–426. doi: 10.1146/annurev-pharmtox-011112-140320

Marioni, R. E., Strachan, M. W., Reynolds, R. M., Lowe, G. D., Mitchell, R. J., Fowkes, F. G., et al. (2010). Association between raised inflammatory markers and cognitive decline in elderly people with type 2 diabetes: the edinburgh type 2 diabetes study. *Diabetes* 59, 710–713. doi: 10.2337/db09-1163

Michailidis, M., Moraitou, D., Tata, D. A., Kalinderi, K., Papamitsou, T., and Papaliagkas, V. (2022). Alzheimer's disease as type 3 diabetes: common pathophysiological mechanisms between Alzheimer's disease and type 2 diabetes. *Int. J. Mol. Sci.* 23:2687. doi: 10.3390/ijms23052687

Pang, X., Makinde, E. A., Eze, F. N., and Olatunji, O. J. (2021). Securidaca inappendiculata polyphenol rich extract counteracts cognitive deficits, neuropathy, neuroinflammation and oxidative stress in diabetic encephalopathic rats via p38 MAPK/Nrf2/HO-1 pathways. *Front. Pharmacol.* 12:737764. doi: 10.3389/fphar.2021.737764

Piatkowska-Chmiel, I., Herbet, M., Gawronska-Grzywacz, M., Ostrowska-Lesko, M., and Dudka, J. (2021). The role of molecular and inflammatory indicators in the assessment of cognitive dysfunction in a mouse model of diabetes. *Int. J. Mol. Sci.* 22:3878. doi: 10.3390/ijms22083878

Qiao, Y., Fan, C. L., and Tang, M. K. (2017). Astragaloside IV protects rat retinal capillary endothelial cells against high glucose-induced oxidative injury. *Drug Des. Devel. Ther.* 11, 3567–3577. doi: 10.2147/DDDT.S152489

Rojo, A. I., Pajares, M., Rada, P., Nuñez, A., Nevado-Holgado, A. J., Killik, R., et al. (2017). NRF2 deficiency replicates transcriptomic changes in Alzheimer's patients and worsens APP and TAU pathology. *Redox Biol.* 13, 444–451. doi: 10.1016/j.redox.2017.07.006

Song, M. T., Ruan, J., Zhang, R. Y., Deng, J., Ma, Z. Q., and Ma, S. P. (2018). Astragaloside IV ameliorates neuroinflammation-induced depressive-like behaviors in mice via the PPARγ/NF-κB/NLRP3 inflammasome axis. *Acta Pharmacol. Sin.* 39, 1559–1570. doi: 10.1038/aps.2017.208

Srikanth, V., Sinclair, A. J., Hill-Briggs, F., Moran, C., and Biessels, G. J. (2020). Type 2 diabetes and cognitive dysfunction-towards effective management of both comorbidities. *Lancet Diabetes Endocrinol.* 8, 535–545. doi: 10.1016/S2213-8587(20)30118-2

Valko, M., Leibfritz, D., Moncol, J., Cronin, M. T., Mazur, M., and Telser, J. (2007). Free radicals and antioxidants in normal physiological functions and human disease. *Int. J. Biochem. Cell Biol.* 39, 44–84. doi: 10.1016/j.biocel.2006.07.001

Wang, B. N., Wu, C. B., Chen, Z. M., Zheng, P. P., Liu, Y. Q., Xiong, J., et al. (2021). DL-3-n-butylphthalide ameliorates diabetes-associated cognitive decline by enhancing PI3K/Akt signaling and suppressing oxidative stress. *Acta Pharmacol. Sin.* 42, 347–360. doi: 10.1038/s41401-020-00583-3

Wang, E., Wang, L., Ding, R., Zhai, M., Ge, R., Zhou, P., et al. (2020). Astragaloside IV acts through multi-scale mechanisms to effectively reduce diabetic nephropathy. *Pharmacol. Res.* 157:104831. doi: 10.1016/j.phrs.2020.104831

Wang, G., Zhang, X., Lu, X., Liu, J., Zhang, Z., Wei, Z., et al. (2020). Fish oil supplementation attenuates cognitive impairment by inhibiting neuroinflammation in STZ-induced diabetic rats. *Aging (Albany NY)* 12, 15281–15289. doi: 10.18632/aging.103426

Wang, X., Wang, Y., Hu, J. P., Yu, S., Li, B. K., Cui, Y., et al. (2017). Astragaloside IV, a natural PPARγ agonist, reduces aβ production in Alzheimer's disease through inhibition of BACE1. *Mol. Neurobiol.* 54, 2939–2949. doi: 10.1007/s12035-016-9874-6

Wu, M., Liao, M., Huang, R., Chen, C., Tian, T., Wang, H., et al. (2022). Hippocampal overexpression of TREM2 ameliorates high fat diet induced cognitive impairment and modulates phenotypic polarization of the microglia. *Genes Dis.* 9, 401–414. doi: 10.1016/j.gendis.2020.05.005

Xia, M. L., Xie, X. H., Ding, J. H., Du, R. H., and Hu, G. (2020). Astragaloside IV inhibits astrocyte senescence: implication in Parkinson's disease. *J. Neuroinflammation* 17:105. doi: 10.1186/s12974-020-01791-8

Yoshizaki, K., Asai, M., and Hara, T. (2020). High-fat diet enhances working memory in the Y-maze test in male C57BL/6J mice with less anxiety in the elevated plus maze test. *Nutrients* 12:2036. doi: 10.3390/nu12072036

You, S., Jang, M., and Kim, G. H. (2020). Mori cortex radicis attenuates high fat diet-induced cognitive impairment via an IRS/Akt signaling pathway. *Nutrients* 12:1851. doi: 10.3390/nu12061851

Zhang, C., Deng, J., Liu, D., Tuo, X., Xiao, L., Lai, B., et al. (2018). Nuciferine ameliorates hepatic steatosis in high-fat diet/streptozocin-induced diabetic mice through a PPARα/PPARγ coactivator-1α pathway. *Br. J. Pharmacol.* 175, 4218–4228. doi: 10.1111/bph.14482

Zhang, L., Ma, Q., and Zhou, Y. (2020). Strawberry leaf extract treatment alleviates cognitive impairment by activating Nrf2/HO-1 signaling in rats with streptozotocin-induced diabetes. *Front. Aging Neurosci.* 12:201. doi: 10.3389/fnagi.2020.00201

Zhang, Y., Tao, C., Xuan, C., Jiang, J., and Cao, W. (2020). Transcriptomic analysis reveals the protection of astragaloside IV against diabetic nephropathy by modulating inflammation. *Oxid. Med. Cell Longev.* 2020:9542165. doi: 10.1155/2020/9542165

Zhang, W. J., and Frei, B. (2015). Astragaloside IV inhibits NF-κB activation and inflammatory gene expression in LPS-treated mice. *Mediators Inflamm.* 2015:274314. doi: 10.1155/2015/274314

Zhao, Q., Zhang, F., Yu, Z., Guo, S., Liu, N., Jiang, Y., et al. (2019). HDAC3 inhibition prevents blood-brain barrier permeability through Nrf2 activation in type 2 diabetes male mice. *J. Neuroinflammation* 16:103. doi: 10.1186/s12974-019-1495-3

Zhao, Y., Zhang, J., Zheng, Y., Zhang, Y., Zhang, X. J., Wang, H., et al. (2021). $NAD^+$ improves cognitive function and reduces neuroinflammation by ameliorating mitochondrial damage and decreasing ROS production in chronic cerebral hypoperfusion models through Sirt1/PGC-1α pathway. *J. Neuroinflammation* 18:207. doi: 10.1186/s12974-021-02250-8

Zhu, D. Y., Lu, J., Xu, R., Yang, J. Z., Meng, X. R., Ou-Yang, X. N., et al. (2022). FX5, a non-steroidal glucocorticoid receptor antagonist, ameliorates diabetic cognitive impairment in mice. *Acta Pharmacol. Sin.* doi: 10.1038/s41401-022-00884-9. [Online ahead of print].

frontiers | Frontiers in Aging Neuroscience

TYPE Original Research
PUBLISHED 10 October 2022
DOI 10.3389/fnagi.2022.1008780



OPEN ACCESS

EDITED BY
Jun Xu,
Beijing Tiantan Hospital, Capital Medical University, China

REVIEWED BY
Xingshun Xu,
The First Affiliated Hospital of Soochow University, China
Jin-Tai Yu,
University of California, San Francisco, United States

*CORRESPONDENCE
Zuo-Teng Wang
wzt20150818@163.com
Lan Tan
dr.tanlan@163.com

†These authors have contributed equally to this work

SPECIALTY SECTION
This article was submitted to Alzheimer's Disease and Related Dementias, a section of the journal Frontiers in Aging Neuroscience

RECEIVED 01 August 2022
ACCEPTED 21 September 2022
PUBLISHED 10 October 2022

CITATION
Fu Y, Wang Z-T, Huang L-Y, Tan C-C, Cao X-P and Tan L (2022) Heart fatty acid-binding protein is associated with phosphorylated tau and longitudinal cognitive changes.
*Front. Aging Neurosci.* 14:1008780.
doi: 10.3389/fnagi.2022.1008780



# Heart fatty acid-binding protein is associated with phosphorylated tau and longitudinal cognitive changes

Yan Fu[1†], Zuo-Teng Wang[1*†], Liang-Yu Huang[1], Chen-Chen Tan[1], Xi-Peng Cao[2] and Lan Tan[1*]

[1]Department of Neurology, Qingdao Municipal Hospital, Qingdao University, Qingdao, China, [2]Clinical Research Center, Qingdao Municipal Hospital, Qingdao University, Qingdao, China

**Background:** Perturbation of lipid metabolism is associated with Alzheimer's disease (AD). Heart fatty acid-binding protein (HFABP) is an adipokine playing an important role in lipid metabolism regulation.

**Materials and methods:** Two datasets separately enrolled 303 and 197 participants. First, we examine the associations of cerebrospinal fluid (CSF) HFABP levels with cognitive measures [including Mini-Mental State Examination (MMSE), Clinical Dementia Rating sum of boxes (CDRSB), and the cognitive section of Alzheimer's Disease Assessment Scale] and AD biomarkers (CSF amyloid beta and tau levels). Second, we examine the longitudinal associations of baseline CSF HFABP levels and the variability of HFABP with cognitive measures and AD biomarkers. Structural equation models explored the mediation effects of AD pathologies on cognition.

**Results:** We found a significant relationship between CSF HFABP level and P-tau (dataset 1: $\beta = 2.04$, $p < 0.001$; dataset 2: $\beta = 1.51$, $p < 0.001$). We found significant associations of CSF HFABP with longitudinal cognitive measures (dataset 1: ADAS13, $\beta = 0.09$, $p = 0.008$; CDRSB, $\beta = 0.10$, $p = 0.003$; MMSE, $\beta = -0.15$, $p < 0.001$; dataset 2: ADAS13, $\beta = 0.07$, $p = 0.004$; CDRSB, $\beta = 0.07$, $p = 0.005$; MMSE, $\beta = -0.09$, $p < 0.001$) in longitudinal analysis. The variability of HFABP was associated with CSF P-tau (dataset 2: $\beta = 3.62$, $p = 0.003$). Structural equation modeling indicated that tau pathology mediated the relationship between HFABP and cognition.

**Conclusion:** Our findings demonstrated that HFABP was significantly associated with longitudinal cognitive changes, which might be partially mediated by tau pathology.

KEYWORDS

**Alzheimer's disease, HFABP, lipid metabolism, cognition, cerebrospinal fluid**

# Introduction

Alzheimer's disease (AD) is the primary cause of dementia in the elderly worldwide, and its prevalence is projected to triple over the next 20 years (Alzheimer's Association, 2011; Prince et al., 2013). AD is characterized by neuropathological markers of neurofibrillary tangles made of filamentous hyperphosphorylated tau and neuritic amyloid-β plaques (Kirkitadze et al., 2002; Selkoe and Hardy, 2016). The underlying mechanisms of extensive and considerable neuropathology of AD are still unclear. Genome-wide association studies implicated lipid metabolism in several neurodegenerative diseases, including AD, and several studies demonstrated the association between lipid/lipoprotein metabolism and AD pathology (Hamilton et al., 2015; Marschallinger et al., 2020).

Changes in lipid metabolism during aging are crucial for a variety of biological processes (Papsdorf and Brunet, 2019). Dysfunction of lipid metabolism affects membrane lipid composition and fluidity, thus contributing to age-related neuronal cell dysfunction and neurologic disease (Mori et al., 2001; Siino et al., 2018). Therefore, lipid-binding proteins seem to be involved in the pathogenesis of AD. Recent studies suggested that heart fatty acid-binding protein (HFABP or FABP3), a lipid-binding protein facilitating the intracellular transport of fatty acids, may contribute to AD diagnosis and prognosis in the earliest stages (Rosén et al., 2011). A study found that the association between elevated levels of HFABP and longitudinal atrophy of crucial brain structures was significant among amyloid positive individuals and occurred irrespective of tau pathology (Chiasserini et al., 2017). However, other studies found that increased cerebrospinal fluid (CSF) HFABP was related to tau pathology and neurodegeneration (Chiasserini et al., 2010, 2017). There is a dearth of research investigating the longitudinal association of HFABP with cognition functioning and AD biomarkers and the mediational role of AD pathology in the relationship between lipid metabolism and cognition.

Here, in this investigation, we examined the association of AD biomarkers and cognition with HFABP from Alzheimer's Disease Neuroimaging Initiative (ADNI) dataset. We evaluated whether CSF HFABP is associated with CSF AD biomarkers and cognition at baseline and follow-up and whether CSF HFABP change is associated with AD biomarkers and cognition over time. We also examined whether AD pathology is a potential mediator of the relationship between HFABP and cognition.

# Materials and methods

## Data description

The data used in the preparation of this were downloaded from the ADNI dataset[1] (Weiner et al., 2010, 2012). The ADNI was launched in 2003 by the National Institute on Aging (NIA), the National Institute of Biomedical Imaging and Bioengineering (NIBIB), the Food and Drug Administration (FDA), private pharmaceutical companies, and non-profit organizations, as a $60 million, 5-year public-private partnership. For up-to-date information, see text footnote 1. Written consent was obtained at enrollment from all participants and the study was approved by each participating site's institutional review board.

## Alzheimer's disease neuroimaging initiative participants

Our study population consisted of all patients, including cognitively healthy control (CN), patients with mild cognitive impairment (MCI), and patients with AD dementia, with available CSF HFABP data from the ADNI cohort. Inclusion and exclusion criteria are described in detail online (see text footnote 1) (Petersen et al., 2010). Finally, participants 55–90 years of age have been included, among whom individuals had available follow-up information. CN participants had a MMSE score of >24 and a clinical dementia rating score of 0. Patients with early MCI had a MMSE score of ≥24, a clinical dementia rating score of 0.5, preserved activities of daily living, and absence of dementia. Patients with AD dementia fulfilled the National Institute of Neurological Communicative Disorders and Stroke–Alzheimer Disease and Related Disorders Association criteria for probable AD (McKhann et al., 1984), had MMSE scores of 20–26, and had CDR scores of 0.5–1.0.

## Measurements of cerebrospinal fluid biomarkers analysis

We download the first data set of participants whose CSF HFABP protein levels were evaluated using a Myriad Rules Based Medicine platform (Human Discovery MAP, v1.0; see ADNI "Materials and methods" Section). A second data set from the Foundation for the National Institutes of Health (FNIH) Biomarker Consortium CSF Proteomics Project included 197 participants with CSF HFABP protein concentrations which were evaluated with the multiple Multi Reaction Monitoring (MRM) targeted mass spectroscopy at baseline and during follow-up.

Alzheimer's Disease Neuroimaging Initiative CSF protocols, including Aβ1–42, tau, and p-tau181, have previously been described in detail (Shaw et al., 2009). The CSF Aβ1–42, tau, and p-tau181 levels were measured with the multiplex xMAP Luminex platform and Innogenetics INNO-BIA AlzBio3 (Innogenetics-Fujirebio, Ghent, Belgium) immunoassay

1 https://adni.loni.usc.edu/

reagents. The intra-assay coefficient of variation (CV) of duplicate determinations for concentration ranged from 2.5 to 5.9% for Aβ1–42, 2.2–6.3% for tau, and the inter-assay CV for CSF pool samples ranged from 5.1 to 14% for Aβ1–42, 2.7–11.2% for tau. Further information on standard operation procedures was described in previous publications (Shaw et al., 2009, 2011) and online (see text footnote 1).

## Cognitive measures

In ADNI, all participants received detailed cognitive evaluations, including the global cognition by Mini-Mental State Examination (MMSE), Clinical Dementia Rating sum of boxes (CDRSB), and the cognitive section of Alzheimer's Disease Assessment Scale (ADAS13).

## Statistical analyses

All data management and analyses were conducted using R version 4.0.1 using the data. Table package version 1.14.0, the dplyr package version 1.0.2, the lme4 package version 1.1.29, the lmerTest package version 3.1.3, and the car package version 3.0.10. Figures were plotted using ggplot2 version 3.2.1. Additionally, stringr package version 1.4.0 and fst package version 0.9.4 were used for data management. All variables were log-transformed to improve normality.

First, multiple linear regression models were used to examine the cross-sectional relationship among CSF HFABP and cognition after adjusting for age, sex, education, and Apolipoprotein E (APOE) ε4 status, and AD core biomarkers after adjusting for age, sex, education, APOE ε4 status, and diagnosis. Second, to assess the association of baseline CSF HFABP levels with the longitudinal cognitive measures and AD core biomarkers. Linear mixed-effect models were used for the analysis, adjusting for the same covariables as the baseline models and additionally including time as an interacting variable with CSF HFABP levels. Third, estimated slopes for changes in the CSF HFABP concentrations were calculated for each individual using linear mixed-effect models for repeated measures. After that, the HFABP change rate was included in the linear mixed-effect models as independent variables to investigate the association between longitudinal CSF HFABP changes and longitudinal cognitive and AD core biomarkers changes. Finally, mediation models were conducted in the current study to investigate whether the association of HFABP with cognition was mediated by AD pathology. These models were adjusted for age, sex, education, and APOE ε4 status. Two other mediation analyses were used to determine whether the association of baseline and longitudinal CSF HFABP with longitudinal clinical outcomes were mediated respectively by baseline and longitudinal AD biomarkers. The same covariates as in the first model were used in two other models.

# Results

## Characteristics of participants

As for the ADNI dataset 1, 303 participants aged 56–89 years (mean age 75.14 years) were included in the present study at baseline. The mean education years of the study sample were 15.66, 39.4% were female, and 48.0% were APOE4 carriers (Table 1). As for ADNI dataset 2, 197 participants aged 55–89 years (mean age 72.69 years) were included in the present study at baseline. The mean education years of the study sample were 16.16, 44.4% were female, and 39.3% were APOE4 carriers (Table 1).

## The cross-section association of heart fatty acid-binding protein with cognition measures and Alzheimer's disease biomarkers

In dataset 1, multivariate analyses showed the strong association of CSF HFABP with cognition measures and AD biomarkers. Individuals with higher HFABP levels had lower cognition measures, as indicated by higher ADAS13 score ($\beta = 0.68$, $p < 0.001$), higher CDRSB score ($\beta = 0.69$, $p < 0.001$), and lower MMSE score ($\beta = -0.60$, $p = 0.002$), and had higher concentration of P-tau ($\beta = 2.04$, $p < 0.001$). In dataset 2, similar results were observed in the relationship between HFABP and P-tau ($\beta = 1.51$, $p < 0.001$). However, there were no significant

TABLE 1 Baseline characteristics of participants.

| Characteristic | ADNI data 1 | ADNI data 2 |
|---|---|---|
| N | 303 | 197 |
| Age [mean (SD)] | 75.14 (6.73) | 72.69 (7.05) |
| Female (%) | 129 (39.4) | 87 (44.4) |
| Education [mean (SD)] | 15.66 (3.04) | 16.16 (2.81) |
| APOE carrier (%) | 157 (48.0) | 77 (39.3) |
| MMSE score [mean (SD)] | 26.76 (2.56) | 28.26 (1.86) |
| CDRSB score [mean (SD)] | 1.71 (1.77) | 0.88 (1.04) |
| ADAS13 score [mean (SD)] | 18.54 (9.14) | 13.05 (7.09) |
| **CSF AD biomarkers [mean (SD)]** | | |
| Aβ42 | 905.26 (562.07) | 1,162.69 (635.32) |
| Tau | 307.76 (118.97) | 281.17 (116.08) |
| P-tau | 30.22 (13.63) | 26.64 (13.07) |

ADAS13, Alzheimer's Disease Assessment Scale; ADNI, Alzheimer's Disease Neuroimaging Initiative; CSF, cerebrospinal fluid; MMSE, Mini-Mental State Examination; CDRSB, clinical Dementia Rating sum of boxes; P-tau, phosphorylated tau; Aβ, Amyloid beta.

10.3389/fnagi.2022.1008780

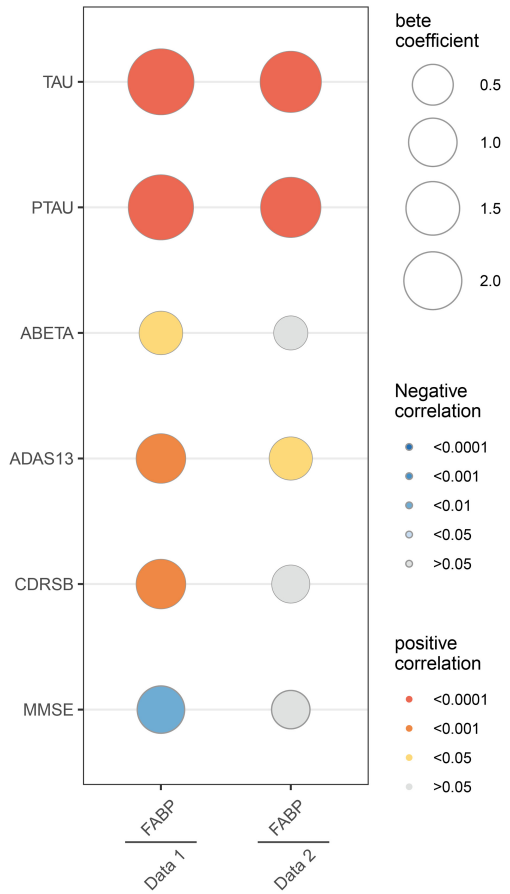


FIGURE 1
Linear associations between fatty acid binding protein and Mini-Mental State Examination (MMSE), Clinical Dementia Rating sum of boxes (CDRSB), ADAS13, Amyloid beta (ABETA), TAU, and PTAU. The size of the bubble represents the correlation levels. The color of the bubble represents the beta coefficient levels. Red: positive correlation. Blue: negative correlation. MMSE, Mini-Mental State Examination; CDRSB, Clinical Dementia Rating sum of boxes; ADAS13, the cognitive section of Alzheimer's Disease Assessment Scale; ABETA, Amyloid beta; P-tau, phosphorylated tau.

relationships between cognition measures, except ADAS13 score ($\beta = 0.39$, $p = 0.021$). This demonstrated the positive association of HFABP with P-tau and the negative association with cognition (Figure 1 and Supplementary Table 1).

## The longitudinal association of heart fatty acid-binding protein with cognition measures and Alzheimer's disease biomarkers

To examine the association of baseline HFABP with cognitive measures and AD biomarkers, we constructed mixed effects models of these measures and biomarkers and observed that HFABP was associated with rate of cognitive change (interacted with time) in both datasets (dataset 1: ADAS13, $\beta = 0.09$, $p = 0.008$; CDRSB, $\beta = 0.10$, $p = 0.003$; MMSE, $\beta = -0.15$, $p < 0.001$; dataset 2: ADAS13, $\beta = 0.07$, $p = 0.004$; CDRSB, $\beta = 0.07$, $p = 0.005$; MMSE, $\beta = -0.09$, $p < 0.001$). However, the results for the association between HFABP and AD biomarkers were inconsistent of both dataset 1 and dataset 2. Baseline HFABP level was associated with P-tau ($\beta = -0.06$, $p = 0.015$) on dataset 1 and Aβ42 ($\beta = -0.04$, $p = 0.008$) on dataset 2 in a longitudinal model. To determine whether HFABP variability is associated with cognitive measures and AD biomarkers, we calculated the difference in CSF HFABP levels between baseline and follow-up and associated this difference with cognitive measures and AD biomarkers. HFABP variability was associated with increased CSF protein level of P-tau ($\beta = 3.62$, $p = 0.003$). This is consistent with the association between baseline HFABP and P-tau in cross-section and longitudinal models (Figure 2 and Supplementary Table 2).

## Causal mediation analyses

Considering the association of HFABP with cognition and tau pathology shown above, HFABP was associated with not only cognitive impairment but also CSF P-tau concentration. We investigate whether high HFABP levels contribute to cognitive impairment *via* tau pathology. In dataset 1, we found that the relationship between HFABP and cognition (MMSE: IE = −0.36, $p = 0.038$; ADAS13: IE = 4.64, $p = 0.002$; CDRSB: IE = 0.73, $p = 0.028$) and longitudinal cognition change (MMSE change: IE = −0.09, $p = 0.000$; ADAS13 change: IE = 0.08, $p = 0.000$; CDRSB change: IE = 0.09, $p = 0.000$) was mediated by tau pathology (Figures 3, 4 and Supplementary Tables 3, 4). However, in dataset 2, we only found tau pathology mediated the relationship between HFABP and longitudinal cognition change (MMSE change: IE = −0.05, $p = 0.001$; ADAS13 change: IE = 0.05, $p = 0.000$; CDRSB change: IE = 0.05, $p = 0.001$) (Figures 3, 4 and Supplementary Tables 3, 4).

# Discussion

The present study found that (1) HFABP was associated with baseline tau pathology; (2) HFABP was associated with longitudinal cognition change; (3) HFABP variability was associated with an increased CSF protein level of P-tau; and (4) the influence of HFABP on cognition was mediated by tau pathology. These findings consolidated the close relationships

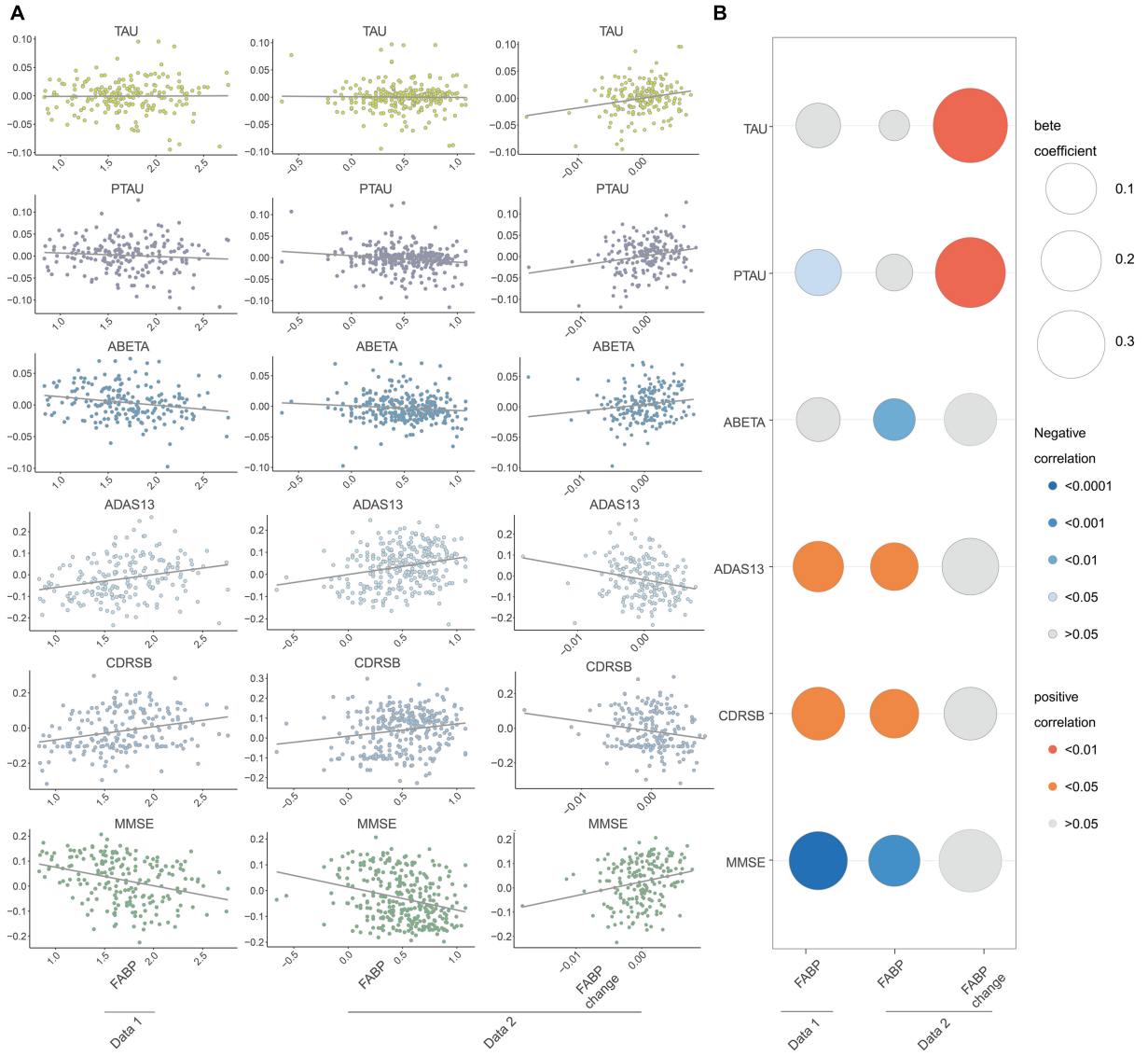


FIGURE 2
Longitudinal association between fatty acid binding protein and Mini-Mental State Examination (MMSE), Clinical Dementia Rating sum of boxes (CDRSB), ADAS13, Amyloid beta (ABETA), TAU, and PTAU. **(A)** Scatter plots of the association of heart fatty acid-binding protein (HFABP) and HFABP change with cognition and AD biomarkers changes; **(B)** standardized coefficients for the association of HFABP and HFABP change with cognitive measures and AD biomarkers. The size of the bubble represents the correlation levels. The color of the bubble represents the beta coefficient levels (interacted with time). Red: positive correlation. Blue: negative correlation. MMSE, Mini-Mental State Examination; CDRSB, Clinical Dementia Rating sum of boxes; ADAS13, the cognitive section of Alzheimer's Disease Assessment Scale; ABETA, Amyloid beta; P-tau, phosphorylated tau.

of HFABP with AD pathology and cognition, supporting the validity of the biomarker-based diagnosis of preclinical AD.

Previous studies found that CSF levels of HFABP in AD patients were higher than in MCI subjects and older people without cognition impairment (Chiasserini et al., 2017; Höglund et al., 2017; Dulewicz et al., 2021). Furthermore, other studies found significantly elevated CSF HFABP levels have been described in MCI subjects compared with the cognitively healthy group, but no difference between the dementia group and the progressive MCI subgroup (Guo et al., 2013). These results demonstrated that CSF levels of HFABP are already increased in the early stages of AD and increased with the progress of AD. This is in line with our studies, as we observed the association between baseline CSF HFABP and longitudinal cognition change. These findings suggested that changes in the CSF levels of HFABP may reflect the roles of lipid-related metabolism in the development of AD. High HFABP levels might result from increasing pathological

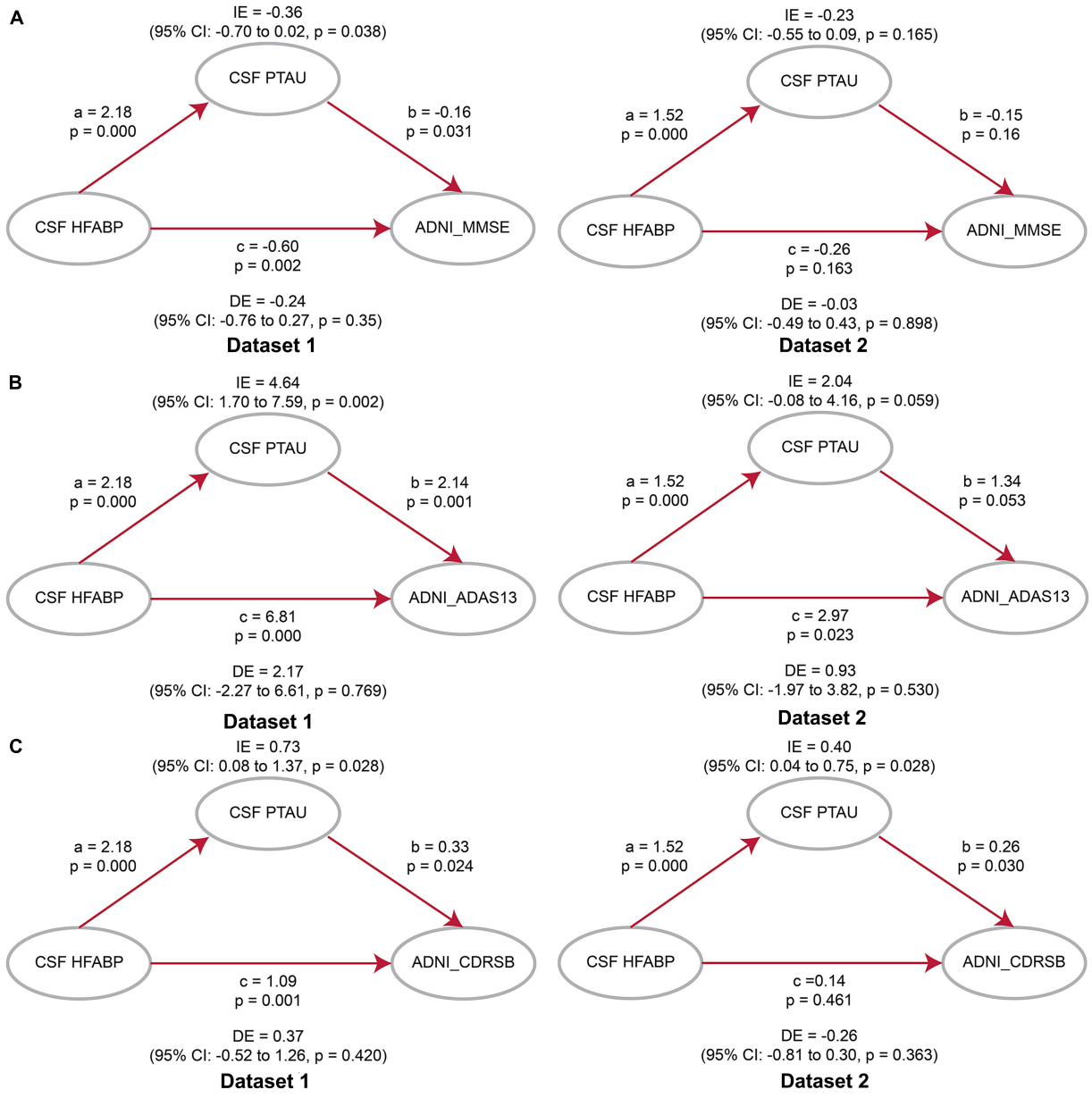


FIGURE 3
Mediation analyses showed that the relationship between heart fatty acid-binding protein (HFABP) and cognitive measures were mediated by tau pathology. **(A)** Global cognition measured by Mini-Mental State Examination (MMSE); **(B)** global cognition measured by ADAS13; **(C)** global cognition measured by CDRSB. MMSE, Mini-Mental State Examination; CDRSB, Clinical Dementia Rating sum of boxes; ADAS13, the cognitive section of Alzheimer's Disease Assessment Scale; ABETA, Amyloid beta; P-tau, phosphorylated tau; IE, Indirect effects; DE, Direct effects.

processes and associate with the neurodegeneration process. Previous studies found that HFABP was significantly correlated with tau pathology (Chiasserini et al., 2010, 2017). The results of these studies are consistent with our research. We also found the longitudinal link between HFABP and tau pathology. Additionally, a study suggested a relationship between HFABP and neurodegeneration-related amyloid pathology and brain atrophy, while we failed to identify the association in the present study (Desikan et al., 2013).

The mechanisms underlying the association between HFABP and cognition remain unknown. Several possible mechanisms might be implicated. First, HFABP in the brain may regulate the lipids components of neuronal cell membranes, thereby affecting synaptic degeneration and regeneration and involving in a number of neurodegeneration diseases (Sellner et al., 1995; Mauch et al., 2001; Shioda et al., 2010; Yamamoto et al., 2018). Second, lipid rafts might mediate pathogenesis-related proteins, including α-synuclein

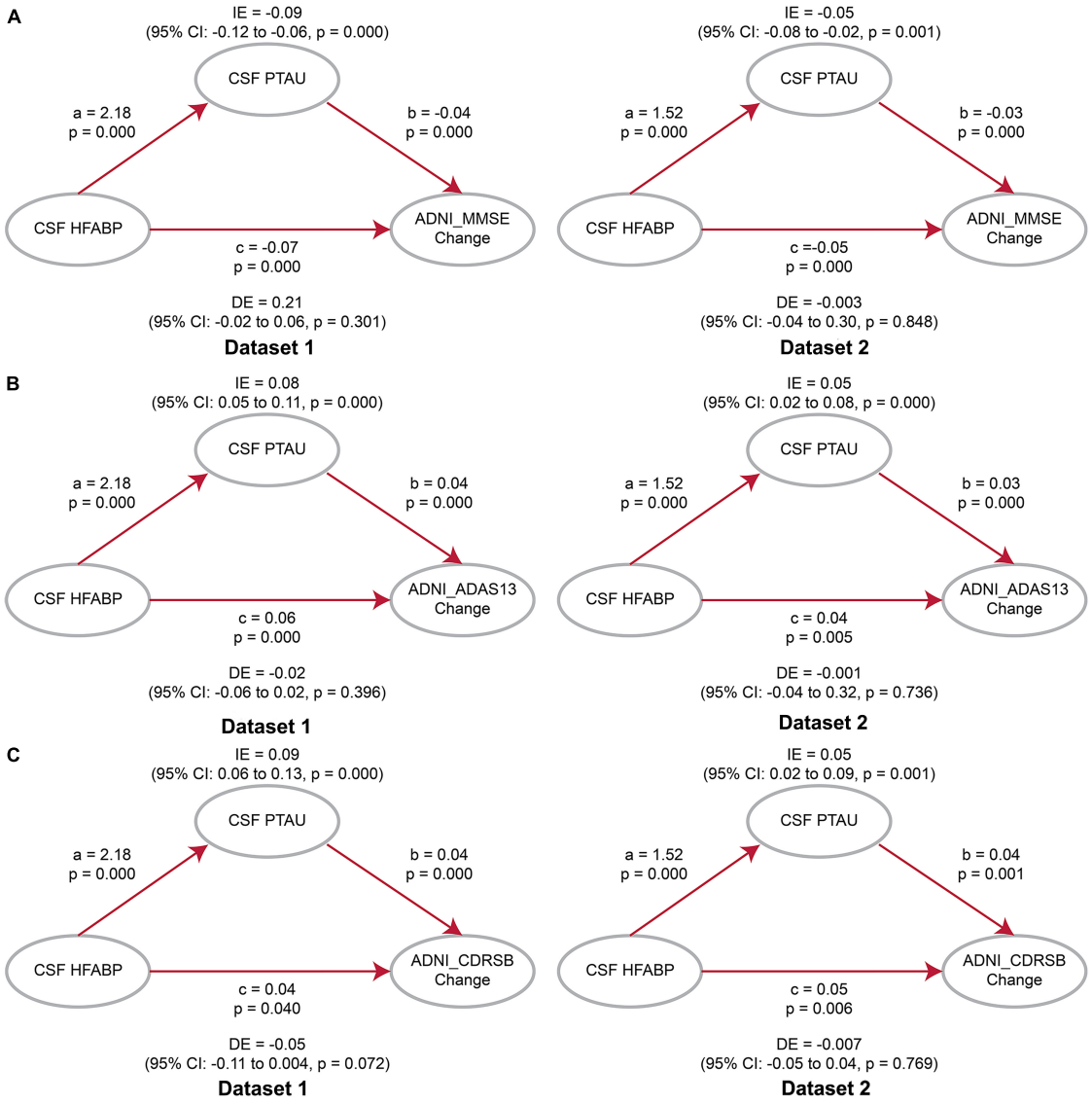


FIGURE 4
Mediation analyses showed that the relationship between heart fatty acid-binding protein (HFABP) and longitudinal cognition change was mediated by tau pathology. **(A)** Global cognition measured by Mini-Mental State Examination (MMSE); **(B)** global cognition measured by ADAS13; **(C)** global cognition measured by Clinical Dementia Rating sum of boxes (CDRSB). MMSE, Mini-Mental State Examination; CDRSB, Clinical Dementia Rating sum of boxes; ADAS13, the cognitive section of Alzheimer's Disease Assessment Scale; ABETA, Amyloid beta; P-tau, phosphorylated tau; IE, Indirect effects; DE, Direct effects.

(Fortin et al., 2004; Yabuki et al., 2020) and prions (Hooper, 2005; Taylor and Hooper, 2007), in a number of protein-misfolding neurodegenerative disorders. Thus, we speculated that HFABP and tau pathology have synergistic effects on AD development. Third, HFABP may also regulate dopamine D2R (dopamine receptor 2) function in the striatum and anterior cingulate cortex and mediates αSyn neurotoxicity in septal GABAergic neurons to affect cognitive function and emotional behavior (Yamamoto et al., 2018; Matsuo et al., 2021). Finally, recent studies suggested HFABP was associated with specific features of brain atrophy and white matter Hyperintensities burden, independently of amyloid and tau pathology biomarkers (Clark et al., 2022; Vidal-Piñeiro et al., 2022).

There are several limitations to this work. First, our study was limited by sample size. The sample size was too small for performing subgroup analyses to detect significant differences. Second, our study included patients with and without dementia to maximize the sample size, which might introduce heterogeneity and slight bias. Finally, we did not determine the plasma levels of HFABP, which will likely influence the CSF levels of HFABP.

## Conclusion

In summary, the present study demonstrated that HFABP was associated with tau pathology and longitudinal cognitive function. Tau pathology might partially mediate the association between HFABP and cognition. Further analyses in large cohorts are needed to validate such findings. Our findings suggested that tau pathology may mediate the role of lipid metabolism in AD development.

## Data availability statement

Publicly available datasets were analyzed in this study. This data can be found in the ADNI at http://adni.loni.usc.edu.

## Ethics statement

Ethical approval was obtained by the ADNI investigators. All participants provided written informed consent. The study conformed with the Declaration of Helsinki.

## Alzheimer's disease neuroimaging initiative

The data used in this article were obtained from the Alzheimer's Disease Neuroimaging Initiative (ADNI) database (adni.loni.usc.edu). As such, the investigators within the ADNI contributed to the design and implementation of ADNI and/or provided data but did not participate in the analysis or writing of this report. A complete listing of ADNI investigators can be found at: http://adni.loni.usc.edu/wpcontent/uploads/how_to_apply/ADNI_Acknowledgement_List.pdf.

## Author contributions

Z-TW and LT conceptualized the study and revised the manuscript. YF, L-YH, C-CT, and X-PC analyzed and interpreted the data, drafted and revised the manuscript, did the statistical analysis, and prepared all the figures. All authors contributed to wrote and revised the manuscript and approved the final version.

## Funding

This study was supported by grants from the National Natural Science Foundation of China (81771148). Data collection and sharing for this project was funded by the Alzheimer's Disease Neuroimaging Initiative (ADNI) (National Institutes of Health Grant U01 AG024904). ADNI is funded by the National Institute on Aging, the National Institute of Biomedical Imaging and Bioengineering, and through generous contributions from the following: Abbott; Alzheimer's Association; Alzheimer's Drug Discovery Foundation; Amorfix Life Sciences Ltd.; AstraZeneca; Bayer HealthCare; BioClinica, Inc.; Biogen Idec Inc.; Bristol-Myers Squibb Company; Eisai Inc.; Elan Pharmaceuticals Inc.; Eli Lilly and Company; F. Hoffmann-La Roche Ltd. and its affiliated company Genentech, Inc.; GE Healthcare; Innogenetics, N.V.; IXICO Ltd.; Janssen Alzheimer Immunotherapy Research & Development, LLC.; Johnson & Johnson Pharmaceutical Research & Development LLC.; Medpace, Inc.; Merck & Co., Inc.; Meso Scale Diagnostics, LLC.; Novartis Pharmaceuticals Corporation; Pfizer Inc.; Servier; Synarc Inc.; and Takeda Pharmaceutical Company. The Canadian Institutes of Health Research is providing funds to support ADNI clinical sites in Canada. Private sector contributions are facilitated by the Foundation for the National Institutes of Health (www.fnih.org). The grantee organization is the Northern California Institute for Research and Education, and the study is coordinated by the Alzheimer's Disease Cooperative Study at the University of California, San Diego. ADNI data are disseminated by the Laboratory for Neuro Imaging at the University of California.

## Conflict of interest

The authors declare that the research was conducted in the absence of any commercial or financial relationships that could be construed as a potential conflict of interest.

## Publisher's note



## Supplementary material

The Supplementary Material for this article can be found online at: https://www.frontiersin.org/articles/10.3389/fnagi.2022.1008780/full#supplementary-material

# References

Alzheimer's Association (2011). 2011 Alzheimer's disease facts and figures. *Alzheimers Dement.* 7, 208–244. doi: 10.1016/j.jalz.2011.02.004

Chiasserini, D., Biscetti, L., Eusebi, P., Salvadori, N., Frattini, G., Simoni, S., et al. (2017). Differential role of CSF fatty acid binding protein 3, α-synuclein, and Alzheimer's disease core biomarkers in Lewy body disorders and Alzheimer's dementia. *Alzheimers Res. Ther.* 9:52. doi: 10.1186/s13195-017-0276-4

Chiasserini, D., Parnetti, L., Andreasson, U., Zetterberg, H., Giannandrea, D., Calabresi, P., et al. (2010). CSF levels of heart fatty acid binding protein are altered during early phases of Alzheimer's disease. *J. Alzheimers Dis.* 22, 1281–1288. doi: 10.3233/jad-2010-101293

Clark, A. L., Haley, A. P., Duarte, A., and O'Bryant, S. (2022). Fatty acid-binding protein 3 is a marker of neurodegeneration and white matter hyperintensity burden in Mexican American older adults. *J. Alzheimers Dis.* doi: 10.3233/jad-220524 [Epub ahead of print].

Desikan, R. S., Thompson, W. K., Holland, D., Hess, C. P., Brewer, J. B., Zetterberg, H., et al. (2013). Heart fatty acid binding protein and Aβ-associated Alzheimer's neurodegeneration. *Mol. Neurodegener.* 8:39. doi: 10.1186/1750-1326-8-39

Dulewicz, M., Kulczyńska-Przybik, A., Słowik, A., Borawska, R., and Mroczko, B. (2021). Fatty acid binding protein 3 (FABP3) and apolipoprotein E4 (ApoE4) as lipid metabolism-related biomarkers of Alzheimer's disease. *J. Clin. Med.* 10:3009. doi: 10.3390/jcm10143009

Fortin, D. L., Troyer, M. D., Nakamura, K., Kubo, S., Anthony, M. D., and Edwards, R. H. (2004). Lipid rafts mediate the synaptic localization of alpha-synuclein. *J. Neurosci.* 24, 6715–6723. doi: 10.1523/jneurosci.1594-04.2004

Guo, L. H., Alexopoulos, P., and Perneczky, R. (2013). Heart-type fatty acid binding protein and vascular endothelial growth factor: Cerebrospinal fluid biomarker candidates for Alzheimer's disease. *Eur. Arch. Psychiatry Clin. Neurosci.* 263, 553–560. doi: 10.1007/s00406-013-0405-4

Hamilton, L. K., Dufresne, M., Joppé, S. E., Petryszyn, S., Aumont, A., Calon, F., et al. (2015). Aberrant lipid metabolism in the forebrain niche suppresses adult neural stem cell proliferation in an animal model of Alzheimer's disease. *Cell Stem Cell* 17, 397–411. doi: 10.1016/j.stem.2015.08.001

Höglund, K., Kern, S., Zettergren, A., Börjesson-Hansson, A., Zetterberg, H., Skoog, I., et al. (2017). Preclinical amyloid pathology biomarker positivity: Effects on tau pathology and neurodegeneration. *Transl. Psychiatry* 7:e995. doi: 10.1038/tp.2016.252

Hooper, N. M. (2005). Roles of proteolysis and lipid rafts in the processing of the amyloid precursor protein and prion protein. *Biochem. Soc. Trans.* 33(Pt 2), 335–338. doi: 10.1042/bst0330335

Kirkitadze, M. D., Bitan, G., and Teplow, D. B. (2002). Paradigm shifts in Alzheimer's disease and other neurodegenerative disorders: The emerging role of oligomeric assemblies. *J. Neurosci. Res.* 69, 567–577. doi: 10.1002/jnr.10328

Marschallinger, J., Iram, T., Zardeneta, M., Lee, S. E., Lehallier, B., Haney, M. S., et al. (2020). Lipid-droplet-accumulating microglia represent a dysfunctional and proinflammatory state in the aging brain. *Nat. Neurosci.* 23, 194–208. doi: 10.1038/s41593-019-0566-1

Matsuo, K., Yabuki, Y., Melki, R., Bousset, L., Owada, Y., and Fukunaga, K. (2021). Crucial role of FABP3 in αSyn-induced reduction of septal GABAergic neurons and cognitive decline in mice. *Int. J. Mol. Sci.* 22:400. doi: 10.3390/ijms22010400

Mauch, D. H., Nägler, K., Schumacher, S., Göritz, C., Müller, E. C., Otto, A., et al. (2001). CNS synaptogenesis promoted by glia-derived cholesterol. *Science* 294, 1354–1357. doi: 10.1126/science.294.5545.1354

McKhann, G., Drachman, D., Folstein, M., Katzman, R., Price, D., and Stadlan, E. M. (1984). Clinical diagnosis of Alzheimer's disease: Report of the NINCDS-ADRDA work group under the auspices of department of health and human services task force on Alzheimer's disease. *Neurology* 34, 939–944. doi: 10.1212/wnl.34.7.939

Mori, T., Paris, D., Town, T., Rojiani, A. M., Sparks, D. L., Delledonne, A., et al. (2001). Cholesterol accumulates in senile plaques of Alzheimer disease patients and in transgenic APP(SW) mice. *J. Neuropathol. Exp. Neurol.* 60, 778–785. doi: 10.1093/jnen/60.8.778

Papsdorf, K., and Brunet, A. (2019). Linking lipid metabolism to chromatin regulation in aging. *Trends Cell Biol.* 29, 97–116. doi: 10.1016/j.tcb.2018.09.004

Petersen, R. C., Aisen, P. S., Beckett, L. A., Donohue, M. C., Gamst, A. C., Harvey, D. J., et al. (2010). Alzheimer's disease neuroimaging initiative (ADNI): Clinical characterization. *Neurology* 74, 201–209. doi: 10.1212/WNL.0b013e3181cb3e25

Prince, M., Bryce, R., Albanese, E., Wimo, A., Ribeiro, W., and Ferri, C. P. (2013). The global prevalence of dementia: A systematic review and metaanalysis. *Alzheimers Dement.* 9, 63–75.e62. doi: 10.1016/j.jalz.2012.11.007

Rosén, C., Mattsson, N., Johansson, P. M., Andreasson, U., Wallin, A., Hansson, O., et al. (2011). Discriminatory analysis of biochip-derived protein patterns in CSF and plasma in neurodegenerative diseases. *Front. Aging Neurosci.* 3:1. doi: 10.3389/fnagi.2011.00001

Selkoe, D. J., and Hardy, J. (2016). The amyloid hypothesis of Alzheimer's disease at 25 years. *EMBO Mol. Med.* 8, 595–608. doi: 10.15252/emmm.201606210

Sellner, P. A., Chu, W., Glatz, J. F., and Berman, N. E. (1995). Developmental role of fatty acid-binding proteins in mouse brain. *Brain Res. Dev. Brain Res.* 89, 33–46. doi: 10.1016/0165-3806(95)00099-y

Shaw, L. M., Vanderstichele, H., Knapik-Czajka, M., Clark, C. M., Aisen, P. S., Petersen, R. C., et al. (2009). Cerebrospinal fluid biomarker signature in Alzheimer's disease neuroimaging initiative subjects. *Ann. Neurol.* 65, 403–413. doi: 10.1002/ana.21610

Shaw, L. M., Vanderstichele, H., Knapik-Czajka, M., Figurski, M., Coart, E., Blennow, K., et al. (2011). Qualification of the analytical and clinical performance of CSF biomarker analyses in ADNI. *Acta Neuropathol.* 121, 597–609. doi: 10.1007/s00401-011-0808-0

Shioda, N., Yamamoto, Y., Watanabe, M., Binas, B., Owada, Y., and Fukunaga, K. (2010). Heart-type fatty acid binding protein regulates dopamine D2 receptor function in mouse brain. *J. Neurosci.* 30, 3146–3155. doi: 10.1523/jneurosci.4140-09.2010

Siino, V., Amato, A., Di Salvo, F., Caldara, G. F., Filogamo, M., James, P., et al. (2018). Impact of diet-induced obesity on the mouse brain phosphoproteome. *J. Nutr. Biochem.* 58, 102–109. doi: 10.1016/j.jnutbio.2018.04.015

Taylor, D. R., and Hooper, N. M. (2007). Role of lipid rafts in the processing of the pathogenic prion and Alzheimer's amyloid-beta proteins. *Semin. Cell Dev. Biol.* 18, 638–648. doi: 10.1016/j.semcdb.2007.07.008

Vidal-Piñeiro, D., Sørensen, Ø, Blennow, K., Capogna, E., Halaas, N. B., Idland, A. V., et al. (2022). Relationship between cerebrospinal fluid neurodegeneration biomarkers and temporal brain atrophy in cognitively healthy older adults. *Neurobiol. Aging* 116, 80–91. doi: 10.1016/j.neurobiolaging.2022.04.010

Weiner, M. W., Aisen, P. S., Jack, C. R. Jr., Jagust, W. J., Trojanowski, J. Q., Shaw, L., et al. (2010). The Alzheimer's disease neuroimaging initiative: Progress report and future plans. *Alzheimers Dement.* 6, 202–211.e207. doi: 10.1016/j.jalz.2010.03.007

Weiner, M. W., Veitch, D. P., Aisen, P. S., Beckett, L. A., Cairns, N. J., Green, R. C., et al. (2012). The Alzheimer's disease neuroimaging initiative: A review of papers published since its inception. *Alzheimers Dement.* 8(Suppl. 1), S1–S68. doi: 10.1016/j.jalz.2011.09.172

Yabuki, Y., Matsuo, K., Kawahata, I., Fukui, N., Mizobata, T., Kawata, Y., et al. (2020). Fatty acid binding protein 3 enhances the spreading and toxicity of α-synuclein in mouse brain. *Int. J. Mol. Sci.* 21:2230. doi: 10.3390/ijms21062230

Yamamoto, Y., Kida, H., Kagawa, Y., Yasumoto, Y., Miyazaki, H., Islam, A., et al. (2018). FABP3 in the anterior cingulate cortex modulates the methylation status of the glutamic acid decarboxylase(67) promoter region. *J. Neurosci.* 38, 10411–10423. doi: 10.1523/jneurosci.1285-18.2018

frontiers | Frontiers in Aging Neuroscience

TYPE Original Research
PUBLISHED 14 October 2022
DOI 10.3389/fnagi.2022.1032917



OPEN ACCESS

EDITED BY
Yuzhen Xu,
Tongji University, China

REVIEWED BY
Jian Su,
Nanjing University of Information Science and Technology, China
Catherine Backman,
University of British Columbia, Canada
Alex Liu,
Michigan State University,
United States

*CORRESPONDENCE
Haichun Ma
mahc@jlu.edu.cn
Min Cheng
chengmin4566@163.com

SPECIALTY SECTION
This article was submitted to Alzheimer's Disease and Related Dementias, a section of the journal Frontiers in Aging Neuroscience

RECEIVED 31 August 2022
ACCEPTED 26 September 2022
PUBLISHED 14 October 2022

CITATION
Zhang C, Dong N, Xu S, Ma H and Cheng M (2022) Identification of hub genes and construction of diagnostic nomogram model in schizophrenia. *Front. Aging Neurosci.* 14:1032917. doi: 10.3389/fnagi.2022.1032917



# Identification of hub genes and construction of diagnostic nomogram model in schizophrenia

Chi Zhang[1], Naifu Dong[1], Shihan Xu[2], Haichun Ma[1]* and Min Cheng[1]*

[1]Department of Anesthesiology, The First Hospital of Jilin University, Changchun, China, [2]College of Basic Medical Sciences, Jilin University, Changchun, China

Schizophrenia (SCZ), which is characterized by debilitating neuropsychiatric disorders with significant cognitive impairment, remains an etiological and therapeutic challenge. Using transcriptomic profile analysis, disease-related biomarkers linked with SCZ have been identified, and clinical outcomes can also be predicted. This study aimed to discover diagnostic hub genes and investigate their possible involvement in SCZ immunopathology. The Gene Expression Omnibus (GEO) database was utilized to get SCZ Gene expression data. Differentially expressed genes (DEGs) were identified and enriched by Gene Ontology (GO), Kyoto Encyclopedia of Genes and Genomes (KEGG), and disease ontology (DO) analysis. The related gene modules were then examined using integrated weighted gene co-expression network analysis. Single-sample gene set enrichment (GSEA) was exploited to detect immune infiltration. SVM-REF, random forest, and least absolute shrinkage and selection operator (LASSO) algorithms were used to identify hub genes. A diagnostic model of nomogram was constructed for SCZ prediction based on the hub genes. The clinical utility of nomogram prediction was evaluated, and the diagnostic utility of hub genes was validated. mRNA levels of the candidate genes in SCZ rat model were determined. Finally, 24 DEGs were discovered, the majority of which were enriched in biological pathways and activities. Four hub genes (NEUROD6, NMU, PVALB, and NECAB1) were identified. A difference in immune infiltration was identified between SCZ and normal groups, and immune cells were shown to potentially interact with hub genes. The hub gene model for the two datasets was verified, showing good discrimination of the nomogram. Calibration curves demonstrated valid concordance between predicted and practical probabilities, and the nomogram was verified to be clinically useful. According to our research, NEUROD6, NMU, PVALB, and NECAB1 are prospective biomarkers in SCZ and that a reliable nomogram based on hub genes could be helpful for SCZ risk prediction.

KEYWORDS

**schizophrenia, biomarker, neuroimmune, diagnosis, nomogram, drug prediction**

# Introduction

Schizophrenia (SCZ) is a multifaceted mental illness with a broad variety of clinical and physiological manifestations; this disorder affects 20 million people and ranks among the top 25 leading causes of disability worldwide (Roy, 1986; GBD 2019 Diseases and Injuries Collaborators, 2020). SCZ is related with an approximately 15-year reduction in life expectancy in comparison to the gross population and a 5–10 percent lifetime risk of suicide. The low quality of life caused by cognitive impairment and mortality risks make SCZ a severe public health burden (Cloutier et al., 2016; Avramopoulos, 2018; Wahbeh and Avramopoulos, 2021). Despite the abundance of literature of SCZ manifestations, its exact etiology and pathogenesis are poorly known. Therefore, research on the pathogenesis and genetic mechanisms of SCZ is crucial.

The whole-transcriptome gene expression profiling study has been extensively utilized to discover SCZ-associated genes, identify disease-associated biomarkers, and anticipate treatment benefit. FOS was found to be a biomarker related to central and peripheral changes in SCZ (Huang et al., 2019), with NFKBIA, CDKN1A, BTG2, and GADD45B being recognized as core SCZ genes (Feng et al., 2022). Autophagy-related competing endogenous RNAs have been found to exhibit diagnostic efficacy in SCZ (Li R. et al., 2021). Moreover, S100B is regarded as a marker of nervous system impairment, and elevated levels have been seen in individuals with SCZ at illness onset as well as in drug-naive patients (Langeh et al., 2021). Several additional immunological indicators in microglia cells, such as cyclooxygenase-2 (COX-2) and prostaglandin E2 (PGE2), have been proposed as possible new therapeutic targets for SCZ treatment (Najjar et al., 2013). However, due to a lack of objective diagnostic methods, definitive assessment and therapy selection for SCZ remain problematic. To increase the efficacy of treatment methods, it is critical to develop innovative biomarkers that are strongly connected with SCZ.

Our research intended to investigate gene expression alterations in the pathophysiology of SCZ and to develop new possible diagnostic biomarkers. In this work, we scrutinized two Gene Expression Omnibus (GEO) datasets and sorted out 24 differentially expressed genes (DEGs) from prefrontal cortex (PFC) samples. The essential modules associated with SCZ were identified and four hub genes, NEUROD6, NMU, PVALB, and NECAB1, were sorted using the support vector machine–recursive feature elimination (SVM-RFE), random forest (RF), and least absolute shrinkage and selection operator (LASSO) algorithms. Then, utilizing hub genes, we developed and validated a predictive nomogram for clinical SCZ diagnosis. The diagnostic values of the four hub genes and the nomogram model were validated with good accuracy per receiver operating characteristics (ROC) curves. The selected four hub genes and nomogram could help improve SCZ diagnosis in high-risk patients, thereby helping to elucidate the neuropsychiatric etiology of SCZ.

# Materials and methods

## Data processing

GSE21138[1] and GSE53987[2] [GPL570 platform (HG-U133_Plus_2) Affymetrix Human Genome U133 Plus 2.0] were obtained from the GEO database. We collected datasets including PFC samples, of which GSE21138 contained 29 normal and 30 SCZ samples and GSE53987 contained 19 normal and 15 SCZ samples. Then, the R packages limma and sva were applied for profiles combination and the normalization. Probes not matching any known gene were eliminated. If more than one probe matched to a gene, the average expression was aggregated. The Perl programming language was used to remove lncRNA profiles and identify mRNA matrix files. The R package ggplot2 was used to normalize data after processing. Information of datasets is listed in **Supplementary Table 1**. The study's flow diagram is shown in **Figure 1**.

## Differentially expressed genes identification

To find DEGs between SCZ and healthy samples, the limma R package was employed. The cutoff criteria were adjusted $P < 0.05$ and $|\log \text{fold change (FC)}| > 0.5$. Using the ggplots package, the heatmap and volcano diagram were generated.

## Enrichment analysis

To determine the biological implications of genes and functions, DEGs were subjected to GO, Kyoto Encyclopedia of Genes and Genomes (KEGG), and DO analyses using clusterProfiler and DOSE package. A *P*-value of less than 0.05 was set as the cutoff criterion.

## Gene set enrichment

GSEA is a computer tool to determine the accordance of a highly enriched gene set. The reference gene set, "c2.cp.kegg.v6.2. symbols.gmt," was downloaded from the

1 https://www.ncbi.nlm.nih.gov/geo/query/acc.cgi?acc=gse21138
2 https://www.ncbi.nlm.nih.gov/geo/query/acc.cgi?acc=gse53987

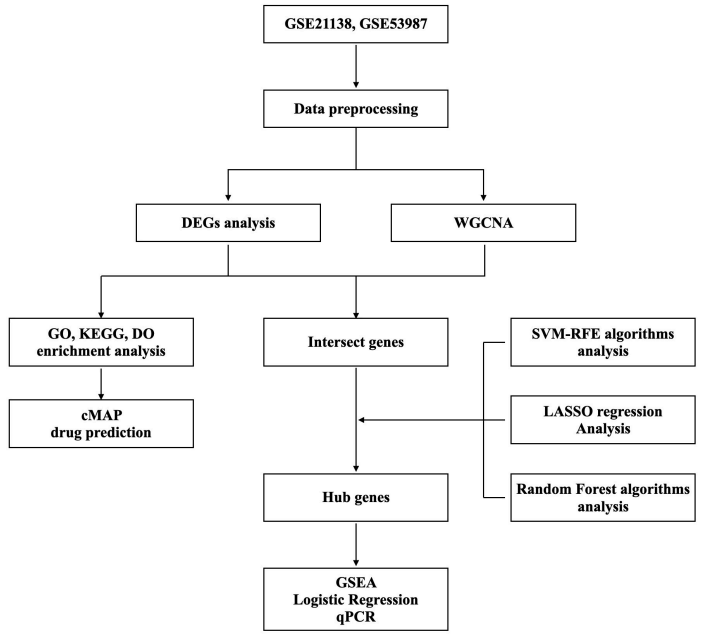


FIGURE 1
Study workflow.

Molecular Signature Database (MSigDB). Enrichment sets comprising fewer than 10 or more than 200 genes were omitted. The upregulated pathways had a normalized enrichment score (NES) greater than zero, whereas the downregulated pathways had a NES less than zero. Five of the most essential pathways were determined (FDR $< 0.05$).

## Weighted gene co-expression network analysis

We combined and batch-processed the data from GSE21138 and GSE53987. Weighted gene co-expression network analysis (WGCNA) package was used to assess the trait-related modules. A topological overlap matrix was constructed from the expression profile. The soft-thresholding power of 5 and minimum module size of 30 were set to screen core modules. A height limit of 0.25 was used as a guideline for modules combination. The modules were then tested using Pearson's correlation test at a significance threshold of $P$ 0.05.

## Support vector machine, random forest, and least absolute shrinkage and selection operator model construction

First, candidate genes were found by crossing DEGs with genes of WGCNA hub module. Next, hub genes were classified by overlapping genes from the SVM-RFE method with the e1071 package (Noble, 2006), the RF algorithm with the randomForest R package (Paul et al., 2018), and the LASSO algorithm with glmnet package (Vasquez et al., 2016).

## Single sample gene set enrichment analysis

Single sample gene set enrichment analysis (ssGSEA), using the GSVA package, was performed to compare the infiltration of 28 immune cells within normal and SCZ samples (Hänzelmann et al., 2013). We identified 28 immunocytes: immature dendritic cells, type 1 T helper cells, activated CD4 + T cells, T follicular helper cells, activated dendritic cells, CD56 dim NK cells, central memory CD4 + T cells, effector memory CD4 + T cells, eosinophils, gamma delta T cells, activated CD8 + T cells, CD56 bright natural killer (NK) cells, mast cells, myeloid-derived suppressor cells, B cells, effector memory CD8 + T cells, monocytes, natural killer cells, natural killer T cells, macrophages, neutrophils, plasmacytoid dendritic cells, regulatory T cells, central memory CD8 + T cells, immature B cells, type 17 T helper cells, and type 2 T helper cells, memory B cells.

## Nomogram model construction

To forecast the incidence of SCZ, rms package was applied to develop the diagnostic nomogram model. "Points"

denotes scores of the corresponding factor. Following that, the nomogram model's predictive ability was evaluated using a calibration curve (Chen et al., 2019). Finally, the practical applicability of the model was assessed using decision curve analysis (DCA) (Vickers and Elkin, 2006). We used the pROC package (Wolbers et al., 2009) to conduct ROC curve and the diagnostic capacities of hub genes and the nomogram model were examined using the area under the curve (AUC).

## qRT-PCR validation

SCZ models were obtained from rats injected intraperitoneally with saline or MK801 (Sigma-Aldrich, St.) (0.5 mg/kg body weight) for 6 days continuously. Total RNA from the rat PFCs was extracted with TRIzol reagent (Takara, Shiga, Japan). 500 ng mRNA in total was transcribed reversely using a Prime-Script RT reagent Kit (Takara), and qRT-PCR was performed at a final volume of 20 μL. Thermal settings were 95°C for 30 s, 40 cycles of 95°C for 10 s, and 60°C for 30 s. Hub gene expression was determined using the $2^{-\Delta\Delta CT}$ methodology. Primers information is shown in **Table 1**.

## Connectivity map analysis

The online platform Connectivity Map (CMap)[3] was used to measure the connectivity between illnesses gene expression features and compound-induced gene signatures to better comprehend drug mechanisms and uncover novel therapeutic compounds. Thus, DEGs were uploaded to the CMap database to anticipate the possible therapeutic small-molecule medicines on SCZ.

3 https://clue.io/

**TABLE 1** Primer sequences used in this study.

| | |
|---|---|
| Primers | NEUROD6 |
| Forward | TCTAGAGGCTCCAGGAGAC |
| Reverse | GACTCGTCAAACGGTAGTG |
| Primers | NMU |
| Forward | CAAAGTGAATGAATACCAGGGTC |
| Reverse | GTTGACCTCTTCCCATTGC |
| Primers | PVALB |
| Forward | GCTAAGGAAACAAAGACGCT |
| Reverse | CAGAGTGGAGAATTCTTCAACC |
| Primers | NECAB1 |
| Forward | AACTCCTCAGAAGAGCTCAG |
| Reverse | GTCTGCTCTCCTCAGTATGTC |
| Primers | GAPDH |
| Forward | AACTCCCATTCTTCCACCT |
| Reverse | TTGTCATACCAGGAAATGAGC |

## Statistical analysis

R software (version 4.1.3) was used for data examination. The Wilcoxon test was performed for groups comparation, and $P < 0.05$ was defined as a significant difference.

# Results

## Differentially expressed genes identification in schizophrenia and healthy control groups

In this study, two microarray datasets (GSE21138 and GSE53987) were used to analyze differential expression. The expression matrix before and after normalization is shown in **Supplementary Figure 1**. In the integrated expression matrix, there were 24 DEGs revealed, with 10 upregulated and 14 downregulated, as shown in **Figures 2A,B**. The protein–protein interactions of the DEGs are shown in **Supplementary Figure 2**.

## Functional analysis

GO analysis revealed 232 biological processes (BP), 29 cellular components (CC), and 28 molecular functions (MF), as shown in **Supplementary Table 2**. **Figure 3A** lists the top 10 GO items. DEGs were significantly enriched in neuropeptide pathways, adult behavior, aging, pallium development, axon terminals, neuron projection terminals, and receptor-ligand activity. According to KEGG analysis, DEGs were enriched in neurofunctional ligand-receptor interactions, as shown in **Figure 3B**. DO analysis revealed 54 items, as shown in **Supplementary Table 3**. **Figure 3C** shows the top ten items revealed by each functional and enrichment analysis. GSEA as shown in **Supplementary Table 4** demonstrated the genes upregulated were primarily enriched in the Notch and TGF-beta signaling pathway, as shown in **Figures 4A,B**; downregulated genes were enriched in neurofunctional processes, as shown in **Figure 4A**, including GABAergic synapses, serotonergic synapses, circadian entrainment, synaptic vesicle cycle, morphine addiction, and dopaminergic synapses. **Figure 4C** shows the top five items.

## Overlap between schizophrenia-related module genes with differentially expressed genes

A scale-free network with a soft threshold of 5 ($R^2 = 0.91$) was built, as shown in **Figure 5A** and **Supplementary Figure 3**. Subsequently, we computed module eigengenes, which indicate

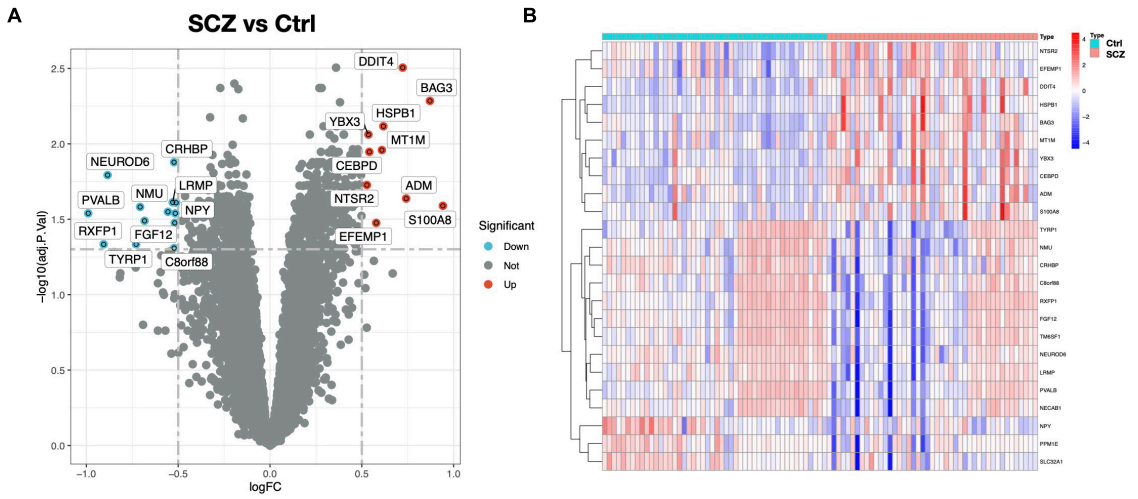


FIGURE 2
DEG screening between SCZ and healthy control. **(A)** Volcano graphic visualizing DEGs of SCZ and normal samples. **(B)** Heatmap of DEGs among normal and SCZ samples.

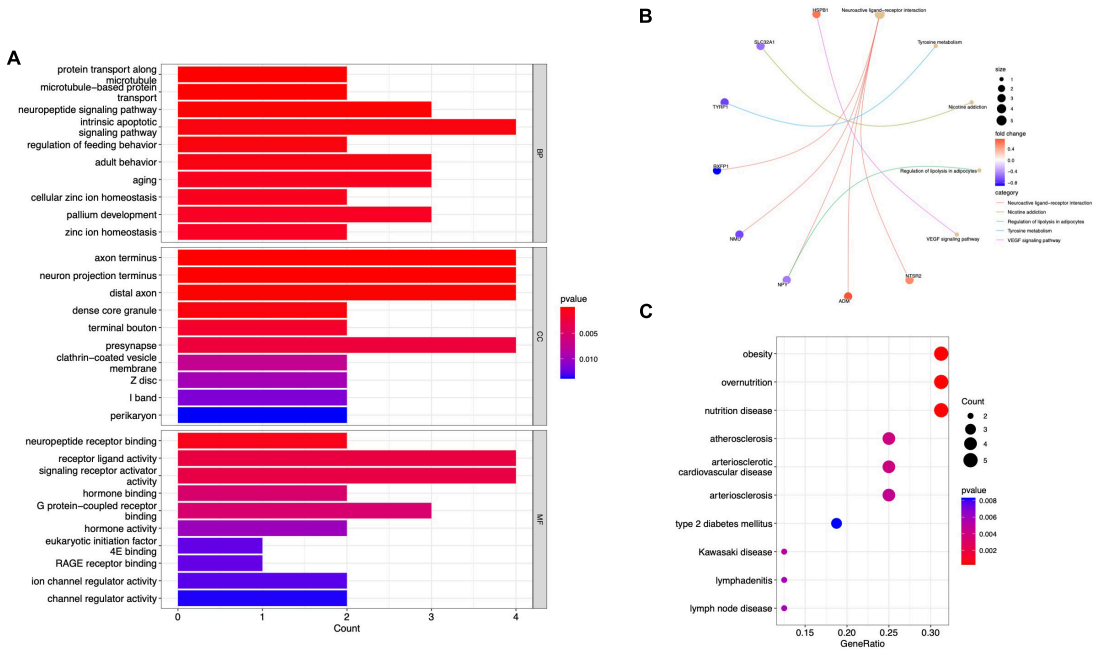


FIGURE 3
Functional DEG enrichment. **(A)** GO analysis. **(B)** KEGG pathway analysis. **(C)** DO analysis.

the total gene expression level of each module and were grouped based on their association. Three modules were identified, as shown in Figure 5B. Only one module was correlated with SCZ (turquoise; cor = -0.27, $P$ = 0.01). The 64 genes related with SCZ identified in this module were maintained for future investigation, as shown in Figures 5C,D. Finally, eight genes were determined to overlap between DEGs and the selected Genes in MEturquoise and are also shown in Figure 5E.

## Hub gene identification

To discover gene signatures, the eight candidate genes were submitted into SVM-RFE, RF, and LASSO. We identified an eight-gene signature using SVM with a precision of 0.711, as shown in Figures 6A,B. The random forest method sorted eight genes with importance scores greater than four, as shown in Figures 6C,D. LASSO regression analyses identified

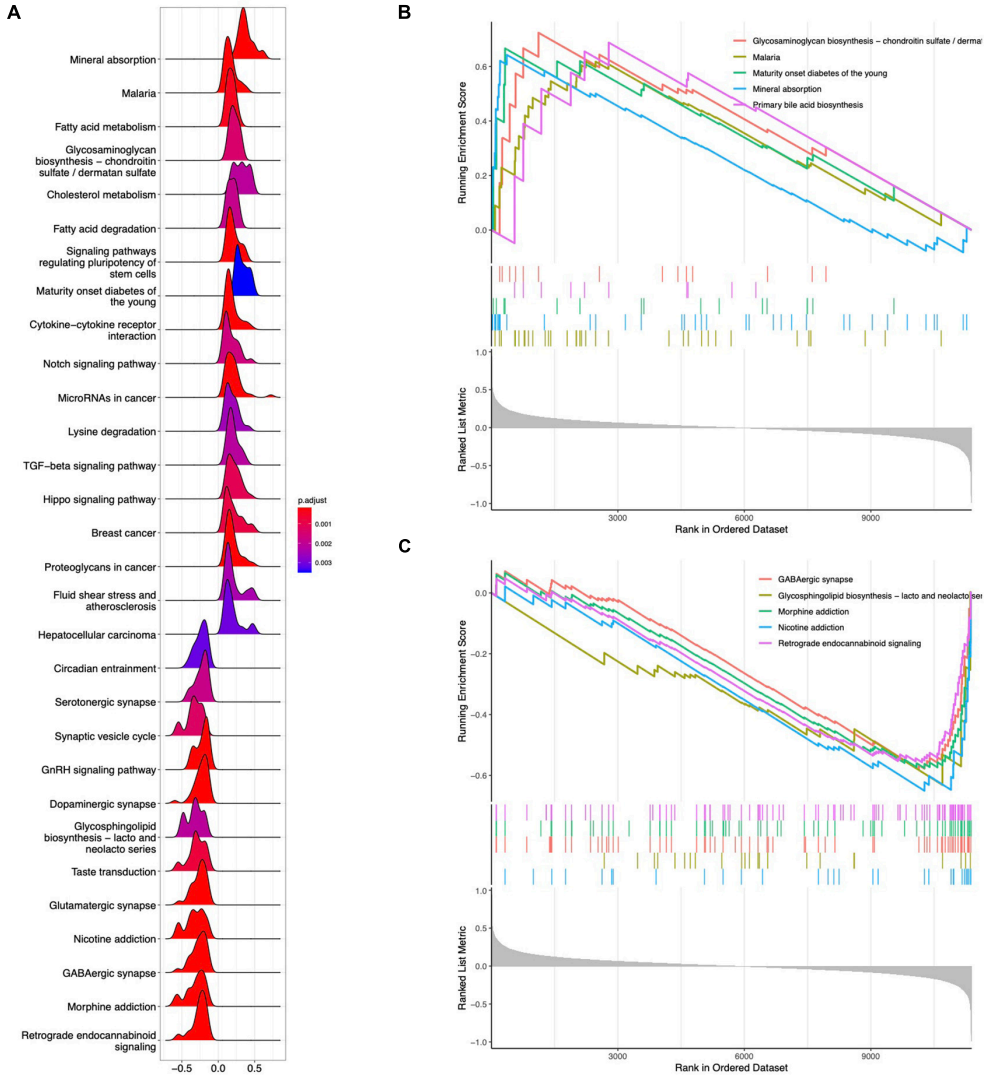


FIGURE 4
GSEA analysis for DEGs. **(A)** Ridgeline plot of GSEA analysis results. **(B)** Top five enrichment terms for upregulated DEGs. **(C)** Top five enrichment terms for downregulated DEGs.

four gene signatures, as shown in Figures 6E,F. To obtain a robust gene signature for SCZ, we determined which genes overlapped from the three methods and obtained four hub genes: NEUROD6, NMU, PVALB, and NECAB1, as shown in Figure 6G. NEUROD6, NMU, PVALB, and NECAB1 were significantly decreased in SC samples compared to control, as shown in Figures 7A,B. Correlation analysis showed that the four genes had robust positive correlations with each other, as shown in Figure 7C.

## Gene set enrichment of the hub genes

To further uncover the probable roles of NEUROD6, NMU, PVALB, and NECAB1, we conducted GSEA. Genes in the low expression categories of the four hub genes were significantly enriched in allograft rejection, autoimmune thyroid disease, graft vs. host disease, antifolate resistance, and glycosaminoglycan biosynthesis, as shown in Figure 8.

## Correlation of hub genes and immunocyte infiltration

We investigated the pattern of immunocytes infiltration using ssGSEA and found that the abundance of CD56 bright NK cells, gamma delta T cells, mast cells, follicular T helper cells, and central memory CD8 + T cells were much greater in SCZ samples than in normal samples, whereas the regulatory T cells and effector memory CD8 + T cells was significantly

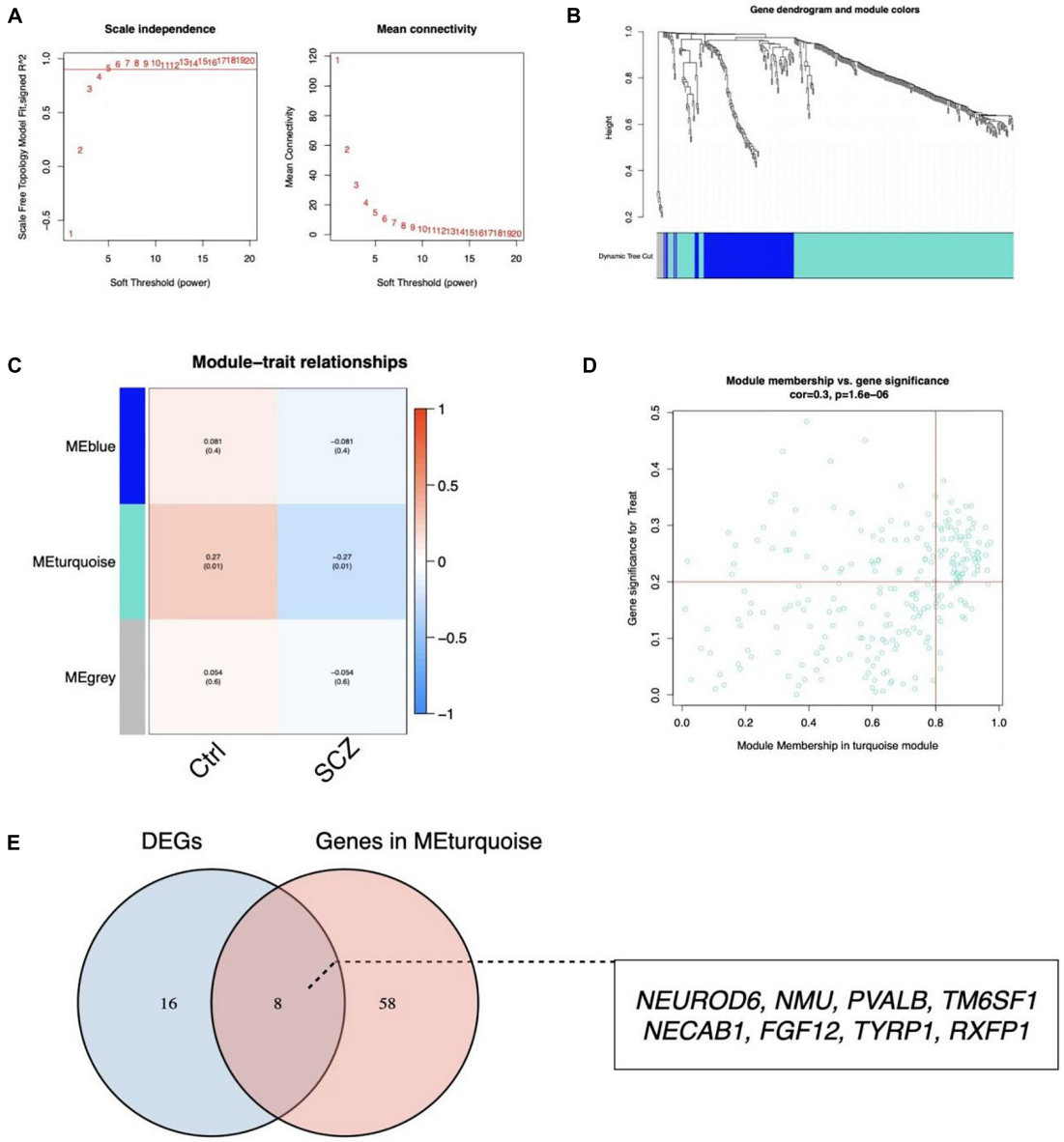


FIGURE 5
Identification of critical modules by WGCNA. **(A)** Scale-free fit index and mean connectivity for different soft-thresholding powers. **(B)** Topological overlap dissimilarity aggregation of DEGs clusters. **(C)** Module-feature correlations Each row represents a module list, whereas each column represents a clinical characteristic. The first line of each cell includes the associated correlation, while the second line gives the *P*-value. **(D)** Scatter plot of the turquoise module. **(E)** Venn diagram for overlapped genes.

reduced, as shown in Figure 9A and Supplementary Figure 4. Furthermore, we calculated the correlation between hub gene expression and infiltrating immune cells, and the results showed that most immunocytes had a significant negative connection with hub genes, as shown in Figure 9B. These results imply that the inflammatory components may play an essential role in the development of SCZ, and hub genes may have a novel regulatory role in immune function.

## Diagnostic model construction

A nomogram model for SCZ diagnosis was established based on NEUROD6, NMU, PVALB, and NECAB1, as shown in Figure 10A. The calibration curve indicated that the variance between observed and predicted risk was limited, indicating that the nomogram model performed very well in predicting SCZ, as shown in Figure 10B. At the risk threshold of 0.1–1.0, DCA showed that the hub genes curve was above the gray line and

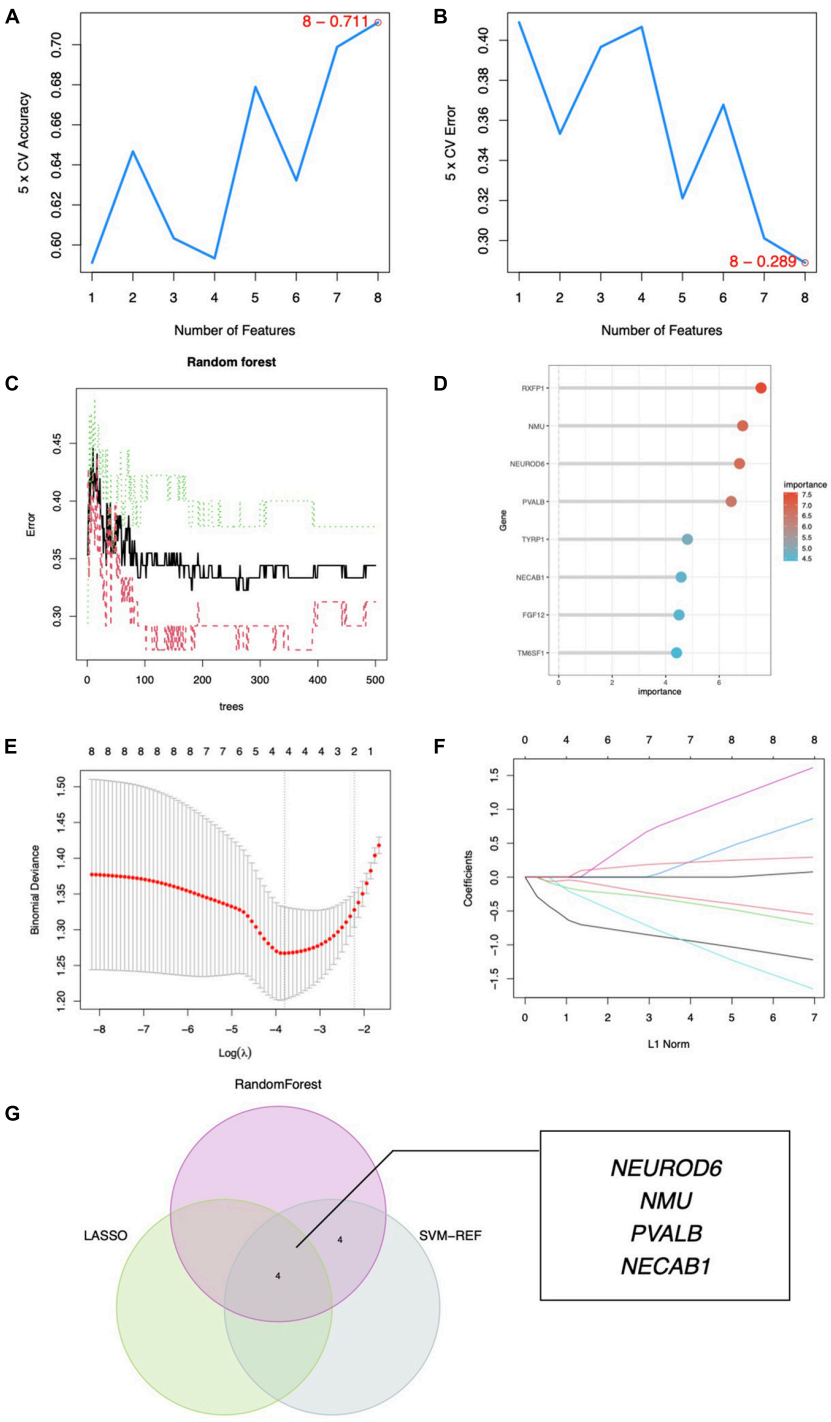


FIGURE 6
Hub gene identification. **(A)** Eight gene signatures were identified by SVM-RFE analysis with an accuracy of 0.711. **(B)** Error of 0.289. **(C)** Prediction accuracy of the RF model. **(D)** Gene importance scores of RF model. **(E)** Cross-validation to select the optimal tuning parameter log (Lambda) in LASSO regression analysis. **(F)** LASSO coefficient profiles of candidate genes. **(G)** Venn diagram of four hub genes shared by the SVM-RFE, RF, and LASSO algorithms.

indicated a significant net benefit from using nomograms to forecast SCZ risk, as shown in Figure 10C. The AUC of the nomogram reached at 0.724, and the 95% confidence interval (CI) ranged from 0.622 to 0.827, as shown in Figure 10D. High-accuracy risk prediction of the diagnostic nomogram for SCZ was observed.

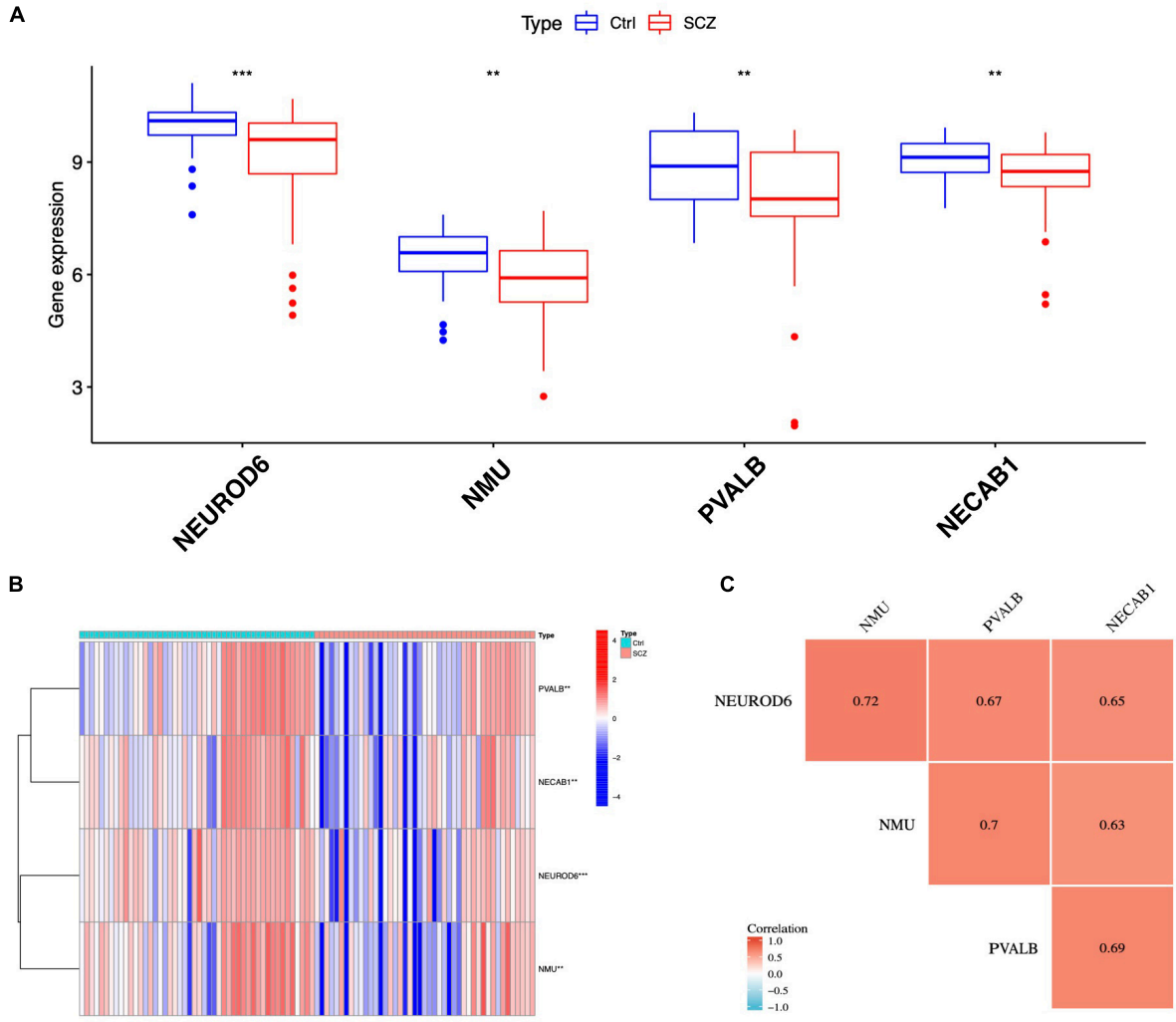


FIGURE 7
Expression analysis of hub genes. **(A)** Expression of four hub genes in SCZ and control groups. **(B)** Heatmap of hub gene expression. **(C)** Correlation between hub genes. $^{**}P < 0.01$, $^{***}P < 0.001$ vs. Ctrl.

## Diagnostic evaluation of hub genes

We further evaluated the diagnostic values of the four hub genes (NEUROD6, NMU, PVALB, and NECAB1) and nomogram model scores in GSE21138 and GSE53987 using ROC curves. The AUC values of hub genes in SCZ and healthy samples measured in GSE21138 were NEUROD6:0.731 (95% CI, 0.600–0.862), NMU: 0.737 (95% CI, 0.602–0.871), PVALB: 0.739 (95% CI, 0.613–0.865), and NECAB1:0.668 (95% CI, 0.526–0.810). The AUC of the nomogram model score was 0.813 (95% CI, 0.702–0.923), as shown in Figure 11A. In GSE53987, the AUC of hub genes were NEUROD6: 0.867 (95% CI, 0.739–0.995), NMU: 0.758 (95% CI, 0.572–0.994), PVALB: 0.877 (95% CI, 0.764–0.990), and NECAB1: 0.723 (95% CI, 0.535–0.911). The AUC of the nomogram model score was 0.937 (95% CI, 0.863–1.000), as shown in Figure 11B. These results indicate that the four hub genes may have significant diagnostic value for SCZ. The AUC of the nomogram model based on the four hub genes was larger than that of a single hub gene, suggesting that when hub genes were regarded together, the diagnostic value was greater, which is more conducive to clinical SCZ prediction.

## Hub gene validation

The experimental design was approved by the Animal Ethics Committee of the First Hospital of Jilin University (NO: 20210637). NEURO6, NMU, and NECAB1 were downregulated in the MK801-induced SCZ rat model compared to the control. Nevertheless, no significant changes were observed in PVALB expression, as shown in Figure 12.

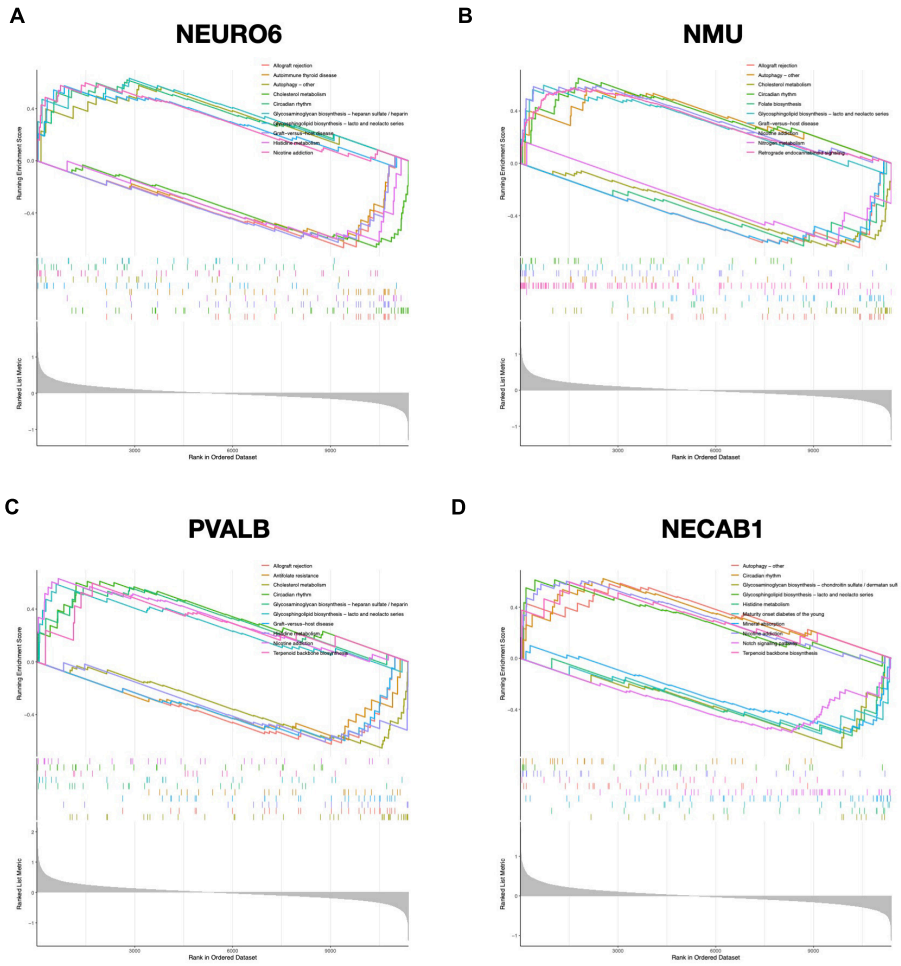


FIGURE 8
GSEA analysis of hub genes. Top 5 GSEA enrichment in the high and low expression gene set of **(A)** NEURO6, **(B)** NMU, **(C)** PVALB, and **(D)** NECAB1.

## Drug prediction for schizophrenia treatment

Differentially expressed mRNAs in SCZ were submitted to the CMap database to predict prospective small-molecule compounds with SCZ therapeutic potential. Drugs exhibiting negative correlations have the potential to improve SCZ symptoms. The top ten small molecular drugs (all connectivity scores > 0.7) are shown in **Figure 13**. Among these, LE-300 is a dopamine receptor antagonist, WAY-161503 is a serotonin receptor agonist, and endo-IWR-1 is an inhibitor of the Wnt/-catenin signaling pathway.

# Discussion

SCZ is a psychiatric disorder with high global prevalence and a multifactorial biological etiology. The mechanics of SCZ are yet to be completely understood. Clinical manifestations of SCZ include hallucinations, disordered emotions, and social isolation caused by disruptions of the immunological, metabolic, and endocrine systems (McCutcheon et al., 2020). Owing to the likelihood of developing disability and rising prevalence, SCZ not only significantly impacts patient health but also has major public health implications (Carpenter and Buchanan, 1994). Therefore, understanding the critical pathways and gene signatures in SCZ could aid in the assessment of risk evaluation, pathogenesis, and personalized therapy.

In this work, we conducted a comprehensive examination of SCZ using PFC samples, which was revealed as a hub region correlated with SCZ. Impaired cognitive functions and aberrant behaviors have been consistently implicated in patients with SCZ with decreased PFC volumes (Tomasik et al., 2016). Despite the complexity of PFC functional regions, the connectivity between the basal ganglia, inferior frontal gyrus, hippocampus,

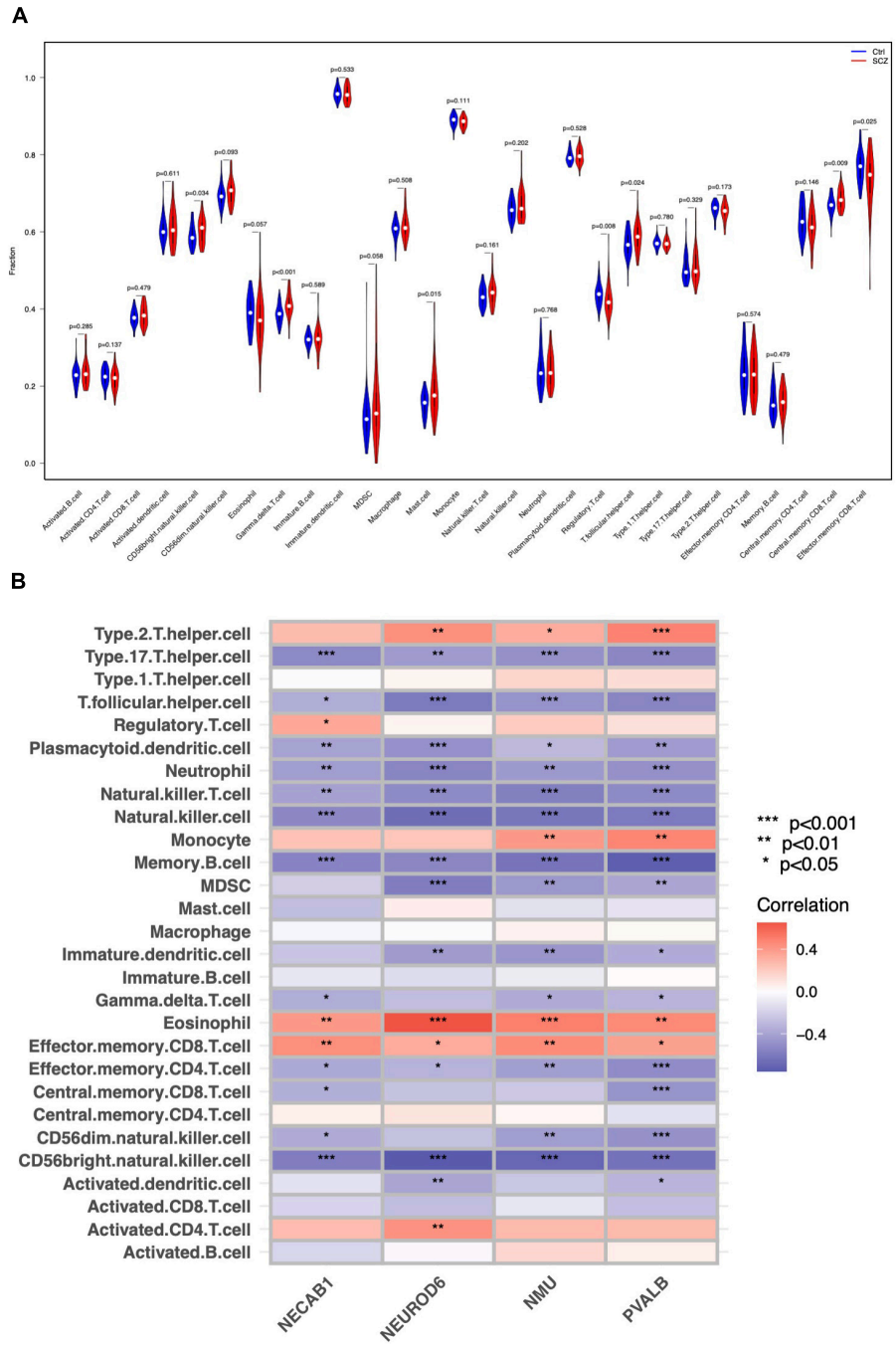


FIGURE 9
Immune cell distribution in SCZ. **(A)** Differences in infiltrated immune cells between SCZ and control groups. **(B)** Correlation analysis between hub genes and immune cells.

lateral habenular, and other brain atlases is characterized by extremely complex anatomical networks and variability in behavior and activation (Zhou et al., 2015; Brady et al., 2019; Mathis et al., 2021). However, both hypo- and hyperfrontality have been hypothesized as valid and informative reflections of PFC dysfunction in SCZ. The basis of this dysfunction and its exact contributions remain unclear (Manoach, 2003). These variables may also impact the co-prevalence of certain autoimmune illnesses and some instances of SCZ (Tomasik et al., 2016).

Cells of the immune system and the central nervous system can interact. The immune system responds to infection,

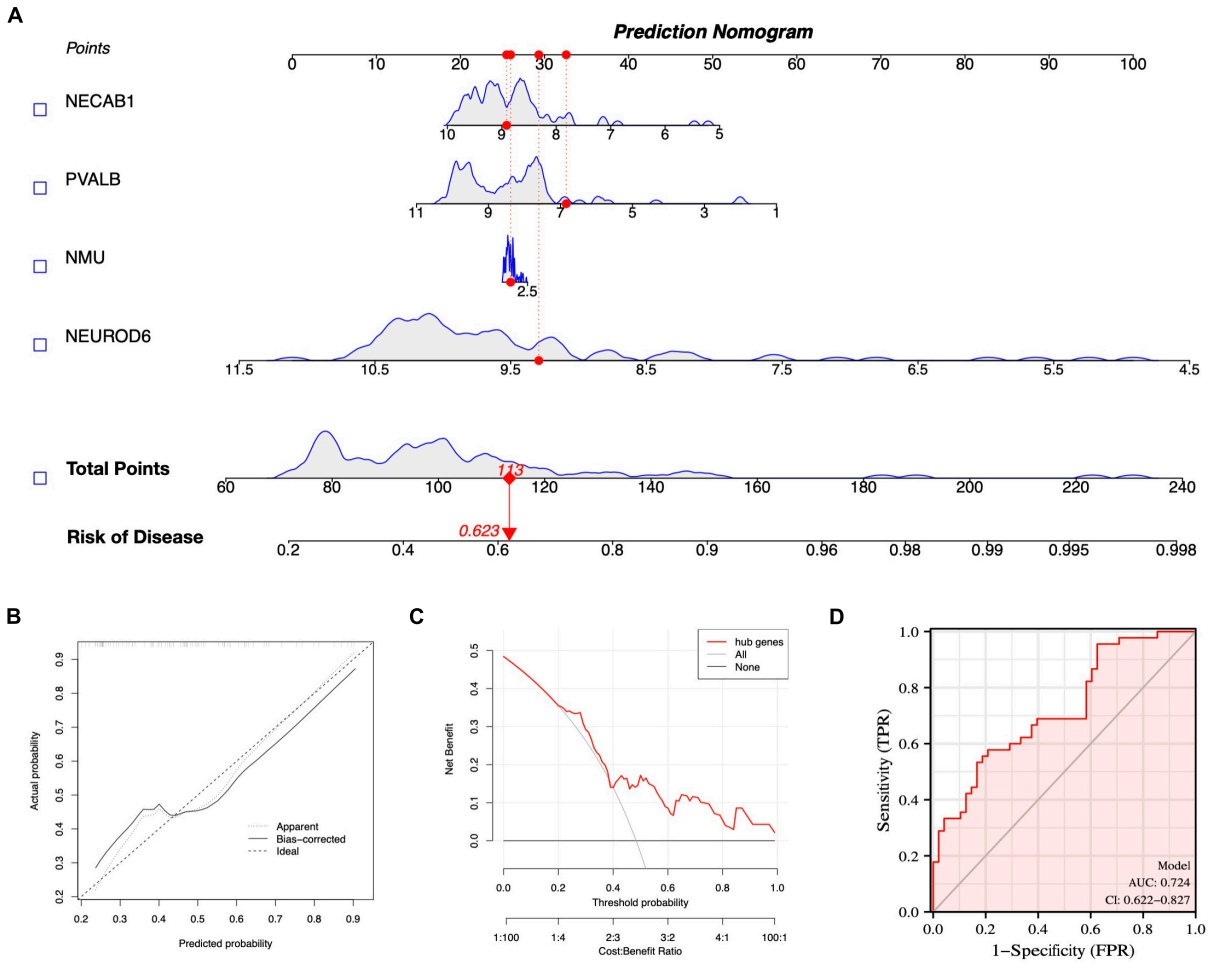


FIGURE 10
Nomogram model construction for SCZ diagnosis. **(A)** Nomogram to predict SCZ risk. **(B)** Calibration curve evaluation for the diagnostic potential of the nomogram model. **(C)** DCA curve to assess the nomogram practical efficacy. **(D)** ROC curve to evaluate prediction accuracy.

tissue damage and trauma by releasing substances that trigger an inflammatory response. Inflammatory cytokines released by the immune system are considered to be a key feature of neurological pathology, such as chronic pain, neurodegenerative diseases, spinal cord injuries, and neuropsychiatric disorders, particularly SCZ (Skaper et al., 2014). Immune infiltration impairment was found in the SCZ PFC, which is consistent with previous findings (Maas et al., 2017). A higher CD56 bright NK cells proportion has been observed in SCZ patients, with activation to secrete TNF-α and IFN-γ, which causes damage to the central nervous system (Miller et al., 2013). Mast cell infiltration may also affect cognitive performance (Skaper et al., 2014). Increased gamma/delta T lymphocytes in unmedicated patients with SCZ impair the blood–brain barrier (Wo et al., 2020). Abundant increases in any of these cell types of influence SCZ pathology. Moreover, the number of regulatory T cells (Treg) was found to decrease in SCZ samples. Inflammatory disorders and SCZ have been linked throughout the recent decades. Immunological-mediated neuropathology is a rising issue, and new research emphasizes the significance of innate immune signaling in SCZ (Hartwig et al., 2017; Yang and Tsai, 2017). Tregs may contribute to the improvement of negative symptoms in SCZ (Kelly et al., 2018). Elevated Tregs in SCZ are correlated with fewer negative symptoms, possibly by counteracting ongoing inflammatory processes (Corsi-Zuelli and Deakin, 2021). Recent studies have demonstrated regulatory connections between microglia, astrocytes, and Tregs. Treg cell dysfunction relates to glial damage, low-level inflammation, and reduced life expectancy in SCZ (Kelly et al., 2018; Corsi-Zuelli et al., 2021). Tregs are also capable of promoting oligodendrocyte differentiation and (re)myelination. Treg knockout mice had markedly reduced remyelination and oligodendrocyte differentiation, resulting in cognitive impairment (Dombrowski et al., 2017). Our study revealed the immune infiltration landscape of SCZ, which paved the

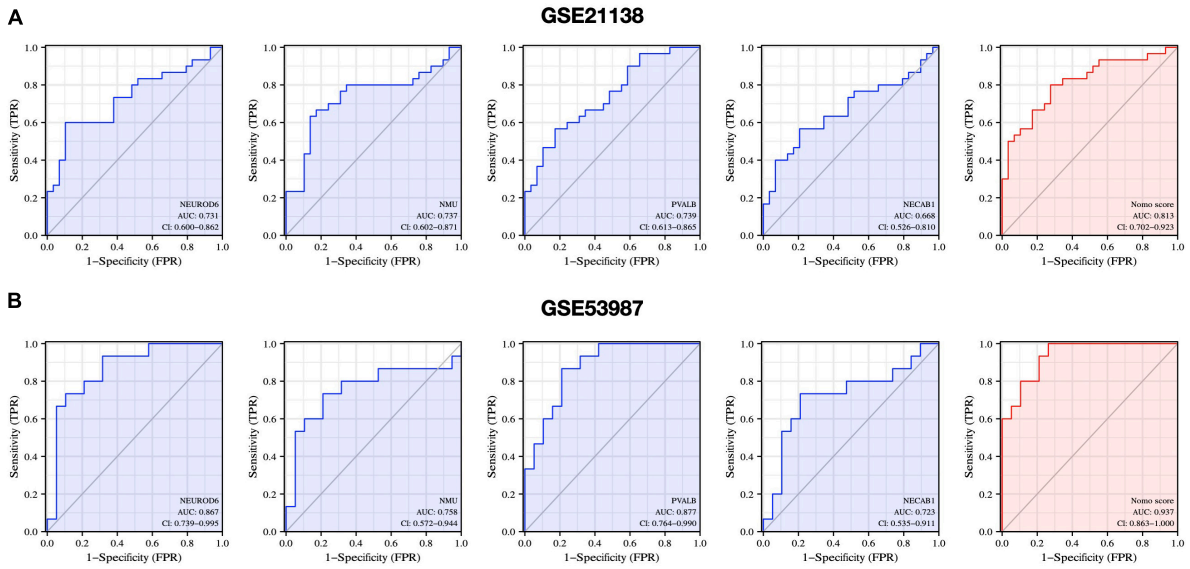


FIGURE 11
Diagnostic evaluation of hub genes and nomogram score. ROC curve to evaluate prediction accuracy in **(A)** GSE21138 and **(B)** GSE53987.

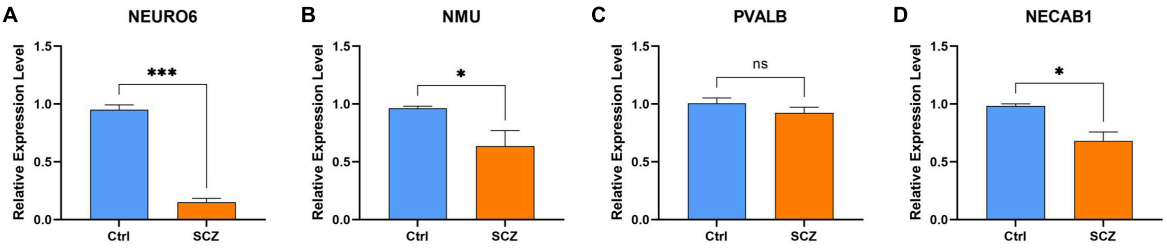


FIGURE 12
qPCR validation. Comparison of gene expression between SCZ rat model and control in **(A)** NEURO6, **(B)** NMU, **(C)** PVALB, and **(D)** NECAB1. $^{*}P < 0.05$, $^{***}P < 0.001$ vs. Ctrl.

way for designing immunotherapy for SCZ based on molecular alterations.

For decades, pathophysiological investigations on SCZ have concentrated on dopaminergic and glutamatergic neurotransmission abnormalities, with scant clinical advancements. Microarray data may now be utilized to uncover hub genes, interaction networks, and pathways that interpret SCZ, according to the tremendous progress of bioinformatics. In this study, DEGs were mainly enriched for neurofunctional activities. The CMap database predicted highly correlated molecular drugs (connectivity scores > 0.7) for SCZ treatment. Bumetanide is a selective antagonist of Na-K-Cl cotransporter (NKCC1) which can reduce intracellular chloride concentrations and enhances the inhibitory effect of GABAergic neurons, an FDA-approved drug with the potential to treat or prevent cognitive impairment in SCZ syndrome (Lemonnier et al., 2016). CCL2 levels are significantly higher in patients with SCZ, dysregulated CCL2 may be one of the important reasons for the negative symptoms of SCZ, and the duration of the disease is closely related to the negative symptoms (Hong et al., 2017). CCL2 inhibition by oral administration of bindarit may potentially improve symptoms of SCZ (Raghu et al., 2017). Rifaximin can reduce gut-derived inflammation, which may also contribute to the relief of SCZ (Li H. et al., 2021; Patel et al., 2022). The brain-gut axis refers to the two-way communication network between the brain and the gut. Different signals from the gastrointestinal tract can regulate brain function through neural, endocrine, immune, metabolic and other pathways (Lach et al., 2018). When the types of intestinal microbes change, the central nervous system will also change accordingly, which is mainly due to the change of metabolites of intestinal microbes (Erny et al., 2015). Although the reasons for this are not fully understood, altering the gut microbiome can improve mental activity, emotional and cognitive processes and behavior in animals (Zheng et al., 2016; Valles-Colomer et al., 2019). Further analyses are necessary to analyze the effect of these

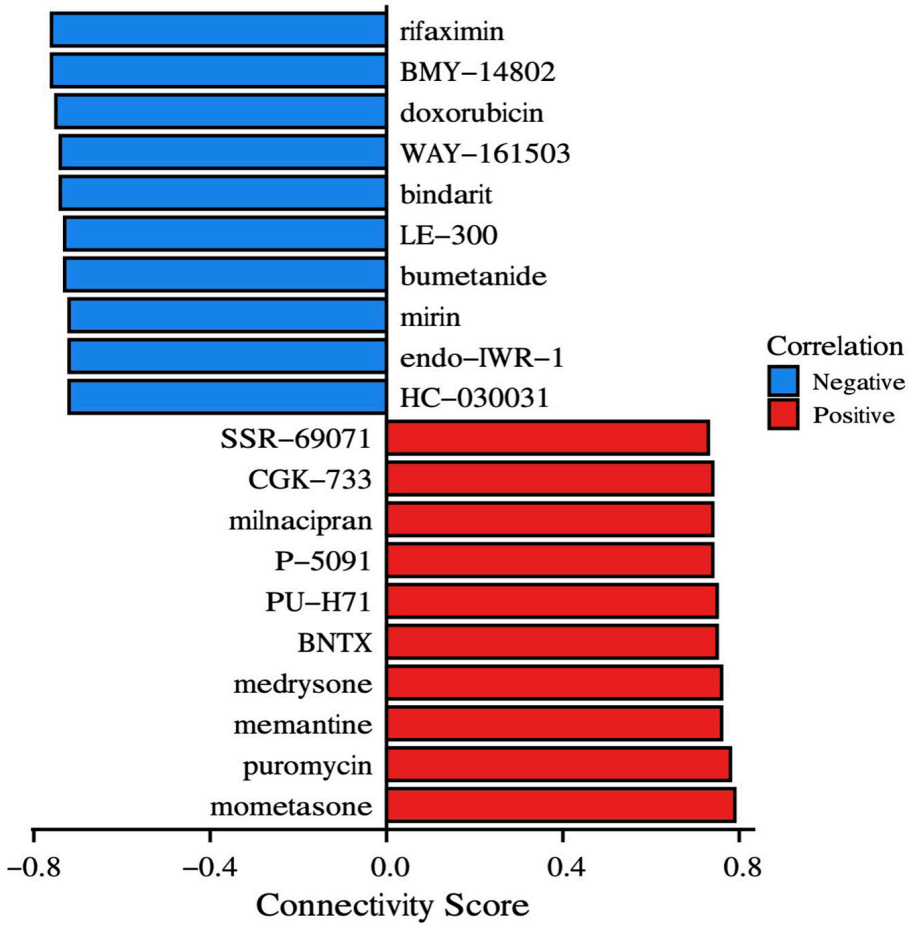


FIGURE 13
Drugs prediction. CMap instances organized by compounds and cell lines depict the most significant positive and negative correlations to the impact on SCZ. The connection score, shown on the x-axis, represents the strength of the association.

molecules on behavioral tests in animal models of SCZ and patients with SCZ.

Based on bioinformatics methods, this is the first study to find four hub genes closely related to SCZ (NEUROD6, NMU, PVALB, and NECAB1). Enrichment and immune infiltration analyses showed that these genes might lead to the onset of SCZ by regulating the genetic process of cells or affecting the immune environment. The NEUROD family (NEUROD1, 2, 4, 6) is a key regulator of neural progenitor cell differentiation (Tutukova et al., 2021). NEUROD6 plays a role in cytoskeletal protein function, mitochondrial trafficking, membrane potential regulation, and mitochondrial chaperoning (Cherry et al., 2011). NEUROD6 may also improve cellular resistance to oxidative stress, which is important in neurodegenerative illness prevention including Parkinson's disease and autism spectrum disorder (Viereckel et al., 2016). Recently, NEUROD6 was revealed as a potential biomarker for of Alzheimer's disease (AD) diagnosis. Alzheimer's animal models and postmortem Alzheimer's patients have both shown low levels of NEUROD6 expression (Satoh et al., 2014). Locomotion was dramatically increased in NEUROD6-KO mice with repeated psychostimulant administration, and optogenetic stimulation of NEUROD6-Cre VTA neurons was found to trigger glutamatergic postsynaptic currents as well as DA secretion in nucleus accumbens (Bimpisidis et al., 2019). Information processing is affected by γ-aminobutyric acid (GABA) neurons that produce parvalbumin, somatostatin, or vasoactive intestinal peptides (Fachim et al., 2018). Parvalbumin (PVALB) deficits or downregulation are common in patients with SCZ (Tsubomoto et al., 2019). PV-deficient (PV-/-) mice exhibit a strong autism-like behavioral phenotype. PVALB neurons exhibit precise control over spike timing, leading to the formation and regulation of gamma rhythms, which are necessary for sensory perception and awareness (Janickova et al., 2021). NMDA receptor hypofunction in pyramidal cells results in decreased activity of PVALB neurons, thus reducing network gamma oscillatory activity (Kaur et al., 2020). Neuromedin U (NMU) is widely distributed neuropeptide. NMU is involved in

physiological activities, including feeding behavior, metabolism, physiological stress, circadian rhythmicity, and inflammatory processes (Ly and Root, 2021; Sasaki-Hamada et al., 2021), as well as reward circuits (Anan et al., 2020). The ability of neuropeptides to reduce food intake in rodents prompted the modification of peptide ligands (Vallöf et al., 2020). NMU receptor activation promotes GABAergic neurons in the hippocampus (Ghashghayi et al., 2022). Recent research indicates that NMU may regulate psychomotor activity. NMU-21 elicits anxiolytic-like effects in the goldfish brain (Matsuda et al., 2020). As the major calcium-binding protein in CB1/CCK-positive interneurons, neuronal calcium-binding protein 1 (NECAB1) is found in several excitatory neuron populations in the rat spinal cord. The soma volume of pyramidal cells immunoreactive for NECAB1 is significantly reduced in SCZ (Maldonado-Avilés et al., 2006).

Correlation analysis found that the four hub genes were highly positively correlated with one another (all cor $>$ 0.6). Therefore, we suspect that they play a vital role in SCZ pathology. Furthermore, we established a nomogram model for SCZ risk prediction. The diagnosis and treatment of SCZ currently are mostly dependent on clinical surveys with inadequate response rates. Recurrence of symptoms is typical among people who cease treatment. Precise diagnosis and early precautions for SCZ are essential to help reduce suffering and enhance the prognosis of the condition. In the present two datasets of SCZ, the AUCs of the four hub genes were greater than 0.65. These results suggest that NEUROD6, NMU, PVALB, and NECAB1 have good diagnostic values. Moreover, the AUC of the nomogram model reached 0.813 (GSE21138) and 0.937 (GSE53987), which exhibited excellent accuracy for disease prediction. Collectively, NEUROD6, NMU, PVALB, NECAB1, and the nomogram model of the four hub genes have great potential as diagnostic biomarkers and therapeutic targets for SCZ.

This study was subjected to the following limitations. First, four hub genes were identified by qPCR, and their localization and distribution should be verified, and the model method may cannot completely simulate SCZ. This may be one of the reasons that the results of qPCR were not completely consistent with expectations. Second, the scope of this study was insufficient to include detailed validation of *in vivo* and *in vitro*. Third, more clinical and demographic characteristics of patients with SCZ should be included in the study for further subgroup analysis.

## Conclusion

Based on bioinformatics methods, a gene signature of NEUROD6, NMU, PVALB, and NECAB1 that intimately associated to SCZ were initially identified. A predictive nomogram for the clinical diagnosis of SCZ was established. This predictive nomogram can be applied clinically to identify patients at high risk of SCZ.

## Data availability statement

The original contributions presented in this study are included in the article/**Supplementary material**, further inquiries can be directed to the corresponding author/s.

## Ethics statement

The animal study was reviewed and approved by the Animal Ethics Committee of The First Hospital of Jilin University (Approval No. 20210637).

## Author contributions

HM, MC, and CZ: conceptualization. SX: methodology. MC: software. ND: validation. CZ and HM: writing—original draft preparation. All authors have read and agreed to the published version of the manuscript.

## Conflict of interest

The authors declare that the research was conducted in the absence of any commercial or financial relationships that could be construed as a potential conflict of interest.

## Publisher's note



## Supplementary material

The Supplementary Material for this article can be found online at: https://www.frontiersin.org/articles/10.3389/fnagi.2022.1032917/full#supplementary-material

# References


Anan, M., Higa, R., Shikano, K., Shide, M., Soda, A., Carrasco Apolinario, M. E., et al. (2020). Cocaine has some effect on neuromedin U expressing neurons related to the brain reward system. *Heliyon* 6:e03947. doi: 10.1016/j.heliyon.2020.e03947

Avramopoulos, D. (2018). Recent Advances in the Genetics of Schizophrenia. *Mol. Neuropsychiatry* 4, 35–51. doi: 10.1159/000488679

Bimpisidis, Z., König, N., Stagkourakis, S., Zell, V., Vlcek, B., Dumas, S., et al. (2019). The NeuroD6 Subtype of VTA Neurons Contributes to Psychostimulant Sensitization and Behavioral Reinforcement. *eNeuro* 6:ENEURO.0066–19. doi: 10.1523/ENEURO.0066-19.2019

Brady, R. O. Jr., Gonsalvez, I., Lee, I., Öngür, D., Seidman, L. J., Schmahmann, J. D., et al. (2019). Cerebellar-Prefrontal Network Connectivity and Negative Symptoms in Schizophrenia. *Am. J. Psychiatry* 176, 512–520. doi: 10.1176/appi.ajp.2018.18040429

Carpenter, W. T. Jr., and Buchanan, R. W. (1994). Schizophrenia. *N. Engl. J. Med.* 330, 681–690. doi: 10.1056/NEJM199403103301006

Chen, S., Liu, Y., Yang, J., Liu, Q., You, H., Dong, Y., et al. (2019). Development and Validation of a Nomogram for Predicting Survival in Male Patients With Breast Cancer. *Front. Oncol.* 9:361. doi: 10.3389/fonc.2019.00361

Cherry, T. J., Wang, S., Bormuth, I., Schwab, M., Olson, J., and Cepko, C. L. (2011). NeuroD factors regulate cell fate and neurite stratification in the developing retina. *J. Neurosci.* 31, 7365–7379. doi: 10.1523/JNEUROSCI.2555-10.2011

Cloutier, M., Aigbogun, M. S., Guerin, A., Nitulescu, R., Ramanakumar, A. V., Kamat, S. A., et al. (2016). The Economic Burden of Schizophrenia in the United States in 2013. *J. Clin. Psychiatry* 77, 764–771. doi: 10.4088/JCP.15m10278

Corsi-Zuelli, F., and Deakin, B. (2021). Impaired regulatory T cell control of astroglial overdrive and microglial pruning in schizophrenia. *Neurosci. Biobehav. Rev.* 125, 637–653. doi: 10.1016/j.neubiorev.2021.03.004

Corsi-Zuelli, F., Deakin, B., de Lima, M. H. F., Qureshi, O., Barnes, N. M., Upthegrove, R., et al. (2021). T regulatory cells as a potential therapeutic target in psychosis? Current challenges and future perspectives. *Brain Behav. Immun. Health* 17:100330. doi: 10.1016/j.bbih.2021.100330

Dombrowski, Y., O'Hagan, T., Dittmer, M., Penalva, R., Mayoral, S. R., Bankhead, P., et al. (2017). Regulatory T cells promote myelin regeneration in the central nervous system. *Nat. Neurosci.* 20, 674–680. doi: 10.1038/nn.4528

Erny, D., Hrabe de Angelis, A. L., Jaitin, D., Wieghofer, P., Staszewski, O., et al. (2015). Host microbiota constantly control maturation and function of microglia in the CNS. *Nat. Neurosci.* 18, 965–977. doi: : 10.1038/nn.4030

Fachim, H. A., Srisawat, U., Dalton, C. F., and Reynolds, G. P. (2018). Parvalbumin promoter hypermethylation in postmortem brain in schizophrenia. *Epigenomics* 10, 519–524. doi: 10.2217/epi-2017-0159

Feng, S., Sun, P., Qu, C., Wu, X., Yang, L., Yang, T., et al. (2022). Exploring the Core Genes of Schizophrenia Based on Bioinformatics Analysis. *Genes* 13:967. doi: 10.3390/genes13060967

GBD 2019 Diseases and Injuries Collaborators (2020). Global burden of 369 diseases and injuries in 204 countries and territories, 1990-2019: A systematic analysis for the Global Burden of Disease Study 2019. *Lancet* 396, 1204–1222. doi: 10.1016/S0140-6736(20)30925-9

Ghashghayi, E., Zendehdel, M., Khodadadi, M., and Rahmani, B. (2022). Central dopaminergic, serotoninergic, as well as GABAergic systems mediate NMU-induced hypophagia in newborn chicken. *Int. J. Neurosci.* doi: 10.1080/00207454.2022.2102980 [Epub ahead of print].

Hänzelmann, S., Castelo, R., and Guinney, J. (2013). GSVA: Gene set variation analysis for microarray and RNA-seq data. *BMC Bioinform.* 14:7. doi: 10.1186/1471-2105-14-7

Hartwig, F. P., Borges, M. C., Horta, B. L., Bowden, J., and Davey Smith, G. (2017). Inflammatory biomarkers and risk of Schizophrenia: A 2-Sample mendelian randomization study. *JAMA Psychiatry* 74, 1226–1233. doi: 10.1001/jamapsychiatry.2017.3191

Hong, S., Lee, E. E., Martin, A. S., Soontornniyomkij, B., Soontornniyomkij, V., Achim, C. L., et al. (2017). Abnormalities in chemokine levels in schizophrenia and their clinical correlates. *Schizophr. Res.* 181, 63–69. doi: 10.1016/j.schres.2016.09.019

Huang, J., Liu, F., Wang, B., Tang, H., Teng, Z., Li, L., et al. (2019). Central and Peripheral Changes in FOS Expression in Schizophrenia Based on Genome-Wide Gene Expression. *Front. Genet.* 10:232. doi: 10.3389/fgene.2019.00232

Janickova, L., Rechberger, K. F., Wey, L., and Schwaller, B. (2021). Correction to: Absence of parvalbumin increases mitochondria volume and branching of dendrites in inhibitory Pvalb neurons in vivo: A point of convergence of autism spectrum disorder (ASD) risk gene phenotypes. *Mol. Autism.* 12:7. doi: 10.1186/s13229-020-00404-8

Kaur, C., Saini, S., Pal, I., Kumar, P., Chandra Sati, H., Jacob, T. G., et al. (2020). Age-related changes in the number of cresyl-violet-stained, parvalbumin and NMDAR 2B expressing neurons in the human spiral ganglion. *Hear. Res.* 388:107883. doi: 10.1016/j.heares.2020.107883

Kelly, D. L., Li, X., Kilday, C., Feldman, S., Clark, S., Liu, F., et al. (2018). Increased circulating regulatory T cells in medicated people with schizophrenia. *Psychiatry Res.* 269, 517–523. doi: 10.1016/j.psychres.2018.09.006

Lach, G., Schellekens, H., Dinan, T. G., and Cryan, J. F. (2018). Anxiety, depression, and the microbiome: A role for gut peptides. *Neurotherapeutics* 15, 36–59. doi: : 10.1007/s13311-017-0585-0

Langeh, U., Singh, S., and Targeting, S. (2021). 100B Protein as a Surrogate Biomarker and its Role in Various Neurological Disorders. *Curr. Neuropharmacol.* 19, 265–277. doi: 10.2174/1570159X18666200729100427

Lemonnier, E., Lazartigues, A., and Ben-Ari, Y. (2016). Treating Schizophrenia With the Diuretic Bumetanide: A Case Report. *Clin. Neuropharmacol.* 39, 115–117. doi: 10.1097/WNF.0000000000000136

Li, H., Xiang, Y., Zhu, Z., Wang, W., Jiang, Z., Zhao, M., et al. (2021). Rifaximin-mediated gut microbiota regulation modulates the function of microglia and protects against CUMS-induced depression-like behaviors in adolescent rat. *J. Neuroinflammation* 18:254. doi: 10.1186/s12974-021-02303-y

Li, R., Wang, Q., Qiu, Y., Meng, Y., Wei, L., Wang, H., et al. (2021). A Potential Autophagy-Related Competing Endogenous RNA Network and Corresponding Diagnostic Efficacy in Schizophrenia. *Front. Psychiatry* 12:628361. doi: 10.3389/fpsyt.2021.628361

Ly, A., and Root, D. H. (2021). Neuromedin U: A neuropeptide modulator of GABA transmission contributes to cocaine seeking. *Neuropsychopharmacology* 47, 1873–1874. doi: 10.1038/s41386-021-01253-6

Maas, D. A., Vallès, A., and Martens, G. J. M. (2017). Oxidative stress, prefrontal cortex hypomyelination and cognitive symptoms in schizophrenia. *Transl. Psychiatry* 7:e1171. doi: 10.1038/tp.2017.138

Maldonado-Avilés, J. G., Wu, Q., Sampson, A. R., and Lewis, D. A. (2006). Somal size of immunolabeled pyramidal cells in the prefrontal cortex of subjects with schizophrenia. *Biol. Psychiatry* 60, 226–234. doi: 10.1016/j.biopsych.2005.10.028

Manoach, D. S. (2003). Prefrontal cortex dysfunction during working memory performance in schizophrenia: Reconciling discrepant findings. *Schizophr. Res.* 60, 285–298. doi: 10.1016/s0920-9964(02)00294-3

Mathis, V. P., Williams, M., Fillinger, C., and Kenny, P. J. (2021). Networks of habenula-projecting cortical neurons regulate cocaine seeking. *Sci. Adv.* 7:eabj2225. doi: 10.1126/sciadv.abj2225

Matsuda, K., Watanabe, K., Miyagawa, Y., Maruyama, K., Konno, N., and Nakamachi, T. (2020). Distribution of neuromedin U (NMU)-like immunoreactivity in the goldfish brain, and effect of intracerebroventricular administration of NMU on emotional behavior in goldfish. *Peptides* 156:170846. doi: 10.1016/j.peptides.2022.170846

McCutcheon, R. A., Reis Marques, T., and Howes, O. D. (2020). Schizophrenia-An Overview. *JAMA Psychiatry* 77, 201–210. doi: 10.1001/jamapsychiatry.2019.3360

Miller, B. J., Gassama, B., Sebastian, D., Buckley, P., and Mellor, A. (2013). Meta-analysis of lymphocytes in schizophrenia: clinical status and antipsychotic effects. *Biol. Psychiatry* 73, 993–999. doi: 10.1016/j.biopsych.2012.09.007

Najjar, S., Pearlman, D. M., Alper, K., Najjar, A., and Devinsky, O. (2013). Neuroinflammation and psychiatric illness. *J. Neuroinflammation* 10:43. doi: 10.1186/1742-2094-10-43

Noble, W. S. (2006). What is a support vector machine? *Nat. Biotechnol.* 24, 1565–1567. doi: 10.1038/nbt1206-1565

Patel, V. C., Lee, S., McPhail, M. J. W., Da Silva, K., Guilly, S., Zamalloa, A., et al. (2022). Rifaximin-α reduces gut-derived inflammation and mucin degradation in cirrhosis and encephalopathy: RIFSYS randomised controlled trial. *J. Hepatol.* 76, 332–342. doi: 10.1016/j.jhep.2021.09.010

Paul, A., Mukherjee, D. P., Das, P., Gangopadhyay, A., Chintha, A. R., and Kundu, S. (2018). Improved Random Forest for Classification. *IEEE Trans. Image Process.* 27, 4012–4024. doi: 10.1109/TIP.2018.2834830

Raghu, H., Lepus, C. M., Wang, Q., Wong, H. H., Lingampalli, N., Oliviero, F., et al. (2017). CCL2/CCR2, but not CCL5/CCR5, mediates monocyte recruitment, inflammation and cartilage destruction in osteoarthritis. *Ann. Rheum. Dis.* 76, 914–922. doi: 10.1136/annrheumdis-2016-210426

Roy, A. (1986). Depression, attempted suicide, and suicide in patients with chronic schizophrenia. *Psychiatr. Clin. North Am.* 9, 193–206.

Sasaki-Hamada, S., Maeno, Y., Yabe, M., and Ishibashi, H. (2021). Neuromedin U modulates neuronal excitability in rat hippocampal slices. *Neuropeptides* 89:102168. doi: 10.1016/j.npep.2021.102168

Satoh, J., Yamamoto, Y., Asahina, N., Kitano, S., and Kino, Y. (2014). RNA-Seq data mining: downregulation of NeuroD6 serves as a possible biomarker for alzheimer's disease brains. *Dis. Markers* 2014:123165. doi: 10.1155/2014/123165

Skaper, S. D., Facci, L., and Giusti, P. (2014). Neuroinflammation, microglia and mast cells in the pathophysiology of neurocognitive disorders: a review. *CNS Neurol. Disord. Drug Targets* 13, 1654–1666. doi: 10.2174/1871527313666141130224206

Tomasik, J., Rahmoune, H., Guest, P. C., and Bahn, S. (2016). Neuroimmune biomarkers in schizophrenia. *Schizophr. Res.* 176, 3–13. doi: 10.1016/j.schres.2014.07.025

Tsubomoto, M., Kawabata, R., Zhu, X., et al. (2019). Expression of Transcripts Selective for GABA Neuron Subpopulations across the Cortical Visuospatial Working Memory Network in the Healthy State and Schizophrenia. *Cereb. Cortex* 29, 3540–3550. doi: 10.1093/cercor/bhy227

Tutukova, S., Tarabykin, V., and Hernandez-Miranda, L. R. (2021). The Role of Neurod Genes in Brain Development, Function, and Disease. *Front. Mol. Neurosci.* 14:662774. doi: 10.3389/fnmol.2021.662774

Valles-Colomer, M., Falony, G., Darzi, Y., Tigchelaar, E. F., Wang, J., Tito, R. Y., et al. (2019). The neuroactive potential of the human gut microbiota in quality of life and depression. *Nat. Microbiol.* 4, 623–632. doi: 10.1038/s41564-018-0337-x

Vallöf, D., Kalafateli, A. L., and Jerlhag, E. (2020). Brain region-specific neuromedin U signalling regulates alcohol-related behaviours and food intake in rodents. *Addict. Biol.* 25:e12764. doi: 10.1111/adb.12764

Vasquez, M. M., Hu, C., Roe, D. J., Chen, Z., Halonen, M., and Guerra, S. (2016). Least absolute shrinkage and selection operator type methods for the identification of serum biomarkers of overweight and obesity: simulation and application. *BMC Med. Res. Methodol.* 16:154. doi: 10.1186/s12874-016-0254-8

Vickers, A. J., and Elkin, E. B. (2006). Decision curve analysis: A novel method for evaluating prediction models. *Med. Decis. Making* 26, 565–574. doi: 10.1177/0272989X06295361

Viereckel, T., Dumas, S., Smith-Anttila, C. J., Vlcek, B., Bimpisidis, Z., and Lagerström, M. C. (2016). Midbrain Gene Screening Identifies a New Mesoaccumbal Glutamatergic Pathway and a Marker for Dopamine Cells Neuroprotected in Parkinson's Disease. *Sci. Rep.* 6:35203. doi: 10.1038/srep35203

Wahbeh, M. H., and Avramopoulos, D. (2021). Gene-Environment Interactions in Schizophrenia: A Literature Review. *Genes* 12:1850. doi: 10.3390/genes12121850

Wo, J., Zhang, F., Li, Z., Sun, C., Zhang, W., and Sun, G. (2020). The Role of Gamma-Delta T Cells in Diseases of the Central Nervous System. *Front. Immunol.* 11:580304. doi: 10.3389/fimmu.2020.580304

Wolbers, M., Koller, M. T., Witteman, J. C., and Steyerberg, E. W. (2009). Prognostic models with competing risks: methods and application to coronary risk prediction. *Epidemiology* 20, 555–561. doi: 10.1097/EDE.0b013e3181a39056

Yang, A. C., and Tsai, S. J. (2017). New Targets for Schizophrenia Treatment beyond the Dopamine Hypothesis. *Int. J. Mol. Sci.* 18:1689. doi: 10.3390/ijms18081689

Zheng, P., Zeng, B., Zhou, C., Liu, M., Fang, Z., Xu, X., et al. (2016). Gut microbiome remodeling induces depressive-like behaviors through a pathway mediated by the host's metabolism. *Mol. Psychiatry* 21, 786–796. doi: 10.1038/mp.2016.44

Zhou, Y., Fan, L., Qiu, C., and Jiang, T. (2015). Prefrontal cortex and the dysconnectivity hypothesis of schizophrenia. *Neurosci. Bull.* 31, 207–219. doi: 10.1007/s12264-014-1502-8

frontiers | Frontiers in Aging Neuroscience

TYPE Systematic Review
PUBLISHED 24 October 2022
DOI 10.3389/fnagi.2022.1036676



OPEN ACCESS

EDITED BY
Yuzhen Xu,
Tongji University, China

REVIEWED BY
Shi-Bin Wang,
Guangdong Mental Health Center, China
Lei Xia,
Chaohu Hospital of Anhui Medical University, China

*CORRESPONDENCE
Wei Zheng
zhengwei0702@163.com
Ze-Zhi Li
biolpsychiatry@126.com

†These authors have contributed equally to this work

SPECIALTY SECTION
This article was submitted to Alzheimer's Disease and Related Dementias, a section of the journal Frontiers in Aging Neuroscience

RECEIVED 05 September 2022
ACCEPTED 10 October 2022
PUBLISHED 24 October 2022

CITATION
Zheng W, Zhang X-Y, Xu R, Huang X, Zheng Y-J, Huang X-B, Li Z-Z and Chen H-D (2022) Adjunctive accelerated repetitive transcranial magnetic stimulation for older patients with depression: A systematic review. *Front. Aging Neurosci.* 14:1036676. doi: 10.3389/fnagi.2022.1036676



# Adjunctive accelerated repetitive transcranial magnetic stimulation for older patients with depression: A systematic review

Wei Zheng[1*†], Xin-Yang Zhang[1], Rui Xu[1], Xiong Huang[1], Ying-Jun Zheng[1], Xing-Bing Huang[1], Ze-Zhi Li[1*†] and Huo-Di Chen[2]

[1]The Affiliated Brain Hospital of Guangzhou Medical University, Guangzhou, China, [2]Laboratory of Laser Sports Medicine, School of Sports Science, South China Normal University, Guangzhou, China

**Objective:** We performed this systemic review to investigate the therapeutic potential and safety of adjunctive accelerated repetitive transcranial magnetic stimulation (aTMS) for older patients with depression.

**Methods:** We included published randomized clinical trials (RCTs) and observational studies targeting adjunctive aTMS for older patients with depression.

**Results:** Two open-label self-controlled studies ($n = 29$) fulfilled the criteria for inclusion. The included studies reported significant improvements in depressive symptoms from baseline to post-aTMS (all $Ps < 0.05$). One study reported a dropout rate of 10.5% (2/19). Mild headache was the most common adverse reaction.

**Conclusion:** The currently available evidence from two open-label self-controlled studies indicates that adjunctive aTMS is a safe and effective therapy for older patients with depression.

KEYWORDS

**accelerated TMS, depression, systematic review, older patients, response**

## Introduction

Depression is a leading cause of disability (World Health Organization, 2017), and occurs in 7% of the elderly population worldwide (World Health Organization, 2016). A diagnosis of depression in old age is often associated with poorer long-term prognoses, higher recurrence rates, lower quality of life, and a greater likelihood of morbidity and early mortality (Mitchell and Subramaniam, 2005; Aziz and Steffens, 2013). Up to 1/3 of individuals experiencing major depressive disorder (MDD), particularly in the elderly population, fail to achieve clinical remission after acute pharmacological treatment (Rush et al., 2006). Because comorbid physical diseases are common, elderly patients with depression are highly likely to experience side effects of medication

(Kok and Reynolds, 2017). Thus, non-pharmacological treatments, such as electroconvulsive therapy (ECT) (Dong et al., 2018; Jiang et al., 2020), transcranial magnetic stimulation (TMS) (Blumberger et al., 2015; Conelea et al., 2017), transcranial direct current stimulation (tDCS) (Kumar et al., 2020; Brooks et al., 2021), vagus nerve stimulation (VNS) (van Rooij et al., 2020), deep brain stimulation (DBS) (McDonald, 2016) and theta-burst stimulation (TBS) (Cristancho et al., 2020), may be reasonable alternatives for older patients with depression.

A type of non-invasive brain stimulation, repetitive transcranial magnetic stimulation (rTMS), was approved by the FDA as a treatment for MDD in 2008 (Holtzheimer et al., 2010). A network meta-analysis of 81 randomized clinical trials (RCTs) found that active rTMS showed a significantly higher clinical response and remission rates than non-active rTMS (Brunoni et al., 2017). A typical course for rTMS involves five days of treatment/week over a period of 3–6 weeks (Holtzheimer et al., 2010). However, this schedule may be inconvenient for patients and can hinder compliance (Frey et al., 2020). Thus, consolidating the treatment (e.g., over 2–3 days) may make it more accessible and could potentially increase compliance.

Accelerated rTMS (aTMS) protocols have been studied as a potential solution for this problem (Sonmez et al., 2019). Recent meta-analyses have found that aTMS protocols may be effective for individuals suffering from depression (Sonmez et al., 2019) and post-stroke depression (PSD) (Frey et al., 2020). A randomized controlled study (RCT) of twice-daily rTMS for the treatment of MDD found that rTMS given twice daily was effective and safe (Loo et al., 2007). Two open-label studies have also reported positive findings for adjunctive aTMS as a therapy in addition to antidepressants for older patients with depression (Dardenne et al., 2018; Desbeaumes Jodoin et al., 2019). For example, Dardenne et al. reported that aTMS was safe and well-tolerated in older patients with MDD (≥65 years old) (Dardenne et al., 2018). Similarly, a recent study reported that aTMS protocol (two sessions per day) is a safe and effective treatment for older patients (≥60 years old) suffering from treatment-resistant depression (TRD) (Desbeaumes Jodoin et al., 2019).

To date, no systematic review examining the therapeutic role and safety of adjunctive aTMS for older patients with depression has been published. In view of this important gap, we conducted this review to systematically investigate the efficacy and safety of adjunctive aTMS for older patients with depression.

# Methods

## Search strategy and selection criteria

Two investigators (X-YZ and RX) independently searched electronic databases (including PsycINFO, Cochrane Library, PubMed, EMBASE, Chinese Journal Net, and WanFang) and manually checked reference lists of the included studies (Dardenne et al., 2018; Desbeaumes Jodoin et al., 2019) and relevant reviews (Mutz et al., 2019; Sonmez et al., 2019) for eligible studies on adjunctive aTMS for older patients with depression. The initial search was completed by two investigators (XYZ and RX) on December 16, 2021, using the following search terms: (accelerated TMS OR accelerated rTMS OR aTMS OR accelerated transcranial magnetic stimulation OR accelerated repetitive transcranial magnetic stimulation) AND (depression OR depressed OR depressive) AND (aged OR elderly OR older adult OR aging).

In line with PRISMA guidelines (Moher et al., 2009), we included studies that fulfilled the following ***PICOS*** criteria. ***P***articipants: older patients (≥60 years old) suffering from uni- or bi-polar depression, as defined by the respective studies. ***I***ntervention *vs.* ***C***omparison: real aTMS with antidepressants *vs.* antidepressant monotherapy or sham aTMS wiht antidepressants; aTMS added to antidepressants (observational studies). ***O***utcomes: the primary outcome was changed in depressive symptoms as measured by depression scales [i.e., the Montgomery-Asberg Depression Rating Scale (MADRS) (Montgomery and Asberg, 1979; Zhong et al., 2011)]. Key secondary outcomes reported in this systematic review were study-defined response and remission, dropout rate, and adverse events. ***S***tudy: only published RCTs or observational studies (single-group, before-after design) investigating the efficacy and safety of aTMS in combination with antidepressants for older patients with uni- and bi-polar depression were eligible for inclusion. As reported previously (Mutz et al., 2019), TBS included the following three different treatment strategies: intermittent TBS, continuous TBS, or bilateral TBS. Thus, studies with at least two rTMS sessions rather than one TBS session per day were included. Review articles, retrospective studies, and case reports/series were excluded.

## Data extraction

Two independent investigators (X-YZ and RX) extracted relevant data from each included study. Any disagreements were resolved through consensus or, if needed, through discussion with the senior author (WZ). Missing data were requested by contacting first and/or corresponding authors and/or searching for the data from other reviews (Sonmez et al., 2019).

## Quality assessment

The quality of RCT were independently evaluated by two investigators (X-YZ and RX) using the Cochrane risk of bias (Higgins et al., 2011).

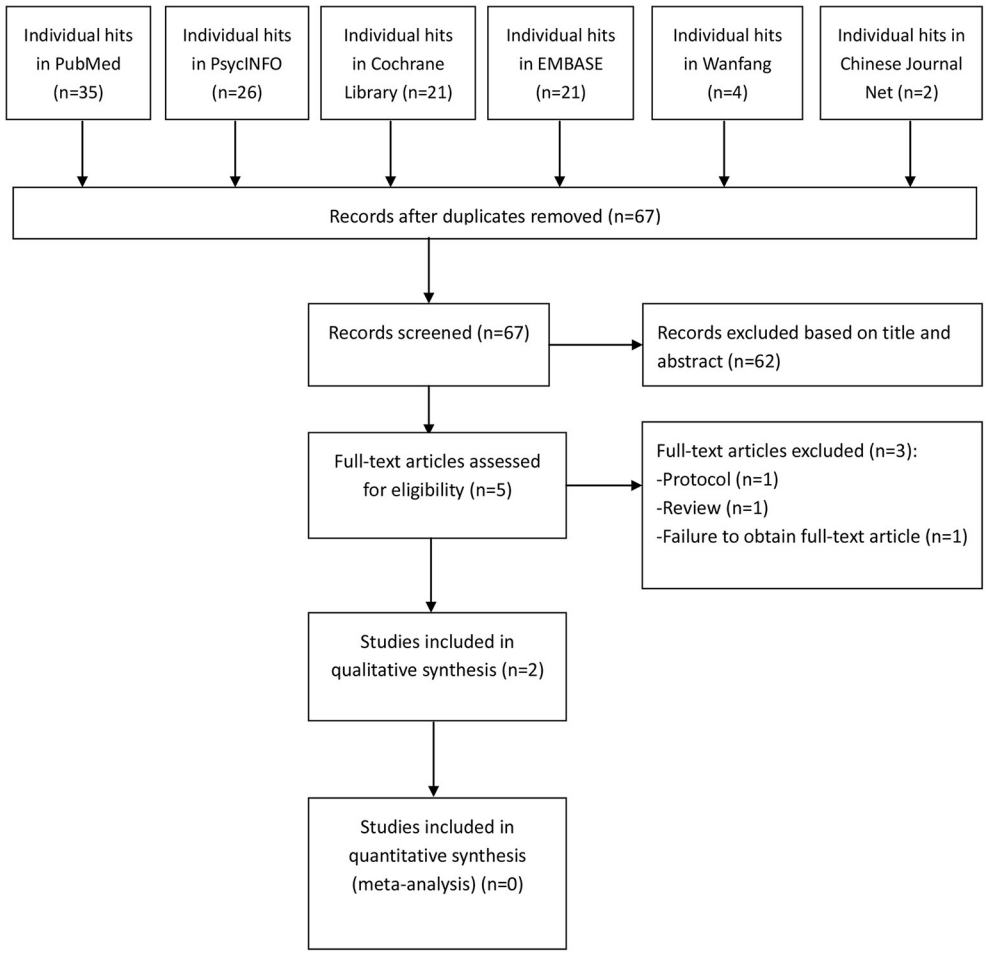


FIGURE 1
PRISMA flow diagram.

TABLE 1 Summary of characteristics of included studies.

| References (country) | *N* (♂/♀) | Study design | - Diagnosis - Diagnostic criteria | Age: yrs (range) | Medication status | Type site; Frequency (intensity) | Total stimuli (stimuli/session); - Total days (sessions/day, Total sessions) | - Trains/ session - Train length - Intertrain |
|---|---|---|---|---|---|---|---|---|
| Dardenne et al. (2018) (Belgium) | 10 (0/10) | Open-label | - MDD<br>- DSM-IV | 73.9 (65–82) | Psychotro pic -allowed | HF-rTMS L-DLPFC; 20 Hz (110%) | 31200 (1560 pluses); 4 (5, 20) | - 39 s<br>- 2 s<br>- 12 s |
| Desbeaumes Jodoin et al. (2019) (Canada) | 19 (10/9)[a] | Open-label | - TRD (17 unipolar, 2 bipolar)<br>- DSM-5 | 71.0 (60–89) | Psychotro pic -allowed | HF-rTMS L-DLPFC; 20 Hz (110%) | 60000–90000 (3000 pluses); 10–15 (2, 20–30) | - 150 s<br>- 5 s<br>- 25 s |

[a]Data were extracted only focusing on older patients (≥60 years old) with depression.
DSM, Diagnostic and Statistical Manual of Mental Disorders; HF, high frequency; L-DLPFC, left dorsolateral prefrontal cortex; MDD, major depressive disorder; N, number of patients; NR, not reported; NOS, newcastle-ottawa scale; rTMS, repetitive transcranial magnetic stimulation; TRD, treatment-resistant depression.
♂ = Male; ♀ = Female.

TABLE 2 The improvement of depressive symptoms after aTMS.

| References | Assessment tools | At baseline (mean ± SD, *n*) | At end of study (mean±SD, n) | *P-value* |
|---|---|---|---|---|
| Dardenne et al. (2018) | HDRS scores | 22.6 ± 4.1 ($n = 10$) | 10.6 ± 7.9 ($n = 10$)[a] | **0.004** |
| | BDI scores | 25.9 ± 7.0 ($n = 10$) | 10.8 ± 7.1 ($n = 10$)[a] | **0.004** |
| Desbeaumes Jodoin et al. (2019) | MADRS scores | 21.7 ± 9.3 ($n = 19$) | 9.4 ± 7.6 ($n = 19$)[b] | **<0.001** |

[a]Patients were assessed at post-aTMS.
[b]Patients were assessed at seven days after the last aTMS session.
Bolded values are $P < 0.05$.
aTMS, accelerated transcranial magnetic stimulation; BDI, Beck Depression Inventory; HDRS, Hamilton Depression Rating Scale; MADRS, Montgomery-Asberg Depression Rating Scale; n, number of patients.

TABLE 3 Dropout rate and adverse events.

| References | Sample size | Dropout rate | Adverse events | |
|---|---|---|---|---|
| | | Total (%) | Events | Total (%) |
| **Observational studies ($n = 29$)** | | | | |
| Dardenne et al. (2018) | 10 | 0 (0) | Local discomfort | 1 (10) |
| | | | Mild headache | 4 (40) |
| Desbeaumes Jodoin et al. (2019) | 19 | 2 (10.5) | Headache | 3 (15.8) |
| | | | Local sensitivity | 3 (15.8) |
| | | | Fatigue | 1 (5.3) |

# Results

## Study selection

As shown in Figure 1, we identified a total of 109 hits in this systematic review. In the end, two open-label self-controlled studies met the inclusion criteria and were included in our qualitative analysis (Dardenne et al., 2018; Desbeaumes Jodoin et al., 2019).

## Study characteristics

The characteristics of the two observational studies (Dardenne et al., 2018; Desbeaumes Jodoin et al., 2019), covering 29 older patients with MDD ($n = 27$) or bipolar depression ($n = 2$), are summarized in Table 1. One of the studies ($n = 10$) (Dardenne et al., 2018) was conducted in Belgium; the other ($n = 19$) (Desbeaumes Jodoin et al., 2019) was conducted in Canada.

## Assessment of study quality

We did not use the Cochrane risk of bias assessment because no RCTs fulfilled the inclusion criteria.

## Depressive symptoms

As shown in Table 2, the two included studies consistently reported significant improvements in depressive symptoms from baseline to post-aTMS (all *Ps* $< 0.05$). In Dardenne et al.'s (2018) study, 40% (4/10) of older patients with MDD showed responses, and 20% (2/10) met the remission criteria. In Desbeaumes Jodoin, Miron and Lespérance (2019) study, 14 out of 19 older patients (73.7%) responded to aTMS, and 63.2% (12/19) met remission criteria.

## Dropout rate and adverse events

Dropout rate and adverse events are summarized in Table 3. The dropout rate was 10.5% (2/19) in Desbeaumes Jodoin, Miron and Lespérance (2019) study and 0% (0/10) in Dardenne et al.'s (2018) study. Mild headaches were the most common adverse events, accounting for 40% of side effects (Dardenne et al., 2018).

# Discussion

This article is the first systematic review to examine the potential therapeutic role and safety of adjunctive aTMS for older patients (≥60 years old) suffering from depression. Only two observational studies (Dardenne et al., 2018; Desbeaumes Jodoin et al., 2019) involving 29 older patients with depression

were included in this systematic review. The two studies (Dardenne et al., 2018; Desbeaumes Jodoin et al., 2019) were published within the last three years, indicating that this is a novel and clinically important topic. This systematic review provides preliminary support for the utility of aTMS for reducing depressive symptoms in older patients with depression. Furthermore, adjunctive rTMS was safe and well-tolerated in elderly depressed patients. However, aTMS may have resulted in higher discomfort rates than standard daily rTMS (Fitzgerald et al., 2018).

According to this systematic review, adjunctive aTMS appears to be effective in treating older patients suffering from depression, although the long-term efficacy was not reported. The rationale for an accelerated approach comes from the idea that repeated application of stimulation within short time intervals could be associated with greater antidepressant effects (Sonmez et al., 2019). A recent review reported that high-frequency (HF) rTMS delivered over the left dorsolateral prefrontal cortex (DLPFC) could reduce suicidal behavior in individuals with the treatment-resistant depression (Godi et al., 2021).

The response rates of HF rTMS tended to range from 20 to 30% (O'Reardon et al., 2007; Avery et al., 2008; George et al., 2010), which was far lower than the response rate to aTMS (73.7%) (Desbeaumes Jodoin et al., 2019). However, a recent RCT, involving 115 outpatients with MDD who randomly received either aTMS or standard daily rTMS, found that aTMS and rTMS had comparable efficacy for treating depression (Fitzgerald et al., 2018). Although this systematic review found that aTMS may be an effective therapy in elderly patients with depression, a variety of parameters have been applied to the two included studies (Dardenne et al., 2018; Desbeaumes Jodoin et al., 2019). For example, the total stimuli of aTMS ranged between 31,200 and 90,000, and the optimal parameters for aTMS remain unclear.

The following limitations must be considered. First, only two open-label self-controlled studies (single-group, before-after design) examining the efficacy and safety of adjunctive aTMS for older patients with depression were included (Dardenne et al., 2018; Desbeaumes Jodoin et al., 2019). Second, the relatively small sample sizes in both studies potentially reduced their power and increased the possibility of type II error. Third, this systematic review on adjunctive aTMS for older patients with depression has not been registered. Fourth, given that the heterogeneity between the studies, a quantitative analysis could not be performed in this study. Finally, some important outcome measures, such as cognitive functioning, were not reported in the included studies.

## Conclusions

The current evidence from open-label self-controlled studies, while limited, indicates that adjunctive aTMS is a safe and effective therapy for older patients with depression. Further RCTs with rigorous methodology need to be performed in order to confirm and extend these findings.

## Data availability statement

The original contributions presented in the study are included in the article/supplementary material, further inquiries can be directed to the corresponding authors.

## Author contributions

X-YZ and RX selected studies and extracted the data. WZ reviewed all the data, helped mediate disagreements, and wrote the first draft. All authors contributed to the interpretation of data and approved the final manuscript.

## Funding

This study was funded by the the Science and Technology Planning Project of Liwan District of Guangzhou (202004034), National Natural Science Foundation of China (82101609), Scientific Research Project of Guangzhou Bureau of Education (202032762), Science and Technology Program Project of Guangzhou (202102020658), Guangzhou Health Science and Technology Project (20211A011045), Guangzhou science and Technology Project of traditional Chinese Medicine and integrated traditional Chinese and Western medicine (20212A011018), China International Medical Exchange Foundation (Z-2018-35-2002), Guangzhou Clinical Characteristic Technology Project (2019TS67), science and Technology Program Project of Guangzhou (202102020658), and Guangdong Hospital Association (2019ZD06). The funders had no role in study design, data collection and analysis, decision to publish, or preparation of the manuscript.

## Conflict of interest

The authors declare that the research was conducted in the absence of any commercial or financial relationships that could be construed as a potential conflict of interest.

## Publisher's note

# References


Avery, D. H., Isenberg, K. E., Sampson, S. M., Janicak, P. G., Lisanby, S. H., Maixner, D. F., et al. (2008). Transcranial magnetic stimulation in the acute treatment of major depressive disorder: clinical response in an open-label extension trial. *J. Clin. Psychiatry* 69, 441–451. doi: 10.4088/JCP.v69n0315

Aziz, R., and Steffens, D. C. (2013). What are the causes of late-life depression? *Psychiatr. Clin. North Am.* 36, 497–516. doi: 10.1016/j.psc.2013.08.001

Blumberger, D. M., Hsu, J. H., and Daskalakis, Z. J. (2015). A Review of brain stimulation treatments for late-life depression. *Curr. Treat Options Psychiatry* 2, 413–421. doi: 10.1007/s40501-015-0059-0

Brooks, H., Oughli, H. A., Kamel, L., Subramanian, S., Morgan, G., Blumberger, D. M., et al. (2021). Enhancing cognition in older persons with depression or anxiety with a combination of mindfulness-based stress reduction (MBSR) and transcranial direct current stimulation (tDCS): results of a pilot randomized clinical trial. *Mindfulness*12, 3047–3059. doi: 10.1007/s12671-021-01764-9

Brunoni, A. R., Chaimani, A., Moffa, A. H., Razza, L. B., Gattaz, W. F., Daskalakis, Z. J., et al. (2017). Repetitive transcranial magnetic stimulation for the acute treatment of major depressive episodes: a systematic review with network meta-analysis. *JAMA Psychiatry* 74, 143–152. doi: 10.1001/jamapsychiatry.2016.3644

Conelea, C. A., Philip, N. S., Yip, A. G., Barnes, J. L., Niedzwiecki, M. J., Greenberg, B. D., et al. (2017). Transcranial magnetic stimulation for treatment-resistant depression: naturalistic treatment outcomes for younger *versus* older patients. *J. Affect Disord.* 217, 42–47. doi: 10.1016/j.jad.2017.03.063

Cristancho, P., Kamel, L., Araque, M., Berger, J., Blumberger, D. M., Miller, J. P., et al. (2020). iTBS to relieve depression and executive dysfunction in older adults: an open label study. *Am. J. Geriatr. Psychiatry* 28, 1195–1199. doi: 10.1016/j.jagp.2020.03.001

Dardenne, A., Baeken, C., Crunelle, C. L., Bervoets, C., Matthys, F., and Herremans, S. C. (2018). Accelerated HF-rTMS in the elderly depressed: a feasibility study. *Brain Stimul.* 11, 247–248. doi: 10.1016/j.brs.2017.10.018

Desbeaumes Jodoin, V., Miron, J. P., and Lespérance, P. (2019). Safety and efficacy of accelerated repetitive transcranial magnetic stimulation protocol in elderly depressed unipolar and bipolar patients. *Am. J. Geriatr. Psychiatry* 27, 548–558. doi: 10.1016/j.jagp.2018.10.019

Dong, M., Zhu, X. M., Zheng, W., Li, X. H., Ng, C. H., Ungvari, G. S., et al. (2018). Electroconvulsive therapy for older adult patients with major depressive disorder: a systematic review of randomized controlled trials. *Psychogeriatrics* 18, 468–475. doi: 10.1111/psyg.12359

Fitzgerald, P. B., Hoy, K. E., Elliot, D., Susan Mcqueen, R. N., Wambeek, L. E., and Daskalakis, Z. J. (2018). Accelerated repetitive transcranial magnetic stimulation in the treatment of depression. *Neuropsychopharmacology* 43, 1565–1572. doi: 10.1038/s41386-018-0009-9

Frey, J., Najib, U., Lilly, C., and Adcock, A. (2020). Novel TMS for stroke and depression (NoTSAD): accelerated repetitive transcranial magnetic stimulation as a safe and effective treatment for post-stroke depression. *Front. Neurol.* 11:788. doi: 10.3389/fneur.2020.00788

George, M. S., Lisanby, S. H., Avery, D., Mcdonald, W. M., Durkalski, V., Pavlicova, M., et al. (2010). Daily left prefrontal transcranial magnetic stimulation therapy for major depressive disorder: a sham-controlled randomized trial. *Arch. Gen. Psychiatry* 67, 507–516. doi: 10.1001/archgenpsychiatry.2010.46

Godi, S. M., Spoorthy, M. S., Purushotham, A., and Tikka, S. K. (2021). Repetitive transcranial magnetic stimulation and its role in suicidality—a systematic review. *Asian J. Psychiatr.* 63:102755. doi: 10.1016/j.ajp.2021.102755

Higgins, J. P., Altman, D. G., Gotzsche, P. C., Juni, P., Moher, D., Oxman, A. D., et al. (2011). The cochrane collaboration's tool for assessing risk of bias in randomised trials. *BMJ* 343:d5928. doi: 10.1136/bmj.d5928

Holtzheimer, P. E. 3rd, Mcdonald, W. M., Mufti, M., Kelley, M. E., Quinn, S., Corso, G., and Epstein, C. M. (2010). Accelerated repetitive transcranial magnetic stimulation for treatment-resistant depression. *Depress. Anxiety* 27, 960–963. doi: 10.1002/da.20731

Jiang, X., Xie, Q., Liu, L. Z., Zhong, B. L., Si, L., and Fan, F. (2020). Efficacy and safety of modified electroconvulsive therapy for the refractory depression in older patients. *Asia Pac. Psychiatry* 12:e12411. doi: 10.1111/appy.12411

Kok, R. M., and Reynolds, C. F. 3rd (2017). Management of depression in older adults: a review. *JAMA* 317, 2114–2122. doi: 10.1001/jama.2017.5706

Kumar, S., Batist, J., Ghazala, Z., Zomorrodi, R. M., Brooks, H., Goodman, M., et al. (2020). Effects of bilateral transcranial direct current stimulation on working memory and global cognition in older patients with remitted major depression: a pilot randomized clinical trial. *Int. J. Geriatr. Psychiatry* 35, 1233–1242. doi: 10.1002/gps.5361

Loo, C. K., Mitchell, P. B., Mcfarquhar, T. F., Malhi, G. S., and Sachdev, P. S. (2007). A sham-controlled trial of the efficacy and safety of twice-daily rTMS in major depression. *Psychol. Med.* 37, 341–349. doi: 10.1017/S0033291706009597

McDonald, W. M. (2016). Neuromodulation treatments for geriatric mood and cognitive disorders. *Am. J. Geriatr. Psychiatry* 24, 1130–1141. doi: 10.1016/j.jagp.2016.08.014

Mitchell, A. J., and Subramaniam, H. (2005). Prognosis of depression in old age compared to middle age: a systematic review of comparative studies. *Am. J. Psychiatry* 162, 1588–1601. doi: 10.1176/appi.ajp.162.9.1588

Moher, D., Liberati, A., Tetzlaff, J., and Altman, D. G. (2009). Preferred reporting items for systematic reviews and meta-analyses: the PRISMA statement. *BMJ* 339:b2535. doi: 10.1136/bmj.b2535

Montgomery, S. A., and Asberg, M. (1979). A new depression scale designed to be sensitive to change. *Br. J. Psychiatry* 134, 382–389. doi: 10.1192/bjp.134.4.382

Mutz, J., Vipulananthan, V., Carter, B., Hurlemann, R., Fu, C. H. Y., and Young, A. H. (2019). Comparative efficacy and acceptability of non-surgical brain stimulation for the acute treatment of major depressive episodes in adults: systematic review and network meta-analysis. *BMJ* 364:l1079. doi: 10.1136/bmj.l1079

O'Reardon, J. P., Solvason, H. B., Janicak, P. G., Sampson, S., Isenberg, K. E., Nahas, Z., et al. (2007). Efficacy and safety of transcranial magnetic stimulation in the acute treatment of major depression: a multisite randomized controlled trial. *Biol. Psychiatry* 62, 1208–1216. doi: 10.1016/j.biopsych.2007.01.018

Rush, A. J., Trivedi, M. H., Wisniewski, S. R., Nierenberg, A. A., Stewart, J. W., Warden, D., et al. (2006). Acute and longer-term outcomes in depressed outpatients requiring one or several treatment steps: a STAR*D report. *Am. J. Psychiatry* 163, 1905–1917. doi: 10.1176/ajp.2006.163.11.1905

Sonmez, A. I., Camsari, D. D., Nandakumar, A. L., Voort, J. L. V., Kung, S., Lewis, C. P., et al. (2019). Accelerated TMS for depression: a systematic review and meta-analysis. *Psychiatry Res.* 273, 770–781. doi: 10.1016/j.psychres.2018.12.041

van Rooij, S. J. H., Riva-Posse, P., and Mcdonald, W. M. (2020). The efficacy and safety of neuromodulation treatments in late-life depression. *Curr. Treat Options Psychiatry* 7, 337–348. doi: 10.1007/s40501-020-00216-w

World Health Organization (2016). *Mental Health and Older Adults*. Geneva: World Health Organization. Available online at: http://www.who.int/mediacentre/factsheets/fs381/en/

World Health Organization (2017). *Depression and Other Common Mental Disorders: Global Health Estimates*. Geneva: World Health Organization.

Zhong, B. L., Wang, Y., Chen, H. H., and Wang, X. H. (2011). Reliability, validity and sensitivity of Montgomery-Åsberg Depression Rating Scale for patients with current major depressive disorder [in Chinese]. *Chin. J. Behav. Med. Brain Sci.* 20, 85–87. doi: 10.3760/cma.j.issn.1674-6554.2011.01.032

frontiers | Frontiers in Aging Neuroscience

TYPE Review
PUBLISHED 03 March 2023
DOI 10.3389/fnagi.2023.1035376



OPEN ACCESS

EDITED BY
Zhengzhe Lan,
Zhejiang University, China

REVIEWED BY
Yuanxiang Zhang,
Wannan Medical College, China
Mei Wang,
First Affiliated Hospital of Wannan Medical College, China
Huaping Chen,
Hangzhou First People's Hospital, China
Yuan Zhang,
First Affiliated Hospital of Wannan Medical College, China

*CORRESPONDENCE
Yong Chen
✉ chenyong@cdutcm.edu.cn

†These authors have contributed equally to this work and share first authorship

SPECIALTY SECTION
This article was submitted to Alzheimer's Disease and Related Dementias, a section of the journal Frontiers in Aging Neuroscience

RECEIVED 02 September 2022
ACCEPTED 13 February 2023
PUBLISHED 03 March 2023

CITATION
Wu L, Dong Y, Zhu C and Chen Y (2023) Effect and mechanism of acupuncture on Alzheimer's disease: A review. *Front. Aging Neurosci.* 15:1035376. doi: 10.3389/fnagi.2023.1035376



# Effect and mechanism of acupuncture on Alzheimer's disease: A review

Liu Wu[1†], Yuting Dong[2†], Chengcheng Zhu[3] and Yong Chen[4*]

[1]Department of Tuina, Hospital of Chengdu University of Traditional Chinese Medicine, Chengdu, China, [2]School of Acupuncture and Tuina, Chengdu University of Traditional Chinese Medicine, Chengdu, China, [3]Department of Galactophore, Hospital of Chengdu University of Traditional Chinese Medicine, Chengdu, China, [4]Department of Emergency, Hospital of Chengdu University of Traditional Chinese Medicine, Chengdu, China

With the development trend of an aging society, Alzheimer's disease (AD) has become an urgent problem in the field of medicine worldwide. Cognitive impairment in AD patients leads to a decline in the ability to perform daily living and abnormalities in behavior and personality, causing abnormal psychiatric symptoms, which seriously affect the daily life of patients. Currently, mainly drug therapy is used for AD patients in the clinic, but a large proportion of patients will experience drug efficacy not working, and even some drugs bring severe sleep disorders. Acupuncture, with its unique concept and treatment method, has been validated through a large number of experiments and proved its reliability of acupuncture in the treatment of AD. Many advances have been made in the study of the neurobiological mechanisms of acupuncture in the treatment of AD, further demonstrating the good efficacy and unique advantages of acupuncture in the treatment of AD. This review first summarizes the pathogenesis of AD and then illustrates the research progress of acupuncture in the treatment of AD, which includes the effect of acupuncture on the changes of biochemical indicators in AD *in vivo* and the specific mechanism of action to exert the therapeutic effect. Changes in relevant indicators of AD similarly further validate the effectiveness of acupuncture treatment. The clinical and mechanistic studies of acupuncture in the treatment of AD are intensified to fit the need for social development. It is believed that acupuncture will achieve new achievements in the treatment of AD as research progresses.

KEYWORDS

**Alzheimer's disease, senile dementia, mechanism of action, acupuncture therapy, curative effect**

## Introduction

Alzheimer's disease (AD) is a chronic brain degenerative disease characterized by progressive distant and near memory impairment, decreased ability of analysis and judgment, emotional changes, behavioral disorders, and even disturbance of consciousness. it is one of the major diseases seriously endangering the health of the elderly (Pfundstein et al., 2022; Rodini et al., 2022). The etiology of AD is related to many factors. The typical pathological changes are a large number of senile plaques (SP) between nerve cells,

neurofibrillary tangles (NFTs) in nerve cells, and neuronal loss. Among all dementia patients, AD patients are the most common and account for the vast majority (about 60–70% of the total number of dementia). Autopsy studies of dementia show that 50 of 70% of the patients are AD (Aborode et al., 2022; Flores et al., 2022). Recent reports have shown that there are about 46 million AD patients worldwide, which will double every 20 years in the future. AD poses a serious threat to the health and safety of the elderly. Thirty years later, it is estimated that the global number of AD patients will reach an alarming 131.5 million. The incidence of AD was positively correlated with age, and there were more females than males. Since the 1980s, the epidemiological survey data on the prevalence of AD in various countries around the world are relatively similar, and the prevalence of dementia in people over 65 years old is about 5% (Eid et al., 2022; Kishino et al., 2022). AD is present at a higher prevalence of 20% in individuals older than 80 years, and the prevalence increases with age. The highest prevalence of AD in people aged 60 and over in Europe and North America was 5.4 and 6.4%, respectively; 4.9% in Latin America; 3.8 and 3.9% in Eastern Europe; China 4%.

At present, for this intractable type of disease, there are no effective drugs and technical means for clinical treatment given at home and abroad (Martersteck et al., 2022; Ruengchaijatuporn et al., 2022). There are currently several claims in the clinic to the related pathogenesis of Alzheimer's disease, namely the cholinergic doctrine, the tau protein hypothesis, the neurovascular doctrine, the oxidative stress doctrine, the β- Amyloid theory, the brain-gut axis theory, etc., whether brain extracellular amyloid peptide exists β (Aβ) Deposition and intracellular tau protein (Tau) hyperphosphorylation while neurofibrillary tangles are the pathological diagnostic criteria of the disease, but the exact etiology of the AD is not well understood, and an effective cure for the AD is lacking to date. AD is a multi-factor and multi-mechanism disease, which has posed a serious threat to human health. As an important part of traditional medicine, acupuncture has the characteristics of multi-target, multi-way, and multi-level functions. Similarly, there are many clinical studies on acupuncture for the treatment of AD. Li R. et al. (2020) randomized 60 AD patients into treatment and control groups, 30 each. Patients in both groups were treated with oral donepezil hydrochloride and conventional therapy. The control group was given conventional acupuncture. In the treatment group, "Fengchi," "Tianzhu," "Wangu," "Panfeng," "Fengfu," and "Zhongwan" acupoints were sampled. In the control group, they were treated with common acupuncture, including "Baihui," "Sishencong," "Intang," "Shenting," "Taixi," and "Xuanzhong" acupoints. The overall response rate was 82.1% in the treatment group and 72.4% in the control group. Moreover, cognition and memory were significantly improved after treatment.

This article reviews the recent studies on acupuncture and moxibustion in the treatment of AD at home and abroad. It is found that acupuncture can regulate the overall regulation of AD by regulating abnormal protein expression in the brain, regulating the physiological and pathological state of microglia, regulating mitochondrial autophagy, regulating epigenetic modification, giving full play to neuron protection, improving synaptic plasticity, regulating oxidative stress and regulating energy metabolism. In-depth analysis of the effect mechanism of acupuncture and moxibustion in the treatment of AD, and reveal its deep action principle, to provide a scientific and reasonable theoretical basis for clinical diagnosis and treatment of AD.

## Research status of action mechanism

### Pathways and effects of acupuncture in the treatment of AD

From the perspective of traditional Chinese medicine, neurodegenerative diseases are diseases of the brain. At present, numerous studies have shown that acupuncture at the "Baihui" acupoint can promote the treatment of encephalopathy. The acupoint selection criteria for the treatment of memory disorders, except the "Baihui" acupoint, are based on the symptoms of the brain disease itself and associated underlying diseases (de Pins et al., 2019; Li G. et al., 2019).

Acupuncture stimulation intensity and frequency are also important for the treatment of diseases. Found that high-intensity acupuncture at "Baihui," and "Dazhui" acupoints improved the learning and memory function of AD rats better than low-intensity acupuncture. Wang et al. (2020c) studied the therapeutic effects of acupuncture "Baihui" and "Shenshu" at different frequencies (50, 30, and 2 Hz) on AD rats and the underlying mechanisms. The results showed that acupuncture downregulated GSK-3β levels in the hippocampus of AD Rats, upregulated GAP-43 levels, and 50 Hz acupuncture improved learning and memory function and repaired synaptic damage in AD rats better than 30 and 2 Hz (Lin et al., 2018).

Combination drugs have also tried to improve the effect of acupuncture on memory impairment. Yang et al. (2021) explored the efficacy and mechanism of a combination of electroacupuncture at "Baihui," and "Yintang" acupoints and donepezil in the treatment of AD. The results showed that acupuncture enhanced the effect of donepezil on improving learning and memory function in AD rats and facilitated the transport of donepezil through the blood-brain barrier by regulating the expression of matrix metalloproteinase nine, low-density lipoprotein receptor-related protein one and PGP Aβ (Wegmann et al., 2018).

Acupuncture at the acupoints "Baihui," "Dazhui," and "Zusanli" combined with gastrodin in the treatment of learning and memory impairment in AD rats. Acupuncture or gastrodin both improved cognitive function and upregulated SIRT1, Bcl2, and PGC-1$\alpha$ in AD rats expression, inhibiting the expression of Bax, and protecting hippocampal neurons, but the effect of combined acupuncture and gastrodin was better than that of acupuncture or gastrodin alone. Interestingly, laser acupuncture improved cognitive impairment induced by cerebral ischemia and modulated the expression of CREB, BDNF, Bcl2, and Bax genes, exerting neuroprotective effects. In addition, some physical therapies, such as transcranial magnetic stimulation, moxibustion, massage, and rehabilitation therapy, can also improve the effect of acupuncture, which needs attention (Jiang et al., 2017; Guo et al., 2020; Hang et al., 2022).

As shown in **Figure 1**, the mechanism of action of acupuncture is closely related to the repair of synaptic plasticity in the hippocampus. This review focuses on the pathogenesis of AD (synaptic proteins, ad signature proteins, gut flora,

neuroinflammation, neuronal apoptosis, and changes in energy metabolism) and the role of acupuncture in the treatment of AD. It is also worth highlighting that synaptic plasticity in the hippocampus may be a central and common link to the above mechanisms.

## Acupuncture intervention modulates central neurotransmitter release

Neurobiochemistry reveals that amino acid neurotransmitters are hardly related to learning and memory (Al-Nasser et al., 2022). Glutamate (Glu) is the capital excitatory neurotransmitter of pyramidal neurons, which acts an essential role in learning and memory, synaptic plasticity in development, neuronal survival, and dendritic growth and degeneration. Its function is regulated by N-methyl-D-aspartate (NMDA) receptor. Long-term synaptic enhancement (LTP) is considered to be a physiological mechanism of information storage and memory formation in the brain (Khavinson et al., 2021). DMNA receptors are considered to be closely related to learning and memory due to the existence of LTP. The relationship between Glu and LTP can be summarized as follows: stimulation-> postsynaptic NMDA receptor activation-> channel opening-> $Ca^{2+}$ influx-> cell membrane depolarization-> LTP (Catarzi et al., 2007). There are excitatory amino acids and inhibitory amino acids in the brain, which play the role of neurotransmitters and act a crucial role in the process of learning and memory (Noda, 2016; Du et al., 2020).

The pathogenesis of AD associated with changes in excitatory amino acid content in brain tissue has long been demonstrated. Tang et al. (2005) used alginic acid injection to make a rat dementia model, acupuncture "Dazhui," "Shenshu," "Taixi," and "Housanli" acupoints to observe the function of acupuncture on the content of Glu and aspartic acid (Asp) in the brain of senile dementia rats. It was detected by high-performance liquid chromatography and ultraviolet spectrophotometer colorimetry. The results showed that the level of Glu and Asp in the brain tissue of the model group were significantly lower than those of the sham operation group ($P < 0.01$), suggesting that the changes in Glu and Asp contents were closely related to the pathogenesis of AD, which was consistent with the related experiment outcome (Hynd et al., 2004; Natale et al., 2006). After acupuncture and dihydroergotamine methanesulfonamide (Hydergine) treatment, the level of Glu and ASP in the brain of model rats decreased significantly ($P < 0.05$), suggesting that increasing the content of excitatory amino acids in the brain of senile dementia rats may be one of the effective mechanisms of acupuncture in the treatment of senile dementia. According to AD's glutamatergic hypothesis, the increase of synthesis and release of excitatory amino acids (EAAS), especially Glu, leads to excitatory neurotoxicity, which leads to neuronal degeneration and death is an important mechanism of AD brain degeneration (O'Neill et al., 2004). Shi and Zhuang (2020) observed the synthesis and release of EAAS in different brain regions by acupuncture at "Shuigou" and "Neiguan" acupoints of SAM-P/8 mice, the results point out that acupuncture could decrease the abnormally increased content of Glu, Asp, and glutamine, suggesting that the regulating effect of acupuncture on EAAS metabolism may be one of the important mechanisms in the treatment of AD.

## Acupuncture intervention modulates the activity of acetylcholine (ACh), acetylcholine transferase (ChAT), and acetylcholinesterase (AChE)

It has been found that the cholinergic projection system from the basal forebrain nucleus to the cerebral cortex and hippocampus is called the forebrain cholinergic system, which is closely related to advanced neural activities such as learning and memory (Zhang et al., 2022). The most obvious changes in the central cholinergic system of AD are the basal forebrain cholinergic system, including the basal nucleus of Meynert and the medial septal nucleus, which project to an extensive region of the hippocampus and cerebral cortex. About 90% of cholinergic neurons are lost in the basal forebrain of patients with AD (Li, 2022). Neurobiochemical studies have shown that Ach synthesis and ChaT activity are decreased in patients with AD, which is inextricably linked to the progression of dementia.

The degeneration of the cholinergic system in the basal forebrain may be the major cause of cognitive impairment in patients with AD (Gu and Wang, 2021; Letsinger et al., 2022). Wang and Zhou (2009) established the AD model by microinjection of Aβ1-40 into bilateral Meynert basal nuclei of rats to study the effect of acupuncture on the contents of Ach, ChAT, and AchE in the brain of AD model rats. After acupuncture at "Baihui," "Zusanli," and "Shenshu" acupoints for 1 month, to test the function of acupuncture on the synthesis and decomposition of ACh in the hippocampus and cortex, it is important to detect the activity and content of ache, ACh, and chat It was found that the activity of ChAT and the content of Ach in the cortex and hippocampus of AD rats induced by Aβ1-40 decreased significantly, while the activity of AchE increased significantly, and the rate of AchE and Ach in brain tissue increased significantly, which was consistent with AD's cholinergic theory (Vecchio et al., 2021). The outcome points out that the level of activities of Ach, ChAT, and AchE in the cortex and hippocampus in the acupuncture group were different from those in the model group ($P < 0.01$). It has been proved that acupuncture can increase the activity of ChAT, inhibits the activity of AchE, promote the synthesis of Ach, inhibit the decomposition of Ach, increases the content of Ach in brain tissue, and reverse memory loss (Reale and Costantini, 2021). Yu et al. (2021) used scopolamine injection to make a senile dementia model in rats and mice, and acupuncture at the "Yongquan" acupoint was carried out alternately for 30 days. The activity of AchE in the brain of senile dementia mice and the hippocampus of senile dementia rats were detected, respectively. The experimental demonstration that the activity of AchE in the brain of mice in the scopolamine model group was significantly lower than that in the control group ($P < 0.05$), and the brain AchE in the model group was significantly higher than that in the model group after acupuncture ($P < 0.05$). The hippocampal AchE of senile dementia model rats was significantly lower than that of the control group, and acupuncture had a significant effect on hippocampal AchE

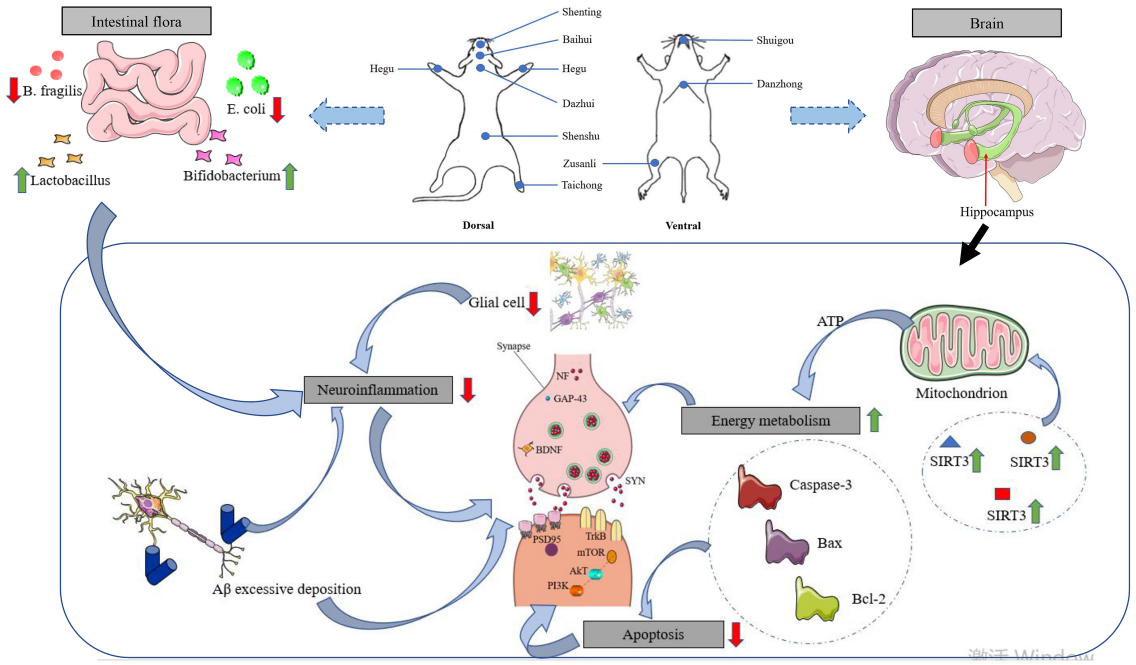


FIGURE 1
Effects of acupuncture intervention on neuroplasticity in AD pathogenesis. With the focus on synaptic plasticity in the hippocampus, the mechanisms by which acupuncture affects memory impairment are reviewed in terms of synaptic proteins, ad signature proteins, gut microflora, neuroinflammation, and energy metabolism.

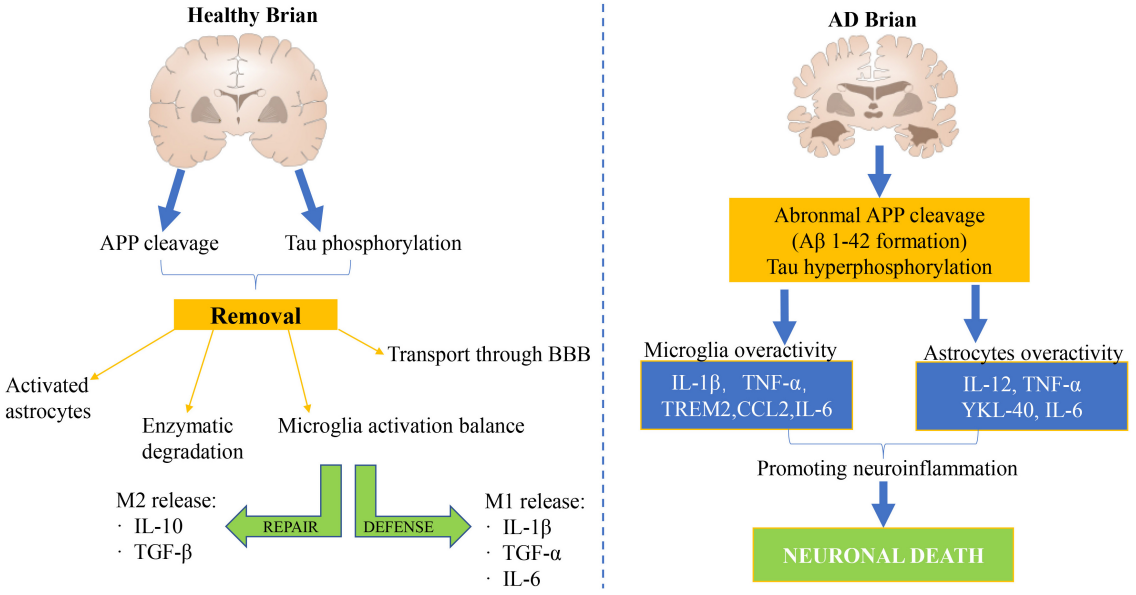


FIGURE 2
Mechanism of cerebral nerve inflammation in healthy people and patients with AD. A large number of genetic and immunological analyses have demonstrated a significant link between inflammation and AD pathology.

response of senile dementia model rats, which was significantly different from that of the model group. In a word, it is suggested that acupuncture has a significant function on the activity of acetylcholinesterase in the brain of senile dementia mice and the hippocampus of senile dementia rats (Sutalangka et al., 2013; Yang Q. et al., 2019; Zhang et al., 2019).

## Acupuncture modulates monoamine neurotransmitter release

Monoamine neurotransmitters in brain tissue include: 5-HT, NA, and DA, 5-HT are important neurotransmitters for maintaining normal intelligence. The brain system of patients with

AD was severely damaged, with an average reduction of 61% of the concentration of 5-HT in the frontal lobe (Plini et al., 2021; Tripathi and Mazumder, 2021). NA is widely projected to the entire central nervous system through axonal connections, participates in the regulation of the excited state of the entire cerebral cortex, and has a wide range of effects on arousal, sensory, emotional, and higher cognitive functions.

The activity of NA in the cerebral cortex of AD decreased significantly, and the loss of NA neurons and the change in NA activity were related to the severity of AD. Ma et al. (2020) made an AD model by microinjection of 6-hydroxydopamine into the ascending dorsal tract of NA in the rat brain, resulting in the decrease of learning and memory function in rats, which proved that the levels of central NA and DA were closely related to learning and memory. Bao and Lv (2003) used Alcl3 to replicate the senile dementia model of chronic aluminum poisoning, acupuncture at "Fengfu" acupoint for 14 days, and drug control treatment with nimodipine tablet (NM), intragastric administration once a day for 14 days (Kaur et al., 2021). The contents of monoamine neurotransmitters 5-HT, NA, and DA in brain tissue were determined, and the behavior test was carried out by a Y-type electric maze. The results showed that acupuncture at the "Fengfu" acupoint could significantly improve the memory impairment of dementia-like mice, and significantly increase the low contents of 5-HT, NA, and DA in brain tissue ($P < 0.05$). It is suggested that the mechanism of acupuncture at "Fengfu" acupoint in the treatment of senile dementia may be to increase the content of monoamine neurotransmitters in brain tissue (Von Linstow et al., 2017; Wang et al., 2018; Babić Leko et al., 2021). Zhao et al. (1999) the aged SD rats were stochastically divided into the aged group and the aged acupuncture group, the young SD rats were the young control group, and the elderly acupuncture group was treated with acupuncture at "Yongquan" acupoints of both hindlimbs alternately every other day for 30 days (Esteban et al., 2017). The results prove that the level of monoamine neurotransmitters in the brain of aged acupuncture rats and aged rats were significantly lower than that of young rats ($P < 0.05$). The content of monoamine neurotransmitters in the brain of aged acupuncture rats was significantly higher than that of aged rats ($P < 0.05$). It shows that the excitability of central nervous system activity which is closely related to learning and memory ability decreases after aging, and acupuncture can reduce the extent of its decline (Nazarali and Reynolds, 1992; Storga et al., 1996; Trabace et al., 2007; Dekker et al., 2015; Gruden et al., 2016; Vermeiren et al., 2016).

## Mechanisms of inflammatory action in the brain of patients with AD and acupuncture inhibition of inflammatory responses in brain tissue

A large number of research have demonstrated that the inflammatory mechanism acts a vital role in the pathogenesis of AD (Cheng et al., 2022; Sun et al., 2022). The neuroinflammatory mechanism of AD has been studied for more than 20 years, but it is still not fully understood. A large number of genetic and immunological analyses show that there is a significant link between inflammation and AD pathology, as shown in **Figure 2** (Wang et al., 2022). Modern medical studies have shown that the core pathological mechanism of AD is that Aβ deposition activates microglia to cause inflammation in neuroinflammatory plaques. In the early stage of inflammation, microglia express phagocytic receptors to clear Aβ (An et al., 2022). With the increase of Aβ, Aβ blocks phagocytosis receptors and makes microglia lose phagocytosis. On the contrary, microglia are activated to release inflammatory cytokines, such as IL-1β, IL-6, TNF-α, and so on. These inflammatory factors in turn activate microglia and astrocytes to produce APP and Aβ, forming a malignant positive feedback loop, resulting in a sharp increase in the amount of APP and Aβ (Yousaf et al., 2022). Recent studies have shown that cytokines IL-1 and IL-6 are not only important immune regulatory factors but also have a wide range of central regulatory effects. IL-1 is a kind of cytokine with an immunomodulatory function.

In patients with AD, IL-1 is overexpressed in the receptive area of the cerebral cortex, and the concentration in the tissue increases accordingly (Yue et al., 2022). Tang et al. (2005) used the method of chemical damage to establish the AD rat model, and selected acupoints: "Dazhui," "Shenshu," "Taixi," and "Housanli" acupoints (Wang et al., 2020c). A total of 30 days was a course of treatment. The level of IL-1 and IL-6 in rat brain tissue were tested by radioimmunoassay. The experimental results indicated that the levels of IL-1 and IL-6 in the sham operation group were significantly lower than those in the model group ($P < 0.01$), while the content of IL-1 and IL-6 in the acupuncture group and Hydergine group were significantly lower than those in the model group ($P < 0.05$), but significantly higher than those in the sham operation group ($P < 0.05$) (Cai et al., 2019). The results suggest that the increase of IL-1 and IL-6 levels in brain tissue is closely related to the pathogenesis of AD, which is consistent with the conclusions of previous studies. And acupuncture can significantly reduce the levels of IL-1 and IL-6 in the brain tissue of AD model rats, its effect is similar to that of Hydergine (Jiang et al., 2021; Liao et al., 2022). It is suggested that acupuncture can reduce the levels of IL-1 and IL-6 in the brain tissue of AD rats, which may be one of the effective mechanisms of acupuncture in the treatment of AD. Huang et al. (1998) observe the effect of acupuncture on the inflammatory reaction of AD. RT-PCR (reverse transcriptase polymerase chain reaction) was used to detect the expression of IL-1β and IL-6 in the brain of AD model rats induced by bacterial lipopolysaccharide (Li Y. et al., 2020; Wang et al., 2020b,c; Xie et al., 2021). Acupuncture can reduce the expression of IL-1β and IL-6, suggesting that acupuncture can play a therapeutic role by inhibiting the specific inflammatory reaction in the brain of AD (Fang et al., 2013; He et al., 2017; Cai et al., 2019; Wang et al., 2020a; Yang and Dong, 2020).

## Acupuncture ameliorates neuronal antioxidant damage as well as the free radical scavenging effect

Many pieces of evidence suggest that mitochondrial abnormalities are closely related to the disease. However, the significant increase in oxidative damage of neurons is limited to the cytoplasm of susceptible neurons (Aborode et al., 2022;

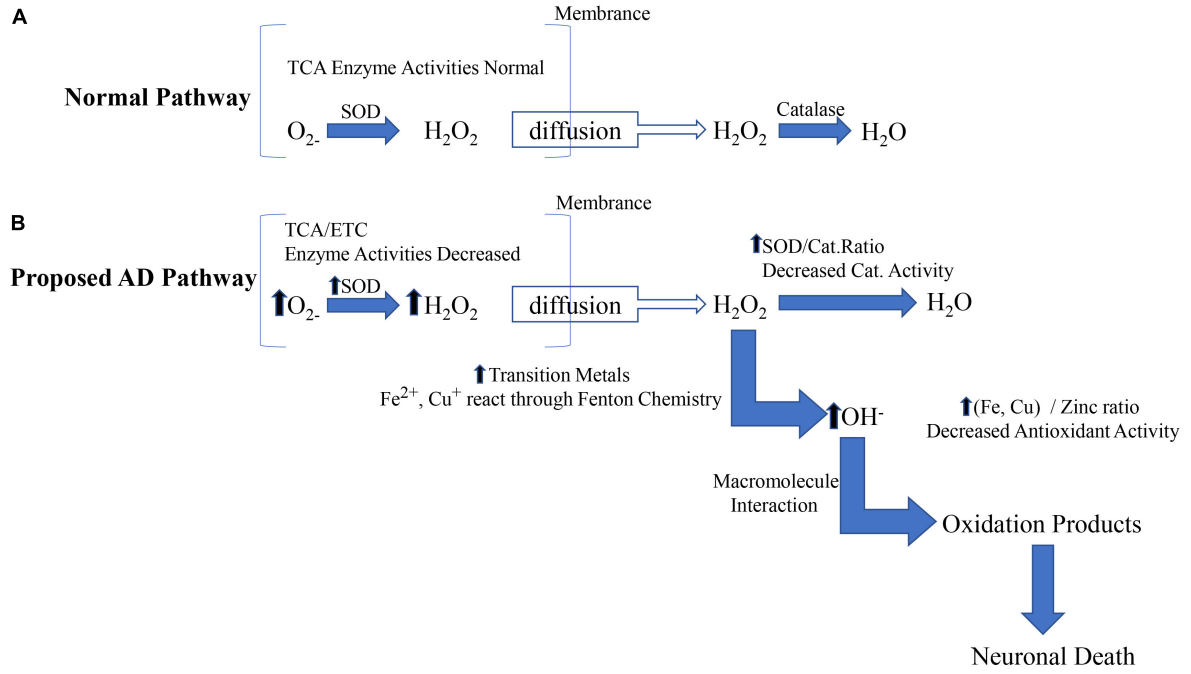


FIGURE 3
The source and mechanism of cytoplasmic oxidative damage are involved in AD. The mitochondrial (intrinsic) apoptotic pathway includes the release of proapoptotic factors located in the mitochondrial intermembrane space *via* the mitochondrial permeability transition (MPT). Once in the cytoplasm, mitochondrial proteins such as cytC, Smac/Diablo, and Omi/HtrA2 mediate caspase-dependent, whereas endog and AIF induce caspase-independent apoptosis.

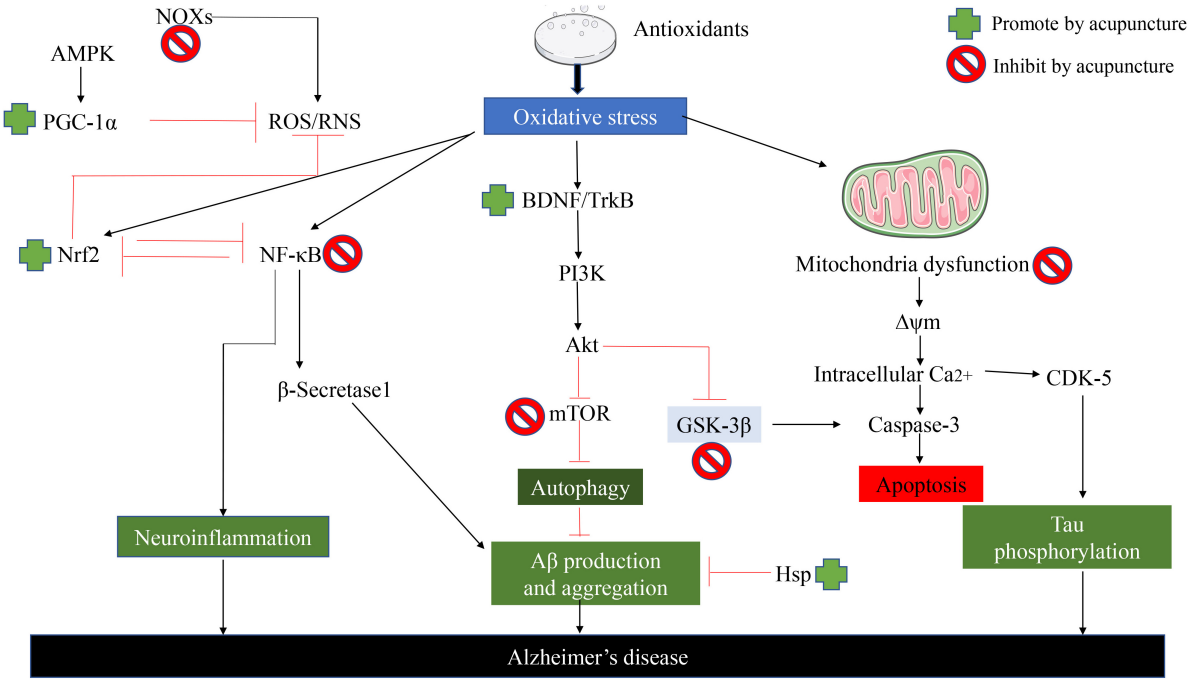


FIGURE 4
Acupuncture ameliorates AD by suppressing the effects of oxidative stress. Acupuncture can reduce oxidative stress and reduce neuroinflammation through multiple signal transduction pathways, Aβ Production, aggregation, and phosphorylation of Tau.

Beura et al., 2022; Estévez-Silva et al., 2022; Maina et al., 2022). We believe that abnormal mitochondria in susceptible neurons play a source role by providing diffusible hydrogen peroxide on the membrane to the surrounding cytoplasm, as shown in **Figure 3**. The cytoplasm is more vulnerable to hydrogen peroxide because: (1) The cytoplasm is less protected than mitochondria (Kaur et al.,

2022); (2) the catalase / SOD ratio decreased in patients with AD, thus reducing the ability to effectively scavenge hydrogen peroxide (Mesa-Herrera et al., 2022; Yoshida et al., 2022); (3) abundant oxidizing metal ions catalyze the Fenton reaction to produce highly active hydroxyl radicals. Therefore, by releasing excess hydrogen peroxide, abnormal mitochondria transmit a series of events involving rich metal ions and cause damage in the cytoplasm (Abu-Elfotuh et al., 2022).

While the current study showed that acupuncture largely improved the symptoms of AD by inhibiting oxidative stress in AD (Wu et al., 2017). As shown in **Figure 4**, it is clear to us that acupuncture specifically ameliorates oxidative stress in AD by which pathways and ways: (1) It further alleviates oxidative stress by increasing the synthesis of antioxidant components in the body, thereby reducing the generation of ROS. (2) Acupuncture exerts its effects against oxidative stress by regulating ROS-related signaling pathways and the generation of downstream proteins, thereby reducing apoptosis. (3) Acupuncture directly affects Aβ Protein generation and packing. (4) Acupuncture repairs proteins, lipids, and DNA that are directly damaged by ROS. (5) Acupuncture similarly inhibits oxidative stress by ameliorating neuroinflammation (Tain and Hsu, 2017). In addition to the specific action pathways of acupuncture described above (Nrf2/ARE related signaling pathway), acupuncture can reduce oxidative stress and reduce neuroinflammation through multiple signal transduction pathways, Aβ Production, aggregation, and phosphorylation of tau. Acupuncture can activate Nrf2 and PGC-1α, Inhibit NOx, thereby reducing ROS production. In addition, acupuncture can reverse mitochondrial dysfunction and further decrease the phosphorylation of Tau (Chang et al., 2019).

Oxidative stress acts an increasingly crucial role in the pathogenesis of AD. Lipid peroxidation is not only the inducement of cell membrane aging but also the result of cell aging (Wei et al., 2022; Xin et al., 2022). Lipid peroxidation is induced by oxygen free radicals, and the cytotoxicity of lipid peroxidation products such as MDA plays a vital role in neuronal degeneration and necrosis, leading to the occurrence and development of AD. Wang et al. (2004) used free radical theory and cholinergic theory, to explore the effects of acupuncture on antioxidation and cholinergic system function of the hippocampus and cerebral cortex of pseudo-AD rats (Chang et al., 2019). It was found that the level of MDA in the cerebral cortex of the acupuncture group was significantly lower than that of the model group ($P < 0.01$), while the activity of SOD was significantly increased ($P < 0.01$). In the determination

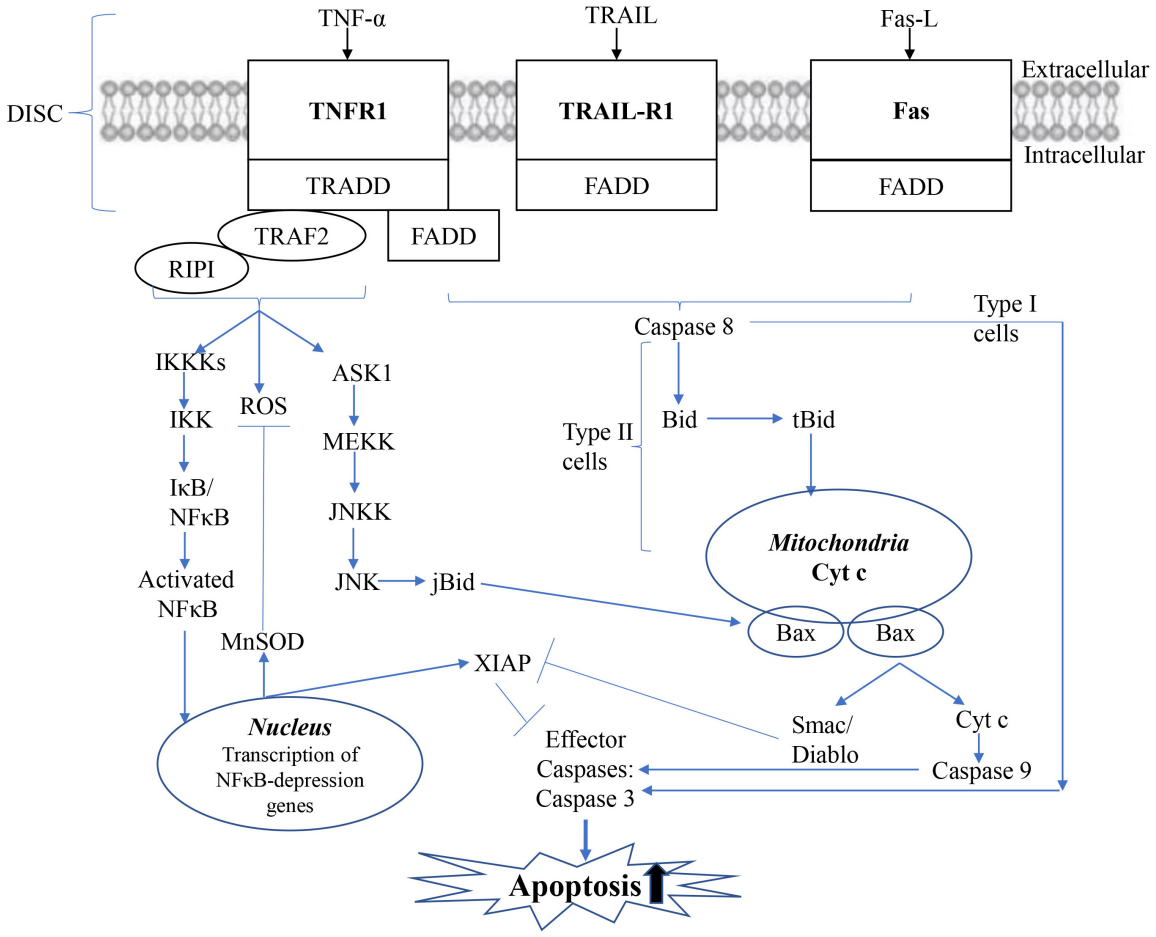


FIGURE 5
Mitochondrial apoptotic pathway. The mitochondrial (intrinsic) apoptotic pathway includes the release of proapoptotic factors located in the mitochondrial intermembrane space *via* the mitochondrial permeability transition (MPT). Once in the cytoplasm, mitochondrial proteins such as cytC, Smac/Diablo, and Omi/HtrA2 mediate caspase-dependent, whereas endog and AIF induce caspase-independent apoptosis.

of AchE, the activity of AchE in the model group was significantly lower than that in the acupuncture group ($P < 0.01$) (Yang J. et al., 2019; Zhang et al., 2019). The experimental results show that acupuncture treatment of AD may be achieved through antioxidation. Liu and Fu (2014) made an AD rat model by intraperitoneal injection of D-galactose. The effects of acupuncture at "Baihui," "Fengfu," "Shenshu," and "Xuanzhong" acupoints on the behavior and the contents of serum MDA and T-AOC in AD rats were observed. It turned out that the acupuncture group and acupuncture combined with the medicine group could prolong the latency of the step-down test, reduce the number of errors ($P < 0.05$), decrease the level of serum MDA and increase the content of T-AOC ($P < 0.05$) (Wu et al., 2017). To summarize the above results, acupuncture can improve the level of serum T-AOC, enhance the ability of antioxidation, and reduce the damage of free radicals in AD rats. Guan et al. (2001) in the observation of the effects of acupuncture at "Baihui," "Dazhui," and "Mingmen" acupoints on the level of nitric oxide (NO), MDA, and the activity of SOD in the brain tissue of subacute aging mice induced by D-galactose, the experiments proved that the level of NO and MDA in the brain tissue of subacute aging mice increased significantly, while the activity of SOD decreased significantly, which could

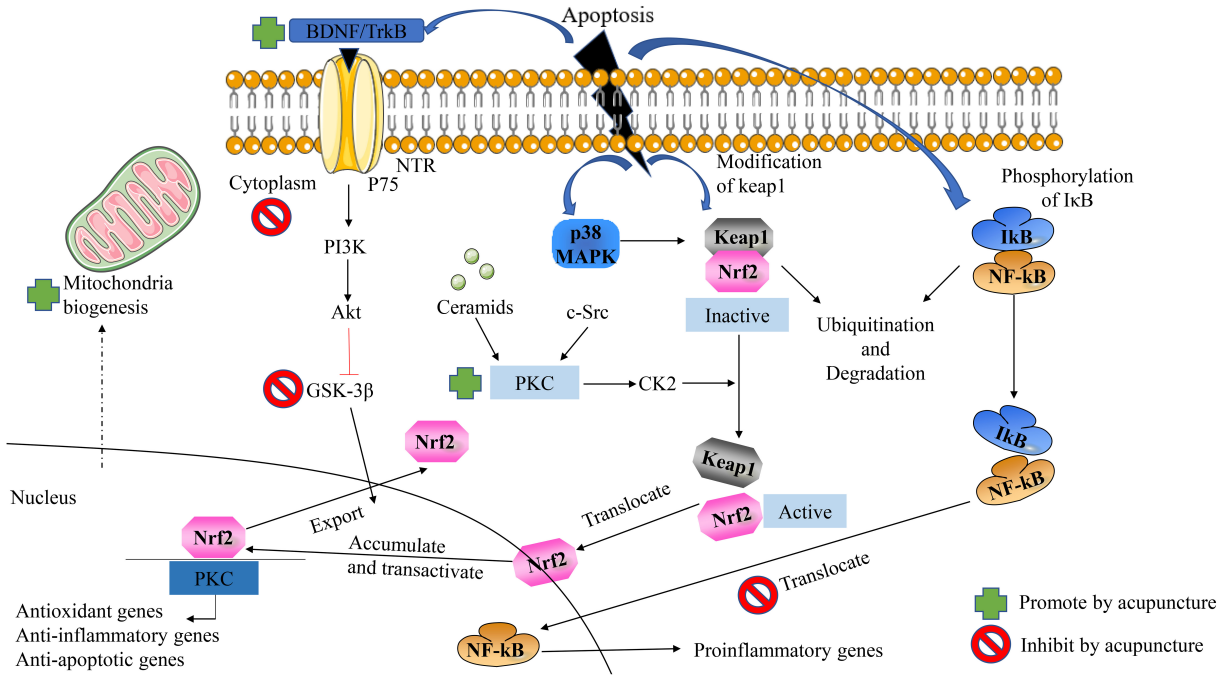


FIGURE 6
Acupuncture ameliorates neuronal apoptosis in AD by regulating the Nrf2/ARE-related pathway *in vivo*. NFκB the antioxidant effect of Nrf2 can be inhibited by blocking the area region and thereby preventing gene transcription.

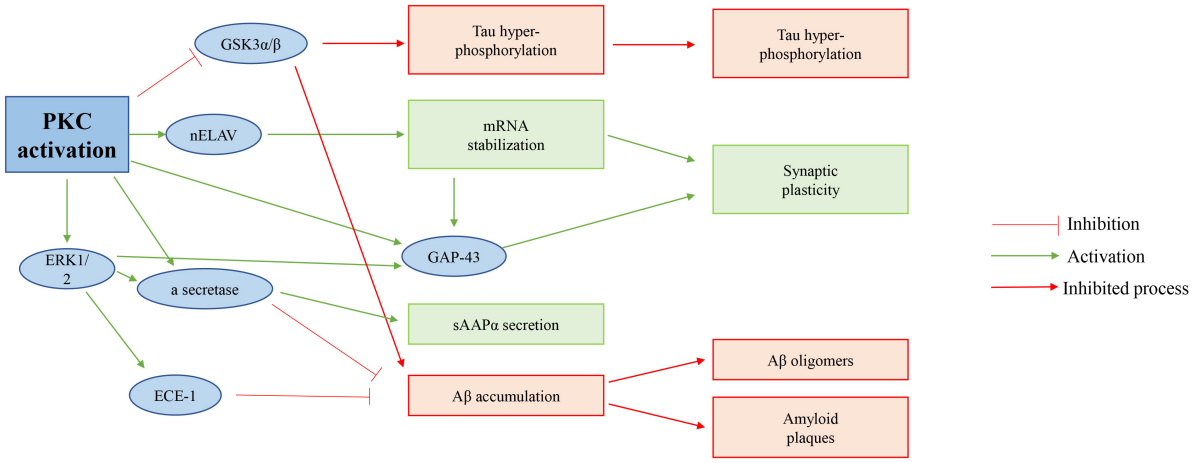


FIGURE 7
Possible role of PKC activation in AD. Activation of PKC directly inhibits GSK 3β of activity, increases APP protein processing, and in turn inhibits Tau hyperphosphorylation; And reduces Aβ accumulation of proteins.

reverse the above indexes after acupuncture, suggesting that acupuncture at "Baihui," "Dazhui," and "Mingmen" acupoints has the effect of anti-brain aging (Ye et al., 2017). Its mechanism may be related to its ability to inhibit the free radical reaction and increase the activity of antioxidant enzymes.

## Inhibition of neuronal apoptosis

Long-term experimental results proved that mitochondria are the critical factors in the early induction and regulation of apoptosis (Li Y. et al., 2022; Weber Boutros et al., 2022). Apoptotic stimuli such as DNA damage, ROS, or Fas signals mediate the death of mitochondrial cells by causing the release of small pro-apoptotic proteins generally located in the intermembrane space of the mitochondria, as shown in **Figure 5** (Xiong et al., 2022). Once in the cytoplasm, pro-apoptotic proteins such as Cytochrome c (Cyt c), mitochondrial-derived second caspase activator/low-PI direct IAP binding protein (Smac/Diablo), AIF, and endonuclease G trigger caspase-dependent or independent apoptotic death pathways. In the caspase-dependent mechanism, Cyt c binds to a junction molecule, apoptotic protein activator-1 (APAF-1), to form an apoptotic body. In the presence of ATP or dATP, Caspase 9 is recruited and activated. Caspase 9 further cleaves and activates effector Caspase 3 and/or 7, which treats substrates such as caspase-activated DNA enzyme (ICAD) or PARP, and leads to DNA fragmentation. AIF translocates to the nucleus in a caspase-independent manner, where it induces DNA fragmentation and chromatin agglutination, while ending induces internucleosomal DNA fragmentation.

It is well known that acupuncture can improve the symptoms of AD patients by inhibiting the apoptosis of nerve cells in a variety of ways and pathways, as shown in **Figure 6**. (1) On the one hand, increasing the synthesis of antioxidants, and on the other hand, reducing the generation of oxidative stress products, thereby exerting a protective effect on nerve cells. (2) Exerts anti-apoptotic effects on nerve cells by regulating ROS-related signaling pathways and the expression of downstream proteins. (3) Acupuncture inhibition α-Synuclein production as well as accelerating its clearance. The effect of acupuncture on improving neuronal apoptosis in AD *via* the Nrf2/ARE-related pathway is shown in **Figure 6** (Ebrahimi-Fakhari et al., 2016). On the other hand, we can also clearly see that acupuncture inhibits GSK-3β by upregulating the expression of BDNF, PI3K/Akt, and Protein Kinase C pathway, further increasing the nuclear translocation, accumulation, and transactivation of Nrf2. In addition, acupuncture can also exert a protective effect on nerve cells by affecting the nuclear translocation of NFkB and thereby downregulating the expression of proinflammatory genes. In addition, acupuncture also promotes

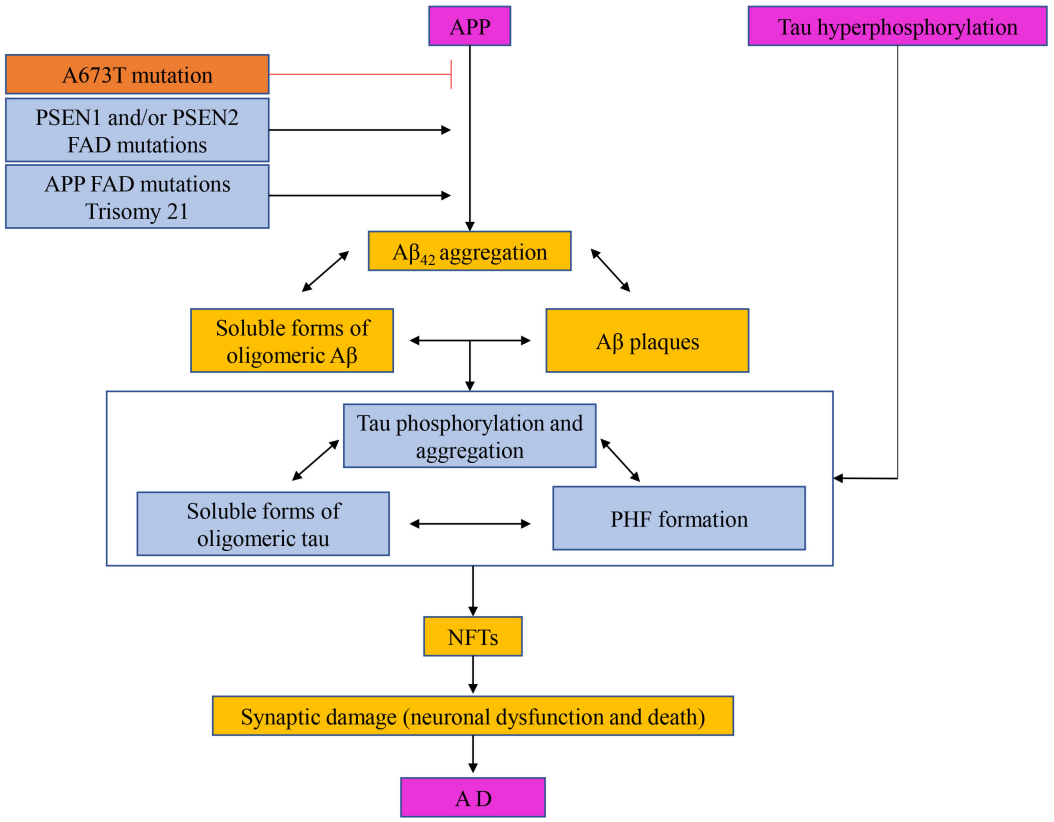


FIGURE 8
The hypothesis of amyloid cascade with the participation of tau protein. Targeting amyloid precursor secretase thereby prevents or reduces Aβ formation, clearance of amyloid deposits from the brain by active or passive immunization, and prevention or reduction of Aβ aggregation and enhancement of Aβ of clearance.

mitochondrial biogenesis. Interestingly, the effect of acupuncture on the p38 MAPK pathway has a duality (Gao et al., 2021).

Apoptosis refers to the orderly, cell-autonomous death of cells controlled by genes that maintain homeostasis (Ynag et al., 2021). The apoptosis of brain neurons in patients with AD is 30–50 times higher than that in normal subjects, resulting in a decrease in neurons in the hippocampus, basal forebrain, and neocortex, so apoptosis is one of the important reasons for the decrease in the number of neurons in AD brain tissue (Song et al., 2020; Zhang et al., 2020). It has been found that the changes in morphological structure and function of mitochondria are the key links leading to the disturbance of energy metabolism in the brain, and the disturbance of energy metabolism is closely related to the loss of AD neurons, the formation of senile plaque, nerve fiber tangles and so on. It is well known that apoptosis refers to the programmed death of cells, and as the key molecule "Bcl" of the apoptosis family, one, in turn, divides it into two categories, Bcl2 and Bax, according to the role it plays. Dong et al., found that acupuncture at the "Baihui" and "Shenting" acupoints could directly inhibit apoptosis of cells and thus ameliorate symptoms (improve memory impairment) in MCAO rats by regulating the interaction of Bax and BCL2. Huang et al. (1998) found that by acupuncture model rats (Aβ-140 stimuli) of "Baihui," "Dazhui," and "Zusanli" acupoints, which can significantly downregulate Bax protein expression in the rat hippocampus, while upregulating Bcl2 protein expression, thereby inhibiting hippocampal neuronal apoptosis (Yang et al., 2021). Zhang et al. (2017) found that acupuncture at "Baihui," "Fengfu," and "Renyu" acupoints significantly decreased the expression levels of Caspase 3 and Bax proteins in the hippocampus of model mice (APP / PS1), which exert protective effects on nerve cells, further improve the symptoms of mice (improved learning and memory ability). In addition to this, numerous studies directly point out that acupuncture exerts anti-apoptotic effects by inhibiting C-Jun amino-terminal protein kinase signaling pathway and thereby inhibiting hippocampal neuronal apoptosis in AD model mice (Huang et al., 2019).

## Activation of hippocampal protein kinase

Protein kinase (PKC) takes part in physiological processes related to cognitive ability (Yang S. et al., 2022). To some degree, PKC is included in so-called cognitive kinases (Lu et al., 2022). It regulates synaptic transmission, and several of its substrates, including Marcks, GAP-43, and NMDA receptors, take part in information processing and storage (Wu et al., 2022). For GAP-43 at least, PKC phosphorylation sites act a crucial role in regulating memory-related tasks, as shown in **Figure 7** (Yamahashi et al., 2022).

In recent years, it has been found that the dysfunction of the signal pathway in the brain of senile dementia is closely related to the decrease in the activity of protein kinase. the imbalance between the activity of protein kinase and phosphatase will lead to the hyperphosphorylation of the tau protein, which aggravates the pathological changes of senile dementia (Ortiz-Sanz et al., 2022). Traditional Chinese medicine and acupuncture have certain advantages in the treatment of senile dementia, and whether their mechanism is related to the activation of the suppressed protein kinase signal pathway in the hippocampus is worthy of in-depth study (Zou et al., 2022). Tang et al. (2005) cut off the fimbria-fornix to establish the model of senile dementia. "Baihui," "Yongquan," "Taixi," and "Xuehai" acupoints were selected in the acupuncture group. After 20 times of treatments, the contents of membrane PKC and tyrosine-protein kinase (PTK) in hippocampal tissue cells of each group were measured by radioimmunoassay (Wang et al., 2021). The results show that acupuncture may activate membrane receptors to activate protein kinases such as PKC through corresponding signal transduction pathways and participate in cell growth factor signal transduction: One may be by activating the intracellular PTK connected to it, which can take the receptor itself as the substrate and transduce the signal of tyrosine phosphorylation by PTK, which converts the growth factor signal into an intracellular signal; and maintains the normal metabolism, proliferation, and growth of cells; promote the regeneration of neurons (Li G. et al., 2019; Zheng et al., 2020). The second is that acupuncture promotes the synthesis of nerve growth factor (NGF) in the hippocampus of senile dementia rats. Together with activated PTK, activating PKC; PKC through PLC or IP3-$Ca^{2+}$ pathway can further promote protein synthesis or related gene expression necessary for the formation of learning and memory, to improve the learning and memory impairment of senile dementia (Lin et al., 2015; Zhang et al., 2017).

## Inhibition of microtubule-associated protein expression

The Aβ cascade hypothesis suggests that the treatment of AD can start with the restoration of the Aβ balance in the brain (Li Q. et al., 2019; Wang et al., 2021). Based on this, there are mainly four ways to reduce the formation of Aβ, that is, to prevent or reduce the formation of Aβ by targeting amyloid precursor secretase, to clear the deposition of amyloid in the brain by active or passive immunity, to prevent or reduce the accumulation of Aβ and to enhance the clearance of Aβ, as shown in **Figure 8** (Zhang et al., 2017).

Current research has demonstrated that the phosphorylation of tau protein is closely related to NFT and AD, and tau protein is the only essential component of NFT (Li R. et al., 2022; Yang B. et al., 2022). Hyperphosphorylation of Tau protein not only reduces its activity of promoting microtubule assembly but also further destroys microtubules by consuming normal tau protein, microtubule-associated protein MAP1, and MAP2, resulting in axoplasmic transport disorder, neuronal process breakage, neuronal degeneration and disintegration, neuronal degeneration and formation of NFT (Teja et al., 2021). Neuronal fiber degeneration caused by NFT act an essential role in the pathogenesis of AD and is parallel to the clinical dementia symptoms of AD patients (Wang et al., 2021). Jiang (2020) taking the AD model rats induced by intraperitoneal injection of D-galactose and intragastric feeding of $AlCl_3$ as the research object, acupuncture at "Baihui," "Dazhui," "Shenshu," "Zusanli," and "Taixi" acupoints (Yu et al., 2020a). The number of Tau protein-positive cells in the hippocampal CA1 region was detected by immunohistochemistry and *in situ* hybridization. The results showed that the expression of Tau protein in the hippocampal CA1 region in the acupuncture group and western medicine group was significantly lower than that in the blank group and model control

group ($P < 0.01$). It is suggested that acupuncture can prevent and treat AD by inhibiting the expression of the microtubule-associated protein Tau (Lee et al., 2009; Liu and Fu, 2014; Zhang et al., 2017; Huang et al., 2020; Ma et al., 2020; Yang et al., 2020; Yu et al., 2020b, 2021).

## Thinking and prospect

As one of the characteristic parts of nonpharmacological therapies and traditional Chinese medicine (TCM), acupuncture plays an effective defensive and therapeutic role for ad with many advantages: (1) It can obviously improve AD symptoms, green and safe with no toxic side effects; (2) Most existing studies of acupuncture have confirmed that acupuncture treatment of ad is not achieved by only one mechanism of action, but by multi-target multi-pathway intervention; (3) All derived from traditional Chinese medicine ideas, according to the characteristics of different etiological disease mechanisms combined with traditional Chinese medicine theory and acupuncture theory as a support based on acupoint selection group formula, is a new idea and method of delaying the progress of AD, and is a new way to prevent and treat AD; (4) Forming a standardized diagnosis and treatment protocol, and making clear the selection of points, operations, parameters, courses, etc., are significant for the promotion of clinical practical applications, it also needs to be continually verified and continually improved in clinical practice, aiming to enrich the means of acupuncture treatment and improve clinical efficacy.

With the development trend of social aging, AD is an urgent problem to be solved in the medical field all over the world. at present, there is no specific drug to treat this disease. Acupuncture with its unique ideas and treatment methods, through a large number of experiments, to verify the reliability of acupuncture treatment of AD. Many advances have been made in the study of the neurobiological mechanism of acupuncture in the treatment of AD, which further proves the good efficacy and unique advantages of acupuncture in the treatment of AD. Animal experiments on related indicators have been widely carried out, but there are few studies on clinical cases, which is also related to the fact that patients and their families do not pay enough attention to the disease. Strengthen the clinical and mechanism research of acupuncture and moxibustion treatment of AD to meet the needs of social development. It is believed that with the progress of research, acupuncture will make new achievements in the treatment of AD.

## Author contributions

All authors listed have made a substantial, direct, and intellectual contribution to the work, and approved it for publication.

## Funding

This work was supported in part by the Sichuan Administration of Traditional Chinese Medicine (grant no. 2020ZD003).

## Conflict of interest

The authors declare that the research was conducted in the absence of any commercial or financial relationships that could be construed as a potential conflict of interest.

## Publisher's note



## References

Aborode, A., Pustake, M., Awuah, W., Alwerdani, M., Shah, P., Yarlagadda, R., et al. (2022). Targeting oxidative stress mechanisms to treat Alzheimer's and Parkinson's disease: A critical review. *Oxid. Med. Cell. Longev.* 2022:7934442. doi: 10.1155/2022/7934442

Abu-Elfotuh, K., Al-Najjar, A., Mohammed, A., Aboutaleb, A., and Badawi, G. (2022). Fluoxetine ameliorates Alzheimer's disease progression and prevents the exacerbation of cardiovascular dysfunction in socially isolated depressed rats through activation of Nrf2/HO-1 and hindering TLR4/NLRP3 inflammasome signaling pathway. *Int. Immunopharmacol.* 104:108488. doi: 10.1016/j.intimp.2021.108488

Al-Nasser, M., Mellor, I., and Carter, W. (2022). Is L-glutamate toxic to neurons and thereby contributes to neuronal loss and neurodegeneration? A systematic review. *Brain Sci.* 12:577. doi: 10.3390/brainsci12050577

An, F., Xuan, X., Liu, Z., Bian, M., Shen, Q., Quan, Z., et al. (2022). HAnti-Inflammatory activity of 4-(4-(Heptyloxy)phenyl)-2,4-dihydro-3-1,2,4-triazol-3-one via repression of MAPK/NF-κB signaling pathways in β-amyloid-induced Alzheimer's disease models. *Molecules* 27:5035. doi: 10.3390/molecules27155035

Babić Leko, M., Hof, P., and Šimić, G. (2021). Alterations and interactions of subcortical modulatory systems in Alzheimer's disease. *Prog. Brain Res.* 261, 379–421. doi: 10.1016/bs.pbr.2020.07.016

Bao, Y., and Lv, G. (2003). Effects of acupuncture on memory impairment and monoamine neurotransmitters in demented mice. *Shang. Acupunc. J.* 7, 23–25.

Beura, S., Dhapola, R., Panigrahi, A., Yadav, P., Reddy, D., and Singh, S. (2022). Redefining oxidative stress in Alzheimer's disease: Targeting platelet reactive oxygen species for novel therapeutic options. *Life Sci.* 306:120855. doi: 10.1016/j.lfs.2022.120855

Cai, M., Lee, J., and Yang, E. (2019). Electroacupuncture attenuates cognition impairment via anti-neuroinflammation in an Alzheimer's disease animal model. *J. Neuroinflammation* 16:264. doi: 10.1186/s12974-019-1665-3

Catarzi, D., Colotta, V., and Varano, F. (2007). Competitive AMPA receptor antagonists. *Med. Res. Rev.* 27, 239–278. doi: 10.1002/med.20084

Chang, S., Guo, X., Li, G., Zhang, X., Li, J., Jia, Y., et al. (2019). Acupuncture promotes expression of Hsp84/86 and delays brain aging in SAMP8 mice. *Acupunct. Med.* 37, 340–347. doi: 10.1136/acupmed-2017-011577

Cheng, X., Wei, Y., Qian, Z., and Han, L. (2022). Autophagy balances neuroinflammation in Alzheimer's disease. *Cell. Mol. Neurobiol.* doi: 10.1007/s10571-022-01269-6 [Epub ahead of print].

de Pins, B., Cifuentes-Díaz, C., Farah, A., López-Molina, L., Montalban, E., Sancho-Balsells, A., et al. (2019). Conditional BDNF delivery from astrocytes rescues memory deficits, spine density, and synaptic properties in the 5xFAD mouse model of Alzheimer disease. *J. Neurosci.* 39, 2441–2458. doi: 10.1523/JNEUROSCI.2121-18.2019

Dekker, A., Coppus, A., Vermeiren, Y., Aerts, T., van Duijn, C., Kremer, B., et al. (2015). Serum MHPG strongly predicts conversion to Alzheimer's disease in behaviorally characterized subjects with down syndrome. *J. Alzheimers Dis.* 43, 871–891. doi: 10.3233/JAD-140783

Du, X., Li, J., Li, M., Yang, X., Qi, Z., Xu, B., et al. (2020). Research progress on the role of type I vesicular glutamate transporter (VGLUT1) in nervous system diseases. *Cell Biosci.* 10:26. doi: 10.1186/s13578-020-00393-4

Ebrahimi-Fakhari, D., Saffari, A., Wahlster, L., Di Nardo, A., Turner, D., Lewis, T. L., et al. (2016). Impaired mitochondrial dynamics and mitophagy in neuronal models of tuberous sclerosis complex. *Cell Rep.* 17, 1053–1070. doi: 10.1016/j.celrep.2016.09.054

Eid, A., Mhatre-Winters, I., Sammoura, F., Edler, M., von Stein, R., Hossain, M., et al. (2022). Effects of DDT on amyloid precursor protein levels and amyloid beta pathology: Mechanistic links to Alzheimer's disease risk. *Environ. Health Perspect.* 130:87005. doi: 10.1289/EHP10576

Esteban, G., Van Schoors, J., Sun, P., Van Eeckhaut, A., Marco-Contelles, J., Smolders, I., et al. (2017). In-vitro and in-vivo evaluation of the modulatory effects of the multitarget compound ASS234 on the monoaminergic system. *J. Pharm. Pharmacol.* 69, 314–324. doi: 10.1111/jphp.12697

Estévez-Silva, H., Cuesto, G., Romero, N., Brito-Armas, J., Acevedo-Arozena, A., Acebes, Á., et al. (2022). Pridopidine promotes synaptogenesis and reduces spatial memory deficits in the Alzheimer's disease APP/PS1 mouse model. *Neurotherapeutics* 19, 1566–1587. doi: 10.1007/s13311-022-01280-1

Fang, J., Zhu, S., Zhang, Y., Wang, F., and Zhu, Q. (2013). Effect of electroacupuncture on expression of phosphorylated P 38 MAPK and IL-1beta in frontal lobe and hippocampus in rats with Alzheimer's disease. *Zhen Ci Yan Jiu* 38, 35–39.

Flores, S., Chen, C., Su, Y., Dincer, A., Keefe, S., McKay, N., et al. (2022). Investigating tau and amyloid tracer skull binding in studies of Alzheimer disease. *J. Nucl. Med.* 64, 287–293. doi: 10.2967/jnumed.122.263948

Gao, S., Zhang, S., Zhou, H., Tao, X., Ni, Y., Pei, D., et al. (2021). Role of mTOR-regulated autophagy in synaptic plasticity related protei ns downregulation and the reference memory Deficits induced by anesthe sia/surgery in aged mice. *Front. Aging Neurosci.* 13:628541. doi: 10.3389/fnagi.2021.628541

Gruden, M., Davydova, T., Wang, C., Narkevich, V., Fomina, V., Kudrin, V., et al. (2016). The misfolded pro-inflammatory protein S100A9 disrupts memory via neurochemical remodelling instigating an Alzheimer's disease-like cognitive deficit. *Behav. Brain Res.* 306, 106–116. doi: 10.1016/j.bbr.2016.03.016

Gu, X., and Wang, X. (2021). An overview of recent analysis and detection of acetylcholine. *Anal. Biochem.* 632:114381. doi: 10.1016/j.ab.2021.114381

Guan, C., Gao, X., and Liang, J. (2001). Effects of acupuncture on nitric oxide, malondialdehyde, and superoxide dismutase in brain tissue of subacute aging mice. *Acupun. Stud.* 2, 111–113.

Guo, F., Zhang, S., Chen, S., Zhang, C., Zhang, X., Gao, F., et al. (2020). Electroacupuncture improved learning-memory ability by reducing hippoc ampal apoptosis and suppressing JNK signaling in rats with vascular dementia. *Zhen Ci Yan Jiu* 45, 21–26.

Hang, Z., Lei, T., Zeng, Z., Cai, S., Bi, W., and Du, H. (2022). Composition of intestinal flora affects the risk relationship between Alzheimer's disease/Parkinson's disease and cancer. *Biomed. Pharmacother.* 145:112343. doi: 10.1016/j.biopha.2021.112343

He, J., Liao, T., Zhong, G., Zhang, J., Chen, Y., Wang, Q., et al. (2017). Alzheimer's disease-like early-phase brain pathogenesis: Self-curing amelioration of neurodegeneration from pro-inflammatory 'Wounding' to anti-inflammatory 'Healing'. *Curr. Alzheimer Res.* 14, 1123–1135.

Huang, C., Chen, H., Qin, X., Zhou, L., and Cheng, J. (1998). Acupuncture suppresses cytokine gene expression in the brain and pituitary of aged rats. *Acupun. Stud.* 1, 24–27.

Huang, R., Gong, X., Ni, J., Jia, Y., and Zhao, J. (2019). Effect of acupuncture plus medication on expression of Bcl-2 and Bax in the hippocampus in rats with Alzheimer's disease. *Zhongguo Zhen Jiu* 39, 397–402.

Huang, X., Huang, K., Li, Z., Bai, D., Hao, Y., Wu, Q., et al. (2020). Electroacupuncture improves cognitive deficits and insulin resistance in an OLETF rat model of Al/D-gal induced aging model via the PI3K/Akt signaling pathway. *Brain Res.* 1740:146834. doi: 10.1016/j.brainres.2020.146834

Hynd, M., Scott, H., and Dodd, P. (2004). Glutamate-mediated excitotoxicity and neurodegeneration in Alzheimer's disease. *Neurochem. Int.* 45, 583–595. doi: 10.1016/j.neuint.2004.03.007

Jiang, X. (2020). Effects of acupuncture on β-AP and tau protein expression in brain tissue of rats with senile dementia. *Heilong. Univ. Chin. Med.*

Jiang, J., Liu, H., Wang, Z., Tian, H., Wang, S., Yang, J., et al. (2021). Electroacupuncture could balance the gut microbiota and improve the learning and memory abilities of Alzheimer's disease animal model. *PLoS One* 16:e0259530. doi: 10.1371/journal.pone.0259530

Jiang, L. G., Zhang, H. W., Zhang, Z., and Shao, Y. (2017). Influence of electroacupuncture stimulation with different intensities and therapeutic intervals on learning-memory ability and expression of aβ 1-40 and arginine vasopressin genes in the hippocampal CA 1 regio n in VD rats. *Zhen Ci Yan Jiu* 42, 20–24.

Kaur, S., Minhas, R., Mishra, S., Kaur, B., Bansal, Y., and Bansal, G. (2022). Design, synthesis and evaluation of benzimidazole hybrids to inhibit acetylcholinesterase and COX for treatment of Alzheimer's disease. *Cent. Nerv. Syst. Agents Med. Chem.* 22, 68–78. doi: 10.2174/1871524922666220428134001

Kaur, S., Raj, K., Gupta, Y., and Singh, S. (2021). Allicin ameliorates aluminium- and copper-induced cognitive dysfunction in Wistar rats: Relevance to neuro-inflammation, neurotransmitters and Aβ analysis. *J. Biol. Inorg. Chem.* 26, 495–510. doi: 10.1007/s00775-021-01866-8

Khavinson, V., Lin'kova, N., and Umnov, R. (2021). Peptide KED: Molecular-genetic aspects of neurogenesis regulation in Alzheimer's disease. *Bull. Exp. Biol. Med.* 171, 190–193. doi: 10.1007/s10517-021-05192-6

Kishino, Y., Sugimoto, T., Kimura, A., Kuroda, Y., Uchida, K., Matsumoto, N., et al. (2022). Longitudinal association between nutritional status and behavioral and psychological symptoms of dementia in older women with mild cognitive impairment and early-stage Alzheimer's disease. *Clin. Nutr.* 41, 1906–1912. doi: 10.1016/j.clnu.2022.06.035

Lee, M., Shin, B., and Ernst, E. (2009). Acupuncture for Alzheimer's disease: A systematic review. *Int. J. Clin. Pract.* 63, 874–879. doi: 10.1111/j.1742-1241.2009.02043.x

Letsinger, A., Gu, Z., and Yakel, J. (2022). α7 nicotinic acetylcholine receptors in the hippocampal circuit: Taming complexity. *Trends Neurosci.* 45, 145–157. doi: 10.1016/j.tins.2021.11.006

Li, G., Zeng, L., Cheng, H., Han, J., Zhang, X., and Xie, H. (2019). Acupuncture administration improves cognitive functions and alleviates inflammation and nuclear damage by regulating phosphatidylinositol 3 kinase (PI3K)/phosphoinositol-dependent kinase 1 (PDK1)/novel protein kinase C (nPKC)/Rac 1 signaling pathway in senescence-accelerated prone 8 (SAM-P8) mice. *Med. Sci. Monit.* 25, 4082–4093. doi: 10.12659/MSM.913858

Li, Q., Wu, X., Na, X., Ge, B., Wu, Q., Guo, X., et al. (2019). Impaired cognitive function and altered hippocampal synaptic plasticity in mice lacking dermatan sulfotransferase Chst14/D4st1. *Front. Mol. Neurosci.* 12:26. doi: 10.3389/fnmol.2019.00026

Li, R., Zhao, Y., and Cai, L. (2020). Effects of donepezil hydrochloride on cognitive function and oxidative stress levels in Alzheimer's disease patients. *China Pharm* 15, 382–385. doi: 10.1007/s40261-014-0235-9

Li, R., He, J., Jiang, Y., and Jia, B. (2022). Progress of experimental researches on acupuncture intervention for Alzheimer's disease based on SAMP8 mice model. *Zhen Ci Yan Jiu* 47, 466–470.

Li, Y., Wang, H., Chen, L., Wei, K., Liu, Y., Han, Y., et al. (2022). Circ_0003611 regulates apoptosis and oxidative stress injury of Alzheimer's disease via miR-383-5p/KIF1B axis. *Metab. Brain Dis.* 37, 2915–2924. doi: 10.1007/s11011-022-01051-z

Li, X. T. (2022). Alzheimer's disease therapy based on acetylcholinesterase inhibitor/blocker effects on voltage-gated potassium channels. *Metab. Brain Dis.* 37, 581–587. doi: 10.1007/s11011-022-00921-w

Li, Y., Jiang, J., Tang, Q., Tian, H., Wang, S., Wang, Z., et al. (2020). Microglia TREM2: A potential role in the mechanism of action of electroacupuncture in an alzheimer's disease animal model. *Neural Plast.* 2020:8867547. doi: 10.1155/2020/8867547

Liao, D., Pang, F., Zhou, M., Li, Y., Yang, Y., Guo, X., et al. (2022). Effect of electroacupuncture on cognitive impairment in APP/PS1 mice based on TLR4/NF-κB/NLRP3 pathway. *Zhen Ci Yan Jiu* 47, 565–572.

Lin, D., Wu, Q., Lin, X., Borlongan, C., He, Z., Tan, J., et al. (2015). Brain-derived neurotrophic factor signaling pathway: Modulation by acupuncture in telomerase knockout mice. *Altern. Ther. Health Med.* 21, 36–46.

Lin, Y., Lee, W., Wang, S., and Fuh, J. (2018). Levels of plasma neurofilament light chain and cognitive function in patients with Alzheimer or Parkinson disease. *Sci. Rep.* 8:17368. doi: 10.1038/s41598-018-35766-w

Liu, Y., and Fu, Y. (2014). Progress of experimental research on treating Alzheimer's disease by acupuncture. *Zhongguo Zhong Xi Yi Jie He Za Zhi* 34, 359–361.

Lu, N., Tan, G., Tan, H., Zhang, X., Lv, Y., Song, X., et al. (2022). Maackiain prevents amyloid-beta-induced cellular injury via priming PKC-Nrf2 pathway. *Biomed. Res. Int.* 2022:4243210.

Ma, R., Kong, L., Qi, F., He, R., Zheng, Q., Lu, W., et al. (2020). Effect of electroacupuncture on cyclin-dependent kinase 5 and Tau protein in hippocampus of SAMP8 mice. *Zhen Ci Yan Jiu* 45, 529–534.

Maina, M., Al-Hilaly, Y., Oakley, S., Burra, G., Khanom, T., Biasetti, L., et al. (2022). Dityrosine cross-links are present in Alzheimer's disease-derived tau oligomers and paired helical filaments (PHF) which promotes the stability of the PHF-core tau (297-391) in vitro. *J. Mol. Biol.* 434:167785. doi: 10.1016/j.jmb.2022.167785

Martersteck, A., Ayala, I., Ohm, D., Spencer, C., Coventry, C., Weintraub, S., et al. (2022). Focal amyloid and asymmetric tau in an imaging-to-autopsy case of clinical primary progressive aphasia with Alzheimer disease neuropathology. *Acta Neuropathol. Commun.* 10:111. doi: 10.1186/s40478-022-01412-w

Mesa-Herrera, F., Marín, R., Torrealba, E., and Díaz, M. (2022). Multivariate assessment of lipoxidative metabolites, trace biometals, and antioxidant and detoxifying activities in the cerebrospinal fluid define a fingerprint of preclinical stages of Alzheimer's disease. *J. Alzheimers Dis.* 86, 387–402. doi: 10.3233/JAD-215437

Natale, N., Magnusson, K., and Nelson, J. (2006). Can selective ligands for glutamate binding proteins be rationally designed? *Curr. Top. Med. Chem.* 6, 823–847. doi: 10.2174/156802606777057535

Nazarali, A., and Reynolds, G. (1992). Monoamine neurotransmitters and their metabolites in brain regions in Alzheimer's disease: A postmortem study. *Cell. Mol. Neurobiol.* 12, 581–587. doi: 10.1007/BF00711237

Noda, M. (2016). Dysfunction of glutamate receptors in microglia may cause neurodegeneration. *Curr. Alzheimer Res.* 13, 381–386.

O'Neill, M., Bleakman, D., Zimmerman, D., and Nisenbaum, E. (2004). AMPA receptor potentiators for the treatment of CNS disorders. *Curr. Drug Targets CNS Neurol. Disord.*3, 181–194. doi: 10.2174/1568007043337508

Ortiz-Sanz, C., Balantzategi, U., Quintela-López, T., Ruiz, A., Luchena, C., Zuazo-Ibarra, J., et al. (2022). Amyloid β / PKC-dependent alterations in NMDA receptor composition are detected in early stages of Alzheimer's disease. *Cell Death Dis.* 13:253. doi: 10.1038/s41419-022-04687-y

Pfundstein, G., Nikonenko, A., and Sytnyk, V. (2022). Amyloid precursor protein (APP) and amyloid β (Aβ) interact with cell adhesion molecules: Implications in Alzheimer's disease and normal physiology. *Front. Cell Dev. Biol.* 10:969547. doi: 10.3389/fcell.2022.969547

Plini, E., O'Hanlon, E., Boyle, R., Sibilia, F., Rikhye, G., Kenney, J., et al. (2021). Examining the role of the noradrenergic locus coeruleus for predicting attention and brain maintenance in healthy old age and disease: An MRI structural study for the Alzheimer's disease neuroimaging initiative. *Cells* 10:1829. doi: 10.3390/cells10071829

Reale, M., and Costantini, E. (2021). Cholinergic modulation of the immune system in neuroinflammatory diseases. *Diseases* 9:29. doi: 10.3390/diseases9020029

Rodini, M., De Simone, M., Caltagirone, C., and Carlesimo, G. (2022). Accelerated long-term forgetting in neurodegenerative disorders: A systematic review of the literature. *Neurosci. Biobehav. Rev.* 141:104815. doi: 10.1016/j.neubiorev.2022.104815

Ruengchaijatuporn, N., Chatnuntawech, I., Teerapittayanon, S., Sriswasdi, S., Itthipuripat, S., and Hemrungrojn, S. (2022). An explainable self-attention deep neural network for detecting mild cognitive impairment using multi-input digital drawing tasks. *Alzheimers Res. Ther.* 14:111. doi: 10.1186/s13195-022-01043-2

Shi, J., and Zhuang, P. (2020). Effects and biological mechanisms of traditional Chinese medicine (TCM) modulating the brain microenvironment to ameliorate cognitive impairment triggered by Alzheimer's disease. *Tian. Trad. Chin. Med.* 37, 475–480.

Song, Y., Xu, W., Zhang, X., and Ni, G. (2020). Mechanisms of electroacupuncture on Alzheimer's disease: A review of animal studies. *Chin. J. Integr. Med.* 26, 473–480. doi: 10.1007/s11655-020-3092-9

Storga, D., Vrecko, K., Birkmayer, J., and Reibnegger, G. (1996). Monoaminergic neurotransmitters, their precursors and metabolites in brains of Alzheimer patients. *Neurosci. Lett.* 203, 29–32. doi: 10.1016/0304-3940(95)12256-7

Sun, J., Zhang, Y., Kong, Y., Ye, T., Yu, Q., Kumaran Satyanarayanan, S., et al. (2022). Microbiota-derived metabolite Indoles induced aryl hydrocarbon receptor activation and inhibited neuroinflammation in APP/PS1 mice. *Brain Behav. Immun.* 106, 76–88. doi: 10.1016/j.bbi.2022.08.003

Sutalangka, C., Wattanathorn, J., Muchimapura, S., Thukham-Mee, W., Wannanon, P., and Tong-un, T. (2013). Laser acupuncture improves memory impairment in an animal model of Alzheimer's disease. *J. Acupunct. Meridian Stud.* 6, 247–251. doi: 10.1016/j.jams.2013.07.001

Tain, Y., and Hsu, C. (2017). Interplay between oxidative stress and nutrient sensing signaling in the developmental origins of cardiovascular disease. *Int. J. Mol. Sci.* 18:841. doi: 10.3390/ijms18040841

Tang, C., Lai, X., Lin, Z., Yang, J., Lin, J., Xian, Z., et al. (2005). Effects of Electroacupuncture on IL-1, IL-6 in brain tissue of rats with senile dementia. *J. Basic Chin. Med.* 7, 532–533.

Teja, Y., Helianthi, D., and Nareswari, I. (2021). The role of medical acupuncture therapy in Alzheimer's disease. *Med. Acupunct.* 33, 396–402. doi: 10.1089/acu.2021.0014

Trabace, L., Cassano, T., Colaianna, M., Castrignanò, S., Giustino, A., Amoroso, S., et al. (2007). Neurochemical and neurobehavioral effects of ganstigmine (CHF2819), a novel acetylcholinesterase inhibitor, in rat prefrontal cortex: An in vivo study. *Pharmacol. Res.* 56, 288–294. doi: 10.1016/j.phrs.2007.07.006

Tripathi, S., and Mazumder, P. (2021). Neuroprotective Efficacy of apple cider vinegar on zinc-high fat diet-induced mono amine oxidase alteration in murine model of AD. *J. Am. Nutr. Assoc.* 41, 658–667. doi: 10.1080/07315724.2021.1948933

Vecchio, I., Sorrentino, L., Paoletti, A., Marra, R., and Arbitrio, M. (2021). The state of the art on acetylcholinesterase inhibitors in the treatment of Alzheimer's disease. *J. Cent. Nerv. Syst. Dis.* 13:11795735211029113. doi: 10.1177/11795735211029113

Vermeiren, Y., Janssens, J., Aerts, T., Martin, J., Sieben, A., Van Dam, D., et al. (2016). Brain serotonergic and noradrenergic deficiencies in behavioral variant frontotemporal dementia compared to early-onset Alzheimer's disease. *J. Alzheimers Dis.* 53, 1079–1096. doi: 10.3233/JAD-160320

Von Linstow, C., Severino, M., Metaxas, A., Waider, J., Babcock, A., Lesch, K., et al. (2017). Effect of aging and Alzheimer's disease-like pathology on brain monoamines in mice. *Neurochem. Int.* 108, 238–245. doi: 10.1016/j.neuint.2017.04.008

Wang, L., and Zhou, L. (2009). Effects of electroacupuncture treatment on ACh, chat, and ache in Alzheimer's disease rats. *Acupunc. Clin.* 25, 40–42.

Wang, J., Zhu, X., Li, Y., Guo, W., and Li, M. (2022). Jiedu-yizhi formula alleviates neuroinflammation in AD rats by modulating the gut microbiota. *Evid. Based Comp. Alternat. Med.* 2022:4023006. doi: 10.1155/2022/4023006

Wang, S., Kang, S., and Li, A. (2004). Analysis of the correlation between the functional effects of acupuncture on the brain free radical system and the cholinergic system in rats with dementia mimicking. *Acupunct. Res.* 102–106.

Wang, Y., Wu, X., Tang, C., Xu, Y., Wang, J., Xu, J., et al. (2020c). Effect of electroacupuncture of different acupoint groups on learning-memory ability and expression of IL-1β and TNF-α in hippocampus and prefrontal cortex in rats with Alzheimer's disease. *Zhen Ci Yan Jiu* 45, 617–622. doi: 10.13702/j.1000-0607.190887

Wang, X., Li, Z., Li, C., Wang, Y., Yu, S., and Ren, L. (2020b). Electroacupuncture with Bushen Jiannao improves cognitive deficits in senescence-accelerated mouse prone 8 mice by inhibiting neuroinflammation. *J. Tradit. Chin. Med.* 40, 812–819.

Wang, L., Zhao, T., Zhou, H., Zhou, Z., Huang, S., Ling, Y., et al. (2020a). Effect of electroacupuncture on recognition memory and levels of Aβ, inflammatory factor proteins and aquaporin 4 in hippocampus of APP/PS1 double transgenic mice. *Zhen Ci Yan Jiu* 45, 431–437.

Wang, S., Yabuki, Y., Matsuo, K., Xu, J., Izumi, H., Sakimura, K., et al. (2018). T-type calcium channel enhancer SAK3 promotes dopamine and serotonin releases in the hippocampus in naive and amyloid precursor protein knock-in mice. *PLoS One* 13:e0206986. doi: 10.1371/journal.pone.0206986

Wang, Y., Zhao, L., Shi, H., Jia, Y., and Kan, B. (2021). RhoA/ROCK pathway involved in effects of Sanjiao acupuncture on learning and memory and synaptic plasticity in Alzheimer's disease mice. *Zhen Ci Yan Jiu* 46, 635–641.

Weber Boutros, S., Unni, V., and Raber, J. (2022). An adaptive role for DNA double-strand breaks in hippocampus-dependent learning and memory. *Int. J. Mol. Sci.* 23:8352. doi: 10.3390/ijms23158352

Wegmann, S., Eftekharzadeh, B., Tepper, K., Zoltowska, K., Bennett, R., Dujardin, S., et al. (2018). Tau protein liquid-liquid phase separation can initiate tau aggregation. *EMBO J.* 37:e98049. doi: 10.15252/embj.201798049

Wei, Y., Zhu, T., Jia, J., and Yan, X. (2022). Research progress on the mechanism of acupuncture intervention on Alzheimer's disease. *Zhen Ci Yan Jiu* 47, 362–368.

Wu, G., Li, L., Li, H. M., Zeng, Y., and Wu, W. C. (2017). Electroacupuncture ameliorate spatial learning and memory impairment via attenuating NOX2-related oxidative stress in a rat model of Alzheimer's disease induced by Aβ1-42. *Cell. Mol. Biol.* 63, 38–45. doi: 10.14715/cmb/2017.63.4.7

Wu, J., Yang, Y., Wan, Y., Xia, J., Xu, J., Zhang, L., et al. (2022). New insights into the role and mechanisms of ginsenoside Rg1 in the management of Alzheimer's disease. *Biomed. Pharmacother.* 152:113207. doi: 10.1016/j.biopha.2022.113207

Xie, L., Liu, Y., Zhang, N., Li, C., Sandhu, A., Williams, G. III, et al. (2021). Electroacupuncture improves M2 microglia polarization and glia anti-inflammation of hippocampus in Alzheimer's disease. *Front. Neurosci.* 15:689629. doi: 10.3389/fnins.2021.689629

Xin, Y., Wang, J., and Xu, A. (2022). Electroacupuncture ameliorates neuroinflammation in animal models. *Acupunct. Med.* 40, 474–483.

Xiong, J., Lu, D., Chen, B., Liu, T., and Wang, Z. (2022). Dimethyl itaconate reduces cognitive impairment and neuroinflammation in APPswe/PS1ΔE9 transgenic mouse model of Alzheimer's disease. *Neuromol. Med.* doi: 10.1007/s12017-022-08725-y [Epub ahead of print].

Yamahashi, Y., Lin, Y., Mouri, A., Iwanaga, S., Kawashima, K., Tokumoto, Y., et al. (2022). Phosphoproteomic of the acetylcholine pathway enables discovery of the PKC-β-PIX-Rac1-PAK cascade as a stimulatory signal for aversive learning. *Mol. Psychiatry* 27, ages3479–ages3492. doi: 10.1038/s41380-022-01643-2

Yang, B., He, M., Chen, X., Sun, M., Pan, T., Xu, X., et al. (2022). Acupuncture Effect Assessment in APP/PS1 Transgenic Mice: On Regulating Learning-Memory Abilities, Gut Microbiota, and Microbial Metabolites. *Comput. Math. Methods Med.* 2022:1527159. doi: 10.1155/2022/1527159

Yang, S., Wang, L., Xie, Z., Zeng, Y., Xiong, Q., Pei, T., et al. (2022). The Combination of Salidroside and Hedysari Radix Polysaccharide Inhibits Mitochondrial Damage and Apoptosis via the PKC/ERK Pathway. *Evid. Based Complement. Alternat. Med.* 2022:9475703. doi: 10.1155/2022/9475703

Yang, J., Wang, X., Ma, S., Yang, N., Li, Q., and Liu, C. (2019). Acupuncture attenuates cognitive impairment, oxidative stress and NF-κB activation in cerebral multi-infarct rats. *Acupunct. Med.* 37, 283–291. doi: 10.1136/acupmed-2017-011491

Yang, Q., Zhu, S., Xu, J., Tang, C., Wu, K., Wu, Y., et al. (2019). Effect of the electro-acupuncture on senile plaques and its formation in APP/PS1 double transgenic mice. *Genes Dis.* 6, 282–289. doi: 10.1016/j.gendis.2018.06.002

Yang, K., Song, X.-G., Ruan, J.-R., Cai, S.-C., Zhu, C.-F., Qin, X.-F., et al. (2021). Effect of moxibustion on cognitive function and proteins related with apoptosis of hippocampal neurons in rats with vascular dementia. *Zhong. Zhen Jiu* 41, 1371–1378.

Yang, W., and Dong, W. (2020). Mechanisms of electroacupuncture for improving Alzheimer's disease from reducing β amyloid protein level. *Zhen Ci Yan Jiu* 45, 426–431.

Yang, Y., Hu, S., Lin, H., He, J., and Tang, C. (2020). Electroacupuncture at GV24 and bilateral GB13 improves cognitive ability via influences the levels of Aβ, p-tau (s396) and p-tau (s404) in the hippocampus of Alzheimer's disease model rats. *Neuroreport* 31, 1072–1083. doi: 10.1097/WNR.0000000000001518

Ye, Y., Zhu, W., Wang, X., Yang, J., Xiao, L., Liu, Y., et al. (2017). Mechanisms of acupuncture on vascular dementia-A review of animal studies. *Neurochem. Int.* 107, 204–210. doi: 10.1016/j.neuint.2016.12.001

Ynag, J., Jiang, J., Tian, H., Wang, Z., Ren, J., Liu, H., et al. (2021). Effect of electroacupuncture on learning-memory ability and expression of IL-1β, IL-6 and TNF-α in hippocampus and spleen in mice with Alzheimer's disease. *Zhen Ci Yan Jiu* 46, 353–361.

Yoshida, N., Kato, Y., Takatsu, H., and Fukui, K. (2022). Relationship between cognitive dysfunction and age-related variability in oxidative markers in isolated mitochondria of Alzheimer's disease transgenic mouse brains. *Biomedicines* 10:281. doi: 10.3390/biomedicines10020281

Yousaf, M., Chang, D., Liu, Y., Liu, T., and Zhou, X. (2022). Neuroprotection of cannabidiol, its synthetic derivatives and combination preparations against microglia-mediated neuroinflammation in neurological disorders. *Molecules* 27:4961. doi: 10.3390/molecules27154961

Yu, C., Du, Y., Wang, S., Liu, L., Shen, F., Wang, L., et al. (2020a). Experimental evidence of the benefits of acupuncture for Alzheimer's disease: An updated review. *Front. Neurosci.* 14:549772. doi: 10.3389/fnins.2020.549772

Yu, C., Wang, J., Ye, S., Gao, S., Li, J., Wang, L., et al. (2020b). Preventive electroacupuncture ameliorates D-galactose-induced Alzheimer's disease-like pathology and memory deficits probably via inhibition of GSK3/mTOR signaling pathway. *Evid. Based Complement. Alternat. Med.* 2020:1428752.

Yu, C., He, C., Du, Y., Gao, S., Lin, Y., Wang, S., et al. (2021). Preventive electroacupuncture reduces cognitive deficits in a rat model of D-galactose-induced aging. *Neural Regen. Res.* 16, 916–923. doi: 10.4103/1673-5374.297090

Yue, Q., Song, Y., Liu, Z., Zhang, L., Yang, L., and Li, J. (2022). Receptor for advanced glycation end products (RAGE): A pivotal hub in immune diseases. *Molecules* 27:4922. doi: 10.3390/molecules27154922

Zhang, H., Wang, Y., Wang, Y., Li, X., Wang, S., and Wang, Z. (2022). Recent advance on carbamate-based cholinesterase inhibitors as potential multifunctional agents against Alzheimer's disease. *Eur. J. Med. Chem.* 240:114606. doi: 10.1016/j.ejmech.2022.114606

Zhang, J., Tang, C., Liao, W., Zhu, M., Liu, M., and Sun, N. (2019). The antiapoptotic and antioxidative stress effects of Zhisanzhen in the Alzheimer's disease model rat. *Neuroreport* 30, 628–636. doi: 10.1097/WNR.0000000000001243

Zhang, M., Xv, G., Wang, W., Meng, D., and Ji, Y. (2017). Electroacupuncture improves cognitive deficits and activates PPAR-γ in a rat model of Alzheimer's disease. *Acupunct. Med.* 35, 44–51. doi: 10.1136/acupmed-2015-010972

Zhang, S., Su, S., and Gao, J. (2020). Electroacupuncture improves learning-memory ability possibly by suppressing apoptosis and down-regulating expression of apoptosis-related proteins in hippocampus and cerebral cortex in immature mice with Alzheimer's disease. *Zhen Ci Yan Jiu* 45, 611–616.

Zhao, J., Yu, S., Zhou, Q., Wang, Z., and Wei, J. (1999). Effects of acupuncture on central neurotransmitters in aged rats and mice. *J. Cheng. Univ. Trad. Chin. Med.* 3, 30–31.

Zheng, Q., Kong, L., Yu, C., He, R., Wang, X., Jiang, T., et al. (2020). [Effects of electroacupuncture on cognitive function and neuronal autophagy in rats with D-galactose induced Alzheimer's disease]. *Zhen Ci Yan Jiu* 45, 689–695.

Zou, D., Li, Q., Pan, W., Chen, P., Sun, M., and Bao, X. (2022). A novel non-selective atypical PKC agonist could protect neuronal cell line from Aβ-oligomer induced toxicity by suppressing Aβ generation. *Mol. Med. Rep.* 25:153. doi: 10.3892/mmr.2022.12669

frontiers | Frontiers in Aging Neuroscience

TYPE Original Research
PUBLISHED 21 March 2023
DOI 10.3389/fnagi.2023.1123456



OPEN ACCESS

EDITED BY
Daojun Hong,
Nanchang University, China

REVIEWED BY
Xiaokuang Ma,
The University of Arizona College of Medicine – Phoenix, United States
Rodolfo Solís-Vivanco,
Manuel Velasco Suárez National Institute of Neurology and Neurosurgery, Mexico

*CORRESPONDENCE
Yasuo Terao
✉ yasuo.terao@gmail.com

SPECIALTY SECTION
This article was submitted to Alzheimer's Disease and Related Dementias, a section of the journal Frontiers in Aging Neuroscience

RECEIVED 14 December 2022
ACCEPTED 06 March 2023
PUBLISHED 21 March 2023

CITATION
Tokushige Si, Matsumoto H, Matsuda Si, Inomata-Terada S, Kotsuki N, Hamada M, Tsuji S, Ugawa Y and Terao Y (2023) Early detection of cognitive decline in Alzheimer's disease using eye tracking.
*Front. Aging Neurosci.* 15:1123456.
doi: 10.3389/fnagi.2023.1123456



# Early detection of cognitive decline in Alzheimer's disease using eye tracking

Shin-ichi Tokushige[1,2], Hideyuki Matsumoto[3], Shun-ichi Matsuda[4], Satomi Inomata-Terada[5], Naoki Kotsuki[2], Masashi Hamada[1], Shoji Tsuji[1,6], Yoshikazu Ugawa[7] and Yasuo Terao[1,5]*

[1]Department of Neurology, Graduate School of Medicine, The University of Tokyo, Tokyo, Japan, [2]Department of Neurology, Kyorin University, Tokyo, Japan, [3]Department of Neurology, Mitsui Memorial Hospital, Tokyo, Japan, [4]Department of Neurology, NTT Medical Center Tokyo, Tokyo, Japan, [5]Department of Medical Physiology, Kyorin University, Tokyo, Japan, [6]Institute of Medical Genomics, International University of Health and Welfare, Chiba, Japan, [7]Department of Human Neurophysiology, Fukushima Medical University, Fukushima, Japan

**Background:** Patients with Alzheimer's disease (AD) are known to exhibit visuospatial processing impairment, as reflected in eye movements from the early stages of the disease. We investigated whether the pattern of gaze exploration during visual tasks could be useful for detecting cognitive decline at the earliest stage.

**Methods:** Sixteen AD patients (age: 79.1 ± 7.9 years, Mini Mental State Examination [MMSE] score: 17.7 ± 5.3, mean ± standard deviation) and 16 control subjects (age: 79.4 ± 4.6, MMSE score: 26.9 ± 2.4) participated. In the visual memory task, subjects memorized presented line drawings for later recall. In the visual search tasks, they searched for a target Landolt ring of specific orientation (serial search task) or color (pop-out task) embedded among arrays of distractors. Using video-oculography, saccade parameters, patterns of gaze exploration, and pupil size change during task performance were recorded and compared between AD and control subjects.

**Results:** In the visual memory task, the number of informative regions of interest (ROIs) fixated was significantly reduced in AD patients compared to control subjects. In the visual search task, AD patients took a significantly longer time and more saccades to detect the target in the serial but not in pop-out search. In both tasks, there was no significant difference in the saccade frequency and amplitude between groups. On-task pupil modulation during the serial search task was decreased in AD. The number of ROIs fixated in the visual memory task and search time and saccade numbers in the serial search task differentiated both groups of subjects with high sensitivity, whereas saccade parameters of pupil size modulation were effective in confirming normal cognition from cognitive decline with high specificity.

**Discussion:** Reduced fixation on informative ROIs reflected impaired attentional allocation. Increased search time and saccade numbers in the visual search task indicated inefficient visual processing. Decreased on-task pupil size during visual search suggested decreased pupil modulation with cognitive load in AD patients,

reflecting impaired function of the locus coeruleus. When patients perform the combination of these tasks to visualize multiple aspects of visuospatial processing, cognitive decline can be detected at an early stage with high sensitivity and specificity and its progression be evaluated.

KEYWORDS

**Alzheimer's disease, cognitive decline, eye tracking, fixation, saccade, pupil**

## Introduction

In the aging population, there is an ever-increasing number of patients with Alzheimer's disease (AD), a common form of dementia characterized by progressive memory disorder (Lopez and Kuller, 2019). Along with the deposition of tau protein and amyloid-beta protein, neurodegeneration occurs in multiple brain areas such as the hippocampus, posterior cingulate gyrus, and the associative areas of the cerebral cortex in AD.

The mainstay therapy using acetylcholine esterase inhibitors and NMDA receptor antagonists is largely symptomatic and provides no real cure. New disease-modifying therapy to stop/remove the amyloid accumulation does not reverse the cognitive impairment that has already set in. Given that disease progression becomes irreversible at some stage of neurodegenerative progression (Viña and Sanz-Ros, 2018), early diagnosis is essential in the context of novel treatment strategies. Reversing cognitive decline by restoring the metabolic process at an early stage has emerged as a novel and promising measure for improving cognitive decline in AD and for improving the quality of life in patients (Bredesen, 2014; Bredesen et al., 2016). In this context, the challenge is how early we can make an accurate diagnosis, that is, at the very beginning of cognitive impairment. Conventional neuroimaging such as computed tomography (CT) and magnetic resonance imaging (MRI) can detect brain atrophy only after neurodegeneration has progressed to a certain stage. Amyloid positron emission tomography (PET) and cerebrospinal fluid tau protein may enable earlier diagnosis by detecting the accumulation of amyloid, but these tests are costly, not performed by all facilities, and only available to a limited number of patients. There is an imminent need for developing methods that can diagnose AD at its earliest stage with high sensitivity and reasonable cost.

Based on the recognition that abnormalities of eye movement appear very early in the disease course of AD, many studies have attempted to use eye movement tasks for the detection of cognitive impairment. Elementary oculomotor tasks for saccades have reported slower reaction times than controls in gap and overlap tasks (Crawford et al., 2015), latency correlating with Mini Mental State Examination (MMSE) score (Yang et al., 2013), decreased accuracy of saccades made toward the instructed target contained in presented photographs or figure sets (Boucart et al., 2014; Lenoble et al., 2015), and an increased proportion of (uncorrected directional) errors made by AD patients as compared to control subjects in antisaccade tasks, in which subjects have to make saccades in the opposite direction of the presented target (Crawford et al., 2013; Heuer et al., 2013). Studies have also demonstrated that eye tracking can be used to detect cognitive decline in AD and assess disease progression (Crawford et al., 2015; Beltrán et al., 2018, for review). Some studies have addressed more cognitive aspects of oculomotor behavior, for example, during a reading task, which involves working memory and memory retrieval function. Researchers have reported failure to recognize targets presented in the center rather than in the periphery (Vallejo et al., 2016), longer or shorter gaze duration compared with controls when reading high, medium, and low predictable sentences (Fernandez et al., 2014a, 2015a,b; Galetta et al., 2017), more fixations, and altered visual exploration while reading sentences, some with lack of context predictability (Fernandez et al., 2013, 2014b, 2015b). However, the impaired performance of patients may reflect subject responses to cognitive impairment hampering task performance that has already appeared but not as a manifestation of cognitive decline to eye movements *per se*; the very fact that patients cannot perform the required task properly is reflected in the way patients look at the targets.

While such tasks require the active cooperation of the subjects and prior knowledge from the context, eye-tracking can also provide a sensitive measure of cognitive impairment by directly looking at the exploration patterns of the eye movements themselves without explicitly giving instructions. For example, by observing the pattern of looking at presented images, we can visualize the abnormalities in attentional deployment (Delazer et al., 2018). Evidence is accumulating that the eye movement pattern can be an effective biomarker of AD. Daffner et al. (1992) compared eye movements of AD patients and control subjects while looking at pairs of regular ("congruous") and irregular ("incongruous") figures. They found that control subjects spend more time viewing irregular figures than regular ones, while AD patients viewed regular and irregular figures equally. This result suggested that AD patients' gaze reflects diminished curiosity, which can be evaluated by their eye movements. Mosimann et al. (2004) found that, when AD patients are reading clocks, their visual explorations were less focused, with fewer fixations inside the informative regions of interest (ROIs), compared to control subjects. Oyama et al. (2019) developed a cognitive assessment utilizing eye-tracking technology that showed good diagnostic performance in detecting patients with dementia, mild cognitive impairment (MCI), and control subjects. Their results demonstrate that observation of the eye movement patterns in visual exploration can be used as a biomarker of AD, although the eye movement patterns may just be the result of cognitive impairment, with subjects responding with their eyes instead of verbally. Thus, any abnormal responses in those tasks may be equal to giving wrong

verbal answers and/or responses to having made an inappropriate response or failure to respond to the question.

For the early diagnosis of cognitive impairment, subtle abnormal exploration patterns should be detected at the very beginning of the cognitive impairment, even before overt deterioration becomes apparent. In addition to memory disorder, patients with AD are known to exhibit various cognitive disorders, including a decline in visuospatial cognition, which is reflected in eye movement patterns. Even when task performance requiring a verbal response is still within the normal range, subtle cognitive impairment can manifest in the form of abnormal attentional deployment, slowed visual information processing speed, and the increased cognitive effort of the subjects when performing the tasks. Based on these premises, we have developed new methods to test visuospatial cognition by eye-tracking (Matsumoto et al., 2011a,b, 2012; Matsuda et al., 2014; Tokushige et al., 2018): a visual memory task and a visual search task. In the visual memory task, the eye movements are recorded while subjects tried to memorize figures in order to visualize the fixation pattern relating to which part of the figure was frequently seen by the subject. In the visual search task, the eye movements while searching for a target among an array of distractions is recorded, which indicates how efficiently the subject can search for the target. Contrary to clinically used cognitive tests requiring verbal responses, which subjects with dementia often fail to perform properly, these are tasks that these subjects can perform to some extent with relative ease. Eye tracking successfully revealed the abnormal visual processing in these subjects, which was correlated with the degree of cognitive decline. This method is expected to be useful in the early detection of cognitive decline in at-risk subjects in the early stage of AD by revealing multiple aspects of cognitive impairment, such as attentional allocation, visual processing, and task engagement.

It is important to note that eye tracking parameters in the visual memory and search tasks cannot be used as a direct measure of impaired cognitive (visuospatial) processing alone, or should be considered reflections of visuospatial processing, visual attention and memory. In this study, to enable early detection of cognitive decline, we aimed to evaluate the earliest changes in eye tracking patterns that occurred at the earliest stage of cognitive decline, rather than differentiating the components one by one, and studied whether these occur in correlation with the cognitive decline.

# Materials and methods

## Participants

Sixteen AD patients and sixteen control subjects were recruited (**Table 1**). Between these groups, there was no significant difference in the age (T-test, $p = 0.914$) or in the gender (Fisher's test, $p = 0.722$). The MMSE score was significantly lower in the AD group (T-test, $p < 0.001$). The diagnosis of AD was clinically made as probable AD by brain MRI and single photon emission computed tomography (SPECT), based on the revised NINCDS (National Institute of Neurological and Communicative Disorders and Stroke)-ADRDA (Alzheimer's Disease and Related Disorders Association) criteria (Dubois et al., 2007). Since positron emission tomography (PET) could not be performed, it was substituted by the results of SPECT. Patients using bilateral intraocular lenses were excluded because light reflection on the lens surface disturbed eye tracking. Patients who could not perform the tasks or could not follow the instructions to perform the tasks due to advanced cognitive decline or loss of visual acuity were also excluded. Written informed consent to participate in the study was obtained from all participants before the experiments. The experimental procedures were approved by the Ethics Committee at the University of Tokyo (No. 2411), which was conducted in accordance with the ethical standards of the Declaration of Helsinki.

TABLE 1 Summary of subjects in the visual memory task.

| | AD ($n = 16$) | Control ($n = 16$) | $p$-value |
|---|---|---|---|
| Age | 79.1 ± 7.9 | 79.4 ± 4.6 | 0.914 |
| Male/female | 8/8 | 10/6 | 0.722 |
| MMSE | 17.7 ± 5.3 | 26.9 ± 2.4 | <0.001 |

## Visual memory task

The procedure has been previously described by Matsumoto et al. (2011a,b, 2012). Briefly, subjects viewed images of various complexities [**Figure 1A**, Image 1: a clock in Western Aphasia Battery (WAB), Image 2: a house in WAB, Image 3: Rey-Osterrieth Complex Figure (Osterrieth, 1944), Image 4: a landscape in WAB] on a 17-inch computer display (1024 × 768 pixels) placed 50 cm in front of their eyes for 10 s trying to memorize them, and after the images disappeared from the screen, drew the images on a paper based on their memory. Eye movements made during task performance were recorded with video-oculography Eyelink1000® (SR Research, Mississauga, Ontario, Canada) (**Figure 1B**).

The ROIs were defined as visually salient positions that have important information in the figure and on which control subjects most frequently fixated according to the methods of Matsumoto et al. (2011a, 2012); they are indicated by blue circles in **Figure 1A** (the blue circles were invisible to the subjects). The radius of the ROI, 50 pixels in the display, corresponded to 1.9 deg in visual angle.

The accuracy of the recalled pictures drawn by the subjects was scored with the following drawing scores: images 1 and 2 (both 0–5 points) were assessed by scores in WAB, and image 3 (0–36 points) was assessed based on Osterrieth (1944). There was no scoring system for image 4, and the number of items the subjects drew was his/her drawing score. For example, if someone drew only a man and a dog, the drawing score was 2.

## Visual search tasks

We employed two visual search tasks, serial search and pop-out, as described by Matsuda et al. (2014), based on the methods of Treisman (1998). Briefly, from among an array of multiple Landolt rings arranged on the display, subjects searched for a sole target ring (target ring) with a different orientation (serial search) or different color (pop-out search) from the other rings. In the

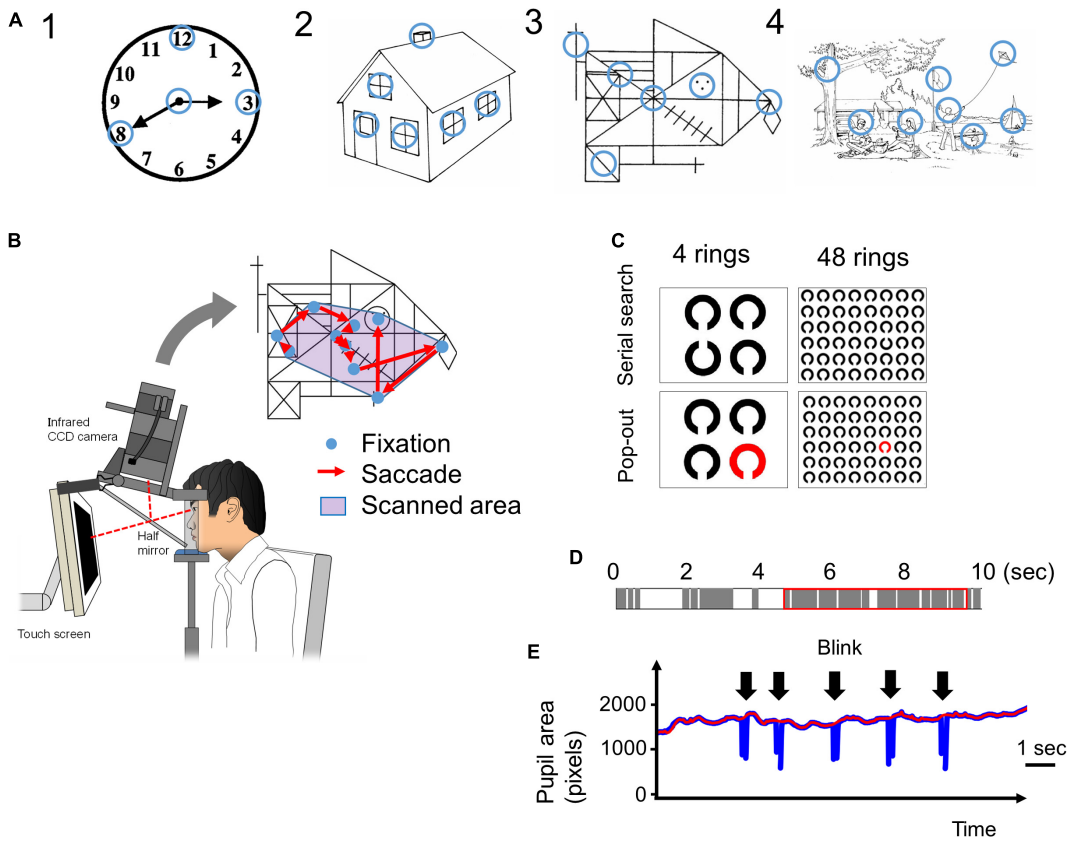


FIGURE 1

**(A)** The four images presented in the visual memory task. Blue circles, which are not visible to the subjects, indicate the informative regions of interest (ROIs) that characterize the image. We determined the locations of these informative regions based on previous studies (Mosimann et al., 2004; Matsumoto et al., 2011b). The radius of these ROIs was 1.9 deg in visual angle. **(B)** The eye-tracking system. A 17-inch computer display is placed 50 cm in front of the subject's eyes. The images are presented on the display, and the subject's eye movements (fixations and saccades) while looking at the image are recorded by the video-oculography camera (Eyelink 1000®). The scanned area is defined by the convex envelope of all fixation points. **(C)** The images used in the visual search tasks. In the serial search task, the target Landolt ring is placed upwards and others are placed downwards. In the pop-out task, the target ring is red and the others are black. In both tasks, the number of rings was 4 or 48. **(D)** An example of time distribution in 10 s while a subject is looking at an image. The gray bars indicate the fixation periods, and the white bars indicate other times (saccades, blinks, face displacements, and so on) that indicate failure of fixation. The red rectangle indicates the 5 s that include the longest total time duration of fixations. **(E)** An example of a pupil size plot during the visual search task. Pupil size data (blue line) cannot be recorded during blinks (arrow). The red line is the upper envelope of pupil size data, which is not influenced by saccades.

serial search task, the cleft of the target Landolt ring was oriented upward, whereas the other non-target Landolt rings were oriented downward. In the pop-out search task, the target Landolt ring was red while the non-target Landolt rings were black (**Figure 1C**). After detection of the target ring, the subjects were instructed to gaze at it and to press the button immediately, at which point the image disappeared from the screen. The time limit for button press was 60 s after the start of image presentation. The trial was automatically terminated in 60 s and the task proceeded to the next trial if no button was pressed.

The number of Landolt rings on the display was either 4 or 48. The number of Landolt rings determines the difficulty of the serial search task. When there are only 4 rings, it is easy to find out the target (there is even no need to search for it), but when there are 48 rings, the search is difficult so that subjects have to look at the rings one by one. Thus the effect of cognitive decline was expected to appear in the 48 ring task, but not in the 4 ring task. The selection of the numbers of stimuli were based on previous reports (Treisman and Gelade, 1980; Matsuda et al., 2014). The reason for the large difference in number of the stimuli, 4 and 48, was because we wanted to detect the slightest cognitive decline through the difference in task performance; a moderate difference in number of stimuli may result in a failure to detect the difference between groups (cognitive impaired and control subjects). By comparing the results of 4 rings task and 48 rings task, we would be able to detect the effect of dementia clearly.

Each trial was repeated 10 times with the target location randomly assigned every time. Eye movements made during task performance were recorded with video-oculography using Eyelink1000. Among the subjects participating in the visual memory task, the data of four AD patients were excluded, since they could not complete the visual search task properly, and thus the data from twelve AD patients and sixteen control subjects (**Table 2**) were analyzed. Between these groups, there was no significant difference in the age (T-test, $p = 0.785$) and in the gender (Fisher's test, $p = 0.702$). The MMSE score was significantly lower in the AD group (T-test, $p < 0.001$).

TABLE 2 Summary of subjects in the visual search task.

| | AD ($n = 12$) | Control ($n = 16$) | $p$-value |
|---|---|---|---|
| Age | 78.7 ± 7.9 | 79.4 ± 4.6 | 0.785 |
| Male/female | 6/6 | 10/6 | 0.702 |
| MMSE | 19.3 ± 3.3 | 26.9 ± 2.4 | <0.001 |

## Data processing

We used the Eyelink Data viewer software (ver1.3.37, SR Research, Mississauga, Ontario, Canada) for data processing. During the visual memory task, images were presented for 10 s for the subjects to memorize, but the pupil data could not necessarily be obtained for the entire 10 s. This was because eye tracking was sometimes truncated as a result of a variety of events, and there were periods during which the gaze and pupil size data were lost within the 10 s. These truncating events included blinks that occluded visual inputs from the camera, and displacement of the face sometimes interrupted the eye tracking transiently. Furthermore, the gaze of some subjects, especially AD patients, occasionally went outside of the display during the trials, possibly due to distraction. Figure 1D shows an example of the composition of a 10 s period during which an image was presented. The gray bars indicate periods of fixation, and the white bars indicate time periods other than fixation with pupil data loss (these included saccades, blinks, face displacements, and so on). For analysis, we took the continuous 5 s period that contained the longest summed time duration of fixation periods among the entire presentation period of 10 s (red rectangle in Figure 1D). During this 5 s period, the density of the fixation period is higher than that during the entire 10 s period, and it excludes the time period with the least pupil data. However, despite selecting the period with the longest summed fixation period, some subjects could not fixate on the images for an adequately long duration. The data of subjects who could not fixate on the screen for 3 s within the selected 5 s (in other words, when the summed durations of gray bars in the red rectangle in Figure 1D were less than 3 s) were excluded.

The total number and mean amplitude of saccades, duration of fixation, proportions of the scanned area, dwell time within ROIs, and number of ROIs fixated were measured for each figure. The subjects were considered to have fixated a ROI if the gaze (i.e., fixation point on the screen) entered the ROI circle (Figure 1A) with the radius of 50 pixels (1.9 deg in visual angle). The proportion of the scanned area was calculated by dividing the area of a minimal convex polygon enclosing all of the fixation points (Figure 1B) by the entire area of the screen. The dwell time within ROIs represents the summed duration of fixations made within the ROI during image presentation. The number of focused ROIs was the number of ROIs (Figure 1A) that the subjects' gaze entered at least once during image presentation. These parameters were calculated individually for every session in all subjects.

For the visual search tasks, in addition to the saccade number and amplitude, we measured the frequency of saccades (number of saccades made per second, counts/s) and the search time (ms), which was the time required for the subjects' eyes to finally reach the target. We judged the eyes to have reached the target when the fixation point on the display approached the center of the target, within a radius twice as large as that of the target ring. Some subjects fixated the target more than once (target re-fixation); the gaze of subjects entered the circle twice as large as the target ring, left the circle, and re-entered the circle again, which occurred more than once during the search. In such cases, the last time the fixation point entered the circle was regarded as the search time.

## Pupil size analysis

From the eye tracking data in the visual search task, we extracted the time-varying data of the pupil size at a sampling rate of 1,000 Hz. The pupil size was given by the count of pixels included within the pupil ellipse detected by the eye tracking camera. An example of a pupil size plot is shown in Figure 1E (blue line). Whenever a blink occurs, the pupil is hidden and the pupil size captured by the camera will be lost; as such, the curve temporarily goes to zero, producing a blink artifact in the pupil size plot (arrow). To compensate for this artifact by interpolating for the lost data, we made upper envelopes of the pupil size plot (Figure 1E, red line). Then we averaged the pupil size for the duration of each figure presentation in each subject. Pupil size in each trial was expressed as a ratio to the average pupil size in the first trial in each subject (pupil size ratio). These analyses of pupils were performed only for the data of serial search task, but not for the visual memory or pop-out tasks.

## Statistical assessment

The parameters of visual search were compared between AD and control subjects. In the visual memory task, for each parameter (number of saccades, saccade amplitude, duration of fixation, scanned area, dwell time in ROI, and number of focused ROIs), repeated measures two-way analysis of variance (ANOVA) was performed with the group (AD vs. control) as a between-subject factor and image (images 1–4) as a within-subject factor. Where necessary, the Greenhouse-Geisser correction was used to evaluate non-sphericity. The correlation between these parameters and the MMSE score or drawing score was assessed by the Pearson correlation coefficient with Bonferroni correction. If there was a significant difference between AD and control groups in a saccade parameter, we performed receiver operating characteristic (ROC) analyses to determine whether these parameters could efficiently differentiate these groups at certain cut-off values.

In the visual search task, each parameter (search time, number of saccades, saccade frequency, and saccade amplitude) was averaged across the images (1–10) for each subject, and compared between AD and control subjects using the $t$-test. Again, the correlation between these parameters and the MMSE score was assessed by the Pearson correlation coefficient with Bonferroni correction. As in the visual memory task, if there was a significant difference between AD and control groups in a saccade parameter, we also performed ROC analyses to determine whether these parameters could effectively differentiate these groups.

The pupil size ratio in the visual search task (serial search), averaged for images 1 to 10, was compared between AD and control subjects using the $t$-test. The correlation between the pupil size

ratio and the MMSE score was assessed by the Pearson correlation coefficient. As in the experiments above, if there was a significant difference between these groups, we performed ROC analyses to determine how efficient this parameter was for the differentiation of these groups.

# Results

## Visual memory task

The results of the visual memory task are shown in Figure 2. Figure 2A shows a representative example of reproduced figures. AD patients tended to be poorer at reproducing any of the images than control subjects. Mann-Whitney's U-test showed that the drawing scores were significantly lower in AD patients for the images (bottom figures of Figure 1; Image 1, AD 2.81 ± 1.38, control 4.75 ± 0.77, $p < 0.001$; Image 2, AD 1.88 ± 1.09, control 3.56 ± 0.81, $p < 0.001$; Image 4, AD 1.69 ± 1.66, control 5.94 ± 2.77, $p < 0.001$) except for image 3, in which the difference showed a trend (AD 3.25 ± 2.58, control 5.19 ± 3.04, $p = 0.057$). For all of the presented images, the drawing score showed a significant positive correlation with MMSE score (Image 1: $R = 0.621$, $p < 0.001$, Image 2: $R = 0.602$, $p < 0.001$, Image 3: $R = 0.548$, $p = 0.00116$, Image 4: $R = 0.682$, $p < 0.001$).

The number of saccades while viewing the images is compared in Figure 2B. Repeated measures two-way ANOVA indicated that the effect of the group ($F[1, 23] = 0.0482$, $p = 0.828$), the image ($F[3, 69] = 0.865$, $p = 0.464$), or their interaction ($F[3, 69] = 0.407$, $p = 0.749$) was not significant, showing that both AD patients and control subjects made a similar number of eye movements (saccades) while viewing the images.

Figure 2C compares the saccade amplitude while viewing the images. The effect of the image (repeated measures two-way ANOVA: $F[3, 69] = 3.11$, $p = 0.0320$) was significant, while the effects of the group ($F[1, 23] = 0.0054$, $p = 0.942$) and their interaction ($F[3, 69] = 0.884$, $p = 0.454$) were not, which suggested that the saccade amplitude depends on the image presented; this did not differ between AD patients and control subjects.

Figure 2D compares the average duration of fixation between the AD patients and control subjects. The effect of the group (repeated measures two-way ANOVA: $F[1, 23] = 0.640$, $p = 0.432$), the image ($F[3, 69] = 1.60$, $p = 0.197$), or their interaction ($F[3, 69] = 1.02$, $p = 0.390$) did not reach significance. This implied that the duration of fixation in AD patients was not significantly different from that of control subjects, regardless of the image viewed.

Figure 2E depicts the total area scanned by the gaze while subjects viewed the images. The scanned area of AD patients appeared to be smaller than that of control subjects. However, by repeated measures two-way ANOVA, the effect of the group (repeated measures two-way ANOVA: $F[1, 23] = 0.760$, $p = 0.393$), the image ($F[3, 69] = 0.839$, $\varepsilon = 0.681$, $p = 0.441$), and their interaction ($F[3, 69] = 0.231$, $\varepsilon = 0.681$, $p = 0.799$) did not reach significance, showing that the total area scanned by the subjects' gaze of AD patients was comparable to that of control subjects across the images presented.

We also compared the dwell time of the gaze within the ROIs (Figure 2F), which refers to the length of time the subjects' gaze stayed within the informative ROIs of each image (blue circles in Figure 1A). Repeated measures two-way ANOVA showed that the effects of the group ($F[1, 23] = 0.382$, $p = 0.543$) or image ($F[3, 69] = 0.704$, $p = 0.553$) were not significant, while their interaction ($F[3, 69] = 2.99$, $p = 0.0370$) was. This suggested that AD patients and control subjects differed in their dwell time within ROIs of different images; AD patients' gaze spent more time within the ROIs while viewing simple images while control subjects' gaze dwelled more in the ROIs while viewing complex images, as depicted in the bar graph for images 1 and 4 in Figure 2F.

The number of ROIs fixated, that is, the number of informative ROIs that their eyes entered within a certain distance (see section "Materials and methods") at least once, is compared in Figure 2G. Here, the effect of the group ($F[1, 23] = 5.42$, $p = 0.0291$) reached significance, but the effect of the image ($F[3, 69] = 2.21$, $\varepsilon = 0.717$, $p = 0.117$) or their interaction ($F[3, 69] = 1.50$, $\varepsilon = 0.717$, $p = 0.234$) did not. This indicated that AD patients look at a smaller number of informative ROIs than control subjects do. AD patients collect information from a smaller number of ROIs within the images compared to control subjects, although subjects in both groups explored each image for the same duration of time and their eye fixation time and saccade frequency made per unit time was similar (Figures 2B, D).

Since AD patients tended to focus on a smaller number of informative ROIs than control subjects, we tested whether this feature could be used to differentiate AD patients from control subjects by ROC analysis (Figure 2H). When the cut-off value was set to 3.125, the sensitivity was 1.0 and the specificity was 0.538.

Table 3 shows the correlation between the drawing score and the saccade parameters. We performed Bonferroni correction with the significance level of $p$ value set at 0.003125, i.e., 0.05 divided by the number of comparisons 16. According to this criterion, none of the parameter significantly correlated with the drawing score. Table 4 shows the correlation between the MMSE score and saccade parameters; again, there were no significant correlations after Bonferroni correction ($p > 0.003125$).

## Visual search task

The results of the visual search task are shown in Figure 3, and the results of the $t$-test are summarized in Table 5. In the serial search task with 4 rings, AD patients required significantly more time and a larger number of saccades to search for the target, while the saccade frequency and amplitude showed no significant difference between AD patients and control subjects. A similar trend was also noted in the serial search task with 48 rings, where AD patients required significantly more time and number of saccades although there was no significant difference in the saccade frequency or amplitude compared to control subjects.

In the pop-out task with 48 rings, there was no significant difference in the search time, saccade counts, frequency, or amplitude between AD patients and control subjects. In the pop-out task with 4 rings, AD patients required more saccades to arrive at the target, but there was no significant difference in the search time, saccade frequency, or amplitude between the two groups.

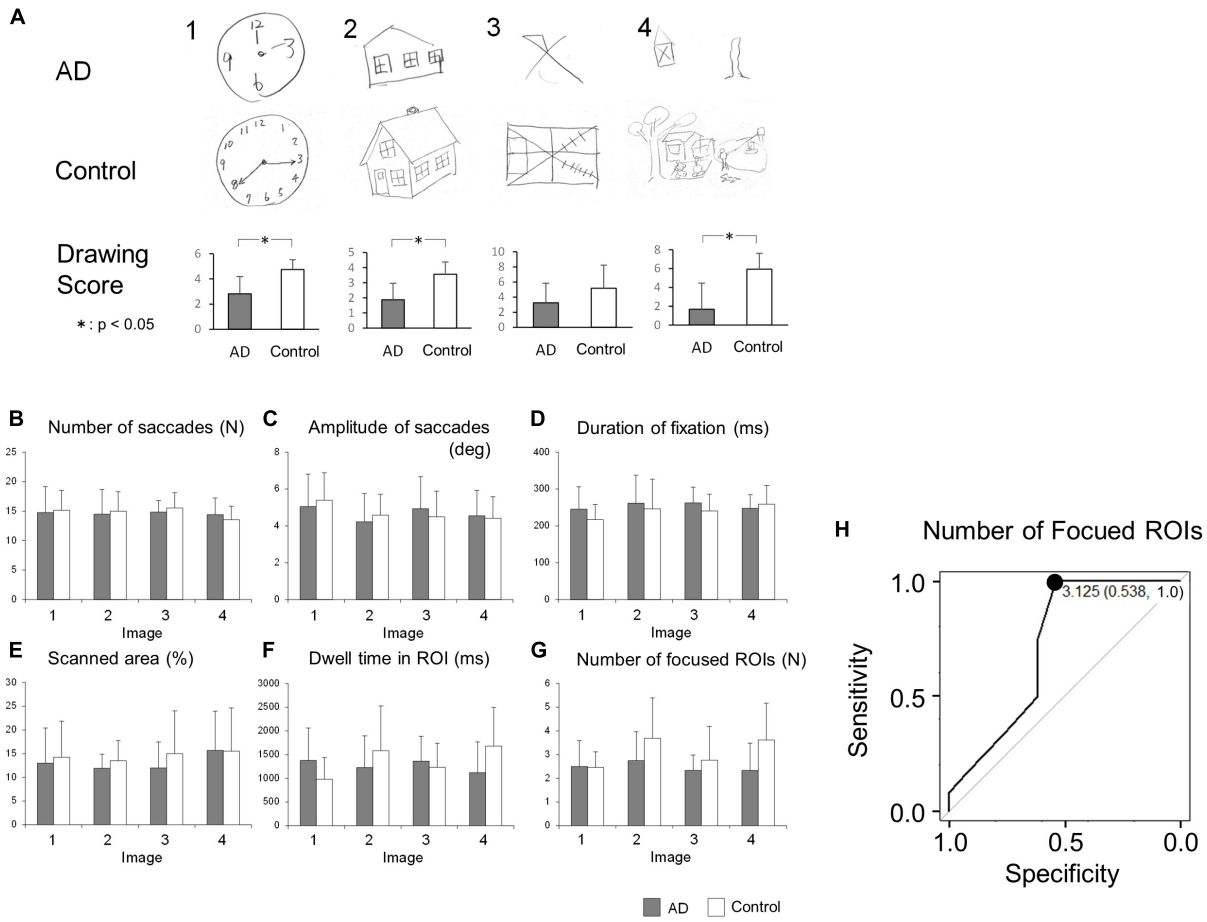


FIGURE 2
**(A)** The result of image drawing of the visual memory task. Examples of images drawn by AD patients and control subjects are shown. The drawing scores tended to be lower in AD patients. **(B–G)** Comparison of saccade parameters in the visual memory task between AD patients and control subjects. By repeated measures two-way ANOVA, the difference between these groups was significant only in panel **(G)** the number of focused ROIs (see the text). **(H)** The ROC analysis of the number of focused ROIs, averaged for images 1-4. When the cut-off was set to 3.125, the sensitivity was 1.0 and the specificity was 0.538. *$p < 0.05$.

TABLE 3 The correlation between the drawing score and saccade parameters in the visual memory task.

| | Image 1 | | Image 2 | | Image 3 | | Image 4 | |
|---|---|---|---|---|---|---|---|---|
| | *R* | *p* value | *R* | *p* value | *R* | *p* value | *R* | *p* value |
| Number of saccades | 0.0685 | 0.714 | −0.026 | 0.893 | 0.0935 | 0.623 | −0.162 | 0.400 |
| Amplitude of saccades | −0.0739 | 0.693 | 0.00641 | 0.974 | 0.00244 | 0.99 | 0.0623 | 0.748 |
| Duration of fixation | −0.269 | 0.143 | −0.0773 | 0.690 | −0.158 | 0.403 | 0.240 | 0.210 |
| Scanned area | 0.137 | 0.462 | 0.462 | 0.0116 | 0.204 | 0.278 | 0.0707 | 0.716 |
| Dwell time in ROI | −0.342 | 0.0598 | 0.242 | 0.205 | 0.0529 | 0.781 | 0.269 | 0.158 |
| Number of focused ROIs | −0.0985 | 0.598 | 0.334 | 0.0769 | 0.254 | 0.176 | 0.369 | 0.0486 |

Table 6 shows the correlations between the MMSE score and saccade parameters in the visual search task. Here again, we performed Bonferroni correction with the significance level of *p* value set at 0.003125. The search time and the number of saccades showed a significant negative correlation with the MMSE score in the serial search tasks ($p < 0.001$), but not in the pop-out tasks. Saccade frequency and amplitude did not correlate significantly with the MMSE score in any of the tasks.

Since the search time and the number of saccades in the serial search task showed significant differences between the AD and control groups, we performed ROC analyses to determine whether these parameters can effectively differentiate the groups by setting certain cut-off values. Figure 4 shows the results of the ROC analyses. Whereas both the search time and the number of saccades effectively differentiate these groups, the search time performed better. In the 4 ring task, when the cut-off time was set at 1070.6 ms,

10.3389/fnagi.2023.1123456

TABLE 4 The correlation between the MMSE score and saccade parameters in the visual memory task.

| | Image 1 | | Image 2 | | Image 3 | | Image 4 | |
|---|---|---|---|---|---|---|---|---|
| | *R* | *p* value | *R* | *p* value | *R* | *p* value | *R* | *p* value |
| Number of saccades | −0.0346 | 0.854 | −0.0965 | 0.619 | 0.00824 | 0.966 | −0.334 | 0.0761 |
| Amplitude of saccades | 0.0784 | 0.675 | 0.0774 | 0.690 | 0.0262 | 0.891 | 0.0421 | 0.828 |
| Duration of fixation | 0.0471 | 0.801 | 0.0456 | 0.814 | −0.0638 | 0.737 | 0.344 | 0.068 |
| Scanned area | −0.220 | 0.234 | 0.158 | 0.414 | 0.029 | 0.879 | 0.0353 | 0.856 |
| Dwell time in ROI | −0.298 | 0.104 | 0.231 | 0.228 | −0.165 | 0.384 | 0.233 | 0.225 |
| Number of focused ROIs | −0.306 | 0.0936 | 0.348 | 0.0641 | 0.111 | 0.558 | 0.315 | 0.096 |

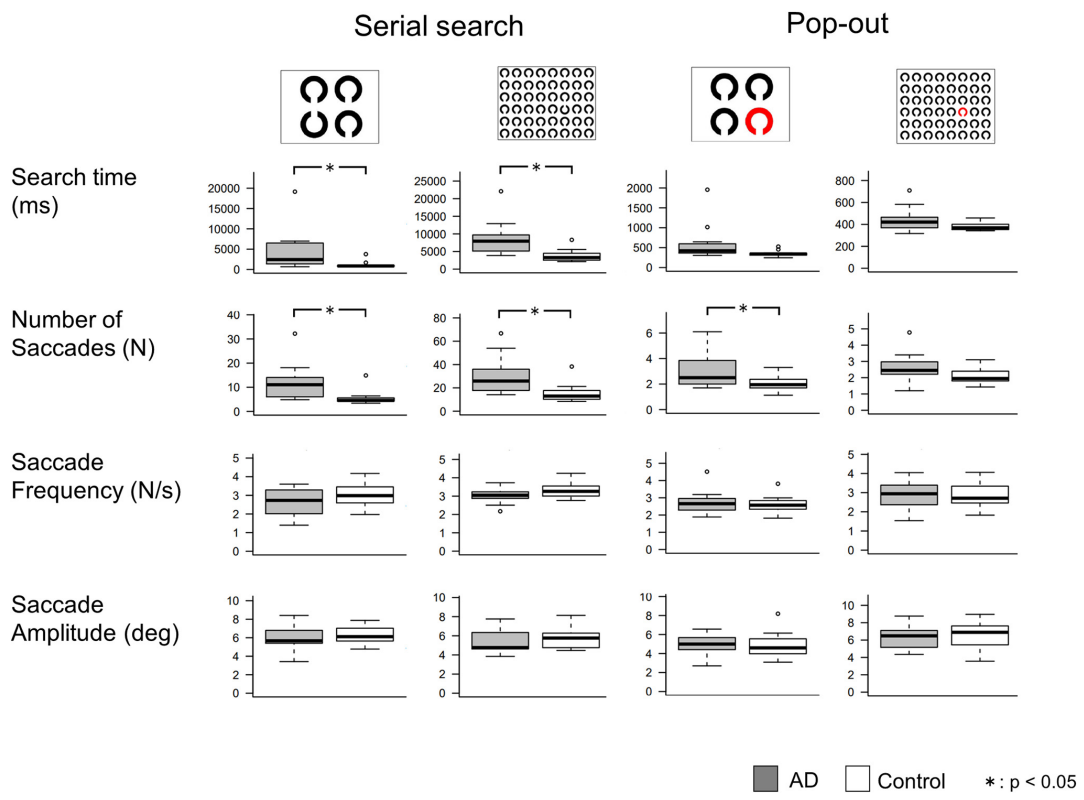


FIGURE 3
Comparisons of saccade parameters in the visual search tasks. *T*-test shows that AD patients required significantly longer search time and more saccades than control subjects, mainly in the serial search task. $^*p < 0.05$.

the sensitivity was 0.917 and the specificity was 0.875. In the 48 ring task, when the cut-off time was set at 3775.106 ms, the sensitivity of the search time was 1.0 and the specificity was 0.688. The results of ROC analysis on the number of saccades were as follows: in the 4 ring task, the sensitivity was 0.75 and the specificity was 0.938 when the cut-off value was 6.45; and in the 48 ring task, the sensitivity was 1.0 and the specificity was 0.625 when the cut-off value was 14.

## Pupil size analysis

Figure 5A shows the change in pupil size in AD patients and control subjects in sequential tasks, which was expressed as a ratio (pupil size ratio) calculated by dividing the mean pupil size during the current by its baseline value, that is, the mean pupil size in the first task for each subject. The pupil size ratio of AD patients was lower than that of control subjects, especially when the number of Landolt rings was 48.

Figure 5B compares the mean pupil size ratio of AD patients and control subjects in the 4 and 48 ring tasks (upper figures) and shows the correlation between the pupil size ratio and the MMSE score (lower figures). In the 4 ring task, the pupil size ratio did not differ significantly between AD patients and control subjects (*t*-test, $p = 0.135$). There was no significant correlation between the pupil size ratio and the MMSE score ($R = 0.338$, $p = 0.0788$). However, in the 48 ring task, the pupil size ratio of AD patients was significantly smaller than that of control subjects (*t*-test, $p = 0.00569$). There was

TABLE 5 The *p* values of T-test of saccade parameters between AD patients and control subjects in the visual search task.

| | Serial search | | Pop-out | |
|---|---|---|---|---|
| | 4 rings | 48 rings | 4 rings | 48 rings |
| Search time | 0.0383* | 0.0059* | 0.0839 | 0.0823 |
| Number of saccades | 0.016* | 0.00878* | 0.0255* | 0.0780 |
| Saccade frequency | 0.169 | 0.0773 | 0.563 | 0.801 |
| Saccade amplitude | 0.515 | 0.389 | 0.943 | 0.571 |

*$p < 0.05$.

a significant positive correlation between the pupil size ratio and the MMSE score ($R = 0.608$, $p < 0.001$).

Since the pupil size ratio in the 48 ring serial search task differed significantly between the AD and the control group, we performed ROC analysis to differentiate these groups using this parameter (**Figure 5C**). When the cut-off value was set at 0.962, the sensitivity was 0.5, the specificity was 1.0, and the area under the curve was 0.771.

# Discussion

In this study, we analyzed the eye movements of AD patients and control subjects performing visual memory and search tasks. In the visual memory task, while saccade parameters such as the frequency or amplitude of saccades did not differ significantly between the two groups, AD patients fixated fewer informative ROIs in the images, even when there was sufficient time to do so. This resulted in a poorer recall of the memorized images, which deteriorated with cognitive decline. In the visual search task, AD patients needed to make more saccades and spent more time before finding the target than control subjects, whereas, again, the saccade frequency (per unit time) and amplitude did not differ significantly from control subjects. The pupil size analysis in the visual search task showed that pupils of control subjects increased in size accumulatively as they performed consecutive trials of the visual search task with 48 rings, although this was not observed in AD patients. Taking these measures together, our visual scanning task could successfully characterize and detect the dysfunction of visuospatial processing in AD patients with high sensitivity and specificity, and could thus become a new biomarker for the early diagnosis and evaluation of cognitive decline.

## Impaired deployment of attention and reduced recall of memory in AD patients

We gather visual information from the outer world by making repeated saccades and fixations on a scene, paying particular attention to the informative areas. Thus, deploying visual attention efficiently over a scene, whether bottom-up or top-down, is important to collect visual information from the scene. In the visual memory task, AD patients became increasingly impaired at recalling the line drawings as cognitive decline progressed; AD patients also tended to view a smaller number of informative, visually salient ROIs in the images during the visual memory task compared to control subjects (**Figure 2G**).

Perceptual salience may emerge mainly under low task constraints, such as during free viewing or scene memorization, as used in this task. For example, when we look at someone's face, our fixation points are concentrated on the eyes, nose, or mouth, and the contour of these components, but not much on the skin in between (Yarbus, 1967). In exploring a scene, subjects may selectively direct attention to objects using both bottom-up, image-based saliency cues or top-down, task-dependent cues (Itti and Koch, 2001). In the bottom-up mode, the gaze is drawn automatically to visually salient regions of the scene. The visually salient and less salient positions, respectively, form a peak and trough in the salience map, and the visually salient locations draw bottom-up attention and saccades toward that location during visual exploration. Instead, in the top-down mode, the ROIs are not visually salient, and the viewer would have to actively deploy their gaze, and possibly their attention as well, over the scene. If subjects fail to pay attention to the informative areas, they would fail to collect visual information from the outer world efficiently, and hence have a lower drawing score. The duration of fixations on individual objects within a scene is shown to affect later recall of the same object (Chapman, 2005).

The inability of AD patients to pay attention to the informative areas of what they are viewing has been reported using a clock reading task. Mosimann et al. (2004) demonstrated that the visual exploration of AD patients was less focused, with fewer fixations on the task-relevant ROIs (the numbers on the clock surface pointing to the time of the clock) compared to control subjects. Normally, while visual search does not leave a memory of its trajectory, an inhibition-of-return mechanism acts on the already-selected locations, and should promote looking at unseen locations of the images (Bridgeman et al., 1975; Horowitz and Wolfe, 1998). Their study and ours both demonstrated that AD patients are poorer at allocating attention broadly to all of the informative areas, even when they had sufficient time to do so, suggesting a restriction in attentional deployment.

AD patients were taking AD medicine (mainly acetylcholinesterase inhibitors such as donepezil). Although the effect of AD drugs on visual memory or search tasks remains to be clarified, a previous study showed that donepezil improves visual working memory performance (Reches et al., 2014). In view of this result, the medicines may have improved the performance of visual memory or search tasks. Even considering this potential drug effect, the performance of the patients was demonstrated to be lower than the age-matched control subjects.

The performance of AD patients may be compared to Parkinson's disease (PD) patients who also showed reduced area of scanning when viewing similar scenes for later recall. PD patients were more restricted in the area scanned within the image, which resulted from reduced saccade amplitude and lower frequency of saccades compared to control subjects (Matsumoto et al., 2011b; Terao et al., 2013). Notably, the performance of PD patients characterized by reduced saccade frequency and amplitude, presumably caused by basal ganglia dysfunction, was most deviated from control subjects for less complex figures, and approached control performance for more complex figures. This improvement in saccade performance was explained by "ocular" kinesie paradoxale, in which the reduced scanning area became

TABLE 6 The correlation between the MMSE score and the saccade parameters in the visual search task.

| | Serial search | | | | Pop-out | | | |
|---|---|---|---|---|---|---|---|---|
| | 4 rings | | 48 rings | | 4 rings | | 48 rings | |
| | *R* | *p* value | *R* | *p* value | *R* | *p* value | *R* | *p* value |
| Search time | −0.664 | <0.001* | −0.752 | <0.001* | −0.298 | 0.123 | −0.371 | 0.0521 |
| Number of saccades | −0.671 | <0.001* | −0.738 | <0.001* | −0.348 | 0.0695 | −0.194 | 0.323 |
| Saccade frequency | 0.289 | 0.136 | 0.134 | 0.496 | 0.0342 | 0.863 | −0.0427 | 0.829 |
| Saccade amplitude | 0.067 | 0.735 | 0.242 | 0.215 | −0.220 | 0.260 | −0.0397 | 0.841 |

*$p < 0.003125$ (Bonferroni correction).

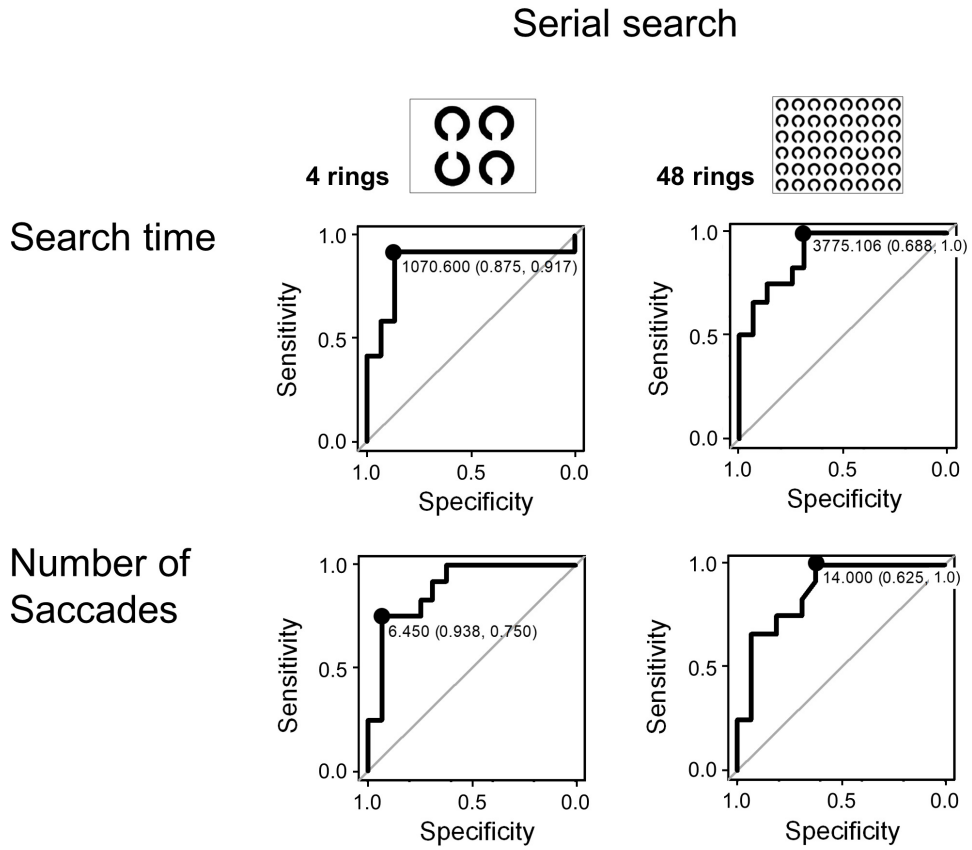


FIGURE 4
The ROC analysis of search time and number of saccades in the visual search task (serial search).

closer to control since PD patients could use the visual cues contained in the figures as a guide to improve the frequency and size of ocular movements (Matsumoto et al., 2011b, 2012), and the smaller scanning area of the images became comparable to control subjects. In contrast, the saccade amplitude and frequency in AD patients was similar to that of control subjects, suggesting that the underlying pathophysiology for the reduced scanning area was different from that of PD patients. Thus, the restriction in attentional deployment may result from dysfunction of the visuospatial processing in the cerebral cortex and working memory in patients, rather than from abnormal basic saccade control by the basal ganglia and/or brainstem. The saccade amplitude of AD patients was not significantly different from that of control subjects (**Figure 2C**).

ROC analysis for the visual memory task showed that the number of ROIs viewed showed a high sensitivity but low specificity for cognitive decline (**Figure 2H**), which can be used as a screening method for AD diagnosis, but not for ruling out subjects with a preserved cognitive functions.

## Inefficient visual processing in AD patients

In the serial but not pop-out visual scanning task, AD patients required more saccades and more time than control subjects before they could detect the target, in both the 4 and 48 ring tasks (**Figure 3**). In AD patients, the search time and number

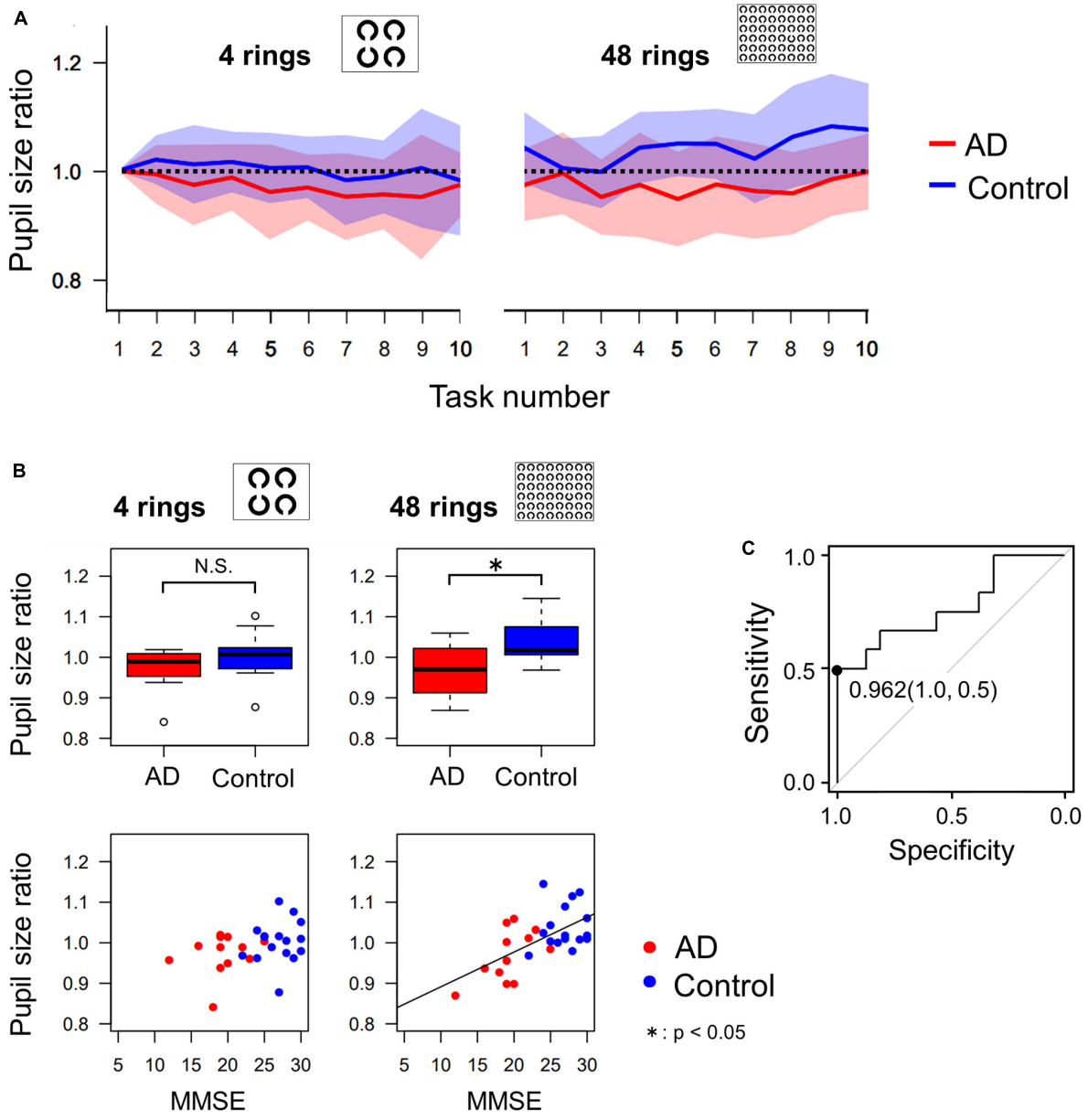


FIGURE 5
**(A)** The change of pupil size ratio during the serial search task as the task progressed. The red and blue lines indicate the average data of AD patients and control subjects, respectively, and the width of the color bars around the red or blue lines indicate their standard deviations. The pupil dilatation of AD patients tended to be less than that of control subjects, especially in the 48 ring task. **(B)** Comparison of pupil size ratio averaged across all 10 images (4 rings or 48 rings) between AD and control groups, which shows that pupil dilatation of AD patients is significantly less than that of control subjects in the 48 ring task, by *t*-test. The correlation between the MMSE score and the pupil size ratio was significant only in the 48 ring task. **(C)** The ROC analysis of the pupil size ratio in the 48 ring task. When the cut-off value is set to 0.962, the sensitivity was 0.5 and the specificity was 1.0. *$p < 0.05$.

of saccades correlated negatively with the MMSE score, that is, it increased with the progression of cognitive decline (Table 6), whereas saccade frequency and amplitude stayed almost constant with disease progression. Thus, the increased search time with increased number of saccades indicated that visual search was inefficient in AD patients. These results are consistent with those of previous studies that showed a relatively preserved single-feature search as opposed to a more impaired feature-conjunction search in AD (Cormack et al., 2004; Hao et al., 2005; Viskontas et al., 2011; Landy et al., 2015; see Ramzaoui et al., 2018 for review). These findings translate here to preserved bottom-up, involuntary engagement of attention (pop-out task) and deficits in top-down, voluntary attention (serial search task).

As in the visual memory task, subjects repeatedly made saccades and fixations during the visual search task to search for the target, but in the visual search task, guidance was also made largely from bottom-up perceptual guidance. The visual search strategy was initially likened to a serial scanning process in which task subjects must judge what he/she is currently looking at every time they look (overt attention) or the covert attentional window

which captures the object included in the search array, either the target or the distractor (Findlay and Gilchrist, 2005). If the subjects recognize that the object that they overtly captured by eye movement or covertly scanned by the attentional window is the target, the search is terminated without further saccade processing. On the other hand, if the subjects judge that they are looking at the distractor, they have to start programming another saccade to the next potential target. In this successive process, the visual search may occur in three stages: (1) judgment of the object as the target or the distractor, (2) seeking out the candidate location for the next potential saccade, and (3) programming and initiation of the saccades. This model posits a covert attentional window (if not the gaze or central visual field themselves) that is scanning the array of objects, including the target and the distractors. However, this model proved to be unable to explain all of the visual search findings to date (see Findlay and Gilchrist, 2005 for review). First, there does not appear to be any apparent discontinuity in the search time between serial and pop-out searches. Second, for large search arrays, there was a close correlation between search time and the number of saccades made before the target is located, and it appears implausible for a rapid attentional scan to be operative with each fixation to seek out the candidate location for the next saccades' destination within the fixation period of around 200 ms. Thus, the prevailing view is a hybrid of parallel processing within each fixation with serial saccade scanning. Items closer to fixation and similar to the target will tend to have higher salience in the saliency map and be more likely to be selected as a next target. If the prolonged search time of AD patients comes from impaired saccade programming, the saccade frequency of AD patients must differ from that of control subjects, which was not the case (**Figure 3**). The longer search time of AD patients may thus arise from the defect in constructing a proper salience map rather than the serial overt or covert attentional scan being defective, because there was no significant difference in the saccade parameters (frequency and amplitude) between AD patients and control subjects.

Problems in low-level visual processes have been reported among the earliest symptoms in AD (Armstrong, 2009; Kirby et al., 2010; Verheij et al., 2012). While AD patients show high reliance on guidance from perceptual features (or saliency, i.e., preserved performance in the pop-out task), they exhibit difficulty in locating targets when target contrast or texture difference with the background was reduced, as in the case of a serial search task with many objects. However, understandably, these tasks tax the cognitive function of AD patients and the difficulty of accomplishing the task itself may affect the gaze pattern during visual search. Our present task did not require much effort on the part of patients, and most of the AD patients could complete the task without much difficulty. Thus, behavioral change was not the result of the subjects being unable to search for the target, but rather, was due to delayed visual scanning caused by inefficient visual processing in the patients.

The inefficient visual search was already compromised in AD patients at an early stage. Remarkably, ROC analysis showed that search time and number of saccades made until target detection in the 48 ring task achieved a high sensitivity (100%, **Figure 4**) and specificity. These measures also showed a significant correlation with the MMSE score (**Table 6**). Because of its high sensitivity and specificity, the search time and saccade number in the visual search task can be effective in detecting subjects sensitively.

## Pupil dilation during visual search in AD patients

In control subjects, accumulating evidence indicates a link between pupil size and visual attention, in which the pupil diameter gets more enlarged as the cognitive load required for task performance increases (Gabay et al., 2011; Geng et al., 2015; Salvaggio et al., 2022). Pupil dilation with performance of the visual search task can be interpreted in terms of the cognitive demand required. Searching for a target from among 48 rings was a more cognitively demanding task than searching from among 4 rings, and required sustained and concentrated visual attention the task-related dilation of pupils during the visual search task was not as prominent as that of control subjects, which was observed in the 48 ring task but not in the 4 ring task (**Figures 5A, B**).

Pupil size modulation is important in the context of AD or even MCI, since task-related pupil dilation reflects the activity of the locus coeruleus (LC), which is one of the initial sites of subcortical tau deposition in early stage AD (Braak et al., 2011). According to Aston-Jones and Cohen (2005), LC neurons exhibit two modes of activity, phasic and tonic. Phasic LC activation is driven by the outcome of task-related decision processes and facilitates strategies for ensuing behaviors and to help optimize task performance (exploitation). Phasic LC activity regulates cortical encoding of salience information, which would be beneficial for the target detection (Vazey et al., 2018). When the utility of exploitation decreases, LC neurons exhibit a tonic activity mode, facilitating disengagement from the current task and switching to an alternative behavior (exploration).

In this context, modulation of pupillary responses is reported as a potential sensitive indicator for early risk for MCI and AD risk prediction, and even as a midlife indicator of risk for AD (Granholm et al., 2017; Kremen et al., 2019). This compensatory enhancement of task-related pupil dilation was observed in the context of a short-memory task such as the digit span. This task required more effort on the side of patients, and can be a response to not being able to memorize and recall properly, or even failed rehearsal of memorized digits during the memorization. Enhanced task-related pupil dilation may represent a compensatory effort to maintain performance through attentional engagement in the exploration mode, especially in amnestic MCI subjects; amnestic MCI patients may exert more effort in performing the task because they are closer to their maximum capacity for compensation (Riediger et al., 2006; Stern et al., 2018). In contrast, our task was performed more easily by most subjects participating and did not incur working memory or executive function, requiring less effort on the part of subjects. The task may be performed more 'automatically' or 'subconsciously' in the exploitation mode, and the task-related pupil dilation was diminished rather than enhanced in AD patients, which may reflect dysfunction of the LC. The modulation also showed a strong correlation with the MMSE score. Since the pupil size modulation in our task exhibited a high selectivity but low sensitivity, it can be useful for confirming diagnosis of dementia rather than screening of dementia in general public.

## Limitations of the study

There are some limitations in our study. First, the statistical power we obtained was relatively weak, which implies that we cannot apply our present experimental procedure directly to the clinical diagnosis of AD.

Second, the images we used in the visual scanning task are all line drawings, with black lines drawn on a white background (**Figure 1A**). Future research should adopt a more ecological or naturalistic design, with images simulating the outer world we see every day, which is much more complex, composed of more complex shapes and full of colors, containing many informative ROIs. For example, if we had used photographs or movies in the visual scanning task, the difference in the visual attention of AD patients and control subjects would be differentiated more clearly (Reading et al., 2012; Ramzaoui et al., 2018).

The third limitation is the small number of participants in this study, both AD patients and control subjects. We should increase the statistical power by studying more large-scale populations in the future.

The fourth limitation concerns the evaluation of pupil size change. In this study, we divided the pupil sizes by the averaged pupil sizes in the first trial of each subject, and this relative pupil size was analyzed. We took the pupil sizes in the first trial as a baseline because they are not affected by the execution of search tasks. Admittedly, the pupil size during the first trial may already be dilated by the cognitive effort and novelty effects, and may not necessarily be used as a reliable baseline. Unfortunately, we have not collected data for pupil size just-before the trials for a sufficient period. During the intersession period, the pupil size often deviated largely from the intrasession pupil size, partially because subjects moved their eyes during the period, and possibly because of distraction and/or mind wandering, i.e., the mental status was not stable during the intrasession period, so that it was difficult to take the intersession pupil size as baseline. As a compromise, we took the pupil sizes in the first trial, which was the period the subjects just started the session, as a baseline because they are not affected by the execution of search tasks. The same analysis was done both for AD patients and control subjects, which allowed comparison between the two groups.

## Conclusions

Most of the AD patients were able to complete the present task without much difficulty. This may be because the present task addressed attentional function related to visuospatial processing using the visual task and visual search in combination with eye tracking, instead of directly requiring responses to asked questions, which would necessitate explicit verbal processing and rely more on memory or executive function. Nevertheless, the task successfully visualized the multiple aspects of attention associated with cognitive decline, making it amenable even to AD patients with apathy and memory disturbance. The reduced fixation on informative ROIs in the visual memory task reflected impaired visuospatial attentional allocation due to defective executive/working memory function, leading to poorer recall of visual content, which could detect cognitive decline in AD patients with high sensitivity. Increased search time and saccade number until target detection in the visual search task indicated inefficient visual scanning, suggesting defective visual processing, especially in the serial search mode with a large number of items, which was related to top-down versus bottom-up attentional engagement. These results showed a high sensitivity in differentiating between AD patients and control subjects. On the other hand, decreased pupil size modulation during the visual search task suggested a diminished ability to increase visual attention to adapt to the cognitive load of the task and to optimize the performance, possibly associated with dysfunction of the LC. Pupil size modulation during the visual search task could be used to differentiate between subjects with normal cognition and those with cognitive decline because of its high specificity. Despite some limitations, considering the multiple aspects of visuospatial processing associated with attention in combination, we were able to detect aspects of early cognitive decline and this may become a new biomarker for the early detection and evaluation of cognitive decline that has high sensitivity and specificity.

## Data availability statement

The original contributions presented in this study are included in the article/supplementary material, further inquiries can be directed to the corresponding author.

## Ethics statement

The studies involving human participants were reviewed and approved by Ethics Committee at the University of Tokyo (approval no. 2411). The patients/participants provided their written informed consent to participate in this study.

## Author contributions

S-iT performed the experiments, collected the data, and prepared the figures. S-iT and YT wrote the main manuscript text and carried out patient recruitment. All authors reviewed the manuscript.

## Funding

S-iT was supported by a Research Project Grant-in-aid for Scientific Research from the Ministry of Education, Culture, Sports, Science, and Technology of Japan (Nos. 19K17046, 21K15687). SI-T was supported by Grant-in-aid for Scientific Research from the Ministry of Education, Culture, Sports, Science, and Technology of Japan (21K11317). MH was supported by MEXT KAKENHI (Nos. 15K19476, 15H01658, 16H01605, and 18K07521). YU received grants from the Ministry of Education, Culture, Sports, Science and Technology of Japan (Nos. 25293206, 15H05881, 16H05322, and 18K10821), The Research Committee on the Medical Basis

of Motor Ataxias, Health and Labour Sciences Research Grants, the Ministry of Health, Labour and Welfare of Japan, the Support Center for Advanced Telecommunications Technology Research, the Association of Radio Industries Businesses, and the Novartis Foundation (Japan) for the Promotion of Science, Nihon Kohden, Ltd., Takeda Pharmaceutical Company Limited, Nippon Boehringer Ingelheim Co., Ltd., and Mitsubishi Tanabe Pharma Corporation. YT was supported by a Research Project Grant-in-aid for Scientific Research from the Ministry of Education, Culture, Sports, Science and Technology of Japan (18H05523) and Communications R&D Promotion Programme from the Ministry of Internal Affairs and Communications, Japan (B203060001). These funders were not involved in the study design, collection, analysis, interpretation of data, the writing of this article or the decision to submit it for publication.

## Acknowledgments

We thank all of the healthy volunteers and patients for their participation.

## Conflict of interest

S-iT has received speaker's honoraria from Otsuka Pharmaceutical Co., Ltd., Daiichi Sankyo Co., Ltd., Dainippon Sumitomo Pharma Co., Ltd., Takeda Pharmaceutical Co., Ltd., Mitsubishi Tanabe Pharma Corporation, Biogen Japan Ltd., FP Pharmaceutical Corporation, and AbbVie Inc. YU received honoraria from the Taiwan Movement Disorders Society, Chinese Neurology Society, Astellas Pharma Inc., Eisai Co., Ltd., FP Pharmaceutical Corporation, Otsuka Pharmaceutical Co., Ltd., Elsevier Japan K.K., Kissei Pharmaceutical Co., Ltd., Kyorin Pharmaceutical Co., Ltd., Kyowa Hakko Kirin Co., Ltd., GlaxoSmithKline K.K., Sanofi-Aventis K.K., Daiichi Sankyo Co., Ltd., Dainippon Sumitomo Pharma Co., Ltd., Takeda Pharmaceutical Co., Ltd., Mitsubishi Tanabe Pharma Corporation, Teijin Pharma Ltd., Nippon Chemiphar Co., Ltd., Nihon Pharmaceutical Co., Ltd., Nippon Boehringer Ingelheim Co., Ltd., Novartis Pharma K.K., Bayer Yakuhin, Ltd., and Mochida Pharmaceutical Co., Ltd., and received royalties from Chugai-Igakusha, Igaku-Shoin Ltd., Medical View Co., Ltd., and Blackwell Publishing K.K.

The remaining authors declare that the research was conducted in the absence of any commercial or financial relationships that could be construed as a potential conflict of interest.

## Publisher's note



## References

Armstrong, R. A. (2009). Alzheimer's disease and the eye. *J. Optom.* 2, 103–111. doi: 10.3921/joptom.2009.103

Aston-Jones, G., and Cohen, J. D. (2005). An integrative theory of locus coeruleus-norepinephrine function: Adaptive gain and optimal performance. *Annu. Rev. Neurosci.* 28, 403–450. doi: 10.1146/annurev.neuro.28.061604.135709

Beltrán, J., García-Vázquez, M. S., Jenny Benois-Pineau, J., Gutierrez-Robledo, L. M., and Dartigues, J.-F. (2018). Computational techniques for eye movements analysis towards supporting early diagnosis of Alzheimer's disease: A review. *Comput. Math. Methods Med.* 2018:2676409. doi: 10.1155/2018/2676409

Boucart, M., Bubbico, G., Szafarczyk, S., and Pasquier, F. (2014). Animal spotting in Alzheimer's disease: An eye tracking study of object categorization. *J. Alzheimers Dis.* 39, 181–189. doi: 10.3233/JAD-131331

Braak, H., Thal, D. R., Ghebremedhin, E., and Del Tredici, K. (2011). Stages of the pathologic process in Alzheimer disease: Age categories from 1 to 100 years. *J. Neuropathol. Exp. Neurol.* 70, 960–969. doi: 10.1097/NEN.0b013e318232a379

Bredesen, D. E. (2014). Reversal of cognitive decline: A novel therapeutic program. *Aging (Albany NY)* 6, 707–717. doi: 10.18632/aging.100690

Bredesen, D. E., Amos, E. C., Canick, J., Ackerley, M., Raji, C., Fiala, M., et al. (2016). Reversal of cognitive decline in Alzheimer's disease. *Aging (Albany NY)* 8, 1250–1258. doi: 10.18632/aging.100981

Bridgeman, B., Hendry, D., and Stark, L. (1975). Failure to detect displacement of the visual world during saccadic eye movements. *Vision Res.* 15:71922. doi: 10.1016/0042-6989(75)90290-4

Chapman, P. (2005). "Remembering what we've seen: Predicting recollective experience from eye movements when viewing everyday scenes," in *Cognitive processes in eye guidance*, ed. G. Underwood (New York, NY: Oxford University Press), 237–258. doi: 10.1093/acprof:oso/9780198566816.003.0010

Cormack, F., Gray, A., Ballard, C., and Tovee, M. J. (2004). A failure of "Pop-Out" in visual search tasks in dementia with Lewy bodies as compared to Alzheimer's and Parkinson's disease. *Int. J. Geriatr. Psychiatry* 19, 763–772. doi: 10.1002/gps.1159

Crawford, T. J., Devereaux, A., Higham, S., and Kelly, C. (2015). The disengagement of visual attention in Alzheimer's disease: A longitudinal eye-tracking study. *Front. Aging Neurosci.* 7:118. doi: 10.3389/fnagi.2015.00118

Crawford, T. J., Higham, S., Mayes, J., Dale, M., Shaunak, S., and Lekwuwa, G. (2013). The role of working memory and attentional disengagement on inhibitory control: Effects of aging and Alzheimer's disease. *Age* 35, 1637–1650. doi: 10.1007/s11357-012-9466-y

Daffner, K. R., Scinto, L. F., Weintraub, S., Guinessey, J. E., and Mesulam, M. M. (1992). Diminished curiosity in patients with probable Alzheimer's disease as measured by exploratory eye movements. *Neurology* 42, 320–328. doi: 10.1212/WNL.42.2.320

Delazer, M., Sojer, M., Ellmerer, P., Boehme, C., and Benke, T. (2018). Eye-tracking provides a sensitive measure of exploration deficits after acute right MCA stroke. *Front. Neurol.* 9:359. doi: 10.3389/fneur.2018.00359

Dubois, B., Feldman, H. H., Jacova, C., Dekosky, S. T., Barberger-Gateau, P., Cummings, J., et al. (2007). Research criteria for the diagnosis of Alzheimer's disease: Revising the NINCDS-ADRDA criteria. *Lancet Neurol.* 6, 734–746. doi: 10.1016/S1474-4422(07)70178-3

Fernandez, G., Castro, L. R., Schumacher, M., and Agamennoni, O. E. (2015a). Diagnosis of mild Alzheimer disease through the analysis of eye movements during reading. *J. Integr. Neurosci.* 14, 121–133. doi: 10.1142/S0219635215500090

Fernandez, G., Schumacher, M., Castro, L., Orozco, D., and Agamennoni, O. (2015b). Patients with mild Alzheimer's disease produced shorter outgoing saccades when reading sentences. *Psychiatry Res.* 229, 470–478. doi: 10.1016/j.psychres.2015.06.028

Fernandez, G., Manes, F., Rotstein, N. P., Colombo, O., Mandolesi, P., Politi, L. E., et al. (2014a). Lack of contextual-word predictability during reading in patients with mild Alzheimer disease. *Neuropsychologia* 62, 143–151. doi: 10.1016/j.neuropsychologia.2014.07.023

Fernandez, G., Laubrock, J., Mandolesi, P., Colombo, O., and Agamennoni, O. (2014b). Registering eye movements during reading in Alzheimers disease: Difficulties in predicting upcoming words. *J. Clin. Exp. Neuropsychol.* 36, 302–316. doi: 10.1080/13803395.2014.892060

Fernandez, G., Mandolesi, P., Rotstein, N. P., Colombo, O., Agamennoni, O., and Politi, L. E. (2013). Eye movement alterations during reading in patients with early Alzheimer disease. *Invest. Ophthalmol. Vis. Sci.* 54, 8345–8352. doi: 10.1167/iovs.13-12877

Findlay, J. M., and Gilchrist, I. D. (2005). "Eye guidance and visual search," in *Cognitive processes in eye guidance*, ed. G. Underwood (New York, NY: Oxford University Press), 259–281. doi: 10.1093/acprof:oso/9780198566816.003.0011

Gabay, S., Pertzov, Y., and Henik, A. (2011). Orienting of attention, pupil size, and the norepinephrine system. *Atten. Percept. Psychophys.* 73, 123–129. doi: 10.3758/s13414-010-0015-4

Galetta, K. M., Chapman, K. R., Essis, M. D., Alosco, M. L., Gillard, D., Steinberg, E., et al. (2017). Screening utility of the King-Devick test in mild cognitive impairment and Alzheimer disease dementia. *Alzheimer Dis. Assoc. Disord.* 31, 152–158. doi: 10.1097/WAD.0000000000000157

Geng, J. J., Blumenfeld, Z., Tyson, T. L., and Minzenberg, M. J. (2015). Pupil diameter reflects uncertainty in attentional selection during visual search. *Front. Hum. Neurosci.* 9:435. doi: 10.3389/fnhum.2015.00435

Granholm, E. L., Panizzon, M. S., Elman, J. A., Jak, A. J., Hauger, R. L., Bondi, M. W., et al. (2017). Pupillary responses as a biomarker of early risk for Alzheimer's disease. *J. Alzheimers Dis.* 56, 1419–1428. doi: 10.3233/JAD-161078

Hao, J., Li, K., Li, K., Zhang, D., Wang, W., Yang, Y., et al. (2005). Visual attention deficits in Alzheimer's disease: An fMRI study. *Neurosci. Lett.* 385, 18–23. doi: 10.1016/j.neulet.2005.05.028

Heuer, H. W., Mirsky, J. B., Kong, E. L., Dickerson, B. C., Miller, B. L., Kramer, J. H., et al. (2013). Antisaccade task reflects cortical involvement in mild cognitive impairment. *Neurology* 81, 1235–1243. doi: 10.1212/WNL.0b013e3182a6cbfe

Horowitz, T. S., and Wolfe, J. M. (1998). Visual search has no memory. *Nature* 394, 575–577.

Itti, L., and Koch, C. (2001). Computational modelling of visual attention. *Nat. Rev. Neurosci.* 2, 194–203. doi: 10.1038/35058500

Kirby, E., Bandelow, S., and Hogervorst, E. (2010). Visual impairment in Alzheimer's disease: A critical review. *J. Alzheimers Dis.* 21, 15–34. doi: 10.3233/JAD-2010-080785

Kremen, W. S., Panizzon, M. S., Elman, J. A., Granholm, E. L., Andreassene, O. A., Dale, A. M., et al. (2019). Pupillary dilation responses as a midlife indicator of risk for Alzheimer's disease: Association with Alzheimer's disease polygenic risk. *Neurobiol. Aging* 83, 114–121. doi: 10.1016/j.neurobiolaging.2019.09.001

Landy, K. M., Salmon, D. P., Filoteo, J. V., Heindel, W. C., Galasko, D., and Hamilton, J. M. (2015). Visual search in dementia with Lewy bodies and Alzheimer's disease. *Cortex* 73, 228–239.

Lenoble, Q., Bubbico, G., Szafarczyk, S., Pasquier, F., and Boucart, M. (2015). Scene categorization in Alzheimer's disease: A saccadic choice task. *Dement. Geriatr. Cogn. Disord. Extra* 5, 1–12.

Lopez, O. L., and Kuller, L. H. (2019). Epidemiology of aging and associated cognitive disorders: Prevalence and incidence of Alzheimer's disease and other dementias. *Handb. Clin. Neurol.* 167, 139–148.

Matsuda, S., Matsumoto, H., Furubayashi, T., Fukuda, H., Emoto, M., Hanajima, R., et al. (2014). Top-down but not bottom-up visual scanning is affected in hereditary pure cerebellar ataxia. *PLoS One* 9:e116181. doi: 10.1371/journal.pone.0116181

Matsumoto, H., Terao, Y., Yugeta, A., Fukuda, A., Emoto, M., Furubayashi, T., et al. (2011a). Where do neurologists look when viewing brain CT images? An eye-tracking study involving stroke cases. *PLoS One* 6:e28928. doi: 10.1371/journal.pone.0028928

Matsumoto, H., Terao, Y., Furubayashi, T., Yugeta, A., Fukuda, H., Emoto, M., et al. (2011b). Small saccades restrict visual scanning area in Parkinson's disease. *Mov. Disord.* 26, 1619–1626. doi: 10.1002/mds.23683

Matsumoto, H., Terao, Y., Furubayashi, T., Yugeta, A., Fukuda, H., Emoto, M., et al. (2012). Basal ganglia dysfunction reduces saccade amplitude during visual scanning in Parkinson's disease. *Basal Ganglia* 2, 73–78.

Mosimann, U. P., Felblinger, J., Ballinari, P., Hess, C. W., and Müri, R. M. (2004). Visual exploration behaviour during clock reading in Alzheimer's disease. *Brain* 127(Pt 2), 431–438.

Osterrieth, P. A. (1944). Le test de copie d'une figure complexe: Contribution à l'étude de la perception et la memoir. *Arch. Psychol.* 30, 206–356.

Oyama, A., Takeda, S., Ito, Y., Nakajima, T., Takami, Y., Takeya, Y., et al. (2019). Novel method for rapid assessment of cognitive impairment using high-performance eye-tracking technology. *Sci. Rep.* 9:12932. doi: 10.1038/s41598-019-49275-x

Ramzaoui, H., Faure, S., and Spotorno, S. (2018). Alzheimer's disease, visual search, and instrumental activities of daily living: A review and a new perspective on attention and eye movements. *J. Alzheimers Dis.* 66, 901–925. doi: 10.3233/JAD-180043

Reading, M. R., Polden, M., Gibbs, M. C., Wareing, L., and Crawford, T. J. (2012). The potential of naturalistic eye movement tasks in the diagnosis of Alzheimer's disease: A review. *Brain Sci.* 11:1503. doi: 10.3390/brainsci11111503

Reches, A., Laufer, I., Ziv, K., Cukierman, G., McEvoy, K., Ettinger, M., et al. (2014). Network dynamics predict improvement in working memory performance following donepezil administration in healthy young adults. *Neuroimage* 88, 228–241. doi: 10.1016/j.neuroimage.2013.11.020

Riediger, M., Li, S.-C., and Lindenberger, U. (2006). "Selection, optimization, and compensation as developmental mechanisms of adaptive resource allocation: Review and preview," in *Handbook of the psychology of aging*, eds J. E. Birren and K. W. Schaie (Amsterdam: Elsevier), 289–313. doi: 10.1016/B9-78-012101-2/64950-0161

Salvaggio, S., Andres, M., Zénon, A., and Masson, N. (2022). Pupil size variations reveal covert shifts of attention induced by numbers. *Psychon. Bull. Rev.* 29, 1844–1853. doi: 10.3758/s13423-022-02094-0

Stern, Y., Arenaza-Urquijo, E. M., Bartres-Faz, D., Belleville, S., Cantilon, M., Chetelat, G., et al. (2018). Whitepaper: Defining and investigating cognitive reserve, brain reserve, and brain maintenance. *Alzheimers Dement.* 16, 1305–1311. doi: 10.1016/j.jalz.2018.07.219

Terao, Y., Fukuda, H., Ugawa, Y., and Hikosaka, O. (2013). New perspectives on the pathophysiology of Parkinson's disease as assessed by saccade performance: A clinical review. *Clin. Neurophysiol.* 124, 1491–1506. doi: 10.1016/j.clinph.2013.01.021

Tokushige, S. I., Matsuda, S. I., Oyama, G., Shimo, Y., Umemura, A., Sasaki, T., et al. (2018). Effect of subthalamic nucleus deep brain stimulation on visual scanning. *Clin. Neurophysiol.* 129, 2421–2432.

Treisman, A. (1998). Feature binding, attention and object perception. *Philos. Trans. R Soc. B Biol. Sci.* 353, 1295–1306. doi: 10.1098/rstb.1998.0284

Treisman, A. M., and Gelade, G. (1980). A feature-integration theory of attention. *Cogn. Psychol.* 12, 97–136. doi: 10.1016/0010-0285(80)90005-5

Vallejo, V., Cazzoli, D., Rampa, L., Zito, G. A., Feuerstein, F., Gruber, N., et al. (2016). Effects of Alzheimer's disease on visual target detection: A peripheral bias. *Front. Aging Neurosci.* 8:200. doi: 10.3389/fnagi.2016.00200

Vazey, E. M., Moorman, D. E., and Aston-Jones, G. (2018). Phasic locus coeruleus activity regulates cortical encoding of salience information. *Proc. Natl. Acad. Sci. U.S.A.* 2115, E9439–E9448. doi: 10.1073/pnas.1803716115

Verheij, S., Muilwijk, D., Pela, J. J. M., van der Cammen, T. J. M., Mattace-Raso, F. U. S., and van der Steena, J. (2012). Visuomotor impairment in early-stage Alzheimer's disease: Changes in relative timing of eye and hand movements. *J. Alzheimers Dis.* 30, 131–143. doi: 10.3233/JAD-2012-111883

Viña, J., and Sanz-Ros, J. (2018). Alzheimer's disease: Only prevention makes sense. *Eur. J. Clin. Invest.* 48:e13005. doi: 10.1111/eci.13005

Viskontas, I. V., Boxer, A. L., Fesenko, J., Matlin, A., Heuer, H. W., Mirsky, J., et al. (2011). Visual search patterns in semantic dementia show paradoxical facilitation of binding processes. *Neuropsychologia* 49, 468–478. doi: 10.1016/j.neuropsychologia.2010.12.039

Yang, Q., Wang, T., Su, N., Xiao, S., and Kapoula, Z. (2013). Specific saccade deficits in patients with Alzheimer's disease at mild to moderate stage and in patients with amnestic mild cognitive impairment. *Age* 35, 1287–1298. doi: 10.1007/s11357-012-9420-z

Yarbus, A. (1967). *Eye movements and vision*. New York, NY: Plenum Press. doi: 10.1007/978-1-4899-5379-7

# Frontiers in
# Aging Neuroscience

**Explores the mechanisms of central nervous system aging and age-related neural disease**

The third most-cited journal in the field of geriatrics and gerontology, with a focus on understanding the mechanistic processes associated with central nervous system aging.

---

## Discover the latest Research Topics

See more →

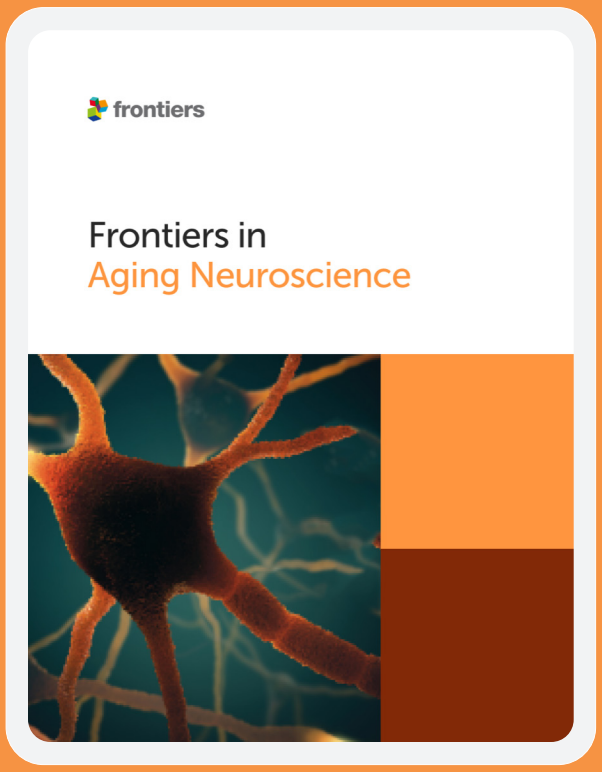


**Frontiers**

Avenue du Tribunal-Fédéral 34
1005 Lausanne, Switzerland
frontiersin.org

**Contact us**

+41 (0)21 510 17 00
frontiersin.org/about/contact